ASYMMETRIC TOTAL SYNTHESIS OF HAVELLOCKATE AND INVESTIGATION INTO CHIRAL PALLADIUM ENOLATES: SYNTHESIS, REACTIVITY, AND APPLICIATIONS

Thesis by

Tsam Mang Melinda Chan

In Partial Fulfillment of the Requirements for

the Degree of

Doctor of Philosophy

CALIFORNIA INSTITUTE OF TECHNOLOGY
Pasadena, California

2024
(Defended May 23rd, 2024)

Melinda Chan
ORCID: 0000-0002-2495-0110

To my dearest Nainai

ACKNOWLEDGEMENTS

If you had asked me a few years ago how graduate school was going, I would have told you that it sucked. It sucked to witness my class/cohort getting significantly affected by the pandemic. It sucked to be amongst the few students dealing with visa complications, preventing me from visiting home where many of my family and friends were throughout my entire graduate school career.

If you were to ask me the same question today, I would still acknowledge the difficulties. However, I've come to realize that everyone in graduate school (and outside of graduate school) faces challenges, whether they are apparent to you or not. What I've learned is the importance of *being kind to everyone and practicing gratitude.* Once I began to shift my perspective, I now recognize that the past five years have probably been the best of my life. As I started to jot down names of people that I needed to thank, I began to feel incredibly grateful for all the support and kindness that I have received along this journey.

The first person I would like to express my upmost gratitude to is my faculty advisor, Brian Stoltz. As an ESL student with a limited vocabulary, I struggle to find adequate words to convey how deeply thankful I am to you. I want to thank you for your unwavering guidance throughout the years, whether it was chemistry-related or life in general. During one of our 'State of the Lab' meetings, Brian shared that during conferences, he often heard colleagues complain about their students, yet he never had anything to complain about any of us. He genuinely believed that we are the best organic chemistry lab in the world. I've been wanting to express to Brian that I (and many others) shared the same sentiment; when I was at conferences or interacting with other graduate students, I often heard people complain about their advisors, but I never had anything negative to say, ever. Perhaps that's

why I've always been so enthusiastic about recruiting for our lab and why I get the biggest smile on my face whenever people ask, 'What's it like working for Brian?'

Brian is not only the smartest and most patient advisor but also one of the funniest and most athletic individuals I know. Over the years, Brian had lived up to his 'fun dad' image, wanting to be a part of every inside joke and also liking to joke around which brought me immeasurable joy. (On a serious note, how is Brian beating us at every sport that our lab decides to play?)

I also want to thank Erna for the emotional support and for the most delicious muffins and pastas! There must have been so many students, visiting students, staff members that you have met but didn't interact with daily over the past several decades. But you managed to remember everyone's name, to be kind to everyone, and to care for everyone. For that, I thank you on behalf of everyone that ever stepped foot in the Stoltz lab. We will not be the same without you, and I hope you know how much you mean to us. I also really appreciated hearing the funny stories of the early days with Brian, about life back home, about Harry and Teddy. Thank you, Erna, you are the best!

Other than Brian and Erna, I've had a lot of other mentors in my life that I would like to thank as well. I want to thank Andrew Nelson for being my mentor at the Siegel lab. You were the first person who got me super excited about organic chemistry, and you are still the person that I aspire to be because of how passionate and hard-working you are. I want to thank Dr. Siegel and Dr. Komives for believing in me and giving me the chance to work in their labs. I want to thank Craig Eberhard for being a mentor to me in my business minor and for all the meals and coffee chats for general life advice. I also need to thank Dr. Nick Hafeman and Dr. Tyler Fulton for being mentors to me when I first came to Caltech.

You guys have taught me so much chemistry that I still benefit from to this day. I am so glad that we were able to have the difficult conversations, talk through our misunderstandings and work out as friends again at the end. I really appreciated that. Lastly, in terms of mentors, I was also fortunate enough to have Professor Sarah Reisman, Professor Hosea Nelson and Professor Harry Gray on my thesis committee. Thank you for all the helpful discussions and recommendations that you all have provided me. I especially want to thank Sarah for her unconditional support and for being a great committee chair. The entire Stoltz lab is very lucky to have her during our group meetings and to have her invaluable feedback. Throughout my years on the third floor, I have also been fortunately enough to see a fun side of Sarah at our yearly holiday party, which I also appreciated deeply.

I want to thank the entire Stoltz Lab – our lab has some of the smartest, funniest, and kindest people that I know, and this lab would not be the same without any single one of you. Specifically, I want to thank my best friend and my nonbiological sister, Veronica Hubble for literally being the person she is. I will forever be grateful that you decided to ask me to hang out and talk about this medical doctor at HMRI and that blossomed into this friendship that got me through every hardship in the past three years. I've told you many times, but I will tell you again that you are family to me, and I will always cherish the softball games, the "snackie times," and panic sessions together at Caltech. Just like how I will always cherish now our little hiking/camping trips, late-night phone calls that can last till sunrise if we let it to, and other adventures. You were a beam of light in my life that guided me through the darkest times. Thank you for being the most understanding, the most considerable, and the most caring person. Thank you for being born, seriously.

Next, I want to thank Dr. Sardini. Thank you for teaching me so much about organic chemistry. You are seriously a walking Wikipedia of organic chemistry and also of many random facts. At the beginning of our friendship, I didn't know the mechanisms of a lot of organometallic transformations, and you didn't know who the Migos and the Weeknd were. We've both come so far. Thank you for keeping me sane during our isolation days at Church and for sending me random Chinese memes every day. I also want to thank Natalie Shum. You have such a beautiful and kind soul, and I thank Stephen all the time for bringing you to our group.

To Chris Reiman, TC, Fa Ngamnithiporn, Eric Alexy, Cus, and Officer Kim, thank you for welcoming me into the Stoltz lab. I knew this was the lab I wanted to join when everyone cared about eating lunch together at 11:30 AM just as much as their chemistry. Everyone was so incredibly nice to me, and I want to thank you all for the memories of eating Ernies together in the COVID months when we could only eat it outdoors in the wildfire ashes.

I especially want to thank Cus for being my quarantine bestie, for the spicy ramen mukbangs, and for the shared Instagram that we have with our stuffed toys Poo and Penelope. You are so smart and funny, and you brought me so much light in my early days in the Stoltz lab. Thank you for teaching me that a Caucasian boy can speak very good Mandarin and Vietnamese, what mice droppings look like, and everything about transition metal catalysis. My only wish is for you to still remember me when you get that Nobel Prize one day. I also need to give a special shoutout to Officer Kim, who built a strong empire of good safety culture in the Stoltz lab. As a fellow female in STEM, you were always an inspiration to me. Thank you for all the game nights during COVID, for the delicious bossam, and for shouting

at karaoke together. I am so grateful to have had you as my Big Sib when I first joined the lab because I wouldn't have traded it with anyone else.

To Joel Monroy, Lexie Beard, Andrea Stegner, and Ally Stanko, thank you all for being in my cohort and for struggling together in classes and during COVID. Joel, you continue being a role model to me for not being afraid to chase your dreams and for knowing what is best for yourself. You were my rock in the Stoltz lab, and I thank you for keeping me sane during some very low points in our first year. I was invited to a panel with the WAVE fellows last year, and someone asked me about untraditional pathways to graduate school and if that will matter in the long run. I told them that I know someone named Joel who took time to explore himself and came to graduate school at the age of 35 and he was one of the smartest, most dedicated scientists that I know. I still remember receiving numerous emails from people who thanked me for sharing your journey and how they always felt the Imposter Syndrome and not a sense of belonging until they heard about you. So, thank you for guiding me and many others. Lexie and Andrea, we probably took every class together for our first two quarters. I want to thank you for the late-night problem-solving sessions and little meals here and there to catch up on life in general. Thank you for being patient with me and for teaching me so much about chemistry. Ally, thank you for becoming my classmate in the Stoltz lab. Thank you for the chemistry and graduating lifetime discussions, the Girly talk of jewelry, clothes, hair, and nails, and the laughs together in the small office. I still can't believe that we have not gone to a rave together, but I am going to make it happen.

To Kali Flesch and Camila Suarez, thank you guys for being the BEST bay mates I could ever ask for. I cannot imagine being in the lab for long hours without you. Thank you for always being willing to help and discuss chemistry together. Thank you for being patient

and listening to me complain about many random little things. Thank you for our little shopping trips, lunches, and wine nights. You both are the little sisters I wish I had, but now I do, and I am so grateful for having you both in my life. Little Kali, thank you for letting me spread over to your side of the hood when I am being chaotic. Thank you for babysitting me during my first camping trip at Yosemite. Thank you for being my rock for our shard projects, our student organization involvement, and our lives in general. Your relationship with Brian (not Stoltz) is the cutest, and I can't wait to go on more adventures with you both. Little Cami, you are probably already tired of hearing me say how much I appreciate your existence and how much I adore you as a person. You are just the coolest, most hard-working, and funniest soul that I've ever met. Thank you for opening up to me, knowing how it is not easy for you to do so with just anyone, and thank you for teaching me how to be a more reserved, calm, and mature person.

To Jay Barbor and Farbod Moghadam, thank you for being great project partners. Thank you for the brainstorming sessions, for being patient with me when I had questions, and for the little laughs that we had while working together. I especially want to thank Jay and Jessie, my fellow cat lovers. Thank you both for all the bbq nights and for making the best toys for Pusheen. Thank you for introducing me to little Maeby and little Tuna. These little troublemakers brought me nothing but joy whenever I saw their pictures.

To Elliot Hicks and Samir Rezgui, thank you for your willingness to hear out my problems and share your intellectual insights over chemistry ideas. You guys are the most humble, hard-working, and funny people I know. Thank you for bringing me so much joy over talking about the "king" (iykyk). I also want to thank Kevin Gonzalez, for the fun year of working on the DICI board together. I still cannot believe you were friends with my middle

school friends in China. What a small world! To Christian Strong and Ruby Chen, thanks for the shenanigans at our side of the big office and for the most random topics of discussion that I never expect to encounter. To Marva Tariq, Kimberly Sharp, Chloe Cerione, and Sara Siddiqui, thank you for continuing to be my inspiration and showing me this girl power in STEM. You all are killing it! To Adrian Samkian, Ben Gross, Hao Yu, Adrian de Almenara, Bryce Gaskin, Jonathan Farhi, Elijah Gonzalez, Dr. Melissa Ramirez, Adam Zoll, and Chris Cooze, thank you all for being my mentors along this journey. I realized that in graduate school, no matter your age and residency, there is always something that you can learn from others, always.

For my CCE friends outside of the Stoltz Lab, Mike He, Molly McFadden, Skylar Osler, and Stella Luo, thank you all for the lessons and conversations that we have regarding graduate school and life in general. You all made my Caltech journey very special, and you continue to remind me how lucky we are to be in one of the best divisions at Caltech.

To my friends outside of CCE, Seola Lee, Shawn Sheng, and Matthew Yao, thanks for all the game and meme nights. I am so grateful for Laura Flower Kim because I was able to meet you all through the international student orientation. Thank you for being there for me in the past few years and I am so proud of how far we've all come.

For the past three years of my graduate career, I have been lucky to be involved with the Diversity in Chemistry Initiative (DICI), and I cannot express how thankful I am to have this separate family outside of my lab family. Professor Doug Rees, thank you for being a great advisor for DICI, DICI would not be here without you, and I would not be here without you. Thank you for all the laughs and advice and for believing in DICI wholeheartedly. Thank you for being our rock. David Cagan, thank you for believing in me

to take over your role in DICI. You are one of the best leaders I have ever came across, and you will always be someone that I aspire to be. To current DICI board members: Cami, Marva, Juliet, Jacob, Omar, Kevin, and Noor, thank you for teaching me how to be better at communication, delegating, and leading. I often feel bad when people associate me with the success of DICI in the past year, but I just happened to be the president last year. It was every one of you that made DICI so special, and I will forever be thankful for everything that you have taught me.

Speaking of my involvement with DICI, throughout the years of organizing events and hosting speakers, I've had the pleasure to work with some amazing staff on campus that I would like to thank. Elyse Garlock is a rockstar admin. She has done so much for DICI and the DEI committee, and I thank you on behalf of everyone who has benefited from your kindness, Elyse. Grace Liang and Paolina Martinez were both someone that I've seen multiple times but did not get the chance to get to know on a deeper level until recently, and they are some of the most talented, patient, and kind people that I know who will stop anything they are doing to help me out. Thank you both for that. I also want to thank Maria from the SFP office for her unconditional support for DICI and for always being willing to host event with us. Every time I see how much she cares about her programs and the students in these programs, I get inspired.

Lastly, I want to thank everyone who had the most important job which is to keep everything running smoothly. Dr. Scott Virgil, thank you for your expertise at the 3CS catalysis. Not only that you are one of the best chemists I know, but you are also so talented with machines and you have helped build so many instruments that many of us could not live without. Thank you for always being there for me and for being willing to drop anything

you're doing to help us out. I really enjoyed the little conversations that we had together while using the HPLC. Silva Virgil, thank you for hosting the best Christmas parties! You are always such a great host and you put your 100% into everything you do, and it shows through the events that you put up. You are also one of the sweetest people I know.

Mona, Mike, and Dave, thank you for all the NMR and crystallography helps. None of our research would have been possible without any single one of you and you deserve all the credit in the world for everything you do on a daily basis.

Leslie, thank you for always putting a smile on my face when I see you in the hallway. Thank you for keeping everything tidy on the third floor. I know we are not the most organized and clean bunch. You never complained about anything, and instead, you showered us with your kindness, your smile, and your amazing home-cooked meals. You were a "mom" to me at Schlinger, and I am so grateful for you.

Tomomi and Alison, thank you for everything that you do day to day. Your jobs are so incredibly important for every student on campus, and we all would not be here without you. I want to especially thank Beth Mitchell. Thank you for spending the last few years of your career helping at Caltech. You helped me so much during my early days at the Stoltz lab. One time, I saw Beth struggle to get down the stairs at Schlinger, and I offered to help. Months later, I remember Beth came to find me in the lab and was so excited to tell me on that day she was able to get down all three flights of stairs without stopping for the first time in decades because she and her husband had been working out together to prepare for some retirement traveling. She was so happy and excited to share that with me. That moment went into my core memory, and it still warms my heart whenever I think about it. Thank you for

your kindness, Beth. I hope you are hiking everywhere in your retirement and going to all the cruises you talked about!

Now, I want to thank my friends outside of Caltech. As an international student with very few family members in the US, I consider all my friends my extended family, and they have proven me right about that repeatedly. No matter the hardship and no matter the time, these following people have always been there for me, and I can only hope that I can repay them with the love and care I give them back.

First, I want to thank my OG best friend, Hiro. We have met probably over 12 years ago now, and for the last 10 years we probably only seen each other less than 10 times because of all the visa/traveling restrictions, but that never stopped him from caring about me and from being there for me whenever I needed a shoulder to lean on, even if it was all virtual WeChat calls. I miss you so much. Thank you for being there to celebrate every little accomplishment with me and thank you for being there during my worst and still love me at the end. You made me a better person, and you will always be my OG bestie.

To my "high school sweethearts" Sisi, Wendy, and Ashley, I want to thank you for also being patient with me for not being able to hang out because of our long-distance friendships. Although I was not able to travel much, a lot of you made efforts to come visit me many times in LA, and it meant so much to me to feel that sense of home while you were here.

To my undergraduate die-hard besties Vania and Cathline, I don't even know where to start when it comes to thanking you both. I wouldn't even be in graduate school without either of you. I don't even think I would have made it out of undergraduate without your friendship and support. Vans, thank you for being my sunshine in the past almost decade of

knowing you. I still remember how you told me that you thought I was intimidating at our Rush event, and now I am attending your wedding as a bridesmaid. You are my inspiration because you are so hard-working, compassionate, and driven. You are one of the only people that I felt connected to on a soul level in life, and I am so grateful to have a soul sister like you. You taught me how to treat friends like family and how to love unconditionally. I can't wait to celebrate your PhD defense and you're wedding with you as well.

Cathline, you showed me the most unconditional love that I can ever ask for in a friend. Every time I had any problem, big or small, you were already there before I even asked. Thank you for co-parenting Poo and Shithead together. Thank you for all the adventures, trips, and food runs that we had together. There were times that I was so down, but you only were able to make me laugh so hard that my abs hurt. You were an angel that was sent to me, and I want to cherish that forever.

Next, I want to thank my LA girls Lindy, Tiff, Joyce, Ashley, and Diana. These girls welcomed me with open arms when I first moved to LA and invited me to every rave, food run, and gossip session. Thank you for being my rock and for keeping me sane during the past few years. These girls are some of the most loving, caring, and funny people I know. Over the past few years, we have shared so many laughs and tears, and that's why you are all family to me, forever. Thank you for all the wine and paint nights, game nights, and hiking trips. Thank you for also being foodies and loving to eat and explore restaurants together. My years in graduate school would not have been the same without you.

I want to give a special shoutout to my favorite couple in the world Nattie and Will, featuring my favorite person, Miss Nattie Srisutthisuriya <3. Thank you both for coming into my life one month into my graduate program. You have been there for me through literally

thick and thin over the past few years, and I am forever grateful for all the trips, meals, and late-night chess sessions we had together. Your love for each other is so touching to witness, and I am so happy that I got to be part of your life journey. I remember a few months after we met, Will thanked me for being Nattie's friend. That will be one of those core memory moments that I can never forget, but also, it is me who should thank Nattie for being my sister for life. Nattie, you are seriously the most kind-hearted person that I know. You taught me what it's like to be compassionate, loving, understanding, and patient. You are the beam of sunshine that lit up my whole world during times when all I could see was darkness. Sometimes when I am in the lab, I randomly think of you, and the thought of you always makes me smile and my day is immediately better. You were there for me without you even knowing it. I love you both so much and I can't wait to travel the whole world together and eat like there is no tomorrow for the rest of our lives.

I want to thank Alex, James, Marie, Evan, Viet, Tanner, Calvin, Kenneth, Megan, Yuri, Justin, Nathan, Ching, Allen, and David for welcoming me into the best friend group and for making the cutest totems at festivals. These will also be the people to blame when one day my ears will inevitably not work as well because of all the loud music that I was exposed to. Thank you for all the bar hopping nights, clubbing nights, and never ending kbbq together. These things made me temporarily forget that I was in graduate school sometimes, which was very much needed.

Recently, through recruitment and job searching, I had the pleasure to meet Bruce and Jackie, who had easily become some of my favorite people in the world, especially after finding out that Jackie was one of the founding members of the sorority that I was a part of in undergrad. What a small world! Bruce, thank you for all your expertise and guidance

during the months of job hunting. Thank you for believing in me even when I didn't myself. Thank you for seeing the best in me and continuing to teach me how to be better. Thank you for being there for me through all the acceptances and rejections that I've received. I would not be here without you. You two are my role models both in the aspect of your loving relationship with each other and the kind-hearted and caring people that you are. I feel so blessed to have you as my friends and I can't wait to go on more adventures together in the future.

Finally, I want to thank my family and almost-biological families, Of course, I want to start by thanking my mom and dad. My mom and dad sacrificed everything they ever had for me to have the life that I have right now, and I will never be able to repay them for what they gave me. Growing up as a single child with a big attitude has not been easy for either me or my parents, but I want to thank them for being patient with me, for believing in me, and for complimenting me on every tiny accomplishment that I had.

妈妈, thank you for teaching me what unconditional love feels like. Thank you for being proud of me and pushing me to be the best version of myself. Thank you for coming to visit me during graduate school and cook delicious food for me. Thank you for being supportive of everything I do. I have always looked up to my mom because of how driven and hard-working she is. She loves hard every person she cares about. She will be there for me and her friends in a heartbeat, and that is why everyone adores her. I love you.

爸爸, thank you for teaching me how to be well-mannered, how to treat every stranger with respect, and how to think from other people's perspectives instead of my own. My dad is a very quiet, reserved, and humble person, and I don't think he gives himself enough credit for the positive influence that he has on the people that he loves. He doesn't

express his emotions easily, but I know he loves me just as much as my mom. I am also not good at expressing my feelings and I don't say this enough to my parents, but I love you so much and I thank you for everything.

I want to thank my grandparents for raising me and influencing me when I was young. To my 公公 and 婆婆, thank you for teaching me how to play Chinese chess, calligraphy, and seal cutting. Thank you for teaching me how to be kind and gracious. To ye ye, thank you for the limited years that we spent together. Thank you for the funny stories that mom and gugu still tell me until this day. Thank you for inspiring me to choose STEM by being a great role model.

To my dearest 奶奶, thank you for being my backbone since the day I was born. Thank you and 武奶奶 for taking good care of me when I was young. I don't have many memories of my younger days, but every memory I still have before I was 6, you were in them. I remember you teaching me my first English word, apple. I remember you teaching me that there is schooling beyond college. I remember you taught me all the characters in Mahjong. Then I got older, and I am grateful that I got to have more memories with you. I remember you would be so happy to see me after school and you would spend all day cooking my favorite dish. I remember sleeping together and staying up to sunrise hearing stories about our family before I was born. I remember that you got sick when I was in high school and had heart issues, but the moment you saw me you began to feel so much better. I remember how proud you were when I got into graduate school, and you would call up all your friends and tell them about it. I remember the year I left China; you were 95 years old, and you told me you would live another 5 years to see me graduate. You kept that promise because I can feel you here with me right now. Thank you for everything nainai. You will forever be the

apple of my eye. I love and miss you every day. This work is dedicated to you nainai, you can rest easy now. You don't have to worry about me not getting enough sleep anymore. I will tell you more about it when we meet again one day.

I want to thank my 姑姑 and 姑父 who were there for me since the day I was born. They took care of me like I was one of their own, and I miss the days when we used to go on walks in Baowen Rd together and see wild animals. I miss the days that my aunt and I would stay up all night and she would tell me stories about her and my dad's childhood. I miss the days that we would spend Christmas and Chinese New Year together as a big family. Gugu, thank you for showering me with your unconditional love and caring for me the way you did. You got such a kind heart and a young soul. Thank you and gufu for supporting me financially over the years especially for college. I can never repay you for the sacrifices that you have done for me, but I can tell you repeatedly how much I appreciate you both. Gufu, you were one of the funniest, kindest, nicest, smartest, and most humble people I have ever met. You taught me to never judge anyone, to always see the best in every person, and to love wholeheartedly the people that you care about. Thank you for being my guardian angel. I miss you so much. To Madeline (Tingchun Jiejie), Baobao gege, and Mindy, thank you for being the best family that I could ever ask for. Growing up, you all have taught me so much and shared so many amazing memories together. I will forever cherish them, and I wouldn't be where I am and who I am without your influence.

I also want to thank my son, Pusheen. You came into my life at a very low point, and your presence immediately made everything better. I remember the first time holding you, and I felt the deepest connection even though I wasn't much of a cat person growing up. You continue to teach me how to be a better mom and how to love unconditionally. You

were always there for me whenever I was happy or when I was down. I feel so lucky to have the opportunity to be your mommy.

To Derek's family – Derek's Mom & Dad, Bonney, Lucas, Mochi, and Bobi, thank you all for welcoming me with open arms and taking care of me. Shushu & Ayi, your kindness continues to warm my heart every time we hang out together. You took me in like I am one of your own, and for someone who doesn't have a lot of family in the LA area, you have no idea how much that meant for me. You taught me so much from how to be a better cook to how to be a better person. You were second parents to me during this challenging chapter of my life, and I loved our dinners, trips, and adventures together. Bonney, thank you for being a great friend to me. You are one of the most talented, caring, and funniest people I know. I love all your witty jokes, creative product/website designs, and passions. You were also an amazing conversationist and listener. Thank you for being willing to listen to my problems and give me great advice on them. I really appreciated it. Lucas, though we haven't met for long, I want to thank you for being part of our little family and for the memories that we have together. You are super considerate and caring, and a great partner to Bonney, and I thank you for that. Bobi, thank you for being the little sweet baby angel you are. Thank you for bringing us so much joy during family gatherings. Hope you rest in peace in doggie heaven. Mochi, thank you for coming into my life and allowing me to be your mommy. You are such a little ball of cuteness who everyone loves. You bring joy to everyone you touch with your beautiful soul. I know you haven't had the smoothest ride in the past several years, but you continue to inspire me with your strength. You endure so much as a small doggie, and I hope your suffering can stop soon, so you can just focus on being cute for the rest of your life.

I want to express my heartfelt gratitude to my boyfriend, Derek Ruan. These past few years wouldn't have been possible without you. I vividly recall Nick's comment during his defense, where he mentioned that the only thing tougher than being a graduate student is being in a relationship with one. I resonated deeply with that sentiment throughout our time together. You've shown me love, patience, and comfort when I needed them the most. You've celebrated all my highs and supported me through all my lows. Your constant showering of love sometimes feels too good to be true. You've helped me become the best version of myself and encouraged me to strive for improvement every day.

You're an incredibly considerate person, always putting others' needs before your own. Your hard work and passion for your interests inspire me endlessly. Your thoughtful little gestures and surprises never failed to warm my heart. I cherish our experiences, from learning to ski together to building LEGO sets and embarking on spontaneous adventures.

Thank you for loving me even when I wasn't at my best, for believing in me when I had lost all faith in myself, and for making me the happiest I've ever been, both in the past and present. Thank you also for being a wonderful parent to Mochi and Pusheen. I love you with all my heart, and I can’t wait for the next chapter of our lives together.

ABSTRACT

Research in the Stoltz group focuses on the synergy of complex natural product synthesis and method development in that we strive to invent new and efficient methodologies that have great synthetic potential in the use for pharmaceuticals and natural products. Herein we describe an asymmetric total synthesis of Havellockate, a polycyclic furanobutenolide-derived cembranoid diterpenoid that exhibits biological activities such as anti-inflammatory, anti-microbial, and cytotoxic. The strategy for this synthesis is highlighted by a convergent Julia–Kocienski olefination, followed by an acylation/intramolecular [4+2] cycloaddition cascade, which furnishes the main core of the natural product in high efficiency.

Another synthetic route toward the total synthesis of Havellocate is presented, using a propargyl ether as a key intermediate. Though the route was unfruitful in compleing the synthesis, the Diels–Alder cascade had significant improvement of yield and stability with this route, and it constitutes tremendous value for the synthesis of other targets within the furanobutenolide-derived natural product family.

Next, the synthesis, isolation, and reactivity of a chiral Pd enolate is described. The Pd enolate is arose by an alpha bromo acetophenone oxidative addition complex with Pd2(dba)3 and PHOX ligand. A crystal structure is obtained to show that the enolate is C-bound and highly regioselective. The novelty of this isolation can shine light on the applications of such Pd enolate for future developments.

Then, we outlined a Pd-catalyzed asymmetric vinylation of γ-lactams to construct all-carbon quaternary stereocenters in high ee and yield. The use of canonically inactive vinyl chloride electrophiles afforded the highest yields and levels of stereoselectivity, and a range

of tri-substituted vinyl chlorides were found to be proficient in promoting this transformation. These stereogenically congested products could be further elaborated to functionally rich scaffolds, proving the synthetic utility of this transformation.

Next, we describe the work of organizing the inaugural Day of Inclusion event of CCE. The event was orchestrated by the Diversity in Chemistry Initiative (DICI), aimed to foster cohesion and to inspire concerted efforts toward Diversity, Equity, and Inclusivity (DEI) within the Chemistry and Chemical Engineering (CCE) division at Caltech. This paper outlines the event's motivation, organization, implementation, and feedback analysis. With support from various collaborators, including the CCE DEI Committee and the Caltech Center for Inclusion and Diversity (CCID), the event featured keynote presentations, guided panels, workshops, and a dinner social. Data collection revealed substantial participation, with over 200 attendees, predominantly graduate students. Encouragingly, post-event surveys indicated strong endorsement and a diverse turnout, affirming the event's significance. This editorial aims to communicate the achievements of the event, welcome feedback, and advocate for initiatives aimed at nurturing diversity and inclusion within the broader chemical sciences community.

Finally, in the Appendixes, several ongoing divergent catalyses of chiral Pd enolate is described including the asymmetric protonation of δ-lactams, the asymmetric formation of spirocyclic lactams with acyl azides, and enantioselective intermolecular Diels–Alder reaction.

PUBLISHED CONTENT AND CONTRIBUTIONS

1. **Chan. M**[†]; Hafeman, N. J.[†]; Fulton, T.J.; Alexy, E.J.; Loskot, S.A; Virgil, S.C.; Stoltz, B.M. Asymmetric Total Synthesis of Havellockate. *J. Am. Chem. Soc.* **2022**, *144*, 44, 20232–20236. DOI: 10.1021/jacs.2c09583.

   [†]These authors contributed equally.

   M.C. participated in product design, synthesis of compounds, data acquisition & analysis, and manuscript preparation.

TABLE OF CONTENTS TABLE OF CONTENTS

LIST OF ABBREVIATIONS

$[\alpha]_D$	specific rotation at wavelength of sodium D line at 23 degrees celsius
AIBN	Azobisisobutyronitrile
aq	aqueous
Bn	Benzyl
CAM	Cerium ammonium molybdate
$CHCl_3$	Chloroform
CO	Carbon monoxide
$Cu(OAc)_2$	Copper(II) acetate
c	Concentration for specific rotation measurements
d	doublet
DMSO	Dimethyl Sulfoxide
dr	Diastereomeric Ratio
ee	enantiomeric excess
ESI	Electrospray Ionization
Et_2O	Diethyl Ether
FcMA	Ferrocenyl Methacrylate

FDA	Food and Drug Administration
FI	Field Ionization
g	grams
GPC	Gel Permeation Chromatography
HPLC	High-Performance Liquid Chromatography
HRMS	High Resolution Mass Spectrometry
IR	Infrared Spectroscopy
$KMnO_4$	Potassium permanganate
LDA	Lithium diisopropylamide
LHMDS	Lithium hexamethyldisilazide
L	Liter; Ligand
MeCN	Acetonitrile
MMA	Methyl Methacrylate
M_n	Number Average Molecular Weight
N	Nitrogen
NO	Nitric oxide
N_2	Nitrogen gas

neoc	Neocuproine
Ni	Nickel
NBS	N-bromosuccimide
NMR	Nuclear Magnetic Resonance
Nu	Nucleophile
o	ortho
OAc	Acetate
OTf	Trifluoromethanesulfonate
PCCs	Palladium catalyzed cascade cyclizations
Pd	Palladium
PHOX	phosphinooxazoline
Ph	Phenyl
PhBr	Bromobenzene
PMMA	Poly(methyl methacrylate)
ppb	Part-per-billion
ppmv	Parts Per Million by Volume
ppq	Part-per-quadrillion

ppt	Parts Per Trillion
q	quartet
R	generic for any atom or functional group
s	singlet
t-Bu	*tert*-butyl
TBS	*tert*-Butyldimethylsilyl
TES	tert-butyldimethylsilyl
TFA	Trifluoroacetic acid
THF	Tetrahydrofuran
TBAF	tetrabutylammonium fluoride
TLC	Thin-Layer Chromatography
UV	Ultraviolet

CHAPTER 1

Asymmetric Total Synthesis of Havellockate[†]

1.1 INTRODUCTION

Marine organisms provide a seemingly endless supply of complex natural products, which have captivated synthetic chemists for decades.[1] Soft corals of the genus Sinularia are no exception, as dozens of macrocyclic and polycyclic molecules have been isolated from their extracts. [2] The polycyclic furanobutenolide-derived cembranoid and norcembranoid classes of natural products have long served as challenging and elusive synthetic targets (Figure 1.1.1).[3,4] The structural complexity of this family of natural products, coupled with the exciting bioactivity associated with several of its members continues to draw synthetic chemists to target these fascinating molecules.

Figure 1.1.1 *Examples of other polycyclic furanobutenolide-derived cembranoid diterpenoids (1).*

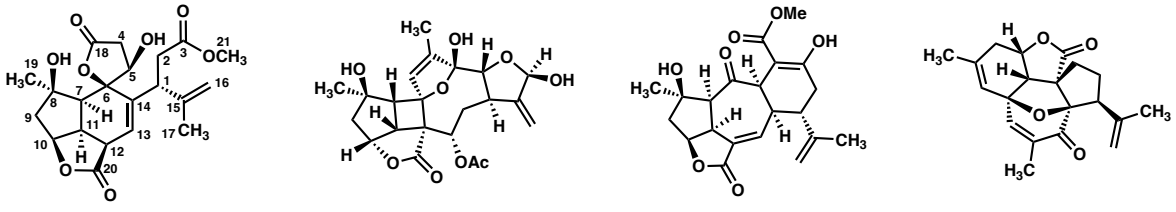

†This research was performed in collaboration with Nicholas J. Hafeman, Tyler J. Fulton, Eric J. Alexy and Steven Loskot. Portions of this chapter have been reproduced with permission from Chan, M.*; Hafeman, N. J.*; Fulton, T.J.; Alexy, E.J.; Loskot, S.A; Virgil, S.C.; Stoltz, B.M. *J. Am. Chem. Soc.* **2022**, 144, 44, 20232–20236.

Havellockate (**1**), a C20-cembranoid first isolated in 1998 from Sinularia granosa, is a prime example of the complexity and synthetic challenge posed by the polycyclic furanobutenolide-derived cembranoid family (Figure 1.1.2).[5] Havellockate (**1**) is characterized by a highly oxygenated cis-fused tricyclic core common to other related natural products. However, it is adorned with a spiro-fused β-hydroxybutanolide ring, a unique feature not found in other members of the polycyclic furanobutenolide-derived cembranoid family. In addition to these topological features, havellockate possesses eight stereocenters, seven of which are contiguous around the highly substituted and densely functionalized core. Although no completed syntheses of havellockate have been reported, previous efforts by Mehta[6] and Barriault[7] highlight the difficulty of accessing this target via total synthesis.

Figure 1.1.2 *Structural features of havellockate (**1**).*

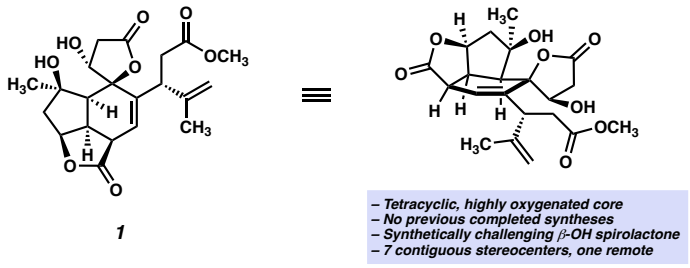

The polycyclic furanobutenolide-derived cembranoids are thought to be biogenically derived from their macrocyclic cembranoid counterparts, however, the details of the biosynthetic formation of havellockate (**1**) remain unclear.[8] After the isolation of havellockate (**1**), Anjaneyulu and coworkers proposed a biosynthetic pathway starting from the hypothetical macrocycle **6**, (where R = CO_2Me, Figure 1.1.3), which is thought to be derived from ether **5**, a naturally occurring cembranoid extracted from Sinularia granosa

(where R = H). From macrocycle **6**, the bridged tetrahydrofuran ring opens to form diketoalcohol **7**, which then enolizes at the C(7) and C(11) position to afford the corresponding dienol. The enol at C(11) undergoes rearrangement to generate diene **8**, followed by an intramolecular Diels–Alder reaction and epoxidation to forge the [5–6–7] tricycle **9**. A bond cleavage between C(3) and C(4) by a retro-Dieckmann type mechanism, lactonization, and opening of the epoxide generates the spiro-lactone and the side chain. Lastly, olefin rearrangement followed by lactonization forms the other gamma lactone unit, affording havellockate (**1**).

Figure 1.1.3 *Proposed biosynthesis of havellockate (**1**).*[8]

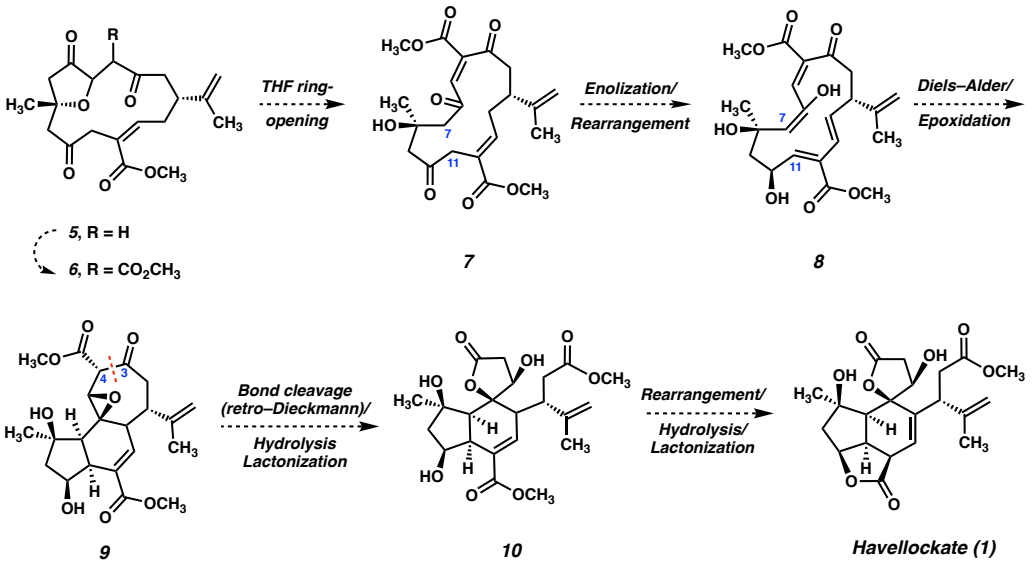

1.2 RETROSYNTHETIC ANALYSIS

When devising a retrosynthetic strategy targeting havellockate, we first opted to disconnect the spirolactone to reveal enone **11** (Figure 1.2.1). In the forward direction, it was envisioned that the β-hydroxybutanolide could be installed via 1,2-addition of a suitable nucleophile into the carbonyl at C(6) (havellockate numbering throughout), with

subsequent elaboration to the requisite lactone. Enone **2**, in turn, could be accessed from tricycle **12** after installation of the C(6) carbonyl and migration of the $\Delta^{12,13}$ olefin. Tricycle **12** was envisaged to arise from the intramolecular Diels–Alder reaction of propiolic ester **13**, which would be formed by esterification of diol **14** with propiolic acid. This key intermediate (**15**) could be forged via a convergent Julia–Kocienski olefination[9] between aldehyde **15** and sulfone **16**, which we imagined could be accessed from commercially available starting materials in enantioenriched form.

Figure 1.2.1 *Retrosynthetic analysis of havellockate (**1**).*

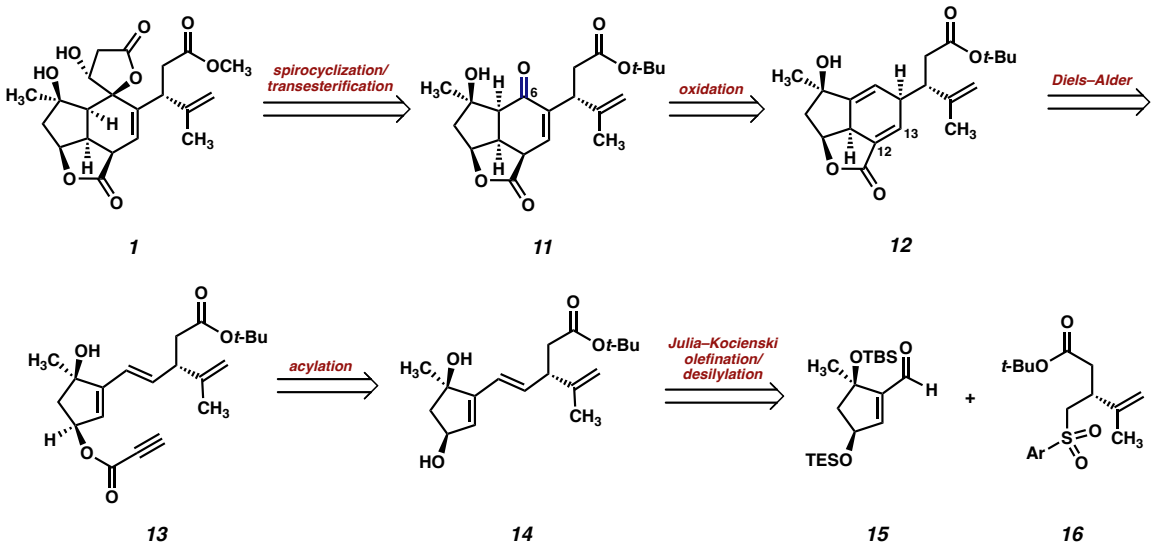

1.3 SYNTHESIS OF THE COUPLING PARTNERS

To proceed with the Julia–Kocienski olefination, we need to prepare the requisite aldehyde **15** and sulfone **16**. The synthesis of aldehyde **15** commences with known enone **18** that could be prepared two steps from (*R*)-linalool ((–)-**XX**) as reported by Maimone. [10] Enone **18** then undergoes bromination followed by conjugate addition/elimination to afford

β-cyanoenone **20** (Scheme 1.3.1). Luche reduction and subsequent alcohol protection furnishes nitrile **21**, which is converted to aldehyde **15** by reduction with DIBAL.

Scheme 1.3.1 *Synthesis of aldehyde* ***15***.

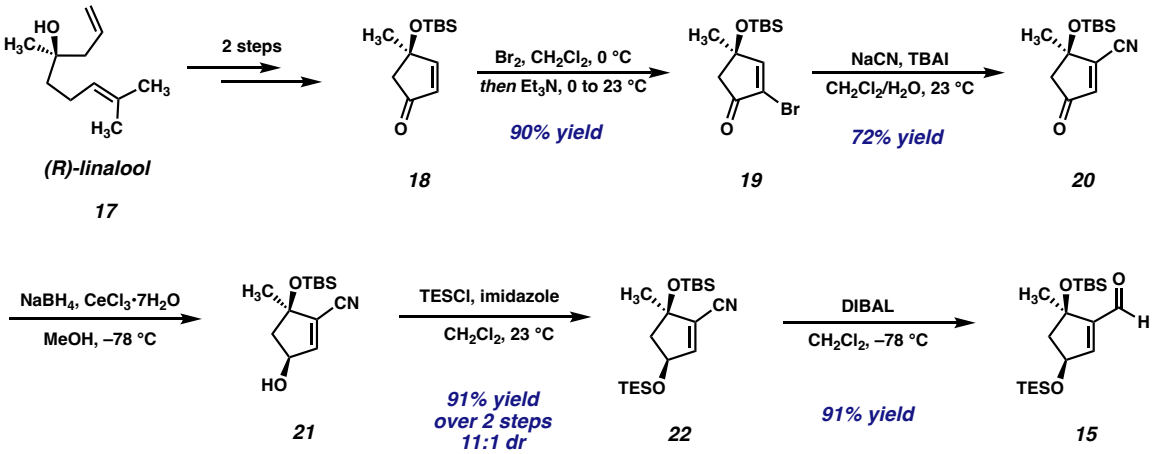

The sulfone coupling partner is accessed in four steps from known acyl oxazolidinone **24**,[11] which can be obtained in two steps from 3,3-dimethyl acrylic acid **23**, by γ-deprotonation followed by α-alkylation with t-Bu bromoacetate, which proceeds in >20:1 dr. [12] Reductive auxiliary removal then affords enantioenriched alcohol **26** (Scheme 1.3.2). A Mitsunobu reaction with 1-phenyltetrazole thiol (PTSH) (**29**) and oxidation of the resultant sulfide (**27**) yields the desired sulfone (**28**).[13]

Scheme 1.3.2 *Synthesis of sulfone* ***28****.*

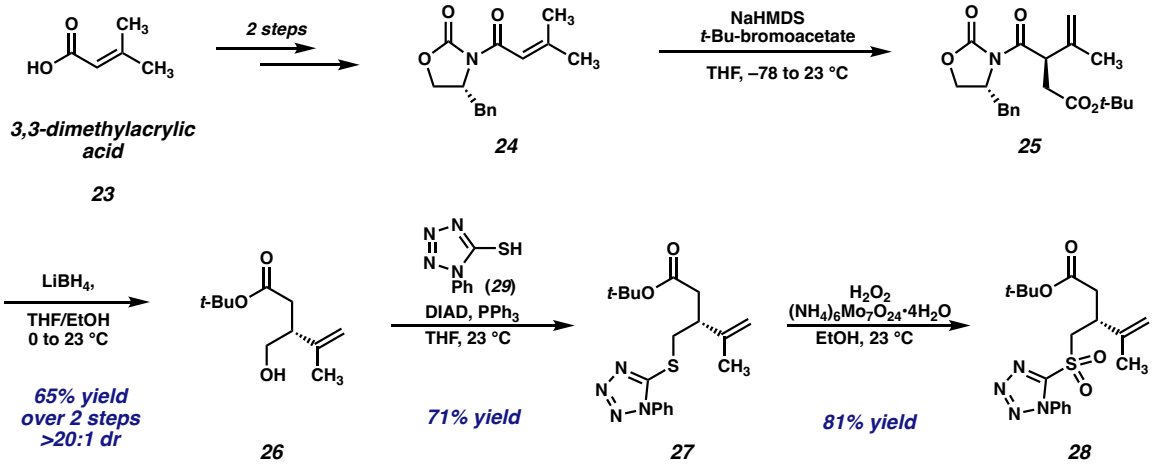

1.4 JULIA-KOCIENSKI OLEFINATION

With both coupling partners in hand, we next investigated the key convergent olefination reaction to unite them (Scheme 1.4.1). Pleasingly, addition of KHMDS to a mixture of aldehyde **15** and sulfone **28** effects the desired Julia–Kocienski olefination and following desilylation of the product, diol **14** is obtained in 40 to 50% yield over the two steps. This key olefination forges the requisite C=C bond with high (>20:1) selectivity for the E-isomer. Although we were able to obtain the desired product, the yield of this transformation is inconsistent and not completely satisfactory. The issue was not ameliorated by employing slightly higher equivalence of the sulfone nor was keeping the deprotonation step at a consistently low temperature. Consequently, not all aldehyde **15** was consumed, and the residual aldehyde was difficult to separate from the olefination product (**14**).

Scheme 1.4.1 *Initial results of the Julia–Kocienski Olefination.*

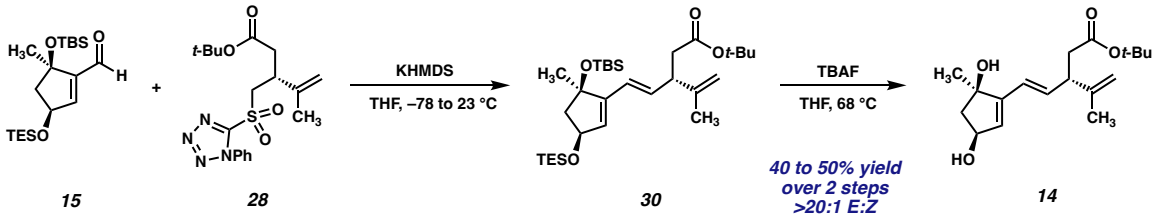

It also been demonstrated that different sulfone groups can also influence the outcome of the olefination, depending on the substrate. Specifically, the phenyl tetrazole- (PT), tert-butyl tetrazole- (TBT), and the benzothiazole (BT) sulfone are shown in Table 1.4.2. Similar to the original protocol, the PT sulfone gave a moderate NMR yield with unreacted aldehyde remaining (entry 1), and the TBT sulfone resulted in a lower yield, albeit with full consumption of the aldehyde (entry 2). To our delight, in comparison with the other sulfone coupling partners, the BT sulfone showed full consumption of the aldehyde with relatively high yield of the product (entry 3).

However, preparing the BT sulfone on scale has proved to be extremely challenging in that the excess BT sulfide used in the Mitsunobu reaction was exceedingly difficult to separate from the desired product. Many purification methods have been attempted to isolate the product such as liquid column chromatography, recrystallization, or automated flash column, but all processes led to the result of losing significant yield of the desired product.

Table 1.4.2 *The effect of different sulfone coupling partners.*

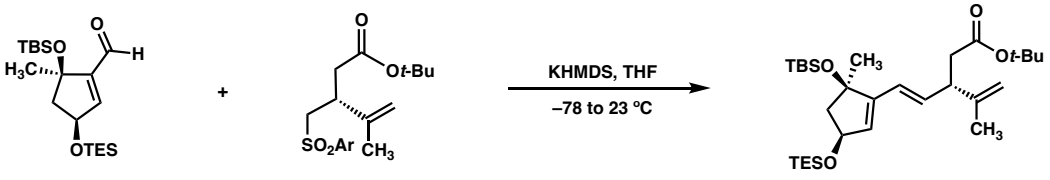

15 ***16*** ***30***

Entry	Ar =	^{1}H NMR Yield (%)	Note
1	PT	45	with unreacted aldehyde
2	TBT	37	complete consumption of aldehyde
3	BT	70	complete consumption of aldehyde but only on small scale

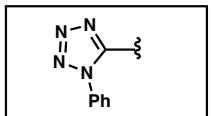

Phenyl Tetrazole (PT)

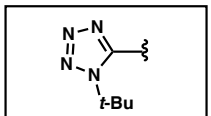

t-Butyl Tetrazole (TBT)

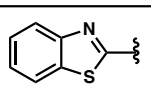

Benzothiazole (BT)

Given these challenges, we turned to the literature and found that, in certain cases, the Julia–Kocienski olefinations could be affected under so-called "Barbier-type" addition conditions (Scheme 1.4.3), wherein the base is added to a mixture of aldehyde and sulfone instead of the more conventional "premetalation" protocol, which involves prestirring of the sulfone with base, followed by addition of the aldehyde after quantitative deprotonation. Presumably, under the Barbier conditions the sulfone anion is consumed as soon as it is generated, and therefore, self-condensation of the sulfone coupling partner would be minimized. Gratifyingly, under the Barbier-type addition approach, we were able to achieve a consistent 68% yield on the transformation with the original PT sulfone (entry 3).

Scheme 1.4.3 *Improved conditions of the Julia–Kocienski olefination.*

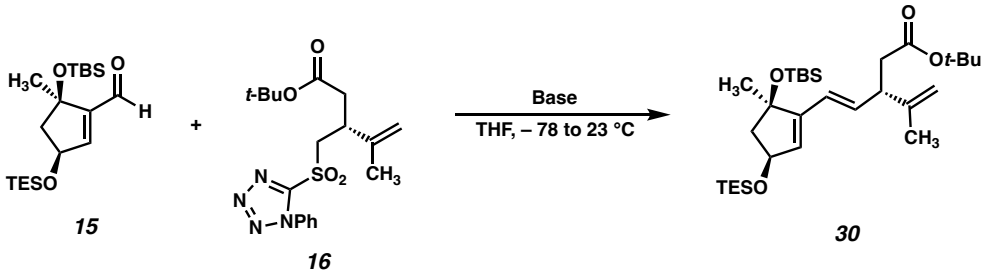

Entry	Base	Ar =	Yield (%)	Addition order	Note
1	NaHMDS	PT	61	Non-Barbier	unreacted aldehyde
2	LiHMDS	PT	70	Non-Barbier	mixture of E/Z isomers
3	KHMDS	PT	68	Barbier	unreacted aldehyde
4	KHMDS	PT	58	Non-Barbier	unrected aldehyde
5	KHMDS	TBT	37	Non-Barbier	complete consumption of aldehyde
6	KHMDS	BT	70	Non-Barbier	complete consumption of aldehyde

Notes:
a) although the yield of entry 6 is slightly higher than entry 3, this yield decreases on scale;
b) Non-Barbier denotes addition of base to sulfone, followed by addition of aldehyde;
c) Barbier denotes addition of base to mixture of sulfone and aldehyde

1.5 INTRAMOLECULAR DIELS–ALDER REACTION

With diol **14** in hand, the stage is set for the key acylation/Diels–Alder sequence. Based upon our experience with similar esterification reactions, we did not anticipate difficulty in preparing Diels–Alder substrate **12**. Upon treatment of diol **14** with propiolic acid under Steglich conditions (Scheme 1.5.1),[14] conversion to ester **13** occurs. However, attempting to isolate and purify this key intermediate resulted in decomposition of this sensitive intermediate (we have observed that ester **13** decomposes after prolonged exposure to silica as well as upon concentration to the neat compound). Consequently, the reaction mixture is rapidly passed through a plug of silica, then the partially purified product is used immediately in the subsequent step. Heating ester **13** to 110 °C in xylenes triggers the [4+2] cycloaddition to afford Diels–Alder adduct **12** as a single diastereomer.

Despite the modest yield of these two steps, this key sequence serves to construct the characteristic [5–5–6] framework of havellockate (**1**).

Scheme 1.5.1 *Intramolecular Diels–Alder sequence.*

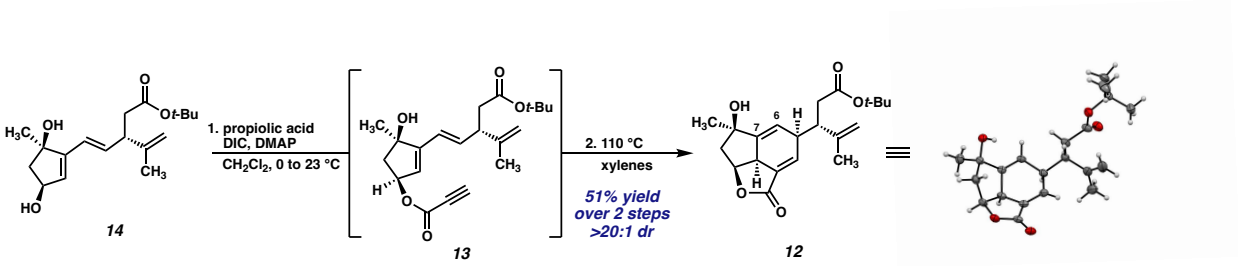

We initially hypothesized that a more traceless acylation process might circumvent the need to purify intermediate ester **13** (Table 1.5.2). Unfortunately, with the acid chloride, the imidazole amide, and the symmetrical propiolic acid anhydride derivative, the acylation reaction either resulted in no reaction or only trace amounts of product.

Table 1.5.2 *Exploring other propiolic acid alternatives.*

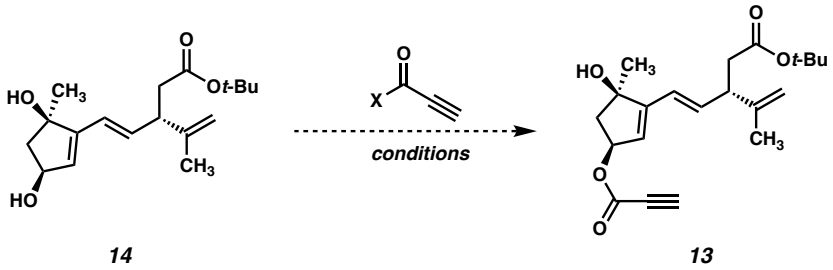

Entry	X =	Conditions	Result
1	Cl	CH_2Cl_2, NEt_3, 0 °C	No Reaction
2	imidazole	CH_2Cl_2, NEt_3, 0 °C	No Reaction
3	OPropiolate	DMAP, py, CH_3CN, 0 °C	traces of product
4	OPiv	DMAP, py, CH_3CN, 0 °C	mixture of products

We believed that these findings were not intrinsic to the acylation step being inadequate, but more due to the complications of successfully synthesizing the acylating reagent. Unlike propiolic acid, these derivatives are less stable and highly prone to

decomposition. Compared to the other acid alternatives, the propynoyl pivaloyl anhydride was a stable compound. The proposed mechanism is shown below for the decomposition pathway of these derivatives (Figure 1.5.3). Unfortunately, the acylation step yielded a mixture of products, potentially due to the poor regioselectivity of the unsymmetrical anhydride reacting with diol **14**.

Figure 1.5.3 *Proposed mechanism of propiolic acid derivative decomposition pathway.*

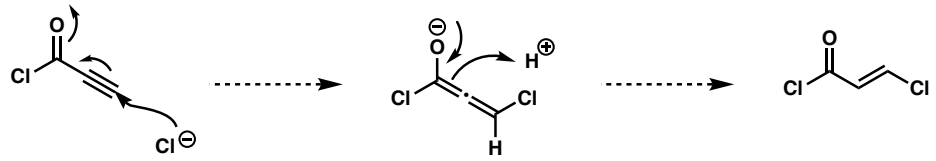

Unable to improve the yield of the intramolecular Diels–Alder reaction, we have also considered the possibility of an intermolecular Diels–Alder reaction to access the [5–6–5] tricycle (Scheme 1.5.4). Unfortunately, by reacting the diol with ethyl propiolate or DMAD, in both cases, no formation of the desired Diels–Alder adduct (**31**) was observed. It is noteworthy to mention that many Lewis-Acid catalyzed Diels–Alder reactions conditions were also attempted for both intra- and intermolecular cases, instead of thermally activated conditions, but have not yet led to promising reactivity.

Scheme 1.5.4 *Attempts for an intermolecular [4+2] disconnection.*

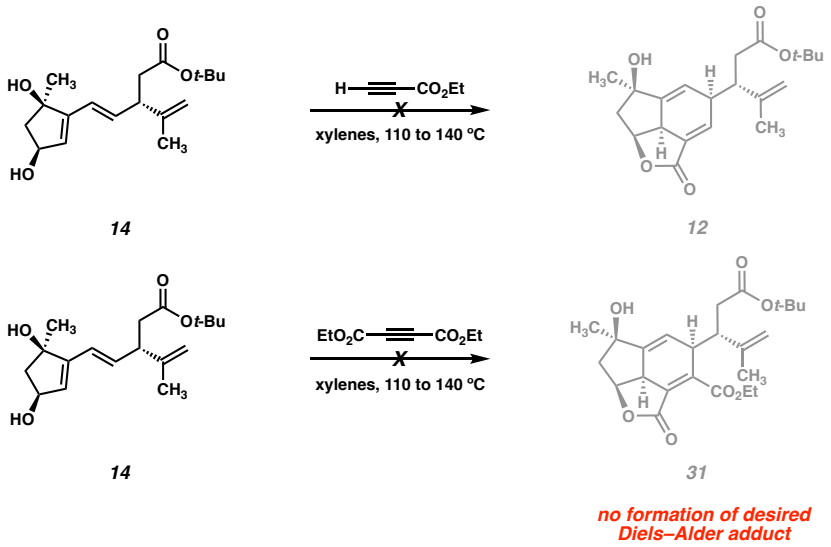

Another hypothesis that we had was that the ester moiety on our acylation product results in a structural constrain for the substrate to access the desired conformation needed for the intramolecular Diels–Alder reaction. Specifically, for the intramolecular Diels–Alder reaction to proceed, the ester needs to be in s-trans conformation. Potentially, due to steric effect of the tethered side chain of the diene in acylation product **13**, the delta G between the s-cis and s-trans conformation is rather high because similar issues were not observed in the scabrolide A synthesis.[4d] Therefore, we targeted a propargyl ether substrate (**32**) instead. To our delight, the subsequent intramolecular Diels–Alder reaction was affected by heating in xylenes in almost quantitative yield, affording the cyclic ether **33** (Scheme 1.5.5).

Scheme 1.5.5 *The propargyl ether route.*

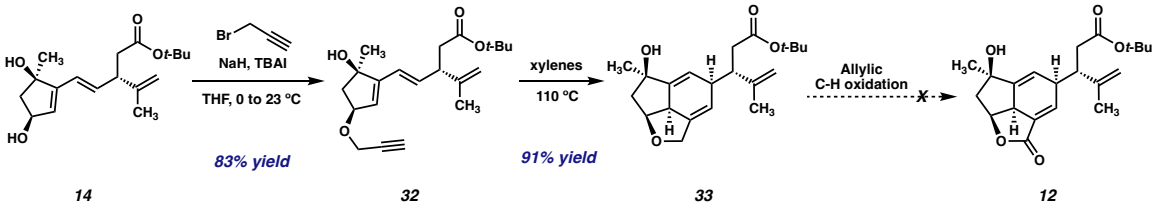

However, in many attempts to oxidize the cyclized product **33** to desired tricycle **12**, we were unable to achieve the desired allylic C-H oxidation (Scheme 1.5.6).[15] Noteworthy to mention that the Diels–Alder product of the propargyl ether substrate was carried forward to the rest of the synthesis in the hopes of oxidizing the allylic position at a later stage, which was also proven to be unfruitful.

Scheme 1.5.6 *Attempts to oxidative the desired allylic C-H bond.*

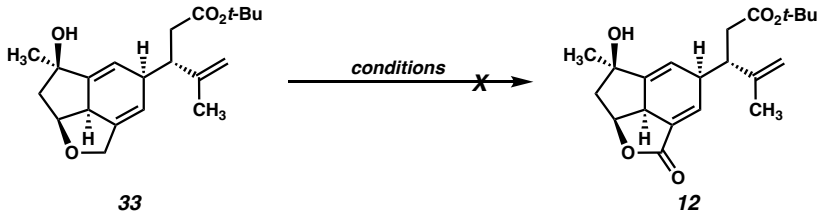

Entry	Conditions	Result
1	CrO_3, 3,5-dimethylpyrazole, CH_2Cl_2, –35 °C to reflux	No reaction
2	$RuCl_3$, tBuOOH, $Mg(OAc)_2$	Decomposition
3	PCC, DCE, 70 °C	undesired oxdized product formed
4	Cr(V), MnO2, 15-crown-5, DCE, 80 °C	Decomposition
5	White Catalyst, benzoquinone, AcOH, 1,4-dioxane	Decomposition

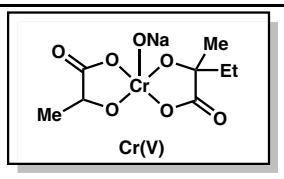

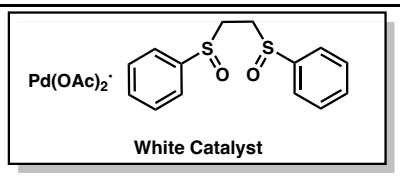

1.6 LATE-STAGE SYNTHESIS

Despite the modest yield of these two steps, this key sequence serves to construct the characteristic [5–5–6] framework of havellockate (**1**). To access enone **11**, Diels–Alder

adduct **12** is subjected to a three-step oxidation protocol. First, a V-catalyzed directed epoxidation of the $\Delta^{6,7}$ olefin furnishes epoxide **34** as a single diastereomer. A Ti-catalyzed reductive epoxide opening of **34** furnishes diol **35** which then undergoes oxidation with IBX. Fortuitously, the oxidation of the C(6) alcohol proceeds with concomitant migration of the $\Delta^{12,13}$ olefin, furnishing the desired enone **11** directly.

Scheme 1.6.1 *Synthesis of Key Enone Intermediate* ***11***.

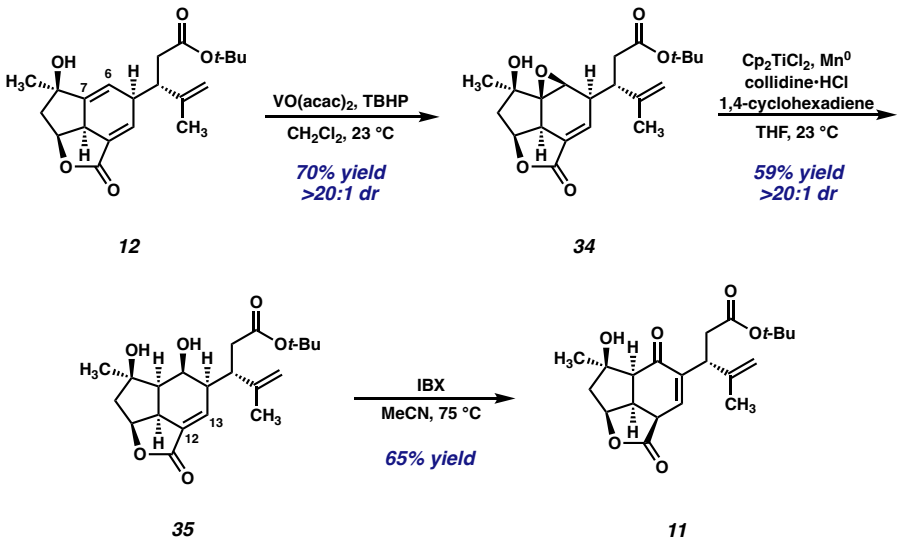

With enone **11** in hand, we set out to explore the installation of the final three carbon atoms of the natural product and the construction of the spiro-fused butanolide ring. We initially envisioned that a diastereoselective 1,2-addition of a Grignard reagent into enone **11** could forge the final C–C bond required and install the three carbon atoms of the butanolide ring. However, to our surprise, no trace of addition product **37** was observed upon addition of vinyl magnesium bromide (as a model nucleophile) to a solution of enone **11** in THF. We attribute this to the basicity of the Grignard reagent, which likely

deprotonates the vinylogous β-ketoester (**11**), proton highlighted in red) forming enolate **36** and rendering the desired 1,2-addition unfeasible.

Scheme 1.6.2 *Failed Grignard addition to enone* ***11***.

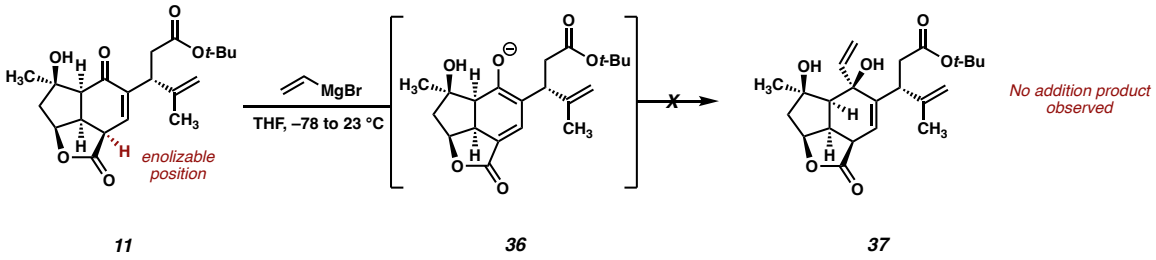

After surveying several classes of nucleophiles,[16] we discovered that exposure of enone **11** to the allylzinc reagent generated from 3-bromo-1-acetoxypropene (**40**)[17] results in productive reaction, generating an inseparable mixture of isomeric addition products.[18] Treatment of this mixture with methanolic ammonia deacetylates the products and renders them separable by flash chromatography (Scheme 1.6.3). After this two-step sequence, triol **38** is isolated in modest yield. Gratifyingly, an X-ray of triol **38** reveals that it possesses the correct stereochemistry at both C(5) and C(6) corresponding to the β-hydroxybutanolide ring of havellockate, with no evidence of the formation of other diastereomers in this reaction. We attribute this high degree of diastereoselectivity to a closed transition state, which is commonly invoked for Zn-mediated allylation reactions, and approach of the nucleophile from the less hindered α-face of the enone (**11**) (see SI for details).[19]

Scheme 1.6.3 *Zn-mediated allylation of enone* ***11*** *to forge triol* ***38****, and failed transesterification.*

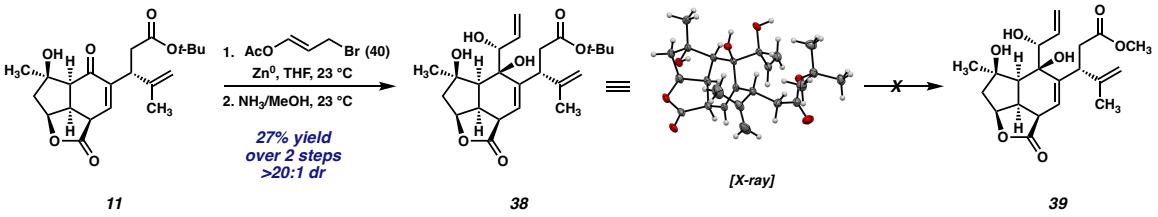

Now in possession of an intermediate containing all the carbon atoms of the natural product and all the stereogenic centers correctly established, we sought to perform a transesterification to replace the t-Bu ester of triol **41** with the requisite methyl ester (i.e. triol **42**). Unfortunately, despite investigating a variety of conditions for the selective removal of the t-Bu ester, we were unable to effect this transformation, and our efforts resulted only in decomposition or undesired side reactivity of this intermediate. After extensive experimentation, we found that enone **11** is a suitable intermediate upon which to carry out the transesterification sequence. This is achieved by cleavage of the t-Bu ester with formic acid,[20] followed by formation of the methyl ester (**41**) using diazomethane.

Scheme 1.6.4 *Successful transesterification of enone* ***11****, and synthesis of tetrol* ***43****.*

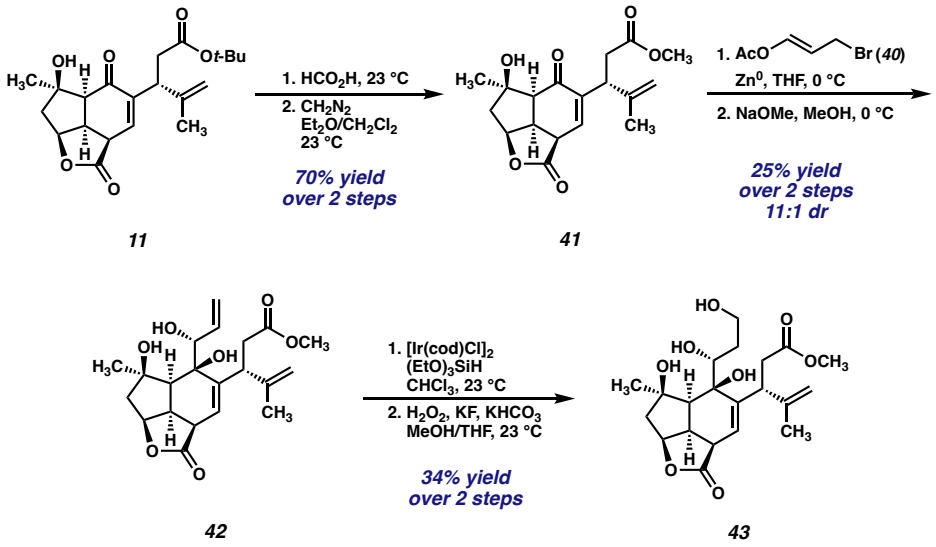

To our delight, methyl ester-bearing enone **41** also serves as a competent substrate for the key allylation reaction (Scheme. 1.6.4). Following deacetylation with NaOMe, triol **42** is furnished in 11:1 dr, and in similar yield to the *t*-Bu system. Elaboration of the newly installed allyl group is accomplished by employing an anti-Markovnikov Ir-catalyzed hydrosilylation of the $\Delta^{4,18}$ olefin, using conditions reported by Ding and coworkers.[21] A subsequent Tamao–Fleming oxidation[21] furnishes tetrol **43**, which comprises all the atoms of havellockate (**1**).[22]

Scheme 1.6.5 *Completion of the total synthesis of havellockate (**1**).*

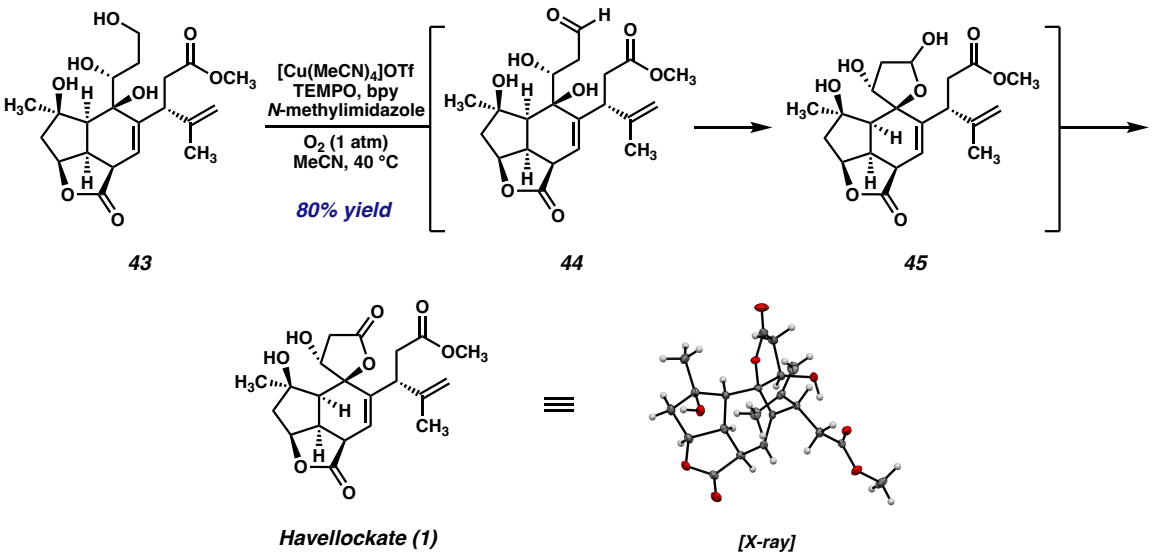

At this stage, the remaining objectives were the oxidation of the C (18) alcohol to the carboxylic acid oxidation state, and the closure of the butanolide ring, which would furnish havellockate (**1**). Given the presence of other oxidation-prone functionality within tetrol **43** (i.e., 2° alcohol, allylic 3° alcohol) we recognized that a protocol for the selective oxidation of 1° alcohols would be required. Consequently, we turned to the Cu-catalyzed aerobic oxidation system reported by Stahl and coworkers.[23] Upon exposure of tetrol **43** to the Stahl oxidation conditions, we were delighted to observe that tetrol **43** undergoes a two-stage oxidation/cyclization to close the butanolide ring and furnish havellockate directly. Presumably, this involves initial oxidation to generate aldehyde **44** which likely undergoes cyclization to lactol **45**. This lactol can then undergo facile oxidation to the lactone yielding the natural product (**1**).[24] All NMR and IR spectral data were in good accordance with the literature values and, additionally, we were able to unambiguously determine the structure of our synthetic material via X-ray crystallography (including absolute stereochemistry).

Unfortunately, the optical rotation of our synthetic sample of havellockate did not match that reported in the literature, either in sign or magnitude (α_D^{25} – 56.7 ° for our synthetic material vs. α_D^{25} + 23.7 ° for the natural material). To date, attempts to secure a sample of the natural product have been met with failure. With no authentic material to compare to we are left in the unenviable situation of not knowing, and potentially never knowing, whether there was an error in the original measurement or whether the absolute stereochemistry of the natural product could be enantiomeric to that depicted in **1**. Should a new sample of natural havellockate become available, this lingering question could be further addressed.

In conclusion, we have completed the first total synthesis of the polycyclic furanobutenolide-derived cembranoid havellockate (**1**). The synthesis begins with the preparation of two enantioenriched fragments which are united via a Julia–Kocienski olefination. This is followed by an intramolecular Diels–Alder reaction that forges the central 6-membered ring of the natural product. Finally, a challenging diastereoselective enone 1,2-acetoxyallylation reaction is employed for the installation of the final carbon-carbon bond and remaining stereogenic centers. A late-stage hydrosilylation/Tamao–Fleming sequence is followed by a Cu-catalyzed oxidative cyclization which closes the butanolide ring and completes the synthesis.

1.7 SUPPORTING INFORMATION

1.7.1 MATERIALS AND METHODS

Unless otherwise stated, reactions were performed in flame-dried glassware under a nitrogen atmosphere using dry, deoxygenated solvents. Solvents were dried by passage through an activated alumina column under argon. Reaction progress was monitored by thin-layer chromatography (TLC). TLC was performed using E. Merck silica gel 60 F254 precoated glass plates (0.25 mm) and visualized by UV fluorescence quenching, p-anisaldehyde, or KMnO4 staining. Silicycle SiliaFlash® P60 Academic Silica gel (particle size 40–63 μm) was used for flash chromatography. 1H NMR spectra were recorded on Varian Inova 500 MHz and 600 MHz and Bruker 400 MHz spectrometers and are reported relative to residual CHCl3 (δ 7.26 ppm), C6D6 (δ 7.16 ppm) or CD3OD (δ 3.31 ppm). 13C NMR spectra were recorded on a Varian Inova 500 MHz spectrometer (125 MHz) and Bruker 400 MHz spectrometers (100 MHz) and are reported relative to CHCl3 (δ 77.16 ppm), C6D6 (δ 128.06 ppm) or CD3OD (δ 49.01 ppm). Data for 1H NMR are reported as follows: chemical shift (δ ppm) (multiplicity, coupling constant (Hz), integration). Multiplicities are reported as follows: s = singlet, d = doublet, t = triplet, q = quartet, p = pentet, sept = septuplet, m = multiplet, br s = broad singlet, br d = broad doublet. Data for 13C NMR are reported in terms of chemical shifts (δ ppm). IR spectra were obtained by use of a Perkin Elmer Spectrum BXII spectrometer or Nicolet 6700 FTIR spectrometer using thin films deposited on NaCl plates and reported in frequency of absorption (cm–1). Optical rotations were measured with a Jasco P-2000 polarimeter operating on the sodium D-line (589 nm), using a 100 mm path-length cell. High resolution mass spectra (HRMS)

were obtained from the Caltech Mass Spectral Facility using a JEOL JMS-600H High Resolution Mass Spectrometer in fast atom bombardment (FAB+) or electron ionization (EI+) mode, or using an Agilent 6200 Series TOF with an Agilent G1978A Multimode source in electrospray ionization (ESI+), atmospheric pressure chemical ionization (APCI+), or mixed ionization mode (MM: ESI-APCI+).

List of Abbreviations:

bpy – bipyridine, DIAD – diisopropylazodicarboxylate, DIC – *N*,*N*'-diisopropylcarbodiimide, DMAP – (4-dimethylamino)pyridine, HMDS – hexamethyldisilazide, HPLC – high-pressure liquid chromatography, IBX – 2-Iodoxybenzoic acid, LCMS – liquid chromatography/mass spectrometry, NMR – nuclear magnetic resonance, TBHP – *tert*-butyl hydroperoxide, TBAF – tetrabutylammonium fluoride, TBAI – tetrabutylammonium iodide, TBS – *tert*-butyl dimethylsilyl, TEMPO – (2,2,6,6-tetramethylpiperidin-1-yl)oxyl, TESCl – triethylsilyl chloride, TES – triethylsilyl, THF – tetrahydrofuran

1.7.2 EXPEPRIMENTAL PROCEDURES AND SPECTROSCOPIC DATA

Experimental Procedures

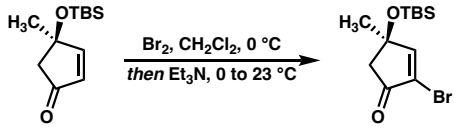

18 ***19***

Bromoenone 19: A flame dried round-bottom flask was charged with enone **18** (2.76 g, 12.2 mmol, 1.0 equiv) in CH_2Cl_2 (122 mL, 0.1 M). The solution was cooled to 0 °C and Br_2 (0.687 mL, 13.4 mmol, 1.1 equiv) was added dropwise over 10 min. The resultant solution was stirred for 30 min at 0 °C. Upon complete consumption of starting material (as determined by TLC), Et_3N (2.5 mL, 18.3 mmol, 1.5 equiv) was added and the mixture was warmed to 23 °C and allowed to stir for 1 h. The reaction was diluted with a saturated solution of $Na_2S_2O_3$ and the product was extracted with EtOAc (3 x 100 mL). The combined organic layers were washed with brine, dried over $MgSO_4$, filtered, and concentrated under reduced pressure. The crude product was purified by column chromatography (SiO_2, 10% EtOAc/Hexanes) to afford enone **19** (3.3 g, 90% yield) as a colorless oil; ^{1}H NMR (400 MHz, $CDCl_3$) δ = 7.51 (s, 1H), 2.64 (d, *J* = 3.6 Hz, 2H), 1.51 (s, 3H), 0.85 (d, *J* = 0.5 Hz, 9H), 0.09 (s, 3H), 0.08 (s, 3H); ^{13}C NMR (100 MHz, $CDCl_3$) δ = 198.9, 165.0, 125.4, 50.4, 29.2, 25.7, 18.0, –2.3, –2.4; IR (thin film, NaCl) 2956, 2930, 2888, 2858, 1733, 1593, 1472, 1463, 1374, 1292, 1254, 1205, 1106, 1081, 1018, 922, 837,

776 cm^{-1}; HRMS (ESI) m/z calc'd $C_{12}H_{22}BrO_2Si$ $[M+H]^+$: 305.0567, found: 305.0567; $[\alpha]_D^{25}$ + 2.3 ° (*c* 0.21, $CHCl_3$).

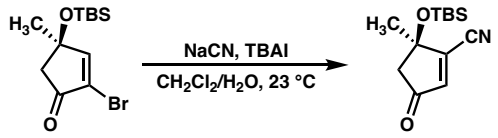

19 ***20***

Cyanoenone 20: A round bottom flask was charged with NaCN (2.3 g, 47 mmol, 2.2 equiv) and TBAI (1.1 g, 3.6 mmol, 0.17 equiv) dissolved in H_2O (66 mL, 0.32 M). Upon complete dissolution, a solution of bromoenone **19** (6.5 g, 21.3 mmol, 1 equiv) in CH_2Cl_2 (107 mL, 0.2 M) was added and the biphasic mixture was stirred vigorously for 16 h. Upon complete consumption of starting material (as determined by TLC) the reaction mixture was allowed to stand until complete separation of the biphasic mixture. The organic layer was drained into an Erlenmeyer flask, and the aqueous layer was extracted with EtOAc (5 x 100 mL). The combined organic layers were washed with brine, dried over $MgSO_4$, filtered, and concentrated under reduced pressure. The crude product was purified by column chromatography (SiO_2, 10% EtOAc/Hexanes) to afford enone **20** (3.8 g, 72% yield) as a pale yellow oil; ^{1}H NMR (400 MHz, $CDCl_3$) δ = 6.56 (s, 1H), 2.65 (d, *J* = 3.7 Hz, 2H), 1.64 (s, 3H), 0.88 (s, 9H), 0.17 (s, 3H), 0.13 (s, 3H); ^{13}C NMR (100 MHz, $CDCl_3$) δ = 203.0, 149.6, 139.6, 113.3, 78.8, 51.1, 28.1, 25.6, 18.1, -2.4, -2.7; IR (thin film, NaCl) 3449, 3087, 2957, 2932, 2888, 2859, 2231, 2736, 1606, 1473, 1378, 1290, 1254, 1217, 1170, 1093, 1006, 838, 778, 673 cm^{-1}; HRMS (FAB+) m/z calc'd $C_{13}H_{22}O_2NSi$ $[M+H]^+$: 252.1420, found: 252.1416; $[\alpha]_D^{23}$ – 34.6 (*c* 0.34, $CHCl_3$).

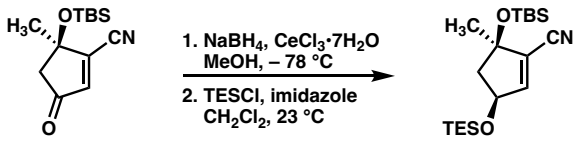

20 ***22***

Nitrile 22: A round bottom flask was charged with enone **20** (9.4 g, 37.3 mmol, 1 equiv) in dissolved in methanol (373 mL, 0.1 M). The solution was stirred for 5 min followed by the addition of $CeCl_3 \bullet 7H_2O$ (13.2 g, 41 mmol, 1.1 equiv). Once homogeneous, the solution was cooled to –78 °C and allowed to stir for 1 h. $NaBH_4$ (1.4 g, 37.3 mmol, 1 equiv) was added slowly in portions to the reaction and was allowed to stir until complete consumption of starting material (as determined by TLC). Upon complete consumption of starting material, the reaction was quenched with a saturated solution of NH_4Cl (300 mL) and the biphasic mixture was allowed to warm to room temperature. The biphasic mixture was extracted with 2:1 Et_2O:hexanes (3 x 300 mL) and the combined organic layers were dried over Na_2SO_4, filtered, and concentrated under reduced pressure. The crude product was used directly into the next reaction without further purification (assuming quantitative yield).

The crude alcohol (37.3 mmol, 1 equiv) was dissolved in CH_2Cl_2 (266 mL, 0.14 M). Once homogeneous, imidazole (7.6 g, 111.9 mmol, 3 equiv) and TESCl (7.1 mL, 55.9 mL, 1.5 equiv) were added. The reaction was allowed to stir until completion at 23 °C. Upon complete consumption of starting material (as determined by TLC), the reaction was quenched with H_2O (200 mL) and the biphasic mixture was extracted with Et_2O (3 x 400 mL). The combined organic layers were washed with brine, dried over $MgSO_4$, filtered and concentrated under reduced pressure. The resultant crude product was purified by column

chromatography (SiO_2, 10% EtOAc/Hexanes) to afford nitrile **22** (12.5 g, 91% yield, 11:1 dr) as a pale yellow oil; ^{1}H NMR (400 MHz, $CDCl_3$) δ 6.41 (d, J = 2.0 Hz, 1H), 4.72 (ddd, J = 7.0, 6.2, 2.0 Hz, 1H), 2.49 (dd, J = 12.8, 7.0 Hz, 1H), 1.98 (dd, J = 12.7, 6.2 Hz, 1H), 1.40 (d, J = 0.9 Hz, 3H), 0.96 (d, J = 8.1 Hz, 11H), 0.89 (s, 10H), 0.61 (d, J = 7.6 Hz, 5H); ^{13}C NMR (101 MHz, $CDCl_3$) δ 147.3, 126.1, 114.9, 82.4, 73.8, 51.5, 28.7, 25.8, 18.1, 6.8, 4.8, –2.2, –2.6; IR (thin film, NaCl) 2957, 2879, 2858, 2224, 1463, 1414, 1360, 1308, 1254, 1198, 1177, 1132, 1099, 1047, 1006, 893, 869, 837, 809, 777 cm^{-1}; HRMS (ESI) m/z calc'd $C_{19}H_{38}NO_2Si_2$ $[M+H]^+$: 268.2436; found: 368.2449; $[\alpha]_D^{25}$ – 52.0 ° (*c* 0.40, $CHCl_3$).

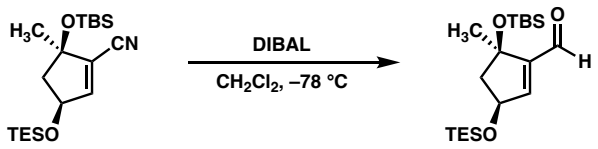

22 ***15***

Aldehyde 15: A round bottom flask was charged with nitrile **11** (250 mg, 0.68 mmol, 1 equiv) in CH_2Cl_2 (6.8 mL, 0.1M) and cooled to –78 °C. DIBAL (1.36 mL, 1 M in DCM, 2 equiv) was added dropwise and allowed to stir for 1 h at –78 °C. Upon complete consumption of starting material (as determined by TLC analysis, 19:1 hexanes:Et_2O) the reaction was quenched with EtOAc (0.5 mL), diluted with Et_2O and warmed to room temperature. A 50% solution of Rochelle's salt (10 mL) was added and the biphasic mixture was allowed to stir for 0.5 h. If the biphasic mixture does not separate completely, another portion of Rochelle's salt is added and stirred for another 0.5 h. The biphasic mixture is separated and the aqueous layer is extracted with Et_2O (3 x 10 mL). The combined organic layers are dried over $MgSO_4$, filtered, and concentrated in vacuo. The resultant crude product was the purified by column chromatography (SiO_2, 5% Et_2O/Hexanes) to afford aldehyde **22** (252 mg, 91% yield, 17:1 dr) as a pale yellow oil; ^{1}H NMR (400 MHz, $CDCl_3$) δ = 9.77 (s, 1H), 6.53 (d, *J* = 1.8 Hz, 1H), 4.70 (td, *J* = 6.9, 1.9 Hz, 1H), 2.49 (dd, *J* = 12.7, 7.1 Hz, 1H), 2.08 (dd, *J* = 12.6, 6.6 Hz, 1H), 1.45 (s, 3H), 0.97 (t, *J* = 7.9 Hz, 9H), 0.84 (d, *J* = 0.9 Hz, 9H), 0.63 (q, *J* = 7.9 Hz, 6H), 0.11 (s, 3H), 0.07 (s, 3H); ^{13}C NMR (100 MHz, $CDCl_3$) δ = 189.7, 149.8, 147.8, 80.6, 72.9, 53.9, 28.6, 25.8, 18.1, 6.9, 4.9, -2.2, -2.4; IR (thin film, NaCl) 2956, 2936, 2879, 2857, 2805, 2708, 1698, 1627, 1472, 1462, 1414, 1359, 1253, 1203, 1172, 1103, 1058, 975, 897, 837, 806, 775, 746,

671; HRMS (FAB+) m/z calc'd $C_{19}H_{37}O_3Si_2$ $[M+H-H_2]^+$: 369.2250, found: 369.2262; $[\alpha]_D^{25}$ – 117.2 ° (*c* 0.20, $CHCl_3$).

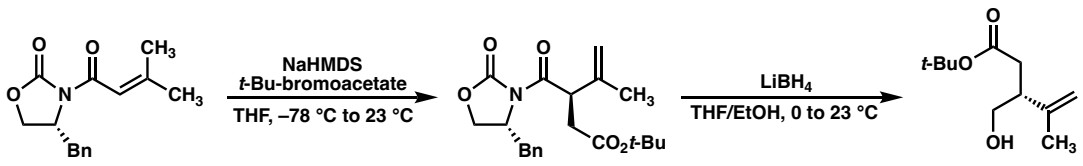

24 ***25*** ***26***

Alcohol 26: A 2L round bottom flask was charged with NaHMDS (1.0 M solution in THF, 100.0 mL, 100.0 mmol, 1.05 equiv) in THF (476 mL). The flask was cooled to –78 °C and oxazolidinone **24** (24.7 g, 95.2 mmol, 1.0 equiv) in THF (125 mL) was added dropwise. The mixture was stirred at –78 °C for 1 h, followed by the addition of *t*-Bu-bromoacetate (35.1 mL, 238.0 mmol, 2.5 equiv). The reaction mixture was stirred for 1 h at –78 °C, then warmed to –40 °C and stirred an additional hour. The reaction was quenched with saturated aqueous $NaHCO_3$, then warmed to 23 °C. The reaction mixture was partitioned between water and Et_2O and the aqueous phase extracted with Et_2O (3x). The organic extracts were combined, washed with brine, dried over $MgSO_4$, filtered and concentrated to afford crude oxazolidinone **25** (>20:1 dr) as a flakey orange solid. This procedure was repeated, and the crude products were combined and used directly in the subsequent step. A sample of oxazolidinone **25** was purified by flash chromatography for characterization: ^{1}H NMR (400 MHz, $CDCl_3$) δ 7.39 – 7.27 (m, 5H), 4.89 – 4.87 (m, 1H), 4.86 – 4.85 (m, 1H), 4.78 (ddd, *J* = 11.2, 3.9, 0.7 Hz, 1H), 4.70 – 4.61 (m, 1H), 4.16 – 4.13 (m, 2H), 3.33 (dd, *J* = 13.4, 3.4 Hz, 1H), 2.98 (dd, *J* = 16.9, 11.5 Hz, 1H), 2.78 (dd, *J* = 13.4, 9.8 Hz, 1H), 2.51 (dd, *J* = 17.0, 3.9 Hz, 1H), 1.83 (s, 3H), 1.44 (s, 9H); ^{13}C NMR (100 MHz, $CDCl_3$) δ 173.00, 171.4, 153.0, 142.3, 135.8, 129.7, 129.1, 127.4, 113.8, 81.0, 65.9, 55.8, 46.8, 37.8, 37.1, 28.2, 21.6; IR (Neat film, NaCl) 2977, 2918, 2849, 1780, 1728, 1697, 1454, 1384, 1351, 1291,

1259, 1206, 1153, 1110, 1011, 947, 904, 844, 761, 702, 683 cm^{-1}; *m/z* calc'd for $C_{21}H_{27}NO_5Na$ $[M+Na]^+$: 396.1781, found 396.1783; $[\alpha]_D^{25}$ – 81.1 ° (*c* 0.12, $CHCl_3$).

A 3 L round bottom flask was charged with the crude oxazolidinone (190.4 mmol assuming quantitative yield) in Et_2O (925 mL). The flask was cooled to 0 °C, and $LiBH_4$ (5.0 g, 228.5 mmol, 1.2 equiv) was added in a single portion. MeOH (9.2 mL, 228.5 mmol, 1.2 equiv) was added slowly, and gas evolution was observed. The reaction was stirred 2 h at 0 °C, after which all starting material had been consumed (as judged by TLC). The reaction was quenched with saturated aqueous $NaHCO_3$, partitioned between water and Et_2O and extracted with Et_2O (3x). The organic extracts were combined, washed with brine, dried over $MgSO_4$, filtered, and concentrated under reduced pressure to afford a yellow oil that was purified by flash chromatography (SiO_2, 20%-30%-40%-50% EtOAc/hexanes) to afford alcohol **26** (24.6 g, 65% yield over 2 steps) as a colorless oil; ^1H NMR (400 MHz, $CDCl_3$) δ 4.91 (dh, *J* = 3.1, 1.6 Hz, 1H), 4.81 (pq, *J* = 1.8, 1.2 Hz, 1H), 3.62 – 3.50 (m, 1H), 2.76 – 2.65 (m, 1H), 2.46 – 2.28 (m, 2H), 1.73 (dq, *J* = 2.3, 1.2 Hz, 3H), 1.42 (d, *J* = 4.0 Hz, 8H); ^{13}C NMR (100 MHz, $CDCl_3$) δ 172.15, 144.4, 113.2 (d, *J* = 4.0 Hz), 80.7 (d, *J* = 1.5 Hz), 64.0, 45.9, 36.8, 28.2 (d, *J* = 2.6 Hz), 20.4; IR (Neat film, NaCl) 3434, 2977, 2932, 1729, 1454, 1367, 1354, 1049, 890, 844 cm^{-1}; HRMS (FD+) m/z calc'd $C_{11}H_{20}O_3$ $[M\bullet]^+$: 200.1412, found: 200.1399; $[\alpha]_D^{25}$ + 3.6 ° (*c* 1.0, $CHCl_3$).

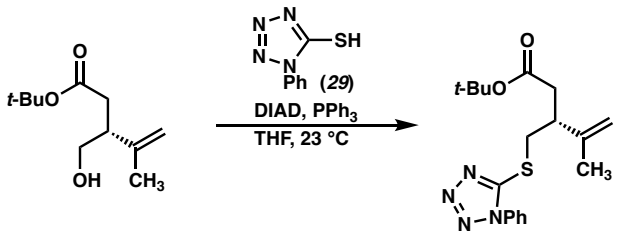

26 *27*

Sulfide 27: To a flame-dried 2 L two-necked round bottom flask with an addition funnel and large stirring bar was added 5-phenyl-1*H*-tetrazole (**29**; 30.70 g, 172.0 mmol, 1.6 equiv), PPh_3 (45.10 g, 172.0 mmol, 1.6 equiv), THF (540 mL), and alcohol **13** (21.50 g, 107.3 mmol, 1.0 equiv). The addition funnel was charged with DIAD (33.9 mL, 172 mmol, 1.6 equiv). The resulting clear, colorless solution was immersed in an ice bath with stirring for 15 min, after which time DIAD was added dropwise over a period of 30 min, resulting in a yellow homogeneous solution. The reaction was then stirred an additional 30 min at 0 °C, at which time consumption of alcohol **26** was observed by TLC analysis. The reaction was quenched at 0 °C with sat. $NaHCO_3$ and the crude mixture was transferred to a separatory funnel with EtOAc. The layers were separated and the aqueous layer was extracted with EtOAc (2x). The combined organics were dried over $MgSO_4$, filtered, and concentrated by rotary evaporation to yield a crude yellow oil. The crude product was dry-loaded on SiO_2 and purified by flash chromatography (5%–30% EtOAc/hexanes) to yield sulfide **27** as a colorless oil (27.51 g, 76.31 mmol, 71% yield). ^{1}H NMR (400 MHz, $CDCl_3$) δ 7.64 – 7.50 (m, 5H), 4.83 (dt, J = 1.6, 0.8 Hz, 1H), 3.61 – 3.54 (m, 1H), 3.54 – 3.48 (m, 1H), 3.04 – 2.93 (m, 1H), 2.51 (dd, J = 15.1, 6.4 Hz, 1H), 2.43 (dd, J = 15.1, 8.3 Hz, 1H), 1.75 (dd, J = 1.5, 0.8 Hz, 3H), 1.42 (s, 9H); ^{13}C NMR (100 MHz, $CDCl_3$) δ 170.7, 154.3, 143.9, 133.7, 130.1, 129.81, 123.9, 113.8, 80.9, 42.8, 39.0, 36.5, 28.1, 19.4; IR (Neat film,

NaCl) 3077, 2976, 2917, 2337, 1731, 1597, 1501, 1391, 1368, 1279, 1246, 1145, 1089, 1074, 1015, 978, 951, 900, 844, 761, 736, 695, 684 cm^{-1}; *m/z* calc'd for $C_{18}H_{25}N_4O_2S$ $[M+H]^+$: 361.1693, found 361.1693; $[\alpha]_D^{25}$ + 9.4 ° (*c* 0.73, $CHCl_3$).

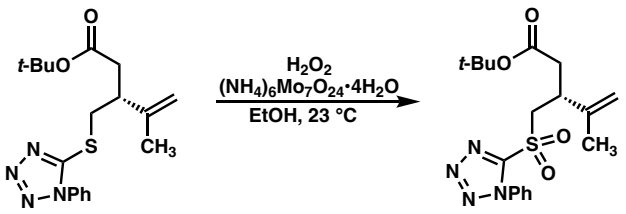

27 ***28***

Sulfone 28: To a 2 L round bottom flask with a large stirring bar was added sulfide **27** (27.51 g, 76.31 mmol, 1.0 equiv) and EtOH (200 proof, 380 mL). The resulting clear, colorless solution was cooled to 0 °C, after which $(NH_4)_6Mo_7O_{24}•4H_2O$ (37.70 g, 30.52 mmol, 0.40 equiv) was added. The flask was then affixed with an addition funnel which was charged with 30% aq. H_2O_2 (156 mL, 1.53 mol, 20.0 equiv). The H_2O_2 was then slowly added to the reaction mixture with vigorous stirring over the course of c.a. 1 h, resulting in a bright yellow suspension. The reaction was slowly allowed to warm to 20 °C over 4 h and maintained at 20 °C in a water bath for an additional 8 h, after which time LC/MS analysis indicated complete consumption of the starting material. *Caution: removal of the 20 °C water bath can result in an unpredictable exothermic reaction.* The reaction mixture was then transferred to a separatory funnel with Et_2O and brine. The layers were separated, and the aqueous layer was extracted with Et_2O (2x). The combined organic extracts were washed with 1:1 brine/sat. $Na_2S_2O_3$. The organics were then dried over $MgSO_4$, filtered, and concentrated by rotary evaporation to yield a crude yellow oil. The crude product was dry loaded on SiO_2 and purified by flash chromatography (5-25% EtOAc/hexanes) to yield sulfone **28** (24.25 g, 61.79 mmol, 81% yield) as a white solid; ^{1}H NMR (500 MHz, $CDCl_3$) δ 7.72 – 7.55 (m, 5H), 4.86 (d, *J* = 2.6 Hz, 2H), 3.99 (dd, *J* = 14.6, 7.5 Hz, 1H), 3.89 (dd, *J* = 14.6, 6.1 Hz, 1H), 3.33 (p, *J* = 7.0 Hz, 1H), 2.61 (dd, *J* = 15.6, 6.6 Hz, 1H), 2.49 (dd, *J*

= 15.5, 8.0 Hz, 1H), 1.76 (s, 3H), 1.42 (s, 9H); ^{13}C NMR (100 MHz, $CDCl_3$) δ 169.9, 153.8, 142.9, 133.0, 131.5, 129.7, 125.3, 114.5, 81.3 58.1, 38.8, 37.7, 28.0, 19.3; IR (Neat film, NaCl) 2978, 2931, 2362, 2341, 1725, 1497, 1348, 1152, 900, 763, 688 cm^{-1}; HRMS (MM: ESI-APCI+) *m/z* calc'd for $C_{18}H_{25}N_4O_4S$ $[M+H]^+$: 393.1597, found 383.1582; $[\alpha]_D^{25}$ + 14.4 ° (*c* 1.0, $CHCl_3$).

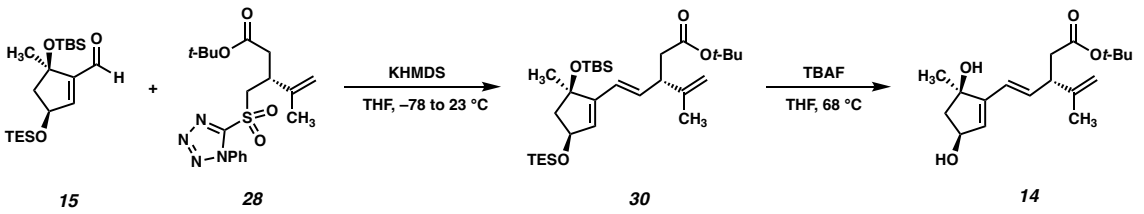

Diol 14: A 250 mL round bottom flask was charged with aldehyde **15** (8.4 g, 22.7 mmol, 1.0 equiv) and sulfone **28** (16.0 g, 40.8 mmol, 1.8 equiv) in THF (227 mL). The mixture was cooled to –78 °C, followed by the addition of KHMDS (0.5 M solution in THF, 77 mL, 38.5 mmol, 1.7 equiv) dropwise. The mixture was allowed to stir for 16 h while gradually warming to 23 °C. TLC indicated a small amount of aldehyde **15** remained. The reaction was quenched with saturated aqueous NH_4Cl, partitioned between water and Et_2O, and extracted with Et_2O (3X). The organic extracts were combined, washed with brine, dried over $MgSO_4$, filtered and concentrated to afford a yellow oil which was subjected to flash chromatography (SiO_2, 0%-5% Et_2O/Hexanes) to afford the product (8.05 g, c.a. 15.0 mmol) as a 11:1 mixture with aldehyde **15**. This mixture was dissolved in THF (300 mL) in a 1 L round bottom flask fitted with a reflux condenser, and TBAF (1.0 M solution in THF, 75 mL, 75.0 mmol, 5.0 equiv) was added. The brown solution was heated to reflux and stirred 5 h, after which no starting material remained, as judged by TLC. The mixture was cooled to 23 °C, partitioned between EtOAc and water, and extracted with EtOAc (3x). The combined organic extracts were washed with brine, dried over Na_2SO_4, filtered and concentrated under reduced pressure to afford a dark brown oil which was purified by flash chromatography (SiO_2, 40%-50%-60%-70% EtOAc/hexanes) to afford diol **24** (4.05 g,

13.1 mmol, 57% yield over two steps, *E:Z* > 20:1) as an orange/white solid. ^{1}H NMR (400 MHz, $CDCl_3$) δ 6.13 (dd, *J* = 16.1, 7.9 Hz, 1H), 6.04 – 5.95 (m, 2H), 5.71 (d, *J* = 2.4 Hz, 1H), 4.82 – 4.79 (m, 1H), 4.77 (dd, *J* = 1.7, 0.8 Hz, 1H), 4.60 (td, *J* = 4.6, 2.3 Hz, 1H), 3.19 (q, *J* = 8.1 Hz, 1H), 2.60 – 2.44 (m, 2H), 2.38 (dd, *J* = 14.5, 8.3 Hz, 1H), 1.90 – 1.80 (m, 1H), 1.71 (d, *J* = 0.6 Hz, 2H), 1.43 (s, 4H), 1.41 (s, 10H), 0.89 (d, *J* = 6.6 Hz, 1H); ^{13}C NMR (100 MHz, $CDCl_3$) δ 171.8, 148.9, 135.4, 130.2, 123.2, 111.3, 81.1, 80.7, 72.9, 52.6, 47.4, 39.6, 28.2, 26.9, 20.9; IR (Neat film, NaCl) 3288, 2975, 2932, 2357, 2106, 1758, 1727, 1636, 1636, 1539, 1506, 1457, 1368, 1290, 1167, 1147, 1026, 963, 847, 751 cm^{-1}; *m/z* calc'd for $C_{18}H_{28}O_4Na$ $[M+Na]^+$: 331.1855, found 331.1877; $[\alpha]_D^{25}$ – 46.1 ° (*c* 1.0, $CHCl_3$).

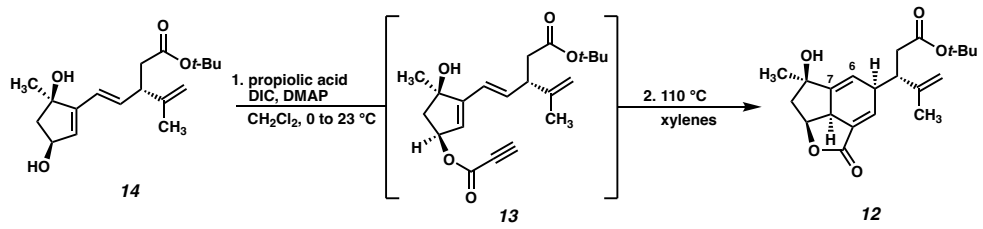

Cyclohexadiene 12: A 250 mL round bottom flask was charged with diol **14** (2.16 g, 7.00 mmol, 1.0 equiv), DMAP (43.0 mg, 0.350 mmol, 0.05 equiv) and propiolic acid (651 µL, 10.5 mmol, 1.5 equiv) in CH_2Cl_2 (70 mL). The solution was cooled to 0 °C, and DIC (1.65 mL, 10.5 mmol, 1.5 equiv) was added dropwise. The reaction mixture was stirred at 0 °C for 2 h, then the reaction mixture was filtered directly over a pad of SiO_2, rinsing with 50% EtOAc/hexanes. The eluent was collected in test tubes, and the fractions containing product were combined in a flame-dried 1 L round bottom flask containing xylenes (700 mL). The lower-boiling solvents (EtOAc, hexanes, CH_2Cl_2) were removed by rotary evaporation, leaving a solution of intermediate ester **13** in xylenes. This solution was sparged with N_2 for 10 min, then heated to 110 °C and stirred for 3 h. The reaction mixture was cooled to 23 °C, and the xylenes removed by rotary evaporation leaving a yellow residue which was purified by flash chromatography (SiO_2, 20%–30% EtOAc/hexanes) to afford tricycle **12** (1.28 g, 3.60 mmol, 51% yield over 2 steps) as a white solid. *Note: the yield of this sequence varied over multiple passes, typically between 40% and 50%.* Crystals suitable for X-ray diffraction were obtained by slow evaporation of a solution in CH_2Cl_2/hexanes**.** ^{1}H NMR (400 MHz, $CDCl_3$) δ 7.06 (dd, *J* = 3.5, 1.6 Hz, 1H), 5.79 – 5.74 (m, 1H), 5.03 (dt, *J* = 9.0, 7.5 Hz, 1H), 4.97 (t, *J* = 1.5 Hz, 1H), 4.89 – 4.86 (m, 1H), 3.39 – 3.29 (m, 1H), 2.86 (dt, *J* = 8.4, 2.8 Hz, 2H), 2.57 – 2.37 (m, 3H), 1.75 – 1.69 (m, 3H), 1.42 (s, 11H); ^{13}C NMR (101

MHz, $CDCl_3$) δ 171.4, 168.2, 152.3, 144.0, 143.1, 133.6, 120.3, 114.9, 80.9, 80.3, 76.0, 49.8, 45.8, 45.6, 37.8, 28.2, 26.7, 19.8.; IR (Neat film, NaCl); 3422, 2976, 1749, 1716, 1636, 1540, 1456, 1368, 1288, 1168, 1149, 758; *m/z* calc'd for $C_{21}H_{28}O_5Na$ $[M+Na]^+$: 383.1834, found 383.1844; $[\alpha]_D^{25}$ – 50.9 ° (*c* 1.0, $CHCl_3$).

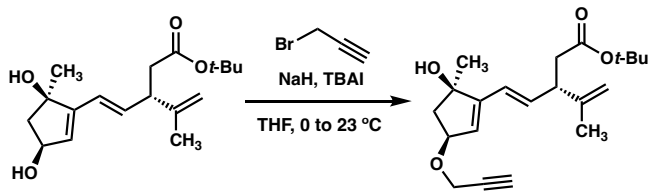

14 ***32***

Ether 32: Flame dried 50mL round bottom flask with stir bar and charged with **14** (300 mg, 0.97 mmol, 1.0 equiv) in THF (9.7 mL, 0.1 M). The solution was cooled to 0 °C and stirred for 30 minutes and NaH (60% in mineral oil) (77.8 mg, 1.94 mmol, 2.0 equiv) was added and stirred for another 30 minutes at 0 ºC. TBAI (35.9 mg, 0.097 mmol, 0.1 equiv) and propargyl bromide (434 μL, 4.85 mmol, 5 equiv) were charged, and the reaction was allowed to warm to room temperature and stirred overnight. Reaction quenched by a mixture of MeOH and NH_4Cl. The product was extracted with EtOAc (2 x 10 mL) and DCM (2 x 10 mL). The combined organic layers were washed with brine, dried over $MgSO_4$, filtered, and concentrated under reduced pressure. The crude product was purified by column chromatography (SiO_2, 5–30% EtOAc/Hexanes, solvent polarity was increased in 5% increments) to afford ether **32** (278.6 mg, 83% yield) as a white solid; 1H NMR (400 MHz, CDCl3) δ 6.15 (dd, J = 16.0, 7.8 Hz, 1H), 6.03 (d, J = 16.1 Hz, 1H), 5.81 (d, J = 2.2 Hz, 1H), 4.81 – 4.74 (m, 2H), 4.50 (ddd, J = 6.7, 4.5, 2.2 Hz, 1H), 4.21 – 4.08 (m, 2H), 3.20 (t, J = 7.7 Hz, 1H), 2.52 – 2.35 (m, 4H), 2.17 (s, 3H), 1.71 (t, J = 1.1 Hz, 3H), 1.41 (s, 9H); 13C NMR (101 MHz, CDCl3) δ 171.47, 149.92, 145.90, 135.73, 127.16, 122.93, 111.33, 80.98, 80.56, 79.36, 60.54, 56.23, 49.50, 47.32, 39.52, 28.24, 26.58, 20.81, 14.33.;

IR (thin film, NaCl) 3450, 2922, 2854, 1713, 1258, 1098, 849, 800, 689 cm^{-1}; HRMS (ESI) m/z calc'd $C_{21}H_{30}O_4$ $[M+Na]^+$: 369.2036, found: 369.2018; $[\alpha]_D^{25}$ –4.1450 ° (*c* 0.2, $CHCl_3$).

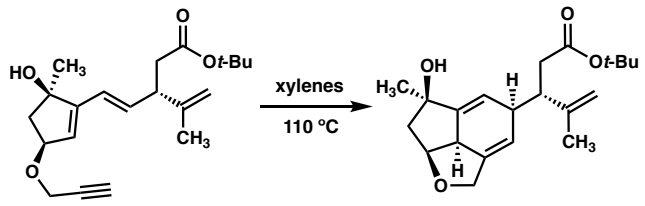

32 ***33***

Cyclohexadiene 33: A flame-dried 50 mL round bottom flask containing xylenes (80 mL) was charged with **32** (277 mg, 0.8 mmol, 1 equiv). This solution was sparged with N_2 for 10 min, then heated to 110 °C and stirred for 3 h. The reaction mixture was cooled to 23 °C, and the xylenes removed by rotary evaporation leaving a yellow residue which was purified by flash chromatography (SiO_2, 5%–40% EtOAc/hexanes with 5% solvent polarity increments) to afford tricycle **33** (265.5 mg, 96% yield) as a white solid; ^{1}H NMR (400 MHz, CDCl3) δ 5.80 – 5.71 (m, 2H), 4.97 – 4.88 (m, 1H), 4.84 (s, 1H), 4.59 (dt, J = 8.9, 6.6 Hz, 1H), 4.40 – 4.32 (m, 2H), 3.03 (t, J = 9.6 Hz, 1H), 2.84 – 2.66 (m, 2H), 2.50 – 2.30 (m, 3H), 2.17 (s, 1H), 1.76 (s, 3H), 1.60 (dd, J = 12.9, 6.2 Hz, 1H), 1.42 (s, 9H), 1.36 (s, 3H); ^{13}C NMR (101 MHz, CDCl3) δ 172.09, 151.37, 145.17, 142.77, 123.42, 119.45, 113.33, 81.28, 80.53, 77.67, 71.67, 50.68, 47.64, 46.37, 39.91, 37.00, 28.23, 27.29, 20.58; IR (thin film, NaCl) 3402, 2972, 2926, 2856, 1714, 1444, 1367, 1256, 1146, 1037, 963, 897, 852, 736 cm^{-1}; HRMS (FAB+) m/z calc'd $C_{21}H_{30}O_4$ $[M+Na]^+$: 369.2036, found: 369.2018; $[\alpha]_D^{23}$ + 5.5844 (*c* 0.9, $CHCl_3$).

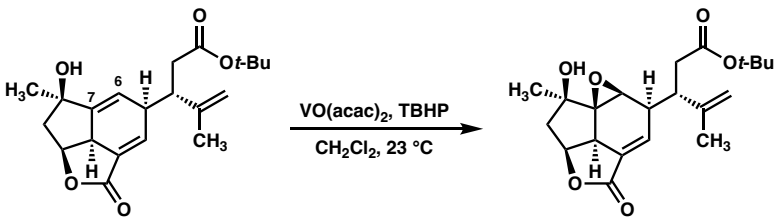

12 ***34***

Epoxide 34: A 500 mL round-bottomed flask was charged with $VO(acac)_2$ (71.6 mg, 0.270 mmol, 0.10 equiv), tricycle **12** (981.1 mg, 2.72 mmol, 1.0 equiv), and CH_2Cl_2 (136 mL). To the resulting green, homogenous reaction mixture was added *t*-BuOOH (990 μL, 5.5 M solution in decane, 5.44 mmol, 2.0 equiv) dropwise over 2 min, causing the reaction solution to turn dark red. The reaction was stirred at 20 ºC for 3 h, after which time it turns from dark red to orange. The reaction solution was concentrated to approximately 10 mL and the resulting solution was purified directly by flash column chromatography (0-100% EtOAc/Hexanes) to provide epoxide **34** (720.2 mg, 1.91 mmol, 70% yield) as a white, semicrystalline solid. ^{1}H NMR (500 MHz, $CDCl_3$) δ 6.46 (dd, *J* = 3.7, 2.3 Hz, 1H), 5.02 – 4.99 (m, 1H), 4.93 – 4.86 (m, 2H), 3.75 (s, 1H), 3.34 (dd, *J* = 8.3, 3.0 Hz, 1H), 2.97 (q, *J* = 7.0 Hz, 1H), 2.72 (dt, *J* = 6.2, 3.0 Hz, 1H), 2.58 (dd, *J* = 13.6, 7.5 Hz, 1H), 2.56 – 2.51 (m, 3H), 1.99 (dd, *J* = 13.7, 6.1 Hz, 1H), 1.79 (s, 3H), 1.45 (s, 3H), 1.43 (s, 9H); ^{13}C NMR (100 MHz, $CDCl_3$) δ 171.1, 169.0, 143.9, 137.1, 127.1, 114.3, 81.0, 77.0, 74.3, 69.0, 53.3, 49.9, 44.6, 44.4, 43.9, 37.0, 28.1, 22.6, 21.2; IR (Neat film, NaCl) 3478, 3076, 3057, 2977, 2035, 1760, 1727, 1648, 1448, 1431, 1392, 1368, 1355, 1312, 1291, 1262, 1196, 1158, 1150, 1100, 1051, 1020, 974, 953, 918, 900, 844, 817, 779, 737, 703, 676 cm^{-1}; HRMS (MM:ESI-APCI+) *m/z* calc'd for $C_{21}H_{29}O_6$ $[M+H]^+$: 377.1964, found 377.1952; $[\alpha]_D^{25}$ – 96.1 ° (*c* 0.40, $CHCl_3$).

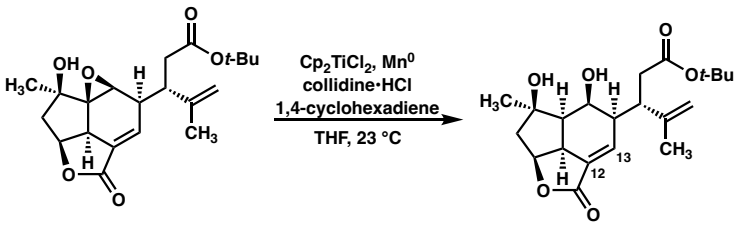

34 ***35***

Alcohol 35: A 250 mL round-bottomed flask was charged with Cp_2TiCl_2 (101.1 mg, 0.406 mmol, 0.20 equiv), Mn^0 (245.6 mg, 4.47 mmol, 2.20 equiv), collidine•HCl (800.8 mg, 5.08 mmol, 2.5 equiv). The flask was then evacuated and back-filled with N_2 gas. To the flask was then added epoxide **34** (765.7 mg, 2.03 mmol, 1.0 equiv) in THF (41 mL). The resulting heterogenous yellow/orange mixture was stirred rapidly and 1,4-cyclohexadiene (865 μL, 9.14 mmol, 4.5 equiv) was added dropwise over 2 min. The reaction was stirred for 2 h at 20 ºC, after which time it turned from yellow/orange to blue. SiO_2 (20 g) was added to the reaction mixture, the solvent was removed by rotary evaporation, and the solid loaded onto a column and purified by flash chromatography (0-100% EtOAc/Hexanes) to provide diol **35** (454.8 mg, 1.20 mmol, 59% yield) as a white, semicrystalline solid. ^{1}H NMR (500 MHz, $CDCl_3$) δ 6.67 (t, *J* = 3.9 Hz, 1H), 4.95 (dt, *J* = 7.8, 5.5 Hz, 1H), 4.90 (s, 2H), 4.43 – 4.37 (m, 1H), 4.33 – 4.29 (m, 1H), 4.24 (s, 1H), 3.20 – 3.10 (m, 1H), 2.91 (ddd, *J* = 12.1, 7.8, 4.5 Hz, 1H), 2.52 (dd, *J* = 16.8, 7.8 Hz, 1H), 2.48 – 2.40 (m, 2H), 2.09 (dd, *J* = 13.7, 4.7 Hz, 1H), 1.98 (dd, *J* = 13.7, 6.6 Hz, 1H), 1.94 – 1.88 (m, 1H), 1.64 (s, 3H), 1.46 (s, 9H), 1.38 (s, 3H); ^{13}C NMR (100 MHz, $CDCl_3$) δ 174.2, 170.0, 144.9, 138.3, 132.6, 114.8, 82.2, 81.3, 80.0, 69.3, 51.1, 47.9, 47.6, 43.5, 41.9, 38.7, 28.6, 28.1, 19.1; IR (Neat film, NaCl) 3380, 2924, 2852, 1742, 1168 cm^{-1}; HRMS (MM:ESI-APCI+) *m/z* calc'd for $C_{21}H_{31}O_6$ $[M+H]^+$: 379.2121, found 379.2110. $[\alpha]_D^{25}$ –2.57 ° (*c* 0.67, $CHCl_3$).

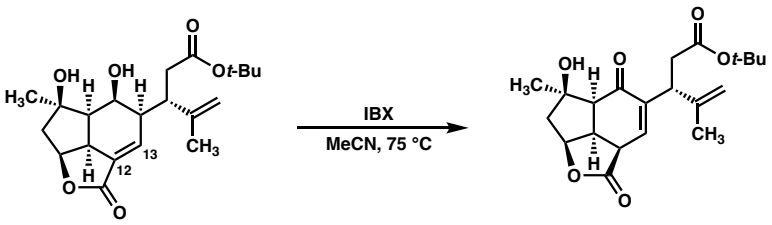

35 ***11***

Enone 11: A 20 mL scintillation vial was charged with diol **35** (71.0 mg, 0.188 mmol, 1.0 equiv) in MeCN (7.5 mL). IBX (263 mg, 0.938 mmol, 5.0 equiv) was added, and the vial was sealed and placed in a preheated 75 °C aluminum block. The suspension was stirred for 2 h at 75 °C, after which no starting material remained (as judged by TLC). The reaction mixture was cooled to 23 °C, then filtered over a pad of SiO_2, rinsing with EtOAc. The filtrate was concentrated by rotary evaporation leaving a crude oil which was purified by flash chromatography (SiO_2, 30%-40%-50% EtOAc/hexanes) to afford enone **11** (46.0 mg, 0.122 mmol, 65% yield) as a white foam; ^{1}H NMR (500 MHz, $CDCl_3$) δ 6.75 (d, J = 3.9 Hz, 1H), 5.11 (t, J = 6.0 Hz, 1H), 4.84 (d, J = 11.2 Hz, 2H), 3.67 – 3.41 (m, 3H), 2.86 (dd, J = 14.7, 10.0 Hz, 1H), 2.61 – 2.44 (m, 2H), 2.31 (d, J = 14.9 Hz, 1H), 1.83 (dd, J = 14.8, 5.7 Hz, 1H), 1.69 (s, 3H), 1.42 (s, 3H), 1.40 (d, J = 1.2 Hz, 10H); ^{13}C NMR (100 MHz, $CDCl_3$) δ 174.4, 172.6, 145.4, 140.0, 139.5, 112.0, 82.8, 81.2, 57.3, 47.1, 44.2, 40.8, 40.2, 37.9, 28.2, 25.6, 21.6; IR (Neat film, NaCl) 3484, 2921, 1742, 1667, 1371, 1229, 1027, 681 cm^{-1}; HRMS (MM:ESI-APCI+) *m/z* calc'd for $C_{21}H_{28}O_6Na$ $[M+Na]^+$: 399.1778, found 399.1788; $[\alpha]_D^{25}$ –22.0 ° (*c* 0.53, $CHCl_3$).

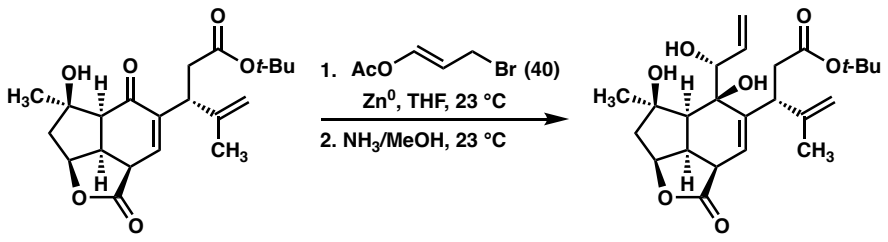

11 ***38***

Triol 38: A 1 dram vial was charged with activated Zn dust (36 mg, 0548 mmol, 6.25 equiv) in THF (890 μL). The suspension was stirred at 23 °C while a solution of allyl bromide **40** (98.0 mg, 0.548 mmol, 6.25 equiv, 9:1 *E:Z* mixture)[25] in THF (250 μL) was added. This suspension was stirred for 10 min at 23 °C, followed by the addition of a solution of enone **11** (33.0 mg, 0.0877 mmol, 1.0 equiv) in THF (1.60 mL). The reaction mixture quickly changed from colorless to yellow/green. This solution was stirred for 30 min at 23 °C, after which no starting material remained (as judged by TLC). The reaction was quenched with saturated aqueous $NaHCO_3$, and extracted with EtOAc (3x). The combined organic extracts were washed with brine, dried over Na_2SO_4, filtered and concentrated to afford a crude oil which was purified by flash chromatography (0%-30%-40%-50% EtOAc/hexanes) to afford a mixture of the branched and linear allylation products (c.a. 1:1 by ^{1}H NMR) which was used directly in the next reaction.

The mixture of allylation products was dissolved in methanolic ammonia (2.0 mL) and stirred 30 min at 23 °C after which no starting material remained (as judged by TLC). The reaction mixture was concentrated, loaded directly onto a column, and purified by flash chromatography (0%-5%-10% EtOAc/CH_2Cl_2) to afford triol **38** (10.4 mg, 0.0239 mmol, 27% yield) as an amorphous white solid. X-ray quality crystals were obtained by

slow diffusion of hexanes into a CH_2Cl_2 solution; ^{1}H NMR (400 MHz, $CDCl_3$) δ 5.98 – 5.76 (m, 2H), 5.50 – 5.34 (m, 1H), 5.26 (dt, *J* = 10.6, 1.5 Hz, 1H), 5.01 – 4.93 (m, 2H), 4.90 (q, *J* = 1.5 Hz, 1H), 4.50 (d, *J* = 3.5 Hz, 1H), 4.16 (ddd, *J* = 6.3, 3.6, 1.6 Hz, 1H), 3.56 (dd, *J* = 11.6, 4.9 Hz, 1H), 3.33 – 3.19 (m, 2H), 2.73 (dd, *J* = 17.2, 11.7 Hz, 1H), 2.53 (dd, *J* = 17.2, 5.0 Hz, 1H), 2.19 – 2.01 (m, 3H), 1.88 – 1.75 (m, 4H), 1.74 (d, *J* = 1.9 Hz, 1H), 1.43 (s, 12H); ^{13}C NMR (100 MHz, $CDCl_3$) δ 176.7, 173.4, 148.3, 142.2, 135.6, 120.7, 117.4, 113.5, 82.2, 81.9, 81.8, 79.2, 48.8, 48.1, 42.9, 39.9, 39.6, 39.6, 29.1, 28.2, 21.5; IR (Neat film, NaCl) 3444, 2920, 2852, 1727, 1659, 1650, 1460, 1453, 1367, 1356, 1265, 1226, 1009, 940, 892, 854, 838, 797, 668 cm^{-1}; HRMS (MM:ESI-APCI+) *m/z* calc'd for $C_{21}H_{32}O_7N$ $[M+NH_4]^+$: 452.2643, found 452.2632; $[\alpha]_D^{25}$ –35.2 ° (*c* 0.20, $CHCl_3$).

The major side product isolated after this reaction sequence has been tentatively assigned as lactol **S5** (Scheme S1), which is isolated as a mixture (presumably epimers at the lactol carbon). This product is hypothesized to arise from the linear allylation product (**S4**), after ammonolysis of the enol acetate. In a typical experiment, putative lactol **S5** is isolated in roughly equal amounts as the desired product, triol **23**. A sample of putative lactol **S5** was purified and characterized: ^{1}H NMR (400 MHz, C_6D_6) δ 6.00 (d, J = 3.7 Hz, 1H), 5.18 (dd, J = 6.8, 5.2 Hz, 1H), 5.15 – 5.13 (m, 1H), 4.78 (p, J = 1.5 Hz, 1H), 4.39 – 4.32 (m, 1H), 3.89 (dd, J = 10.3, 5.7 Hz, 1H), 3.08 (d, J = 7.0 Hz, 1H), 2.72 (tdd, J = 10.3, 3.6, 1.3 Hz, 2H), 2.60 – 2.53 (m, 1H), 2.52 – 2.45 (m, 1H), 2.37 (d, J = 5.7 Hz, 1H), 2.33 (d, J = 5.4 Hz, 1H), 2.12 (d, J = 8.1 Hz, 1H), 2.08 (d, J = 7.9 Hz, 1H), 1.72 (d, J = 1.2 Hz, 3H), 1.36 (s, 3H), 1.33 (s, 9H); ^{13}C NMR (100 MHz, C_6D_6) δ 175.4, 172.4, 148.9, 141.9, 120.6, 113.0, 99.4, 86.2, 80.7, 80.7, 80.1, 52.1, 48.3, 41.9, 40.4, 40.2, 39.7, 39.4, 35.7, 33.3,

28.8, 28.1, 21.3; IR (thin film, NaCl) 3540, 2973, 2916, 2361, 1759, 1731, 1453, 1369, 1294, 1264, 1230, 1192, 1146, 1036, 1008, 957, 905, 842, 737, 680, 651 cm^{-1}; HRMS (ESI) m/z calc'd $C_{24}H_{34}NaO_7$ $[M+Na]^+$: 457.2197; found: 457.2198; $[\alpha]_D^{23}$ – 38.2 (*c* 0.42, $CHCl_3$).

Scheme S1: Schematic of allylation reaction and proposed identity of intermediates and side-products.

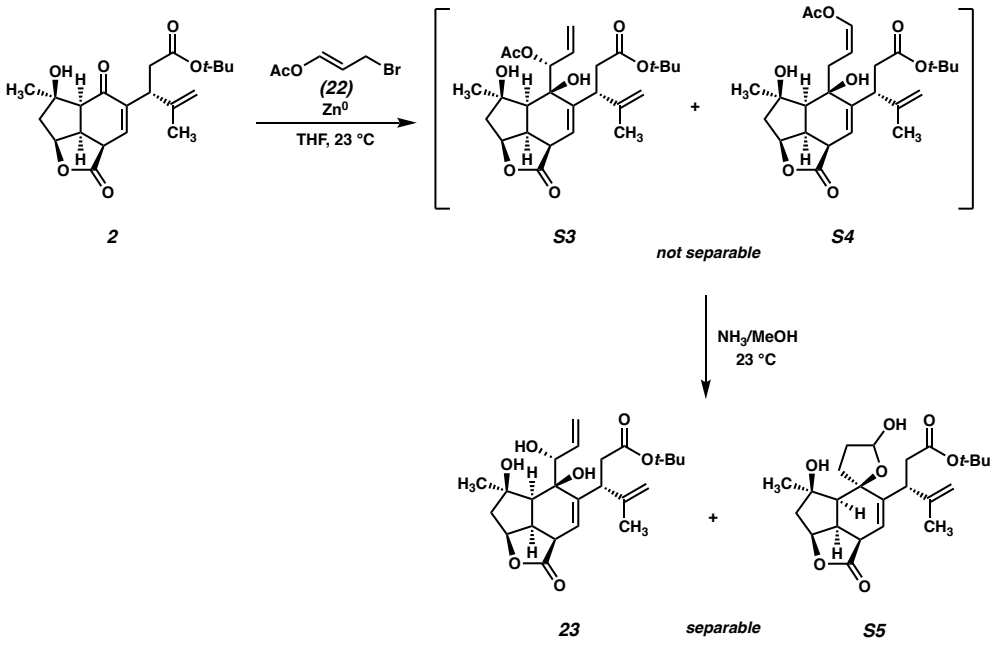

Scheme S2: Stereochemical rationale for the allylation reaction: after metalation of bromide **22** (90:10 mixture E/Z), the allylzinc bromide equilibrates to the *Z*-isomer (**S6**) via metallotropic shift.[26] The nucleophile can engage enone **2** from the less hindered α-face through one of two closed transition states (**S7** or **S8**). **S7** is hypothesized to be favored due to the steric interaction depicted in **S8** (red). Linear isomer **S4** is proposed to arise from a competitive open transition state, due the extreme steric hinderance of enone **2** (typically allyl Zn nucleophiles display branched selectivity).[27]

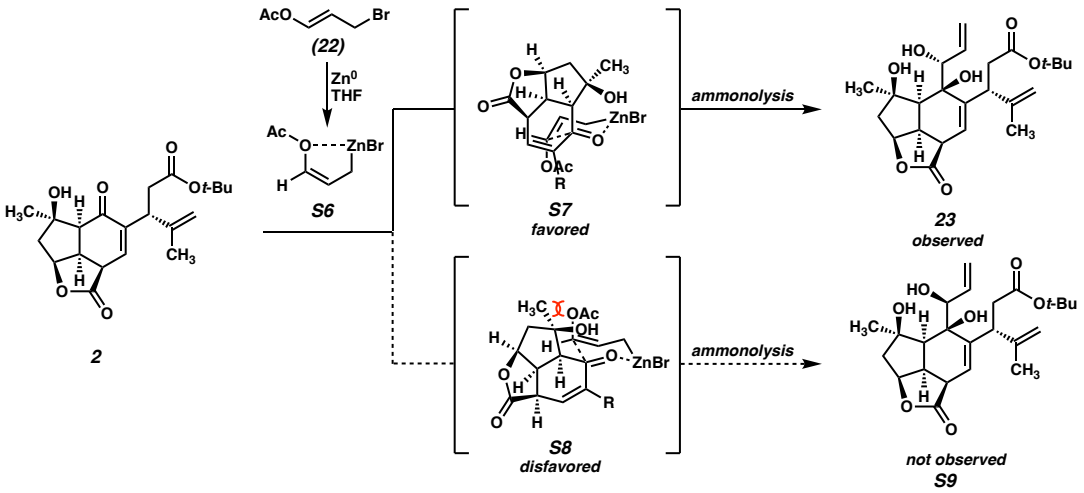

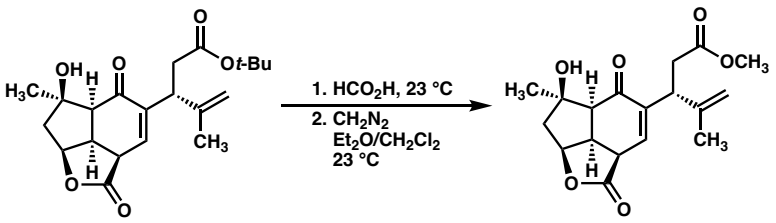

11 ***41***

Methyl Ester 41: A solution of enone **11** (63.0 mg, 0.167 mmol, 1.0 equiv) in HCO_2H (3.3 mL) was stirred for 4 h in a 20 mL scintillation vial, after which no starting material remained (as judged by LCMS). The solvent was removed by rotary evaporation, and then the resulting crude oil was dissolved in CH_2Cl_2 (3.3 mL). This solution was stirred at 23 °C while diazomethane (c.a. 0.5 M solution in Et_2O) was added until the yellow color of the reagent persisted (c.a. 2 mL). At this point, excess diazomethane was quenched by the addition of AcOH (100 μL). The solvent was removed by rotary evaporation, leaving a crude oil which was purified by flash chromatography (SiO_2, 50%-60%-70% EtOAc/Hexanes) to afford methyl ester **41** (39.0 mg, 0.117, 70% yield over 2 steps) as a white foam; ^{1}H NMR (400 MHz, $CDCl_3$) δ 6.74 (d, *J* = 4.3 Hz, 1H), 5.15 – 5.07 (m, 1H), 4.89 – 4.83 (m, 1H), 4.82 (s, 1H), 3.73 – 3.66 (m, 1H), 3.66 – 3.53 (m, 6H), 2.85 (dd, *J* = 15.0, 9.4 Hz, 1H), 2.65 – 2.52 (m, 2H), 2.29 (d, *J* = 14.9 Hz, 1H), 2.04 (s, 1H), 1.90 – 1.78 (m, 1H), 1.67 (s, 4H), 1.41 (s, 3H); ^{13}C NMR (100 MHz, $CDCl_3$) δ 195.5, 174.5, 173.4, 145.3, 140.1, 139.4, 112.1, 82.8, 82.8, 57.0, 52.0, 47.2, 43.3, 40.8, 40.2, 36.8, 25.7, 21.7; IR (Neat film, NaCl) 3486, 2964, 1732, 1661, 1435, 1376, 1256, 1168, 1120, 1107, 652 cm^{-1}, HRMS (MM:ESI-APCI+) *m/z* calc'd for $C_{18}H_{32}O_6$ $[M+H]^+$: 335.1489, found 335.1495; $[\alpha]_D^{25}$ –119.5 ° (*c* 0.40, $CHCl_3$).

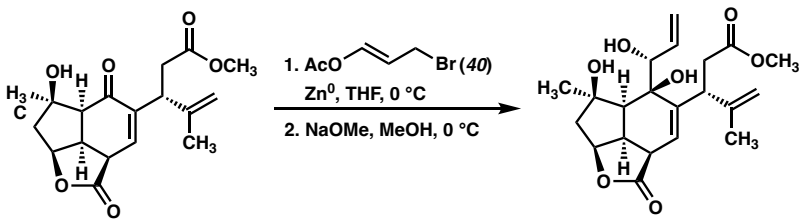

41 *42*

Triol 42: A 1 dram vial was charged with enone **41** (50.0 mg, 0.150 mmol, 1.0 equiv) and Zn dust (58.0 mg, 0.897 mmol, 6.0 equiv) in THF (2.0 mL). The suspension was cooled to 0 °C and stirred vigorously (1500 RMP) while a solution of ally bromide **40** (160 mg, 0.897 mmol, 6.0 equiv, 9:1 *E:Z* mixture) in THF (200 µL) was added dropwise. The reaction mixture was stirred vigorously at 0 °C for 1 h after which a small amount of enone **25** remained (as judged by TLC and LC/MS). A second portion of allyl bromide **40** (80 mg, 0.449 mmol, 3.0 equiv) in THF (100 µL) was added at 0 °C, and the suspension was stirred an additional 20 min at 0 °C. The reaction mixture was quenched with saturated aqueous $NaHCO_3$ and extracted with EtOAc (3x). The organic extracts were combined, washed with brine, dried over Na_2SO_4, filtered and concentrated to afford a crude oil which was purified by flash chromatography (SiO_2, 30%-40%-50% EtOAc/hexanes) to afford a mixture of branched and linear allylation products (39.0 mg total, 0.0898 mmol), which was used directly in the next reaction.

The mixture of allylation products was dissolved in dry MeOH (9.0 mL) in a 20 mL scintillation vial and cooled to 0 °C. A solution of NaOMe/MeOH (c.a. 1.0 M, 144 µL, 0.144 mmol, 1.6 equiv) was added dropwise. The solution was stirred at 0 °C with careful monitoring by TLC. Once the starting material had been consumed (c.a. 10 min), the reaction was quenched at

0 °C with saturated aqueous NH_4Cl and warmed to 23 °C. The mixture was extracted with EtOAc (3x), and the organic extracts were combined, washed with brine, filtered and concentrated to afford a crude oil which was purified by flash chromatography (SiO_2, 60%-70%-80% EtOAc/hexanes) to afford a mixture of triol **42** and putative lactonized product **S10** (18.0 mg total, 4:1 mixture by ^{1}H NMR– 81% triol **42** by mass, 0.0372 mmol triol **42**, 25% yield of triol **42** over 2 steps) as an amorphous white solid which was used in the next step without further purification. An aliquot of this material was subjected to preparative HPLC purification (Agilent Zorbax Rx-Sil (SiO_2) preparative HPLC; IPA/hexanes, 7.0mL/min, monitor wavelength = 206 nm, 20% IPA in hexanes over 4.40 min) to obtain a pure sample of triol **42** for characterization (isolated as an 11.6:1 mixture of epimers at C(5)): ^{1}H NMR (400 MHz, C_6D_6) δ 6.03 (d, *J* = 3.4 Hz, 1H), 5.76 (ddd, *J* = 17.4, 10.8, 4.6 Hz, 1H), 5.46 (dt, *J* = 17.2, 2.1 Hz, 1H), 5.11 (dt, *J* = 10.8, 2.0 Hz, 1H), 5.06 – 5.04 (m, 1H), 4.79 – 4.76 (m, 1H), 4.31 – 4.25 (m, 1H), 4.22 – 4.18 (m, 1H), 3.64 (dd, *J* = 11.1, 5.1 Hz, 1H), 3.27 (s, 3H), 3.26 (d, *J* = 3.2 Hz, 1H), 3.08 (s, 1H), 2.72 – 2.51 (m, 3H), 2.29 (dd, *J* = 16.6, 5.1 Hz, 1H), 1.94 (d, *J* = 9.8 Hz, 1H), 1.75 (d, *J* = 15.2 Hz, 1H), 1.66 – 1.64 (m, 5H), 1.26 (s, 1H), 1.15 (s, 3H), 1.01 (ddd, *J* = 15.2, 6.2, 2.0 Hz, 1H); ^{13}C NMR (100 MHz, C_6D_6) δ 175.3, 173.2, 148.1, 140.4, 136.3, 122.4, 115.9, 113.3, 81.9, 81.5, 77.5, 76.8, 51.4, 48.1, 47.3, 43.2, 40.3, 39.6, 38.3, 29.3, 21.0; IR (Neat film, NaCl) 3455, 2920, 2852, 2359, 1732, 1458, 1370, 1258, 1117, 1013, 805 cm^{-1}; HRMS (MM:ESI-APCI+) *m/z* calc'd for $C_{21}H_{32}O_7N$ $[M+NH_4]^+$: 410.2173, found 410.2191; $[\alpha]_D^{25}$ –130.3 ° (*c* 0.083, $CHCl_3$).

Lactone **S10** was characterized by ^{1}H NMR and HRMS (lactone **10** was found to be unstable to prolonged storage, causing difficulty in further characterization): ^{1}H NMR (400

MHz, C_6D_6) δ 5.86 (d, *J* = 3.2 Hz, 1H), 5.62 (dt, *J* = 17.1, 2.5 Hz, 1H), 5.52 (dddd, *J* = 17.2, 10.6, 3.1, 1.3 Hz, 1H), 5.05 (dt, *J* = 10.4, 2.5 Hz, 1H), 4.92 (s, 1H), 4.68 (t, *J* = 1.4 Hz, 1H), 4.29 (t, *J* = 2.6 Hz, 1H), 4.08 (dd, *J* = 8.0, 6.3 Hz, 1H), 2.75 (d, *J* = 4.4 Hz, 3H), 2.73 – 2.67 (m, 1H), 2.58 (d, *J* = 1.6 Hz, 1H), 2.57 (d, *J* = 4.9 Hz, 2H), 2.47 (dd, *J* = 11.8, 3.2 Hz, 1H), 2.26 (dd, *J* = 10.0, 1.9 Hz, 1H), 1.38 (d, *J* = 1.2 Hz, 3H), 1.11 (s, 3H); HRMS (MM:ESI-APCI+) *m/z* calc'd for $C_{20}H_{25}O_6$ $[M+H]^+$: 361.1646, found 361.1645.

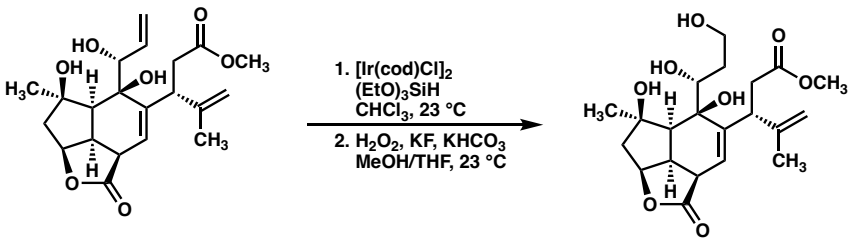

42 ***43***

This step was performed using the c.a. 80% pure product from the previous step. The yield and equivalents are calculated accounting for the purity of the starting material.

Tetrol 43: In a nitrogen-filled glovebox, a 20 mL scintillation vial was charged with triol **42** (18.0 mg, 81% purity, 0.0372 mmol triol **42**, 1.0 equiv) and $[Ir(cod)Cl]_2$ (6.2 mg, 0.00917 mmol, 0.25 equiv) in $CHCl_3$ (4.6 mL). Triethoxysilane (35 µL, 0.228 mmol, 6.1 equiv) was added, and the orange solution was allowed to stir 1 h at 23 °C, after which time it had changed to bright yellow in color. LCMS, TLC and NMR analysis indicated that no starting material remained. The vial was removed from the glovebox and concentrated under vacuum. The remaining orange residue was reconstituted in THF/MeOH (1:1, 11.5 mL). To this solution was added $KHCO_3$ (91.8 mg, 0.917 mmol, 25.0 equiv) followed by KF (53.2 mg, 0.917 mmol, 25.0 equv). To this dark orange suspension was added H_2O_2 (30% aqueous, 312 µL, 2.75 mmol, 74.0 equiv) after which the reaction mixture became deep blue in color. The reaction was stirred 2 h at 23 °C, then quenched with saturated aqueous $Na_2S_2O_3$, and the MeOH and THF were removed by rotary evaporation. The remaining residue was partitioned between EtOAc and water, and extracted with EtOAc (3x) then *i*-PrOH:$CHCl_3$ (1:3). The combined organic extracts were combined, washed with brine, and dried over Na_2SO_4, filtered and concentrated, leaving a crude solid that was purified by flash chromatography (30%-50%-100% EtOAc/hexanes,

then 5% MeOH/EtOAc) to afford tetrol **43**, isolated as a mixture with an unidentified isomeric impurity (7.0 mg total, 3.1:1 mixture by ^{1}H NMR–75% tetrol **43** by mass, 0.0128 mmol tetrol **43**, 34% yield over 2 steps) as a white solid. An aliquot of this material was subjected to preparative HPLC purification (Agilent Zorbax Rx-Sil (SiO_2) preparative HPLC; IPA/hexanes, 4.0mL/min, monitor wavelength = 206 nm, 60% IPA in Hexanes over 4.40 min) to obtain a sample of tetrol **43** for characterization: ^{1}H NMR (600 MHz, CD_3CN) δ 5.82 (d, J = 4.0 Hz, 1H), 4.95 (dd, J = 7.3, 6.1 Hz, 1H), 4.88 – 4.76 (m, 1H), 3.77 (d, J = 10.5 Hz, 1H), 3.62 (s, 3H), 3.59 (t, J = 8.0 Hz, 1H), 3.54 (s, 1H), 3.36 – 3.29 (m, 1H), 3.31 – 3.24 (m, 1H), 2.85 (d, J = 14.5 Hz, 1H), 2.68 – 2.61 (m, 1H), 2.64 – 2.57 (m, 1H), 2.49 – 2.39 (m, 1H), 2.39 (d, J = 9.9 Hz, 1H), 2.10 (dd, J = 9.5, 2.0 Hz, 1H), 1.76 (s, 3H); ^{13}C NMR (100 MHz, CD_3CN) δ 177.5, 173.84, 149.8, 123.5, 111.5, 83.7, 83.2, 78.2, 74.3, 60.7, 52.2, 48.2, 47.0, 42.8, 41.2, 40.3, 39.5, 34.7, 29.8, 22.1; IR (Neat film, NaCl) 3448, 2921, 2852, 1730, 1361, 1168, 681 cm^{-1}; HRMS (MM:ESI-APCI+) *m/z* calc'd for $C_{21}H_{30}O_8Na$ $[M+Na]^+$: 433.1833, found 433.1840; $[\alpha]_D^{25}$ +165.5 ° (*c* 0.53, EtOH).

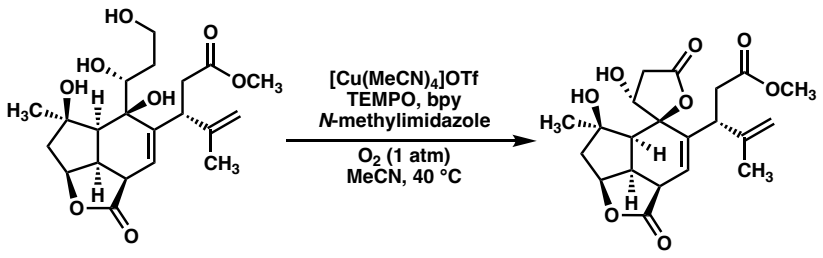

43 ***Havellockate (1)***

This step was performed using the c.a. 75% pure product from the previous step. The yield and equivalents are calculated accounting for the purity of the starting material.

Havellockate (1): A stock solution was prepared which included CuOTf(MeCN)$_4$ (19.0 mg, 0.050 mmol), bipyridine (9.0 mg, 0.050 mmol), TEMPO (9.0 mg, 0.05 mmol) and *N*-methylimidazole (8.0 μL, 0.10 mmol) in MeCN (5.0 mL, 0.01 M with respect to Cu). 1.7 mL (0.0170 mmol, 1.3 equiv based on Cu) of this solution was added to a 1-dram vial containing tetrol **43** (7.0 mg, 75% purity, 0.0128 mmol tetrol **43**, 1.0 equiv). The solution was sparged with O_2 (balloon) for 5 min during which time the solution changed from dark red to green. The vial was affixed with an O_2 balloon and placed in a preheated 40 °C aluminum block. The solution was stirred rapidly at 40 °C for 5 h, after which no starting material remained (as judged by LCMS). The vial was cooled to 23 °C, and the contents purified directly by preparative HPLC (Agilent Eclipse XDB (C8) preparative HPLC; MeCN/H_2O, 7.0mL/min, monitor wavelength = 206 nm, 10% MeCN ramp up to 40% MeCN over 10 min) to afford havellockate (4.2 mg, 0.0103 mmol, 80% yield, 7% total yield over the 5 steps from enone **11**) as a white crystalline solid. Crystals suitable for X-ray diffraction were obtained by layer diffusion of hexanes into CH_2Cl_2; ^{1}H NMR (400 MHz, *d*$_5$-Pyr) δ 6.39 (d, *J* = 3.5 Hz, 1H), 5.31 (s, 1H), 4.89 – 4.87 (m, 1H), 4.84 (s, 1H),

4.75 – 4.69 (m, 1H), 4.18 (dd, J = 10.2, 5.4 Hz, 1H), 3.53 (s, 3H), 3.53 – 3.49 (m, 1H), 3.47 (dd, J = 3.6, 1.2 Hz, 1H), 3.41 (dd, J = 18.0, 6.1 Hz, 1H), 3.20 (dd, J = 14.9, 5.4 Hz, 1H), 3.04 (dd, J = 14.9, 10.6 Hz, 1H), 2.94 (dd, J = 18.1, 1.3 Hz, 1H), 2.24 (d, J = 14.9 Hz, 1H), 2.11 (d, J = 8.9 Hz, 1H), 2.05 (s, 3H), 1.77 (dd, J = 14.9, 6.2 Hz, 1H), 1.56 (s, 3H); ^{13}C NMR (100 MHz, d_5-Pyr) δ 176.6, 176.1, 173.2, 147.9, 138.4, 123.1, 113.0, 91.8, 81.6, 80.1, 76.0, 51.5, 51.4, 49.1, 44.8, 40.5, 40.4, 39.1, 38.2, 28.1, 20.7; IR (Neat film, NaCl) 3347, 2919, 2849, 1762, 1632, 1551, 1460, 1374, 1171, 1102, 1032, 809, 687, 615 cm^{-1}; HRMS (MM:ESI-APCI+) *m/z* calc'd for $C_{21}H_{26}O_8Na$ $[M+Na]^+$: 429.1520, found 429.1528; $[\alpha]_D^{25}$ – 56.7 ° (*c* 0.38, pyridine).

1.7.3 Comparison of Natural and Synthetic Havellockate

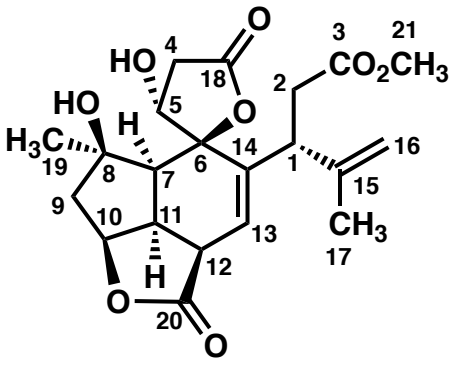

Table S1. ^{1}H NMR shifts of natural and synthetic havellockate. *Note:* synthetic sample was referenced to 7.18 for d_5-Py to match the shifts reported for the natural material.

^{1}H NMR (400 MHz, d_5-Py) Natural[28]	^{1}H NMR (400 MHz, d_5-Py) Synthetic (referenced to 7.18)	Assignment
1.53 (3H, s)	1.52 (3H, s)	19-Me
1.73 (1H, dd, *J* = 13.3, 6.5)	1.73 (1H, dd, *J* = 14.9, 6.2)	9-H_a
2.02 (3H, s)	2.01 (3H, s)	17- Me
2.08 (1H, d, *J* = 8.2)	2.07 (1H, d, *J* = 8.9)	7-H
2.20 (1H, d, *J* = 13.3)	2.20 (1H, d, *J* = 14.9)	9-H_b
2.90 (1H, d, *J* = 16.3)	2.89 (1H, dd, *J* = 18.1, 1.3)	4-H_a
3.02 (1H, dd, *J* = 13.8)	3.00 (1H, dd, *J* = 14.9, 10.6)	2-H_a
3.16 (1H, dd, *J* = 13.4)	3.16 (1H, dd, *J* = 14.9, 5.4)	2-H_b
3.36 (1H, dd, *J* = 19.5, 6.5)	3.37 (1H, dd, *J* = 18.0, 6.1)	4-H_b
3.46 (1H, d, *J* = 3)	3.43 (1H, dd, *J* = 3.6, 1.2)	12-H
3.48 (1H, m)	3.47 (1H, m)	11-H
3.50 (3H, s)	3.49 (3H, s)	21-OMe
4.15 (1H, dd, *J* = 8.3)	4.14 (1H, dd, *J* = 10.2, 5.4)	1-H
4.70 (1H, d, *J* = 6)	4.68 (1H, m)	5-H
4.72 (1H, brs, -OH)	4.80 (1H, brs, –OH)	OH
4.86 (1H, brs)	4.84 (1H, m)	16-H_a
5.02 (1H, m)	5.00 Obscured by water peak (evident in HSQC)	10-H
5.27 (1H, brs)	5.27 (1H, s)	16-H_b
6.34 (1H, d, *J* = 3)	6.35 (1H, d, J = 3.5)	13-H
7.48 (1H, br, –OH)	7.36 (1H, d, J = 4.6)	OH

Figure S2. ^{1}H NMR spectrum of synthetic havellockate (400 MHz, d_5-Py).

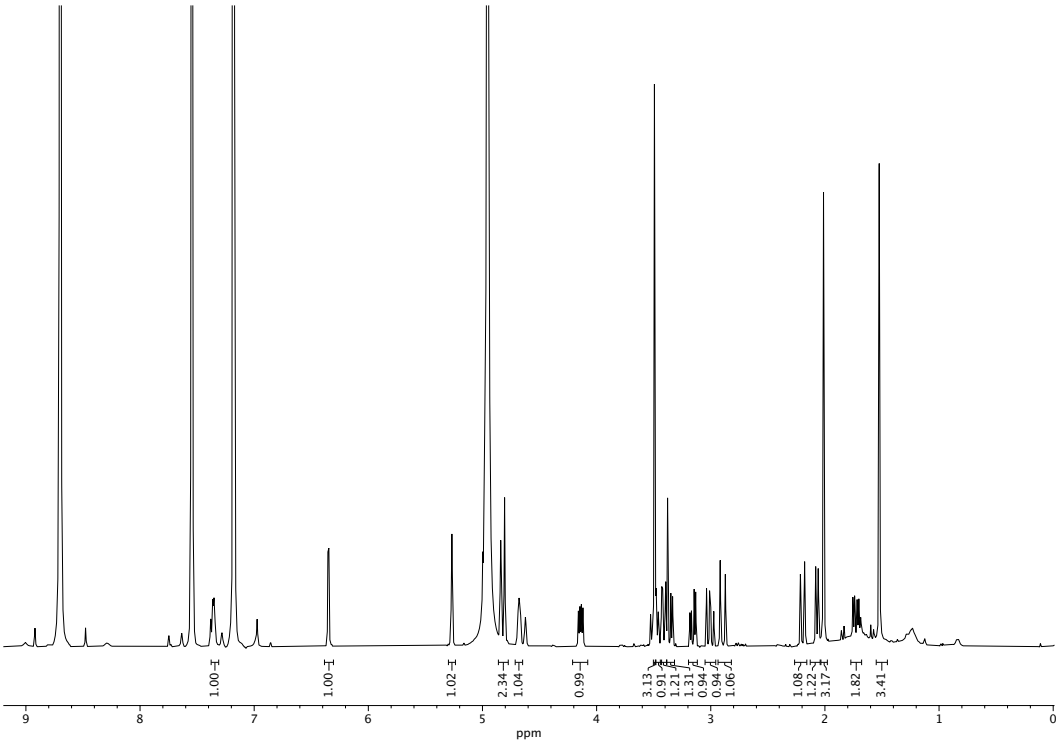

Table S2. ^{13}C NMR shifts of natural and synthetic havellockate. *Note:* synthetic sample was referenced to 123.57 for d_5-Py to match the shifts reported for the natural material.

^{13}C NMR (22.5 MHz, d_5-Py) Natural	^{13}C NMR (125 MHz, d_5-Py) Synthetic[3] (referenced to 123.57)
20.7	20.7
28.1	28.1
38.2	38.2
39.1	39.1
40.3	40.4
40.4	40.5
44.8	44.9
49.0	49.1
"5.10" (presumed error)	51.4
51.3	51.5
76.0	76.0
80.2	80.1
81.8	81.6
91.7	91.8
112.9	113.0
123.1	123.1
138.3	138.4
147.9	147.9
173.1	173.2
176.0	176.0
176.6	176.6

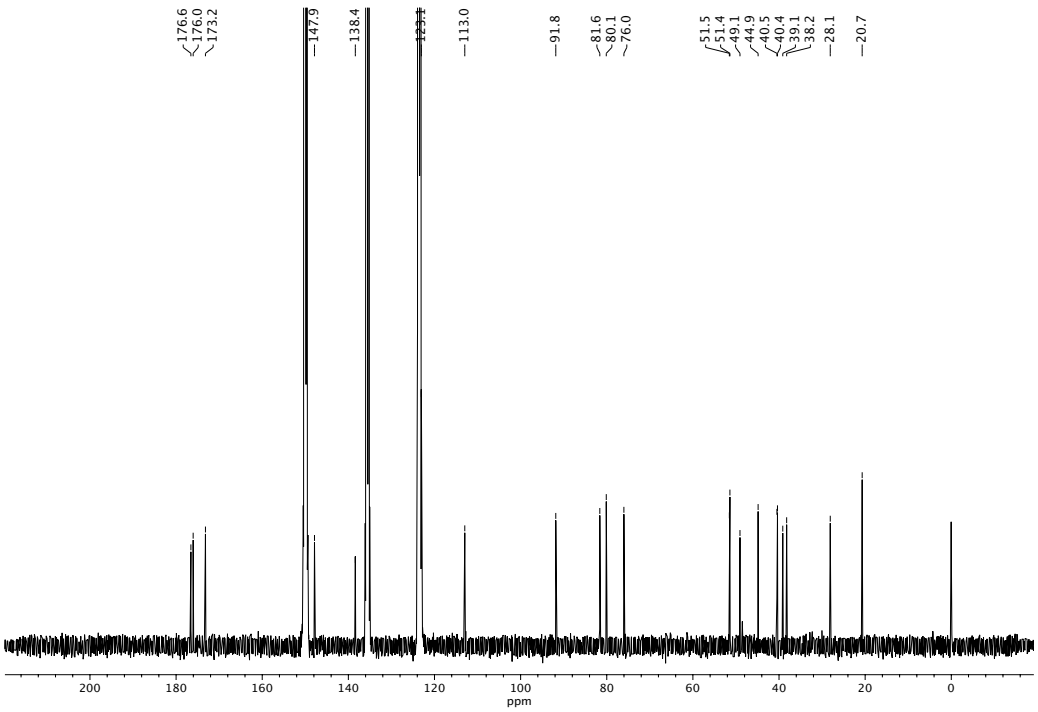

Figure S3. ^{13}C NMR spectrum of synthetic havellockate (100 MHz, d_5-Py).

1.7.4 REFERENCES OF EXPERIMENTALS

1) Pangborn, A. M.; Giardello, M. A.; Grubbs, R. H.; Rosen, R. K.; Timmers, F. J. Safe and Convenient Procedure for Solvent Purification. *Organometallics* **1996**, *15*, 1518–1520.

2) Prepared by "Procedure B" in the following reference: Lombardo, M.; Morganti, S.; Trombini, C. 3-Bromopropenyl Esters in Organic Synthesis: Indium- and Zinc-Mediated Entries to Alk-1-ene-3,4-diols. *J. Org. Chem.* **2003**, *68*, 997–1006. The *E/Z* ratio of the material obtained using this procedure varied from 3:1 to 9:1. Batches of 3-bromo-1-acetoxypropene of different *E/Z* ratios performed similarly in the Zn-mediated allylation chemistry (as noted by Lombardo et al.).

3) Lombardo, M.; Girotti, R.; Morganti, S.; Trombini, C. The First Zinc-promoted, Environmentally Friendly, and Highly Efficient Acetoxyallylation of Aldehydes in Aqueous Ammonium Chloride. *Chem. Commun.* **2001**, 2310–2311.

4) Formation of a similar linear product was observed by Trombini and Lobmardo with allylchromium nucleophiles. They observed that the formation of the linear product increased with steric hinderance of the electrophile. See: Lombardo, M.; Morganti, S.; Licciuli, S.; Trombini, C. 3-Chloro-propenyl Esters in Organic Synthesis: A New Chromium-Catalyzed Homoaldol Reaction. *Synlett* **2003**, *1*, 43–46.

5) Anjaneyulu, A. S. R.; Venugopal, M. J. R. V.; Sarada, P.; Clardy, J.; Lobkovsky, E. Havellockate, A Novel Seco and Spiro Lactone Diterpenoid From the Indian Ocean Soft Coral *Sinularia granosa. Tetrahedron Lett.* **1998**, *39*, 139–142.

1.8 REFERENCES AND NOTES OF CHAPTER

1) Carroll, A. R.; Copp, B. R.; Davis, R. A.; Keyzers, R. A.; Prinsep, M. R. Marine Natural Products. *Nat. Prod. Rep*. **2022**, (Advance Article) and previous articles in this series.

2) Li, Y.; Pattenden, G. Perspectives on the Structural and Biosynthetic Interrelationships Between Oxygenated Furanocembranoids and Their Polycyclic Congeners Found in Corals. *Nat. Prod. Rep*. **2011**, 28, 1269–1310.

3) Craig, R. A., II; Stoltz, B. M. Polycyclic Furanobutenolide-Derived Cembranoid and Norcembranoid Natural Products: Biosynthetic Connections and Synthetic Efforts. *Chem. Rev*. **2017**, 117, 7878−7909.

4) For previous syntheses of the polycyclic furanobutenolide-derived cembranoid intricarene, see (a) Tang, B.; Bray, C. D.; Pattenden, G. A Biomimetic Total Synthesis of (+)-Intricarene. *Tetrahedron Lett*. **2006**, *47*, 6401–6404. (b) Roethle, P. A.; Hernandez, P. T.; Trauner, D. Exploring Biosynthetic Relationships Among Furanocembranoids: Synthesis of (–)-Bipinnatin J, (+)-Intricarene, (+)-Rubifolide, and (+)-Isoepilophodione B. *Org. Lett.* **2006**, *8*, 5901–5904. (c) Stichnoth, D.; Kölle, P.; Kimbrough, T. J.; Riedle, E.; de Vivie-Riedle, R.; Trauner, D. Photochemical Formation of Intricarene. *Nat. Commun.* **2014**, *5*, 5597. For previous syntheses of the polycyclic furanobutenolide-derived norcembranoid scabrolide A, see: (d) Hafeman, N. J.; Loskot, S. A.; Reimann, C. E.; Pritchett, B. P.; Virgil, S. C.; Stoltz, B. M. The Total Synthesis of (–)-Scabrolide A. *J. Am. Chem. Soc*. **2020**, *142*, 8585–8590 (e) Meng, Z.; Fürstner, A. Total Syntheses of Scabrolide

A and Nominal Scabrolide B. *J. Am. Chem. Soc***. 2022***, 144*, 1528–1533. (f) Hafeman, N. J.; Loskot, S.; Reimann, C.; Pritchett, B.; Virgil, S. C.; Stoltz, B. M. Total Synthesis of (−)-Scabrolide A and (−)-Yonarolide. *Chem. Sci*. **2023**, *14*, 4745−4758. (g) Serrano, R.; Boyko, Y. D.; Hernandez, L. W.; Lotuzas, A.; Sar- lah, D. Total Syntheses of Scabrolide A and Yonarolide. *J. Am. Chem. Soc*. **2023**, *145*, 8805−8809. For the recent total synthesis of havellockate see: (h) Hafeman, N. J.; Chan, M.; Fulton, T. J.; Alexy, E. J.; Loskot, S. A.; Virgil, S. C.; Stoltz, B. M. Asymmetric Total Synthesis of Havellockate. *J. Am. Chem. Soc.* **2022**, *144*, 20232−20236 The total synthesis of ineleganolide was also recently disclosed: (i) Tuccinardi, J. P.; Wood, J. L. Total Syntheses of (+)-Ineleganolide and (−)-Sinulochmodin C. *J. Am. Chem. Soc*. **2022**, *144*, 20539−20547. (j) Gross, B. M.; Han, S.-J.; Virgil, S. C.; Stoltz, B. M. A Convergent Total Synthesis of (+)-Ineleganolide. *J. Am. Chem. Soc.* **2023**, *145*, 7763−7767. For the recent total synthesis of rameswaralide see: (k) Truax, N. J.; Ayinde, S.; Liu, J. O.; Romo, D. Total Synthesis of Rameswaralide Utilizing a Pharmacophore-Directed Retrosynthetic Strategy. *J. Am. Chem. Soc*. **2022**, *144*, 18575−18585. For recent synthesis of sinulochmodin C see: Zhang, Y.-P.; Du, S.; Ma, Y.; Zhan, W.; Chen, W.; Yang, X.; Zhang, H. Structure-Unit-Based Total Synthesis of (−)-Sinulochmodin C. *Angew. Chem. Int. Ed*. **2023**, *136*, e202315481.

5) Anjaneyulu, A. S. R.; Venugopal, M. J. R. V.; Sarada, P.; Clardy, J.; Lobkovsky, E. Havellockate, A Novel Seco and Spiro Lactone Diterpenoid from the Indian Ocean Soft Coral Sinularia granosa. Tetrahedron Lett. 1998, 39, 139–142.

6) Mehta, G.; Kumaran, R. S. Studies Toward the Total Synthesis of Novel Marine Diterpene Havellockate. Construction of the Tetracyclic Core. *Tetrahedron Lett*. **2001**, 42, 8097–8100.

7) Beingessner, R. L.; Farand, J. A.; Barriault, L. Progress toward the Total Synthesis of (±)-Havellockate. *J. Org. Chem*. **2010**, 75, 6337–6346.

8) Anjaneyulu, A. R. On the Novel Cembranoids of the Soft Coral Sinularia Granosa of the Indian Ocean and Their Biogenesis. *Indian Journal of Chemistry,* **2000**, 39B, 530-535.

9) Blakemore, P. R. The Modified Julia Olefination: Alkene Synthesis via the Condensation of Metallated Heteroarylalkylsulfones with Carbonyl Compounds. *J. Chem. Soc., Perkin Trans.* 1 **2002**, No. 23, 2563–2585.

10) Brill, Z. G.; Grover, H. K.; Maimone, T. J. Enantioselective Synthesis of an Ophiobolin Sesterterpene via a Programmed Radical Cascade. *Science* **2016**, 352 (6289), 1078–1082.

11) Bauta, W.; Booth, J.; Bos, M. E.; DeLuca, M.; Diorazio, L.; Donohoe, T.; Magnus, N.; Magnus, P.; Mendoza, J.; Pye, P.; Tarrant, J.; Thom, S.; Ujjainwalla, F. New Strategy for the Synthesis of the Taxane Diterpenes: Formation of the BC-Rings of Taxol via a [5+2]-Pyrylium Ylide-Alkene Cyclization, Ring Expansion Strategy. *Tetrahedron Letters* **1995**, 36 (30), 5327–5330.

12) Evans, D. A.; Ennis, M. D.; Mathre, D. J. Asymmetric Alkylation Reactions of Chiral Imide Enolates. A Practical Approach to the Enantioselective Synthesis of a-Substituted Carboxylic Acid Derivatives. *J. Am. Chem. Soc*. **1982**, 104 (6), 1737–1739.

13) Pospíšil, J.; Markó, I. E. Efficient and Stereoselective Synthesis of Allylic Ethers and Alcohols. *Org. Lett.* **2006**, 8 (26), 5983–5986.

14) Neises, B.; Steglich, W. Simple Method for the Esterification of Carboxylic Acids. *Angew. Chem., Int. Ed. Engl*. **1978,** 17, 522−524.

15) (a) Brill, Z. G.; Grover, H. K.; Maimone, T. J. Enantioselective Synthesis of an Ophiobolin Sesterterpene via a Programmed Radical Cascade. *Science* **2016**, 352 (6289), 1078–1082. (b) Patra, T.; Agasti, S.; Akanksha; Maiti, D. Nickel-Catalyzed Decyanation of Inert Carbon–Cyano Bonds. *Chem. Comm.* **2013**, 49 (1), 69–71. (c) (1) Fraunhoffer, K. J.; White, M. C. Syn-1,2-Amino Alcohols via Diastereoselective Allylic C−H Amination. *J. Am. Chem. Soc*. **2007**, 129 (23), 7274–7276. d) (1) Nakayama, Y.; Maser, M. R.; Okita, T.; Dubrovskiy, A. V.; Campbell, T. L.; Reisman, S. E. Total Synthesis of Ritterazine B. *J. Am. Chem. Soc*. **2021**, 143 (11), 4187–4192.

16) Additions with organocerium, chromium, indium, and alkyl and vinyl organozinc nucleophiles were attempted. In all cases no addition product was observed.

17) (a) Lombardo, M.; Morganti, S.; Trombini, C. 3-Bromopropenyl Esters in Organic Synthesis: Indium- and Zinc-Mediated Entries to Alk-1-ene-3,4-diols. *J. Org. Chem*. **2003**, *68*, 997–1006. (b) Lombardo, M.; Morganti, S.; d'Ambrosio, F.; Trombini, C. 3-Bromo-propenyl Acetate in Organic Synthesis. The Zinc-Promoted a-Hydroxyallylation of Ketones. *Tetrahedron Lett.* **2003**, 2823–2826.

18) This mixture has been tentatively characterized as a 1:1 mixture of branched and linear allylation products. See SI for de-tails.

19) Mejuch, T.; Gilboa, N.; Gayon, E.; Wang, H.; Houk, K. N.; Marek, I. Axial Preferences in Allylation Reactions via the Zimmerman–Traxler Transition State. *Acc. Chem. Res.* **2013**, *46*, 1659–1669.

20) (a) Wuts, P. G. M.; Greene, T. W. *Greene's Protective Groups in Organic Synthesis, 5th ed*.; John Wiley & Sons, Ltd: Hoboken, NJ, 2014; pp 752. (b) Chandrasekaran, S.; Kluge, A. F.; Edwards, J. A. Studies in b-Lactams. 6. Synthesis of Substituted b-Lactams by Addition of Nitromethane to 6-Oxopenicillanates and 7-Oxocephalosporanates. *J. Org. Chem.* **1977***, 42* (24), 3972–3974.

21) Xie, X.; Zhang, X.; Yang, H.; Ji, X.; Li, J.; Ding, S. Iridium-Catalyzed Hydrosilylation of Unactivated Alkenes: Scope and Application to Late-Stage Functionalization. *J. Org. Chem.* **2019**, *84* (2), 1085–1093.

22) Triol 26 and tetrol 27 were each isolated with an impurity that were evident in their NMR spectra. See SI for details.

23) Hoover, J. M.; Stahl, S. S. Highly Practical Copper(I)/TEMPO Catalyst System for Chemoselective Aerobic Oxidation of Primary Alcohols. *J. Am. Chem. Soc.* **2011**, *133* (42), 16901–16910.

24) Xie, X.; Stahl, S. S. Efficient and Selective Cu/Nitroxyl-Catalyzed Methods for Aerobic Oxidative Lactonization of Diols. *J. Am. Chem. Soc.* **2015**, *137* (11), 3767–3770.

APPENDIX 1

Spectra Relevant to Chapter 1:

Asymmetric Total Synthesis of Havellockate

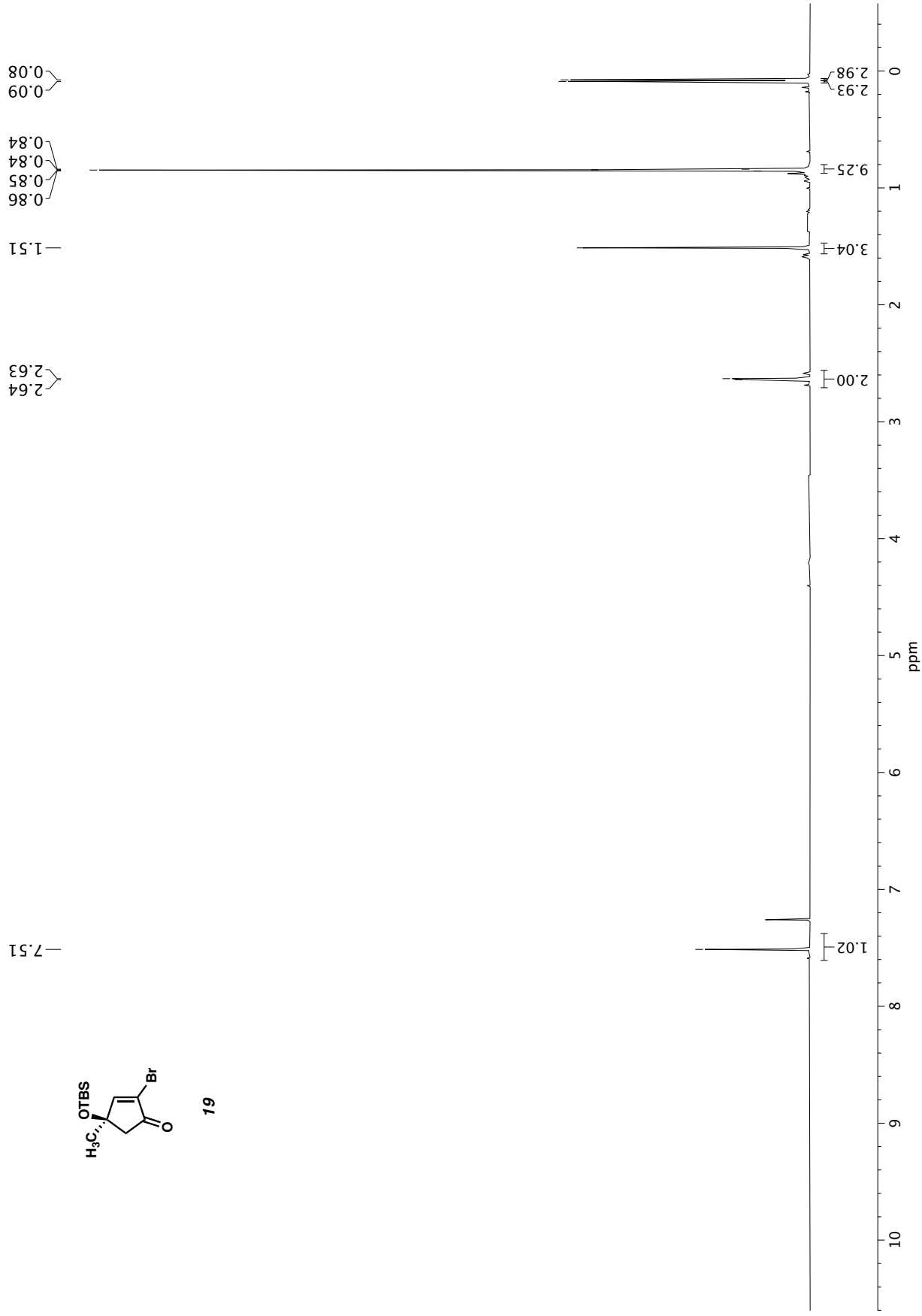

Figure A1.1. *^1H NMR (400 MHz, $CDCl_3$) of compound **19**.*

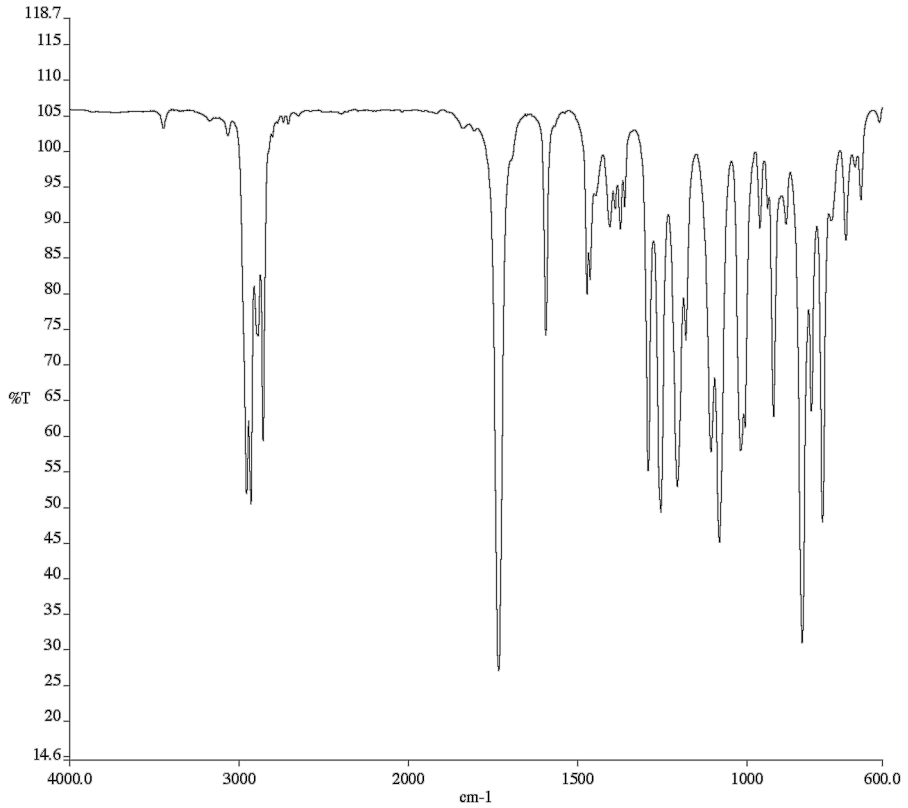

Figure A1.2. *Infrared spectrum (Thin Film, NaCl) of compound* ***19***.

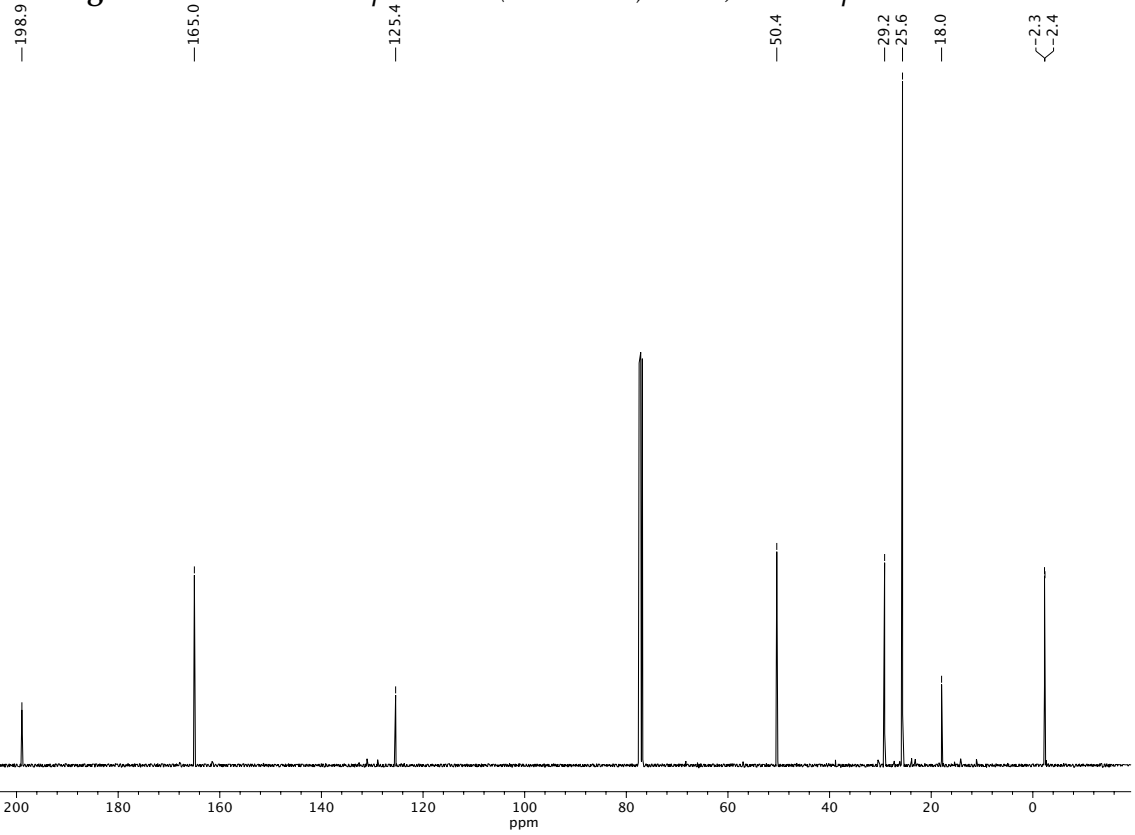

Figure A1.3. *^{13}C NMR (100 MHz, $CDCl_3$) of compound* ***19***.

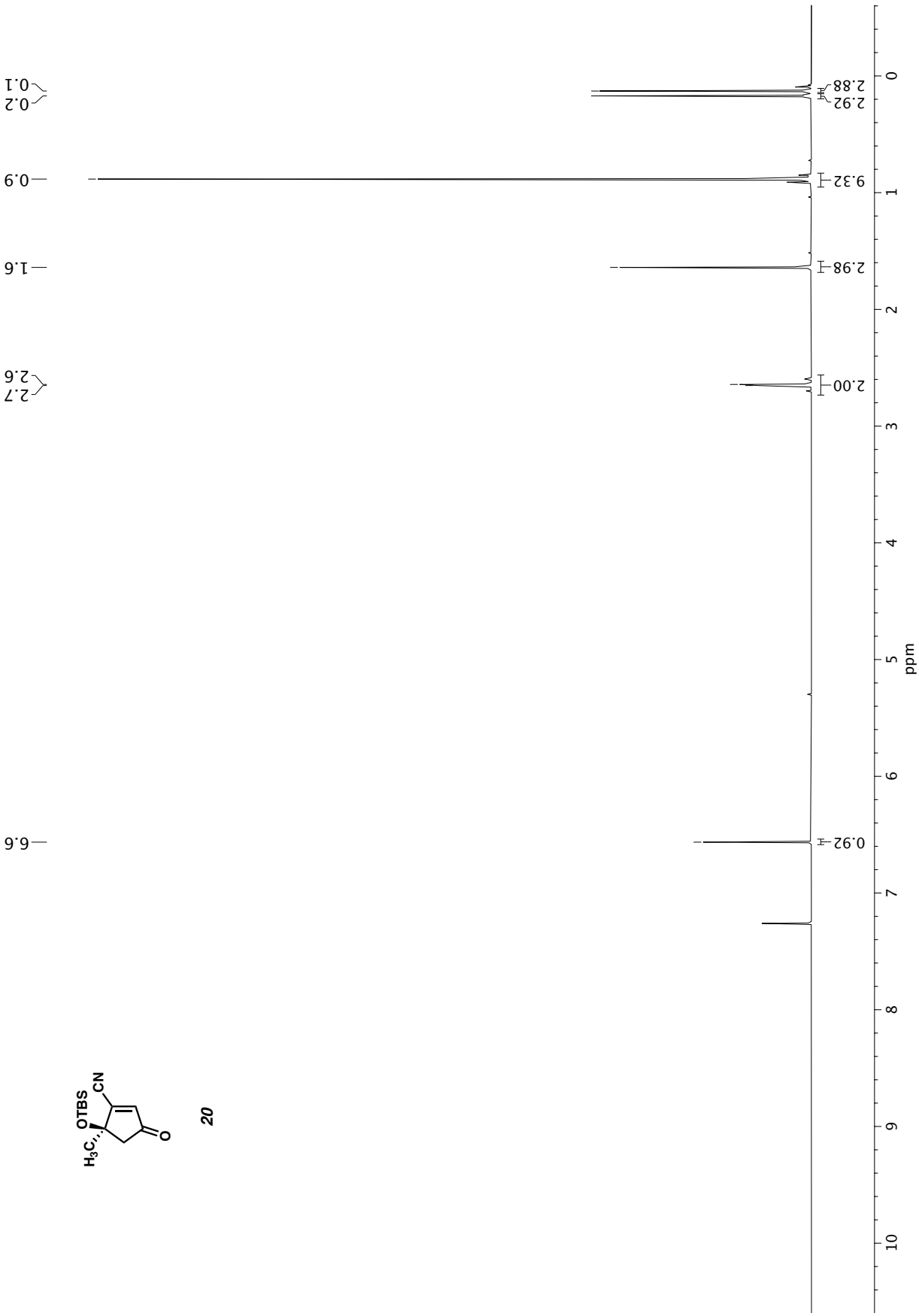

Figure A1.4. *^1H NMR (400 MHz, $CDCl_3$) of compound* ***20****.*

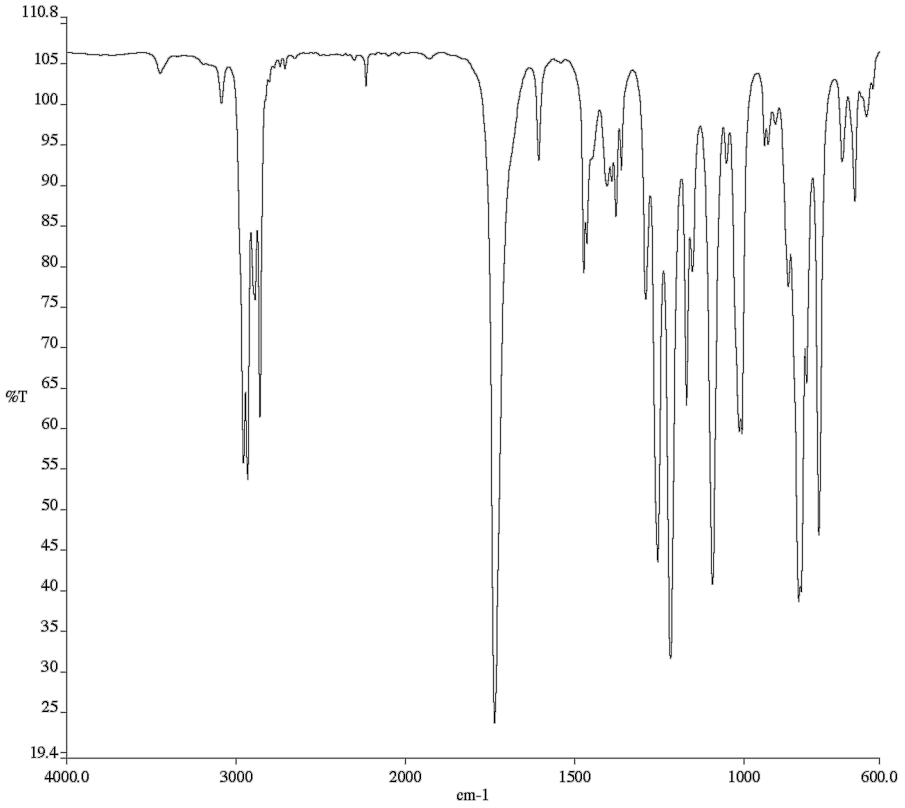

Figure A1.5. *Infrared spectrum (Thin Film, NaCl) of compound* ***20****.*

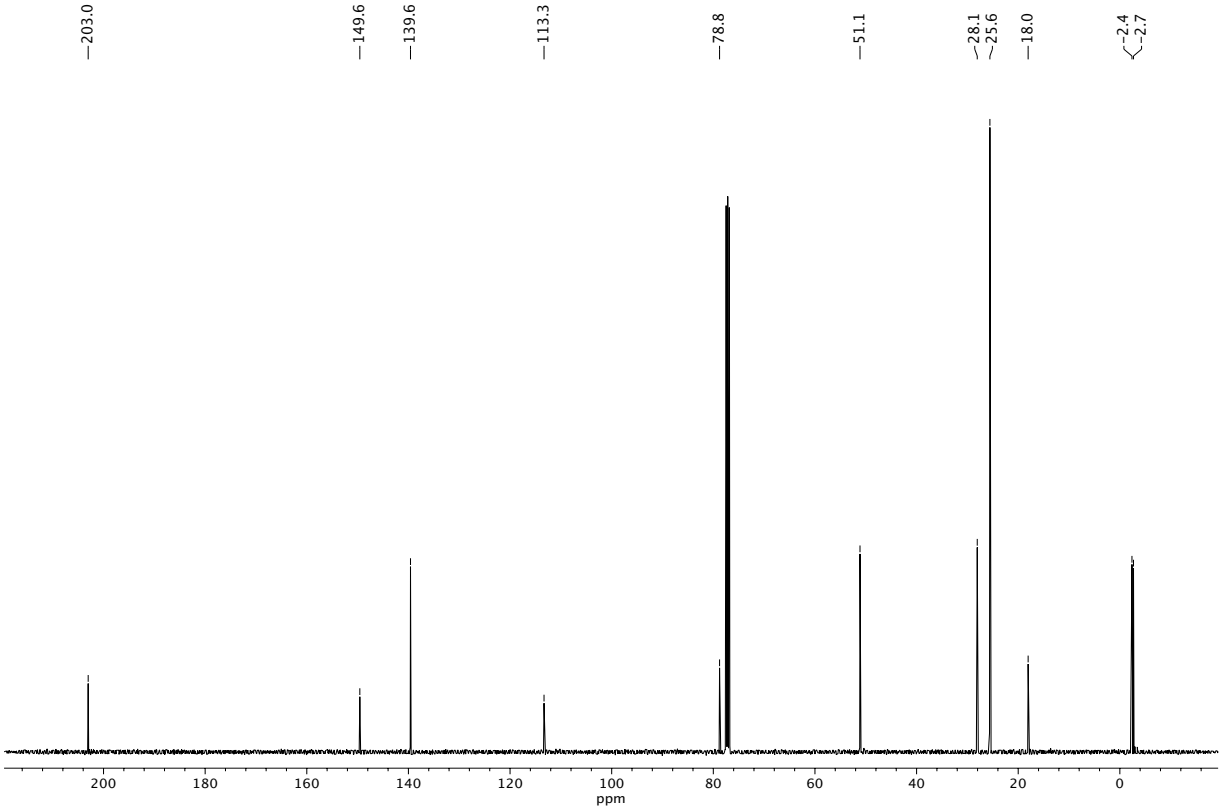

Figure A1.6. *^{13}C NMR (100 MHz, $CDCl_3$) of compound* ***20****.*

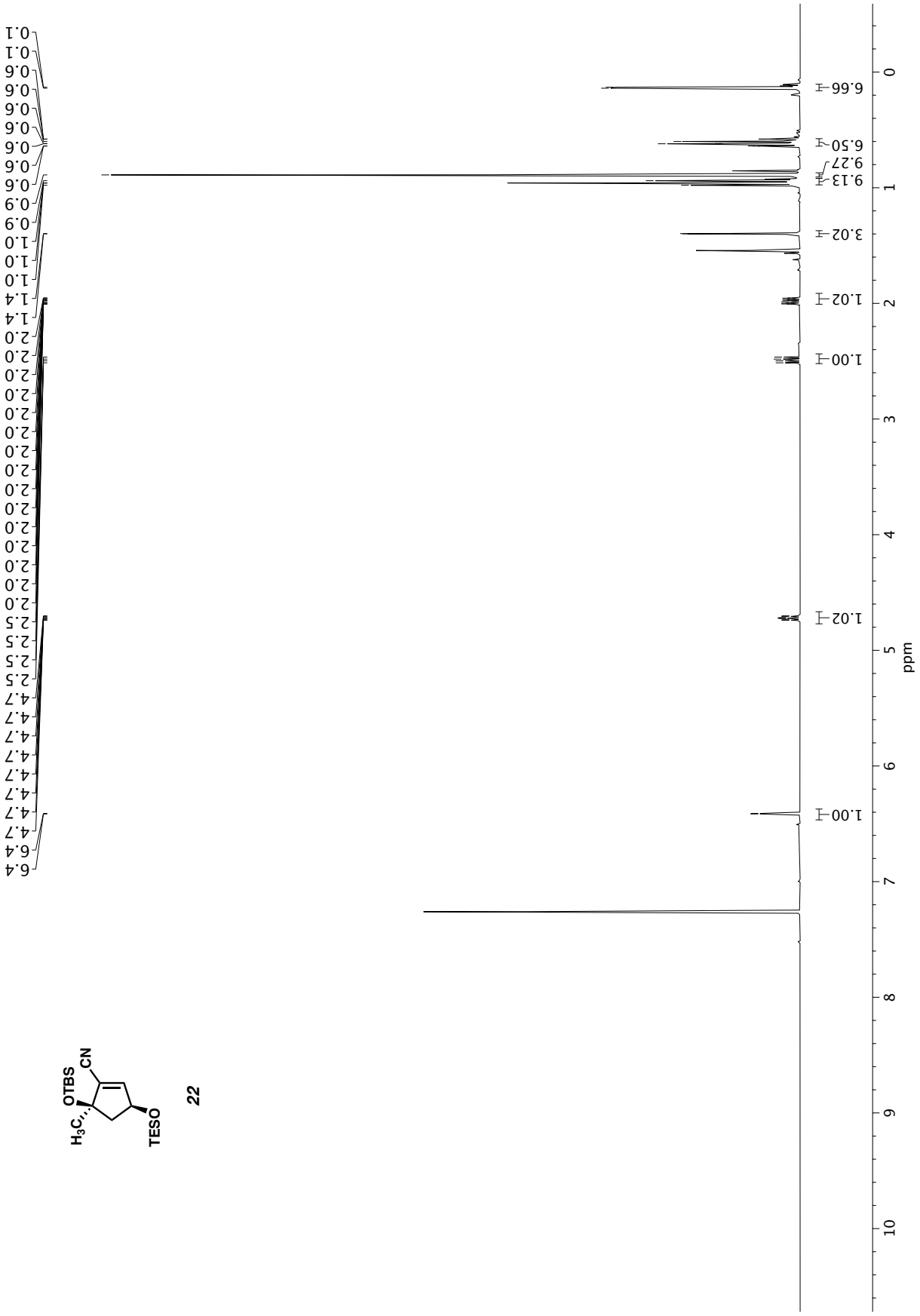
6.66
6.50
9.27
9.13
3.02
1.02
1.00
1.02
1.00
ppm
0 1 2 3 4 5 6 7 8 9 10
6.4 4.7 4.7 4.7 4.7 4.7 4.7 4.7 4.7 2.5 2.5 2.5 2.0 2.0 2.0 2.0 2.0 2.0 2.0 2.0 2.0 2.0 2.0 2.0 2.0 1.4 1.4 1.0 1.0 1.0 0.9 0.9 0.6 0.6 0.6 0.6 0.6 0.6 0.6 0.1 0.1

OTBS
CN
H3C
TESO

22

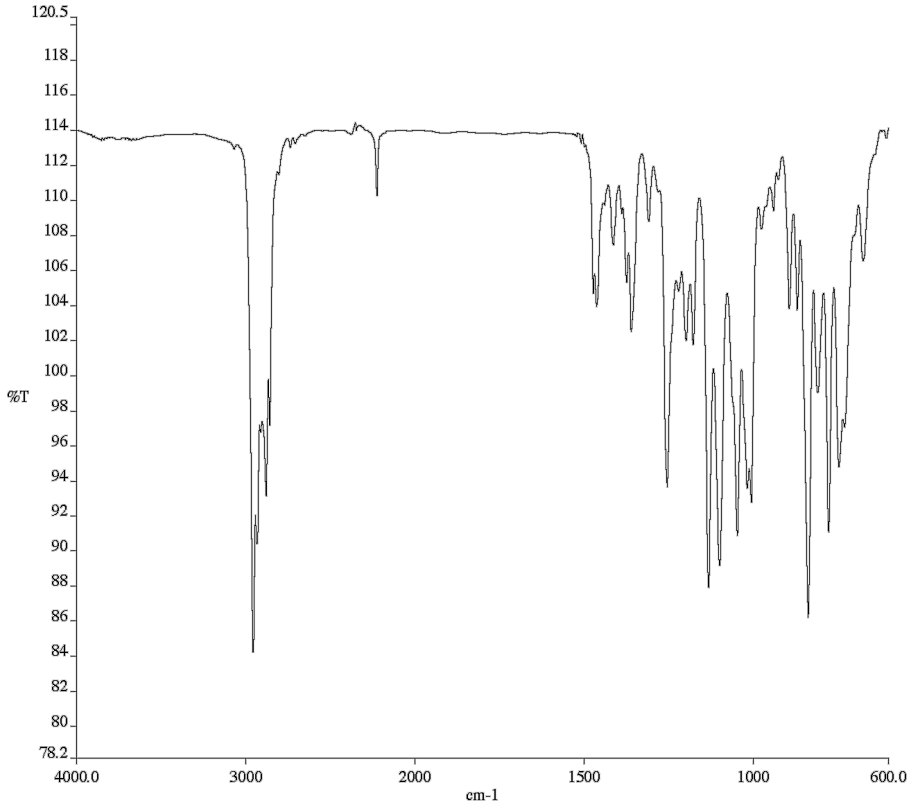

Figure A1.8. *Infrared spectrum (Thin Film, NaCl) of compound* ***22***.

Figure A1.7. *^1H NMR (400 MHz, $CDCl_3$) of compound* ***22***.

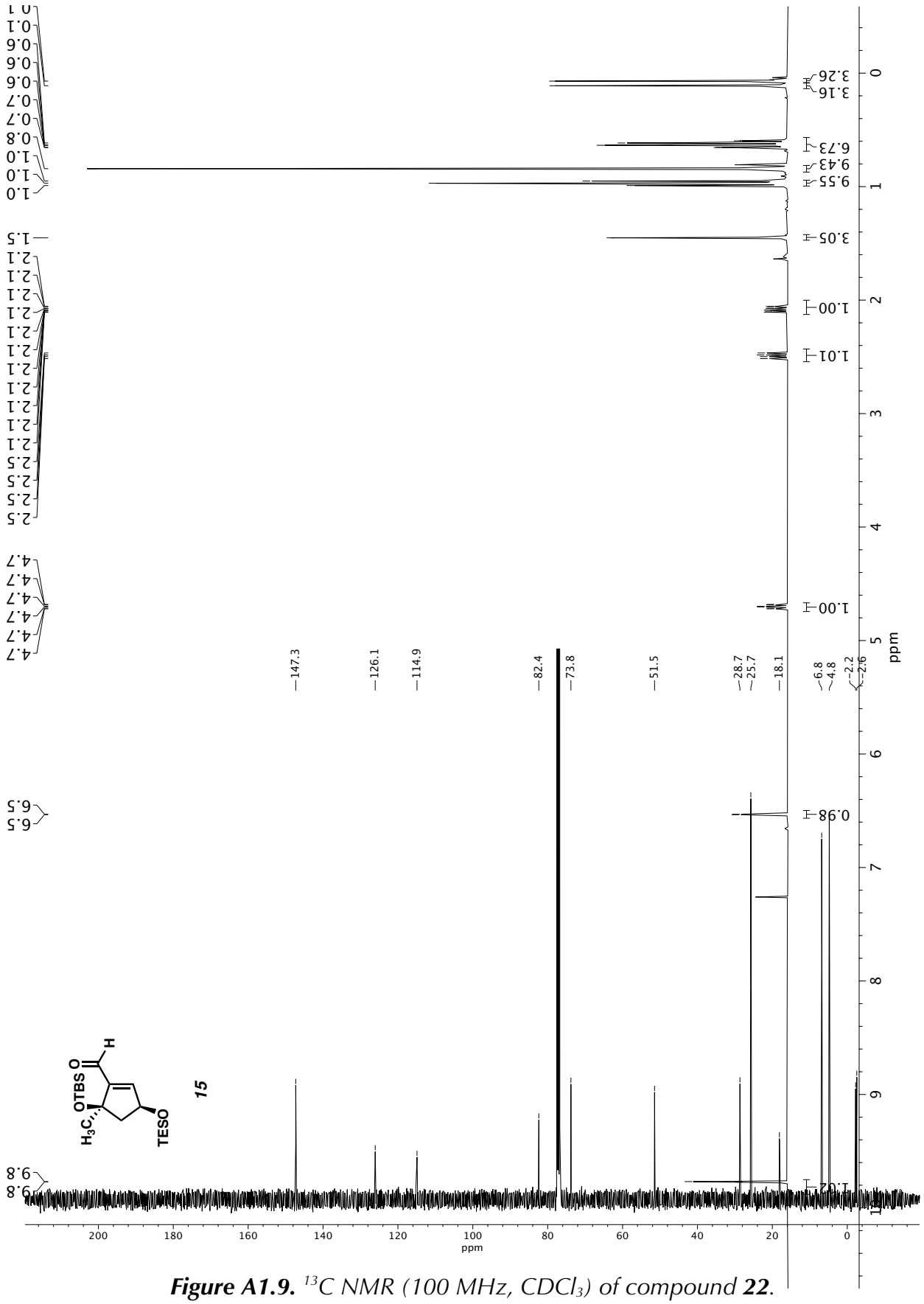

Figure A1.9. *^{13}C NMR (100 MHz, $CDCl_3$) of compound* ***22****.*

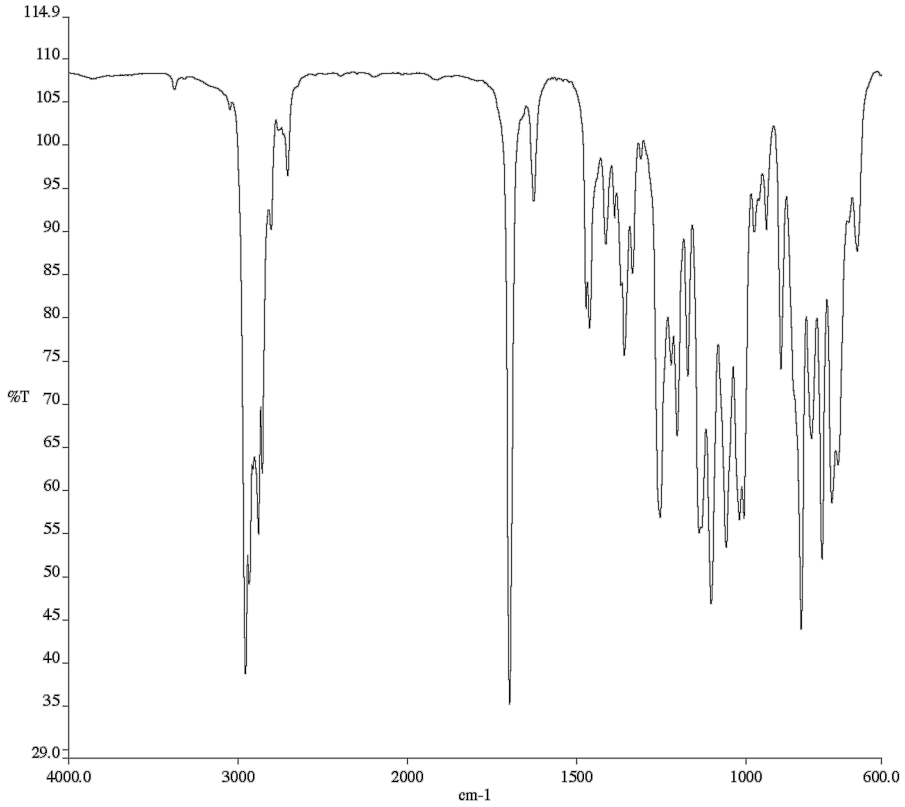

Figure A1.11. *Infrared spectrum (Thin Film, NaCl) of compound* ***15****.*

Figure A1.10. *^1H NMR (400 MHz, $CDCl_3$) of compound* ***15****.*

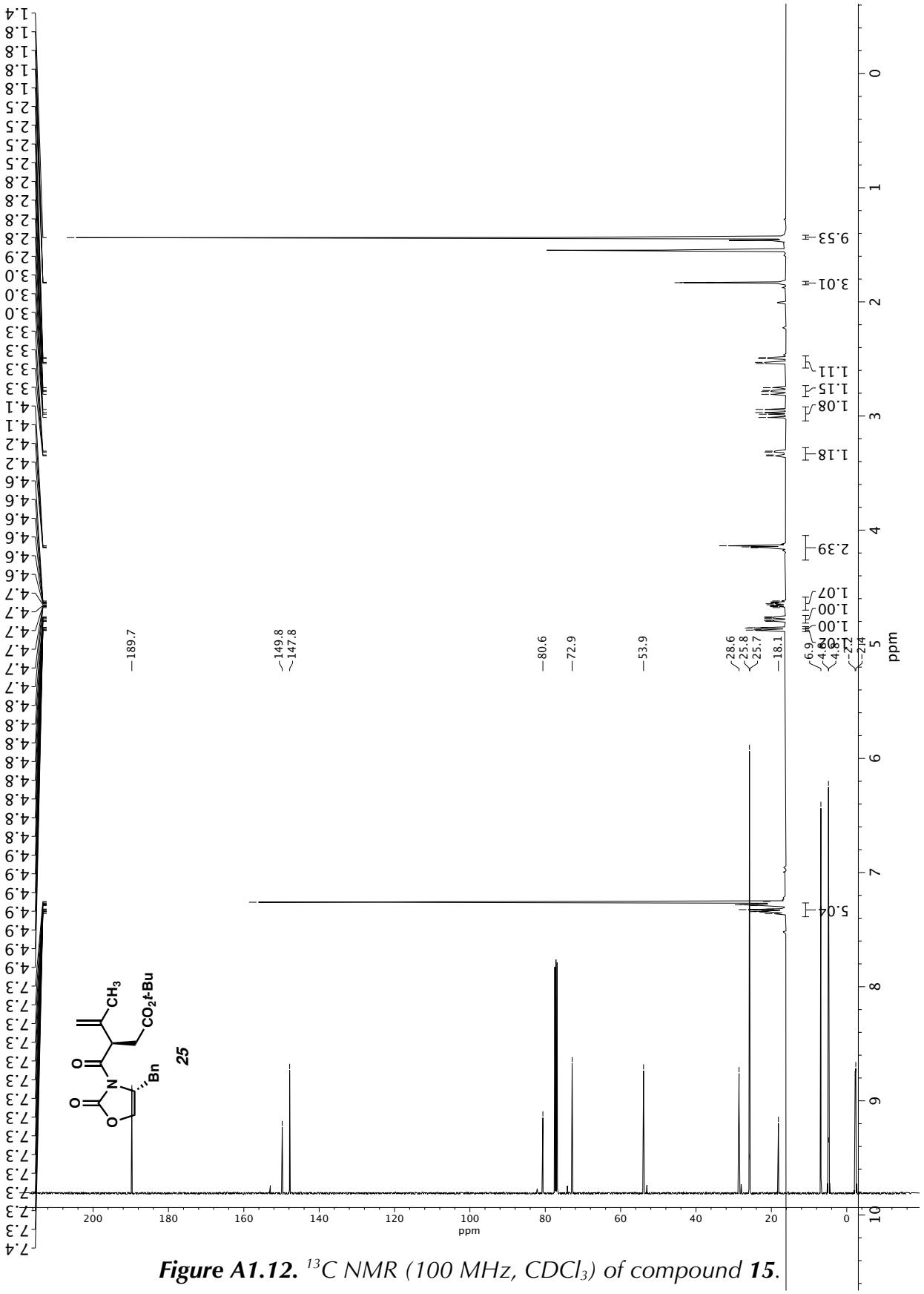

Figure A1.12. *^{13}C NMR (100 MHz, $CDCl_3$) of compound **15**.*

Figure A1.13. *^{1}H NMR (400 MHz, $CDCl_3$) of compound* ***25***.

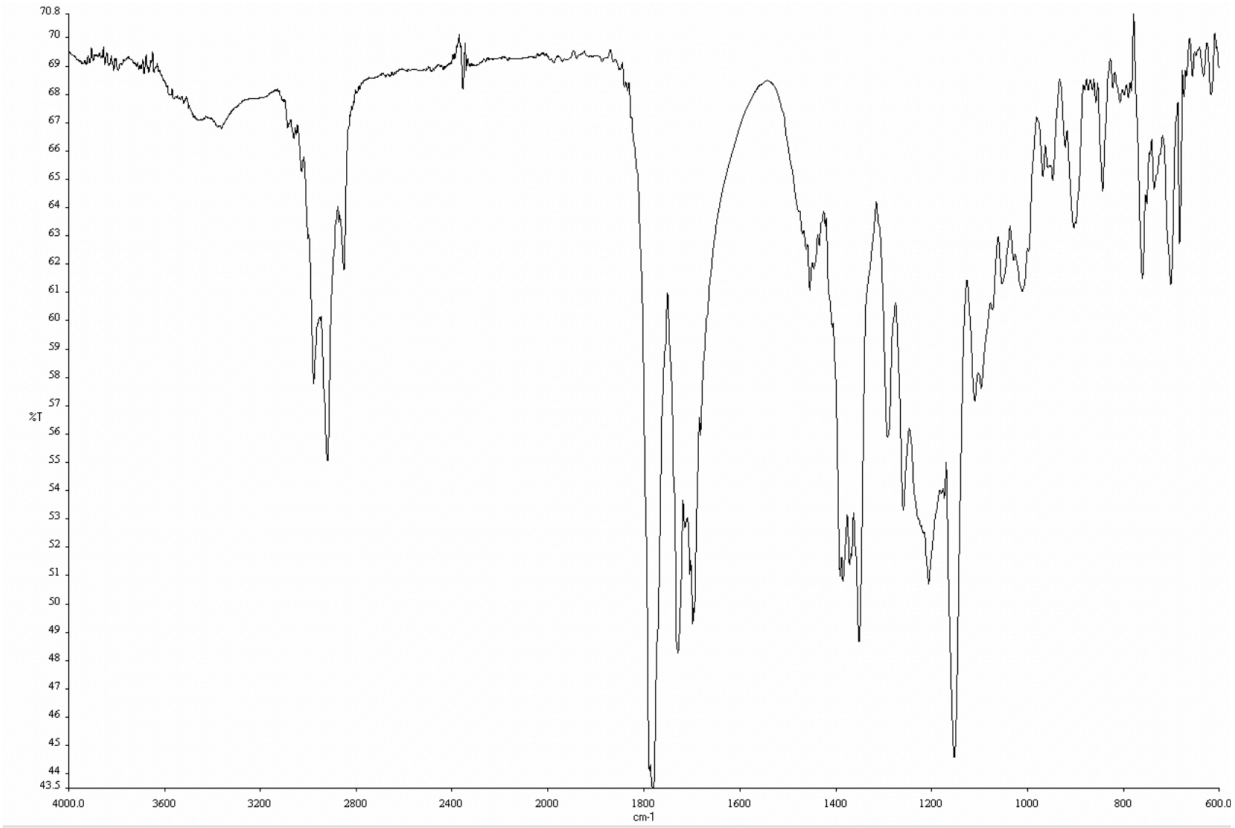

Figure A1.14. *Infrared spectrum (Thin Film, NaCl) of compound* ***25****.*

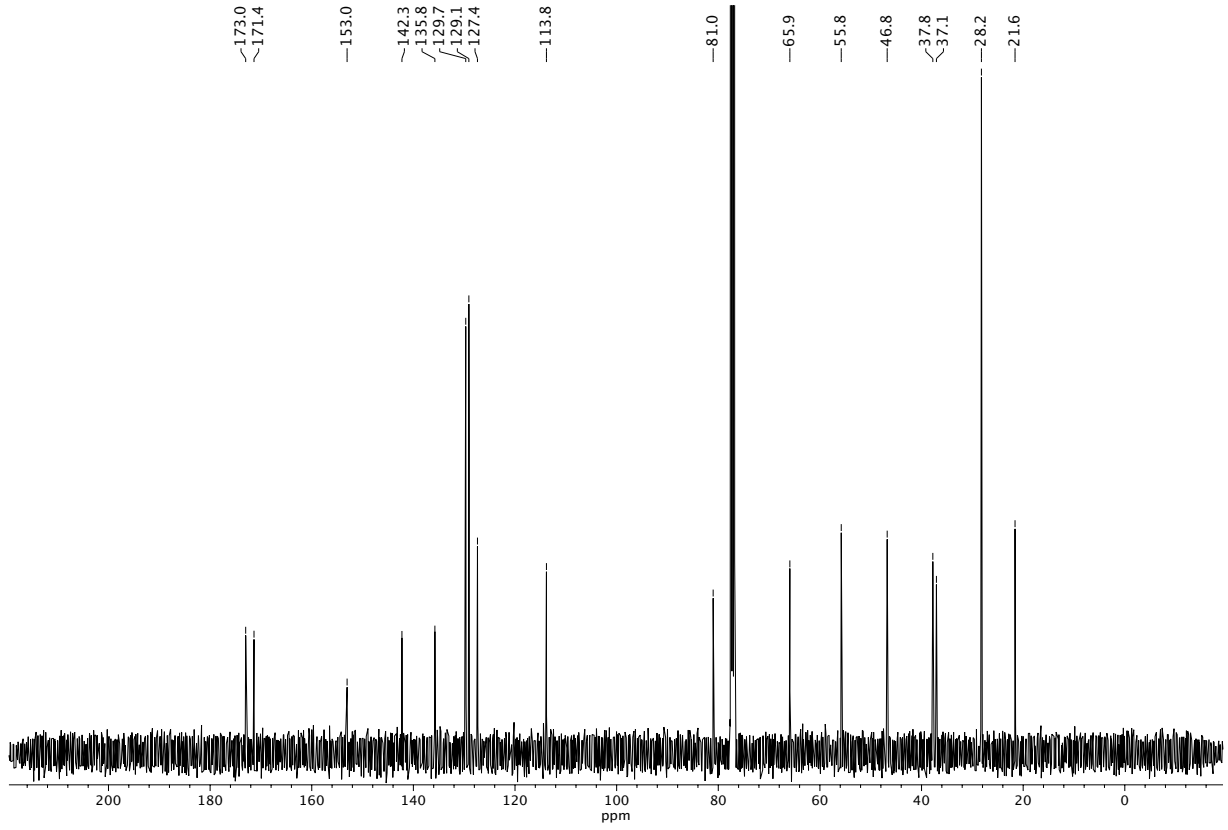

Figure A1.15. *^{13}C NMR (100 MHz, $CDCl_3$) of compound* ***25****.*

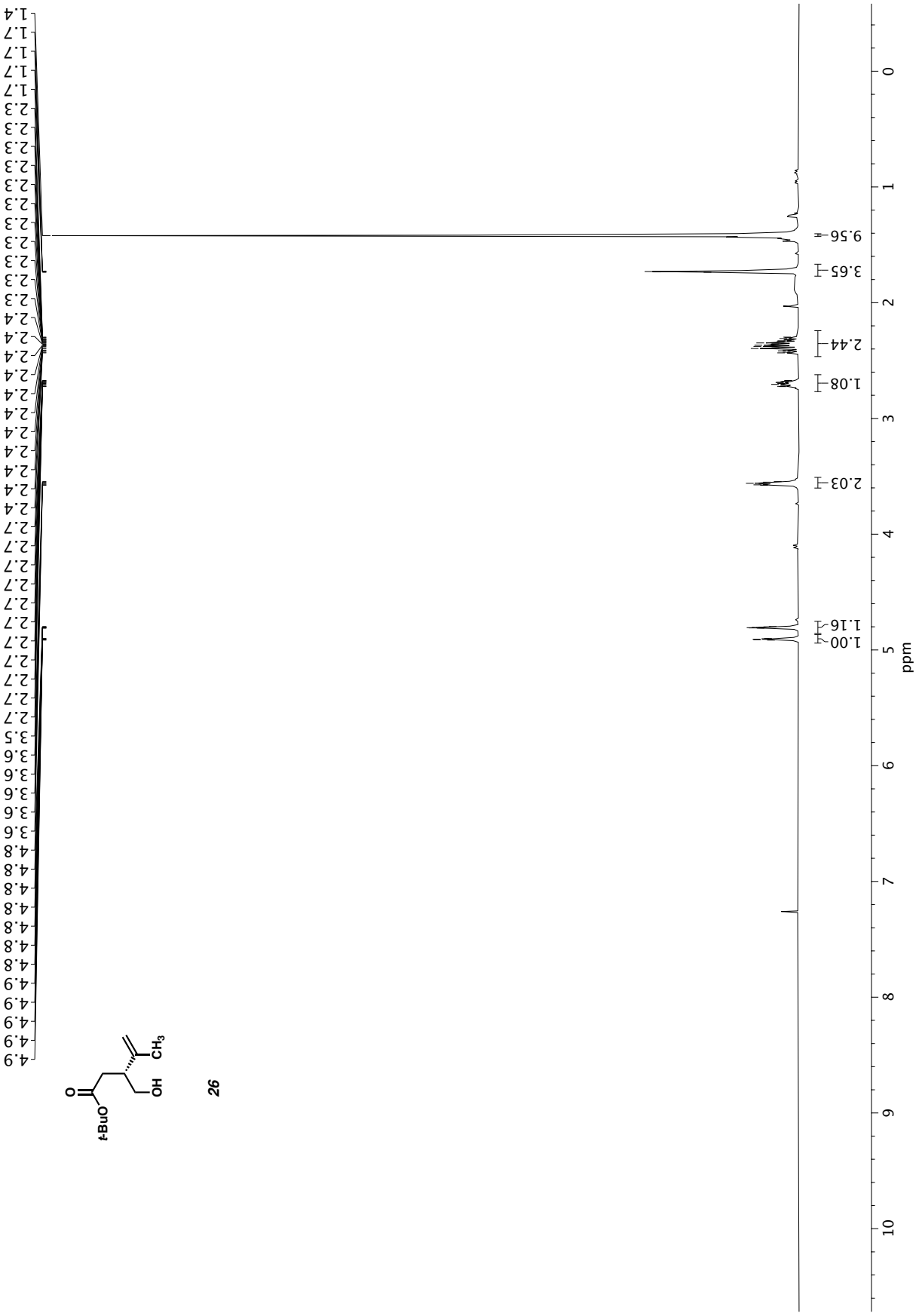

Figure A1.16. *^1H NMR (400 MHz, $CDCl_3$) of compound* ***26****.*

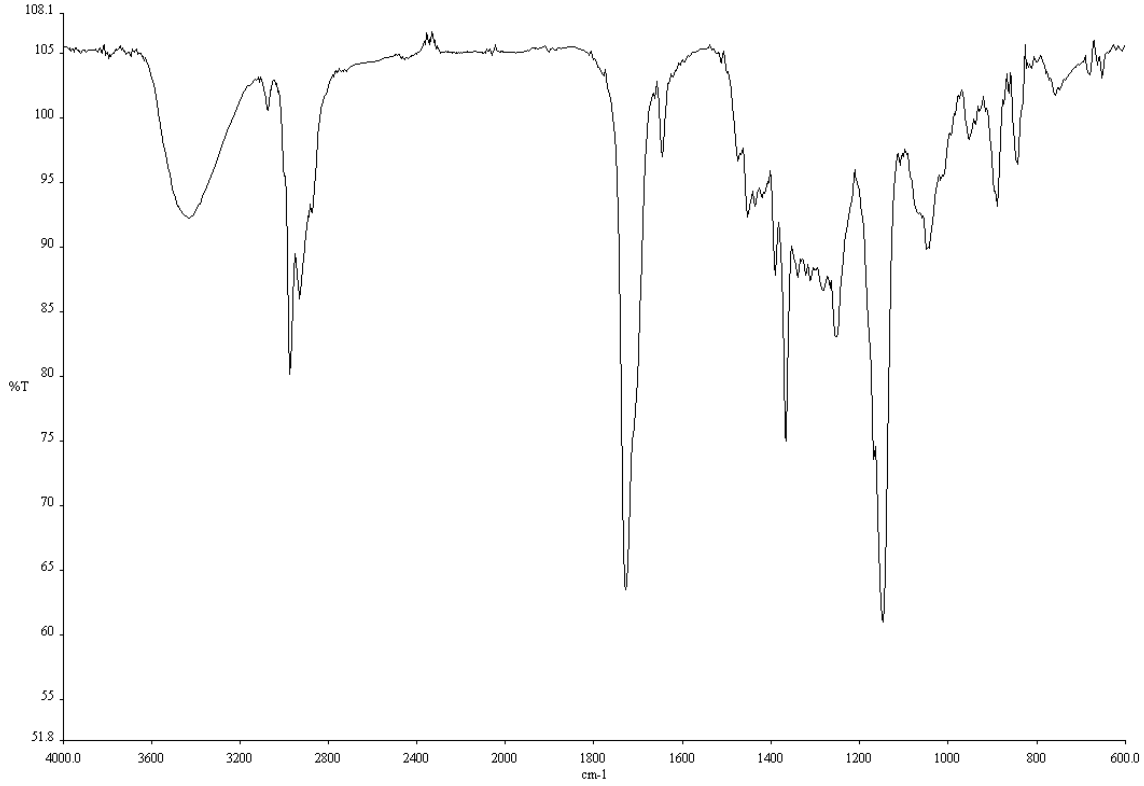

Figure A1.17. *Infrared spectrum (Thin Film, NaCl) of compound* ***26****.*

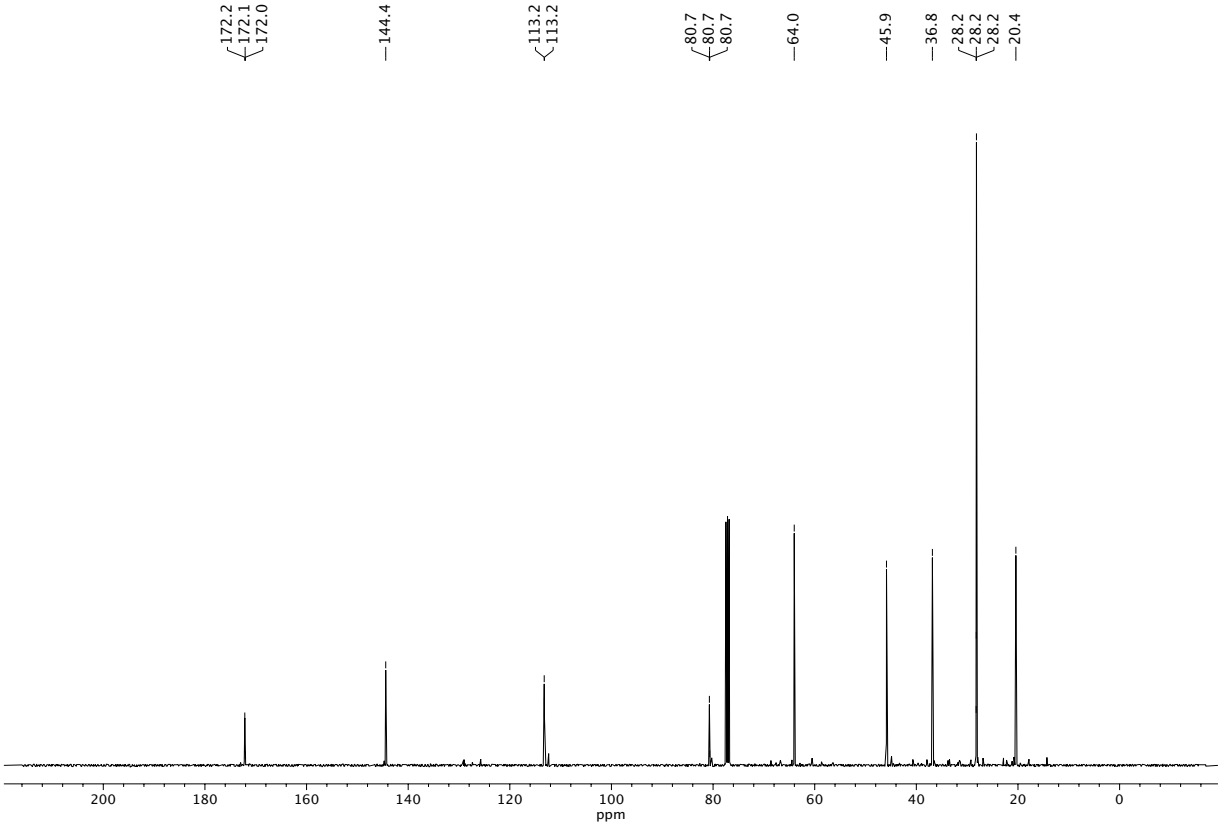

Figure A1.18. *^{13}C NMR (100 MHz, $CDCl_3$) of compound* ***26****.*

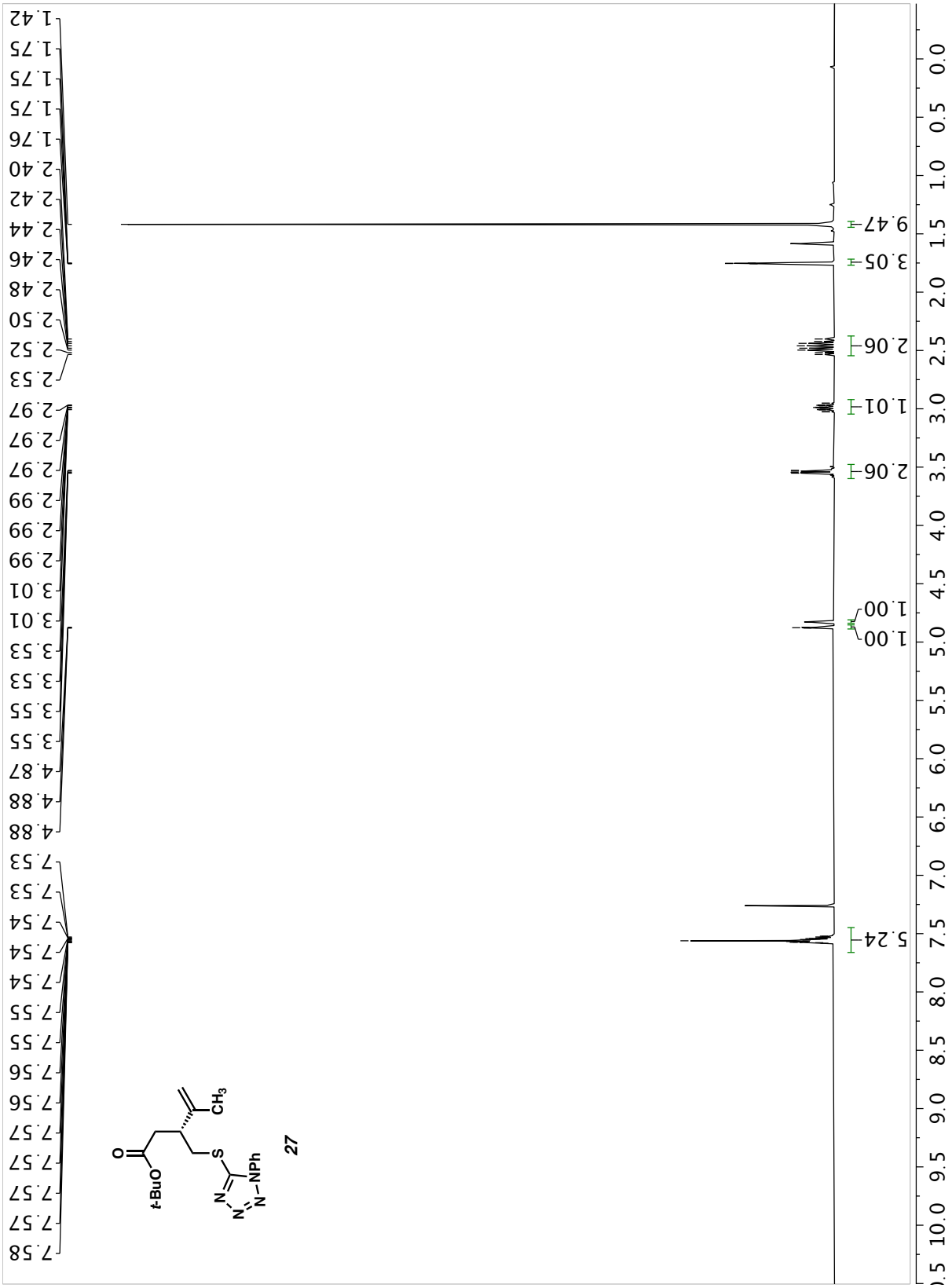

Figure A1.19. *^1H NMR (400 MHz, $CDCl_3$) of compound* ***27****.*

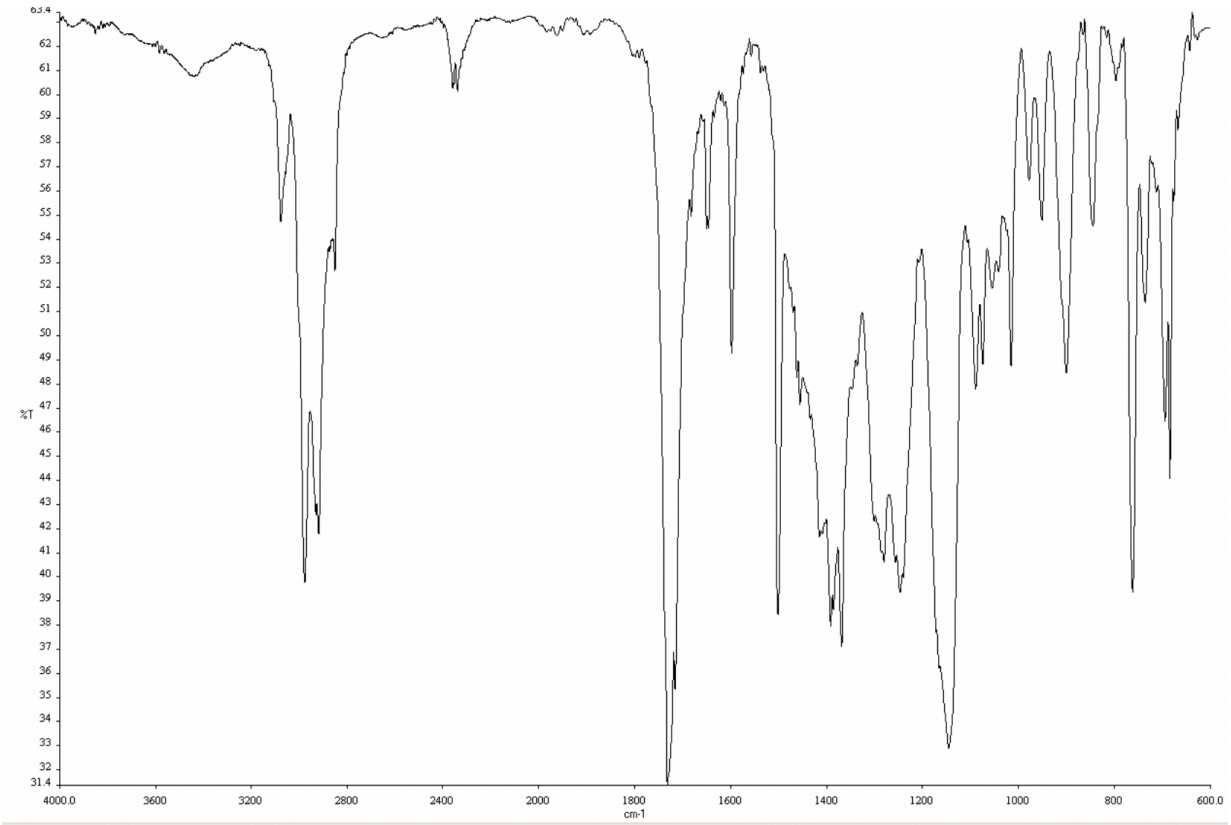

Figure A1.20. *Infrared spectrum (Thin Film, NaCl) of compound* ***27****.*

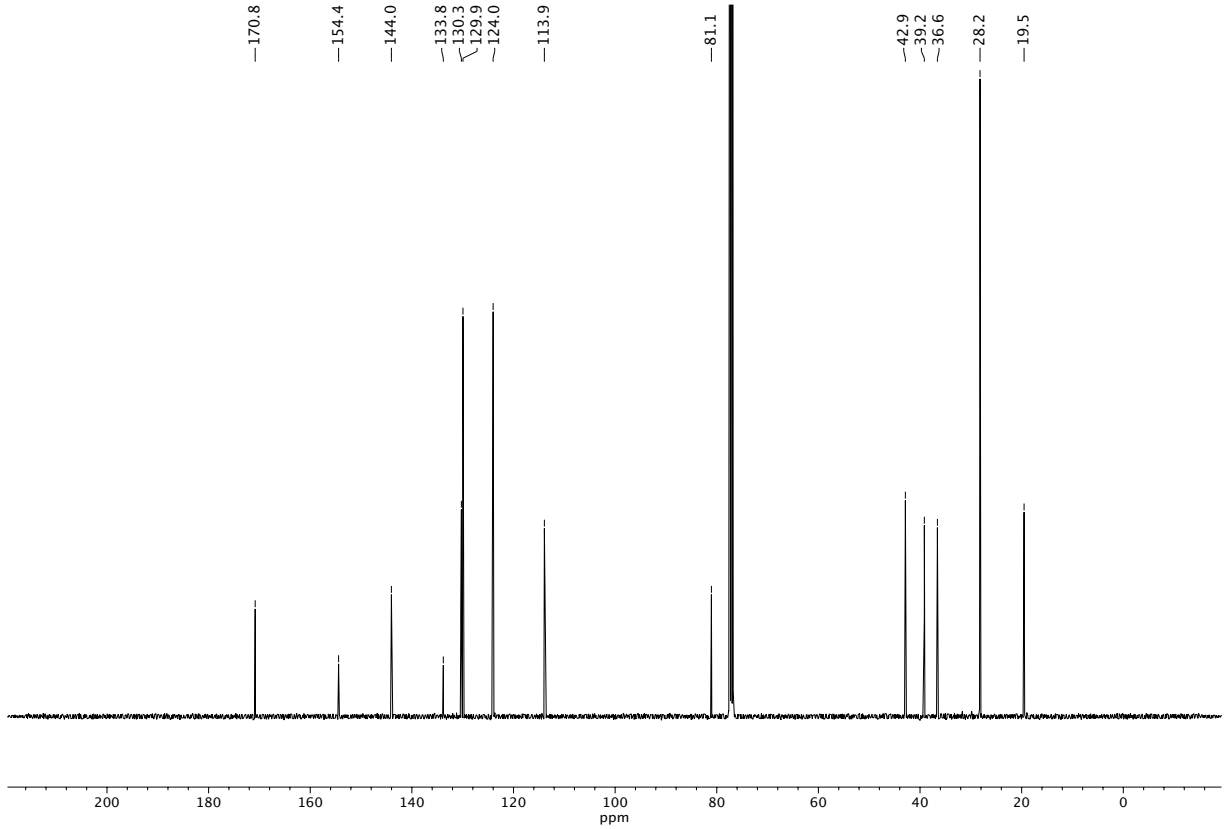

Figure A1.21. *^{13}C NMR (100 MHz, $CDCl_3$) of compound* ***28****.*

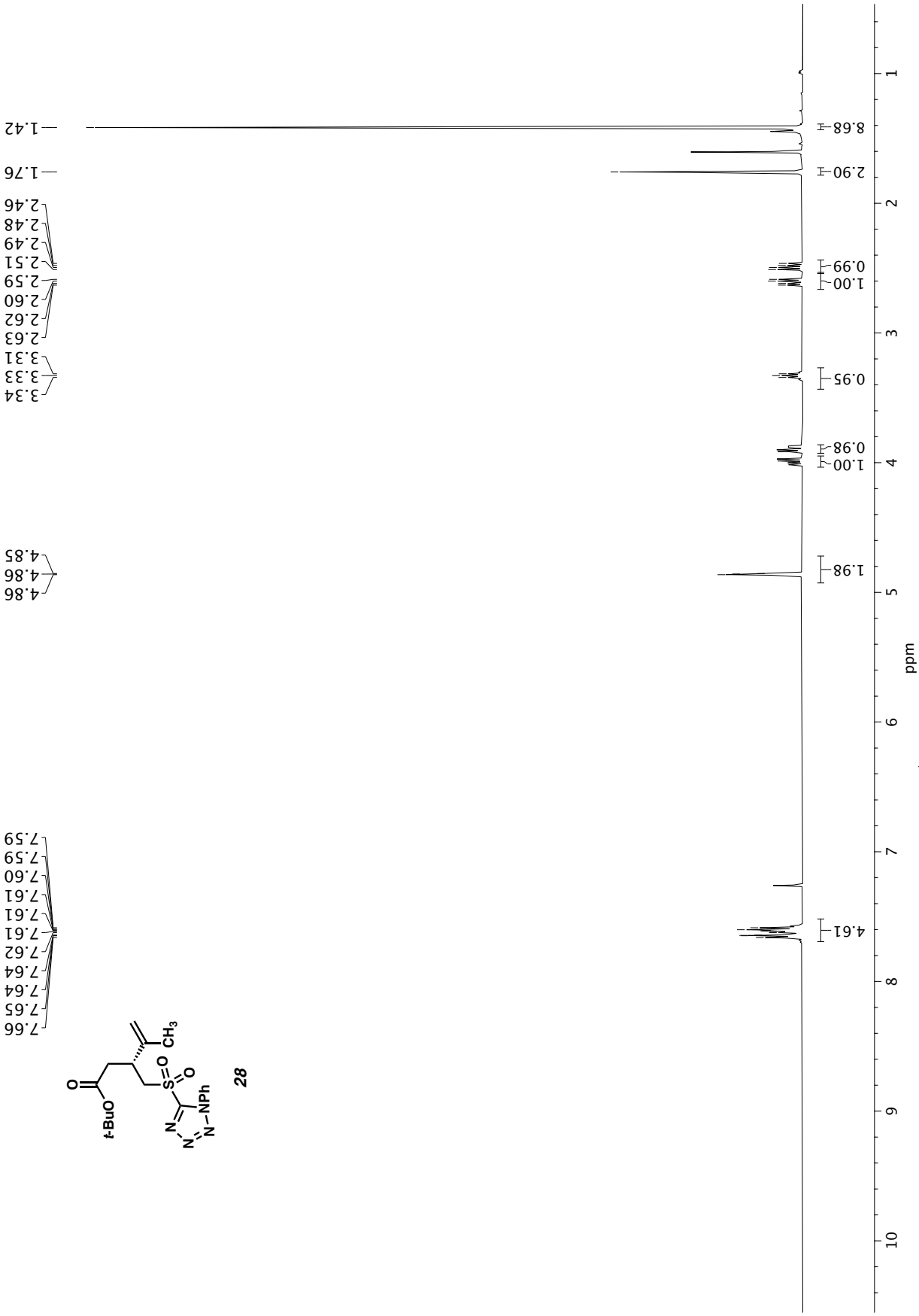

Figure A1.22. *^1H NMR (500 MHz, $CDCl_3$) of compound* ***28****.*

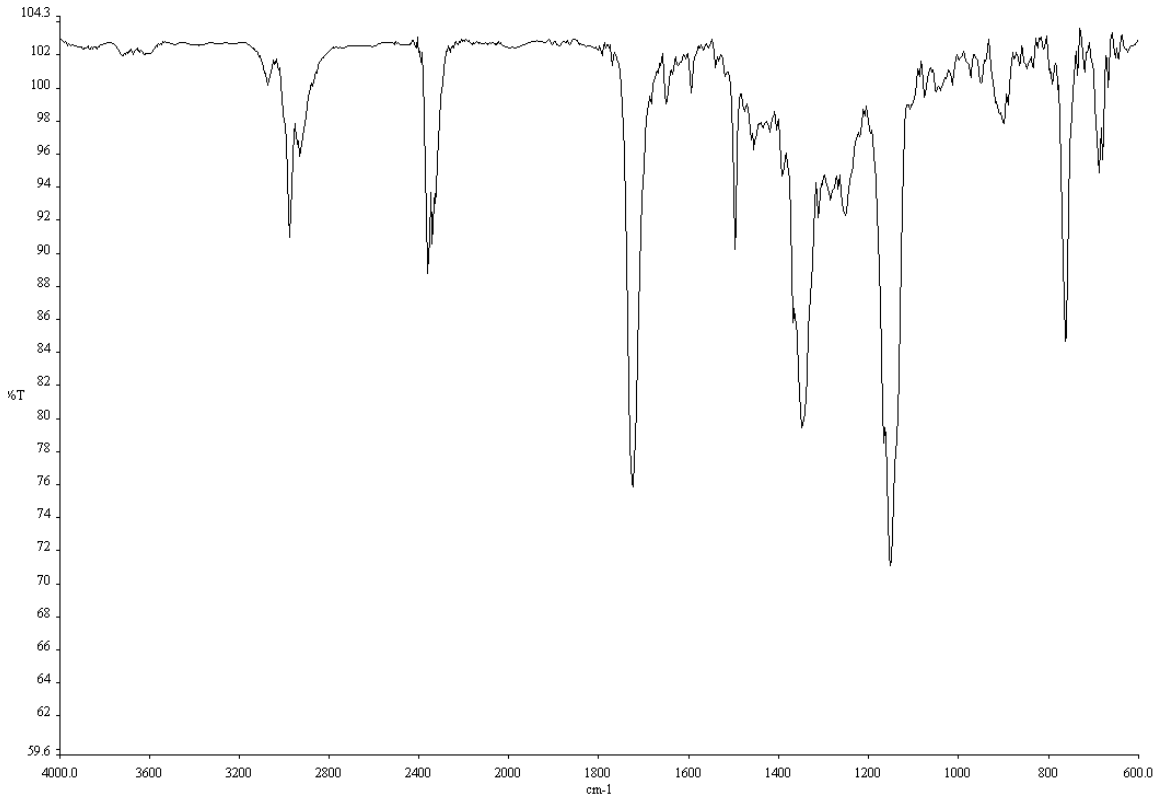

Figure A1.23. *Infrared spectrum (Thin Film, NaCl) of compound* ***28****.*

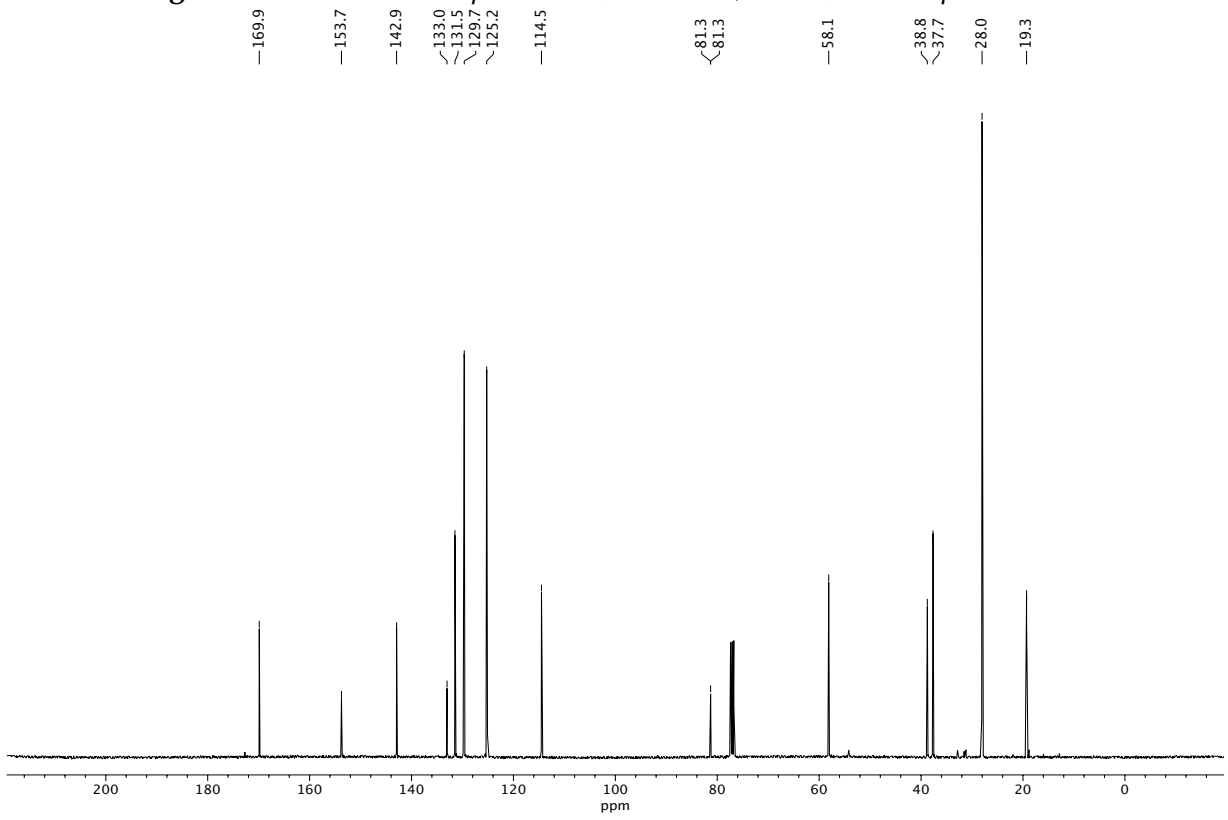

Figure A1.24. *^{13}C NMR (100 MHz, $CDCl_3$) of compound* ***28****.*

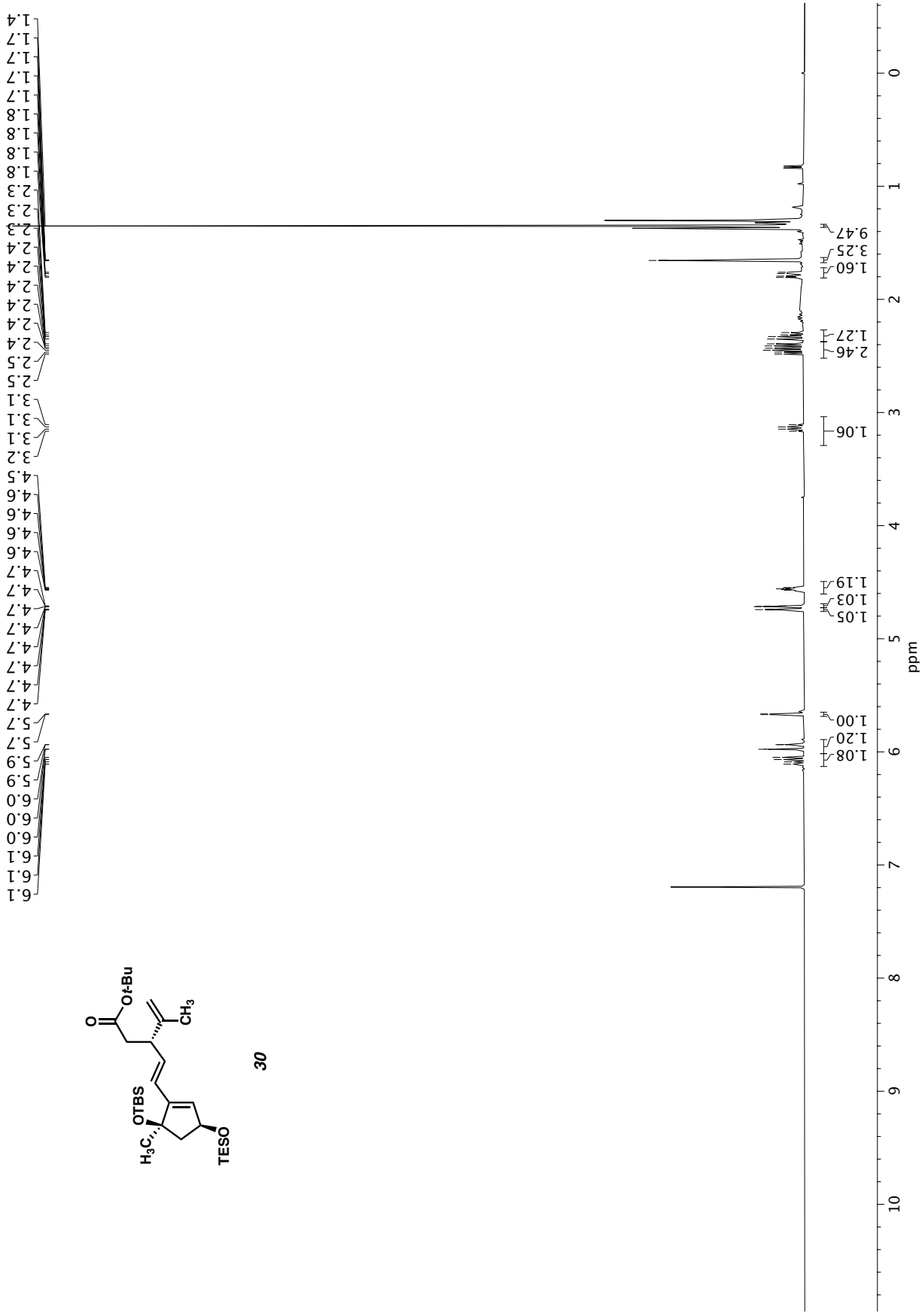

Figure A1.25. *^1H NMR (400 MHz, $CDCl_3$) of compound **30**.*

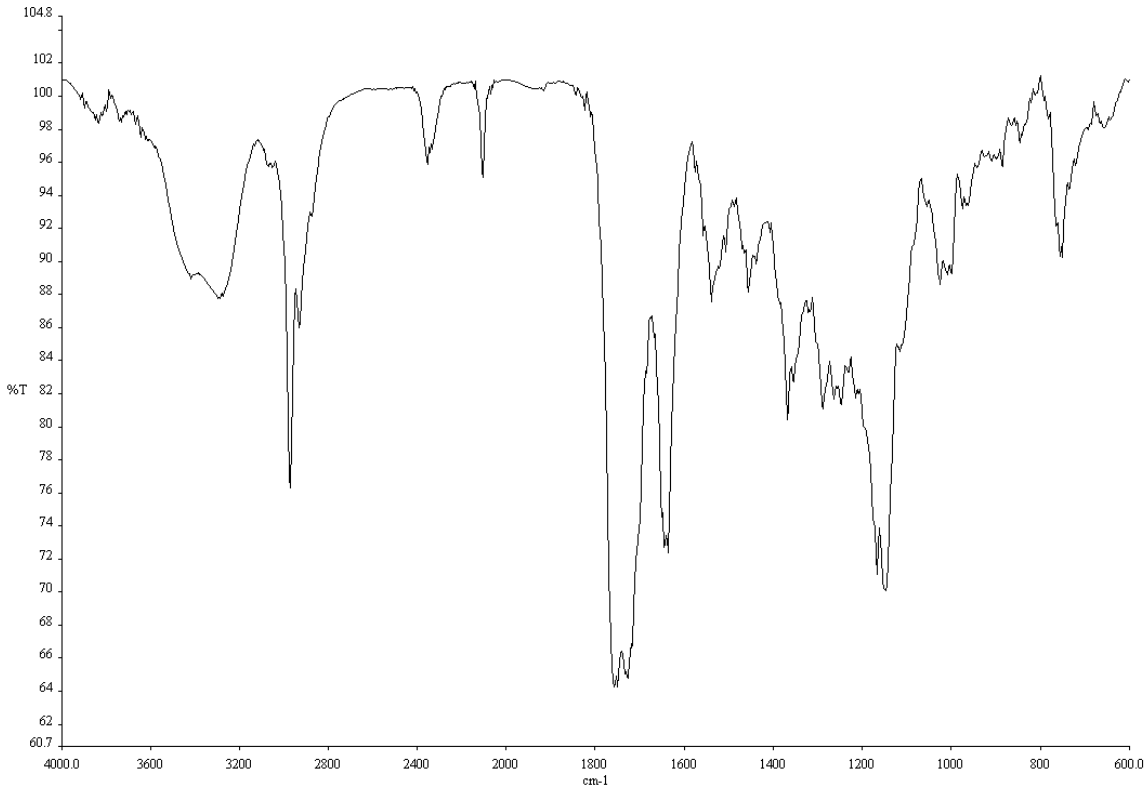

Figure A1.26. *Infrared spectrum (Thin Film, NaCl) of compound* ***30****.*

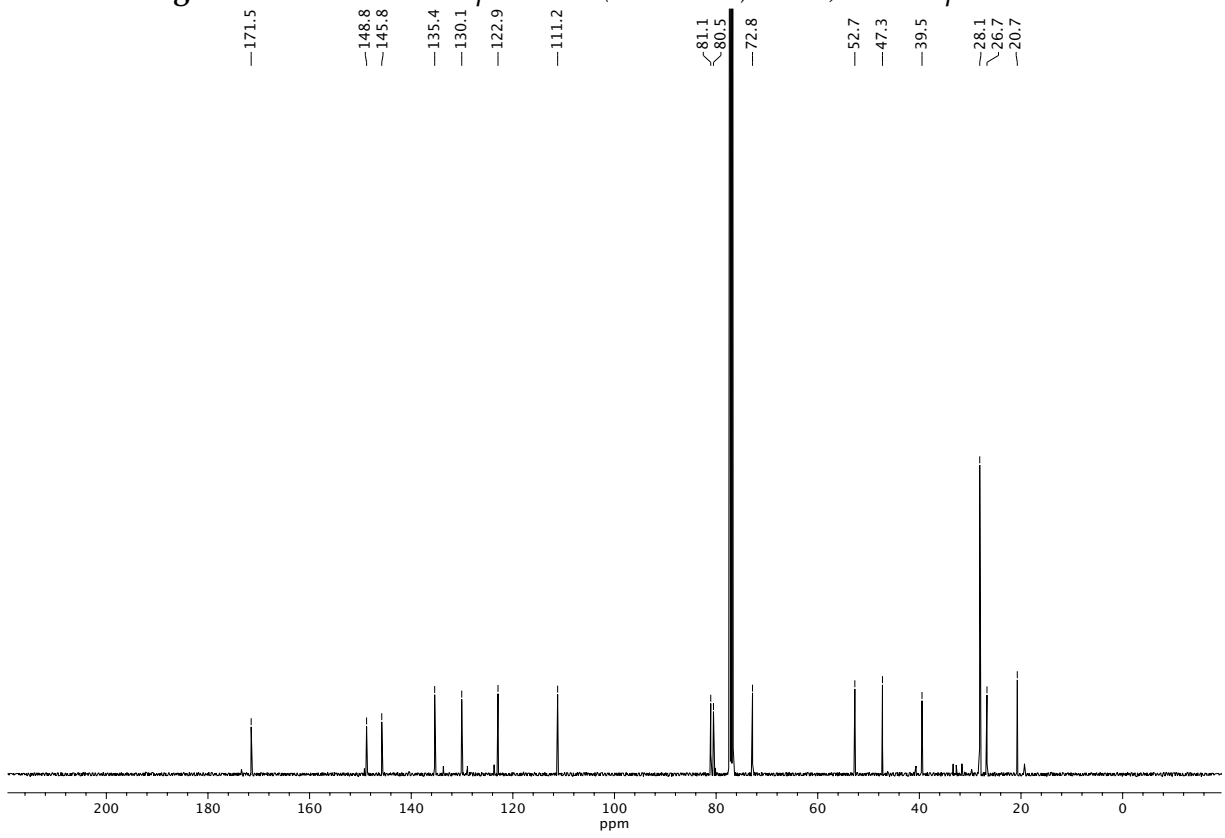

Figure A1.27. *^{13}C NMR (100 MHz, $CDCl_3$) of compound* ***30****.*

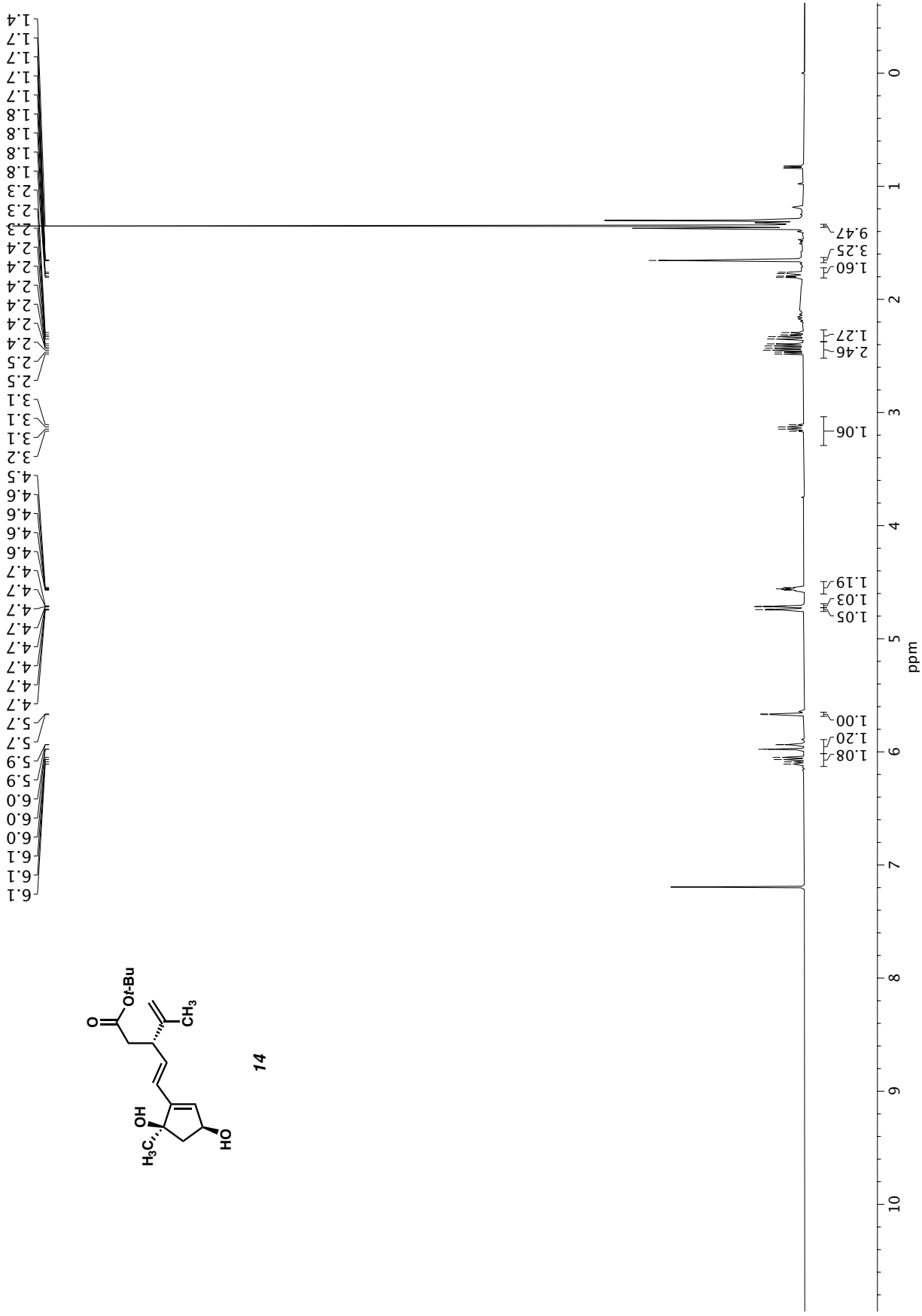

Figure A1.28. *^{13}C NMR (100 MHz, $CDCl_3$) of compound **14***

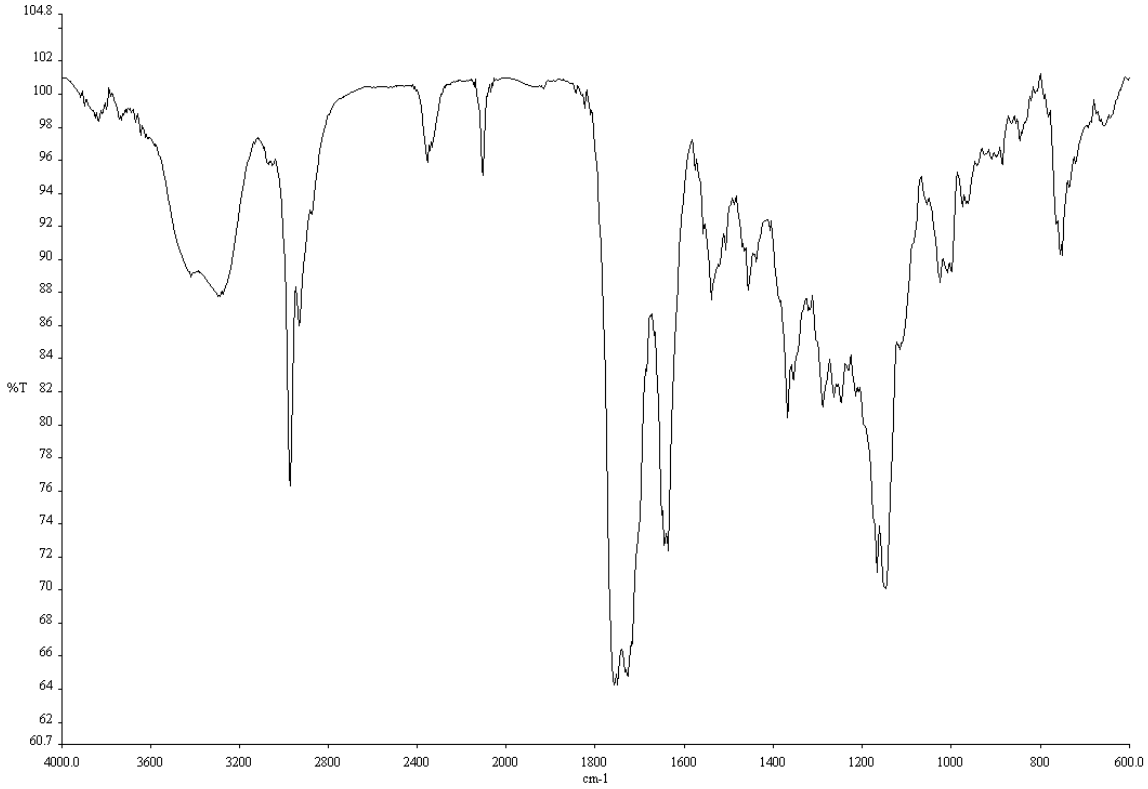

Figure A1.29. *^{13}C NMR (100 MHz, $CDCl_3$) of compound **14**.*

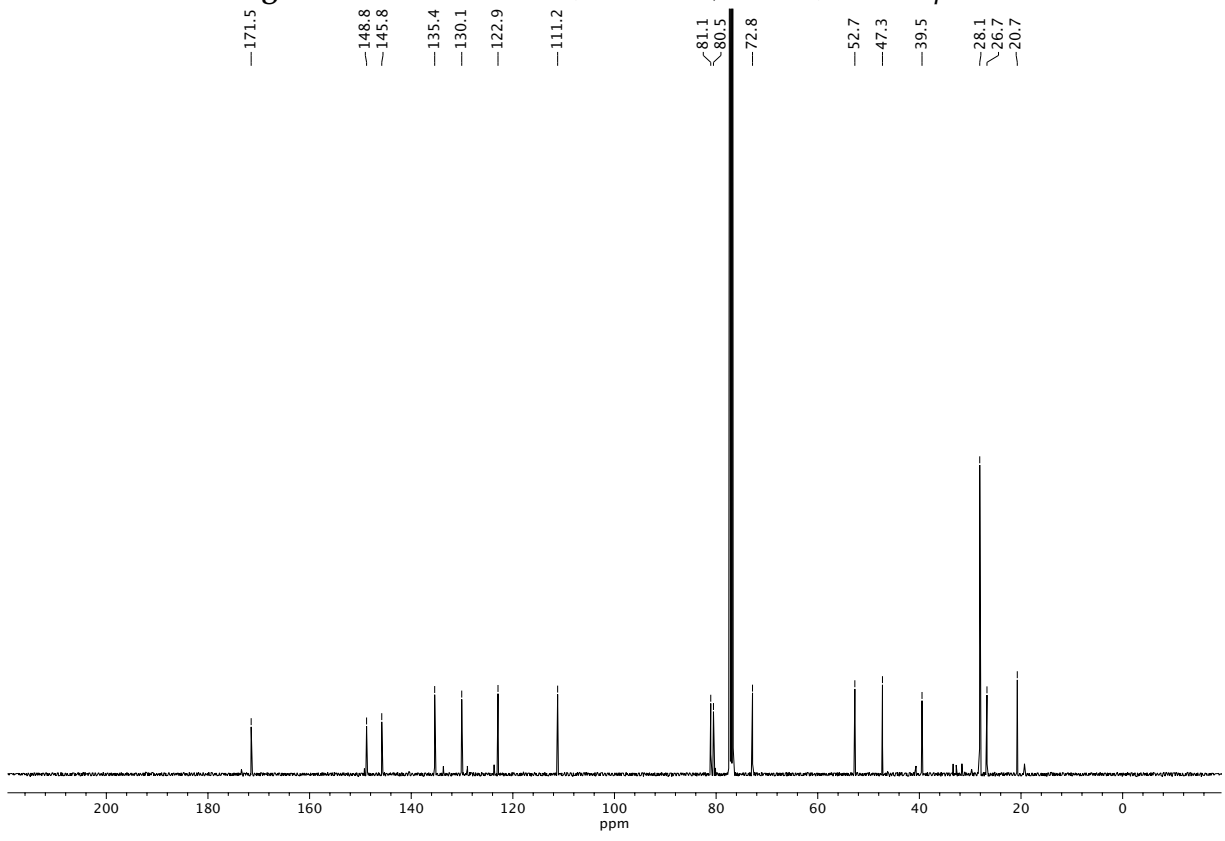

Figure A1.30. *^{13}C NMR (100 MHz, $CDCl_3$) of compound **14**.*

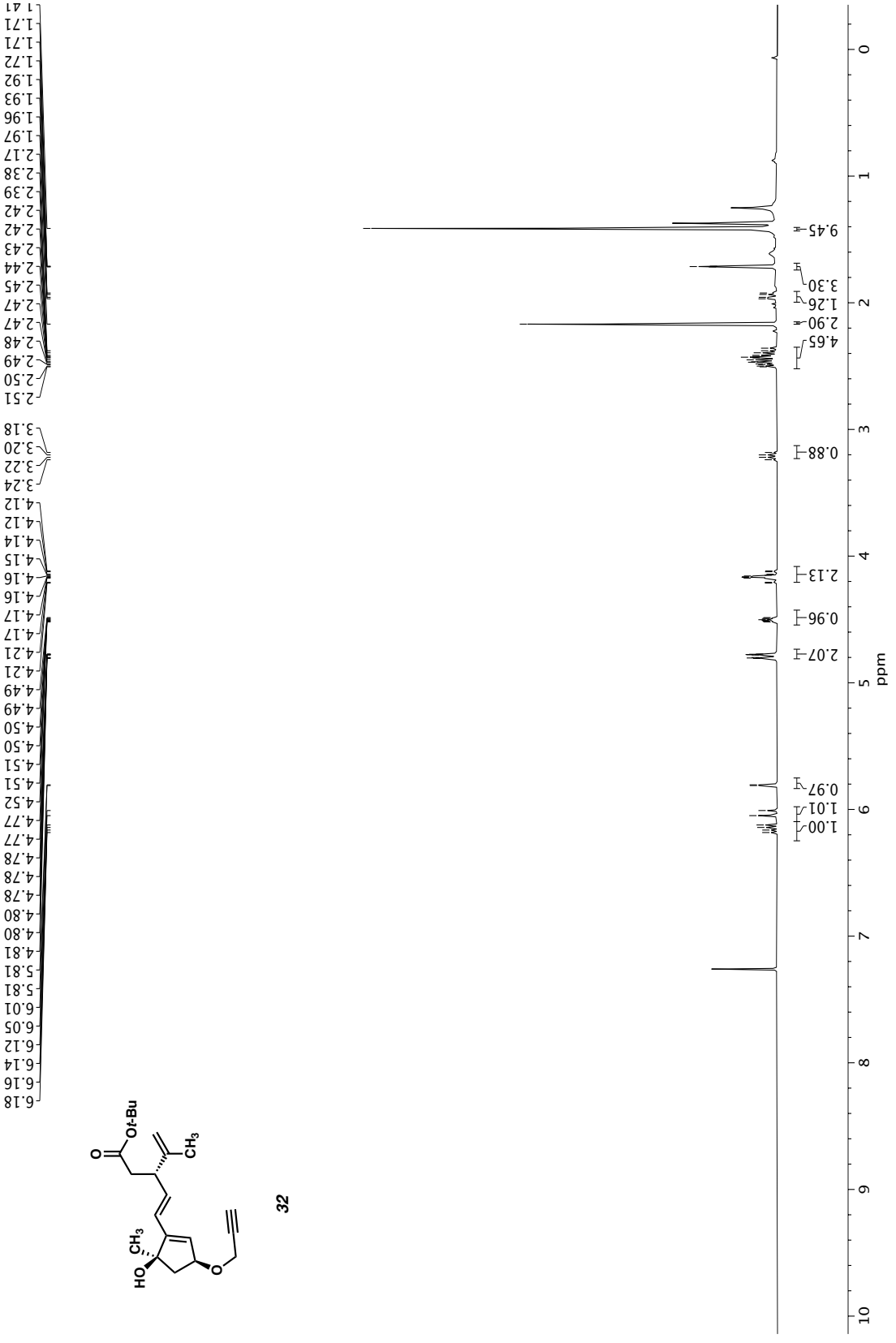

Figure A1.31. *^{1}H NMR (500 MHz, $CDCl_3$) of compound* ***32****.*

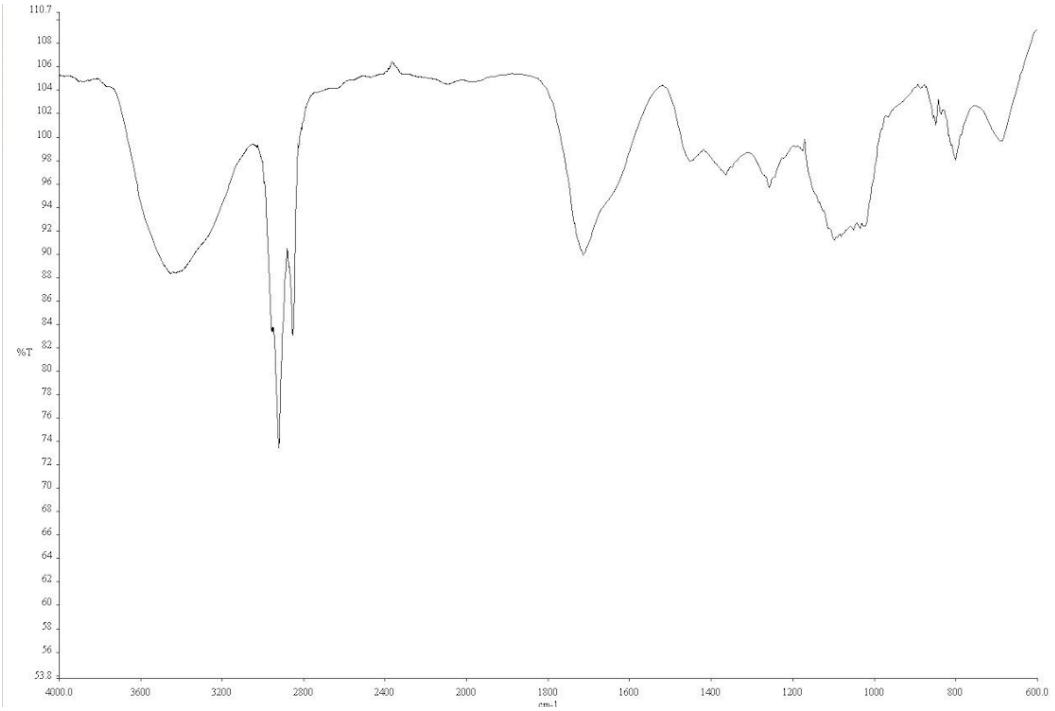

Figure A1.32. *^{13}C NMR (100 MHz, $CDCl_3$) of compound **32**.*

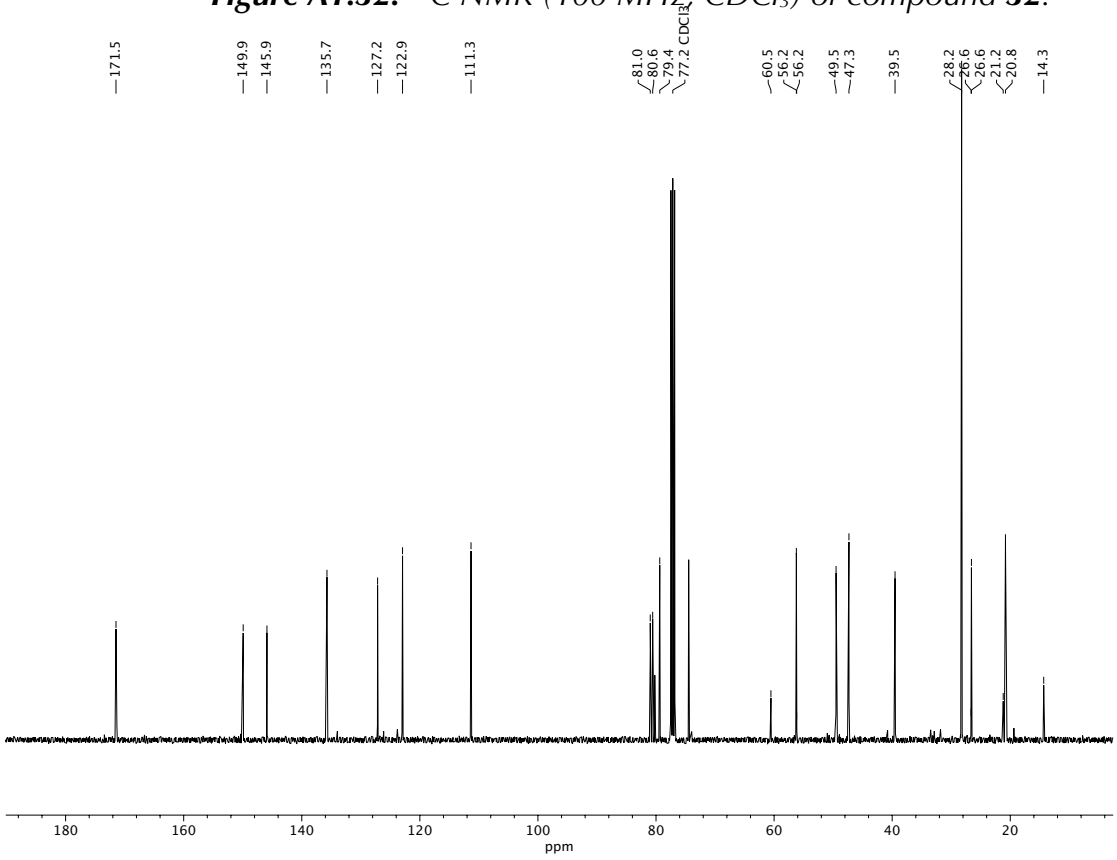

Figure A1.33. *^{13}C NMR (100 MHz, $CDCl_3$) of compound **32**.*

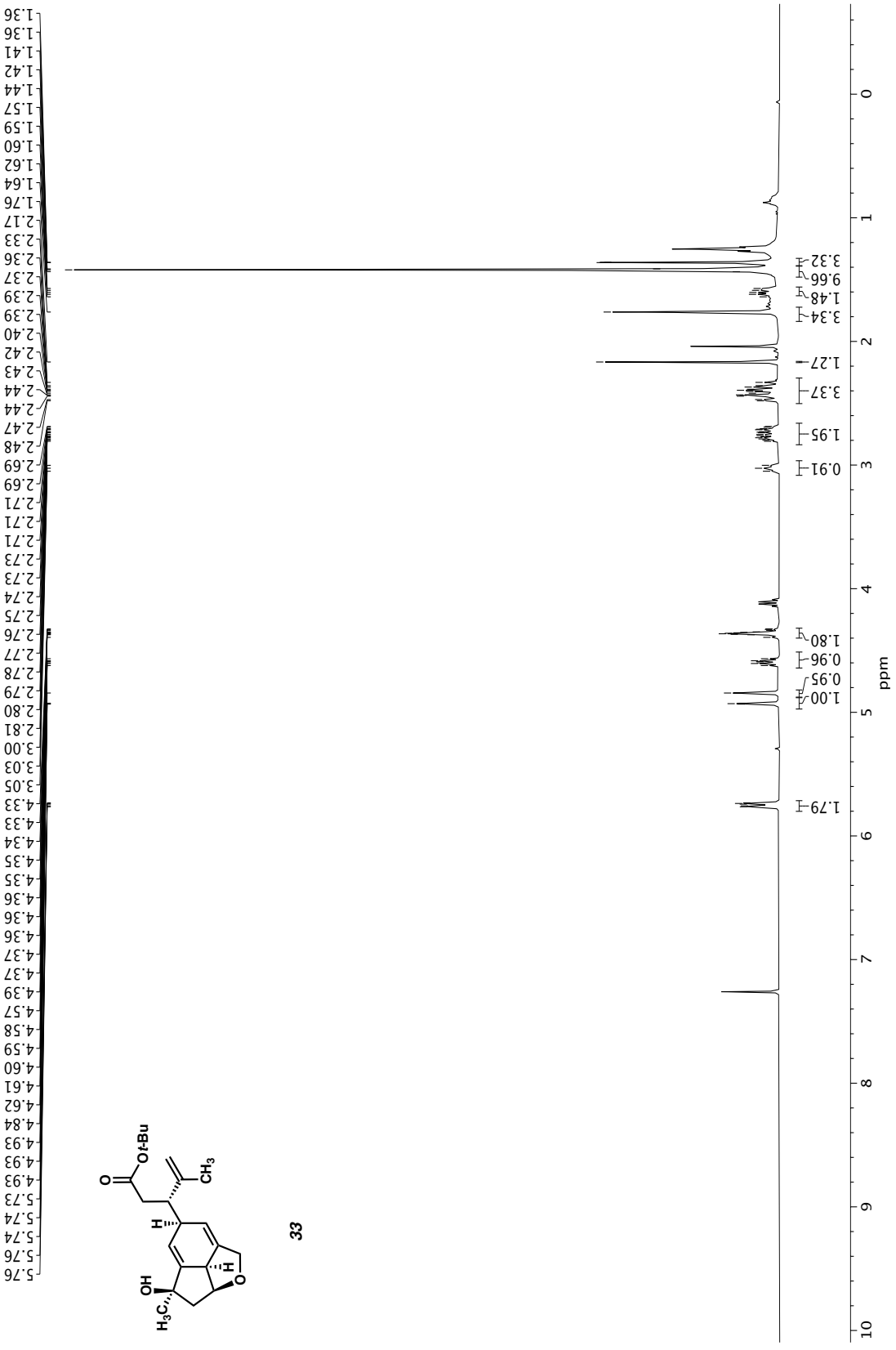

Figure A1.34. *^1H NMR (500 MHz, $CDCl_3$) of compound* ***33****.*

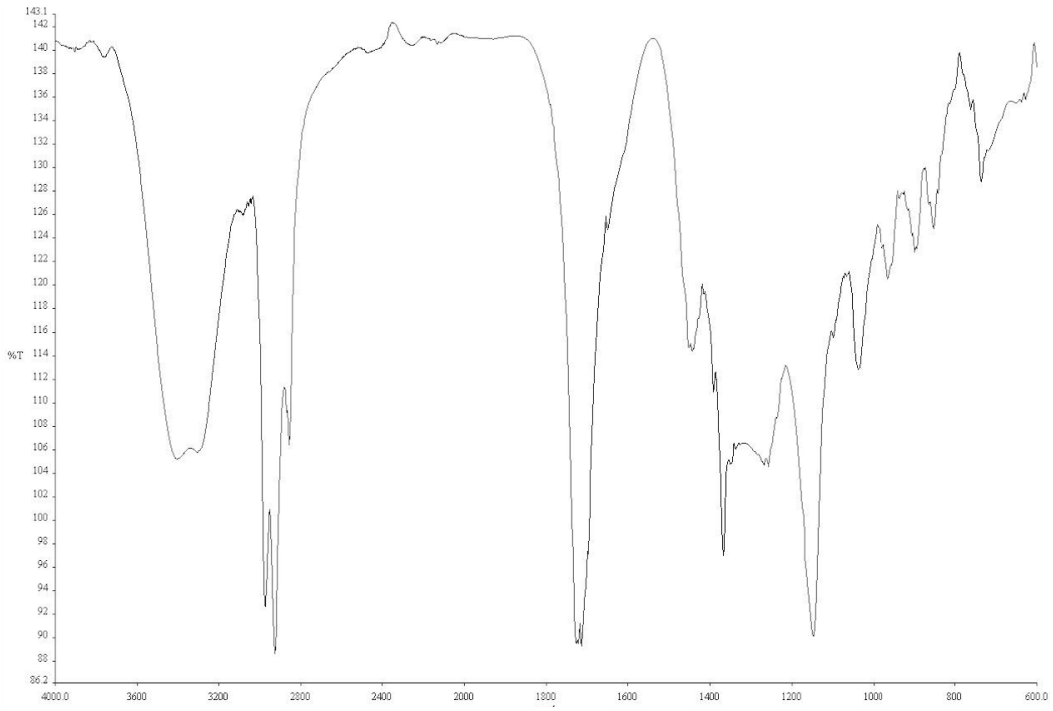

Figure A1.35. *^{13}C NMR (100 MHz, $CDCl_3$) of compound **33**.*

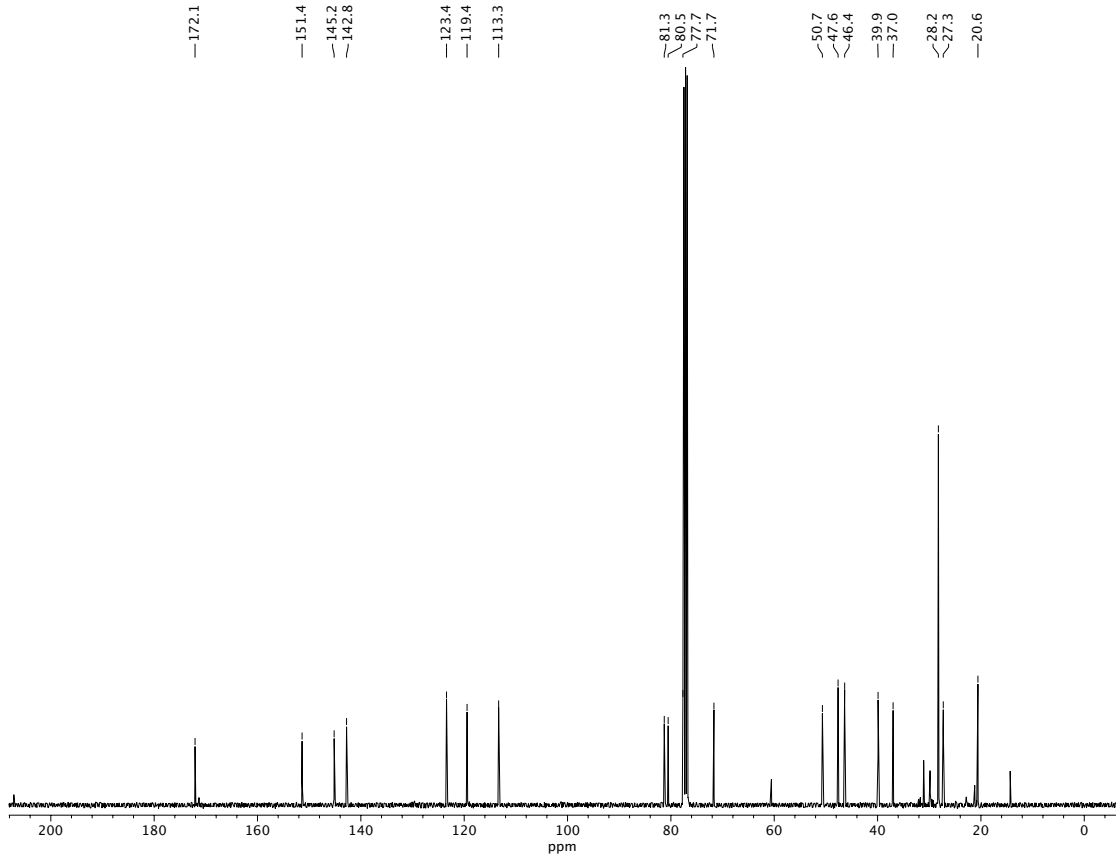

Figure A1.36. *^{13}C NMR (100 MHz, $CDCl_3$) of compound **33**.*

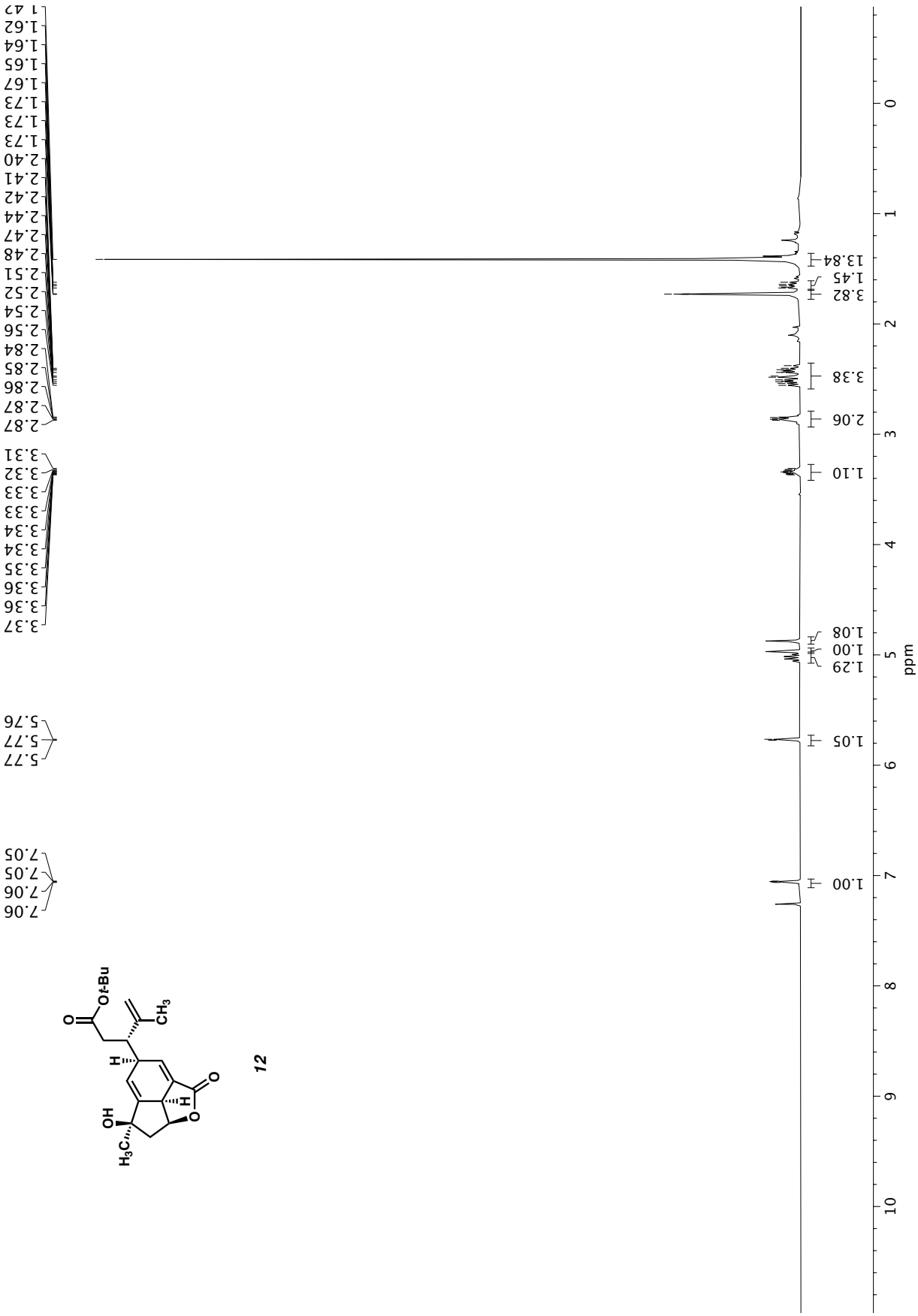

Figure A1.37. *^1H NMR (500 MHz, $CDCl_3$) of compound* ***12****.*

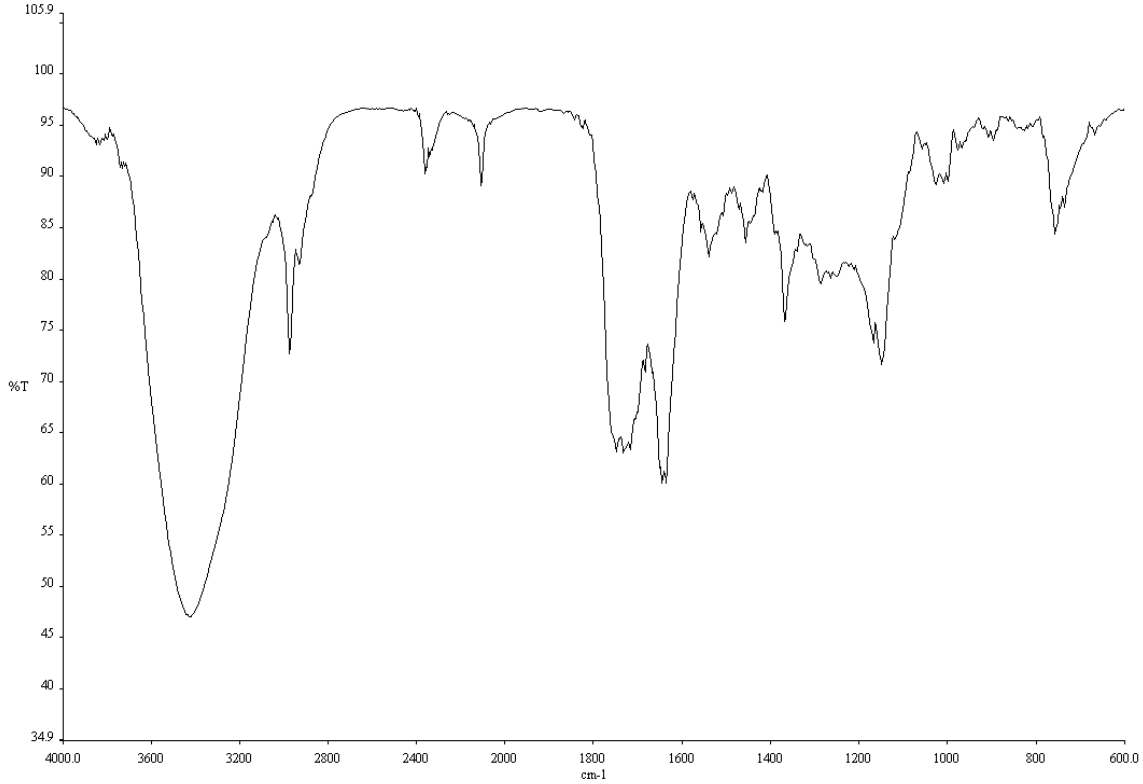

Figure A1.38. *Infrared spectrum (Thin Film, NaCl) of compound* ***12***.

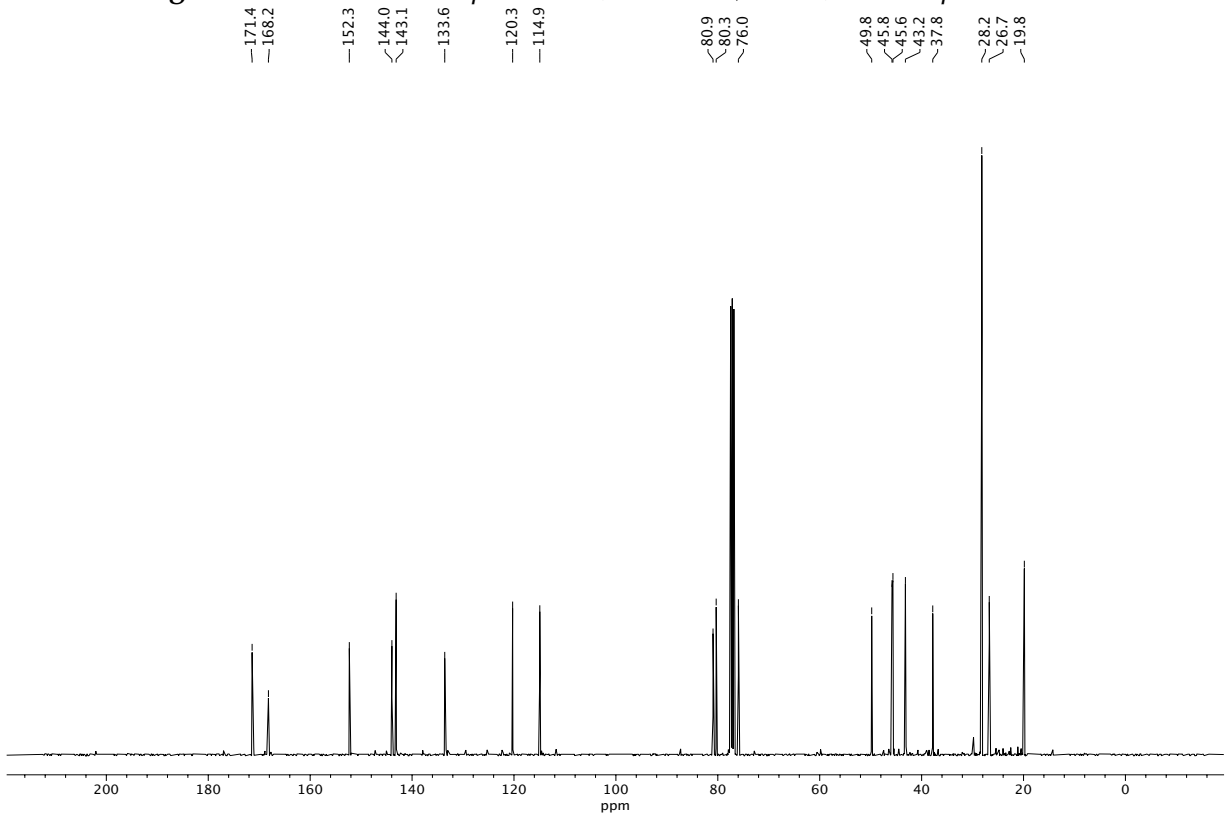

Figure A1.39. *^{13}C NMR (100 MHz, $CDCl_3$) of compound* ***12***.

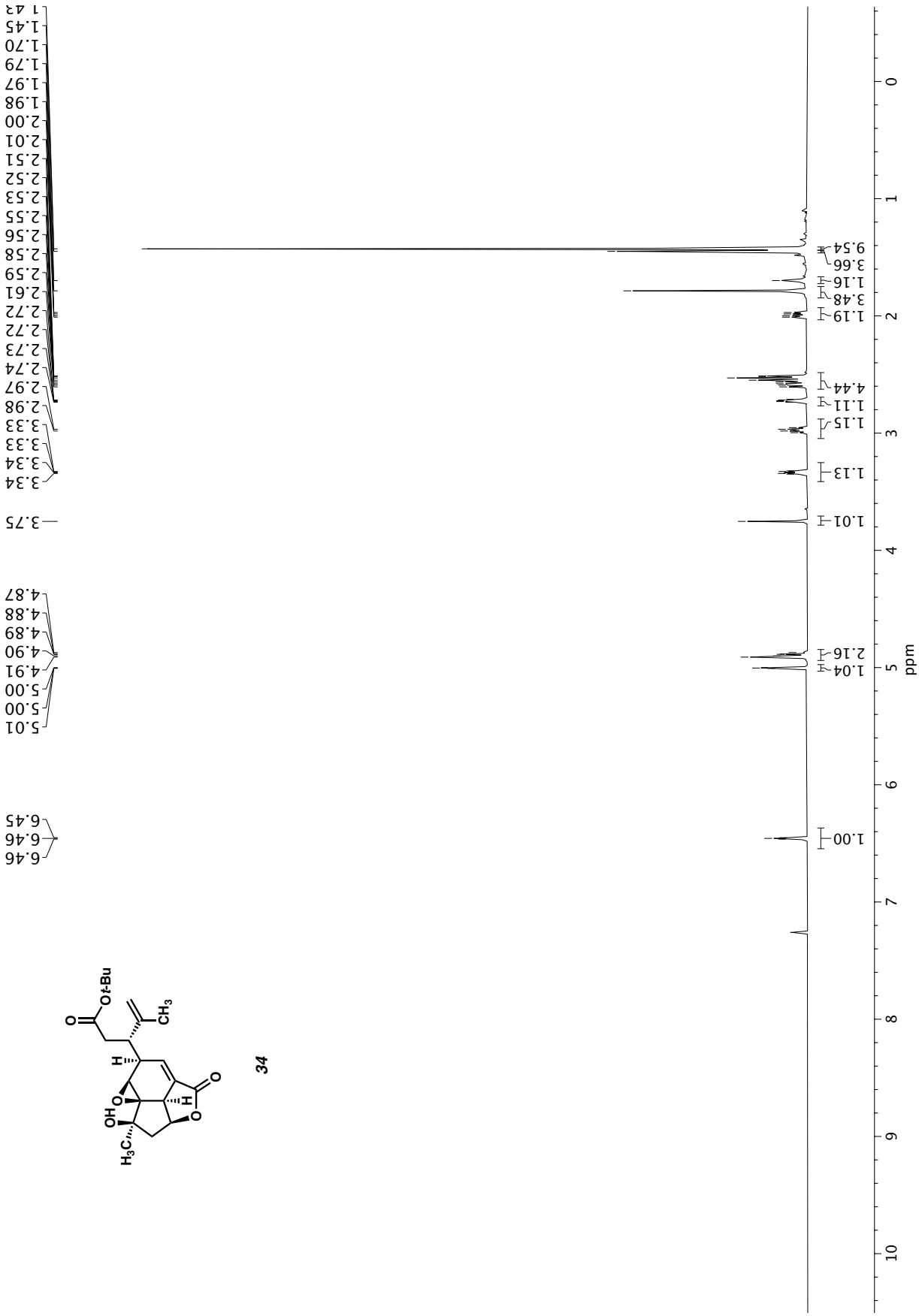

34

Figure A1.40. *^1H NMR (500 MHz, $CDCl_3$) of compound* ***34****.*

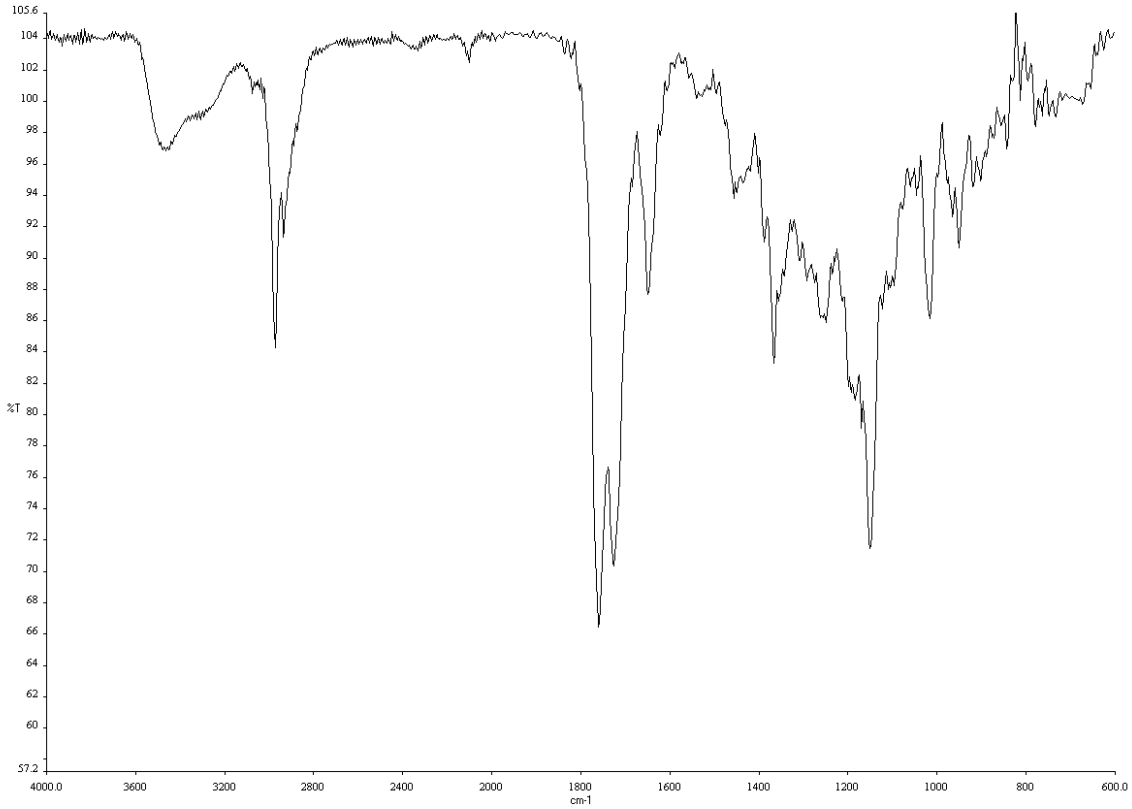

Figure A1.41. *Infrared spectrum (Thin Film, NaCl) of compound* ***34.***

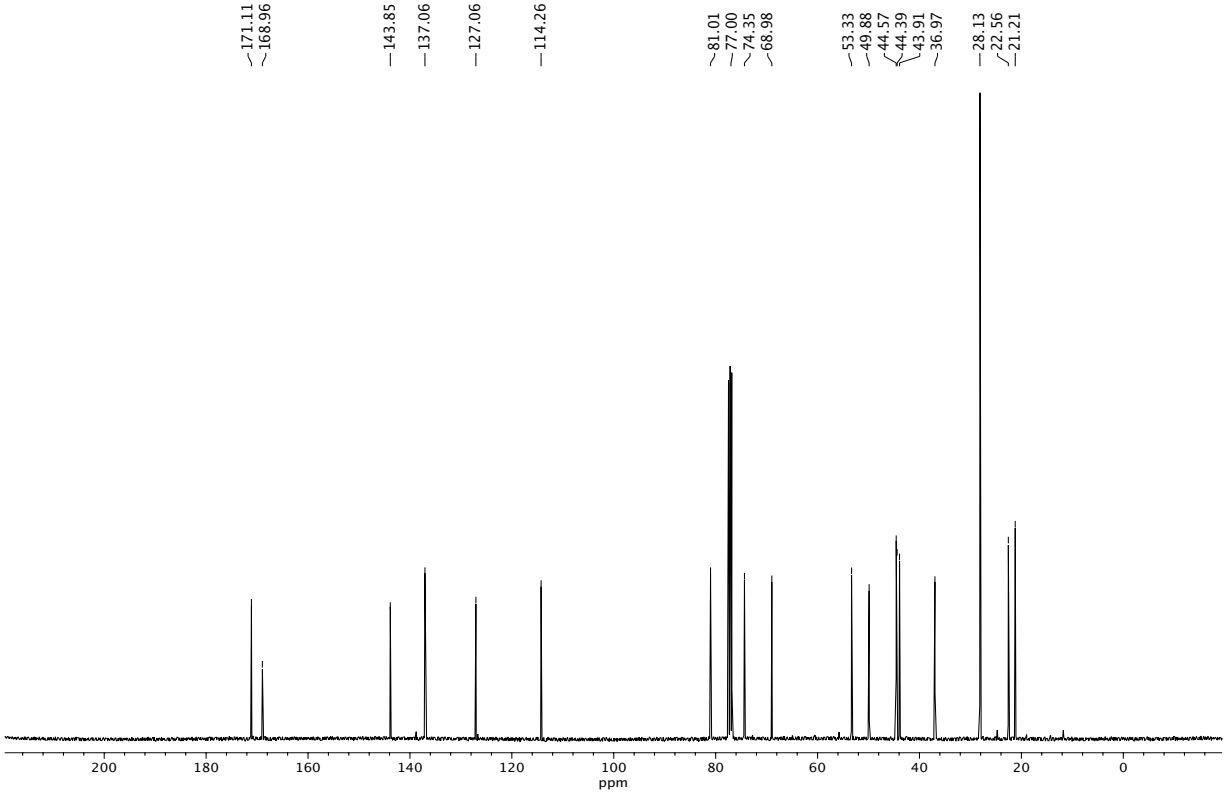

Figure A1.42. *^{13}C NMR (100 MHz, $CDCl_3$) of compound* ***34****.*

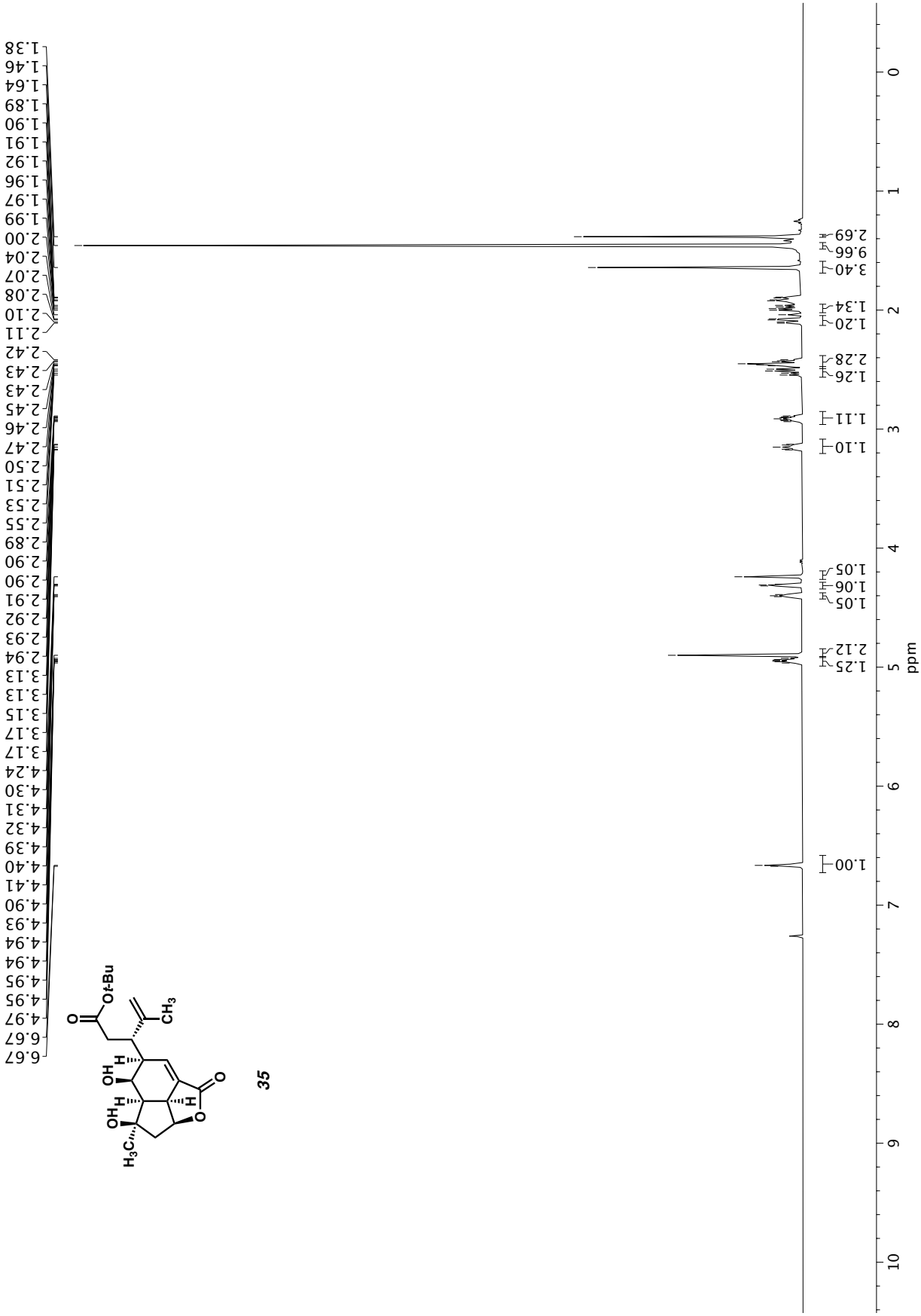

Figure A1.43. *^1H NMR (500 MHz, $CDCl_3$) of compound* ***35****.*

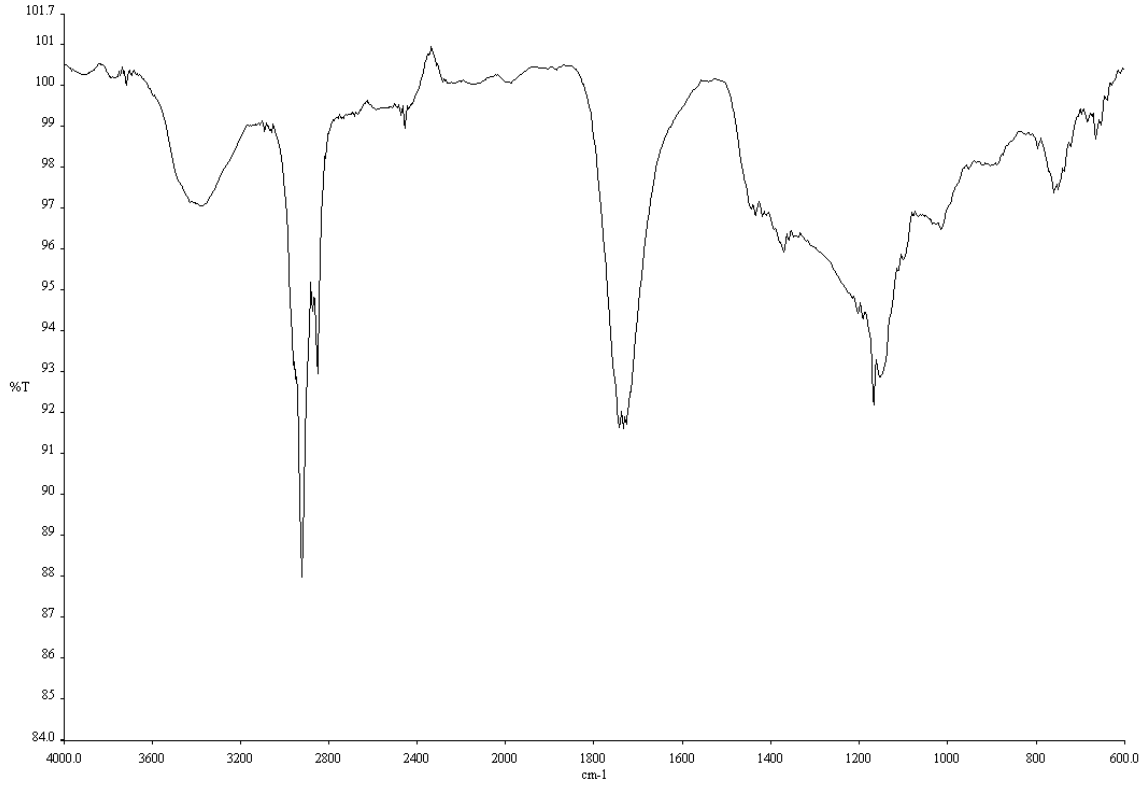

Figure A1.44. *Infrared spectrum (Thin Film, NaCl) of compound* ***35****.*

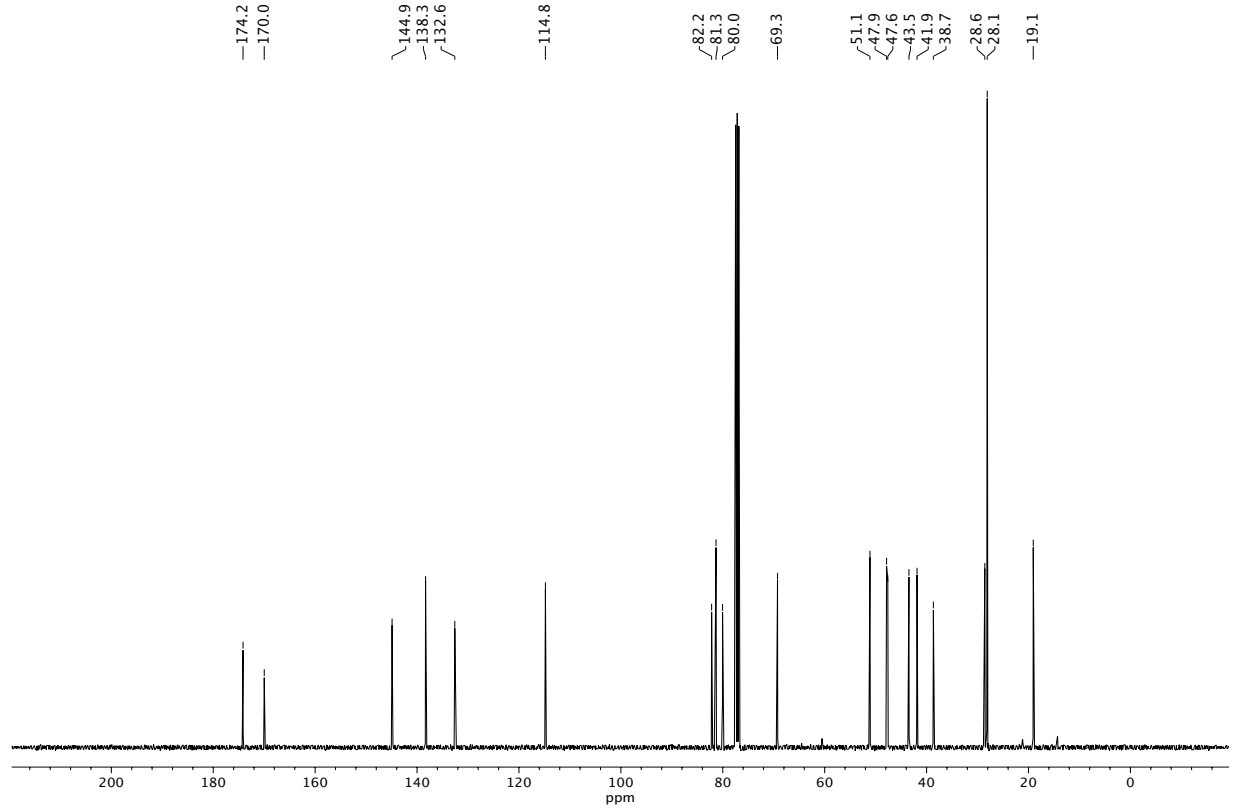

Figure A1.45. *^{13}C NMR (100 MHz, $CDCl_3$) of compound* ***35****.*

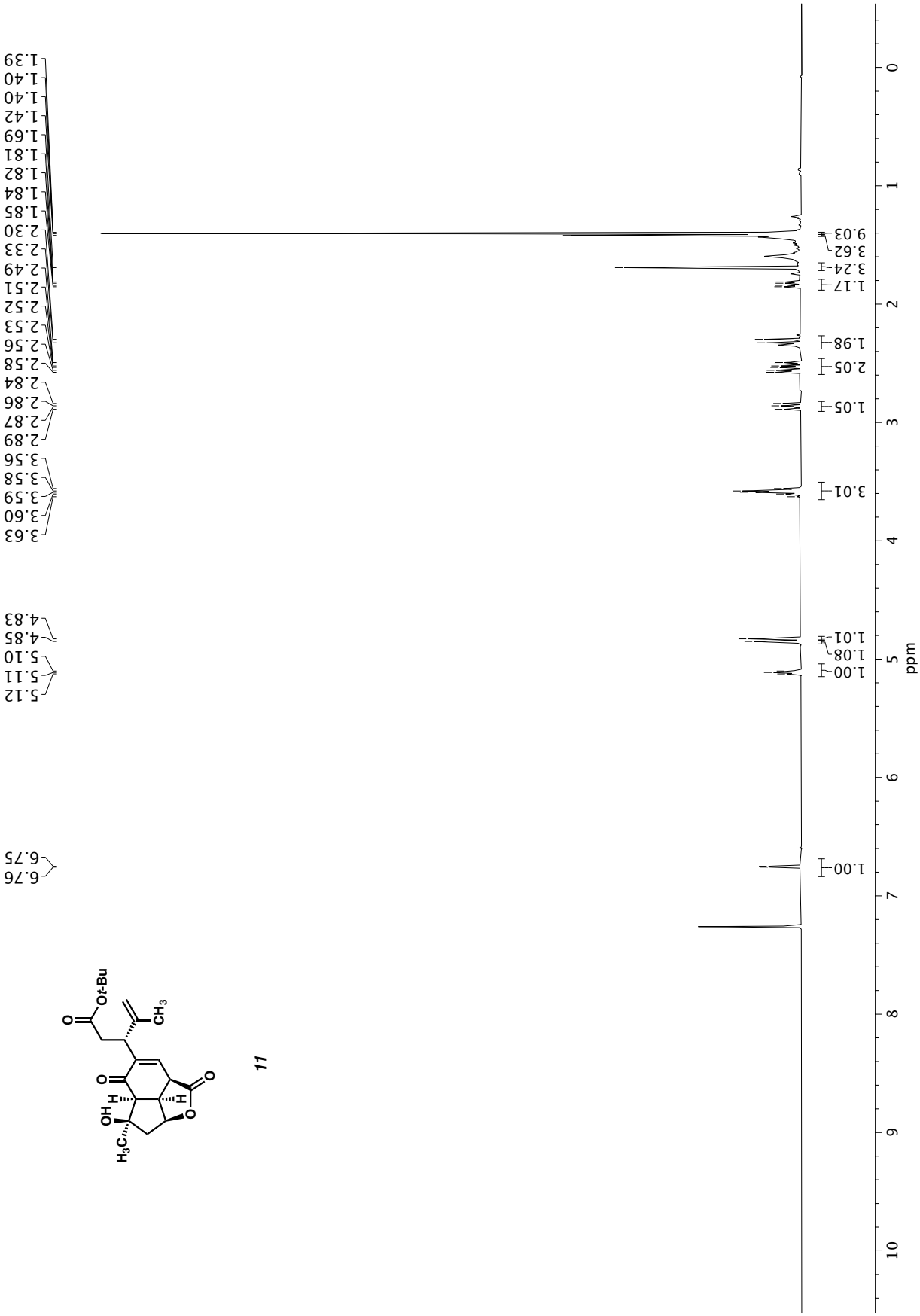

Figure A1.46. *^1H NMR (500 MHz, $CDCl_3$) of compound* ***11****.*

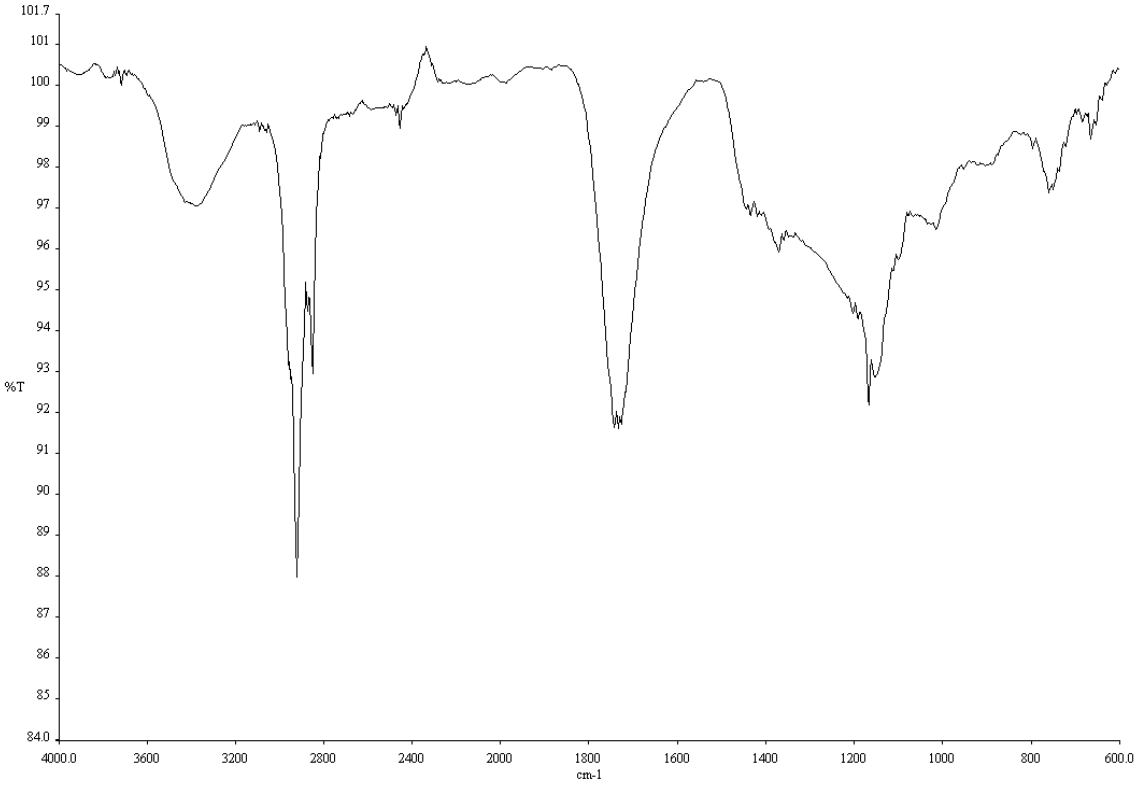

Figure A1.47. *Infrared spectrum (Thin Film, NaCl) of compound* ***11****.*

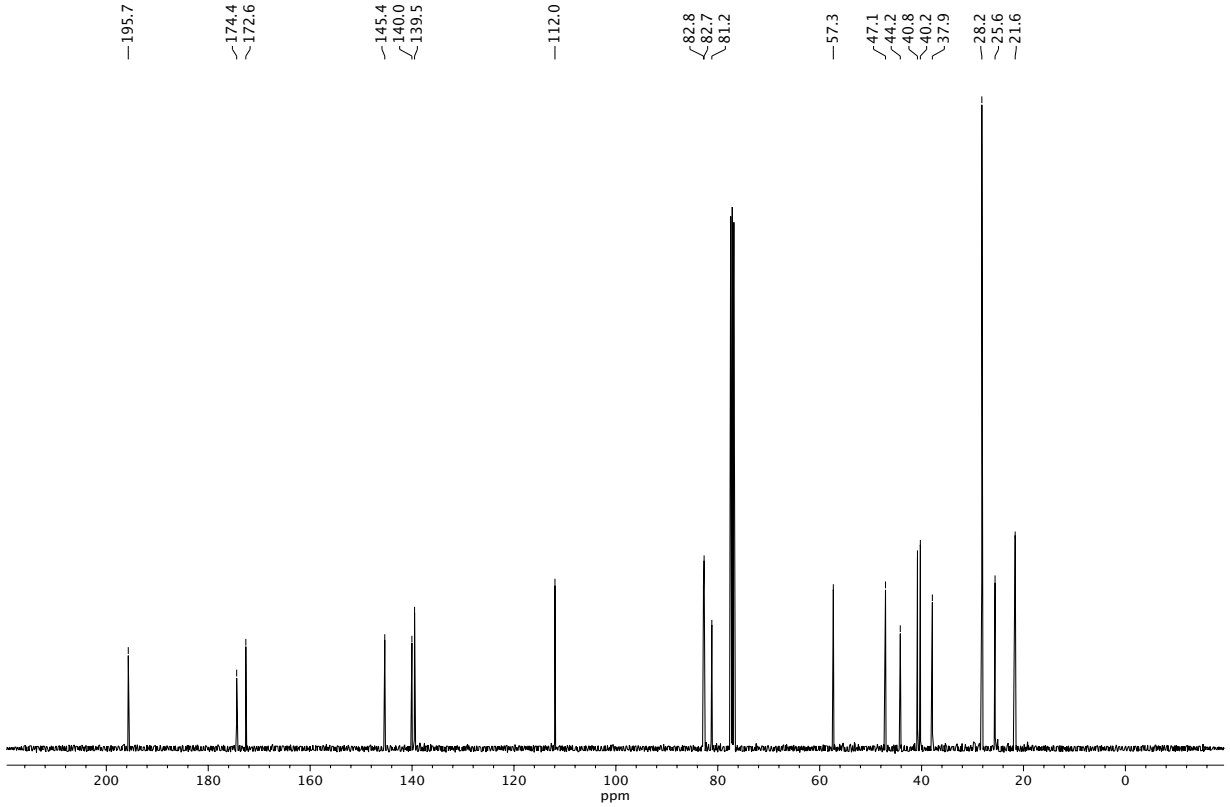

Figure A1.48. *^{13}C NMR (100 MHz, $CDCl_3$) of compound* ***11****.*

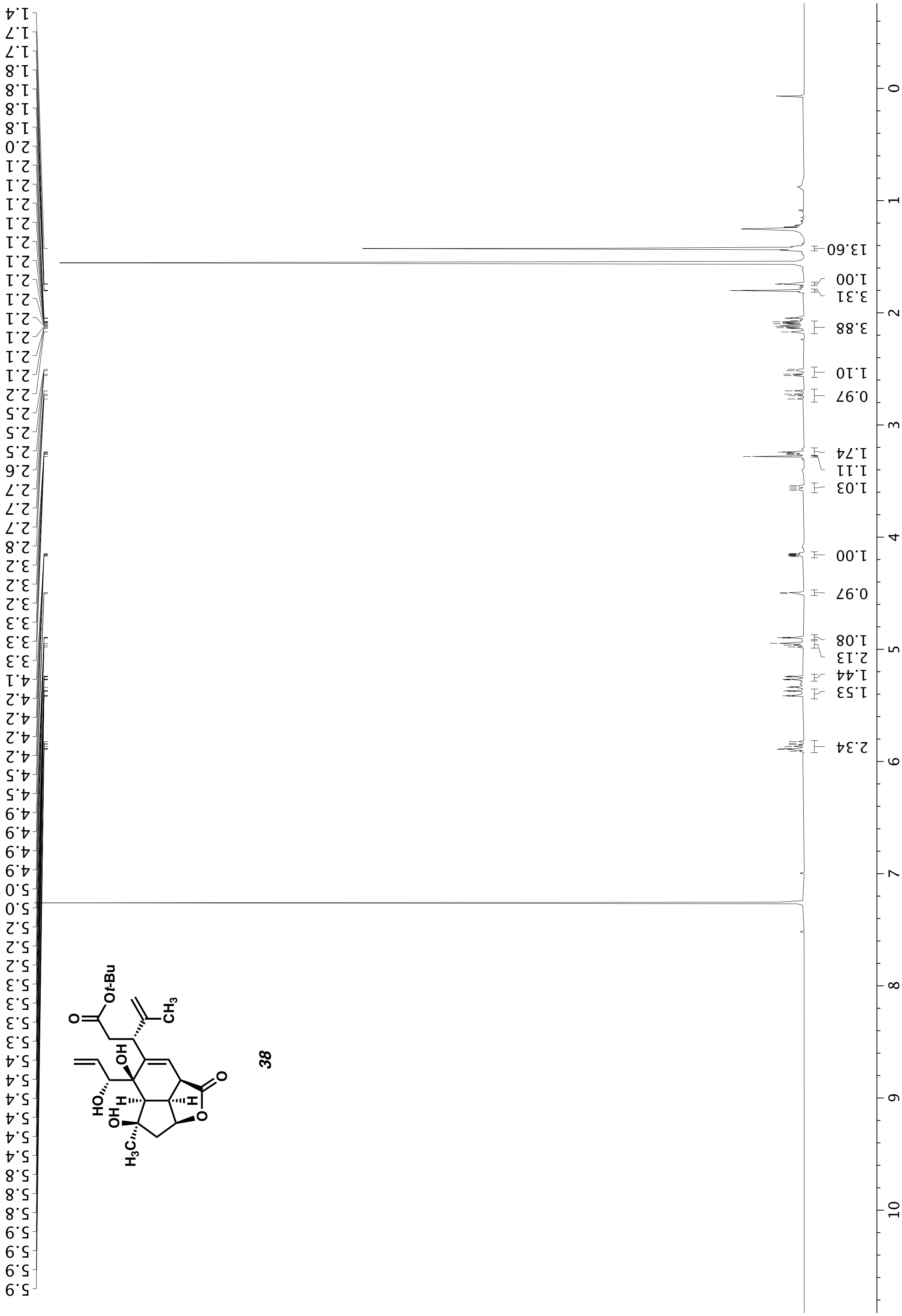

Figure A1.49. *^{1}H NMR (400 MHz, $CDCl_3$) of compound* ***38****.*

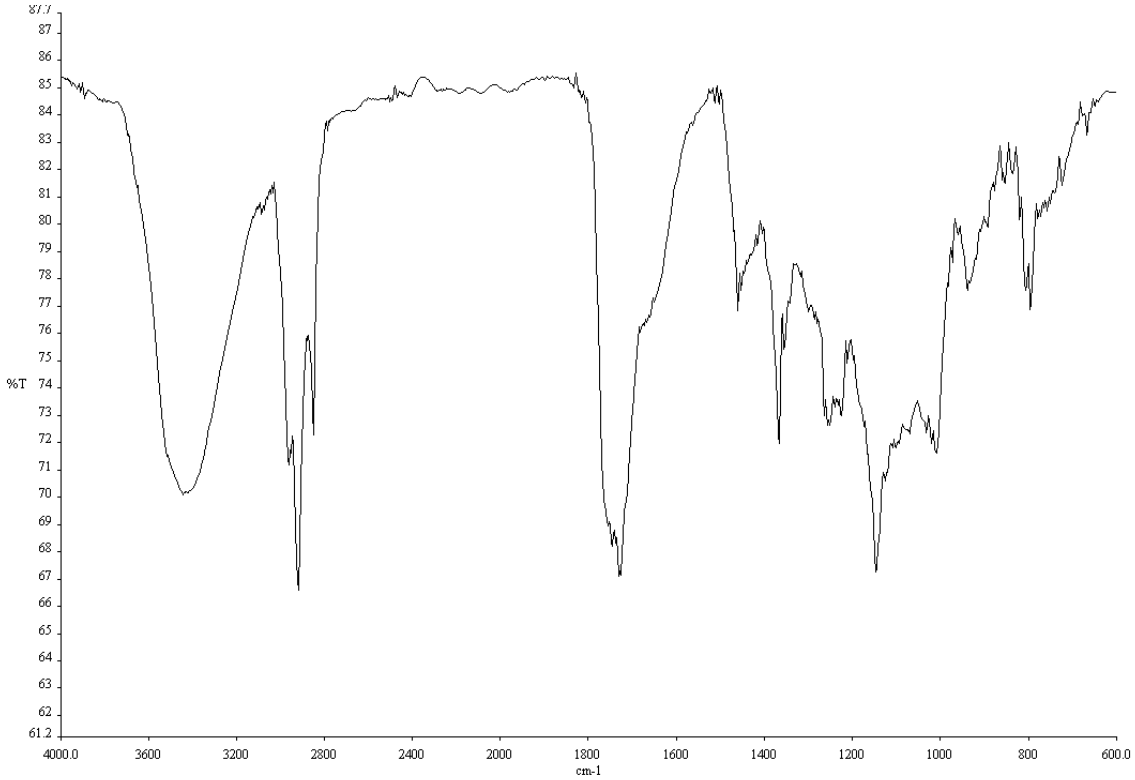

Figure A1.50. *Infrared spectrum (Thin Film, NaCl) of compound* ***38****.*

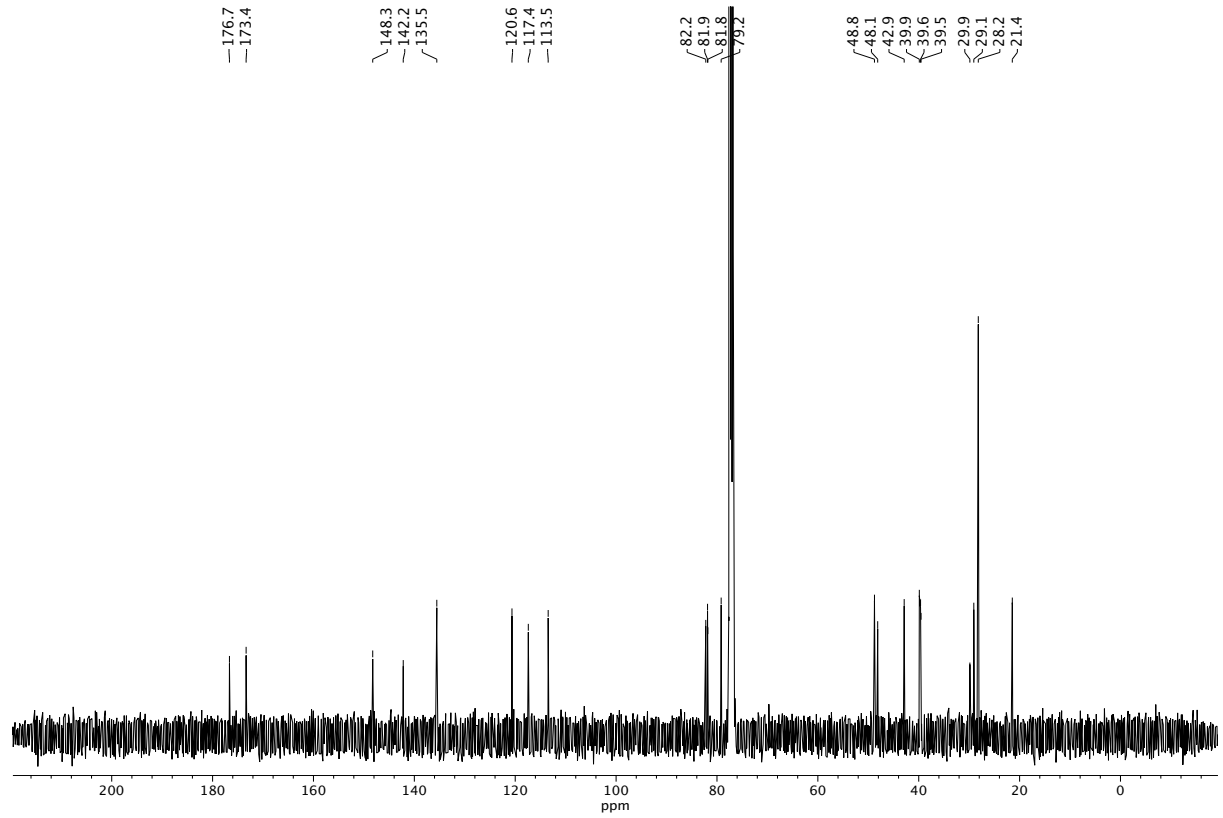

Figure A1.51. *^{13}C NMR (100 MHz, $CDCl_3$) of compound* ***38****.*

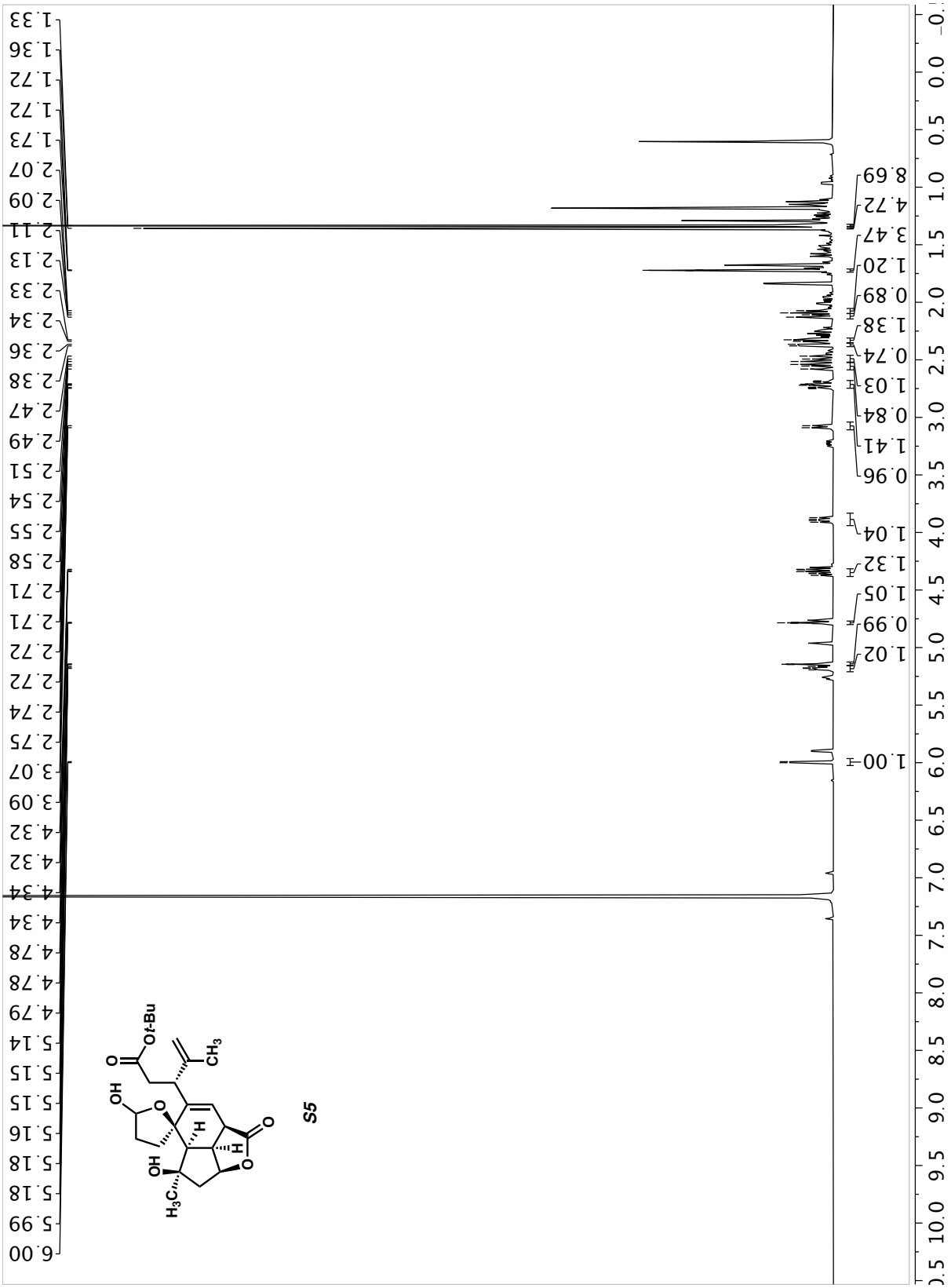

Figure A1.52. *^1H NMR (400 MHz, $CDCl_3$) of compound* ***S5****.*

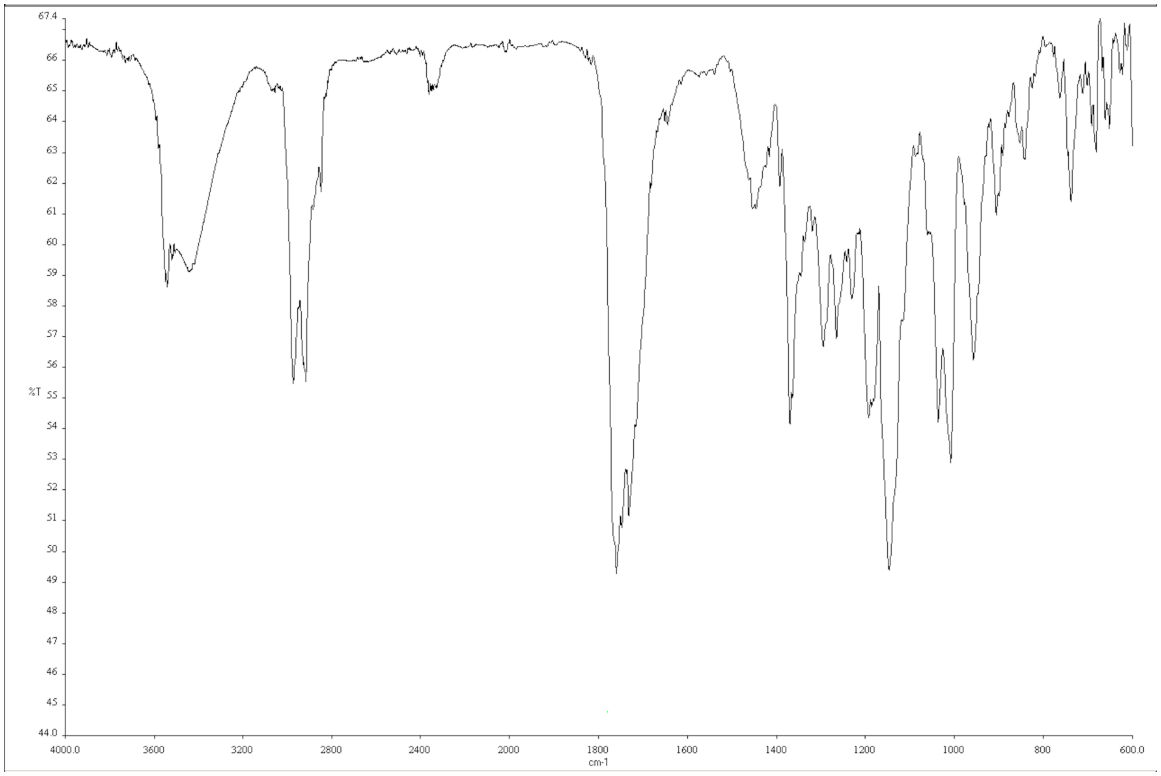

Figure A1.53. *Infrared spectrum (Thin Film, NaCl) of compound* ***S5****.*

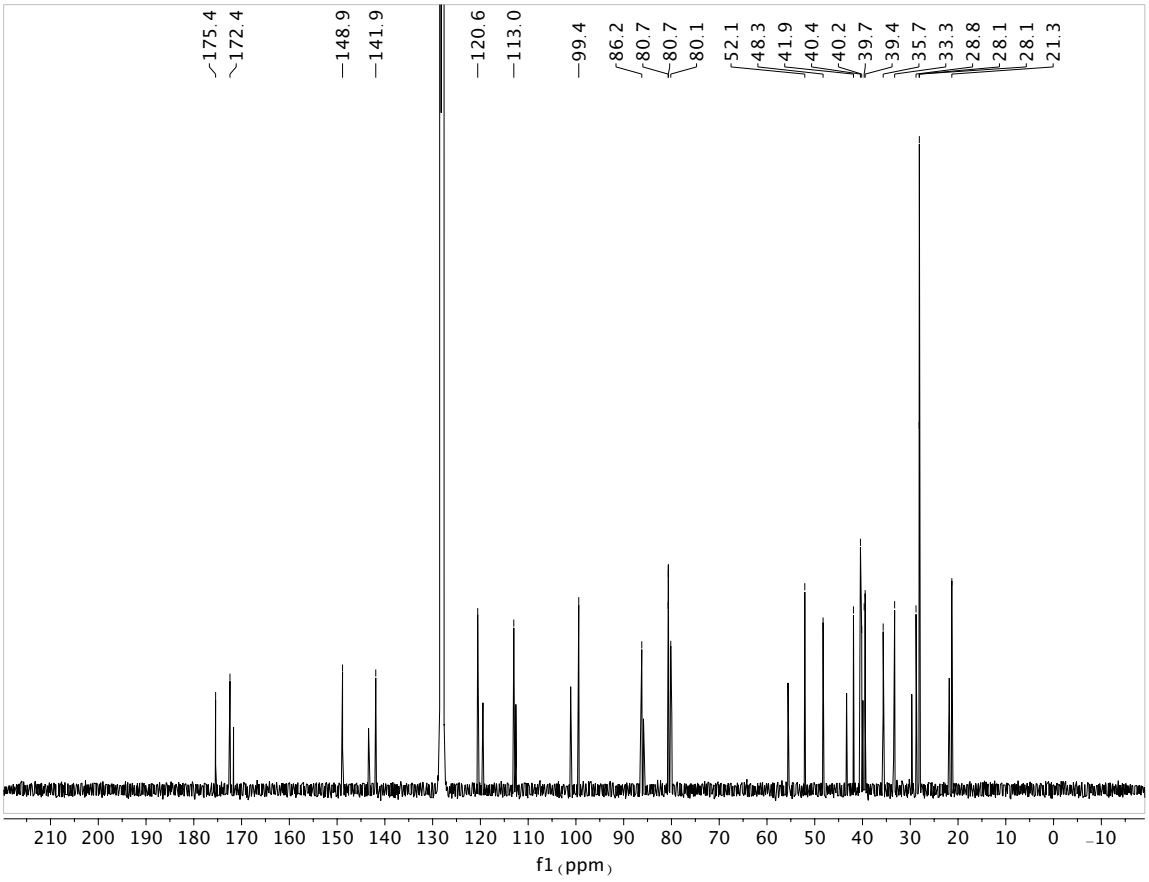

Figure A1.54. *^{13}C NMR (100 MHz, $CDCl_3$) of compound* ***S5****.*

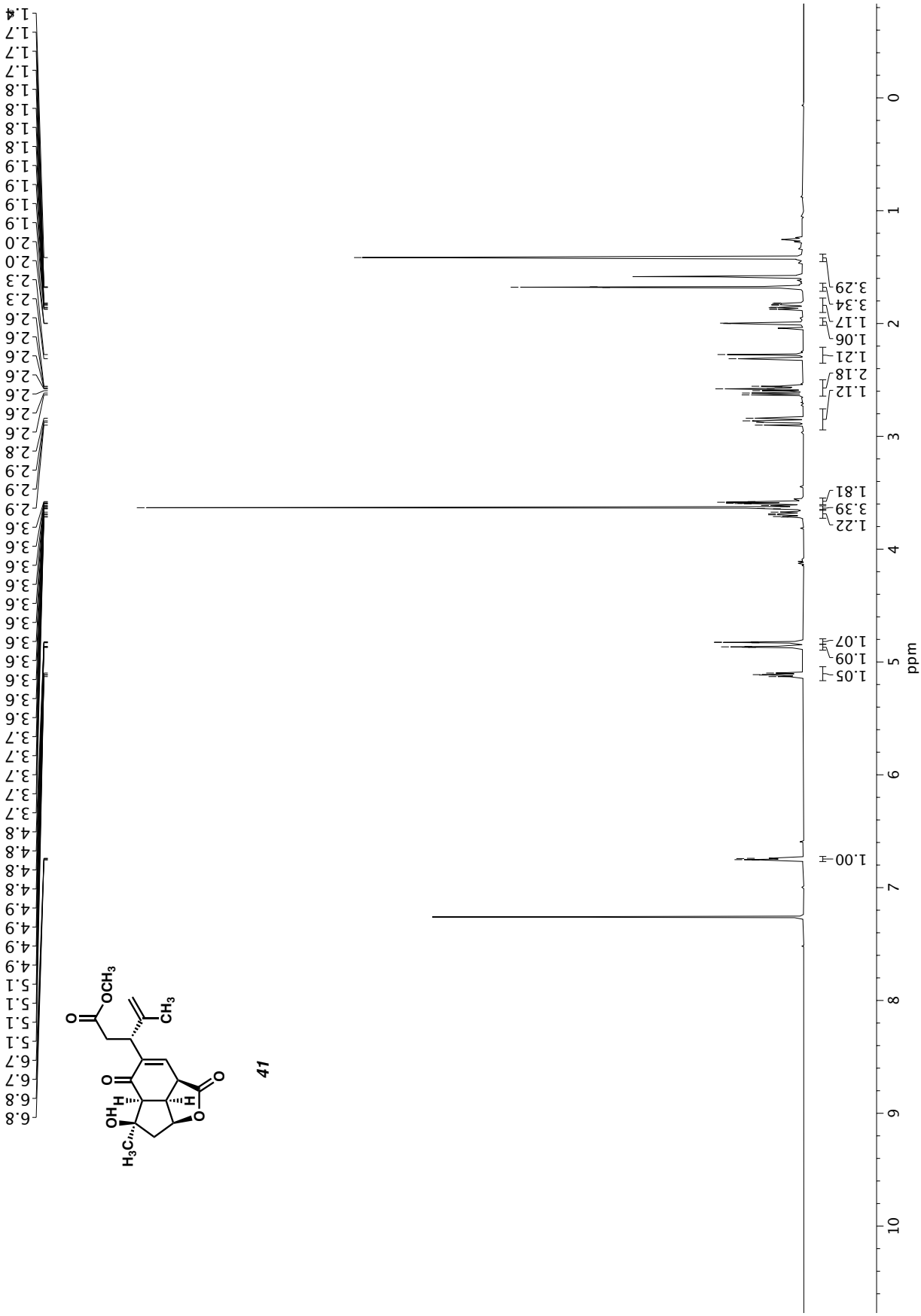

Figure A1.55. *^1H NMR (400 MHz, $CDCl_3$) of compound* ***41****.*

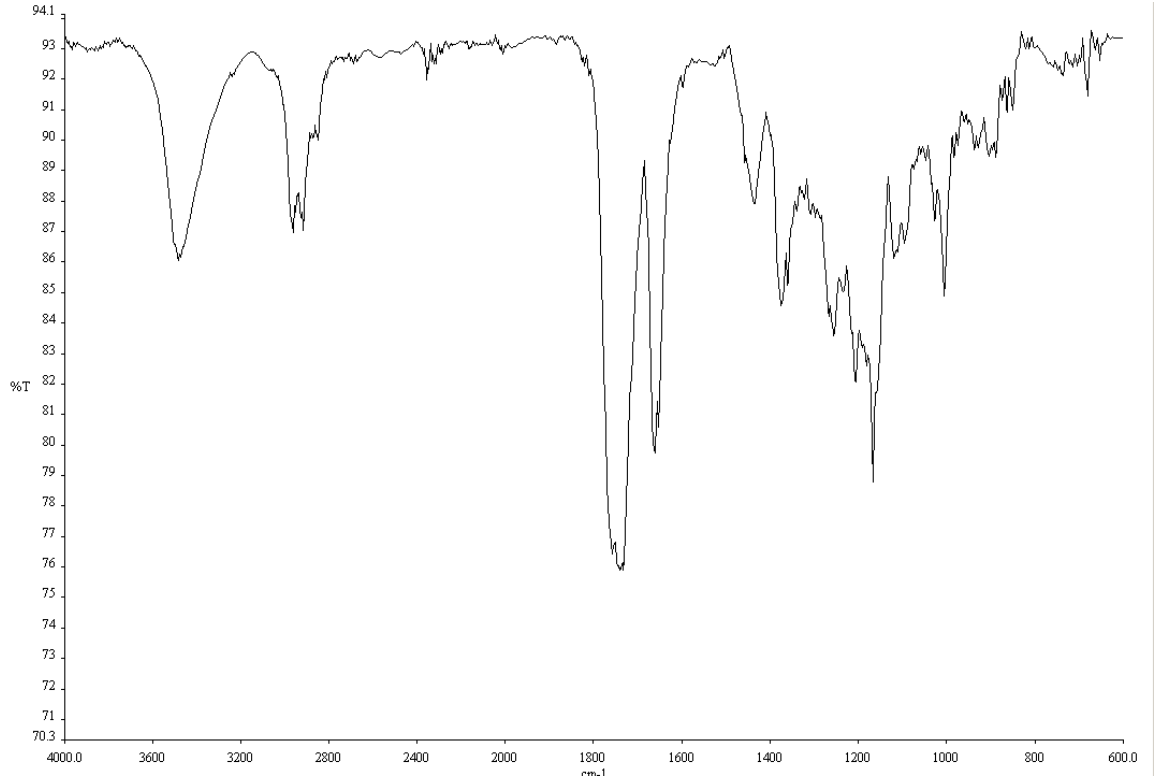

Figure A1.56. *Infrared spectrum (Thin Film, NaCl) of compound* ***41***.

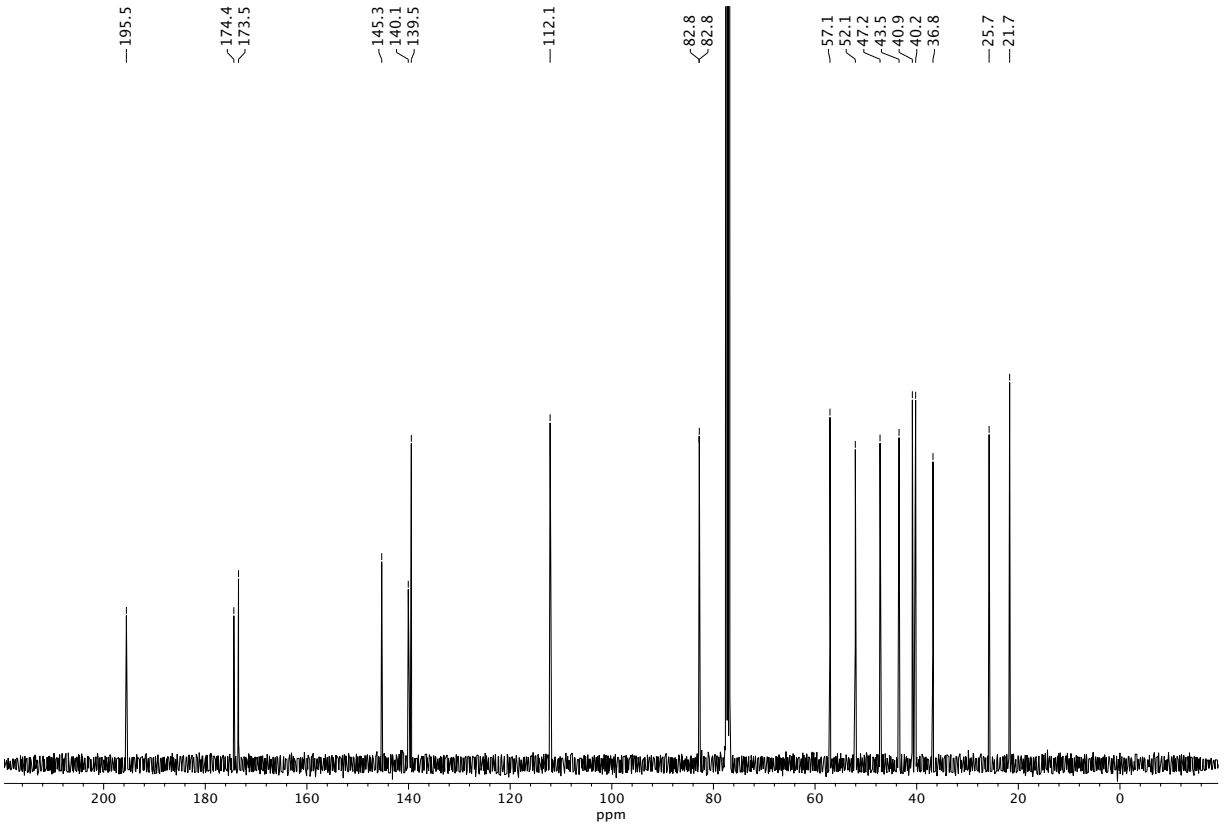

Figure A1.57. *^{13}C NMR (100 MHz, $CDCl_3$) of compound* ***41***.

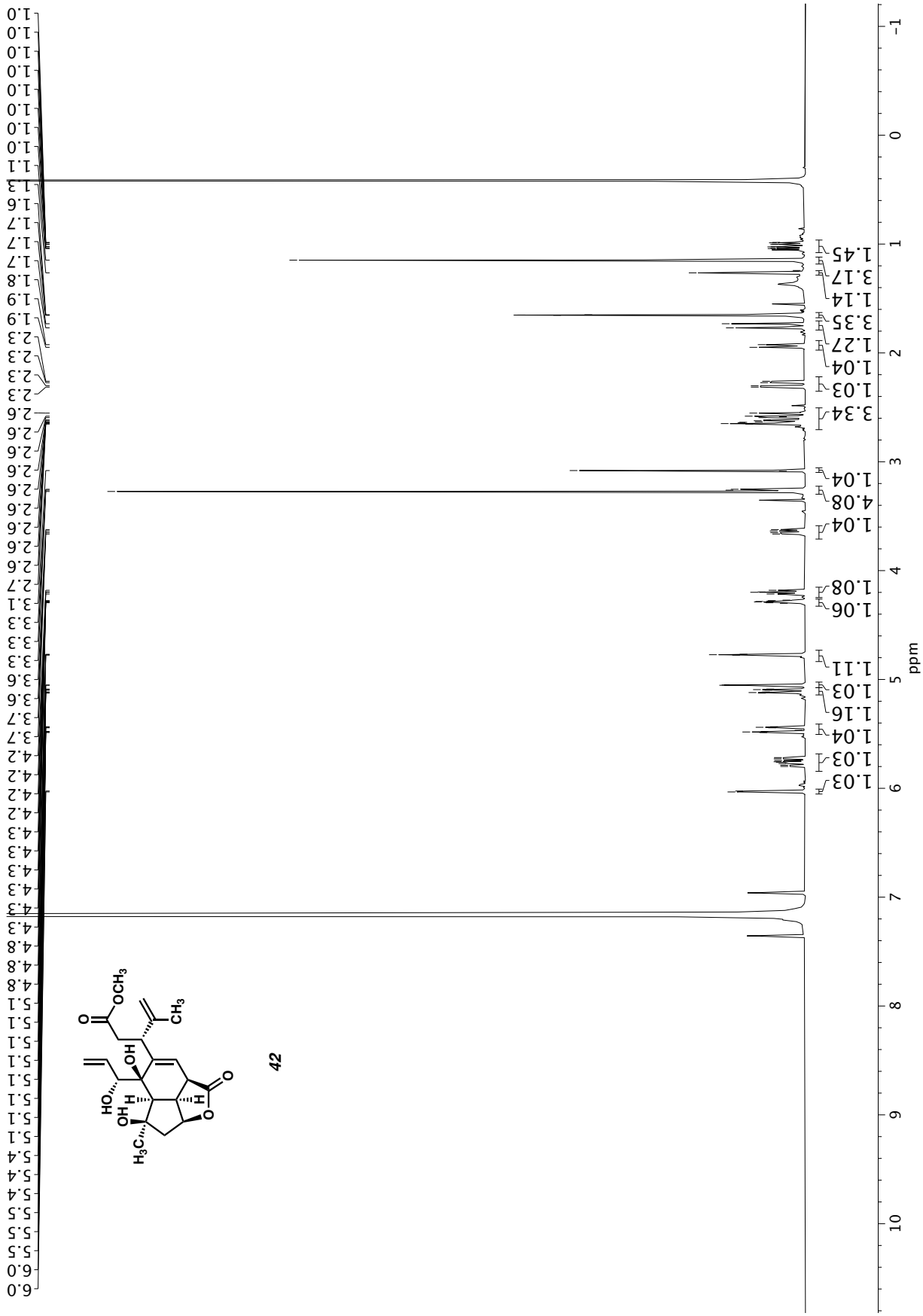

Figure A1.58. *^{1}H NMR (400 MHz, C_6D_6) of compound* ***42****.*

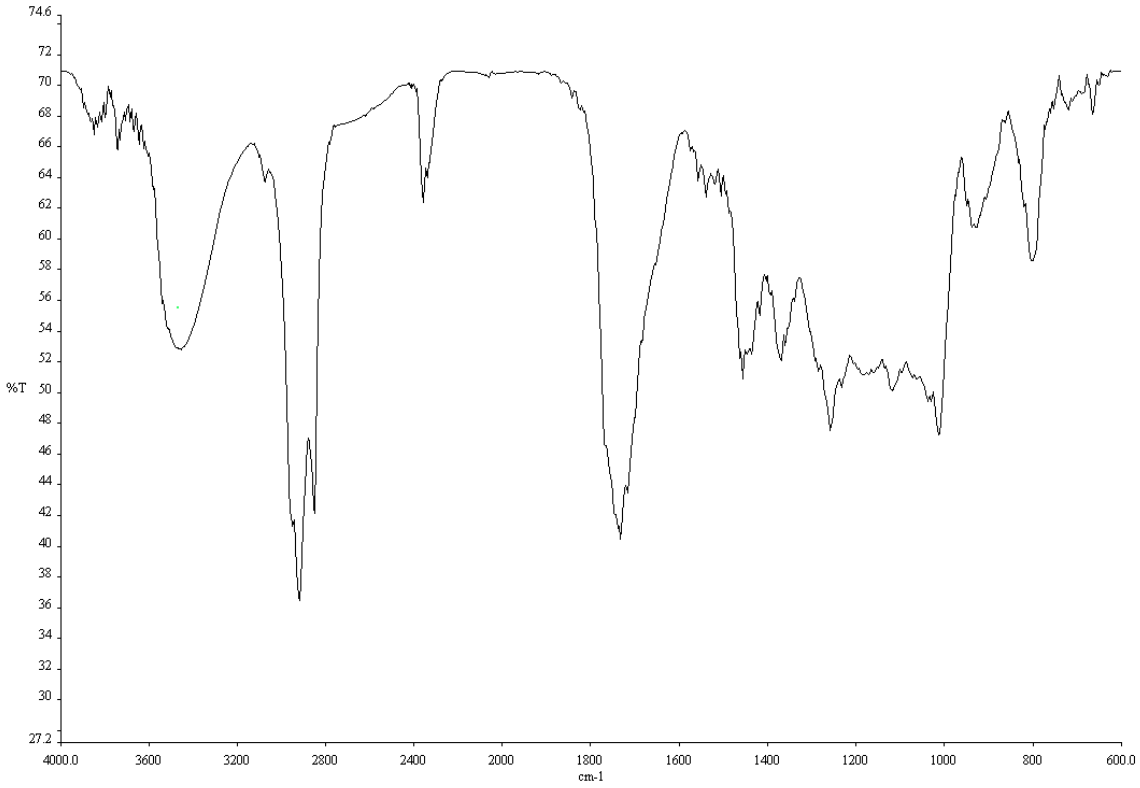

Figure A1.59. *Infrared spectrum (Thin Film, NaCl) of compound* ***42****.*

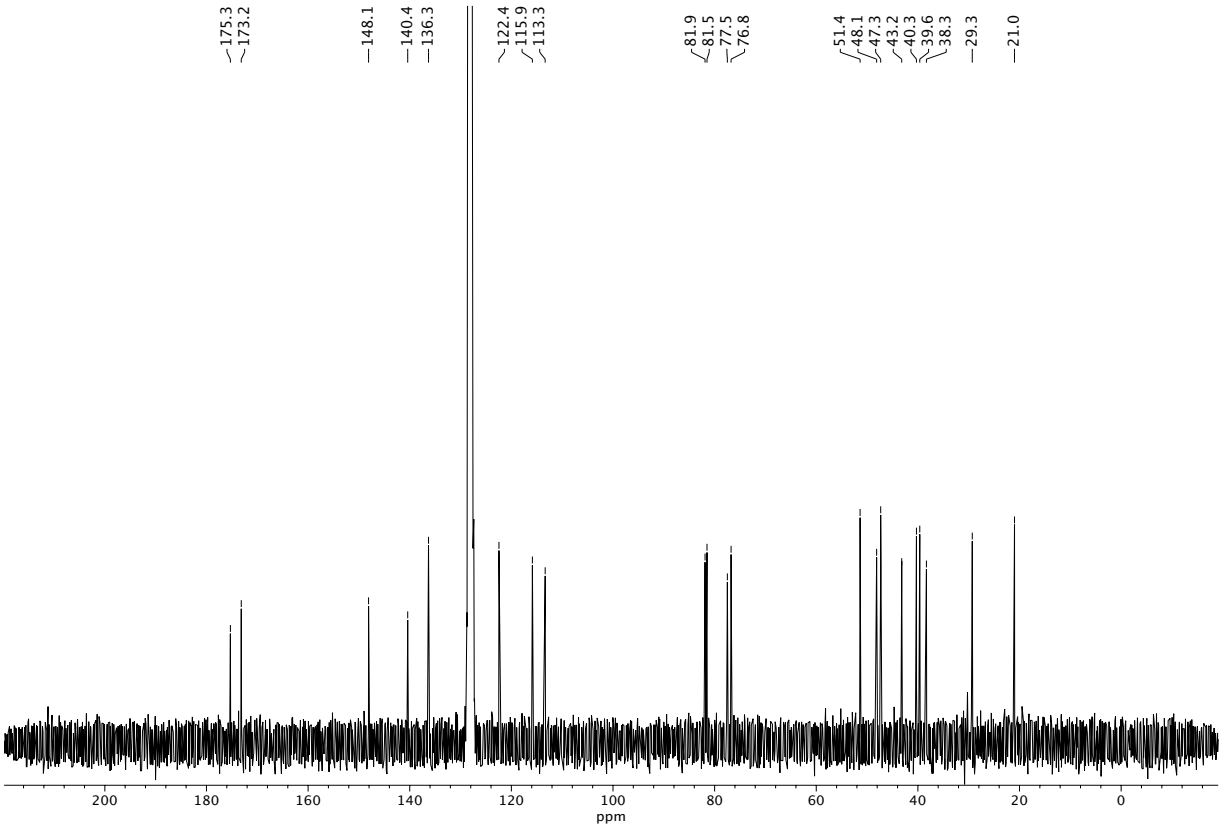

Figure A1.60. *^{13}C NMR (100 MHz, C_6D_6) of compound* ***42****.*

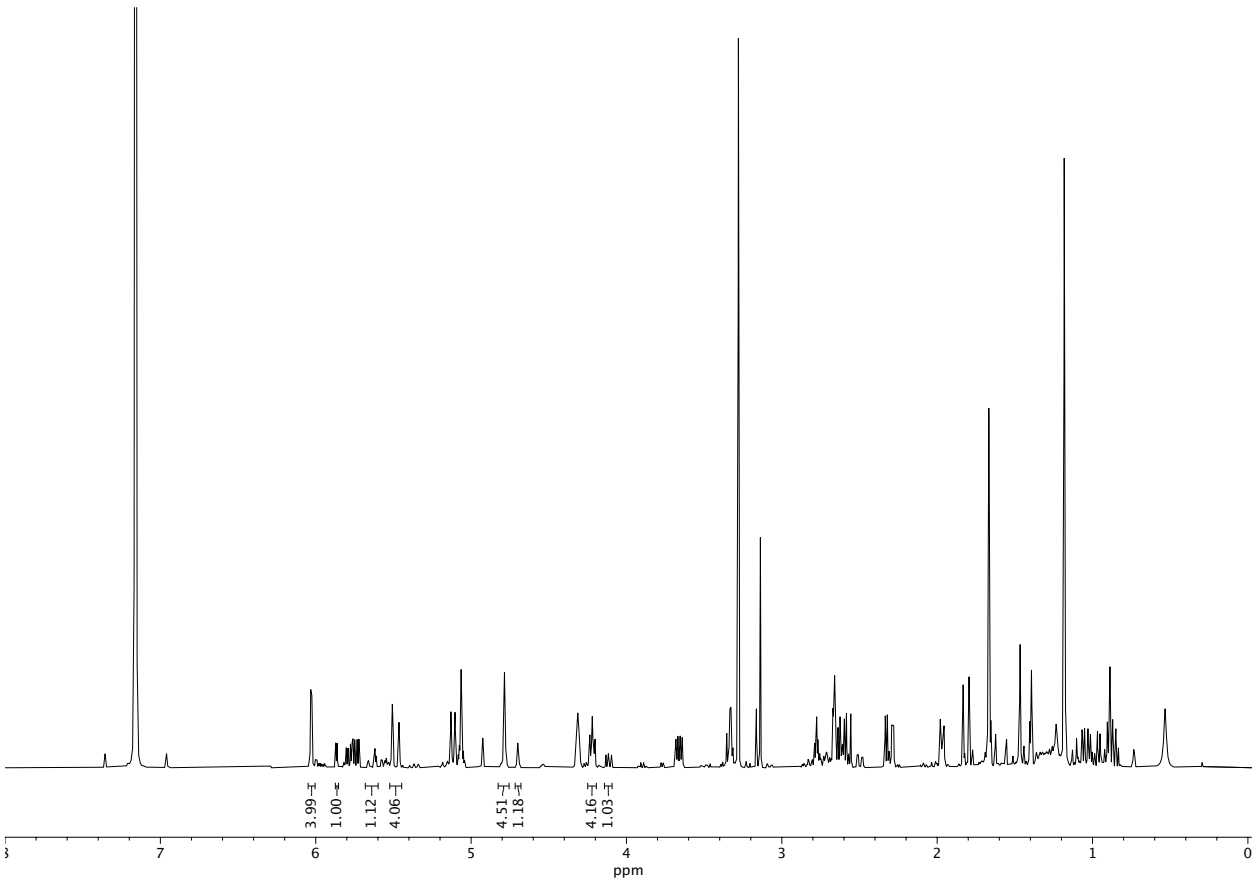

Figure A1.61. *^{1}H NMR (400 MHz, C_6D_6) of compound **42** (80% pure– as isolated by flash chromatography).*

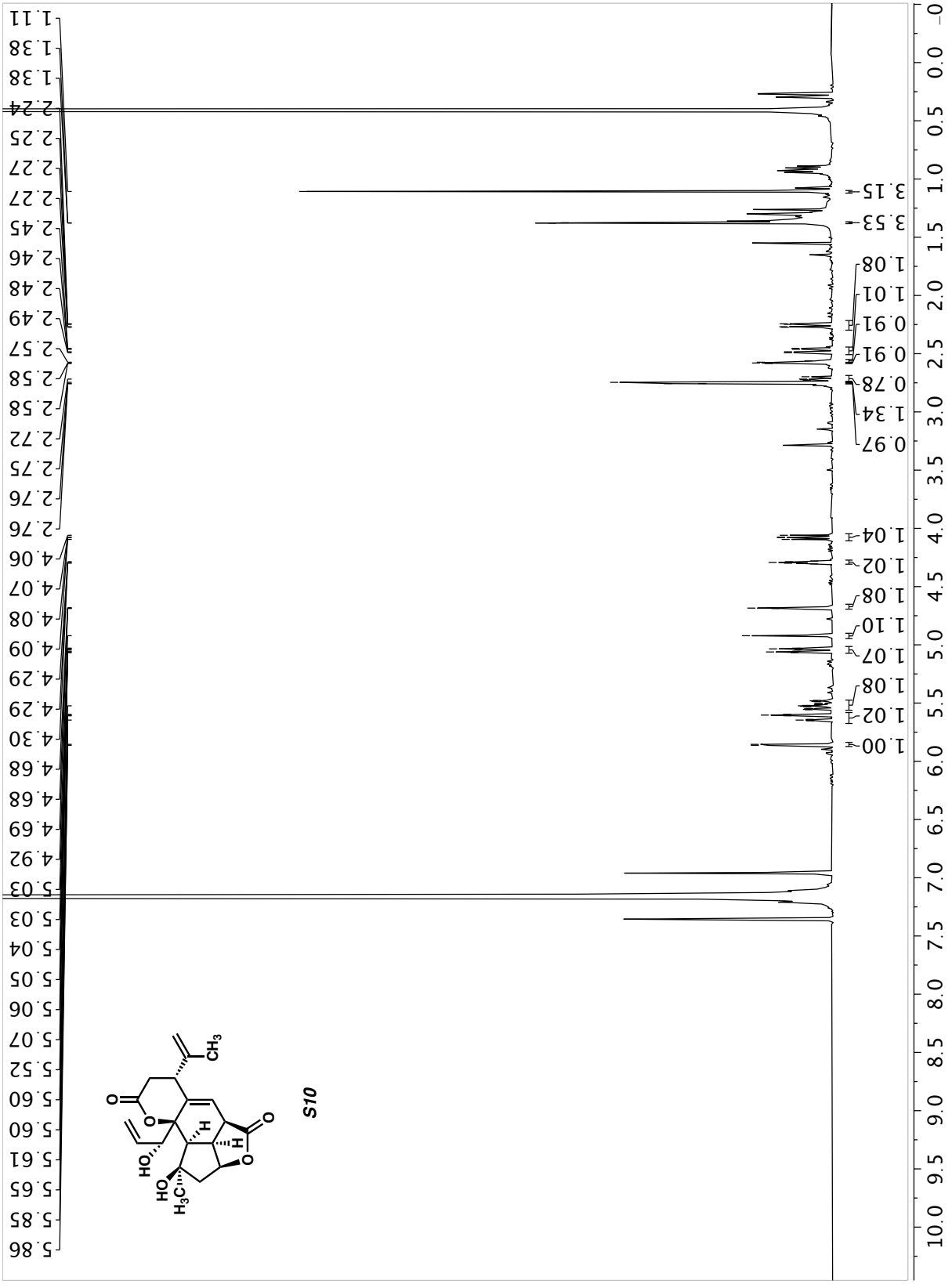

Figure A1.62. *^1H NMR (400 MHz, C_6D_6) of compound* ***S10***.

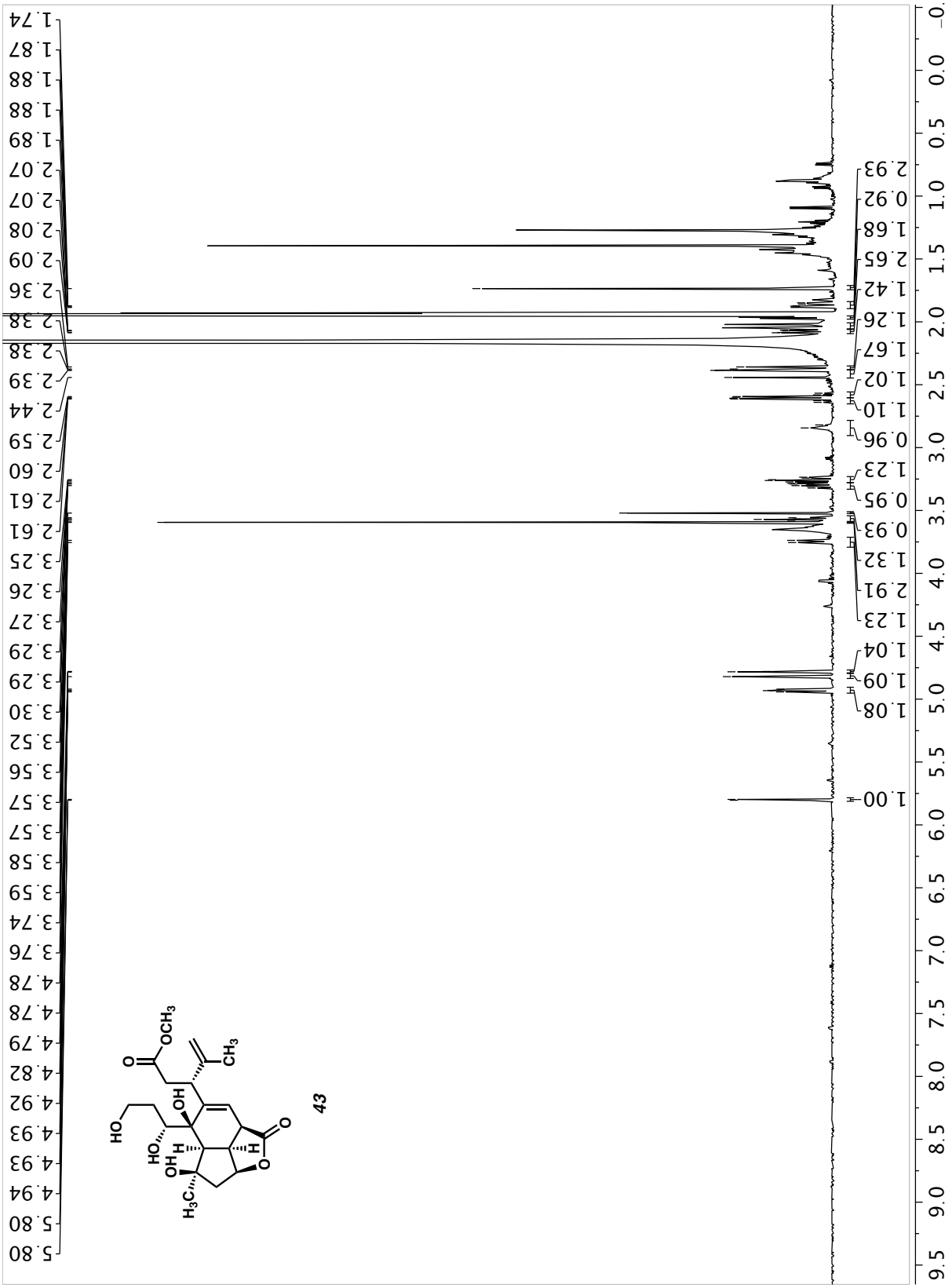

Figure A1.63. *^{1}H NMR (400 MHz, CD_3CN) of compound* ***43***.

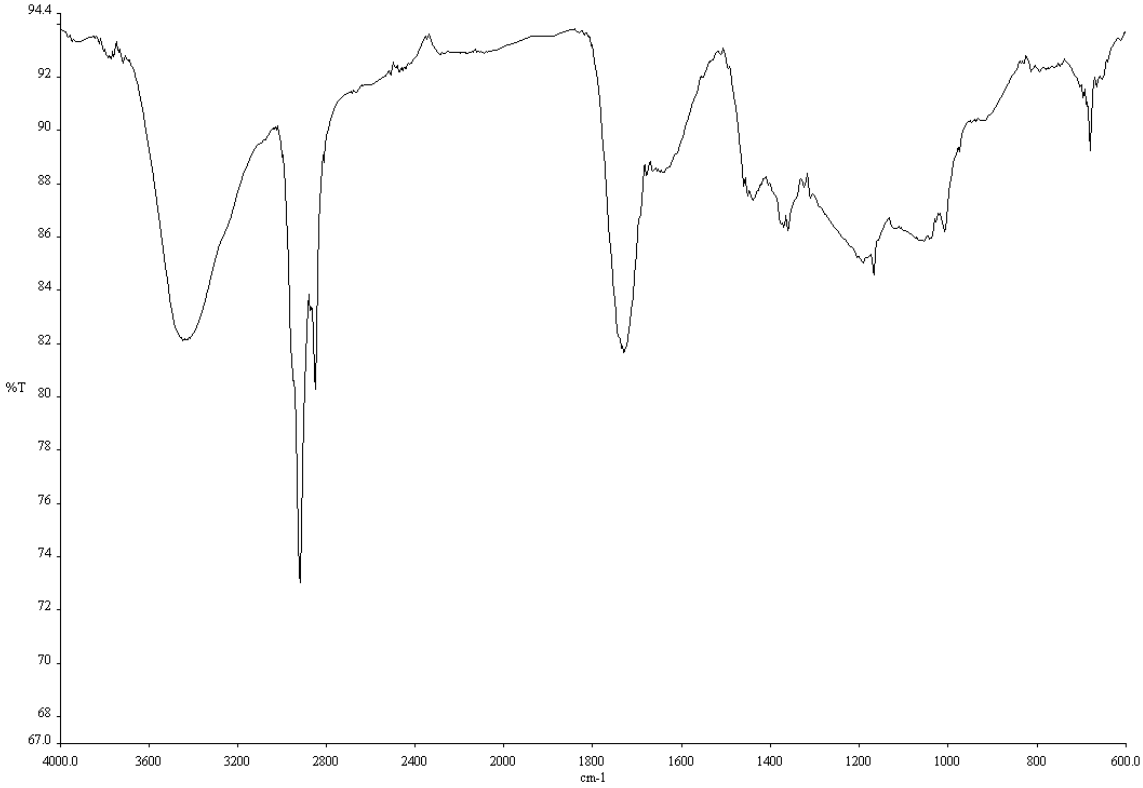

Figure A1.64. *Infrared spectrum (Thin Film, NaCl) of compound* ***43***.

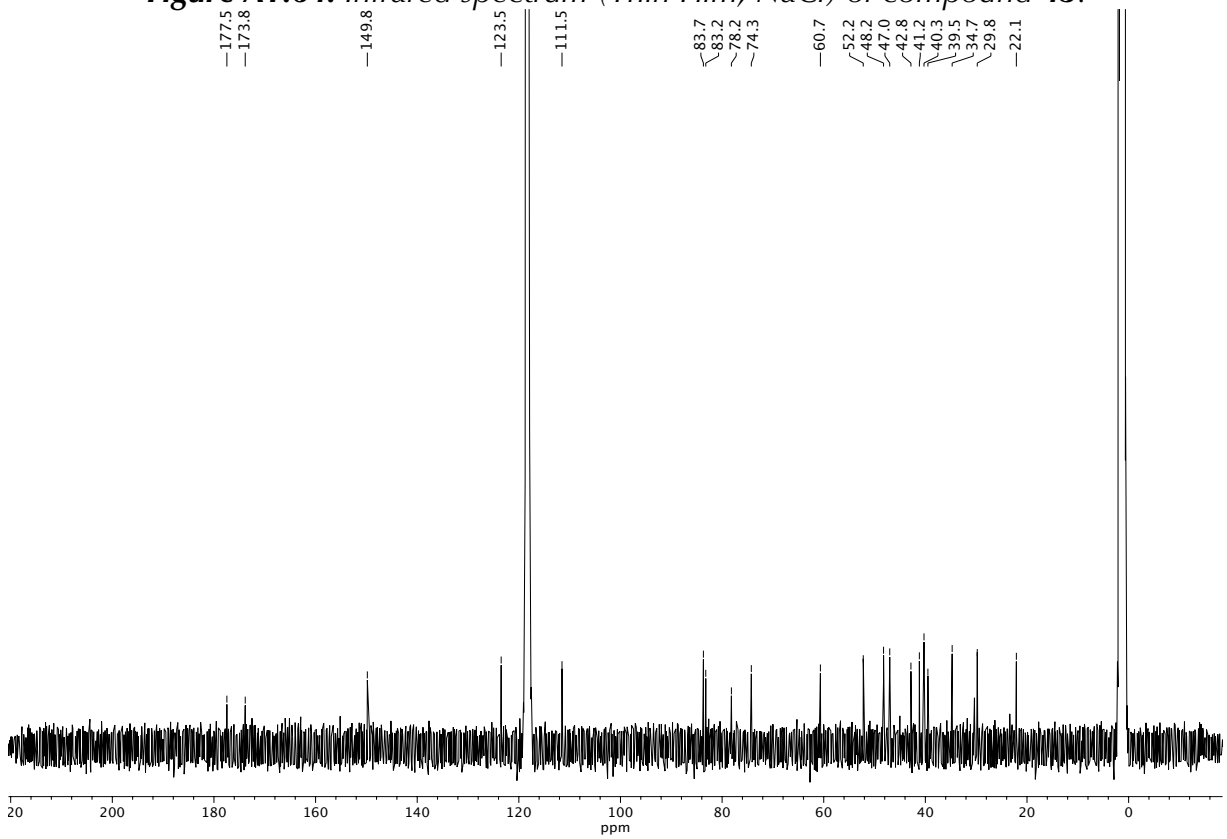

Figure A1.65. *^{13}C NMR (100 MHz, CD_3CN) of compound* ***43***.

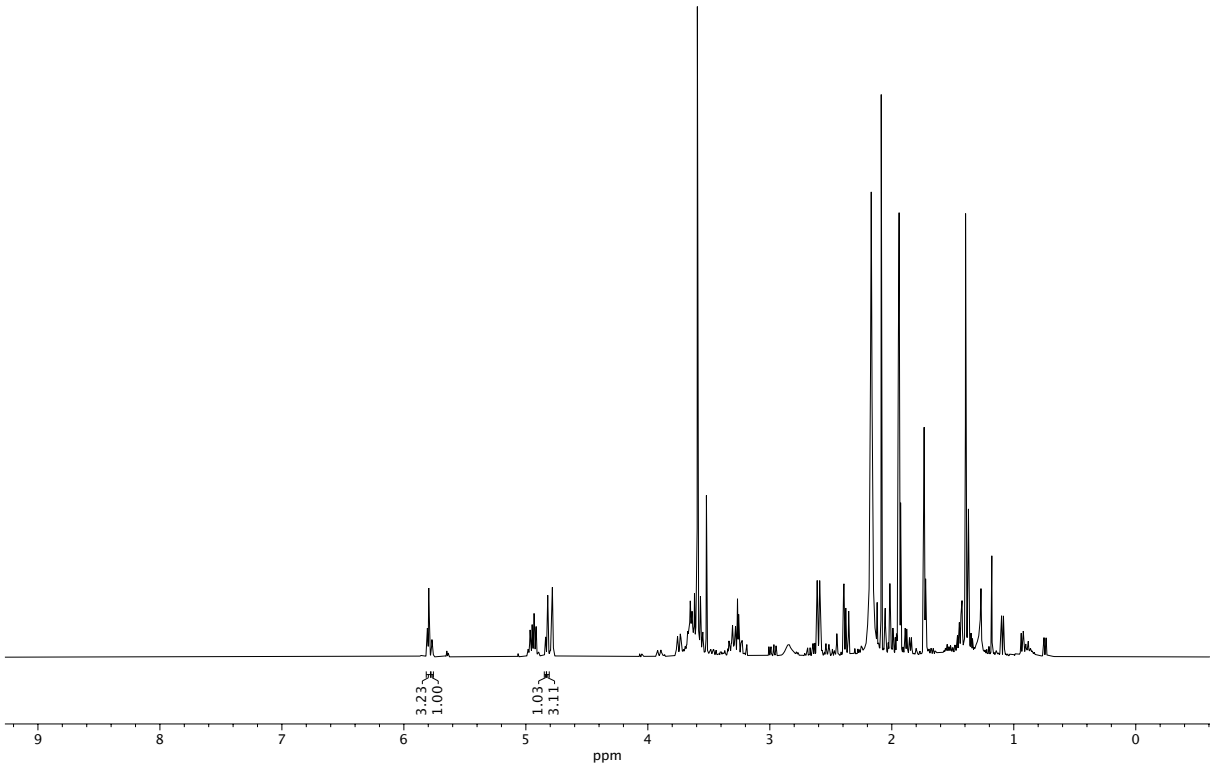

Figure A1.66. *^{1}H NMR (400 MHz, CD_3CN) of compound* ***43*** *(75% pure– as isolated by flash chromatography).*

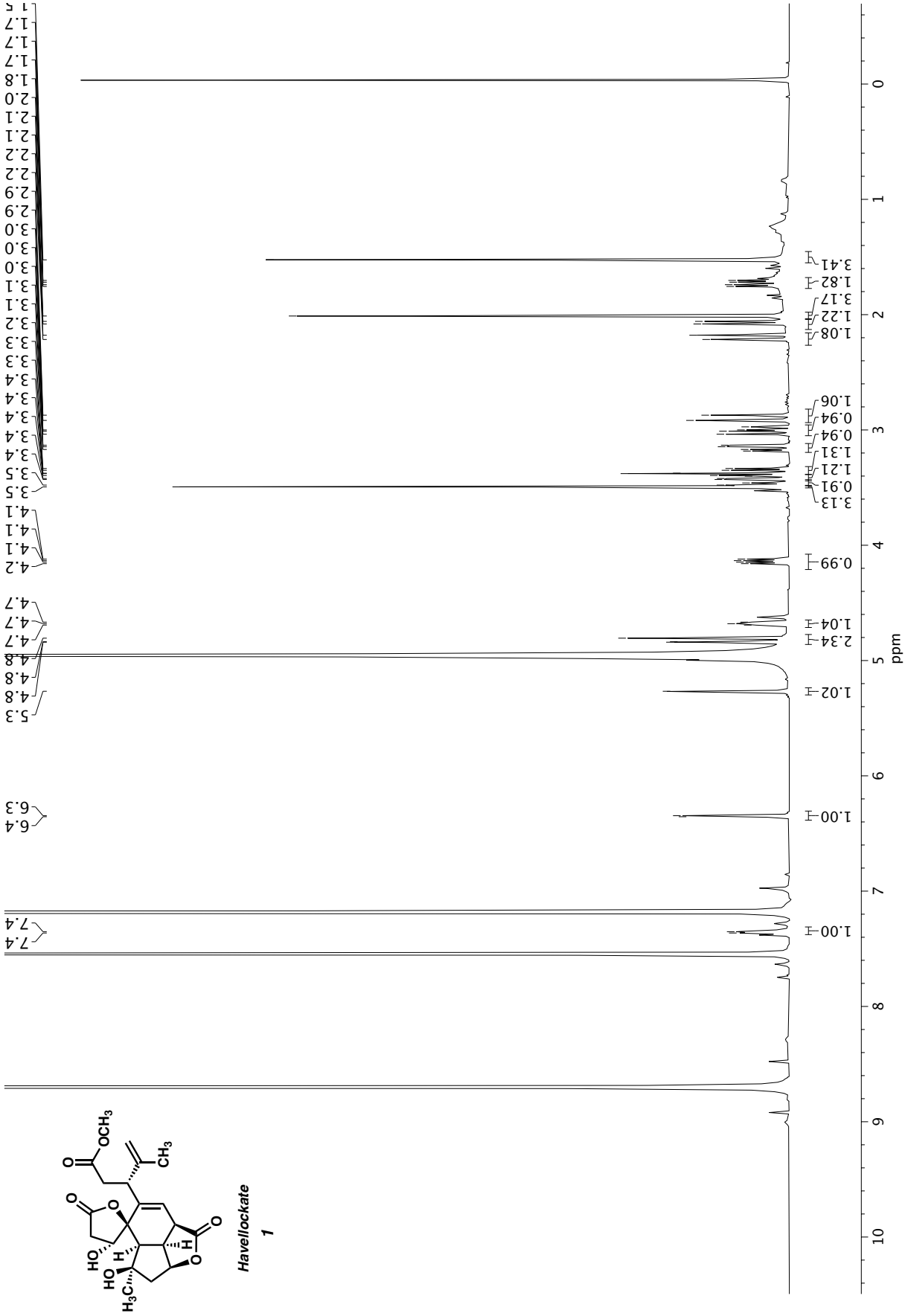

Figure A1.67. *^{1}H NMR (400 MHz, C_5D_5N) of havellockate (**1**).*

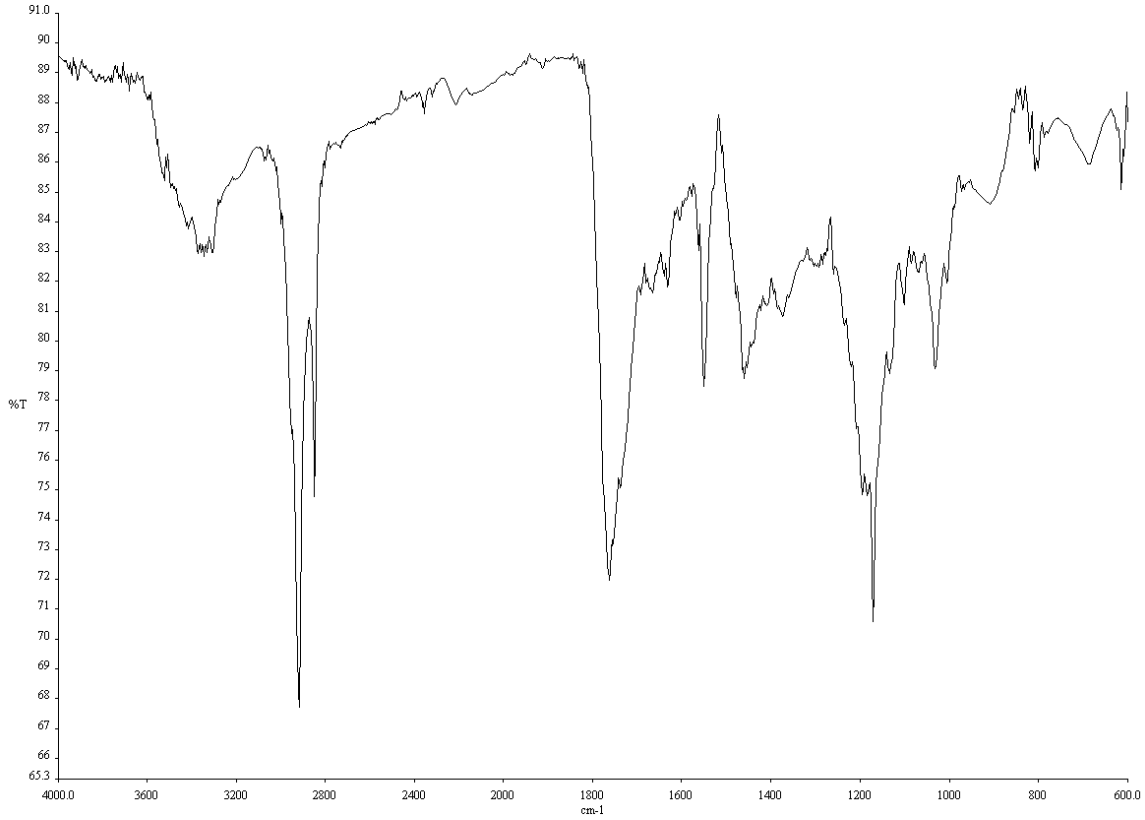

Figure A1.68. *Infrared spectrum (Thin Film, NaCl) of havellockate (**1**).*

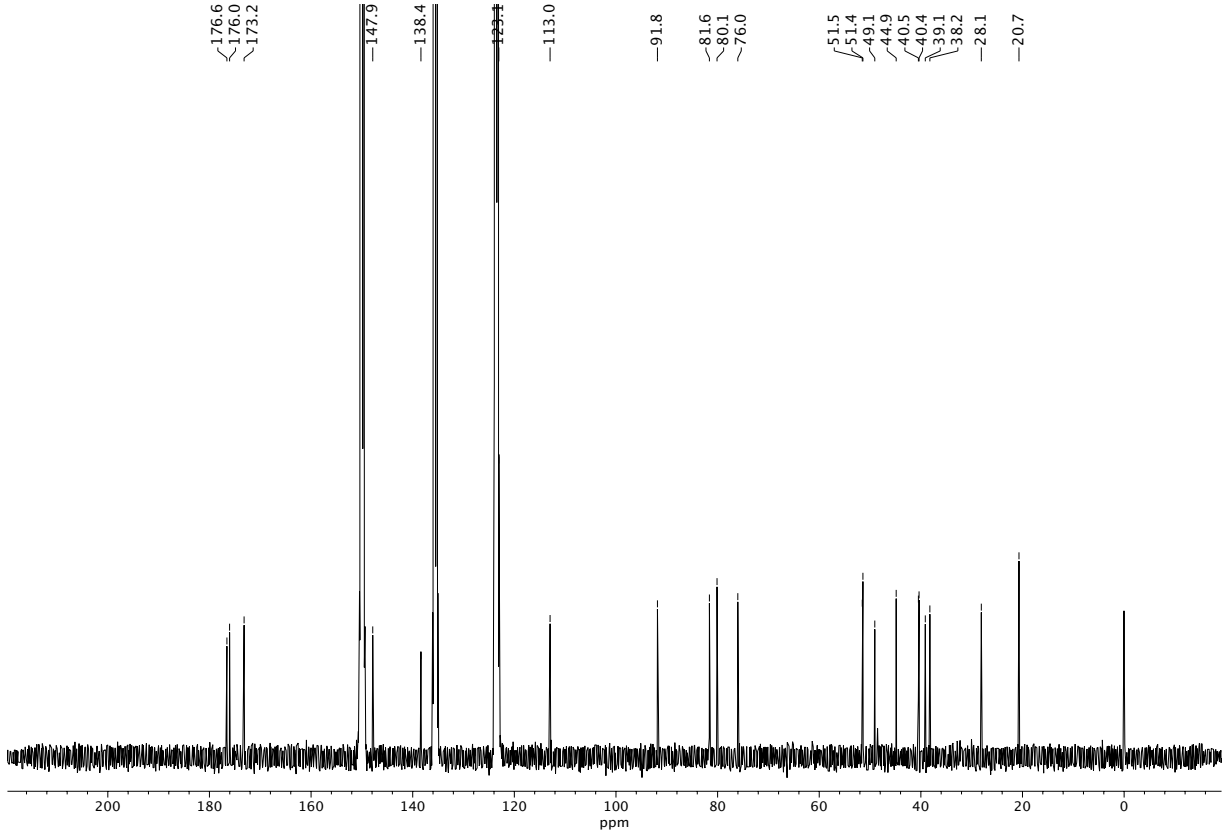

Figure A1.1. *^{13}C NMR (100 MHz, C_5D_5N) of havellockate (**1**).*

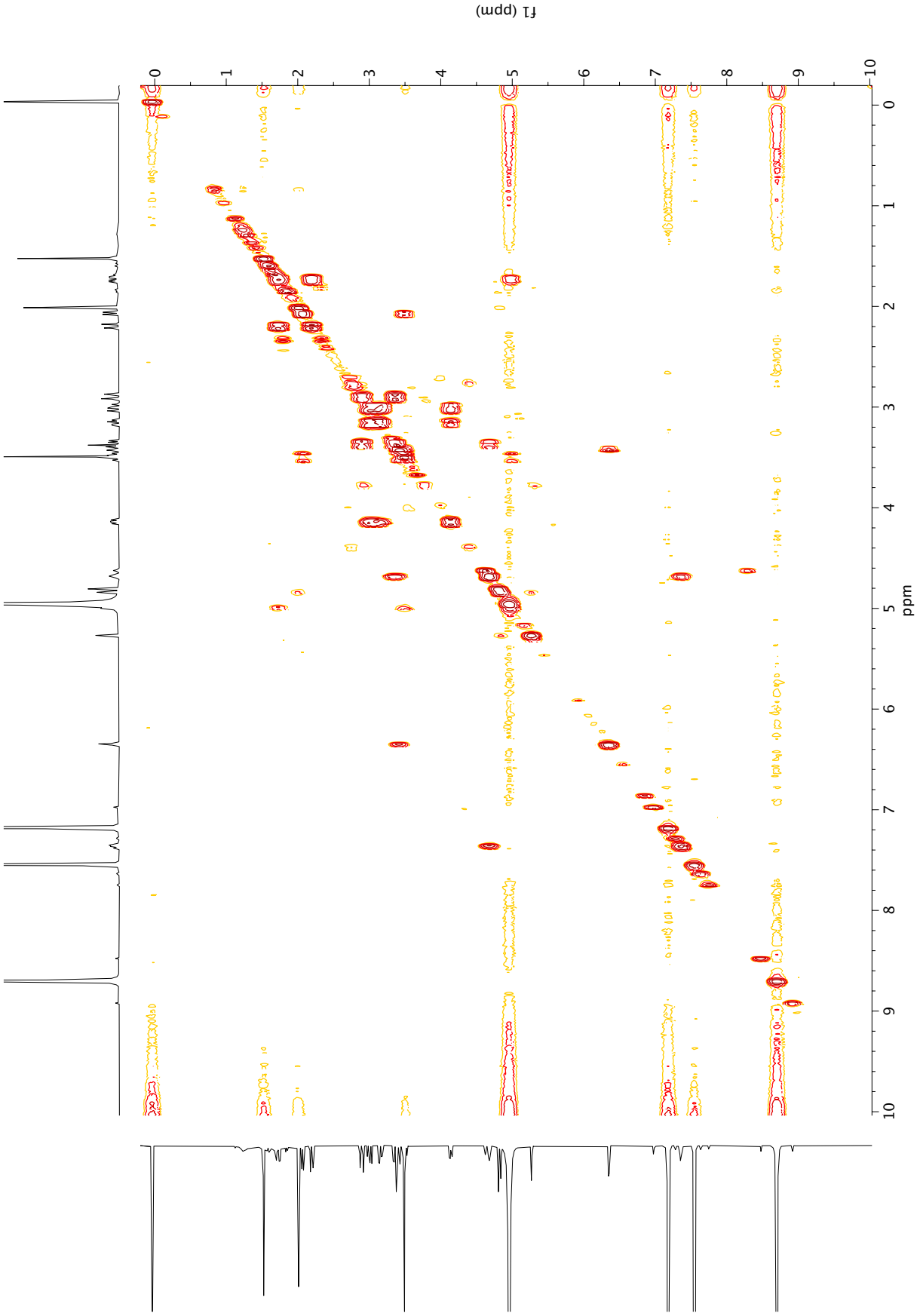

Figure A1.69. *COSY (400 MHz, C_5D_5N) of havellockate (**1**).*

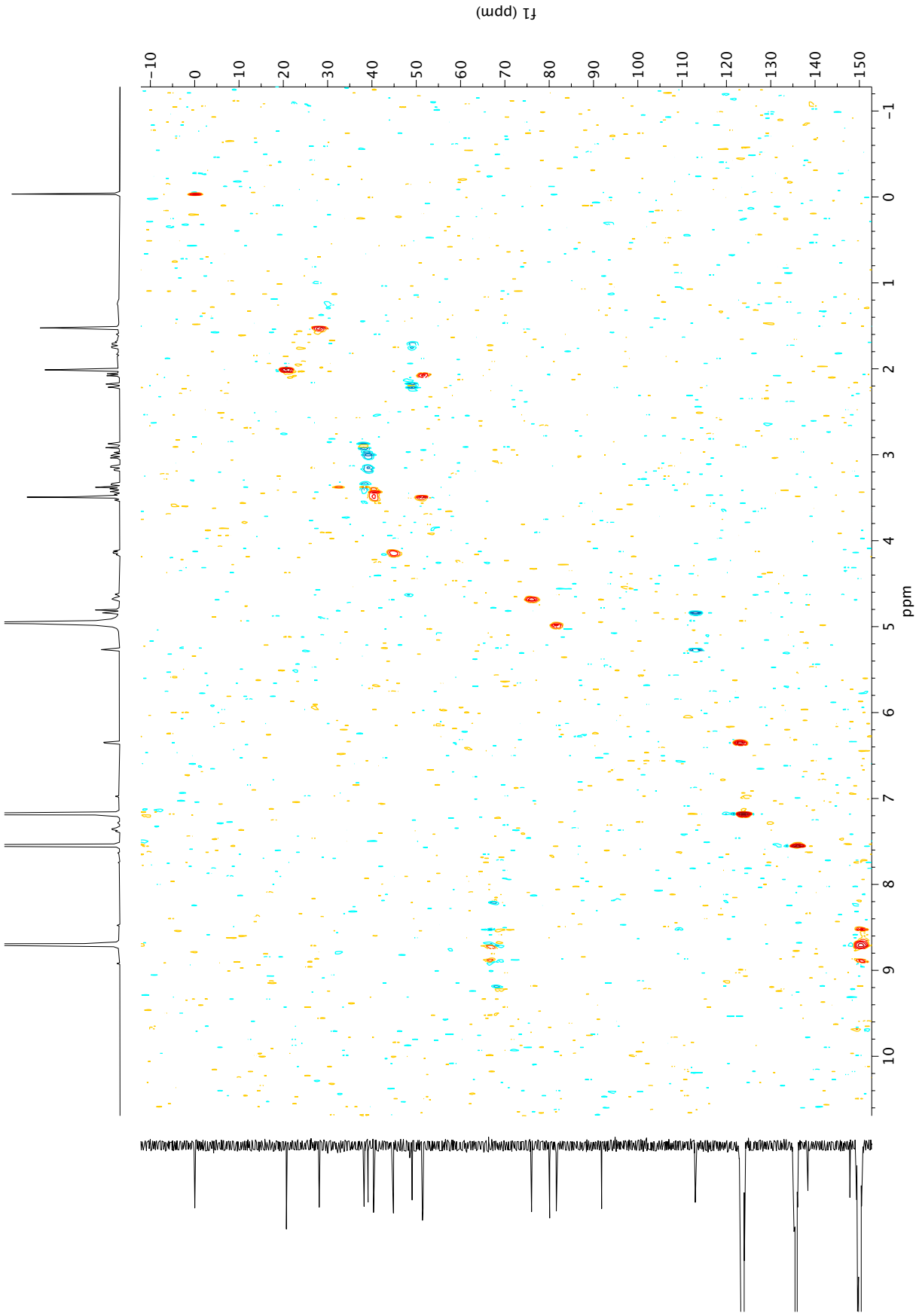

Figure A1.70. *HSQC (400 MHz, C_5D_5N) of havellockate (**1**).*

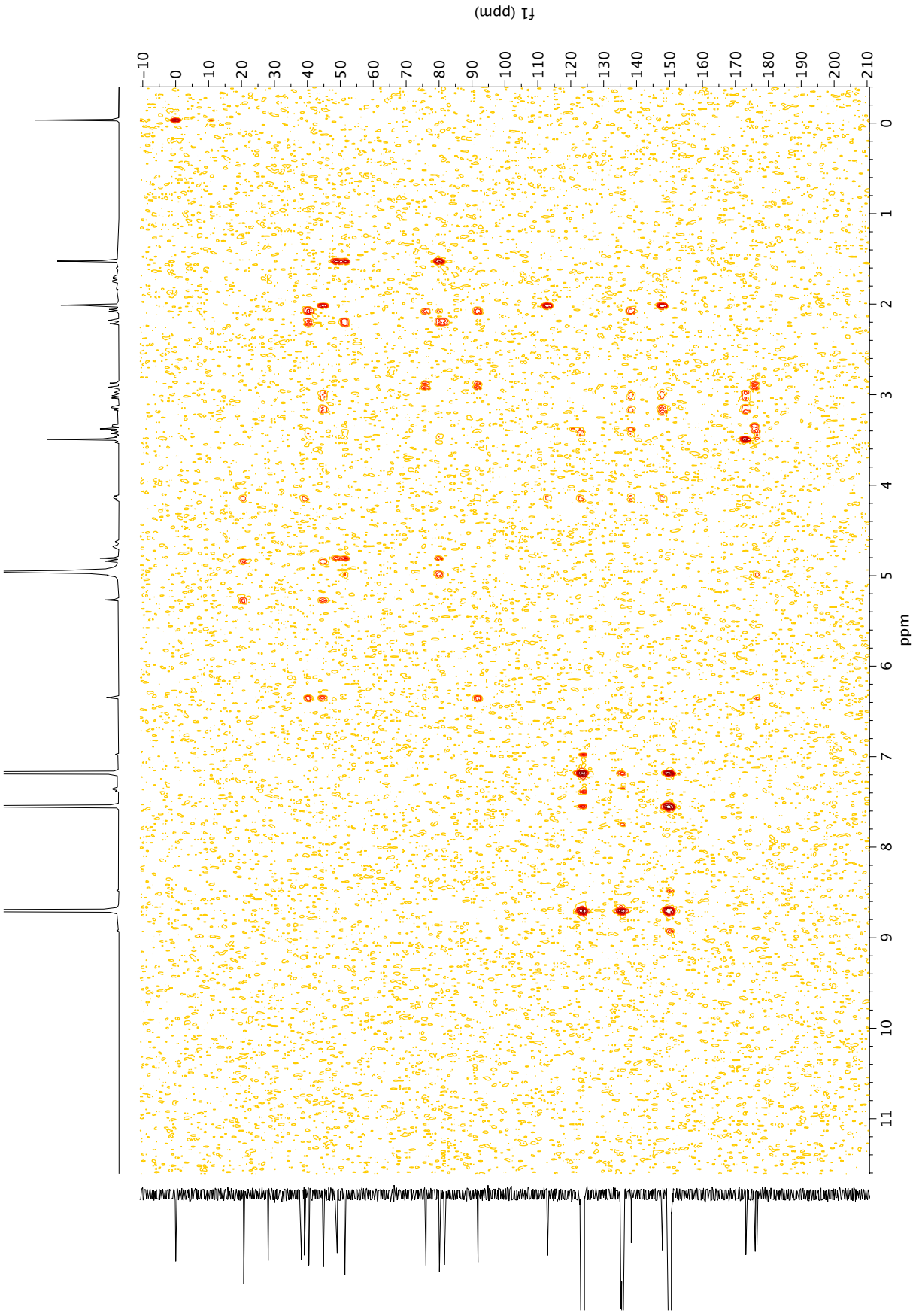

Figure A1.71. *HMBC (400 MHz, C_5D_5N) of havellockate (**1**).*

CHAPTER 2

An Efficient Route to Construct the 6-5-5 Tricyclic Core of Furanobutenolide-Derived Cembranoids and Norcembranoids

2.1 INTRODUCTION

For decades, synthetic chemists have been intrigued by the vast array of complex natural products sourced from marine organisms.[1] Among these, the soft corals of the genus Sinularia have garnered significant attention, offering a wide array of macrocyclic and polycyclic compounds.[2] Notably, the polycyclic furanobutenolide-derived cembranoid and norcembranoid natural products derived from these corals have posed considerable challenges as synthetic targets. The intricate structures coupled with the promising bioactivities exhibited by these compounds continue to lure synthetic chemists toward the pursuit of these intriguing molecules. To date, several total syntheses have been reported in literature.[3,4]

Scheme 2.1.1 *Shortened forward synthesis of Havellockate (**1**)*

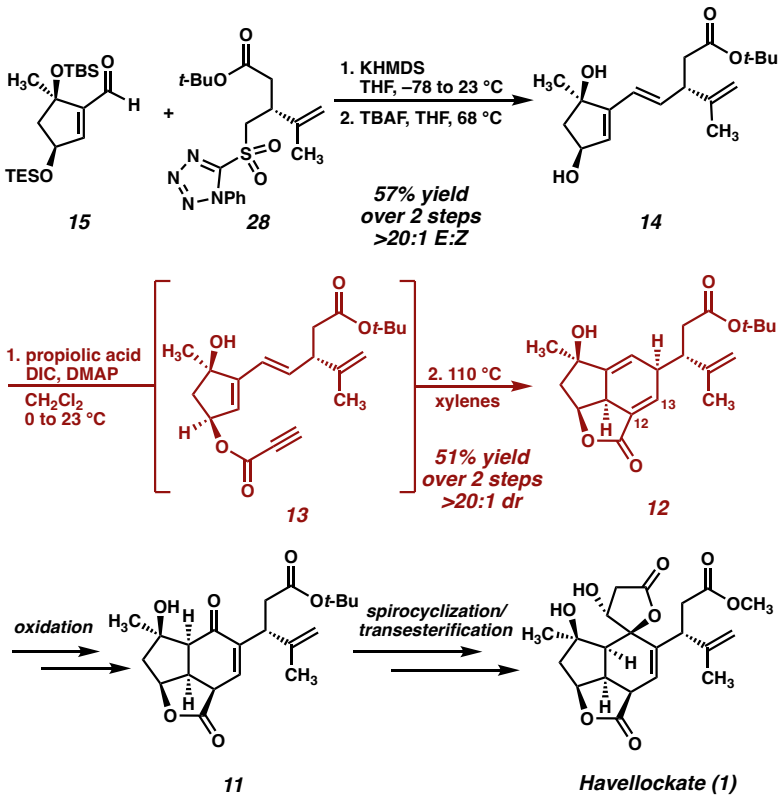

In 2022, our lab reported the first asymmetric total synthesis of havellockate (**1**), a C20-cembranoid first isolated in 1998 from *Sinularia granosa*.[4h, 5] This synthesis utilized starting materials **15** and **28**, both easily accessed via commercially available compounds, in a Julia–Kocienski olefination to afford diol **14**. Diol **14** was subjected to a pivotal esterification/Diels–Alder cascade (illustrated in red in Scheme 2.1.1), which facilitated the efficient construction of the natural product's tricyclic core with high diastereoselectivity. While this key sequence successfully yielded the desired product, it was not without its constraints.

Firstly, subjecting diol **14** to Steglich acylation conditions yields ester **13**, but efforts to isolate and purify it led to decomposition due to its sensitivity to silica, rotovap concentration, and mildly acidic NMR solvents. We have attributed this instability partly to the unsubstituted propiolate alkyne. To address this issue, the reaction mixture is rapidly passed through a silica plug with xylenes, and the partially purified product is promptly utilized in the subsequent Diels–Alder reaction. Furthermore, the intramolecular [4+2] cascade yields only a modest 51% over two steps. Despite various optimization attempts such as exploring alternative propiolic acids (Scheme 2.1.2A), introducing substitutions at the alkyne's terminal position, or attempting the corresponding intermolecular Diels–Alder reaction of diol **14** with propiolate **47** (Scheme 2.1.2B), all endeavors have proven unsuccessful.

Scheme 2.1.2 *A) Representative unsuccessful attempts to enhance the acylation step. B) Failed attempt to improve the cycloaddition sequence.*

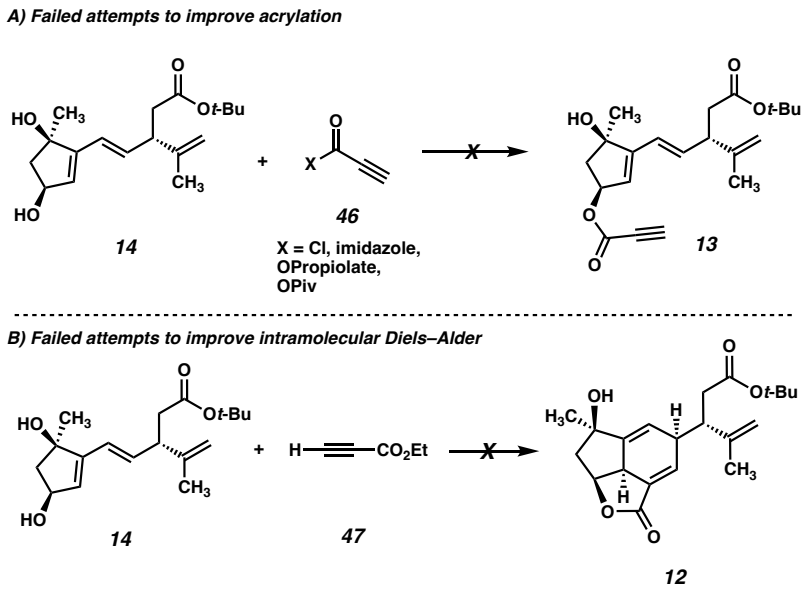

Despite the challenges encountered in this sequence, the tricyclic product (**12**) obtained can be further advanced to enone **11** through a series of high-yielding oxidative manipulations. Upon spirocycle formation and transesterification, the total synthesis of havellockate (**1**) was achieved. The 6-5-5 tricyclic core present in enone **11** constitutes a common structural motif within the polycyclic furanobutenolide-derived natural product family (highlighted in red in Figure 1), exemplified by compounds like scabrolide A (**48**) and dissectolide A (**49**). Consequently, it becomes imperative to find enhancements in the formation of the tricyclic core to establish a uniform approach for accessing other molecules within this natural product family.

Figure 2.1.3 *Common motif of 6-5-5 fused cycle for furano(nor)cembranoids.*

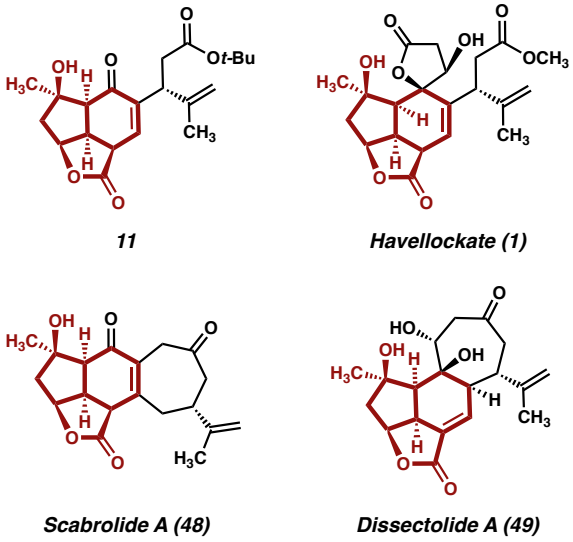

2.2 PROPARGYL ETHER ROUTE DEVELOPMENT

We proposed that the challenges encountered in this transformation are not only attributed to the instability of the acylation product **13**, but also to the structural constraints imposed by its ester moiety. This structural feature appears to hinder the substrate's ability to adopt the requisite conformation for the intramolecular Diels–Alder reaction.[4d] Keeping these considerations in mind, we directed our focus toward a propargyl ether counterpart (32).

Scheme 2.2.1 *Synthesis of tricyclic product 33 from diol 14 via propargyl ether route.*

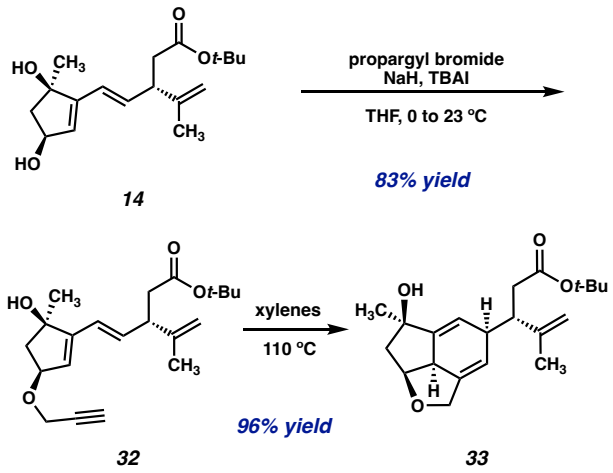

To synthesize the desired ether, our initial approach involved treating diol **14** with propargyl bromide under basic alkylation conditions, affording ether **32** with an impressive 83% yield (Scheme 2.2.1). Subsequently, the intramolecular Diels-–Alder reaction occurred smoothly, forming cyclic ether **33** with an outstanding 96% yield, nearly doubling the productivity achieved from the acylation/cycloaddition sequence presented in Scheme 2.1.1. This discovery brought us considerable satisfaction, not only due to the enhanced yield of the reaction but also because the intermediates proved to be significantly more

stable and easier to handle compared to their propargyl ester counterparts. To propel our synthesis forward, the next pivotal step entailed the allylic oxidation of ether **33** to its corresponding ester (**12**).

Table 2.2.2 *Failed attempts to oxidize ether 33 to ester 12.*

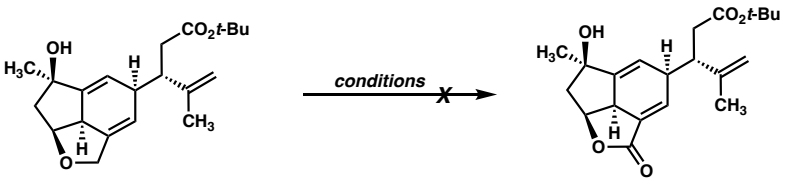

33 ***12***

Entry	Conditions	Result
1	PCC, DCE, 70 °C	Undesired oxidation
2	CrO_3, 3,5-dimethylpyrazole, CH_2Cl_2, –35 °C to reflux	No reaction
3	$RuCl_3$, *t*-BuOOH, $Mg(OAc)_2$, CH_2Cl_2/H_2O	Decomposition
4	Cr(V), MnO_2, 15-crown-5, DCE, 80 °C	Decomposition
5	White Catalyst, benzoquinone, AcOH, 1,4-dioxane	Decomposition

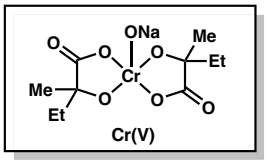

Cr(V)

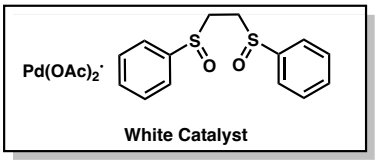

White Catalyst

However, despite our endeavors, we encountered obstacles in achieving this transformation. When employing PCC or other conventional oxidizing agents, we encountered issues such as over-oxidation or undesired allylic oxidation, attributable to the presence of multiple allylic C–H bonds in ether **33**. We then explored an alternative approach involving 3,5-dimethylpyrazole and chromium trioxide, following a procedure documented by Havens and colleagues.[6] However, this method yielded only unreacted starting material (Table 2.2.2, entry 2). Similarly, Maimone and collaborators explored various allylic oxidation conditions in their synthesis of sesterterpenes[7], finding success

with the ruthenium-catalyzed oxidation method described by Merck.[8] Yet, our attempts using these conditions led solely to the decomposition of the starting material (entry 3). Furthermore, a procedure employed in the total synthesis of ritterazine B, as reported by Reisman and colleagues[9], utilizing oxochromate (Cr(V)), also proved ineffective in our hands (entry 4). We also utilized catalysts developed in the White lab for oxidizing this allylic C–H bond, yet these attempts also resulted in decomposition (entry 5).[10]

Despite encountering difficulties in oxidizing at this stage of the synthesis, we proceeded with the remainder of the synthetic pathway, deferring oxidation to a later stage. Thus, we subjected ether **33** to a three-step oxidation protocol previously utlized in our total synthesis of havellocate (**1**).[4h] Initially, employing V-catalyzed directed epoxidation yielded epoxide **50** as a single diastereomer (Scheme 2.2.3). Subsequent Ti-catalyzed reductive epoxide opening afforded diol **51** in excellent yield. Finally, under oxidation conditions with IBX, the secondary alcohol was converted to ketone **52**. It's worth noting that our attempts at allylic oxidation were also extended to epoxide **50** and ketone **52**, yielding similar unsuccessful outcomes.

Scheme 2.2.3 *A) Synthesis of ketone 16 from ether 33. B) Olefin migration observed under oxidation with IBX in our reported havellockate (1) synthesis.*[4h]

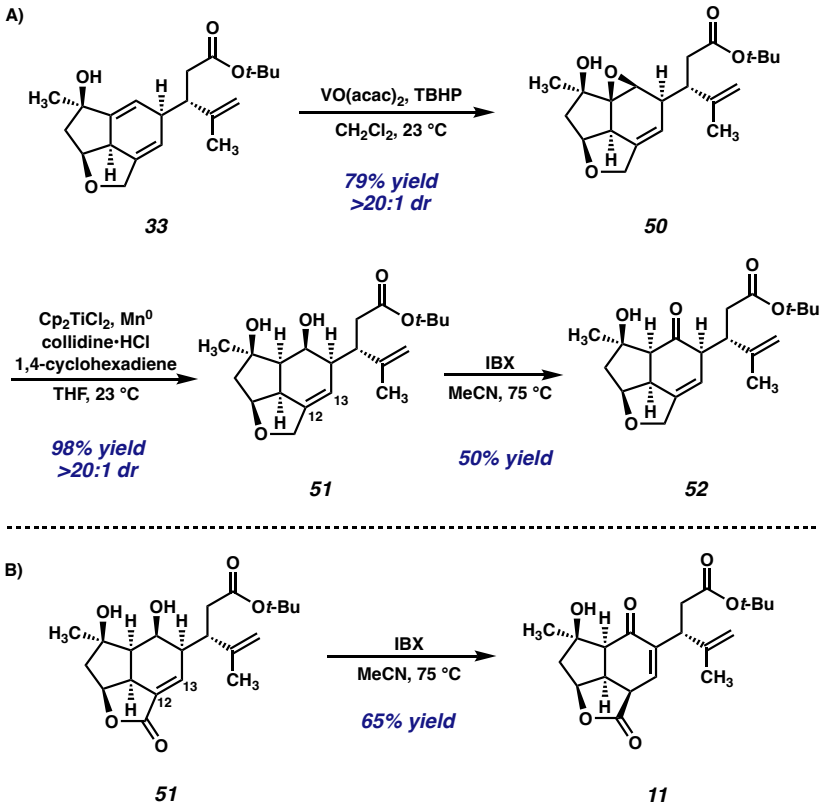

An intriguing observation emerged during our havellockate synthesis: under IBX oxidation conditions, we noted the concurrent migration of the Δ12,13 olefin into conjugation with the newly formed ketone, resulting in the generation of enone **11** (Scheme 4B). However, in the case of diol **51**, such olefin migration did not occur upon IBX oxidation. This observation is particularly noteworthy considering that some natural products within the polycyclic furanobutenolide family, such as dissectolide A (Scheme 2.2.4), feature the Δ12,13 olefin in a similar position as ketone **52**. This phenomenon presents a promising avenue for targeting dissectolide A (**49**) via our synthetic route.

Scheme 2.2.4 *Potential natural product target of ketone 52.*

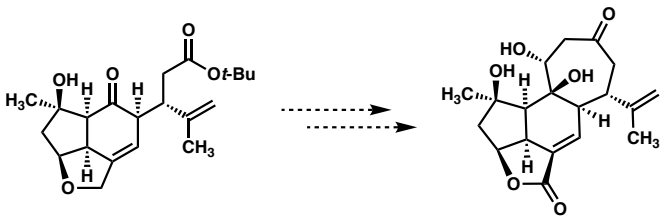

52 ***Dissectolide A (49)***

2.3 CONCLUSION

In summary, we have presented a highly efficient intramolecular Diels–Alder reaction for the rapid assembly of the fused 6-5-5 tricycle found in numerous furanobutenolide-derived cembranoids and norcembranoids. This synthetic pathway not only demonstrated remarkable yield but also exhibited excellent diastereoselectivity. Despite encountering challenges in oxidizing the newly formed ether to its corresponding ester (4), we speculate that enzymatic methods might offer a viable solution for achieving this transformation. Furthermore, the presence of unoxidized substrate effectively prevents olefin migration upon oxidation with IBX, presenting novel opportunities for pursuing synthetic targets within the marine natural product family, such as dissectolide A. This observation underscores the potential of our synthetic approach to unlock new avenues for accessing structurally complex molecules in this intriguing class of compounds.

2.4 SUPPORTING INFORMATION

2.4.1 MATERIALS AND METHODS

Unless otherwise stated, reactions were performed in flame-dried glassware under a nitrogen atmosphere using dry, deoxygenated solvents. Solvents were dried by passage through an activated alumina column under argon. Reaction progress was monitored by thin-layer chromatography (TLC). TLC was performed using E. Merck silica gel 60 F254 precoated glass plates (0.25 mm) and visualized by UV fluorescence quenching, p-anisaldehyde, or KMnO4 staining. Silicycle SiliaFlash® P60 Academic Silica gel (particle size 40–63 μm) was used for flash chromatography. 1H NMR spectra were recorded on Varian Inova 500 MHz and 600 MHz and Bruker 400 MHz spectrometers and are reported relative to residual CHCl3 (δ 7.26 ppm), C6D6 (δ 7.16 ppm) or CD3OD (δ 3.31 ppm). 13C NMR spectra were recorded on a Varian Inova 500 MHz spectrometer (125 MHz) and Bruker 400 MHz spectrometers (100 MHz) and are reported relative to CHCl3 (δ 77.16 ppm), C6D6 (δ 128.06 ppm) or CD3OD (δ 49.01 ppm). Data for 1H NMR are reported as follows: chemical shift (δ ppm) (multiplicity, coupling constant (Hz), integration). Multiplicities are reported as follows: s = singlet, d = doublet, t = triplet, q = quartet, p = pentet, sept = septuplet, m = multiplet, br s = broad singlet, br d = broad doublet. Data for 13C NMR are reported in terms of chemical shifts (δ ppm). IR spectra were obtained by use of a Perkin Elmer Spectrum BXII spectrometer or Nicolet 6700 FTIR spectrometer using thin films deposited on NaCl plates and reported in frequency of absorption (cm–1). Optical rotations were measured with a Jasco P-2000 polarimeter operating on the sodium

D-line (589 nm), using a 100 mm path-length cell. High resolution mass spectra (HRMS) were obtained from the Caltech Mass Spectral Facility using a JEOL JMS-600H High Resolution Mass Spectrometer in fast atom bombardment (FAB+) or electron ionization (EI+) mode, or using an Agilent 6200 Series TOF with an Agilent G1978A Multimode source in electrospray ionization (ESI+), atmospheric pressure chemical ionization (APCI+), or mixed ionization mode (MM: ESI-APCI+).

List of Abbreviations:

bpy – bipyridine, DIAD – diisopropylazodicarboxylate, DIC – *N*,*N*'-diisopropylcarbodiimide, DMAP – (4-dimethylamino)pyridine, HMDS – hexamethyldisilazide, HPLC – high-pressure liquid chromatography, IBX – 2-Iodoxybenzoic acid, LCMS – liquid chromatography/mass spectrometry, NMR – nuclear magnetic resonance, TBHP – *tert*-butyl hydroperoxide, TBAF – tetrabutylammonium fluoride, TBAI – tetrabutylammonium iodide, TBS – *tert*-butyl dimethylsilyl, TEMPO – (2,2,6,6-tetramethylpiperidin-1-yl)oxyl, TESCl – triethylsilyl chloride, TES – triethylsilyl, THF – tetrahydrofuran

2.4.2 EXPEPRIMENTAL PROCEDURES AND SPECTROSCOPIC DATA

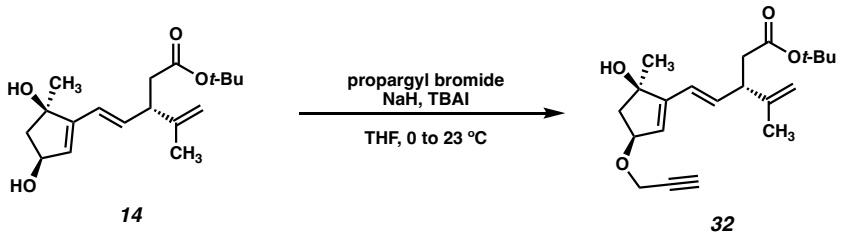

14 *32*

Ether 32: Flame dried 50mL round bottom flask with stir bar and charged with **14** (300 mg, 0.97 mmol, 1.0 equiv) in THF (9.7 mL, 0.1 M). The solution was cooled to 0 °C and stirred for 30 minutes and NaH (60% in mineral oil) (77.8 mg, 1.94 mmol, 2.0 equiv) was added and stirred for another 30 minutes at 0 ºC. TBAI (35.9 mg, 0.097 mmol, 0.1 equiv) and propargyl bromide (434 μL, 4.85 mmol, 5 equiv) were charged, and the reaction was allowed to warm to room temperature and stirred overnight. Reaction quenched by a mixture of MeOH and NH_4Cl. The product was extracted with EtOAc (2 x 10 mL) and DCM (2 x 10 mL). The combined organic layers were washed with brine, dried over $MgSO_4$, filtered, and concentrated under reduced pressure. The crude product was purified by column chromatography (SiO_2, 5–30% EtOAc/Hexanes, solvent polarity was increased in 5% increments) to afford ether **32** (278.6 mg, 83% yield) as a white solid; 1H NMR (400 MHz, CDCl3) δ 6.15 (dd, J = 16.0, 7.8 Hz, 1H), 6.03 (d, J = 16.1 Hz, 1H), 5.81 (d, J = 2.2 Hz, 1H), 4.81 – 4.74 (m, 2H), 4.50 (ddd, J = 6.7, 4.5, 2.2 Hz, 1H), 4.21 – 4.08 (m, 2H), 3.20 (t, J = 7.7 Hz, 1H), 2.52 – 2.35 (m, 4H), 2.17 (s, 3H), 1.71 (t, J = 1.1 Hz, 3H), 1.41 (s, 9H); 13C NMR (101 MHz, CDCl3) δ 171.47, 149.92, 145.90, 135.73, 127.16, 122.93,

111.33, 80.98, 80.56, 79.36, 60.54, 56.23, 49.50, 47.32, 39.52, 28.24, 26.58, 20.81, 14.33.; IR (thin film, NaCl) 3450, 2922, 2854, 1713, 1258, 1098, 849, 800, 689 cm^{-1}; HRMS (ESI) m/z calc'd $C_{21}H_{30}O_4$ $[M+Na]^+$: 369.2036, found: 369.2018; $[\alpha]_D^{25}$ –4.1450 ° (*c* 0.2, $CHCl_3$).

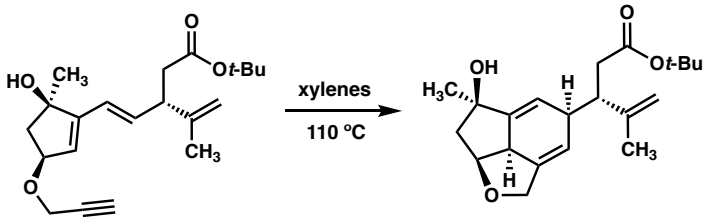

32 ***33***

Cyclohexadiene 33: A flame-dried 50 mL round bottom flask containing xylenes (80 mL) was charged with **32** (277 mg, 0.8 mmol, 1 equiv). This solution was sparged with N_2 for 10 min, then heated to 110 °C and stirred for 3 h. The reaction mixture was cooled to 23 °C, and the xylenes removed by rotary evaporation leaving a yellow residue which was purified by flash chromatography (SiO_2, 5%–40% EtOAc/hexanes with 5% solvent polarity increments) to afford tricycle **33** (265.5 mg, 96% yield) as a white solid; ^{1}H NMR (400 MHz, CDCl3) δ 5.80 – 5.71 (m, 2H), 4.97 – 4.88 (m, 1H), 4.84 (s, 1H), 4.59 (dt, J = 8.9, 6.6 Hz, 1H), 4.40 – 4.32 (m, 2H), 3.03 (t, J = 9.6 Hz, 1H), 2.84 – 2.66 (m, 2H), 2.50 – 2.30 (m, 3H), 2.17 (s, 1H), 1.76 (s, 3H), 1.60 (dd, J = 12.9, 6.2 Hz, 1H), 1.42 (s, 9H), 1.36 (s, 3H); ^{13}C NMR (101 MHz, CDCl3) δ 172.09, 151.37, 145.17, 142.77, 123.42, 119.45, 113.33, 81.28, 80.53, 77.67, 71.67, 50.68, 47.64, 46.37, 39.91, 37.00, 28.23, 27.29, 20.58; IR (thin film, NaCl) 3402, 2972, 2926, 2856, 1714, 1444, 1367, 1256, 1146, 1037, 963, 897, 852, 736 cm^{-1}; HRMS (FAB+) m/z calc'd $C_{21}H_{30}O_4$ $[M+Na]^+$: 369.2036, found: 369.2018; $[\alpha]_D^{23}$ + 5.5844 (*c* 0.9, $CHCl_3$).

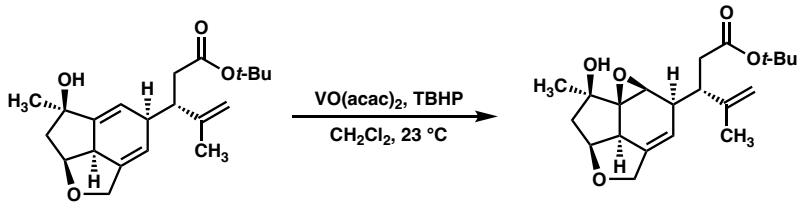

33 ***50***

Epoxide 50: A 100 mL round bottom flask was flame dried and charged with stir bar. $VO(acac)_2$ (17.4 mg, 0.066 mmol, 0.10 equiv) and tricycle **33** (227 mg, 0.66 mmol, 1.0 equiv) were added in CH_2Cl_2 (28.7 mL, 0.023M). To the resulting green, homogenous reaction mixture was added *t*-BuOOH (TBHP) (262 μL, 5.5 M solution in decane, 1.31 mmol, 2.0 equiv) dropwise over 2 min, causing the reaction solution to turn dark red. The reaction was stirred at 20 ºC for 3 h, after which time it turns from dark red to orange. The reaction solution was concentrated and the resultant crude product directly loaded onto a column (SiO_2, 0–35% EtOAc/Hexanes) to afford epoxide **50** (190 mg, 79% yield, >20:1 dr) as a pale yellow solid; ^{1}H NMR (400 MHz, CDCl3) δ 5.22 (dd, J = 2.9, 1.5 Hz, 1H), 4.96 (t, J = 1.5 Hz, 1H), 4.88 (q, J = 1.0 Hz, 1H), 4.54 – 4.45 (m, 1H), 4.43 – 4.39 (m, 1H), 4.21 (ddt, J = 11.3, 3.3, 1.7 Hz, 1H), 3.61 (t, J = 1.0 Hz, 1H), 3.00 (dt, J = 7.3, 2.3 Hz, 1H), 2.86 (dd, J = 10.5, 5.3 Hz, 1H), 2.62 – 2.51 (m, 4H), 2.51 – 2.38 (m, 2H), 1.93 (dd, J = 13.8, 4.5 Hz, 1H), 1.79 (dd, J = 1.4, 0.7 Hz, 3H), 1.42 (s, 9H), 1.39 (d, J = 1.0 Hz, 3H); ^{13}C NMR (101 MHz, CDCl3) δ 171.83, 144.76, 138.00, 117.83, 113.12, 80.59, 77.86, 77.00, 73.04, 69.10, 53.43, 50.12, 47.40, 45.08, 41.59, 36.67, 28.20, 23.37, 21.57. IR (thin film, NaCl) 3467, 3077, 2975, 2930, 1726, 1647, 1453, 1432, 1391, 1366, 1354, 1247, 1167,

1032, 1000, 961, 938, 898, 848, 811, 761, 665 cm^{-1}; HRMS (ESI) m/z calc'd $C_{21}H_{30}O_5$ $[M+Na]^+$: 385.1985; found: 385.1931; $[\alpha]_D^{25}$ – 70.3814 ° (*c* 1.42, $CHCl_3$).

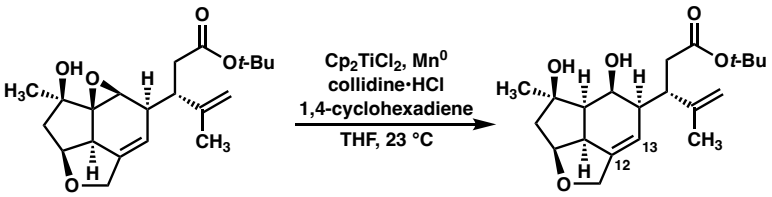

50 ***51***

Diol 51: A 250 mL round bottom flask was flame dried with a stir bar and charged with Cp_2TiCl_2 (185.1 mg, 0.74 mmol, 1.0 equiv), Mn^0 (224.7 mg, 4.09 mmol, 5.5 equiv), collidine•HCl (732.5 mg, 4.64 mmol, 6.25 equiv). The flask was then evacuated and backfilled with N_2 gas. To the flask was then added epoxide **50** (269.5 mg, 0.74 mmol, 1.0 equiv) in THF (39.1 mL). The resulting heterogenous yellow/orange mixture was stirred rapidly and 1,4-cyclohexadiene (316.5 μL, 3.34 mmol, 4.5 equiv) was added dropwise over 2 min. The reaction was stirred for 2 hours at room temperature, after which time it turned from yellow/orange to blue. SiO_2 (20 g) was added to the reaction mixture, the solvent was removed by rotary evaporation, and the solid loaded onto a column and purified by flash chromatography (20–35% EtOAc/DCM) to provide diol **51** (225.3 mg, 84% yield, >20:1 dr) as a pale yellow solid; ^{1}H NMR (400 MHz, CDCl3) δ 5.55 (ddp, J = 3.3, 2.2, 1.0 Hz, 1H), 4.92 – 4.85 (m, 3H), 4.59 (ddd, J = 7.7, 5.2, 2.7 Hz, 1H), 4.48 – 4.39 (m, 2H), 4.27 – 4.11 (m, 1H), 3.99 (s, 1H), 2.93 (ddd, J = 11.4, 9.0, 5.3 Hz, 1H), 2.89 – 2.75 (m, 1H), 2.68 (dd, J = 14.4, 5.4 Hz, 1H), 2.29 (ddd, J = 14.3, 9.3, 7.3 Hz, 2H), 2.10 – 2.01 (m, 1H), 1.86 (dd, J = 13.9, 5.2 Hz, 1H), 1.82 (d, J = 8.5 Hz, 1H), 1.66 (s, 3H), 1.42 (d, J = 3.0 Hz, 12H); ^{13}C NMR (101 MHz, CDCl3) δ 172.46, 145.40, 142.64, 120.51, 114.39, 83.20, 82.70,

80.60, 77.36, 70.88, 67.24, 50.31, 47.63, 45.18, 45.09, 43.61, 38.01, 29.84, 28.26, 28.22, 27.01, 18.76; IR (thin film, NaCl) 3416, 3070, 2971, 2921, 2850, 1722, 1645, 1451, 1391, 1368, 1255, 1146, 1092, 1035, 1019, 952, 892, 847, 806, 736, 636 cm^{-1}; HRMS (FAB+) m/z calc'd $C_{21}H_{32}O_5$ $[M+H]^+$: 365.2323, found: 365.2301; $[\alpha]_D^{25}$ + 0.9675° (*c* 0.20, $CHCl_3$).

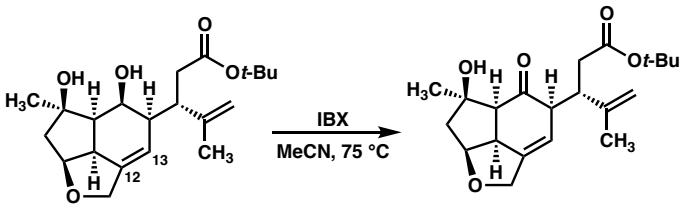

51 ***52***

Ketone 52: A flame dried 20 mL scintillation vial with stir bar was charged with diol **51** (13.7 mg, 0.04 mmol, 1.0 equiv) in MeCN (1.5 mL, 0.025 M). IBX (52.6 mg, 0.19 mmol, 5.0 equiv) was added, and the vial was sealed and placed in a preheated to 75 °C on an aluminum heating block. The suspension was stirred for 1 h at 75 °C, after which no starting material remained (as judged by TLC). The reaction mixture was cooled to 23 °C, then filtered over a pad of SiO_2, rinsing with EtOAc. The filtrate was concentrated by rotary evaporation leaving a crude oil which was purified by flash chromatography (SiO_2, 30–60% EtOAc/hexanes) to afford ketone **52** (7.4 mg, 50% yield) as a foamy yellow solid. Product is suspected to be unstable to air or the impurity is not separable by normal phase chromatography; ^{1}H NMR (400 MHz, C6D6) δ 5.45 (dq, J = 2.9, 1.3 Hz, 1H), 5.00 – 4.95 (m, 2H), 4.32 (dd, J = 7.3, 5.6 Hz, 1H), 4.03 – 3.96 (m, 1H), 3.97 – 3.87 (m, 1H), 3.58 (td, J = 8.6, 5.5 Hz, 1H), 2.94 (dd, J = 14.5, 5.5 Hz, 1H), 2.90 – 2.79 (m, 2H), 2.62 (d, J = 12.0 Hz, 1H), 2.59 – 2.54 (m, 1H), 2.14 – 2.03 (m, 1H), 1.97 (d, J = 8.7 Hz, 1H), 1.79 (dd, J = 1.5, 0.8 Hz, 3H), 1.61 (s, 3H), 1.52 (s, 9H); ^{13}C NMR (101 MHz, C6D6) δ 155.01, 120.48, 94.45, 93.71, 64.66, 63.40, 32.40, 31.02, 28.88, 19.44, 5.90, 0.42, -3.03, -3.43, -9.35, -11.88, -22.70, -23.82, -30.27 IR (thin film, NaCl) 3447, 2972, 2929, 2097, 1714, 1666,

1453, 1391, 1367, 1280, 1256, 1172, 1146, 1092, 1026, 975, 936, 900, 848, 683 cm^{-1}; HRMS (MM:ESI-APCI+) *m/z* calc'd for $C_{21}H_{30}O_5$ $[M+Na]^+$: 385.1927, found 385.1917; $[\alpha]_D^{25}$ + 138.94 ° (*c* 0.2, $CHCl_3$).

2.4.3 REFERENCES FOR EXPERIMENTAL

1) Pangborn, A. M.; Giardello, M. A.; Grubbs, R. H.; Rosen, R. K.; Timmers, F. J. Safe and Convenient Procedure for Solvent Purification. *Organometallics* **1996**, *15*, 1518–1520.

2) Prepared by "Procedure B" in the following reference: Lombardo, M.; Morganti, S.; Trombini, C. 3-Bromopropenyl Esters in Organic Synthesis: Indium- and Zinc-Mediated Entries to Alk-1-ene-3,4-diols. *J. Org. Chem.* **2003**, *68*, 997–1006. The *E/Z* ratio of the material obtained using this procedure varied from 3:1 to 9:1. Batches of 3-bromo-1-acetoxypropene of different *E/Z* ratios performed similarly in the Zn-mediated allylation chemistry (as noted by Lombardo et. al.).

3) Lombardo, M.; Girotti, R.; Morganti, S.; Trombini, C. The First Zinc-promoted, Environmentally Friendly, and Highly Efficient Acetoxyallylation of Aldehydes in Aqueous Ammonium Chloride. *Chem. Commun.* **2001**, 2310–2311.

4) Formation of a similar linear product was observed by Trombini and Lobmardo with allylchromium nucleophiles. They observed that the formation of the linear product increased with steric hinderance of the electrophile. See: Lombardo, M.; Morganti, S.; Licciuli, S.; Trombini, C. 3-Chloro-propenyl Esters in Organic Synthesis: A New Chromium-Catalyzed Homoaldol Reaction. *Synlett* **2003**, *1*, 43–46.

5) Anjaneyulu, A. S. R.; Venugopal, M. J. R. V.; Sarada, P.; Clardy, J.; Lobkovsky, E. Havellockate, A Novel Seco and Spiro Lactone Diterpenoid From the Indian Ocean Soft Coral *Sinularia granosa. Tetrahedron Lett.* **1998**, *39*, 139–142.

2.5 REFERENCES AND NOTES OF CHAPTER

(1) Carroll, A. R.; Copp, B. R.; Davis, R. A.; Keyzers, R. A.; Prinsep, M. R. Marine Natural Products. *Nat. Prod. Rep*. **2022**, *39*, 1122–1171.

(2) Li, Y.; Pattenden, G. Perspectives on the Structural and Biosynthetic Interrelationships Between Oxygenated Furanocembranoids and Their Polycyclic Congeners Found in Corals. *Nat. Prod. Rep***. 2011**, *28*, 1269–1310.

(3) Craig, R. A., II; Stoltz, B. M. Polycyclic Furanobutenolide-Derived Cembranoid and Norcembranoid Natural Products: Biosynthetic Connections and Synthetic Efforts. *Chem. Rev*. **2017**, *117*, 7878−7909.

(4) For previous syntheses of the polycyclic furanobutenolide-derived cembranoid intricarene, see (a) Tang, B.; Bray, C. D.; Pattenden, G. A Biomimetic Total Synthesis of (+)-Intricarene. *Tetrahedron Lett*. **2006**, *47*, 6401–6404. (b) Roethle, P. A.; Hernandez, P. T.; Trauner, D. Exploring Biosynthetic Relationships Among Furanocembranoids: Synthesis of (–)-Bipinnatin J, (+)-Intricarene, (+)-Rubifolide, and (+)-Isoepilophodione B. *Org. Lett.* **2006**, *8*, 5901–5904. (c) Stichnoth, D.; Kölle, P.; Kimbrough, T. J.; Riedle, E.; de Vivie-Riedle, R.; Trauner, D. Photochemical Formation of Intricarene. *Nat. Commun*. **2014**, *5*, 5597. For previous syntheses of the polycyclic furanobutenolide-derived norcembranoid scabrolide A, see: (d) Hafeman, N. J.; Loskot, S. A.; Reimann, C. E.; Pritchett, B. P.; Virgil, S. C.; Stoltz, B. M. The Total Synthesis of (–)-Scabrolide A. *J. Am. Chem. Soc*. **2020**, *142*, 8585–8590 (e) Meng, Z.; Fürstner, A. Total Syntheses of Scabrolide A and Nominal Scabrolide B. *J. Am. Chem. Soc*. **2022**, *144*, 1528–1533. (f) Hafeman, N.

J.; Loskot, S.; Reimann, C.; Pritchett, B.; Virgil, S. C.; Stoltz, B. M. Total Synthesis of (−)-Scabrolide A and (−)-Yonarolide. *Chem. Sci*. **2023**, *14*, 4745−4758. (g) Serrano, R.; Boyko, Y. D.; Hernandez, L. W.; Lotuzas, A.; Sar- lah, D. Total Syntheses of Scabrolide A and Yonarolide. *J. Am. Chem. Soc*. **2023**, *145*, 8805−8809. For the recent total synthesis of havellockate see: (h) Hafeman, N. J.; Chan, M.; Fulton, T. J.; Alexy, E. J.; Loskot, S. A.; Virgil, S. C.; Stoltz, B. M. Asymmetric Total Synthesis of Havellockate. *J. Am. Chem. Soc.* **2022**, *144*, 20232−20236 The total synthesis of ineleganolide was also recently disclosed: (i) Tuccinardi, J. P.; Wood, J. L. Total Syntheses of (+)-Ineleganolide and (−)-Sinulochmodin C. *J. Am. Chem. Soc.* **2022**, *144,* 20539−20547. (j) Gross, B. M.; Han, S.-J.; Virgil, S. C.; Stoltz, B. M. A Convergent Total Synthesis of (+)-Ineleganolide. *J. Am. Chem. Soc*. **2023**, *145*, 7763−7767. For the recent total synthesis of rameswaralide see: (k) Truax, N. J.; Ayinde, S.; Liu, J. O.; Romo, D. Total Synthe- sis of Rameswaralide Utilizing a Pharmacophore-Directed Retrosyn- thetic Strategy. *J. Am. Chem. Soc*. **2022**, *144*, 18575−18585. For recent synthesis of sinulochmodin C see: Zhang, Y.-P.; Du, S.; Ma, Y.; Zhan, W.; Chen, W.; Yang, X.; Zhang, H. Structure-Unit-Based Total Synthesis of (−)-Sinulochmodin C. *Angew. Chem. Int. Ed.* **2023**, *136*, e202315481.

(5) Anjaneyulu, A. S. R.; Venugopal, M. J. R. V.; Sarada, P.; Clardy, J.; Lobkovsky, E. Havellockate, A Novel Seco and Spiro Lactone Diterpenoid from the Indian Ocean Soft Coral Sinularia granosa. *Tetrahedron Lett.* **1998,** *39*, 139–142.

(6) Salmond, W. G.; Barta, M. A.; Havens, J. L. Allylic Oxidation with 3,5-Dimethylpyrazole. Chromium Trioxide Complex Steroidal. DELTA.5-7-Ketones. *J. Org. Chem.* **1978**, *43,* 2057–2059.

(7) Brill, Z. G.; Grover, H. K.; Maimone, T. J. Enantioselective Synthesis of an Ophiobolin Sesterterpene via a Programmed Radical Cascade. *Science*, **2016**, *352*, 1078–1082.

(8) Miller, R. A.; Li, W.; Humphrey, G. R. A Ruthenium Catalyzed Oxidation of Steroidal Alkenes to Enones. *Tetrahedron Letters*. **1996**, *37*, 3429–3432.

(9) Nakayama, Y.; Maser, M. R.; Okita, T.; Dubrovskiy, A. V.; Campbell, T. L.; Reisman, S. E. Total Synthesis of Ritterazine B. *J. Am. Chem. Soc*. **2021**, *143*, 4187–4192.

(10) Fraunhoffer, K. J.; White, M. C. Syn-1,2-Amino Alcohols via Diastereoselective Allylic C−H Amination. *J. Am. Chem. Soc.* **2007**, *129*, 7274–7276.

APPENDIX 2

Spectra Relevant to Chapter 2:

An Efficient Route to Construct the 6-5-5 Tricyclic Core of Furanobutenolide- Derived Cembranoids and Norcembranoids

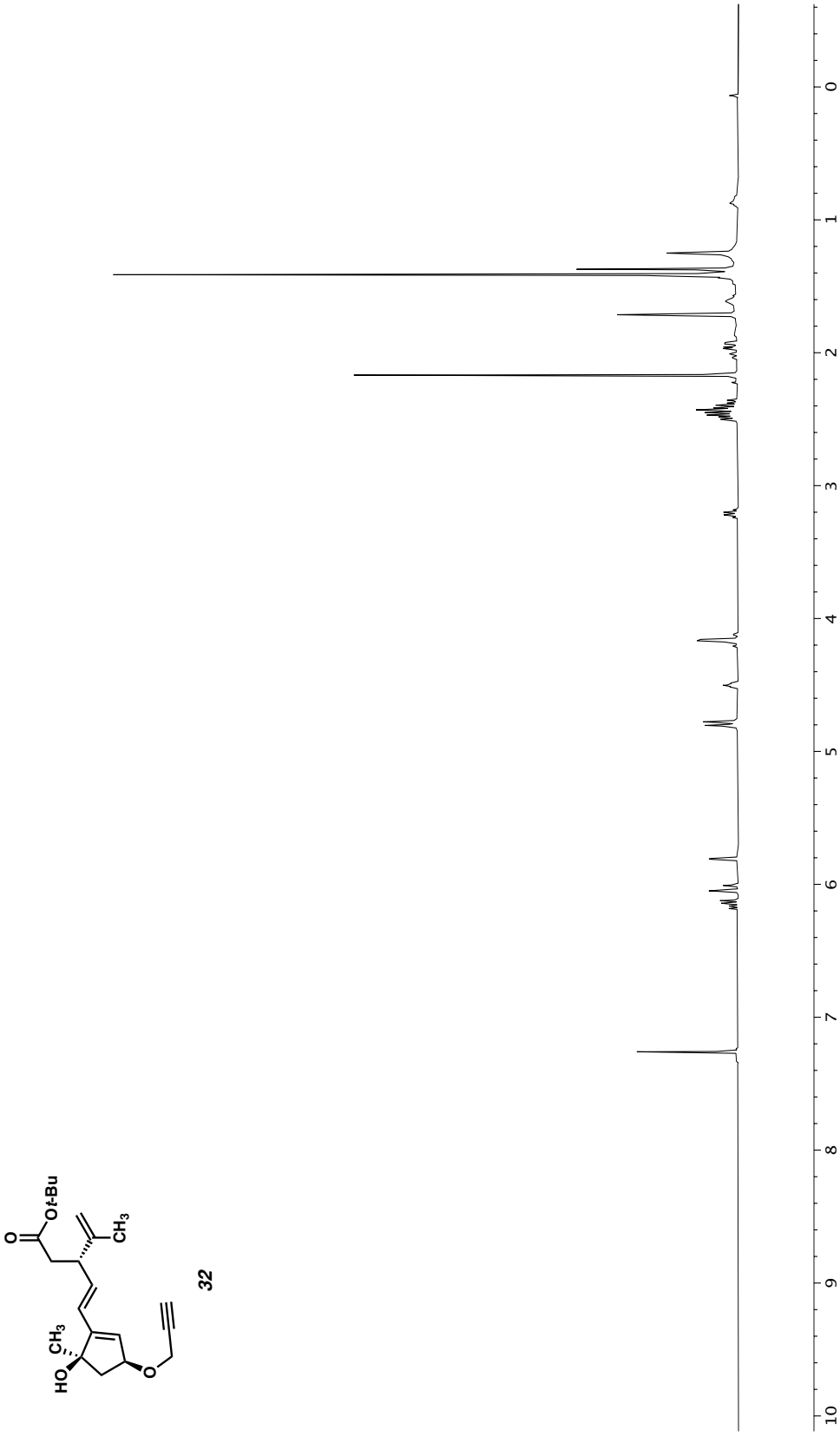

Figure A2.1. *^1H NMR (400 MHz, $CDCl_3$) of compound* ***32***.

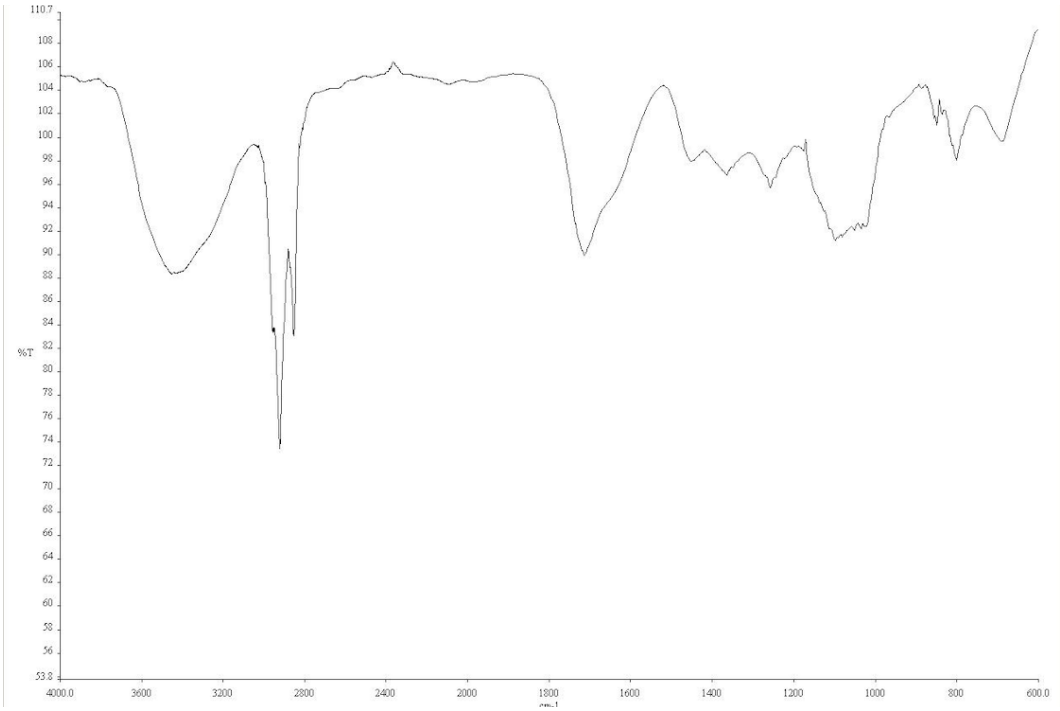

Figure A2.2. *Infrared spectrum (Thin Film, NaCl) of compound* ***32****.*

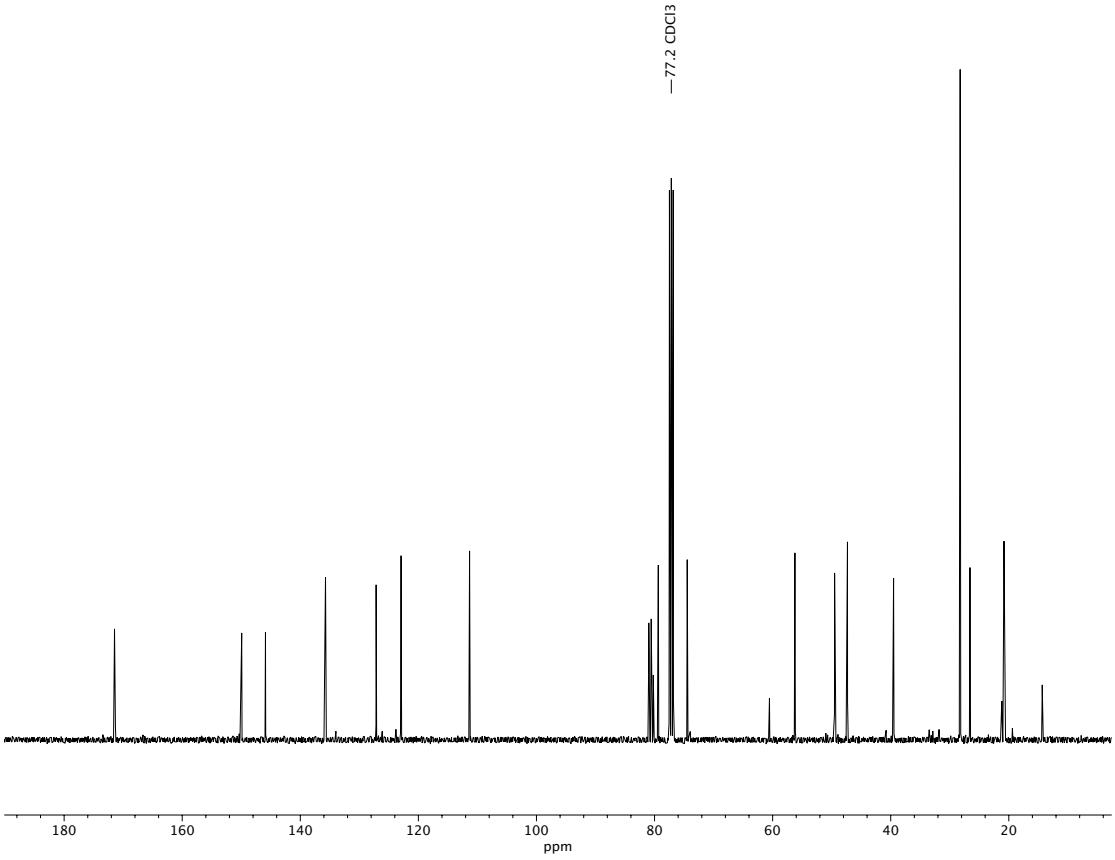

Figure A2.3. *^{13}C NMR (100 MHz, $CDCl_3$) of compound* ***32****.*

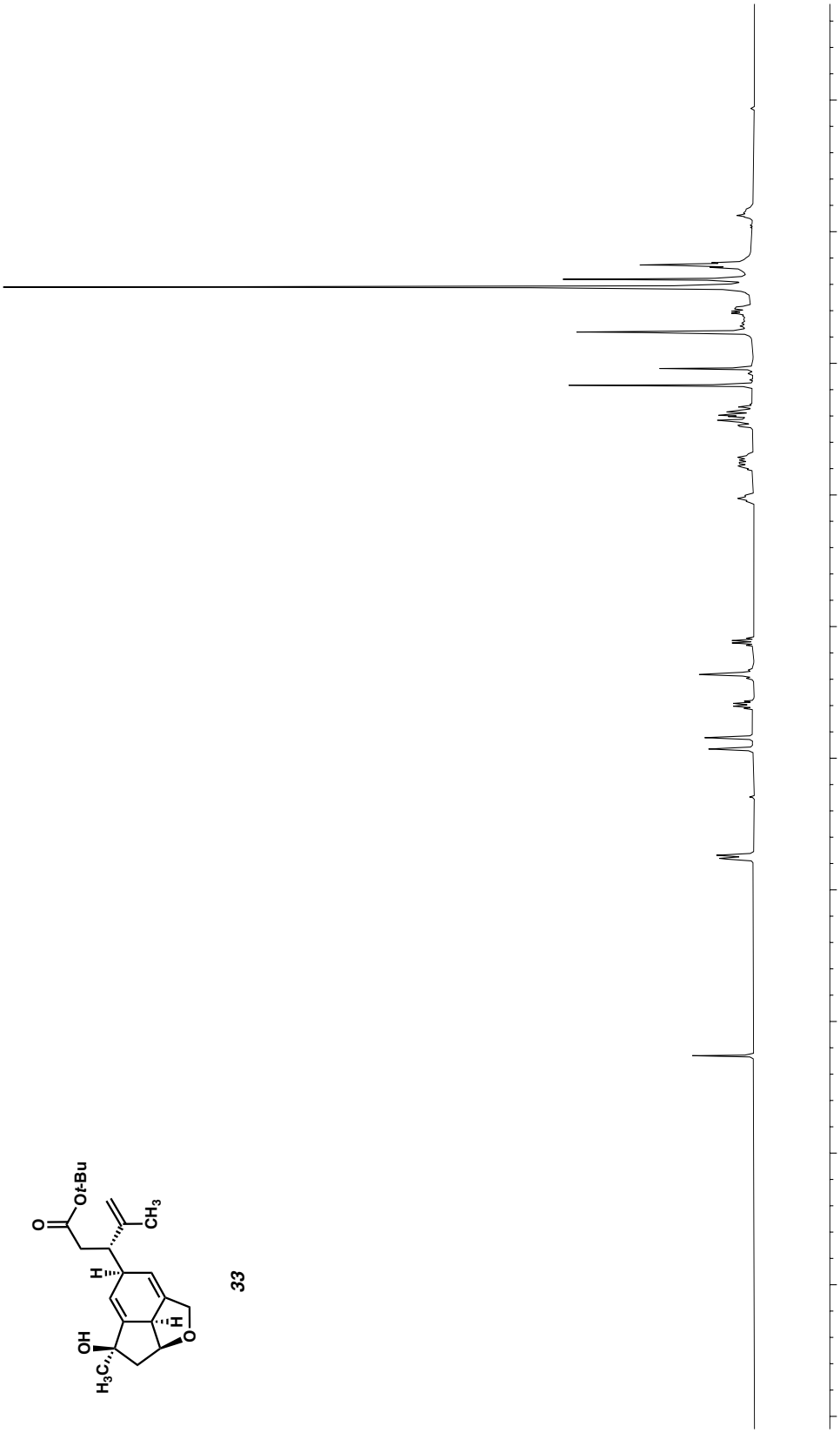

Figure A2.4. *^{1}H NMR (400 MHz, $CDCl_3$) of compound* ***33****.*

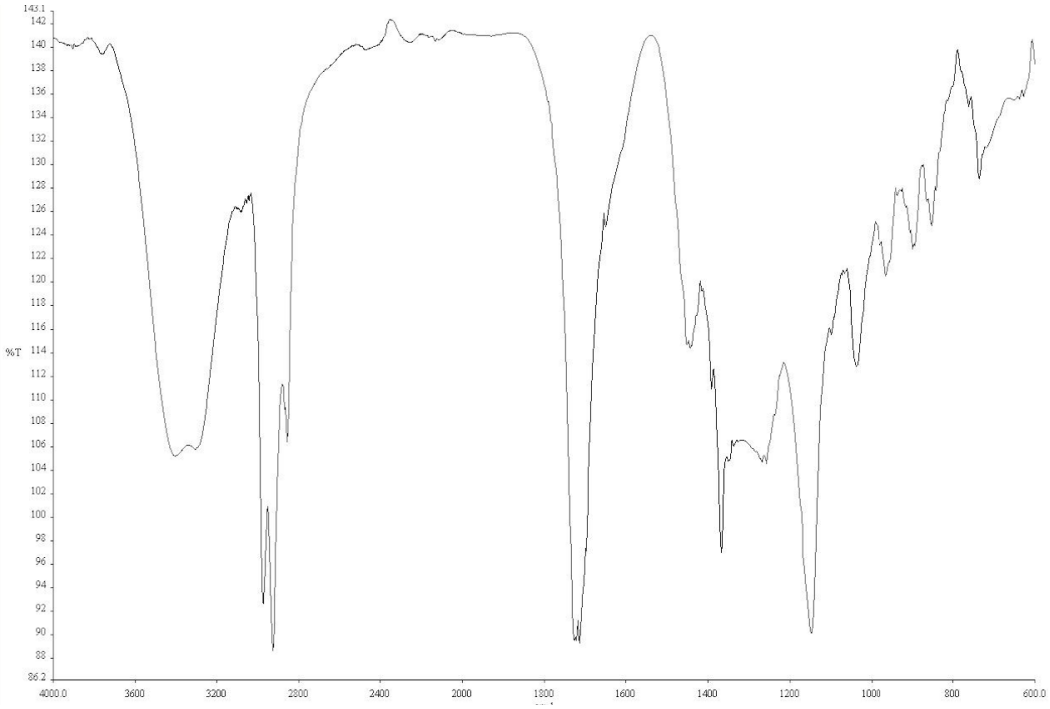

Figure A2.5. *Infrared spectrum (Thin Film, NaCl) of compound* ***33***.

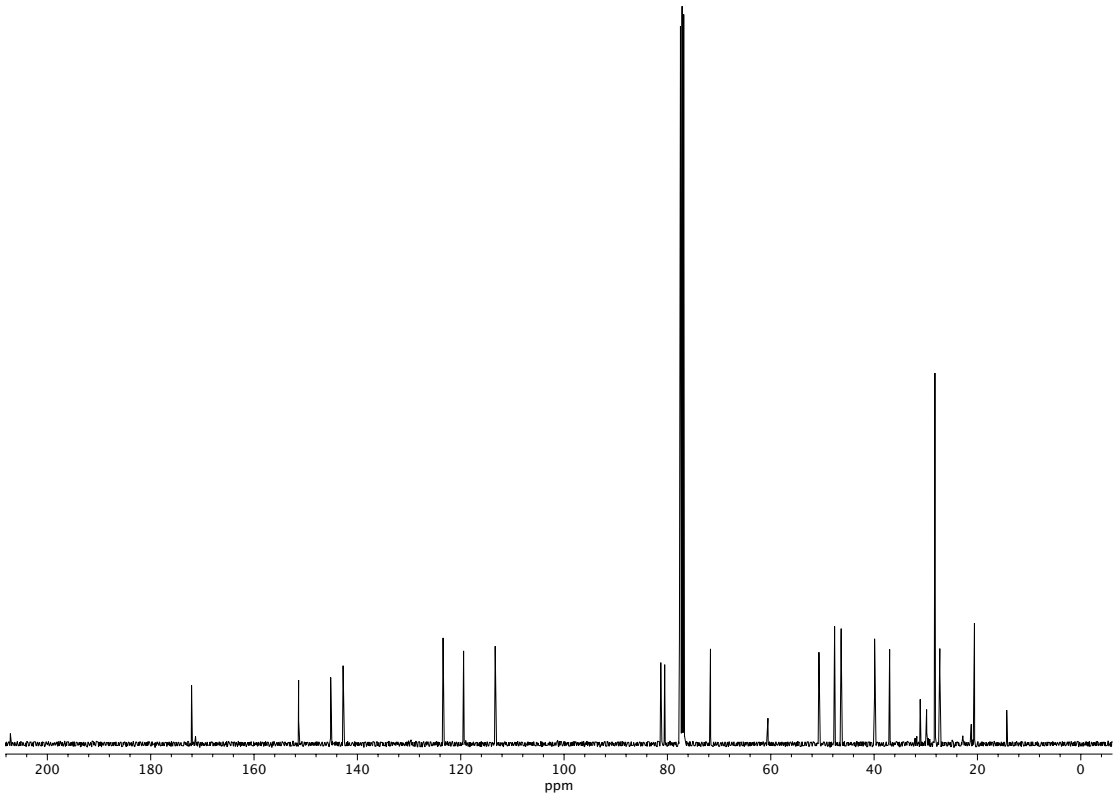

Figure A2.6. *^{13}C NMR (100 MHz, $CDCl_3$) of compound* ***33***.

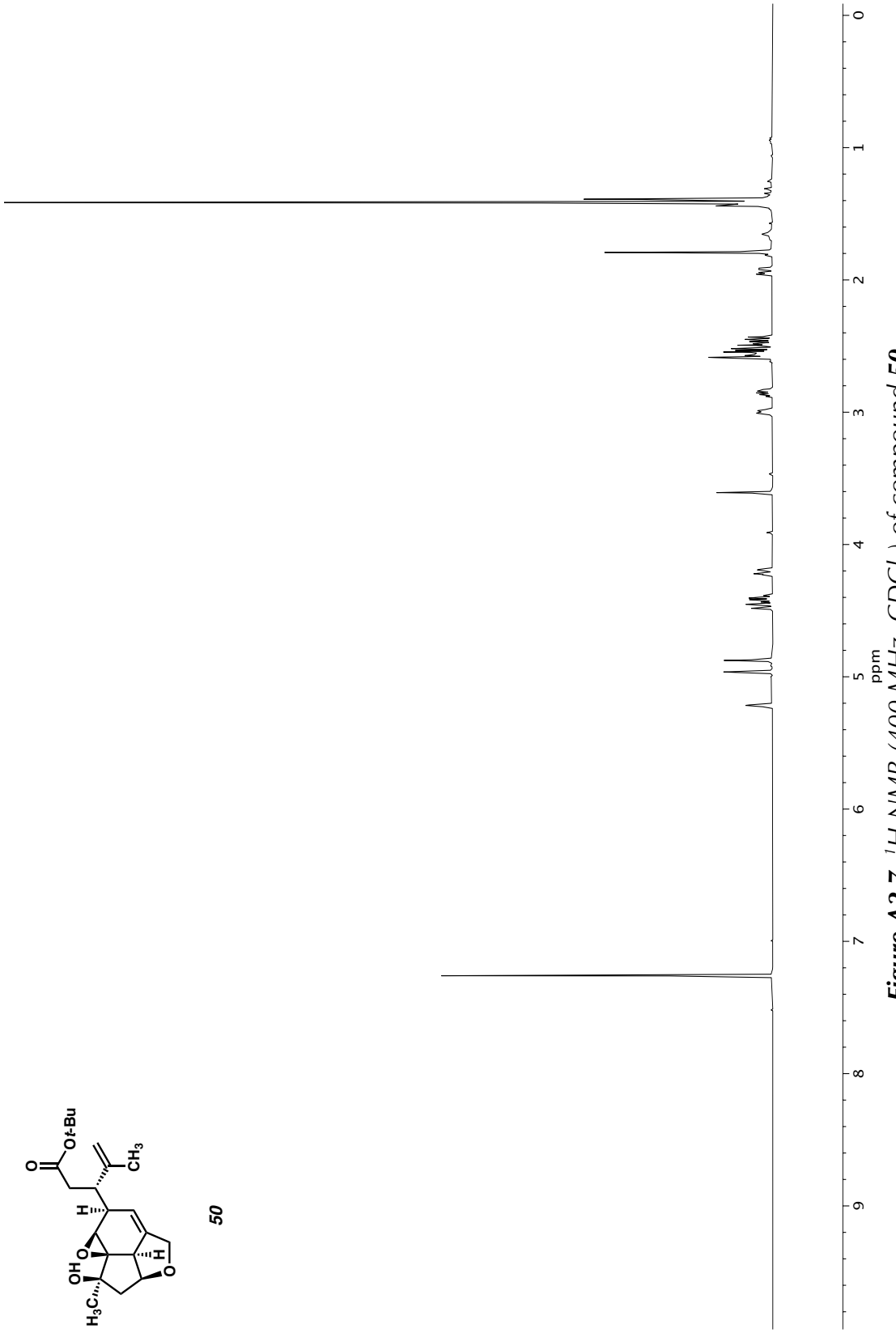

Figure A2.7. *^{1}H NMR (400 MHz, $CDCl_3$) of compound* ***50****.*

50

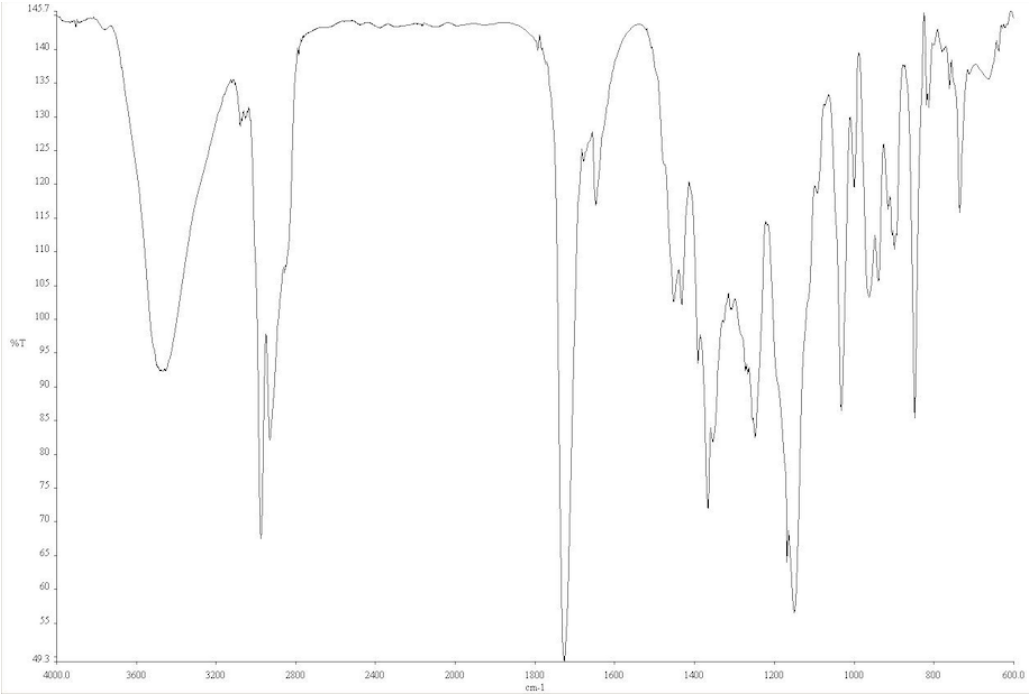

Figure A2.8. *Infrared spectrum (Thin Film, NaCl) of compound* ***50****.*

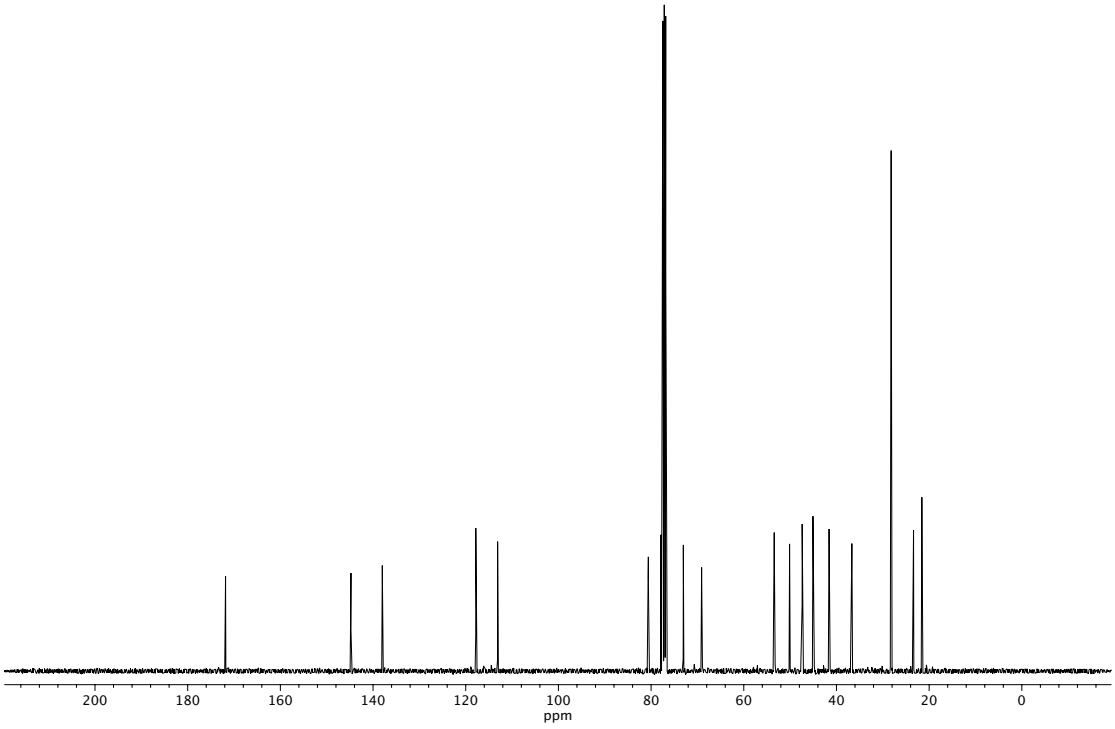

Figure A2.9. *^{13}C NMR (100 MHz, $CDCl_3$) of compound* ***50****.*

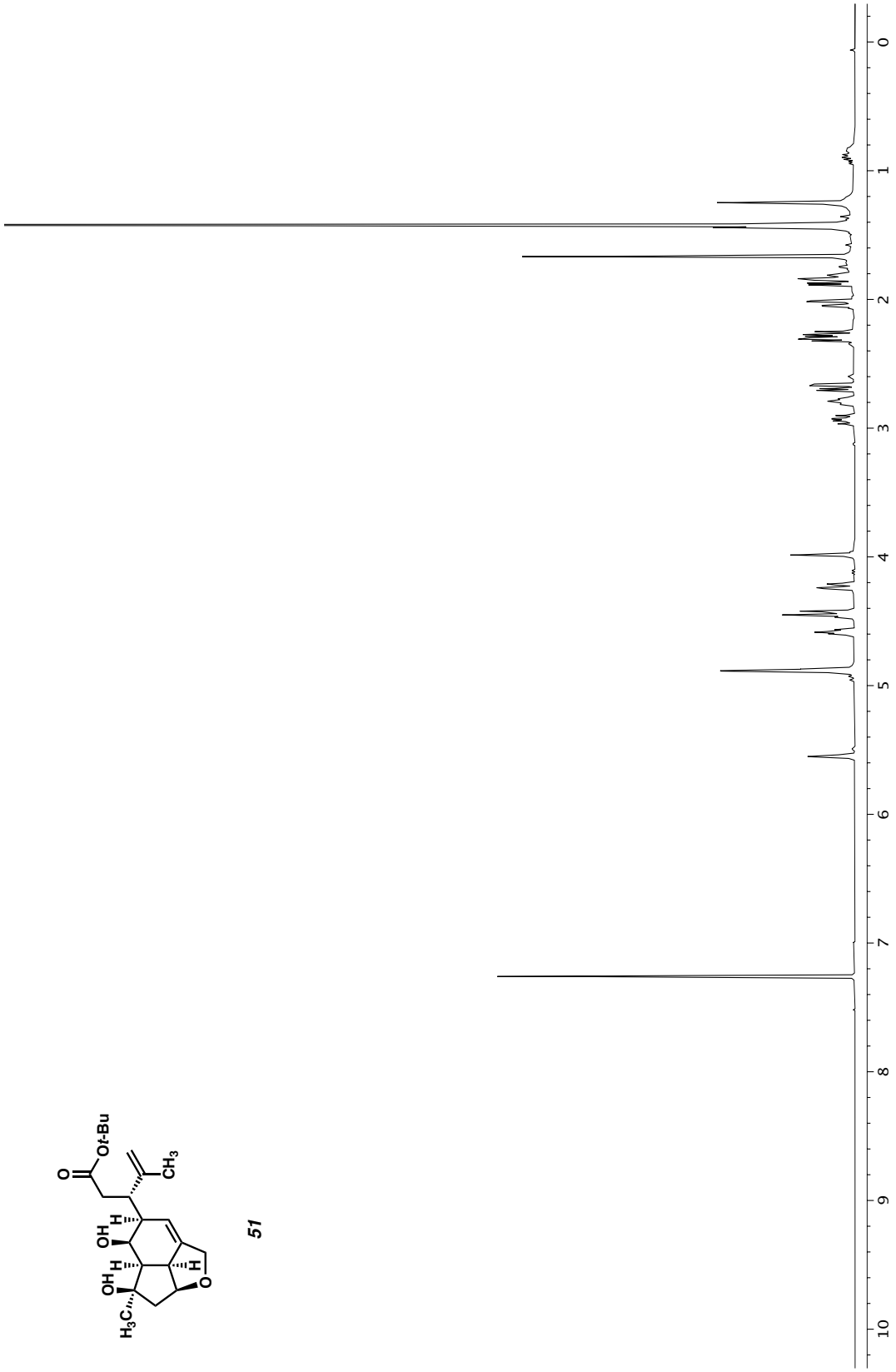

Figure A2.10. *^{1}H NMR (400 MHz, $CDCl_3$) of compound **51**.*

51

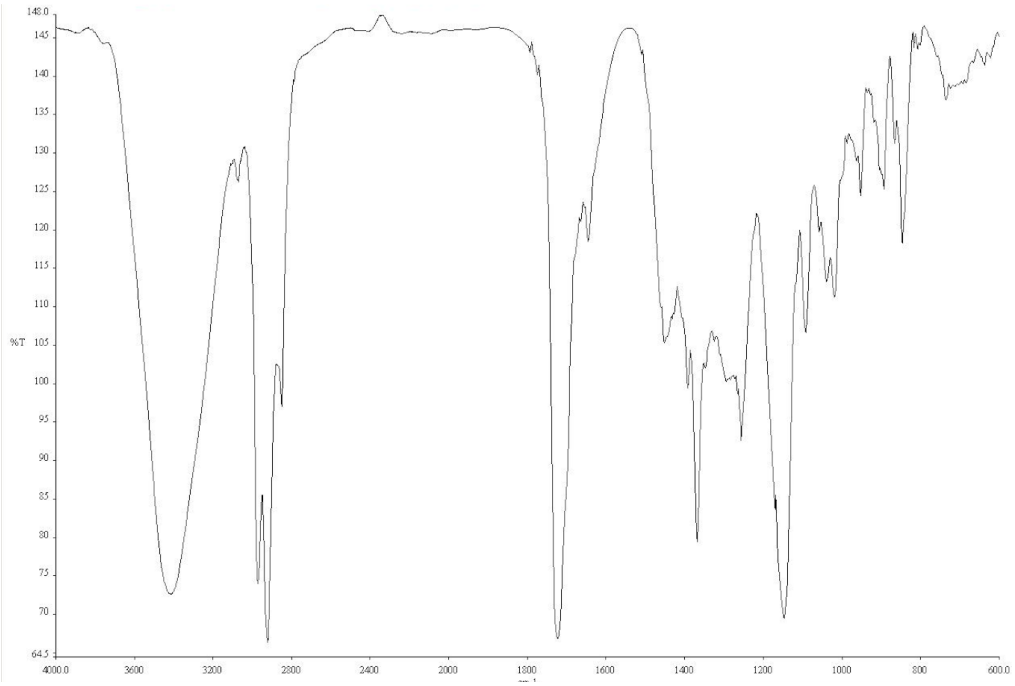

Figure A2.11. *Infrared spectrum (Thin Film, NaCl) of compound* ***51****.*

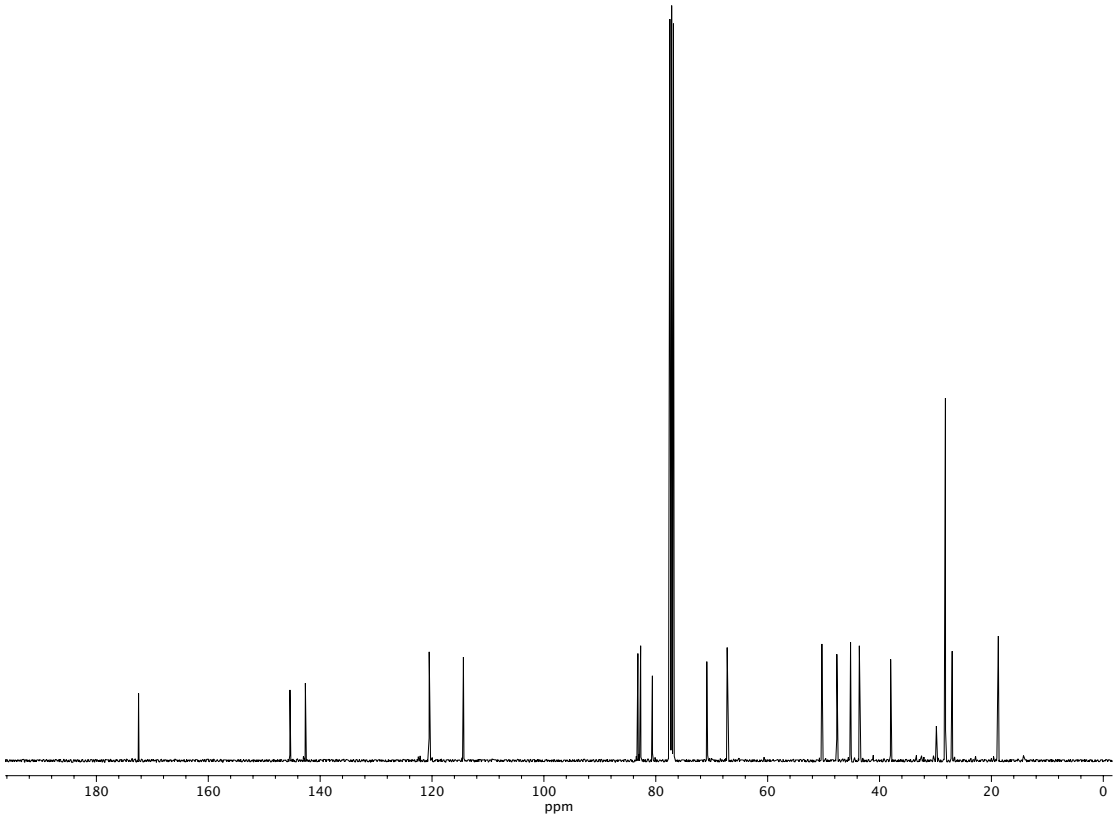

Figure A2.12. *^{13}C NMR (100 MHz, $CDCl_3$) of compound* ***51****.*

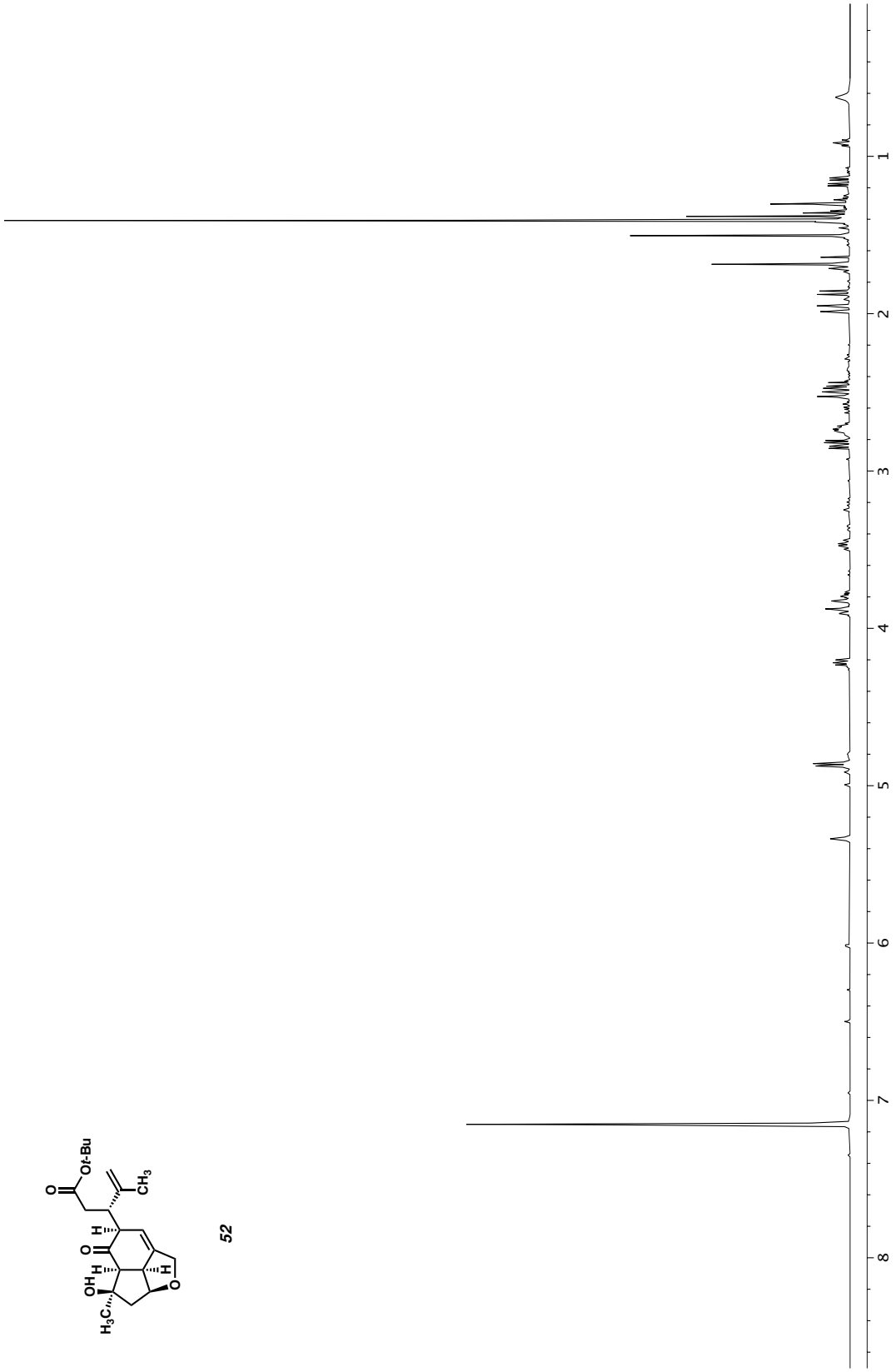

52

Figure A2.13. *^{1}H NMR (400 MHz, $CDCl_3$) of compound **52**.*

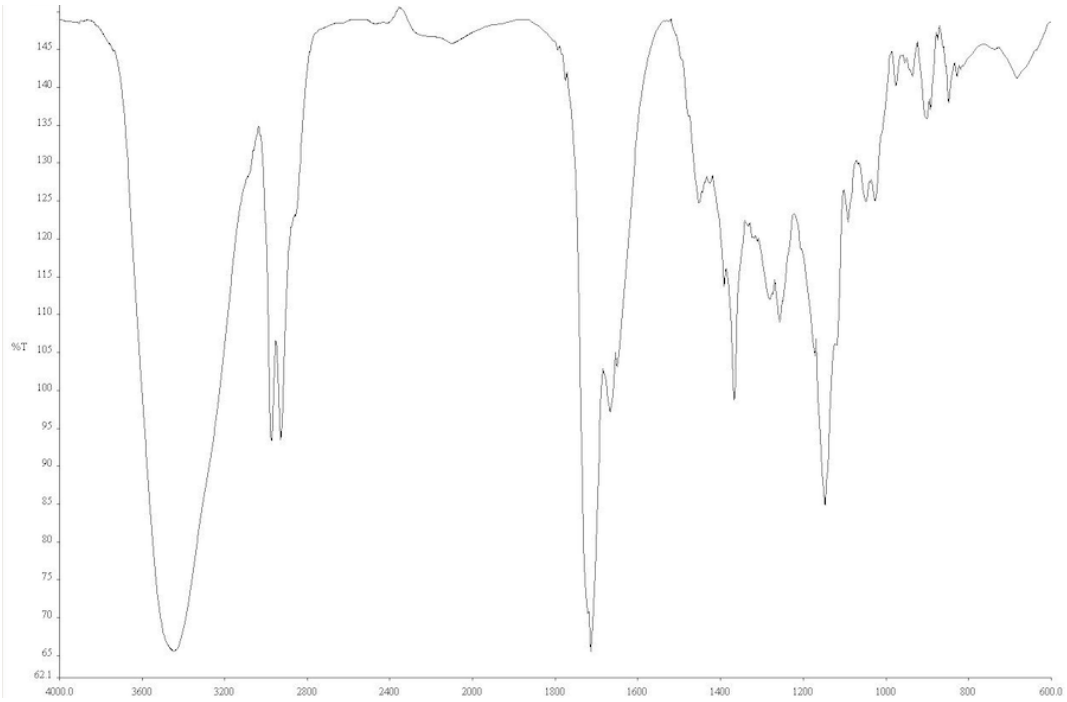

Figure A2.14. *Infrared spectrum (Thin Film, NaCl) of compound* ***52****.*

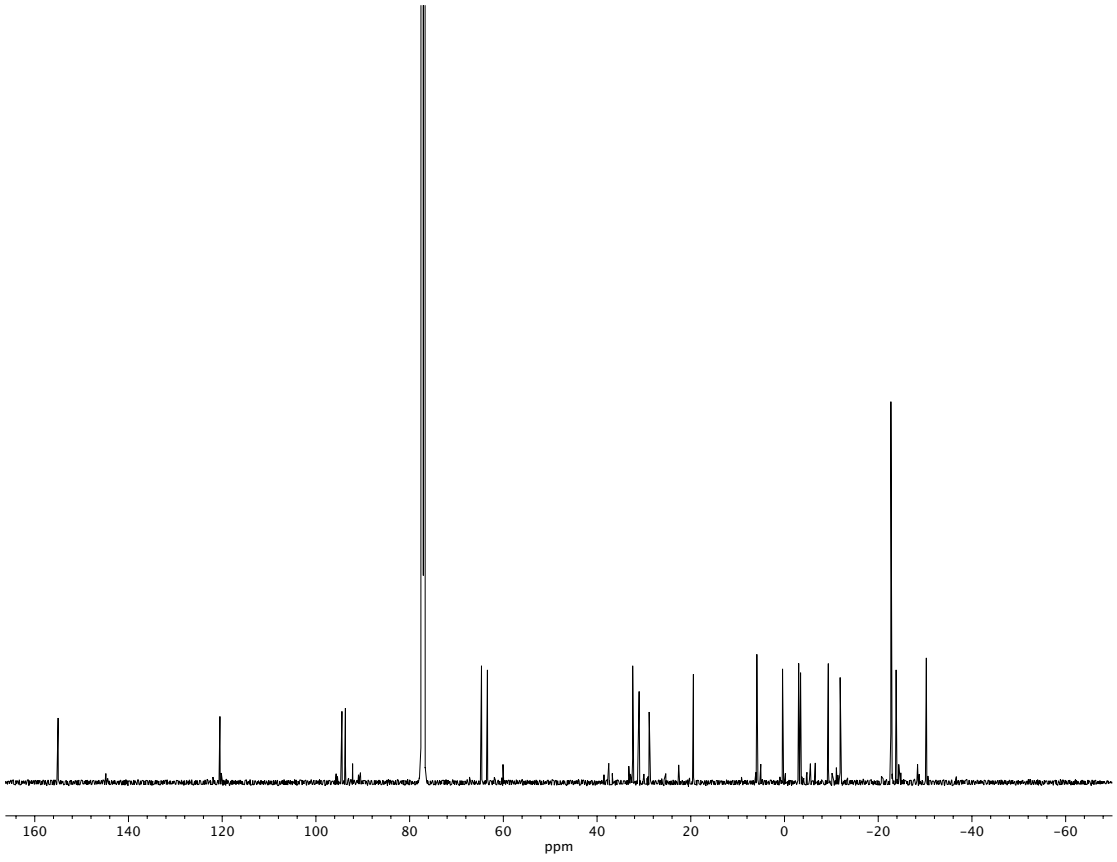

Figure A2.15. *^{13}C NMR (100 MHz, $CDCl_3$) of compound* ***52****.*

CHAPTER 3

Formation of All-Carbon Quaternary Centers via Pd-catalyzed α-Vinylation of γ-Lactams

3.1 INTRODUCTION

γ-lactams are heterocyclic motifs that are overrepresented in pharmaceuticals and natural products alike (Figure 3.1.1).[1,2] The direct vinylation of these materials remains an unsolved problem in organic synthesis, limiting the ability of these structures to be elaborated to more complex scaffolds with potential biological applications. Our group has previously dis-closed a novel, Pd-catalyzed strategy toward the α-arylation of PMP-protected γ-lactams containing pre-existing substitution at the α-position.[3] As such, we successfully achieved the first asymmetric α-arylation of γ-lactams forming enantioenriched all-carbon quaternary centers. We imagined that this success could be translated to the more unprecedented vinylation of these nucleophiles, so we commenced with an optimization campaign aimed to effect a Pd-catalyzed vinylation.

†This research was performed in collaboration with Farbod A. Moghadam,‡ Jay P. Barbor,‡ Carina Jette, and Shunya Sakurai.

Figure 3.1.1 *Selected examples of γ-lactams of pharmaceutical relevance and natural products.*

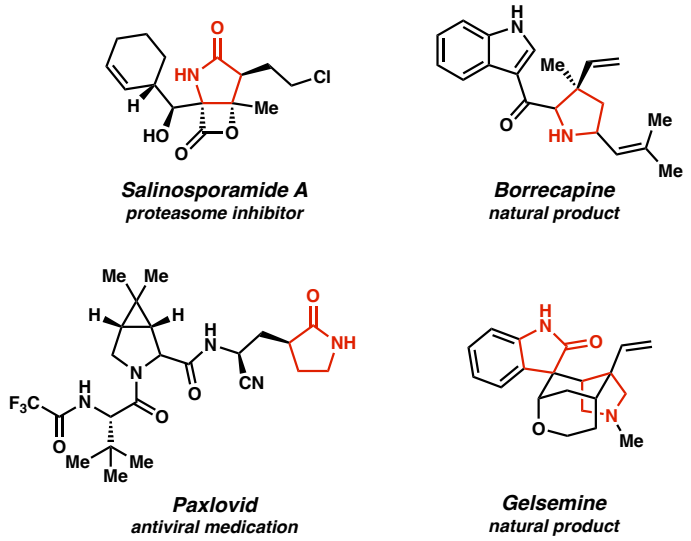

3.2 OPTIMIZATION

Utilizing the same catalytic conditions disclosed in our prior report, initial optimization efforts demonstrated the superiority of vinyl chlorides in the transformation, as vinyl bromide and triflate electrophiles did not result in observable yields of the desired product (Scheme 3.2.1). We found that a counterion effect was operative in the reaction, and use of LiHMDS as the base garnered the desired product in a moderate 46% yield and 90% ee. Dilution of the reaction to 0.05 M diminished the formation of undesired byproducts arising from the addition of the nucleophile to the dba ligand of the Pd precatalyst, allowing for an improved 58% yield.

Scheme 3.2.1 *Optimization.*[a]

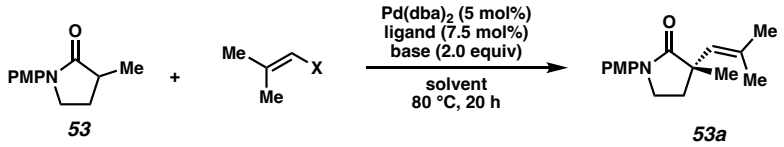

Entry	Ligand	X	Base	Solvent	Yield (%)	ee (%)
1	L1	Cl	NaHMDS	dioxane	0	–
2	L1	Cl	KHMDS	dioxane	0	–
3	L1	Cl	LiHMDS	dioxane	46	90
4	L1	Cl	LiTMP	dioxane	29	ND
5	L1	Br	LiHMDS	dioxane	27	77
6	L2	Cl	LiHMDS	dioxane	43	88
7[b]	L1	Cl	LiHMDS	THF	19	ND
8[b]	L1	Cl	LiHMDS	CPME	43	92
9[c]	L1	Cl	LiHMDS	CPME	38	ND
10[c]	L1	Cl	LiHMDS	dioxane	58	93

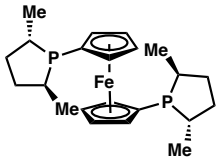

L1
Me-Ferrocelane

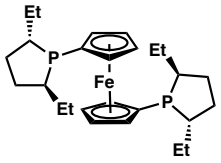

L2
Et-Ferrocelane

[a]Reactions performed at 0.1 mmol scale and 0.1 M. Yields determined by ^{1}H NMR with CH2Br2 internal standard. [b]Reaction performed at 70 ºC for 48h. [c]Reaction performed at 0.05 M concentration.

With optimized conditions in hand, we sought to investigate the range of compatible substitution patterns on the vinyl halide coupling partner. Surprisingly, we found that use of 1,1-disubstituted or trans-1,2-disubstituted substrates resulted in either degraded yield or ee, respectively. Considering the sensitivity of the reaction to these steric parameters, we developed a quadrant model rationalizing the importance of the various substituents of the vinyl electrophile (Figure 3.2.2B). With the hypothesis that reductive

elimination is both inner-sphere and enantiodetermining (Figure 3.2.2A),[4,5] we posit that the diminished yield of the 1,1-disubstituted electrophiles originates from steric congestion at the metal center, which may deter transmetallation of the lithium enolate to palladium. Conversely, we propose that the greatly minimized interactions between the ligand and trans-1,2-disubstituted electrophiles result in high conversion but with poor enantiocontrol. With these observations in mind, we explored an array of 2,2-disubstituted vinyl electrophiles to test the scope of this transformation.

Figure 3.2.2 *A) Proposed catalytic cycle of Pd-catalyzed α-Vinylation of Lactams. B) Proposed quadrant model of the C-C bond formation process.*

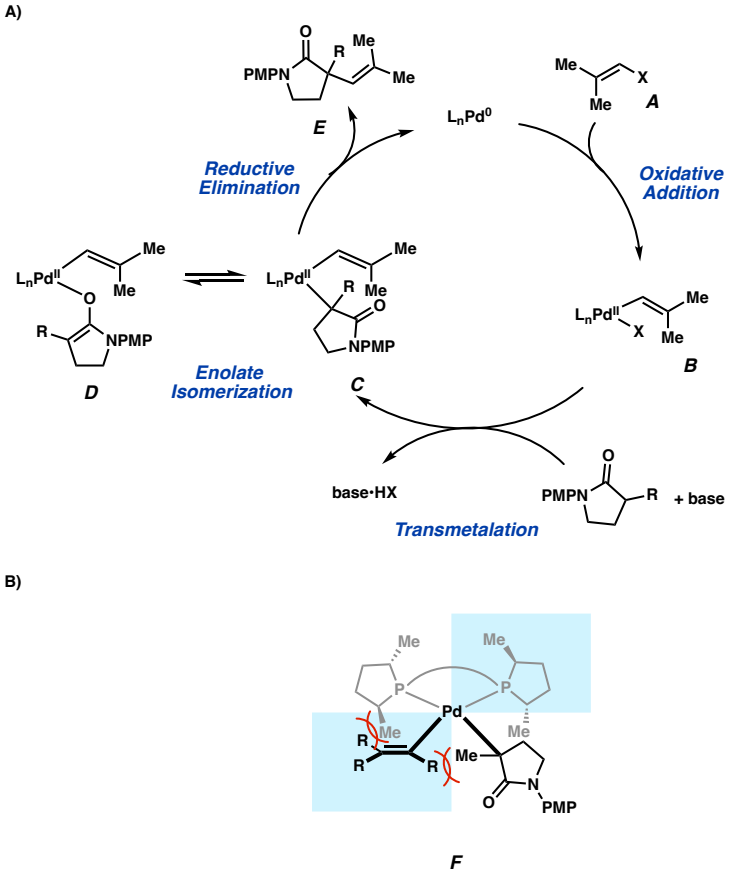

3.3 SUBSTRATE SCOPE & DERIVATIZATION

Vinyl electrophiles featuring a cyclopentyl, cyclohexyl and cycloheptyl substitution at the 2,2-position afforded products with high enantioselectivity, although **53a** suffered from diminished yields likely due to increased steric hindrance (Scheme 3.3.1). Additionally, saturated heterocyclic moieties, such as a pyran and thiopyran, were well tolerated. Acyclic precursor **59a** could also undergo the reaction in comparable yield and ee, while **60a** and **61a** were formed in diminished ee and yield, respectively. We were pleased to find that while differing substitution at the α-position was not well-tolerated, preexisting γ-substitution on the lactam coupling partner resulted in a predictable match/mismatch situation, where enhancement of the dr at the apposition and higher reaction efficiency was observed in case **62a**. We were also able to implement our methodology at a 3 mmol scale for our model system, obtaining over 450 mg of the desired product in a similar 59% yield and 93% ee.

Scheme 3.3.1 *Substrate scope.*

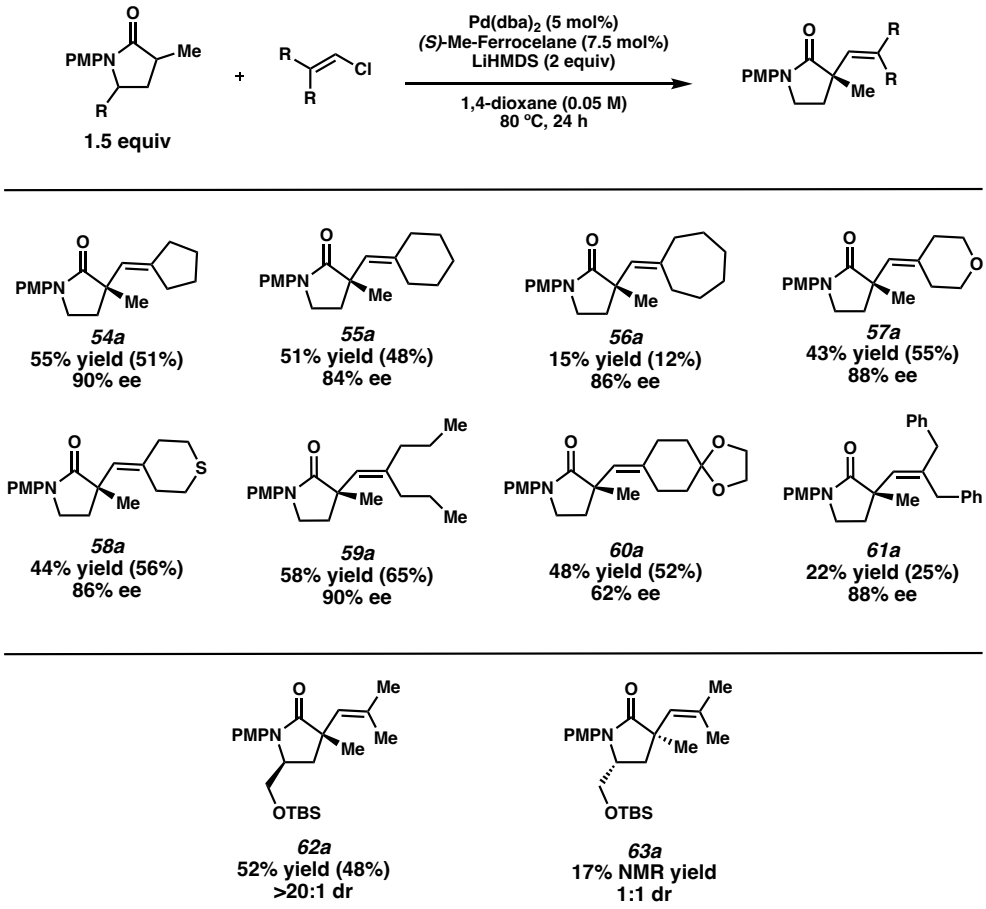

These enantioenriched heterocycles, characterized by highly substituted quaternary centers, exhibit significant potential for pharmaceutical applications and synthetic chemistry pursuits.[6] Recognizing their capacity to efficiently construct the carbon framework of drug molecules or natural products, we embarked on a series of derivatizations of product **53a** to generate differentially substituted five-membered lactam derivatives (Scheme 3.3.2). Our initial strategy involved the hydrogenation of product **53a** using Pd/C and hydrogen gas to yield α-quaternary lactam **64**. Given the inherent

challenges associated with enantioselective α-alkylation of lactams using conventional methods, we believe that this alternative approach to generating product **64** offers tremendous synthetic value.

The reduction of the carbonyl moiety on product **53a** with LAH yields β-substituted pyrrolidine **65**, a moiety of significant pharmaceutical importance. This structural motif is extensively utilized in various existing drug molecules and targets. Oxidation of the newly introduced vinyl group with PTSA produces tertiary alcohol **66**. Additionally, product **53a** can undergo oxidation to yield the corresponding aldehyde through ozonolysis, achieving satisfactory yields. From this aldehyde (**67**), a Wittig reaction can be conducted to yield vinylated lactam **68**, with no substitution at the terminal position. Allylic oxidation using SeO_2 results in the formation of aldehyde **69**, which could be further functionalized via coupling, providing promising benefits for the synthesis of complex molecules. Finally, deprotection of the PMP group with DDQ reveals the unprotected lactam **70**.

Scheme 3.3.2 *Derivatization of vinylation products. Conditions: a) H_2, Pd/C (10 mol%), MeOH, 12h, 74 % yield. b) LAH (5 equiv), Et2O, 0 °C to 18 °C, 21 h, 84 % yield. c) PTSA, AcOH, 70 °C, 12h, 59 % yield. d) ozone, PPh3 CH2Cl2, 15min, 89% yield. e) KOtBu, methyl wittig, THF, 0 ºC to reflux, 12h, 84% yield. f) SeO2, 1,4-dioxane, reflux, 15min, 49% yield. g) CAN, H2O, 60 ºC, 32h, 40% yield.*

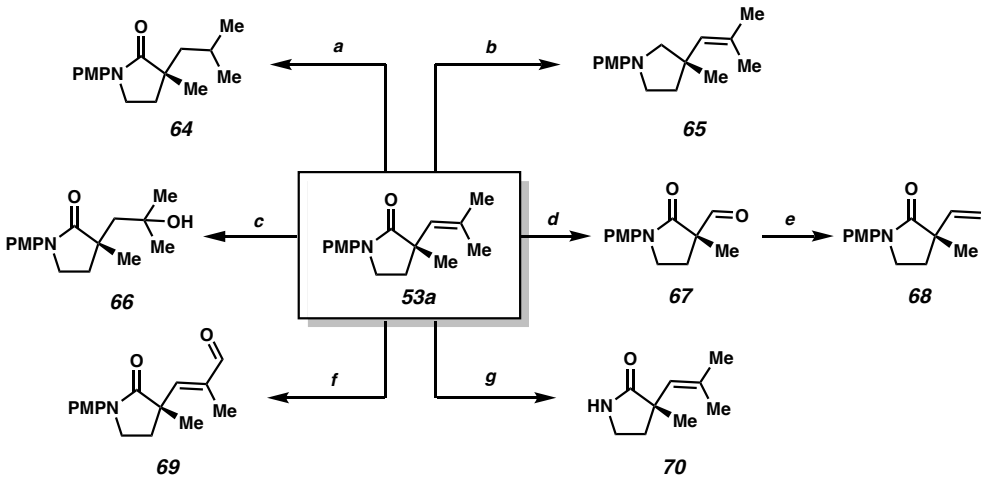

3.4 CONCLUSION

In conclusion, our study showcases an enantioselective vinylation method for γ-lactams, yielding α-quaternary centers with up to 58% yield and 93% ee. Notably, the reaction exhibits distinct preferences among different classes of electrophiles. Particularly, we observed that trisubstituted vinyl chlorides outperformed others under these conditions in both yield and ee. This observation is rationalized through the quadrant model illustrated in Figure 3.2.2B. Moreover, these highly substituted γ-lactams hold significant synthetic

potential, offering diverse functional handles for the synthesis of complex drug molecules or natural products.

3.5 SUPPORTING INFORMATION

3.5.1 MATERIALS AND METHODS

Unless otherwise stated, reactions were performed in flame-dried glassware under a nitrogen atmosphere using dry, deoxygenated solvents. Solvents were dried by passage through an activated alumina column under argon. Reaction progress was monitored by thin-layer chromatography (TLC). TLC was performed using E. Merck silica gel 60 F254 precoated glass plates (0.25 mm) and visualized by UV fluorescence quenching, p-anisaldehyde, or KMnO4 staining. Silicycle SiliaFlash® P60 Academic Silica gel (particle size 40–63 μm) was used for flash chromatography. 1H NMR spectra were recorded on Varian Inova 500 MHz and 600 MHz and Bruker 400 MHz spectrometers and are reported relative to residual CHCl3 (δ 7.26 ppm), C6D6 (δ 7.16 ppm) or CD3OD (δ 3.31 ppm). 13C NMR spectra were recorded on a Varian Inova 500 MHz spectrometer (125 MHz) and Bruker 400 MHz spectrometers (100 MHz) and are reported relative to CHCl3 (δ 77.16 ppm), C6D6 (δ 128.06 ppm) or CD3OD (δ 49.01 ppm). Data for 1H NMR are reported as follows: chemical shift (δ ppm) (multiplicity, coupling constant (Hz), integration). Multiplicities are reported as follows: s = singlet, d = doublet, t = triplet, q = quartet, p = pentet, sept = septuplet, m = multiplet, br s = broad singlet, br d = broad doublet. Data for 13C NMR are reported in terms of chemical shifts (δ ppm). IR spectra were obtained by use of a Perkin Elmer Spectrum BXII spectrometer or Nicolet 6700 FTIR spectrometer using thin films deposited on NaCl plates and reported in frequency of absorption (cm–1). Optical rotations were measured with a Jasco P-2000 polarimeter operating on the sodium

D-line (589 nm), using a 100 mm path-length cell. High resolution mass spectra (HRMS) were obtained from the Caltech Mass Spectral Facility using a JEOL JMS-600H High Resolution Mass Spectrometer in fast atom bombardment (FAB+) or electron ionization (EI+) mode, or using an Agilent 6200 Series TOF with an Agilent G1978A Multimode source in electrospray ionization (ESI+), atmospheric pressure chemical ionization (APCI+), or mixed ionization mode (MM: ESI-APCI+).

List of Abbreviations:

ee – enantiomeric excess, SFC – supercritical fluid chromatography, HPLC – high-performance liquid chromatography, TLC – thin-layer chromatography, Dr – dram

3.5.2 EXPEPRIMENTAL PROCEDURES AND SPECTROSCOPIC DATA

Pd-catalyzed Vinylation Reactions: General Procedure A

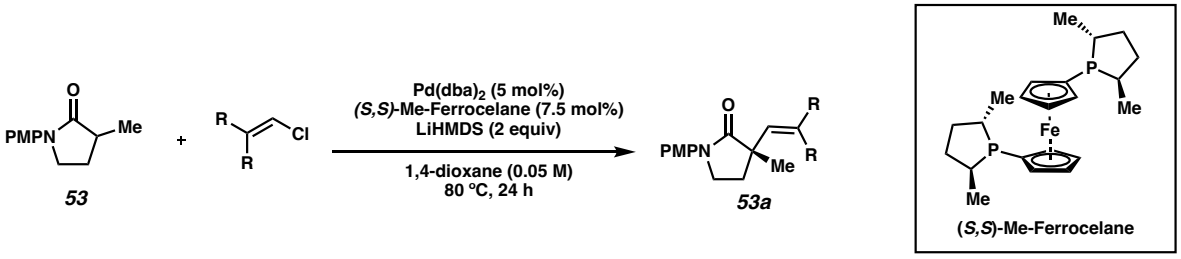

In a nitrogen-filled glovebox, a catalyst solution of $Pd(dba)_2$ (9.6 mg/mL) and (S,S)-Me-Ferrocelane (10.4 mg/mL) in 1,4-dioxane was stirred for 20 min at 40 °C. In a vial, the lactam was dissolved in 1,4-dioxane (1.5 equiv, 0.09 M), and subsequently LHMDS (2 equiv) was added. A 2 Dr vial was charged with neat vinyl chloride (0.1 mmol, 1 equiv) and a magnetic stir bar. After the catalyst pre-stir was complete, 0.4 mL of the catalyst solution was added to the vinyl chloride, followed by 1.6 mL of the nucleophile/base mixture. The vial was sealed with a Teflon-lined cap, removed from the glovebox, and stirred at 80 °C in a metal heating block for 24 h unless noted otherwise. After 24 h, 3 mL 0.5 M HCl or sat. NH4Cl was added to the crude reaction mixture, which was then extracted three times with ethyl acetate, dried over Na−2SO4, concentrated, and purified by silica gel flash chromatography to provide the desired vinylation product.

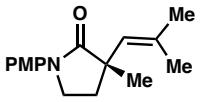

(S)-1-(4-methoxyphenyl)-3-methyl-3-(2-methylprop-1-en-1-yl)pyrrolidin-2-one (53a)

Prepared according to general procedure A using vinyl chloride (0.1 mmol) and lactam **53**. Purification by silica gel chromatography (0-30% EtOAc/Hexanes) provided 13.4 mg (52%) of a yellow oil. The reaction was also performed using 3 mmol vinyl chloride to obtain 456 mg (59%) of a tan solid.

Optical rotation: [α]D25 –79.9 (c 1.0, CHCl3).

1H NMR (400 MHz, CDCl3) δ 7.54 (d, J = 9.2 Hz, 2H), 6.90 (d, J = 9.1 Hz, 2H), 5.46 (t, J = 1.4 Hz, 1H), 3.79 (s, 3H), 3.78 – 3.63 (m, 2H), 2.32 – 2.12 (m, 2H), 1.74 (d, J = 1.5 Hz, 3H), 1.69 (d, J = 1.4 Hz, 3H), 1.36 (s, 3H).

13C NMR (101 MHz, CDCl3) δ 177.76, 156.54, 134.55, 133.25, 128.53, 121.59, 114.13, 55.62, 46.33, 45.73, 34.25, 27.05, 24.38, 19.17.

IR (Neat Film, NaCl) 2965, 1694, 1513, 1400, 1297, 1250, 1170, 1089, 1063, 1033, 828 cm–1.

HRMS (MM:ESI-APCI+) m/z calc'd C16H21NO2 [M+H]+: 260.1645, found 260.1649.

SFC Conditions: 5% MeOH, 2.5 mL/min, Chiralcel OJ-H column, λ = 210 nm, tR (min): major = 1.99, minor = 2.90.

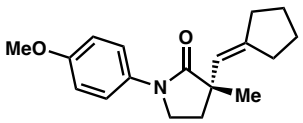

(S)-3-(cyclopentylidenemethyl)-1-(4-methoxyphenyl)-3-methylpyrrolidin-2-one (54a)

Prepared according to general procedure A using **53**. Purification by column chromatography (0–25 % EtOAc/Hexanes) yielded **54a** as a white solid (15.6 mg, 55% yield); 90% ee.

Optical roatation: [α]D25 –56.8 (c 0.75, CHCl3).

1H NMR (400 MHz, CDCl3) δ 7.55 (d, J = 9.1 Hz, 2H), 6.90 (d, J = 9.1 Hz, 2H), 5.53 (p, J = 2.3 Hz, 1H), 3.79 (s, 3H), 3.75 – 3.51 (m, 2H), 2.26 (m, 5H), 2.15 – 1.87 (m, 1H), 1.88 – 1.60 (m, 2H), 1.60 – 1.42 (m, 2H), 1.35 (s, 3H).

13C NMR (101 MHz, CDCl3) δ 177.4, 156.5, 145.1, 133.3, 123.7, 121.5, 114.1, 55.6, 47.1, 45.8, 35.5, 34.0, 28.9, 27.3, 25.8, 23.9.

IR (neat film, NaCl) 3835, 3732, 2951, 2866, 2360, 1693, 1511, 1455, 1395, 1298, 1248, 1181, 1084, 1035, 833, 662 cm–1.

HRMS (MM:ESI-APCI+) m/z calc'd for C18H24NO2 [M+H]+: 286.1802, found 286.1815.

SFC conditions: 30% IPA, 2.5 mL/min, Chiralcel AD-3 column, λ = 254 nm, tR (min): minor = 4.69, major = 7.78.

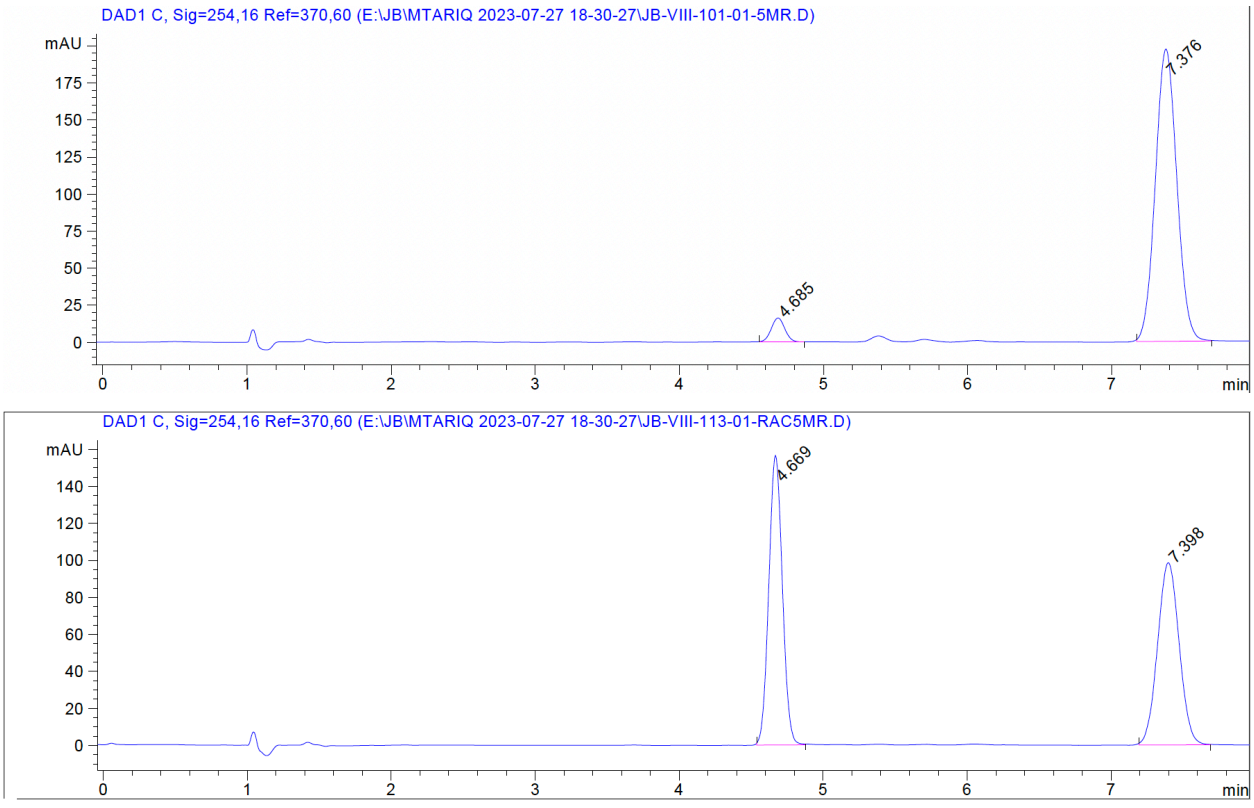

Peak #	RetTime [min]	Type	Width [min]	Area [mAU*s]	Height [mAU]	Area %
1	4.685	BB	0.1012	106.83373	16.14227	17.4045
2	7.376	BB	0.1609	2041.56543	196.96281	332.5955

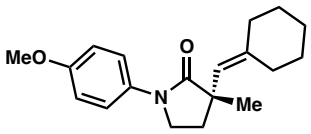

(S)-3-(cyclohexylidenemethyl)-1-(4-methoxyphenyl)-3-methylpyrrolidin-2-one (55a)

Prepared according to general procedure A using **53**. Purification by column chromatography (0–25 % EtOAc/Hexanes) yielded **55a** as a white solid (15.3 mg, 51% yield); 84% ee.

Optical rotation: [α]D25 –64.5 (c 1.0, CHCl3).

1H NMR (400 MHz, CDCl3) δ 7.44 (d, J = 9.1 Hz, 2H), 6.80 (d, J = 9.1 Hz, 2H), 5.36 – 5.31 (m, 1H), 3.69 (s, 3H), 3.67 – 3.34 (m, 2H), 2.12 (m, 2H), 2.08 – 1.94 (m, 4H), 1.55 – 1.32 (m, 6H), 1.25 (s, 3H).

13C NMR (101 MHz, CDCl3) δ 177.9, 156.4, 142.7, 133.2, 125.4, 121.5, 114.0, 55.5, 45.9, 45.6, 37.7, 34.6, 30.2, 28.7, 27.6, 26.5, 24.7.

IR (neat film, NaCl) 3835, 3745, 2925, 2851, 2359, 1693, 1513, 1443, 1396, 1298, 1248, 1179, 1088, 1035, 828 cm^{-1}.

HRMS (MM:ESI-APCI+) m/z calc'd for C19H26NO2 [M+H]+: 300.1958, found 300.1972.

SFC conditions: 30% IPA, 2.5 mL/min, Chiralcel AD-3 column, λ = 254 nm, tR (min): minor = 5.21, major = 9.35.

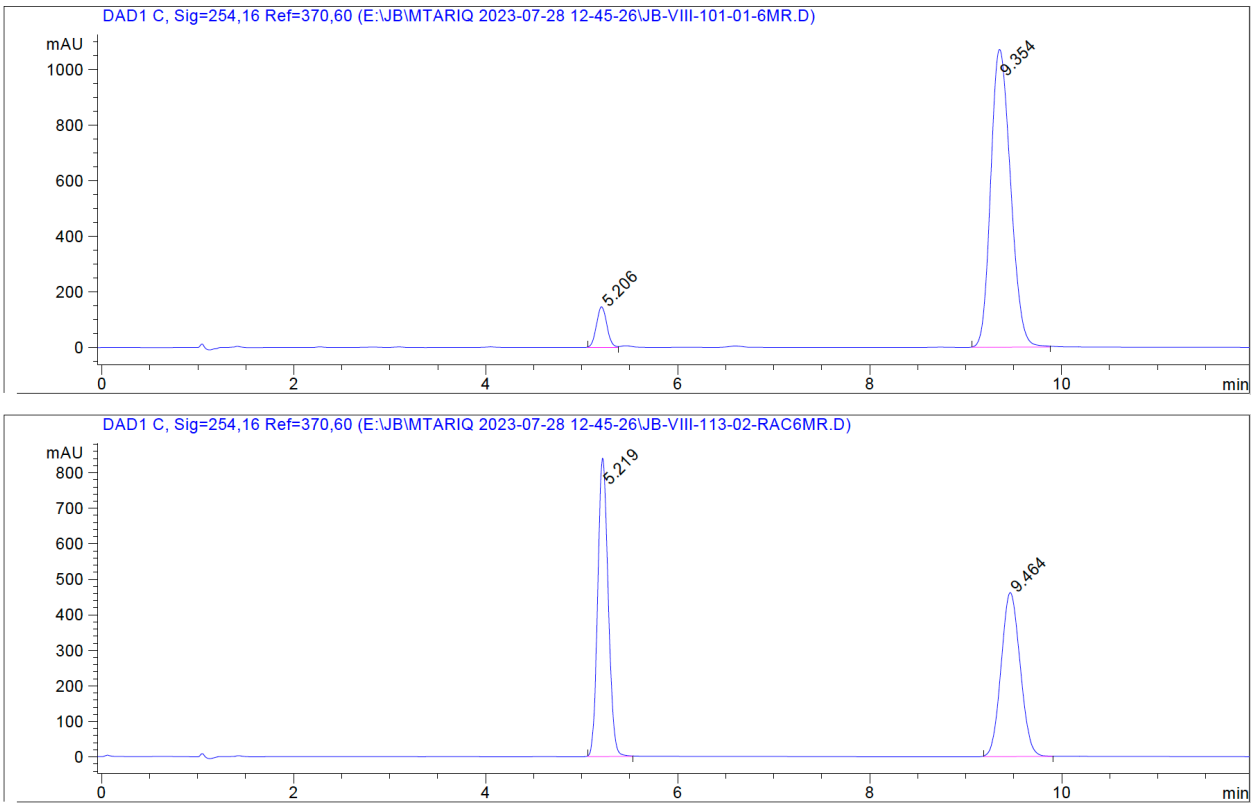

Peak #	RetTime [min]	Type	Width [min]	Area [mAU*s]	Height [mAU]	Area %
1	5.206	BV	0.1200	1104.03723	146.31050	23.4316
2	9.354	BB	0.2276	1.53871e4	1071.06799	326.5684

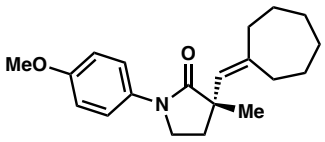

(S)-3-(cycloheptylidenemethyl)-1-(4-methoxyphenyl)-3-methylpyrrolidin-2-one (56a)

Prepared according to general procedure A using **53**. Purification by column chromatography (0–25 % EtOAc/Hexanes) yielded **56a** as a white solid (4.7 mg, 15% yield); 86% ee.

Optical rotation: [α]D25 – 39.4 (c 0.5, CHCl3).

1H NMR (400 MHz, CDCl3) δ 7.54 (d, J = 9.2 Hz, 2H), 6.90 (d, J = 9.1 Hz, 2H), 5.52 (p, J = 1.4 Hz, 1H), 3.80 (s, 3H), 3.77 – 3.32 (m, 2H), 2.86 – 1.98 (m, 6H), 1.84 – 1.40 (m, 8H), 1.36 (s, 3H).

13C NMR (101 MHz, CDCl3) δ 177.9, 156.5, 144.2, 133.3, 128.8, 121.6, 121.6, 114.2, 55.6, 46.3, 45.8, 38.5, 34.1, 31.0, 29.9, 29.7, 29.3, 27.0, 24.4.

IR (neat film, NaCl) 3834, 3732, 2923, 2849, 2341, 1693, 1511, 1395, 1298, 1247, 1087, 1035, 827 cm–1.

HRMS (MM:ESI-APCI+) m/z calc'd for C20H28NO2 [M+H]+: 314.2115, found 314.2029.

SFC conditions: 30% IPA, 2.5 mL/min, Chiralcel AD-3 column, λ = 254 nm, tR (min): minor = 5.32, major = 9.13.

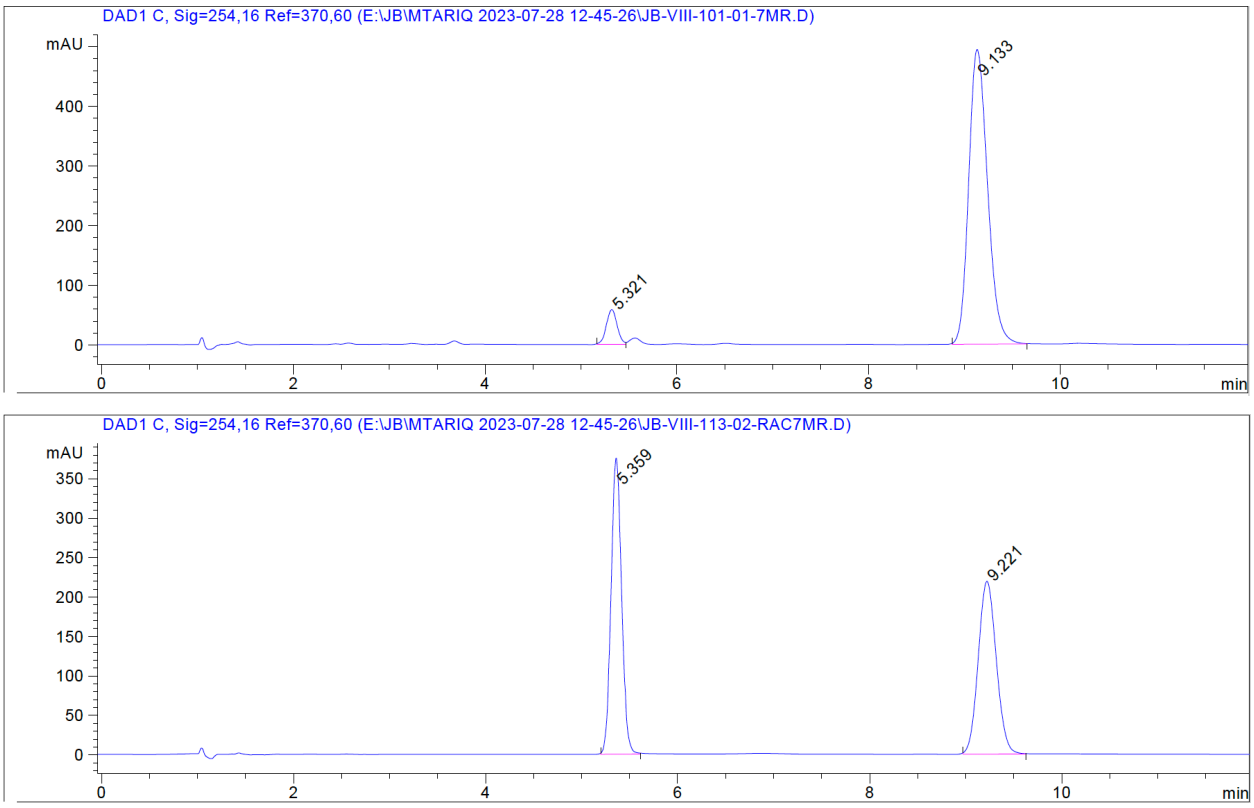

Peak #	RetTime [min]	Type	Width [min]	Area [mAU*s]	Height [mAU]	Area %
1	5.321	BV	0.1235	456.16669	58.17908	22.1449
2	9.133	BB	0.2117	6753.53467	493.49271	327.8551

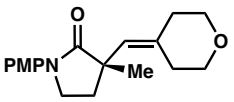

(S)-3-(tetrahydropyranlidenemethyl)-1-(4-methoxyphenyl)-3-methylpyrrolidin-2-one (57a)

Prepared according to general procedure A using **53**. Purification by column chromatography (0–30% EtOAc/Hexanes) yielded **57a** as a colorless oil (13.2 mg, 44%); 88% ee.

Optical rotation: [α]D25 – 41.4 (c 1.0, CHCl3).

1H NMR (400 MHz, CDCl3) δ 7.52 (d, J = 9.0 Hz, 2H), 6.90 (d, J = 9.1 Hz, 2H), 5.54 (d, J = 1.3 Hz, 1H), 3.79 (s, 3H), 3.78 – 3.57 (m, 6H), 2.34 (tt, J = 5.8, 1.2 Hz, 2H), 2.29 – 2.17 (m, 4H), 1.37 (s, 3H);

13C NMR (101 MHz, CDCl3) δ 177.44, 156.64, 137.52, 133.07, 127.53, 121.63, 114.18, 69.80, 68.44, 55.62, 46.01, 45.69, 37.52, 34.88, 31.32, 24.78.

IR (neat film, NaCl) 2958, 2839, 1691, 1511, 1462, 1396, 1286, 1269, 1246, 1087, 1032, 831 cm–1

HRMS (MM:ESI-APCI+) m/z calc'd for C18H23NO3 [M+H]+: 302.1751, found 302.1750.

SFC conditions: 30% IPA, 2.5 mL/min, Chiralcel AD-3 column, λ = 254 nm, tR (min): minor = 8.03, major = 11.15.

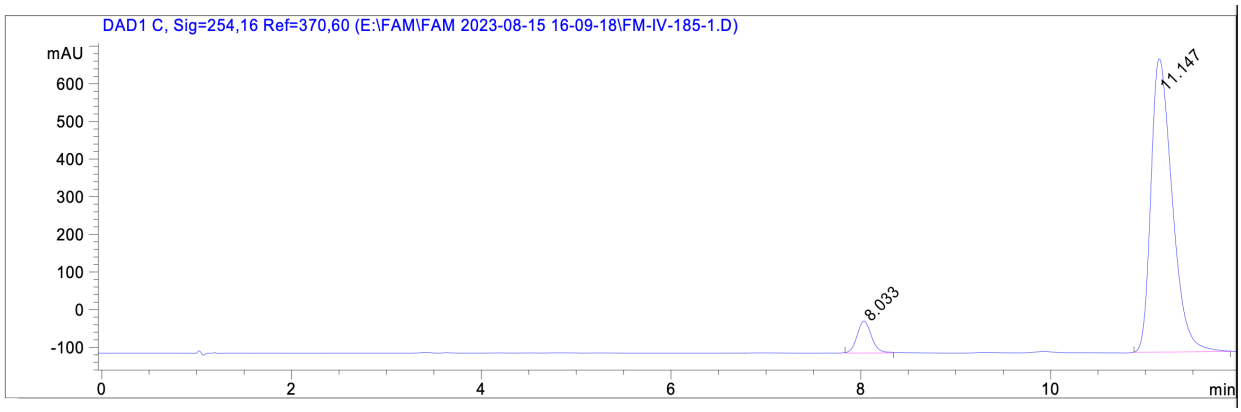

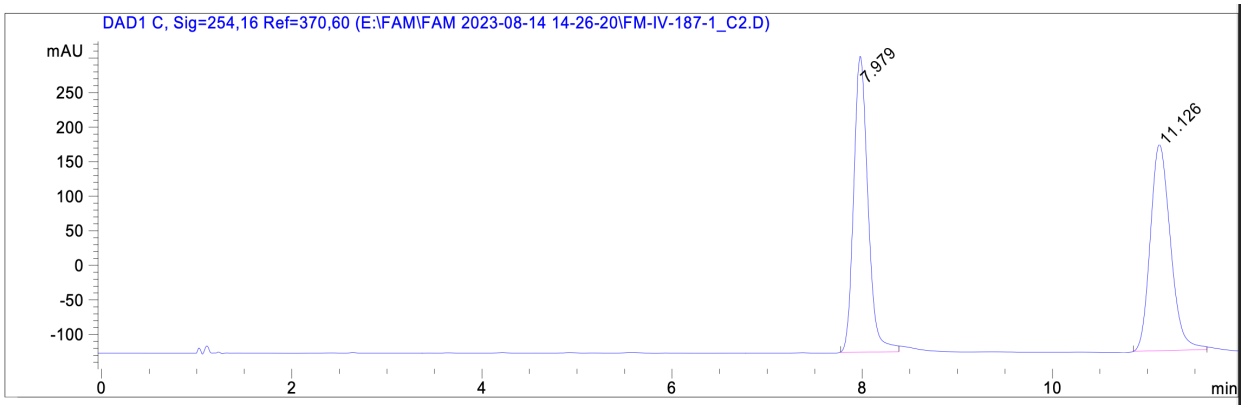

Peak #	RetTime [min]	Type	Width [min]	Area [mAU*s]	Height [mAU]	Area %
1	8.033	BB	0.1634	895.48993	84.67880	24.0017
2	11.147	BB	0.2379	1.21628e4	780.28503	325.9983

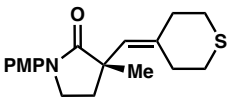

(S)-3-(tetrahydro-thiopyranlidenemethyl)-1-(4-methoxyphenyl)-3-methylpyrrolidin-2-one (58a)

Prepared according to general procedure A using **53**. Purification by column chromatography (0–25 % EtOAc/Hexanes) yielded **58a** as a colorless oil (13.5 mg, 43%); 86% ee.

Optical rotation: [α]D25 –58.3 (c 1.0, CHCl3).

1H NMR (400 MHz, CDCl3) δ 7.52 (d, J = 9.1 Hz, 1H), 6.90 (d, J = 9.1 Hz, 1H), 5.55 (t, J = 1.0 Hz, 1H), 3.80 (s, 2H), 3.78 – 3.68 (m, 1H), 2.76 – 2.48 (m, 4H), 2.44 (td, J = 5.4, 2.5 Hz, 1H), 2.24 – 2.17 (m, 1H), 1.36 (s, 2H).

13C NMR (101 MHz, CDCl3) δ 177.43, 156.64, 139.64, 133.05, 128.95, 121.61, 114.19, 55.62, 45.92, 45.65, 39.36, 34.79, 32.15, 31.22, 29.89, 24.76.

IR (neat film, NaCl) 2953, 1689, 1511, 1428, 1398, 1297, 1247, 1180, 1087, 1034, 821 cm–1.

HRMS (MM:ESI-APCI+) m/z calc'd for C18H23NO2S [M+H]+: 318.1522, found 318.1520.

SFC conditions: 30% IPA, 2.5 mL/min, Chiralcel AD-3 column, λ = 254 nm, tR (min): minor = 7.45, major = 6.32.

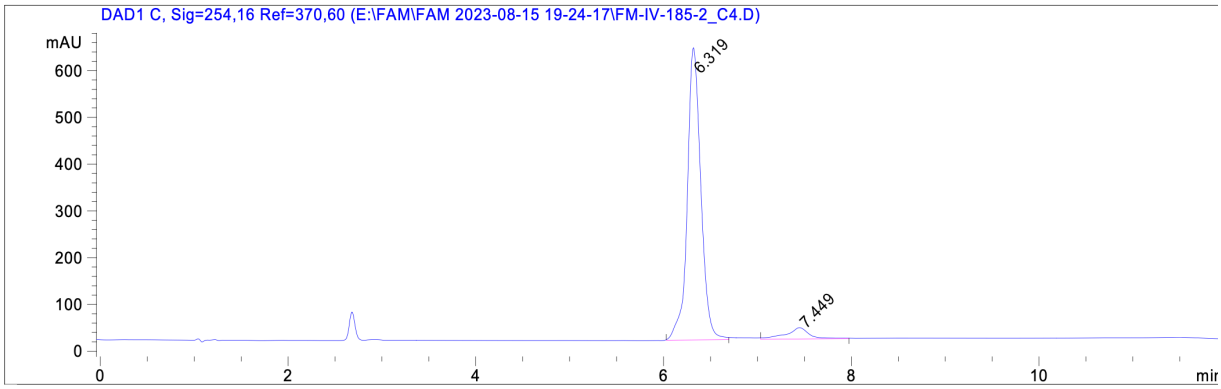

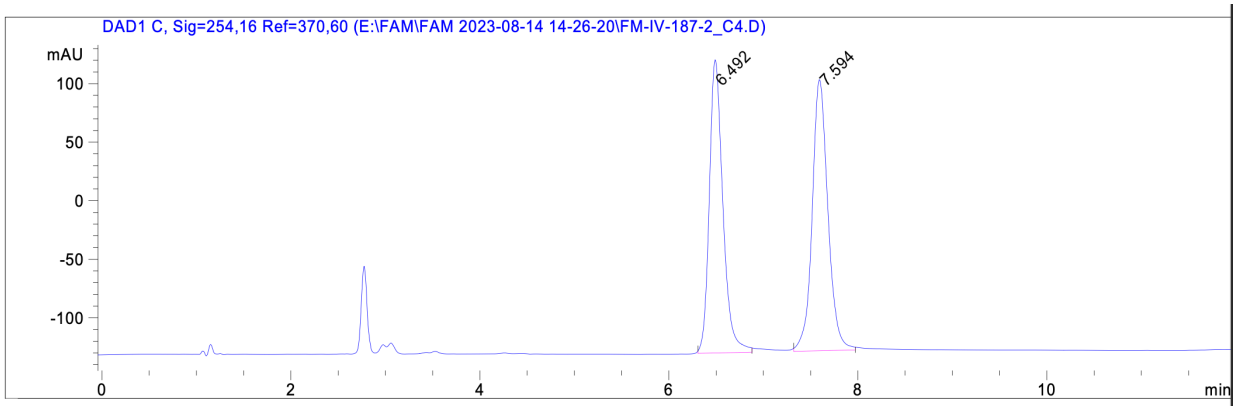

Peak #	RetTime [min]	Type	Width [min]	Area [mAU*s]	Height [mAU]	Area %
1	6.319	BB	0.1536	6285.17188	623.72955	328.2187
2	7.449	BB	0.2366	417.09830	24.25278	21.7813

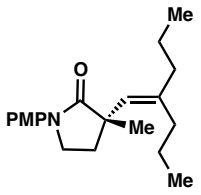

(S)-1-(4-methoxyphenyl)-3-methyl-3-(2-propylpent-1-en-1-yl)pyrrolidin-2-one (59a)

Prepared according to general procedure A using **53**. The crude product was purified by silica gel chromatography (30% EtOAc/Hexanes) to afford vinylated lactam X (58% yield, 90% ee) as a colorless oil.

Optical rotation: [a]D25 – 2.5 ° (c 0.35, CHCl3).

1H NMR (400 MHz, CDCl3) δ 7.54 (d, J = 9.1 Hz, 2H), 6.90 (d, J = 9.1 Hz, 2H), 5.50 (t, J = 1.0 Hz, 1H), 3.80 (d, J = 0.7 Hz, 3H), 3.78 – 3.67 (m, 2H), 2.34 – 2.25 (m, 1H), 2.25 – 2.17 (m, 1H), 2.12 – 2.03 (m, 1H), 2.03 – 1.94 (m, 3H), 1.48 – 1.38 (m, 4H), 1.36 (s, 3H), 0.93 – 0.84 (m, 6H).

13C NMR (101 MHz, CDCl3) δ 177.92, 156.38, 142.39, 133.19, 128.45, 121.44, 114.01, 77.35, 77.23, 77.03, 76.71, 55.51, 46.15, 45.59, 38.79, 34.47, 32.97, 24.74, 21.33, 21.10, 14.58, 13.81.

IR (thin film, NaCl) 2958, 2930, 2870, 1694, 1513, 1469, 1454, 1423, 1398, 1299, 1288, 1248, 1181, 1168, 1122, 1087, 1036, 836, 823, 805, 634 cm^{-1}

HRMS (MM:ESI-APCI+) m/z calc'd C20H29NO2 [M+Na]+: 338.2091, found: 338.2100.

SFC conditions: 30% IPA, 2.5 mL/min, Chiralcel AD-3 column, λ = 254 nm, tR (min): minor = 2.88, major = 3.73.

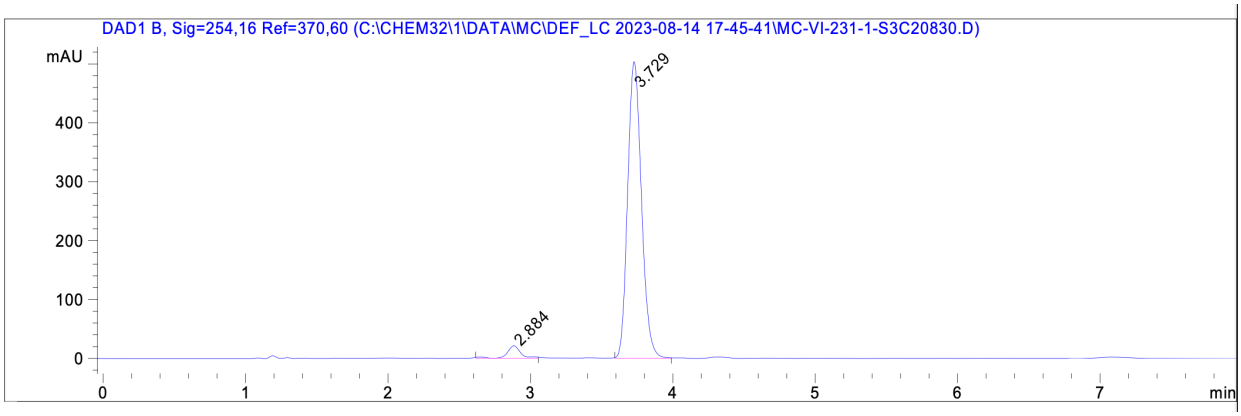

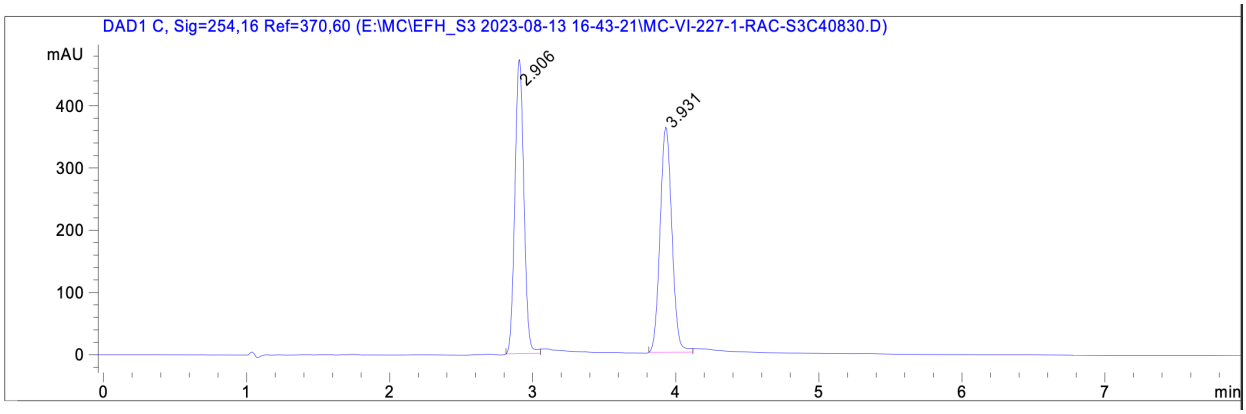

Peak #	RetTime [min]	Type	Width [min]	Area [mAU*s]	Height [mAU]	Area %
1	2.884	BB	0.0977	139.83130	21.00225	3.9512
2	3.729	BB	0.1069	3399.10669	502.66321	96.0488

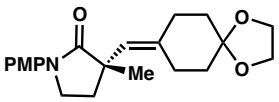

(S)-3-((1,4-dioxaspiro[4.5]decan-8-ylidene)methyl)-1-(4-methoxyphenyl)-3-methylpyrrolidin-2-one (60a)

Prepared according to general procedure A using **53**. The crude product was purified by silica gel chromatography (30% EtOAc/Hexanes) to afford vinylated lactam **60a** (48% yield, 62% ee) as a colorless oil.

Optical rotation: [a]D25 + 4.5 ° (c 0.52, CHCl3).

1H NMR (400 MHz, CDCl3) δ 7.53 (d, J = 9.1 Hz, 2H), 6.90 (d, J = 9.1 Hz, 2H), 5.54 (d, J = 1.7 Hz, 1H), 3.95 (s, 3H), 3.80 (s, 3H), 3.76 – 3.60 (m, 2H), 2.40 – 2.29 (m, 2H), 2.31 – 2.16 (m, 4H), 1.71 (td, J = 6.7, 3.9 Hz, 3H), 1.68 – 1.62 (m, 1H), 1.60 (s, 1H), 1.37 (s, 3H).

13C NMR (101 MHz, CDCl3) δ 177.70, 156.58, 140.01, 133.20, 127.18, 121.62, 114.17, 114.14, 108.72, 77.48, 77.36, 77.16, 76.84, 64.48, 64.45, 55.64, 46.10, 45.72, 36.37, 35.31, 34.67, 34.46, 26.65, 24.72.

IR (thin film, NaCl) 3465, 2950, 2886, 2320, 2009, 1902, 1693, 1681, 1513, 1433, 1401, 1298, 1276, 1248, 1226, 1181, 1171, 1120, 1082, 1032, 944, 906, 826, 738, 728 cm–1;

HRMS (ESI) m/z calc'd C21H27NO4 [M+Na]+: 380.1832, found: 380.1843.

SFC conditions: 30% IPA, 2.5 mL/min, Chiralcel AD-3 column, λ = 254 nm, tR (min): minor = 3.53, major = 5.02.

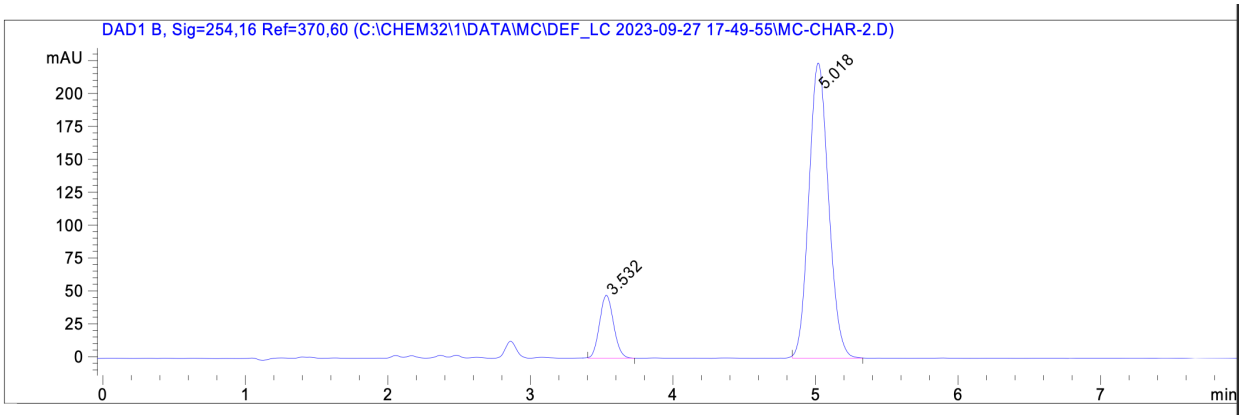

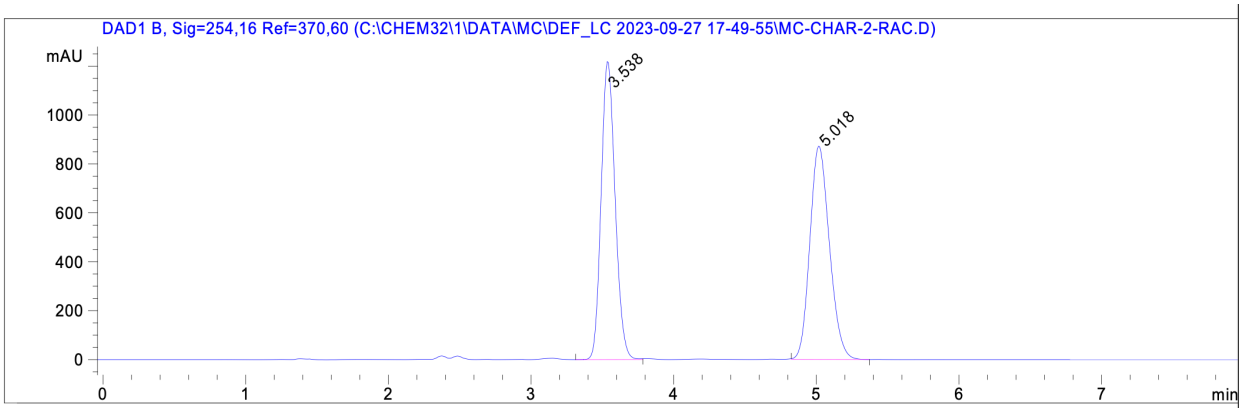

Peak #	RetTime [min]	Type	Width [min]	Area [mAU*s]	Height [mAU]	Area %
1	3.532	BB	0.1077	326.17273	47.72661	13.1365
2	5.018	BB	0.1523	2156.76880	223.97276	86.8635

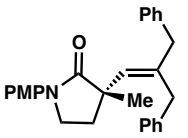

(S)-3-(2-benzyl-3-phenylprop-1-en-1-yl)-1-(4-methoxyphenyl)-3-methylpyrrolidin-2-one (61a)

Prepared according to general procedure A using **53**. The crude product was purified by silica gel chromatography (30% EtOAc/Hexanes) to afford vinylated lactam **61a** (22% yield, 88% ee) as a colorless oil.

Optical rotation: [a]D25 – 12.4 ° (c 0.56, CHCl3).

1H NMR (400 MHz, CDCl3) δ 7.58 (d, J = 9.1 Hz, 2H), 7.38 – 7.32 (m, 2H), 7.30 – 7.23 (m, 3H), 7.23 – 7.17 (m, 2H), 7.17 – 7.10 (m, 2H), 6.95 (d, J = 9.1 Hz, 2H), 6.02 (t, J = 1.0 Hz, 1H), 3.86 (s, 3H), 3.84 – 3.74 (m, 2H), 3.54 – 3.38 (m, 2H), 3.27 (t, J = 1.6 Hz, 2H), 2.43 (dt, J = 12.5, 8.2 Hz, 1H), 2.30 (ddd, J = 12.5, 7.2, 3.6 Hz, 1H), 1.52 (s, 3H).

13C NMR (101 MHz, CDCl3) δ 177.40, 156.53, 139.80, 139.45, 139.03, 132.94, 132.77, 128.97, 128.94, 128.45, 128.32, 128.28, 126.10, 121.61, 114.06, 77.35, 77.24, 77.03, 76.72, 55.51, 46.39, 45.68, 43.33, 35.85, 34.10, 24.79.

IR (thin film, NaCl) 3059, 3025, 2930, 2835,m 2340, 1682, 1600, 1520, 1493, 1453, 1398, 1298, 1240, 1181, 1120, 1088, 1031, 829, 734, 702 cm^{-1}.

HRMS (MM:ESI-APCI+) m/z calc'd C28H29NO2 [M+Na]+: 434.2091, found: 434.2102.

SFC conditions: 30% IPA, 2.5 mL/min, Chiralcel AD-3 column, λ = 254 nm, tR (min): minor = 5.63, major = 7.11.

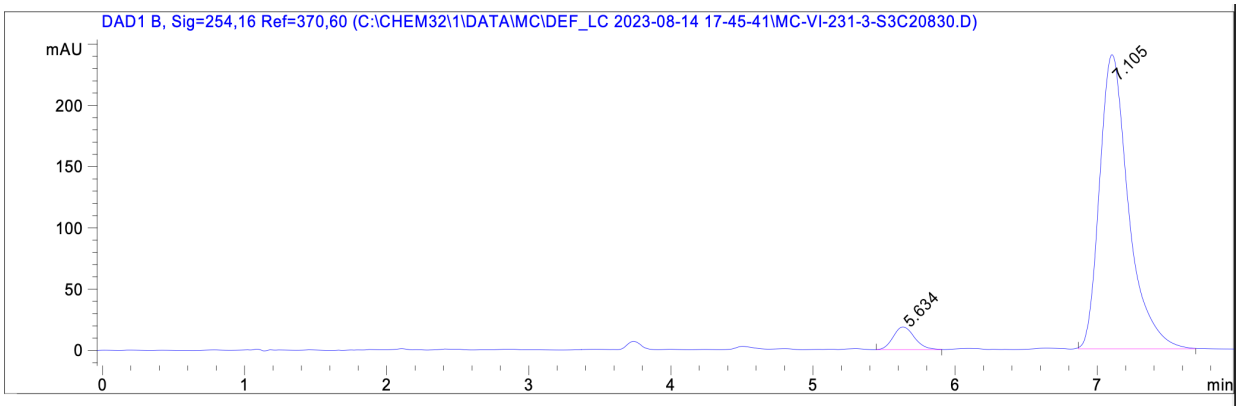

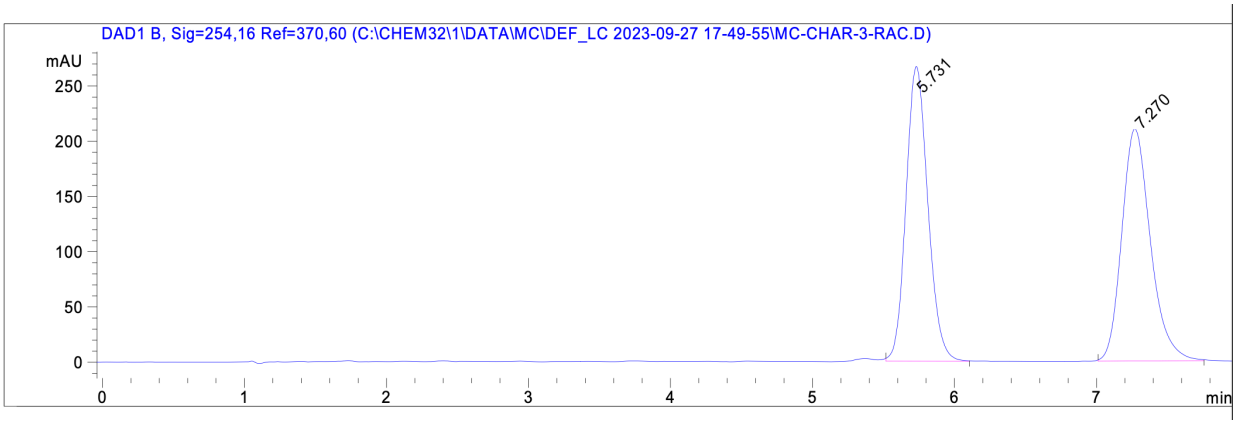

Peak #	RetTime [min]	Type	Width [min]	Area [mAU*s]	Height [mAU]	Area %
1	5.634	BB	0.1609	192.02281	18.53370	5.3335
2	7.105	BB	0.2136	3408.32178	240.14082	94.6665

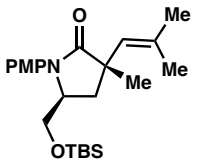

(3S,5S)-5-(((tert-butyldimethylsilyl)oxy)methyl)-1-(4-methoxyphenyl)-3-methyl-3-(2-methylprop-1-en-1-yl)pyrrolidin-2-one (62a)

Prepared according to general procedure A using **53**. The crude product was purified by silica gel chromatography (0-30% EtOAc/Hexanes) to afford vinylated lactam **62a** (21 mg, 52% yield) as a colorless oil; [a]D25 – 36.795 ° (c 1, CHCl3); 1H NMR (400 MHz, CDCl3) δ 7.25 – 7.21 (m, 2H), 6.92 – 6.86 (m, 2H), 5.41 (h, J = 1.4 Hz, 1H), 4.09 (dddd, J = 8.6, 5.8, 4.4, 2.8 Hz, 1H), 3.80 (s, 3H), 3.62 – 3.45 (m, 2H), 2.41 (dd, J = 12.9, 8.6 Hz, 1H), 2.13 (dd, J = 12.9, 5.7 Hz, 1H), 1.70 (dd, J = 3.6, 1.4 Hz, 6H), 1.47 (s, 3H), 0.84 (s, 9H), 0.07 (s, 3H), -0.09 (d, J = 13.5 Hz, 6H); 13C NMR (101 MHz, CDCl3) δ 178.85, 157.83, 134.10, 130.70, 129.77, 126.45, 114.31, 62.55, 58.54, 55.61, 45.31, 37.50, 27.10, 26.99, 25.95, 19.09, 18.38, 1.16, -5.50, -5.51. IR (thin film, NaCl) 2932, 2857, 1693, 1513, 1467, 1401, 1247, 1104, 1043, 826 cm–1; HRMS (MM:ESI-APCI+) m/z calc'd C23H37NO3Si [M+H]+: 404.2615, found 404.2626.

Preparation of Vinyl Chloride Substrates: General Procedure B

To a stirred suspension of (chloromethyl)triphenylphosphonium chloride (2.60 g, 7.50 mmol, 1.5 equiv) in diethyl ether (60 mL) was added sodium bis(hexamethylsilyl)amide (1.38 g, 7.50 mmol, 1.5 equiv) in diethyl ether (15 mL) at –78 °C or 0 ºC, and the resulting mixture was stirred at this temperature for 1 h. Then, ketone (5 mmol, 1.0 equiv) was added dropwise, and the reaction was allowed to slowly warm to room temperature and stirred overnight. After 18 h, the reaction was quenched with water (50 mL), transferred to a separatory funnel, and extracted with diethyl ether (20 mL) three times. The combined organics were washed with brine, dried over anhydrous Na2SO4, filtered, concentrated, and purified by silica gel chromatography to provide the desired vinyl chloride.

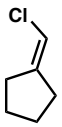

(chloromethylene)cyclopentane (S1)

Prepared according to general procedure B using cyclopentanone. Purification by column chromatography (100% Hexanes) yielded vinyl chloride **S1** as a clear oil (209 mg, 36% yield); 1H NMR (400 MHz, CDCl3) δ 5.86 (p, J = 2.4 Hz, 1H), 2.42 – 2.23 (m, 4H), 1.80 – 1.63 (m, 4H); 13C NMR (101 MHz, CDCl3) δ 146.9, 108.0, 32.6, 30.7, 27.4, 25.8; IR (neat film, NaCl) 3817, 3645, 2955, 2359, 1650, 1455, 772, 653 cm–1; HRMS (FI+) m/z calc'd for C6H9Cl [M]+•: 116.04001, found 116.03928.

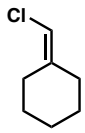

(chloromethylene)cyclohexane (S2)

Prepared according to general procedure B using cyclohexanone. Purification by silica gel chromatography (100% Hexanes) yielded **S2** as a clear oil (419 mg, 64% yield); 1H NMR (400 MHz, CDCl3) δ 5.76 (p, J = 1.2 Hz, 1H), 2.32 (m, 2H), 2.13 (m, 2H), 1.55 (m, 6H); 13C NMR (101 MHz, CDCl3) δ 142.3, 108.5, 34.2, 28.6, 28.0, 26.8, 26.5; IR (neat film, NaCl) 3817, 3732, 3064, 2937, 2356, 1636, 1541, 1455, 1336, 1293, 1231, 986, 786 cm–1; HRMS (FI+) m/z calc'd for C7H11Cl [M]+•: 130.05493, found 130.05581.

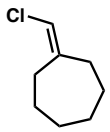

(chloromethylene)cycloheptane (S3)

Prepared according to general procedure B using cycloheptanone. Purification by silica gel chromatography (100% Hexanes) yielded **S3** as a colorless oil (557 mg, 77% yield); 1H NMR (400 MHz, CDCl3) δ 5.81 (p, J = 1.5 Hz, 1H), 2.45 – 2.36 (m, 2H), 2.30 – 2.22 (m, 2H), 1.70 – 1.55 (m, 4H), 1.53 – 1.43 (m, 4H); 13C NMR (101 MHz, CDCl3) δ 144.7, 111.7, 35.2, 30.9, 30.2, 29.4, 29.0, 26.2; IR (neat film, NaCl) 3380, 2921, 2859, 2360, 1674, 1506, 1069, 682 cm–1; HRMS (FI+) m/z calc'd for C8H13Cl [M]+•: 144.07123, found 144.07058.

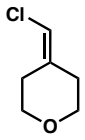

4-(chloromethylene)tetrahydro-2H-pyran (S4)

Prepared according to general procedure B using tetrahydro-4H-pyran-4-one. The crude product was purified by silica gel chromatography (0-20% EtOAc/Hexanes) to afford vinyl chloride **S4** (136 mg, 45%) as a colorless oil; 1H NMR (400 MHz, CDCl3) δ 5.88 (t, J = 1.3 Hz, 1H), 3.69 (dt, J = 7.5, 5.5 Hz, 4H), 2.46 (ddd, J = 6.5, 5.3, 1.3 Hz, 2H), 2.27 (ddd, J = 6.2, 5.0, 1.3 Hz, 2H). 13C NMR (101 MHz, CDCl3) δ 137.23, 110.59, 68.83, 67.97, 34.27, 29.48; IR (thin film, NaCl) 3069, 2961, 2907, 2848, 2747, 2704, 2360, 1954, 1645, 1466, 1432, 1380, 1356, 1323, 1296, 1228, 1165, 1099, 1021, 1000, 923, 859, 822, 792, 749, 663 cm–1; HRMS (FI+) m/z calc'd for C6H9ClO [M]+•: 132.03419, found 132.03478.

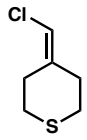

4-(chloromethylene)tetrahydro-2H-thiopyran (S5)

Prepared according to general procedure B using tetrahydro-4H-thiopyran-4-one. The crude product was purified by silica gel chromatography (0-20% EtOAc/Hexanes) to afford vinyl chloride **S5** (189 mg, 81%) as a colorless, malodorous oil. 1H NMR (400 MHz, CDCl3) δ 5.88 (d, J = 1.1 Hz, 1H), 2.71 – 2.62 (m, 6H), 2.51 – 2.45 (m, 2H); 13C NMR (101 MHz, CDCl3) δ 139.26, 111.69, 36.00, 30.52, 30.37, 29.36. IR (thin film, NaCl) 3065, 2949, 2907, 2829, 2360, 1649, 1626, 1425, 1337, 1323, 1291, 1270, 1223, 1171, 991, 975, 938, 822, 797 cm–1; HRMS (FI+) m/z calc'd for C6H9ClS [M]+•: 148.01135, found 148.01232.

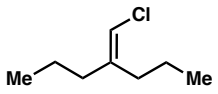

4-(chloromethylene)heptane (S6)

Prepared according to general procedure B using 4-heptanone. The crude product was purified by silica gel chromatography (100% Hexanes) to afford vinyl chloride **S6** (27% yield) as a colorless oil. 1H NMR (400 MHz, CDCl3) δ 5.82 – 5.73 (m, 1H), 2.21 – 2.14 (m, 2H), 2.03 (td, J = 7.6, 1.3 Hz, 2H), 1.58 – 1.34 (m, 4H), 0.91 (dt, J = 16.5, 7.3 Hz, 6H). 13C NMR (101 MHz, CDCl3) δ 142.73, 112.09, 77.48, 77.16, 76.84, 37.00, 32.17, 20.95, 20.52, 14.12, 13.85; IR (thin film, NaCl) 3066, 2980, 2933, 2872, 1911, 1630, 1465, 1456, 1379, 1319, 1169, 1109, 836, 791, 766 cm–1; HRMS (FI+) m/z calc'd C8H15Cl [M+H]+: 146.0862, found: 146.0872.

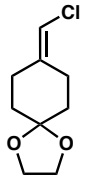

8-(chloromethylene)-1,4-dioxaspiro[4.5]decane (S7)

Prepared according to general procedure B using 1,4-dioxaspiro[4.5]decan-8-one. The crude product was purified by silica gel chromatography (100% Hexanes) to afford vinyl chloride **S7** (79 yield) as a colorless oil. 1H NMR (400 MHz, CDCl3) δ 5.82 (d, J = 1.4 Hz, 1H), 3.97 (s, 4H), 2.53 – 2.43 (m, 2H), 2.30 (td, J = 6.5, 1.3 Hz, 2H), 1.76 – 1.63 (m, 4H). 13C NMR (101 MHz, CDCl3) δ 139.62, 109.97, 108.57, 77.48, 77.16, 76.84, 64.56, 35.59, 34.50, 30.87, 25.39; IR (thin film, NaCl) 3068, 2950, 2930, 2883, 2685, 2728, 2685, 1718, 1654, 1634, 1443, 1366, 1341, 1295, 1272, 1246, 1225, 1186, 1100, 1080, 1034, 962, 943, 908, 828, 797, 770., 748, 678 cm–1; HRMS (FI+) m/z calc'd C9H13ClO2 [M+H]+: 188.0604, found: 188.0619.

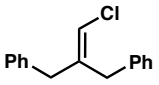

(2-(chloromethylene)propane-1,3-diyl)dibenzene (S8)

Prepared according to general procedure B using 1,3-diphenyl-2-propanone. The crude product was purified by silica gel chromatography (100% Hexanes) to afford vinyl chloride **S8** (68% yield) as a colorless oil; 1H NMR (400 MHz, CDCl3) δ 7.39 – 7.33 (m, 4H), 7.32 – 7.28 (m, 2H), 7.27 – 7.23 (m, 2H), 7.19 – 7.14 (m, 2H), 6.07 – 6.01 (m, 1H), 3.56 (s, 2H), 3.32 (d, J = 1.3 Hz, 2H); 13C NMR (101 MHz, CDCl3) δ 141.17, 138.34, 138.04, 129.07, 128.86, 128.56, 128.54, 126.60, 126.42, 114.88, 77.36, 77.04, 76.72, 40.41, 35.62; IR (thin film, NaCl) 3088, 3062, 3020, 2916, 2845, 2355, 1947, 1872, 1809, 1633, 1601, 1494, 1453, 1433, 1310, 1296, 1178, 1075, 1029, 960, 906, 870, 829,787, 740, 703, 634 cm–1; HRMS (FI+) m/z calc'd C16H15Cl [M+H]+: 242.0862, found: 242.0889.

Synthesis of Substrates 62 and 63

Following a literature protocol, enantiopure alcohol was dissolved in CH2Cl2 (0.86 M). Iteratively, TBSCl (1.2 equiv) and imidazole (1.5 equiv) were added. The reaction was stirred for 4h, after which it was quenched with H¬2O and separated into layers. The aqueous phase was extracted with CH2Cl2 two more times, and the combined organic extracts were dried with Na2SO4. The product was isolated as a colorless oil (quant.) and used in the next step without additional purification.

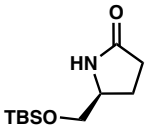

(S)-5-(((tert-butyldimethylsilyl)oxy)methyl)pyrrolidin-2-one (S9)

Prepared according to a literature procedure. Characterization data was in agreement with the literature. 1H NMR (500 MHz, CDCl3) δ 5.71 (s, 1H), 3.92 – 3.70 (m, 1H), 3.63 (dd, J = 10.1, 3.8 Hz, 1H), 3.44 (dd, J = 10.1, 7.9 Hz, 1H), 2.35 (ddd, J = 8.6, 7.2, 2.8 Hz, 2H), 2.25 – 2.09 (m, 1H), 1.73 (dddd, J = 13.2, 9.3, 7.7, 5.5 Hz, 1H), 0.90 (s, 9H), 0.07 (s, 6H).

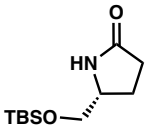

(R)-5-(((tert-butyldimethylsilyl)oxy)methyl)pyrrolidin-2-one (S10)

In a flask equipped with a magnetic stir bar, CuI (0.5 mmol, 10 mol%) was combined with anhydrous K2CO3 (10 mmol, 2 equiv). The vial was purged and backfilled with N2 three times. At this point, 5 mL of toluene was added, followed by N, N'-dimethylethylenediamine (1 mmol, 20 mol%), intermediate XX or XX (6 mmol, 1.2 equiv), and p-Br anisole (5 mmol). The reaction mixture was allowed to react at 100 ºC for 24h. The crude reaction mixture was concentrated and purified by silica gel chromatography (0-100% EtOAc/Hexanes) to afford the product **S10** as a pale yellow oil (1.10 g, 66% yield).

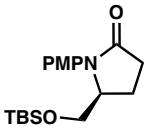

(S)-5-(((tert-butyldimethylsilyl)oxy)methyl)-1-(4-methoxyphenyl)pyrrolidin-2-one (S11)

[α]D25 –48.0º (c 1.0, CHCl3); 1H NMR (400 MHz, CDCl3) δ 7.27 (d, J = 8.9 Hz, 2H), 6.91 (d, J = 8.9 Hz, 2H), 4.12 (dtd, J = 8.6, 3.6, 2.5 Hz, 1H), 3.80 (3, 2H), 3.68 – 3.43 (m, 2H), 2.68 (ddd, J = 16.9, 10.1, 8.1 Hz, 1H), 2.49 (ddd, J = 16.9, 10.2, 4.6 Hz, 1H), 2.26 (ddt, J = 12.8, 10.1, 8.3 Hz, 1H), 2.09 (dddd, J = 12.7, 10.1, 4.6, 3.5 Hz, 1H), 0.86 (s, 9H), -0.04 (d, J = 11.3 Hz, 6H);13C NMR (101 MHz, CDCl3) δ 175.25, 157.89, 130.53, 126.46, 114.47, 62.96, 62.00, 55.61, 31.59, 25.92, 21.51, 18.27, -5.47, -5.51. IR (thin film, NaCl) 2934, 1694, 1513, 1248, 1090, 834, 682 cm–1; HRMS (MM:ESI-APCI+) m/z calc'd C18H29NO3Si [M+H]+: 336.1989, found 336.1999.

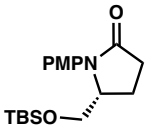

(R)-5-(((tert-butyldimethylsilyl)oxy)methyl)-1-(4-methoxyphenyl)pyrrolidin-2-one (S12)

A solution of LDA was prepared by the slow addition of n-BuLi (1.44 mL, 2.5 M in hexanes) to a solution of diisopropylamine (3.61 mmol) in THF (0.9 M) at -78ºC. After letting the mixture stir for 1h at this temperature, substrate **S10** was added slowly as a solution in THF (0.3 M). 30 min later, MeI (3.61 mmol) was added slowly to the reaction mixture, and it was allowed to warm up to 18 ºC. After 16h, the reaction was quenched with sat. NH4Cl solution and extracted with CH_2Cl_2. The crude compound was concentrated and purified by silica gel chromatography (10-60% EtOAc/Hexanes) to afford the product as a dark solid (703 mg, 61% yield).

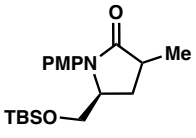

(5S)-5-(((tert-butyldimethylsilyl)oxy)methyl)-1-(4-methoxyphenyl)-3-methylpyrrolidin-2-one (62)

[α]D25 –30.0º (c 1.0, CHCl3); 1H NMR (500 MHz, cdcl3) δ 7.32 (d, J = 9.1 Hz, 2H), 6.90 (d, J = 9.1 Hz, 2H), 4.15 – 4.01 (m, 1H), 3.81 (s, 3H), 3.68 – 3.43 (m, 2H), 2.81 (td, J = 9.1, 7.1 Hz, 1H), 2.33 (ddd, J = 12.7, 9.0, 2.0 Hz, 1H), 1.90 (dt, J = 12.6, 9.1 Hz, 1H), 1.26 (d, J = 7.1 Hz, 3H), 0.86 (s, 9H), -0.03 (d, J = 11.9 Hz, 6H).13C NMR (101 MHz, CDCl3) δ 177.47, 157.52, 130.99, 125.74, 114.37, 62.96, 59.86, 55.60, 36.84, 30.94, 25.94, 18.27, 17.08, -5.45, -5.48; IR (thin film, NaCl) 2928, 1693, 1513, 1463, 1272, 1246, 1171, 1107, 1041, 832, 776, 681 cm–1; HRMS (MM:ESI-APCI+) m/z calc'd C19H31NO3Si [M+H]+: 350.2146, found 350.2143.

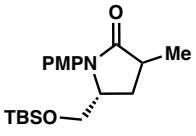

(5R)-5-(((tert-butyldimethylsilyl)oxy)methyl)-1-(4-methoxyphenyl)-3-methylpyrrolidin-2-one (63)

Refer to Compound 62 for 1H NMR, 13C NMR, IR, and HRMS data. [α]D25 32.3º (c 1.0, CHCl3).

3.5.3 Derivitization of Vinylation Products

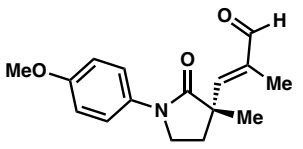

(S,E)-3-(1-(4-methoxyphenyl)-3-methyl-2-oxopyrrolidin-3-yl)-2-methylacrylaldehyde (69)

To a solution of **53a** (26 mg, 0.1 mmol) in dioxane (0.2 M) was added SeO2 (22 mg, 0.2 mmol), and the reaction was heated to reflux. After 15 minutes, starting material was consumed by TLC. The crude reaction was concentrated and passed through a silica plug (ca. 1" silica), eluting with 35% EtOAc/Hexanes, to afford the desired aldehyde **69** as a tan solid (13.4 mg 49% yield).

Optical rotation: [α]D25 –60.6º (c 1.0, CHCl3).

1H NMR (400 MHz, CDCl3) δ 9.44 (s, 1H), 7.53 (d, J = 9.2 Hz, 2H), 6.92 (d, J = 9.2 Hz, 2H), 6.89 (d, J = 1.4 Hz, 1H), 3.88 (m, 1H), 3.81 (s, 4H), 3.78 – 3.35 (m, 1H), 2.43 – 2.31 (m, 2H), 1.84 (d, J = 1.4 Hz, 3H), 1.48 (s, 3H).

13C NMR (101 MHz, CDCl3) δ 195.8, 175.4, 157.0, 156.1, 139.7, 132.5, 121.8, 114.3, 55.6, 47.5, 45.8, 32.5, 22.9, 10.1.

IR (neat film, NaCl) 3834, 3732, 2958, 2359, 1688, 1512, 1396, 1299, 1249, 1178, 1090, 1031, 833 cm–1.

HRMS (FI+) m/z calc'd for C16H19NO3 [M]+•: 273.13649, found 273.13926.

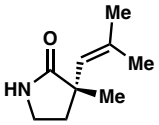

(S)-3-methyl-3-(2-methylprop-1-en-1-yl)pyrrolidin-2-one (70)

A solution of CAN (82 mg, 0.15 mmol) in deionized H2O (0.05 M) was added dropwise to a solution of **53a** (26 mg, 0.1 mmol) at 0 °C, and the reaction was allowed to slowly warm to room temperature. After 12 hours, starting material remained by TLC. CAN (82 mg, 0.15 mmol) added, and the reaction was allowed to continue at 23 °C. After 2 h, the reaction was heated to 60 °C and continued for 18 hours, at which point starting material was consumed by TLC. The reaction was cooled, diluted with ethyl acetate and water, transferred to a separatory funnel, and the organic layer was separated. The aqueous layer was extracted twice with ethyl acetate, the combined organics were dried with Na2SO4, filtered and concentrated. The material was purified with silica gel chromatography (5–10% MeOH/CH2Cl2) to afford the desired lactam **70** as a white solid (6.2 mg, 40% yield).

Optical rotation: [α]D25 –15.7 (c 0.5, CHCl3).

1H NMR (400 MHz, CDCl3) δ 6.37 – 5.97 (bs, 1H), 5.38 (p, J = 1.4 Hz, 1H), 3.32 (ddd, J = 8.2, 5.5, 0.9 Hz, 2H), 2.39 – 1.87 (m, 2H), 1.72 (d, J = 1.5 Hz, 3H), 1.67 (d, J = 1.3 Hz, 3H), 1.29 (s, 3H).

13C NMR (101 MHz, CDCl3) δ 182.8, 134.7, 128.1, 44.0, 39.0, 36.8, 27.0, 24.4, 19.1.

IR (neat film, NaCl) 3835, 3732, 3229, 2964, 2927, 2358, 1697, 1454, 1281, 1062, 832 cm–1.

HRMS (MM:ESI-APCI+) m/z calc'd for C9H16NO [M+H]+: 154.1226, found 154.1230.

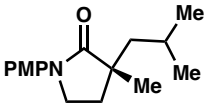

(R)-3-isobutyl-1-(4-methoxyphenyl)-3-methylpyrrolidin-2-one (64)

A one-dram vial was charged with a stir bar and flame dried. Starting material **53a** (15mg, 0.058mmol, 1 equiv) was then added with MeOH (0.421uL, 0.1M), followed by Pd/C (10%) (6.23mg, 0.058 mmol, 1 equiv). Reaction mixture was purged with N2 for 5 minutes and then with H2, and the mixture was stirred overnight with a H2 balloon. Upon complete consumption of starting material as determined by TLC (30% EtOAc in Hexanes), the reaction was quenched by filtering through a pad of celite with DCM. The filtrate was concentrated in vacuo, and the crude product was purified by prep TLC (25% EtOAc/Hexanes) to afford lactam **64** (7.6 mg, 74% yield) as a pale yellow oil.

Optical rotation: [α]D25 – 117.2 ° (c 0.20, CHCl3).

1H NMR (400 MHz, CDCl3) δ 7.65 – 7.44 (m, 2H), 7.04 – 6.81 (m, 2H), 3.80 (s, 3H), 3.77 – 3.65 (m, 2H), 2.17 (ddd, J = 12.7, 8.4, 7.0 Hz, 1H), 1.92 (ddd, J = 12.6, 7.8, 4.7 Hz, 1H), 1.79 (dqd, J = 8.3, 6.6, 4.6 Hz, 1H), 1.68 – 1.58 (m, 2H), 1.49 (dd, J = 14.1, 8.3 Hz, 1H), 1.21 (s, 3H), 0.94 (dd, J = 17.5, 6.7 Hz, 6H).

13C NMR (101 MHz, CDCl3) δ 178.63, 156.49, 133.28, 121.57, 114.13, 55.63, 46.22, 45.67, 45.19, 31.26, 25.17, 25.04, 23.77, 23.42; IR (thin film, NaCl) 3358, 2953, 2930,

2869, 2837, 2058, 1885, 1700, 1610, 1518, 1461, 1453, 1394, 1366, 1313, 1290, 1252, 1233, 1184, 1168, 1121, 1036, 1011, 830, 805, 743, 722.

HRMS (MM:ESI-APCI+) m/z calc'd C16H23NO2 [M+Na]+: 284.1621, found: 284.1628.

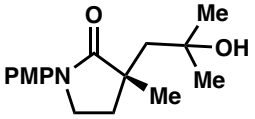

(S)-3-(2-hydroxy-2-methylpropyl)-1-(4-methoxyphenyl)-3-methylpyrrolidin-2-one (66)

In a one-dram vial, starting material **53a** (10.9mg, 0.042 mmol, 1 equiv) was combined with PTSA (4mg, 0.021 mmol, 0.5 equiv) and acetic acid (700uL, 0.06M). The reaction mixture was heated to 70 ºC overnight, and reaction was tracked by LCMS. After completion, saturated aqueous NaHCO3 was added to quench the reaction, and then extracted with DCM and washed with brine. The combined organic layer was dried over MgSO4 and concentrated in vacuo. The crude material was purified via prep TLC (50% EtOAc/Hexanes) to afford alcohol **66** (6.3 mg, 59% yield) as a colorless oil.

Optical rotation: [α]D25 4.1950 ° (c 0.60, CHCl3).

1H NMR (400 MHz, CDCl3) δ 6.78 (d, J = 8.9 Hz, 2H), 6.58 (d, J = 8.9 Hz, 2H), 3.74 (s, 3H), 3.22 (ddd, J = 12.1, 8.7, 5.3 Hz, 1H), 3.12 (ddd, J = 12.1, 8.8, 6.7 Hz, 1H), 2.18 (d, J = 13.4 Hz, 1H), 2.07 – 1.78 (m, 3H), 1.47 (s, 3H), 1.39 (d, J = 5.6 Hz, 6H).

13C NMR (101 MHz, CDCl3) δ 181.58, 152.46, 142.26, 115.04, 114.42, 81.30, 77.48, 77.36, 77.16, 76.84, 55.93, 46.41, 44.08, 41.02, 38.70, 30.35, 30.24, 26.64.

IR (thin film, NaCl) 3369, 2968, 2930, 2834, 2339, 1754, 1681, 1513, 1455, 1401, 1377, 1265, 1249, 182, 1171, 1115, 1098, 1035, 942, 824.

HRMS (MM:ESI-APCI+) m/z calc'd C16H23NO3 [M+H]+: 278.1751, found: 278.1771.

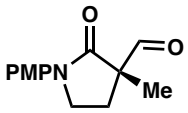

(S)-1-(4-methoxyphenyl)-3-methyl-2-oxopyrrolidine-3-carbaldehyde (67)

Procedure A: A one-dram vial was flame dried and charged with stir bar. Starting material **53a** (50mg, 0.2 mmol, 1 equiv) was added with CH2Cl2 (482uL, 0.4M). The reaction mixture was cooled to – 78 ºC in a dry-ice bath, and ozone (1 atm) was bubbled through until all starting material was consumed as indicated by TLC. Then, O2 gas was bubbled through to quench the residual ozone, and PPh3 (101.2mg, 0.4 mmol, 2 equiv) was added and reaction was warmed to room temperature. The crude mixture was concentrated in vacuo and purified by silica gel chromatography (30% EtOAc/Hexanes) to afford aldehyde **67** (40 mg, 89% yield) as a white solid.

Optical rotation: [α]D25 – 26.8 ° (c 1.0, CHCl3).

1H NMR (400 MHz, CDCl3) δ 9.67 (d, J = 0.7 Hz, 1H), 7.56 – 7.43 (m, 2H), 6.96 – 6.83 (m, 2H), 3.93 – 3.67 (m, 5H), 2.75 (ddd, J = 12.9, 8.0, 4.8 Hz, 1H), 1.91 (dddd, J = 13.1, 8.6, 6.7, 0.7 Hz, 1H), 1.51 (s, 3H).

13C NMR (101 MHz, CDCl3) δ 199.45, 171.26, 157.07, 132.20, 121.87, 114.26, 58.02, 55.62, 45.98, 25.89, 18.80. IR (thin film, NaCl) 2932, 2358, 1731, 1682, 1520, 1455, 1402, 1297, 1248, 1170, 1092, 1032, 825 cm–1.=

HRMS (MM:ESI-APCI+) m/z calc'd C13H15NO3 [M+H]+: 234.1125, found 234.1121.

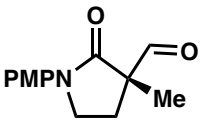

Procedure B: A one dram vial was charged with a stir bar and compound **53a**. To this vial, 2,6-lutidine (2 equiv) and K2OsO4 • 2 H2O was added as a solution in dioxane/H¬2O. To the stirring mixture, NaIO4 was added and the temperature was increased to 50 ºC. After 24 h, the crude mixture was filtered through a pad of celite, eluting with CH2Cl2 and EtOAc. H2O was added and CH2Cl2 was used to perform an extraction. The organic layer was washed with brine and dried with Na2SO4. The crude compound was purified via silica gel chromatography.

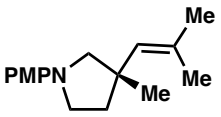

(S)-1-(4-methoxyphenyl)-3-methyl-3-(2-methylprop-1-en-1-yl)pyrrolidine (65)

To a solution of the lactam in Et¬2O (0.1 M) at 0 ºC. The solution was stirred at this temperature for 5 min and then was allowed to warm to 18 ºC. After 21 h, the reaction was quenched with H2O. Extractions were performed with EtOAc 7 times, and the crude product was subjected to silica gel chromatography (0-40% EtOAc/Hexanes) to afford the desired product as a white solid (22.5 mg, 84% yield). [a]D25 5.5° (c 1.0, CHCl3); HRMS (MM:ESI-APCI+) m/z calc'd C16H23NO [M+H]: 245.1780, found: 245.1784.

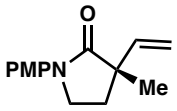

(S)-1-(4-methoxyphenyl)-3-methyl-3-vinylpyrrolidin-2-one (68)

A one-dram vial was charged with stir bar and flame dried. The methyl wittig reagent (51mg, 0.145mmol, 2.5 equiv) was added in THF (300uL, 0.1M) and cooled to 0 ºC. Reaction mixture was then charged with KOtBu (14mg, 0.128 mmol, 2.2 equiv) and stirred at 0 ºC for 20 minutes. Starting material **53a** (13.2 mg, 0.057 mmol, 1 equiv) was added with the remaining THF (about 100uL) and slowly warmed to room temperature and heated to reflux overnight. Second day all starting material was consumed by TLC (50% EtOAc/Hexanes) and reaction was quenched with NH4Cl and extracted with EtOAc (3x) and washed with brine. The organic extracts were combined, washed with brine, dried over MgSO4, and concentrated in vacuo. The resultant crude product was the purified by pipette column chromatography (15% EtOAc/Hexanes) to afford vinylated lactam X (11 mg, 84% yield) as a pale-yellow oil.

Optical rotation: [α]D25 – 0.6 ° (c 0.35, CHCl3).

1H NMR (400 MHz, CDCl3) δ 7.60 – 7.48 (m, 2H), 6.95 – 6.80 (m, 2H), 5.97 (dd, J = 17.5, 10.6 Hz, 1H), 5.24 – 5.11 (m, 2H), 3.80 (s, 3H), 3.73 (ddt, J = 7.8, 5.0, 2.5 Hz, 2H), 2.26 (ddd, J = 12.3, 7.0, 5.0 Hz, 1H), 2.12 – 1.96 (m, 1H), 1.35 (s, 3H).

13C NMR (101 MHz, CDCl3) δ 175.97, 156.63, 140.57, 133.07, 121.61, 114.16, 113.99, 55.63, 48.63, 45.60, 31.95, 23.13.

IR (Neat film, NaCl) 3360, 3077, 2962, 2927, 2060, 1693, 1512, 1504, 1455, 1394, 1315, 1299, 1246, 1182, 1170, 1124, 1111, 1090, 1034, 1005, 924, 913, 883, 825, 807, 731, 636 cm–1.

HRMS (MM:ESI-APCI+) m/z calc'd for C14H17NO2 [M+Na]+ : 252.1151, found 254.1155.

3.5.4 REFERENCES FOR EXPERIMENTAL

1) Pangborn, A. M.; Giardello, M. A.; Grubbs, R. H.; Rosen, R. K.; Timmers, F. J. Safe and Convenient Procedure for Solvent Purification. *Organometallics* **1996**, *15*, 1518–1520.

3.6 REFERENCES AND NOTES

1) Caruano, J.; Muccioli, G.G.; Robiette, R. Biologically active γ-lactams: synthesis and natural sources. Org. Biomol. Chem. 2016, 14, 10134–10156.

2) (a) Lee, H.; Jeong, G. Salinosporamide A, a Marine-Derived Proteasome Inhibitor, Inhibits T Cell Activation through Reg-ulating Proliferation and the Cell Cycle. Molecules 2020, 25, 5031–5044. (b) Beniddir, M.A.; Jagora, A.; Szwarc, S.; Hafidi, W.; Gallard, J.F.; Retailleau, P.; Buevich, A.V.; Le Pogam, P. Unifying the configuration of historical alkaloids from Borre-ria capitata through an extensive spectroscopic reinvestiga-tion. Phytochemistry 2023, 212, 113741–113746. (c) Najjar-Debbiny, R.; Gronich, N.; Weber, G.; Khoury, J.; Amar, M.; Stein, N.; Goldstein, L.H.; Saliba, W. Effectiveness of Paxlovid in Reducing Severe Coronavirus Disease 2019 and Mortality in High-Risk Patients. Clinical Infectious Diseases 2023, 76, 342–349. (d) Chen, L.; Pan, H.; Bai, Y.; Li, H.; Yang, W.; Lin, Z.; Cui, W.; Xian, Y. Gelsemine, a natural alkaloid extracted from Gelsemium elegans Benth. alleviates neuroin-flammation and cognitive impairments in Aβ oligomer-treated mice. Psychopharmacology 2020, 237, 2111–2124.

3) Jette, C.I.; Geibel, I.; Bachman, S.; Hayashi, M.; Sakurai, S.; Shimizu, H.; Morgan, J.B.; Stoltz, B.M. Palladium-Catalyzed Construction of Quaternary Stereocenters by Enantioselective Arylation of γ-Lactams with Aryl Chlorides and Bromides. Angew. Chem. Int. Ed. 2019, 58, 4297–4301.

4) (a) Culkin, D.A.; Hartwig, J.F. Palladium-Catalyzed α-Arylation of Carbonyl Compounds and Nitriles. Acc. Chem. Res. 2003, 36, 234–245. (b) Culkin, D.A.; Hartwig,

J.F. Car-bon-Carbon Bond-Forming Reductive Elimination from Ar-ylpalladium Complexes Containing Functionalized Alkyl Groups. Influence of Ligand Steric and Electronic Properties on Structure, Stability, and Reactivity. Organometallics 2004, 14, 3398–3416. (c) Culkin, D.A.; Hartwig, J.F. C–C Bond-Forming Reductive Elimination of Ketones, Esters, and Am-ides from Isolated Arylpalladium(II) Enolates. J. Am. Chem. Soc. 2001, 123, 5816–5817.

5) (a) Åhman, J.; Wolfe, J. P.; Troutman, M. W.; Palucki, M.; Buchwald, S. L. Asymmetric Arylation of Ketone Enolates. J. Am. Chem. Soc. 1998, 120, 1918– 1919. (b) Hamada, T.; Chieffi, A.; Åhman, J.; Buchwald, S. L. An Improved Cata-lyst for the Asymmetric Arylation of Ketone Enolates. J. Am. Chem. Soc. 2002, 124, 1261– 1268.

6) (a) Christoffers, J.; Mann, A. Enantioselective Construction of Quaternary Stereocenters. Angew. Chem., Int. Ed. 2001, 40, 4591– 4597. (b) Douglas, C. J.; Overman, L. E. Catalytic Asymmetric Synthesis of All-Carbon Quaternary Stereocen-ters. Proc. Natl. Acad. Sci. U.S.A. 2004, 101, 5363– 5367.

7) E. Vitaku, D. T. Smith, J. T. Njardarson, J. Med. Chem. 2014, 57, 10257–10274.

8) Sahu, R.; Shah, K.; Malviya, R.; Paliwal, D.; Sagar, S.; Singh, S.; Prajapati, B. G. Recent Advancement in Pyrrolidine Moiety for the Management of Cancer: A Review. Results in Chemis-try. 2024, 7, 101301.

9) Boonnak, N.; Chantrapromma, S.; Sathirakul, K.; Kaew-piboon, C. Modified Tetra-Oxygenated Xanthones Analogues as Anti-MRSA and P. Aeruginosa Agent and Their

Synergism with Vancomycin. Bioorganic & Medicinal Chemistry Letters. 2020, 30, 127494.

10) Henne, A. L.; Hill, P. The Preparation of Aldehydes, Ketones, and Acids by Ozone Oxidation. J. Am. Chem. Soc. 1943, 65, 752–754.

11) Riley, H. L.; Morley, J. F.; Friend, N. A. C. 255. Selenium Dioxide, a New Oxidising Agent. Part I. Its Reaction with Al-dehydes and Ketones. J. Chem. Soc. 1932, No. 0, 1875–1883.

12) E. Vitaku, D. T. Smith, J. T. Njardarson, J. Med. Chem. 2014, 57, 10257–10274.

APPENDIX 3

Spectra Relevant to Chapter 3:

Formation of All-Carbon Quaternary Centers via Pd-catalyzed α-Vinylation of γ-Lactams

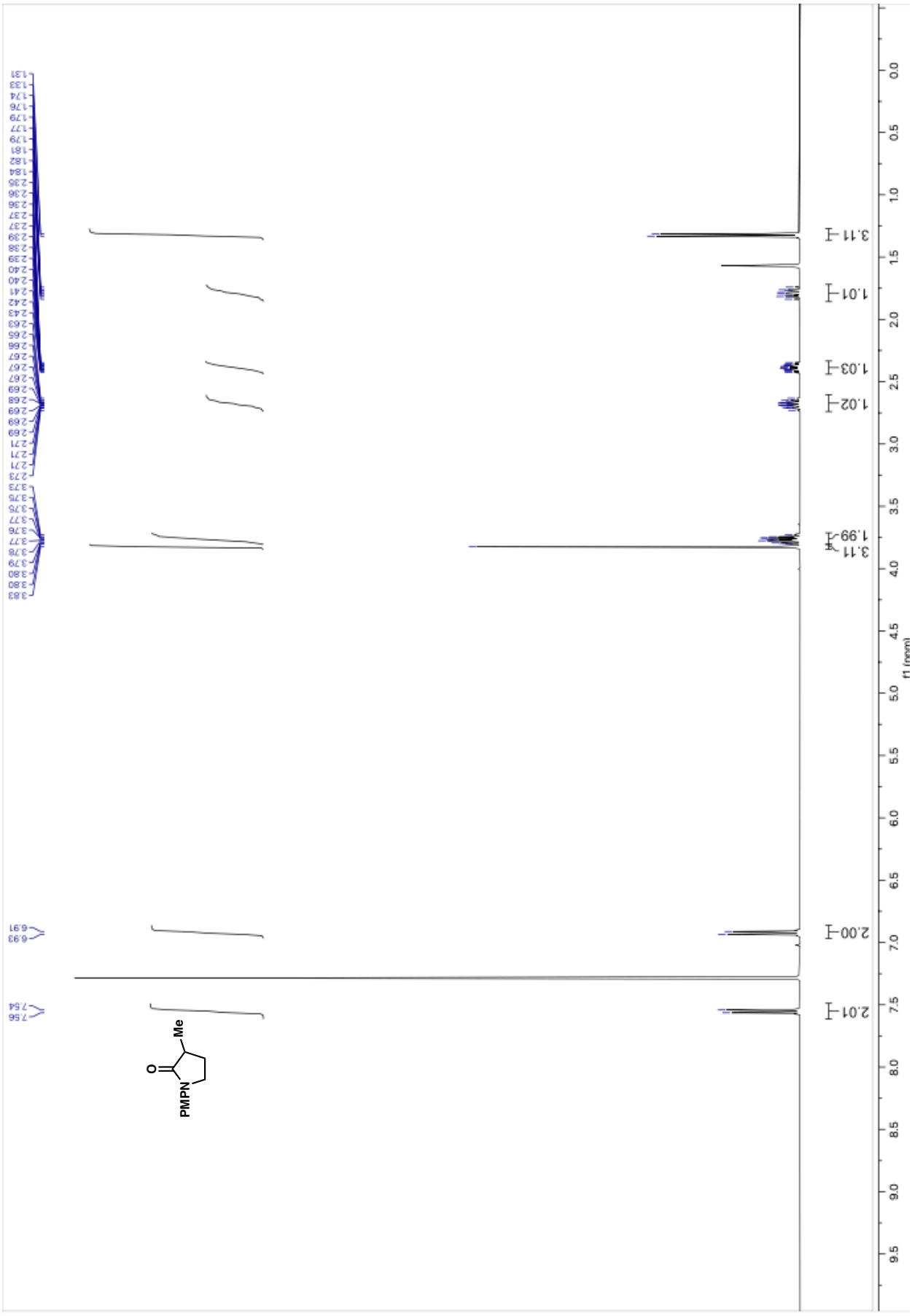

Figure A3.1. *^1H NMR (400 MHz, $CDCl_3$) of compound* ***53****.*

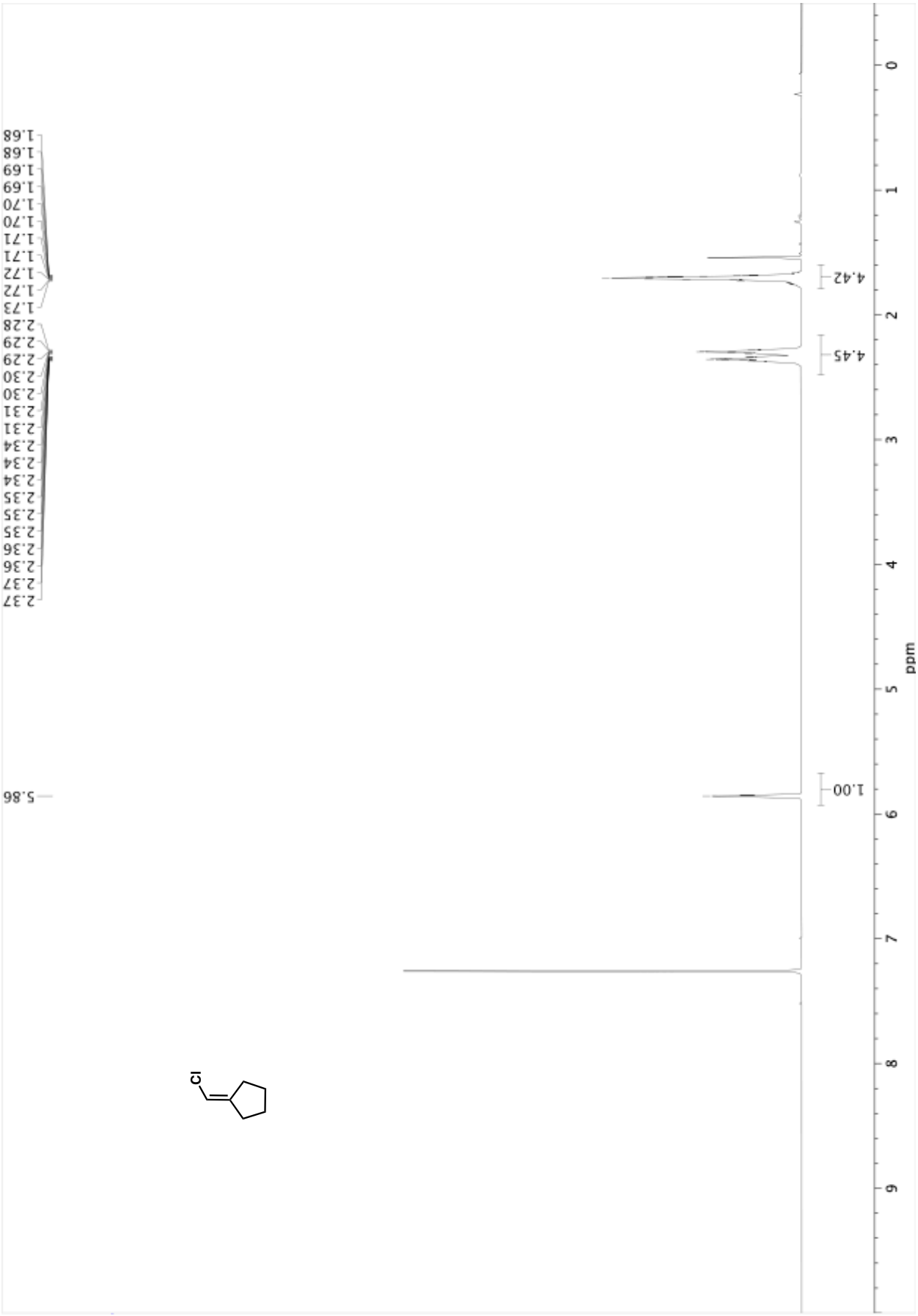

Figure A3.2. *^1H NMR (400 MHz, $CDCl_3$) of compound* ***S1****.*

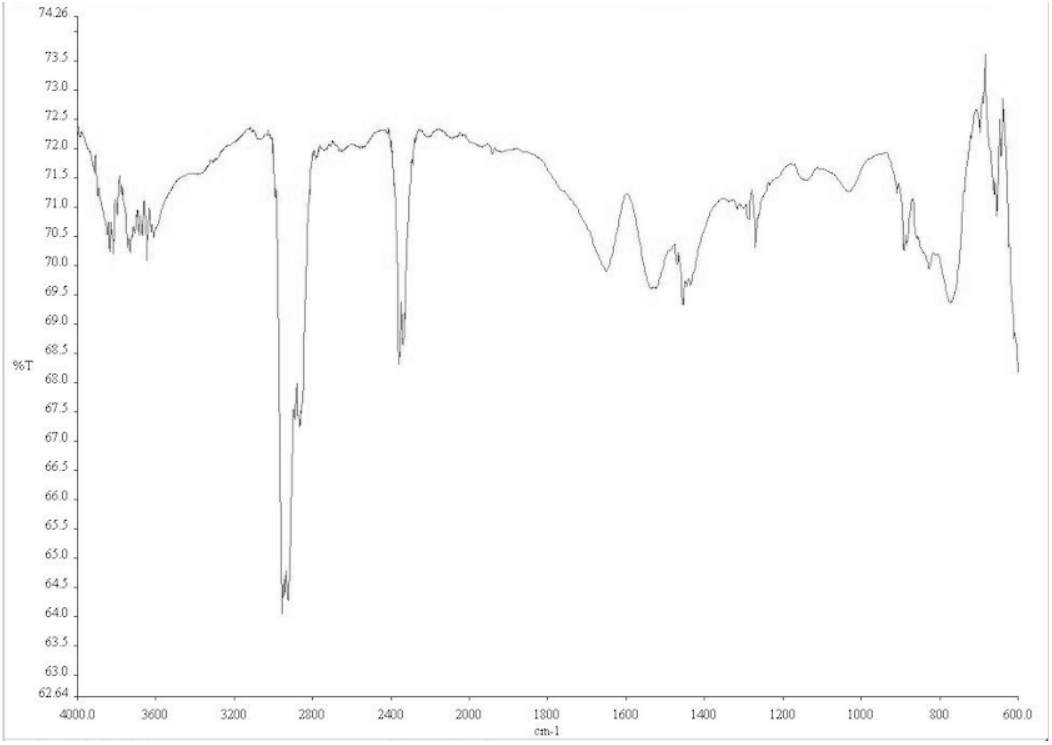

Figure A3.3. *Infrared spectrum (Thin Film, NaCl) of compound* ***S1***.

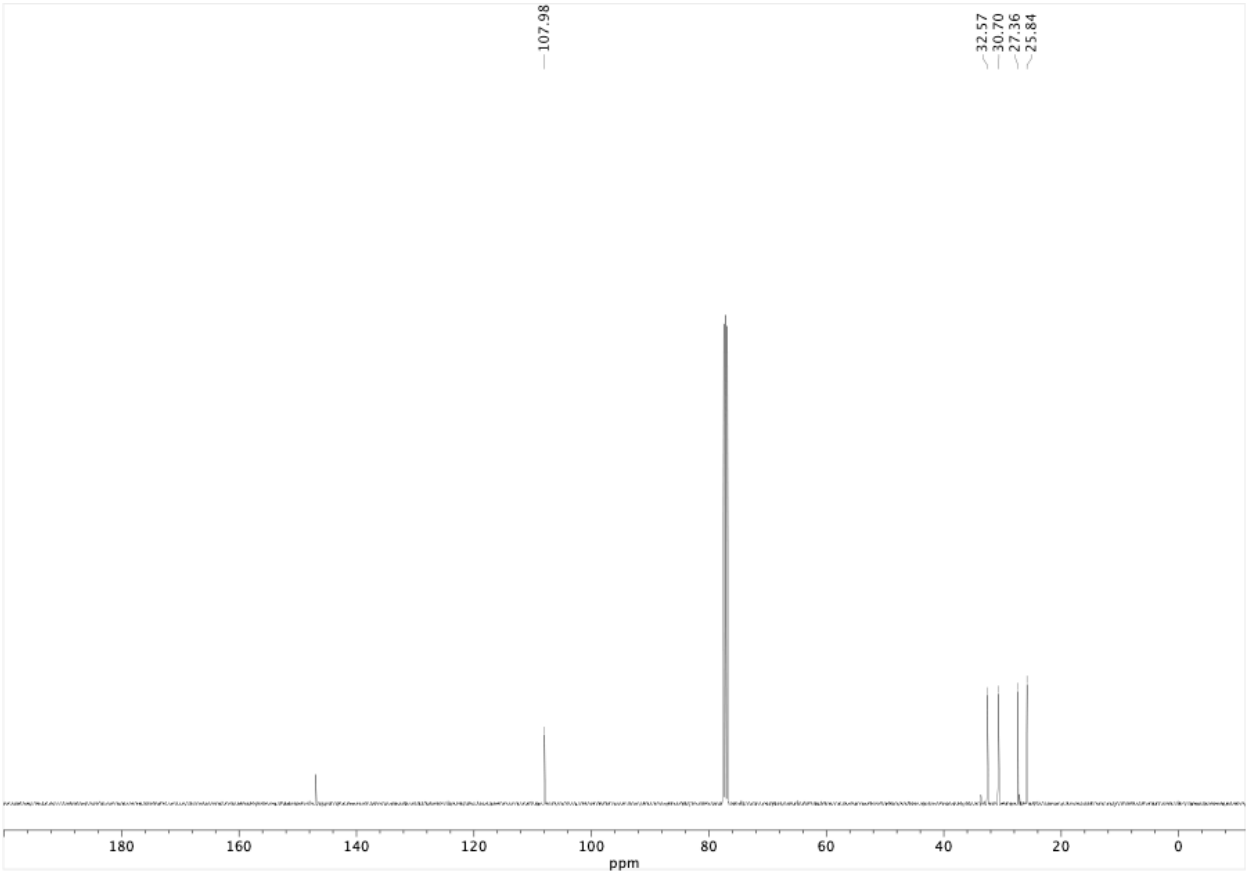

Figure A3.4. *^{13}C NMR (100 MHz, $CDCl_3$) of compound* ***S1***.

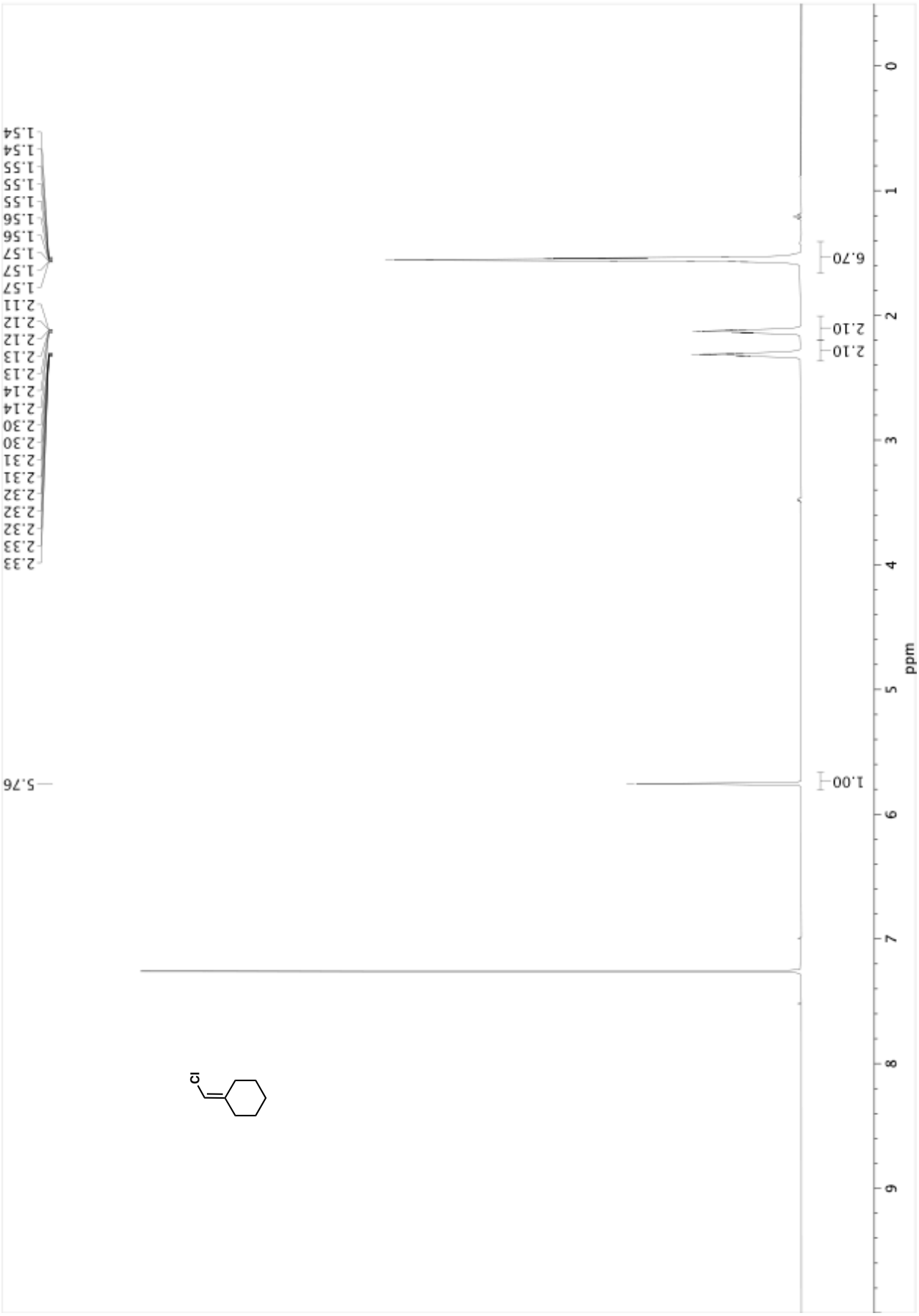

Figure A3.5. *^1H NMR (400 MHz, $CDCl_3$) of compound* ***S2.***

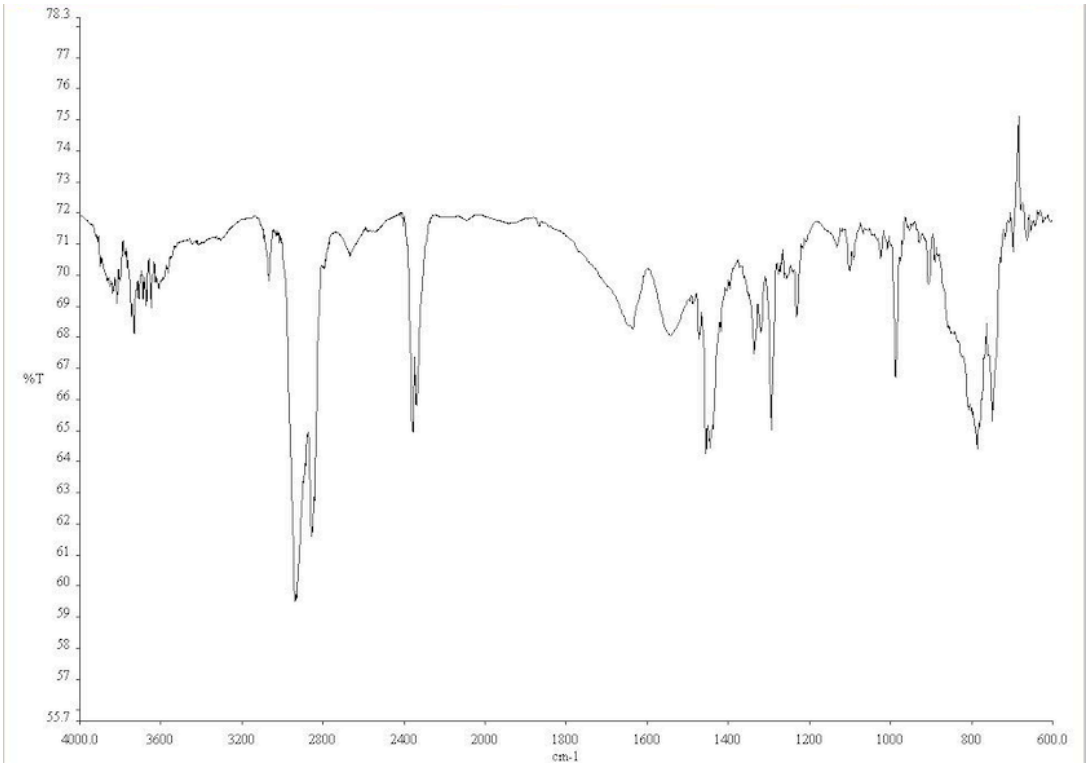

Figure A3.6. *Infrared spectrum (Thin Film, NaCl) of compound* ***S2****.*

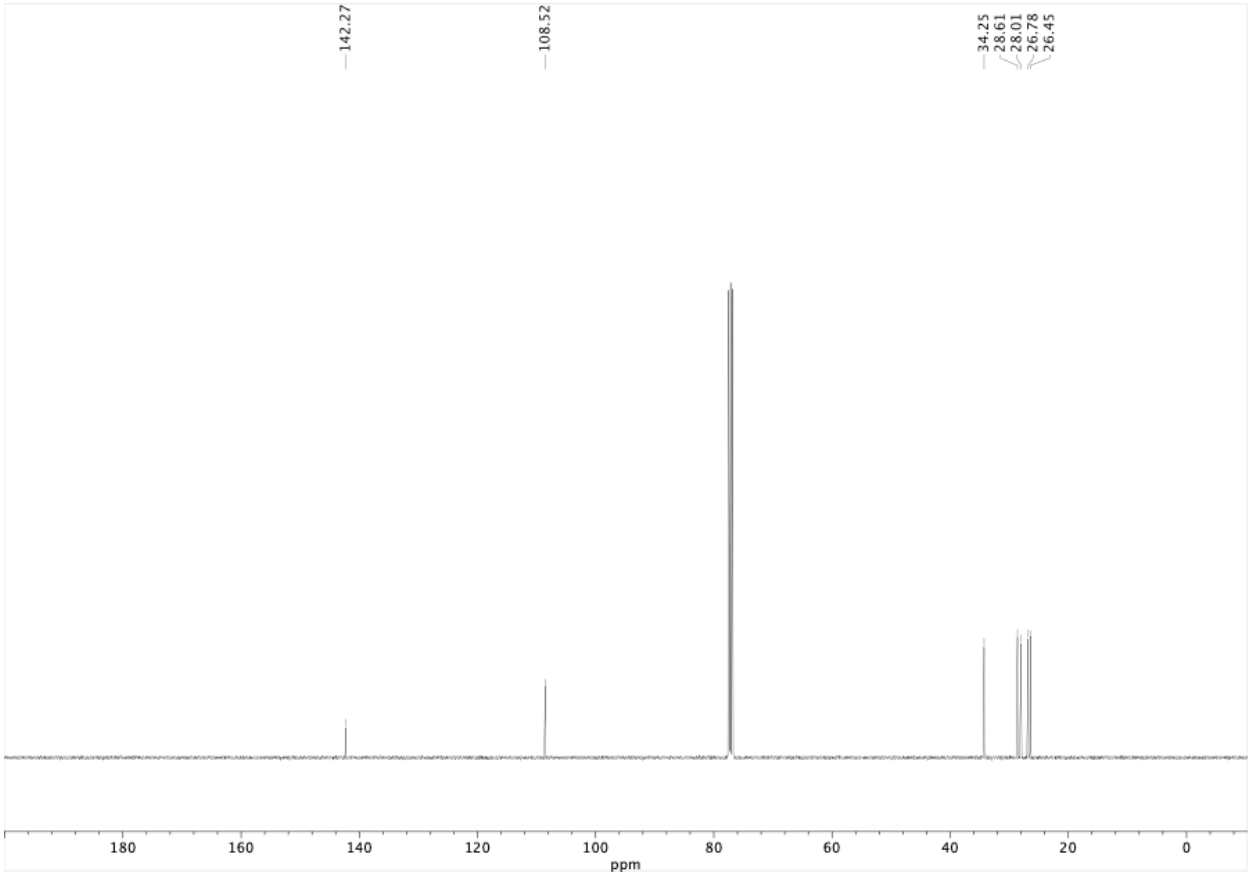

Figure A3.7. *^{13}C NMR (100 MHz, $CDCl_3$) of compound* ***S2****.*

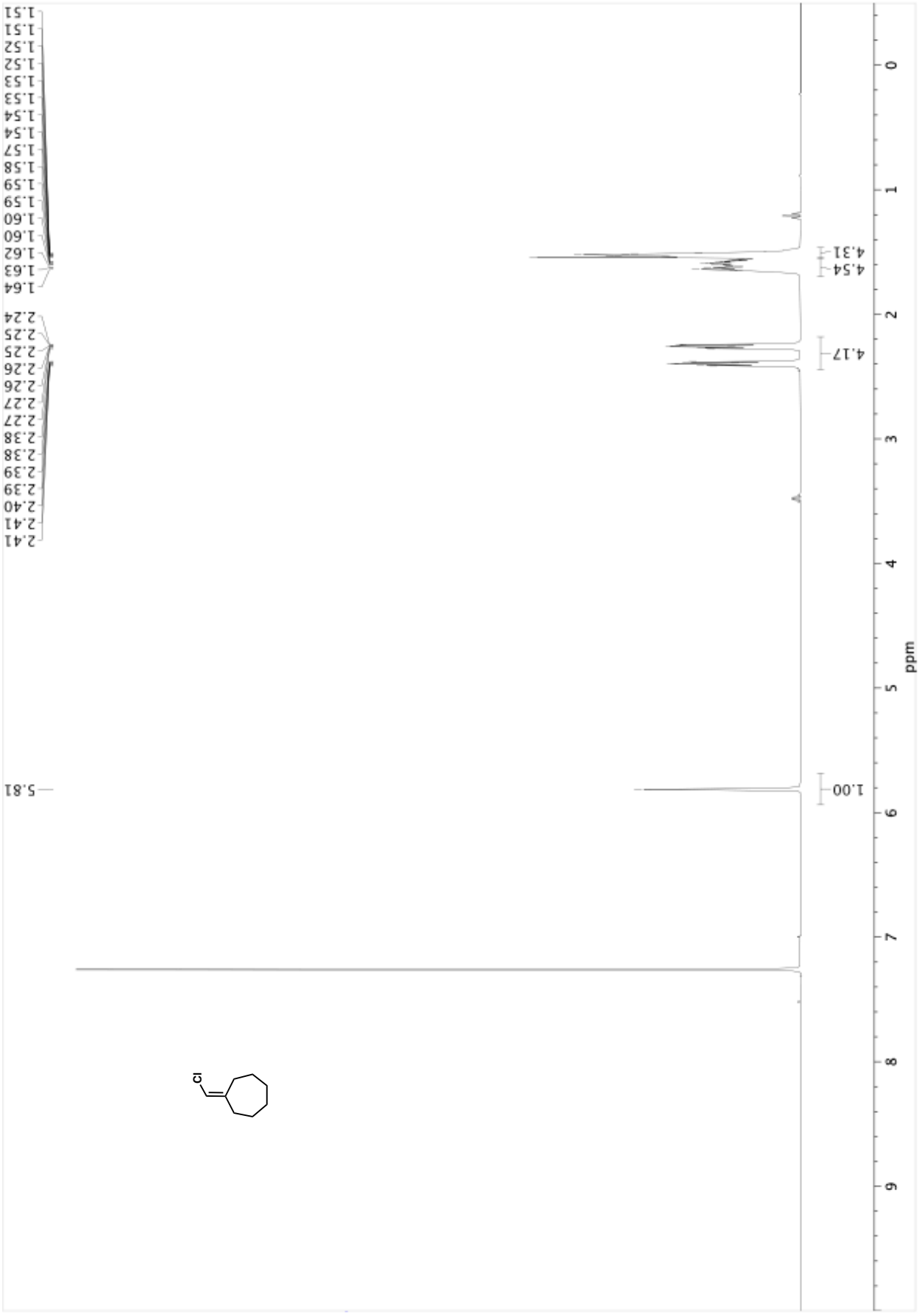

Figure A3.8. *^1H NMR (400 MHz, $CDCl_3$) of compound **S3**.*

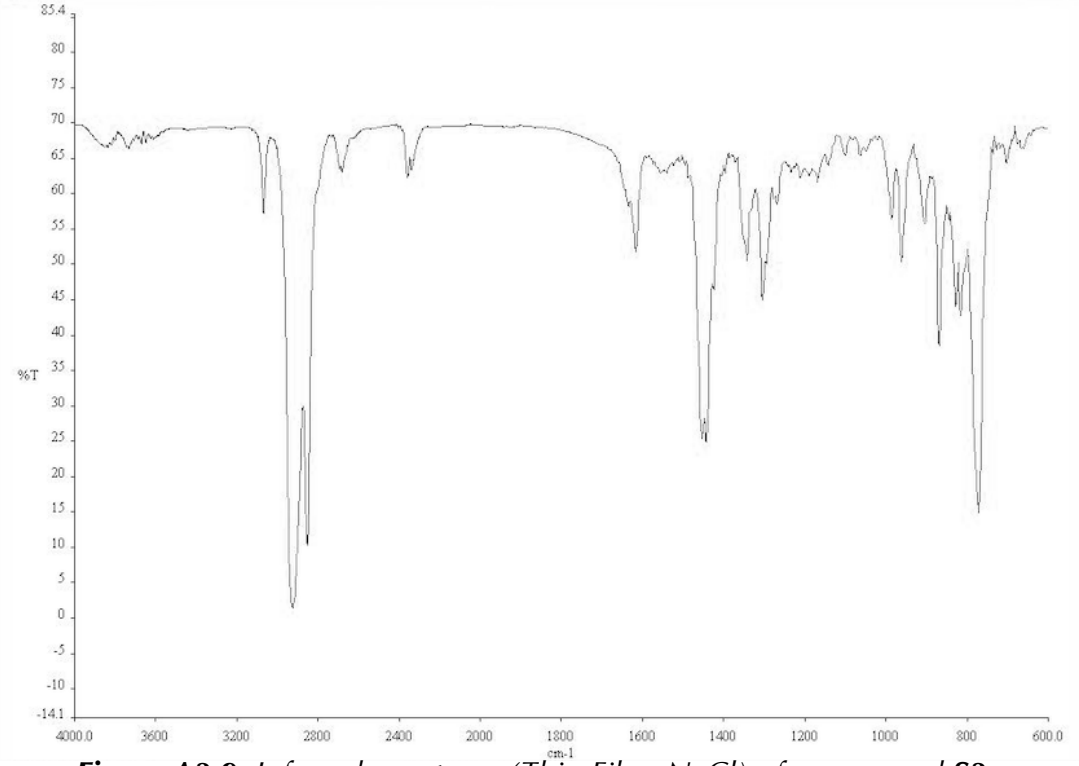

Figure A3.9. *Infrared spectrum (Thin Film, NaCl) of compound* ***S3****.*

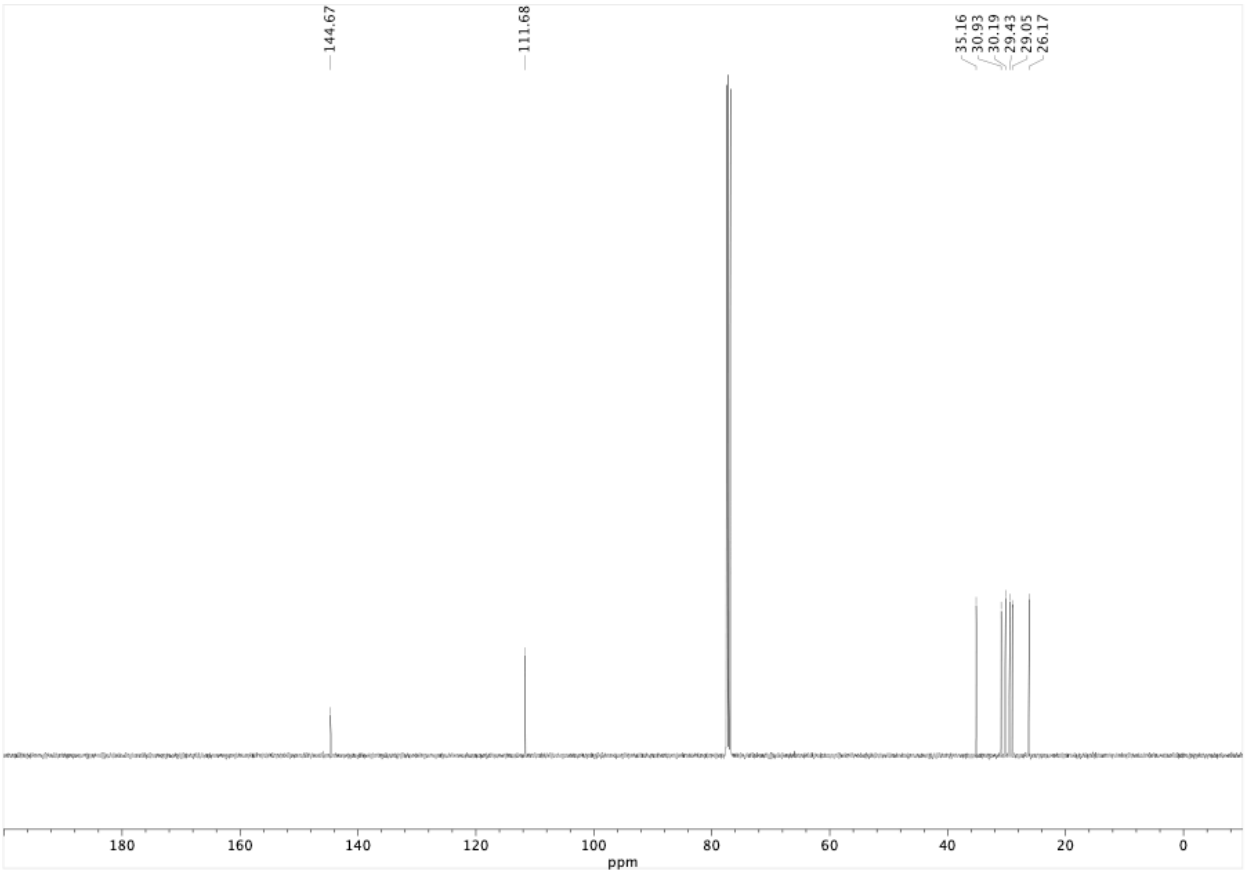

Figure A3.10. *^{13}C NMR (100 MHz, $CDCl_3$) of compound* ***S3****.*

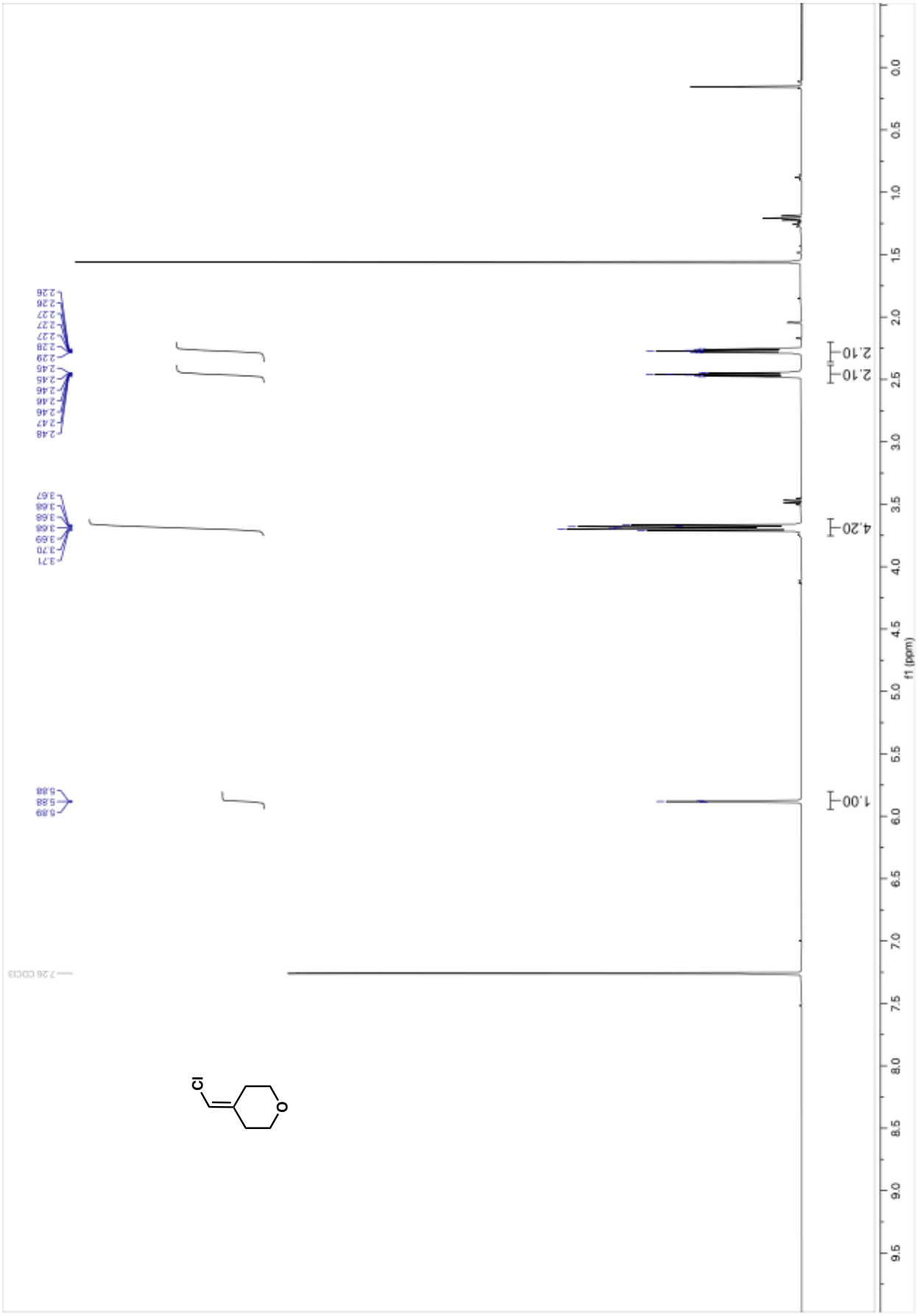

Figure A3.11. *^{1}H NMR (400 MHz, $CDCl_3$) of compound* ***S4****.*

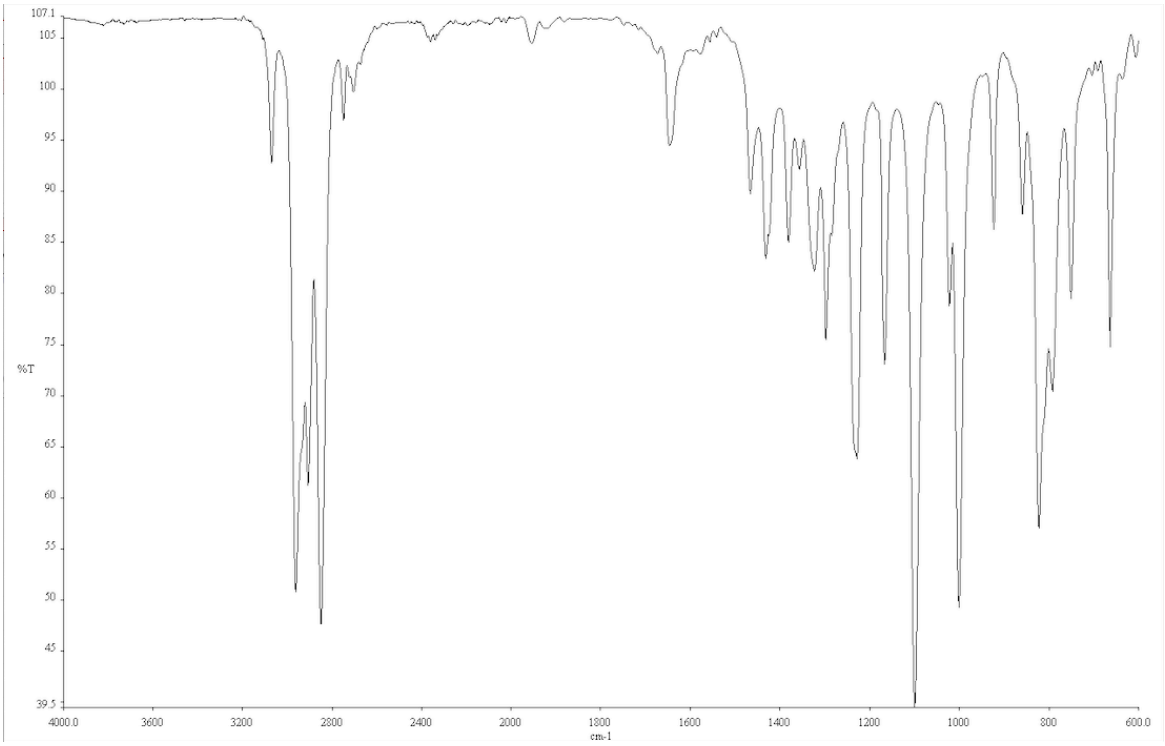

Figure A3.12. *Infrared spectrum (Thin Film, NaCl) of compound* ***S4****.*

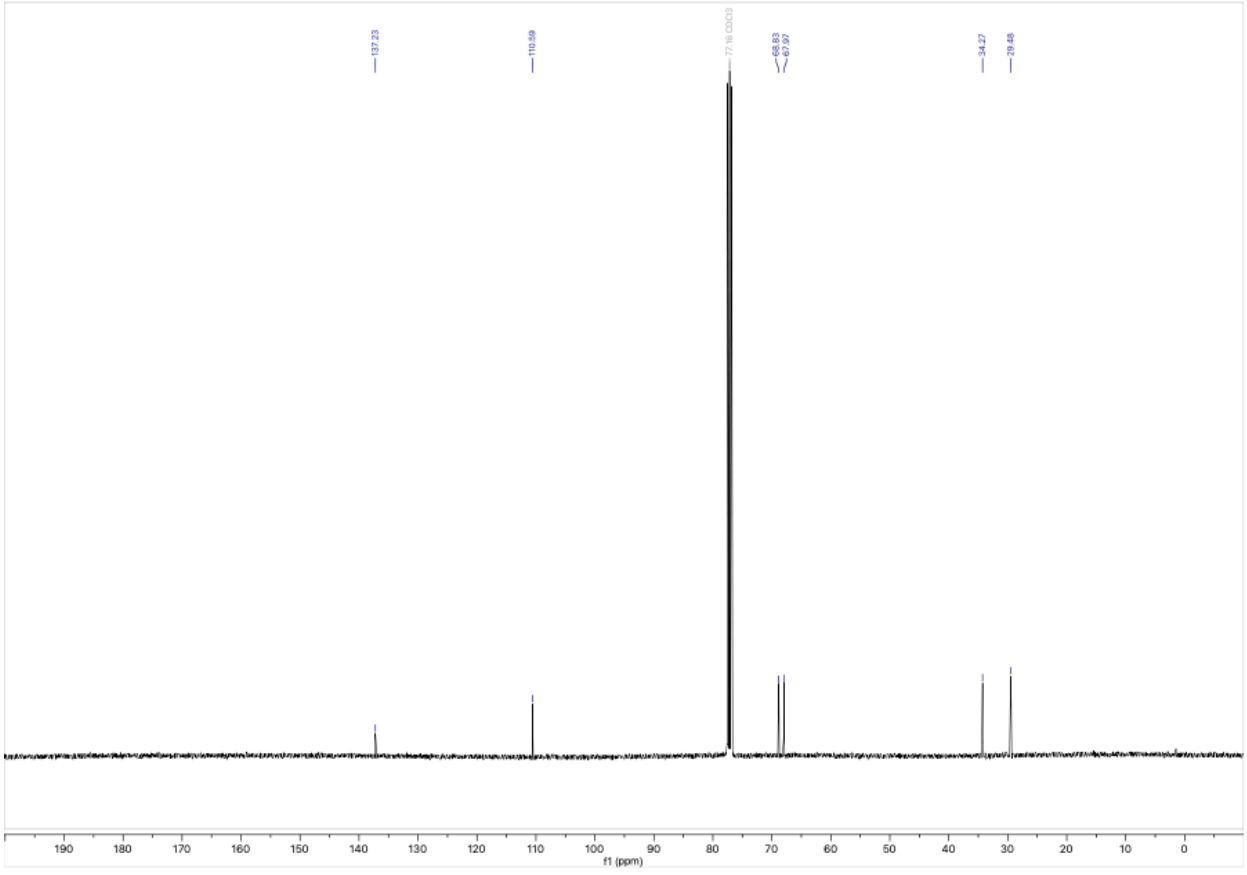

Figure A3.13. *^{13}C NMR (100 MHz, $CDCl_3$) of compound* ***S4****.*

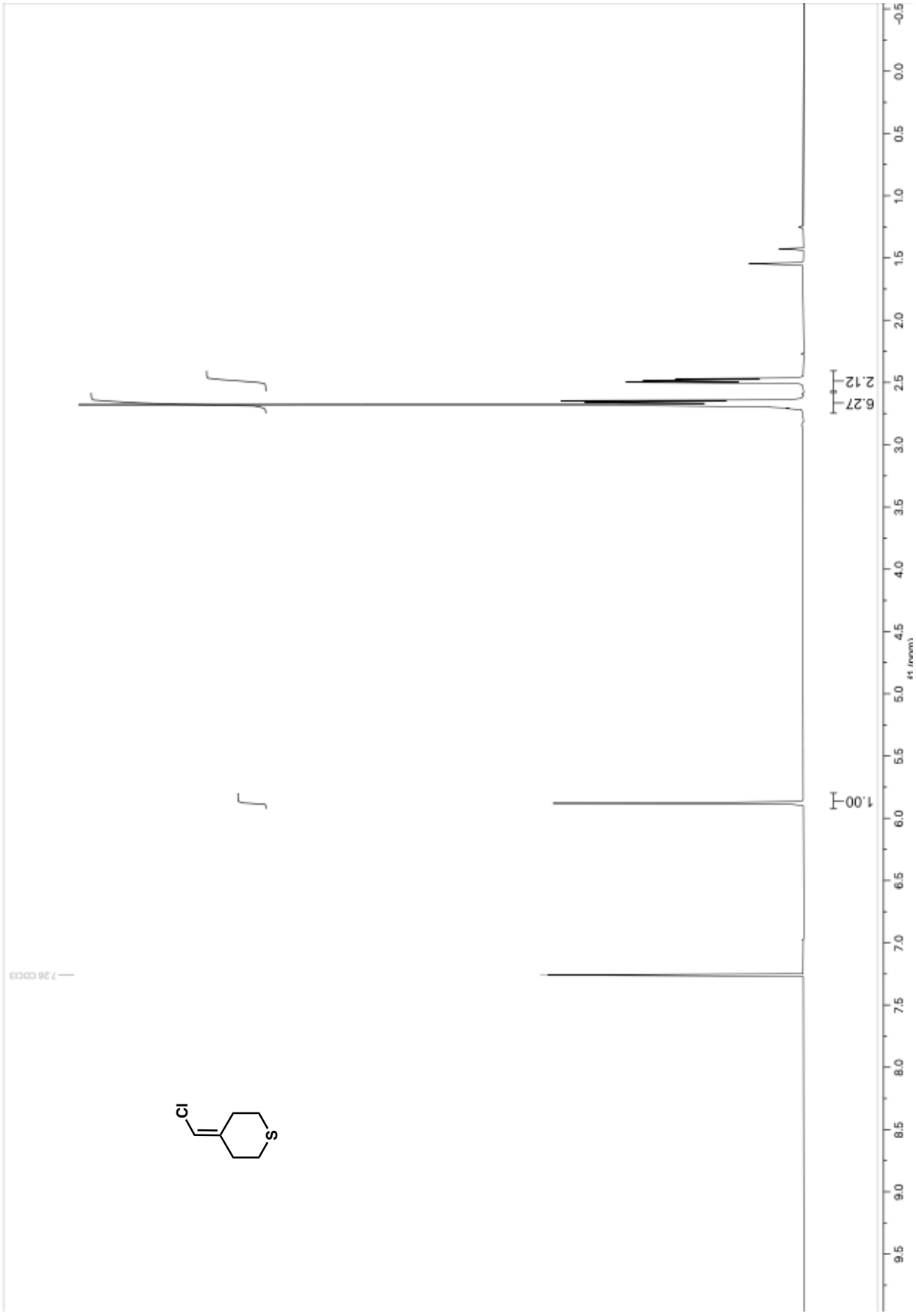

Figure A3.14. *^{1}H NMR (400 MHz, $CDCl_3$) of compound* ***S5****.*

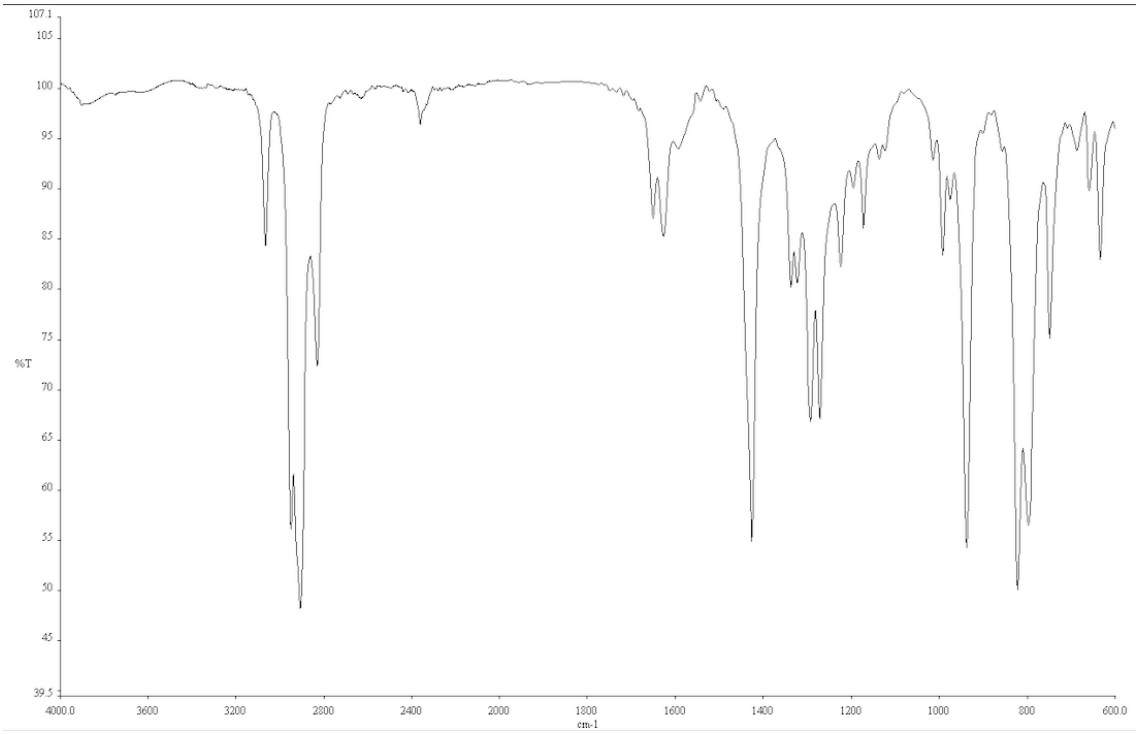

Figure A3.15. *Infrared spectrum (Thin Film, NaCl) of compound* ***S5****.*

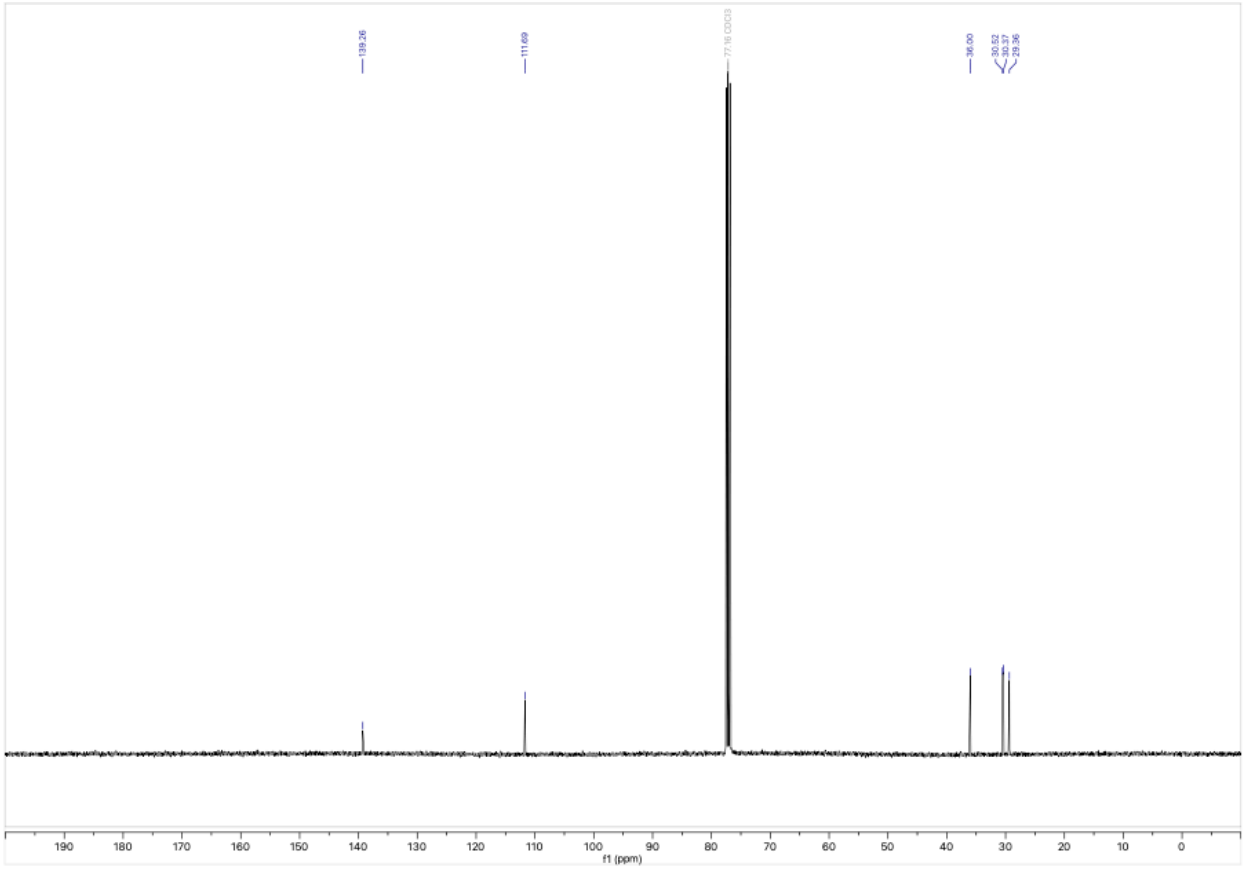

Figure A3.16. *^{13}C NMR (100 MHz, $CDCl_3$) of compound* ***S5****.*

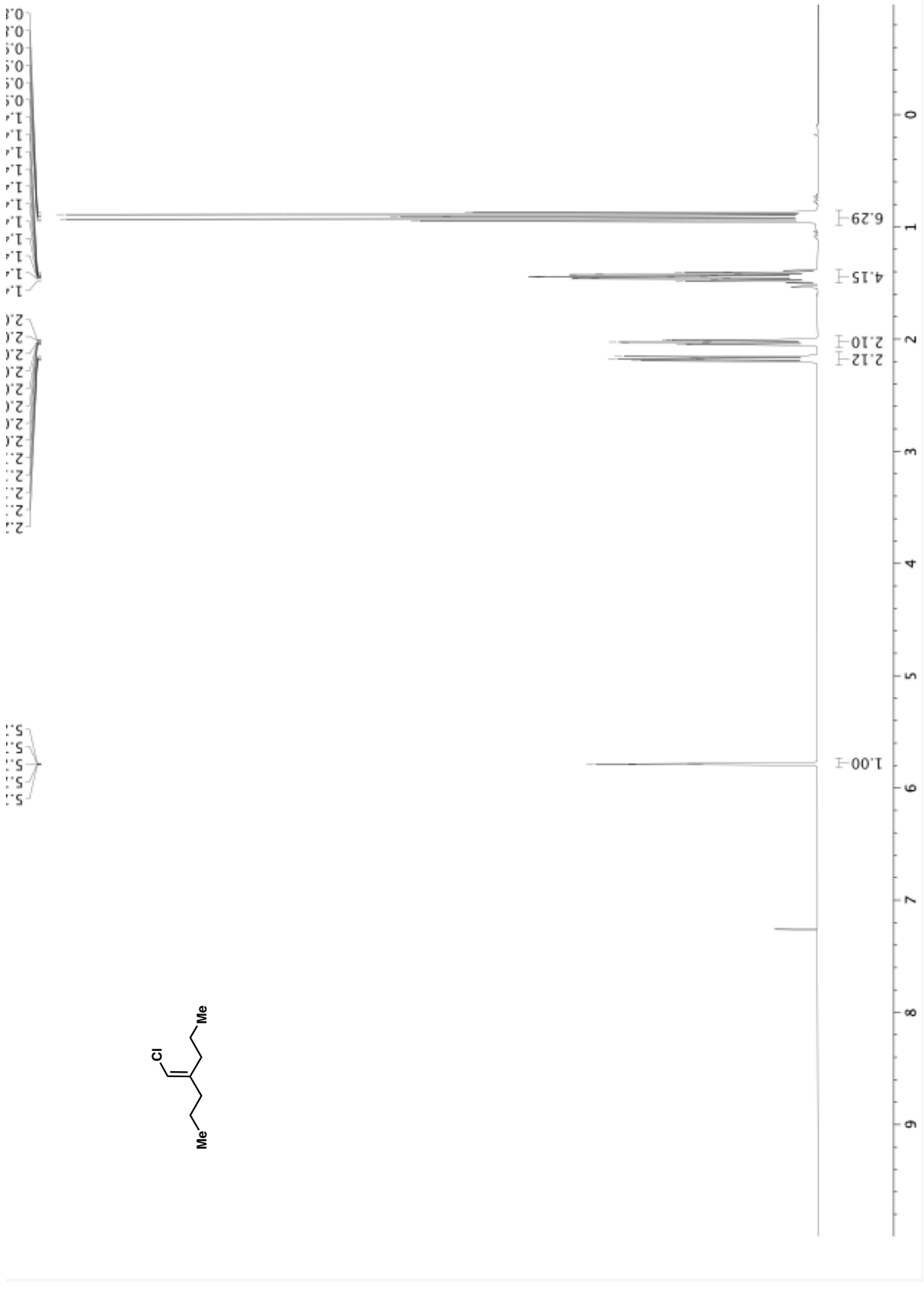

Figure A3.17. *^{1}H NMR (400 MHz, $CDCl_3$) of compound* ***S6****.*

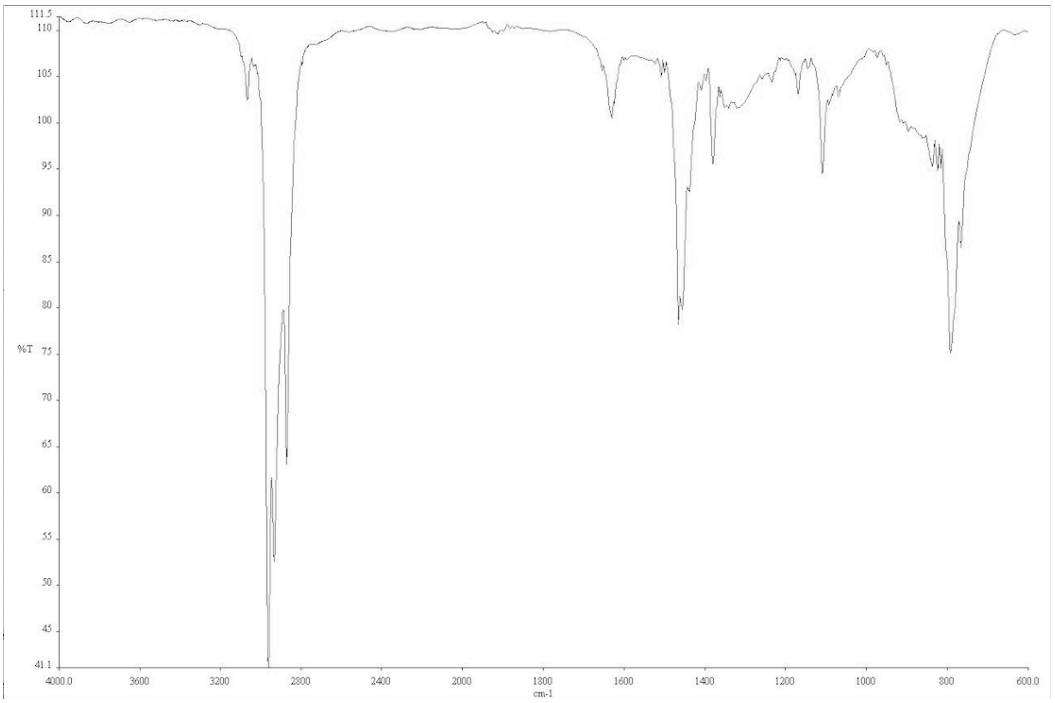

Figure A3.18. *Infrared spectrum (Thin Film, NaCl) of compound* ***S6****.*

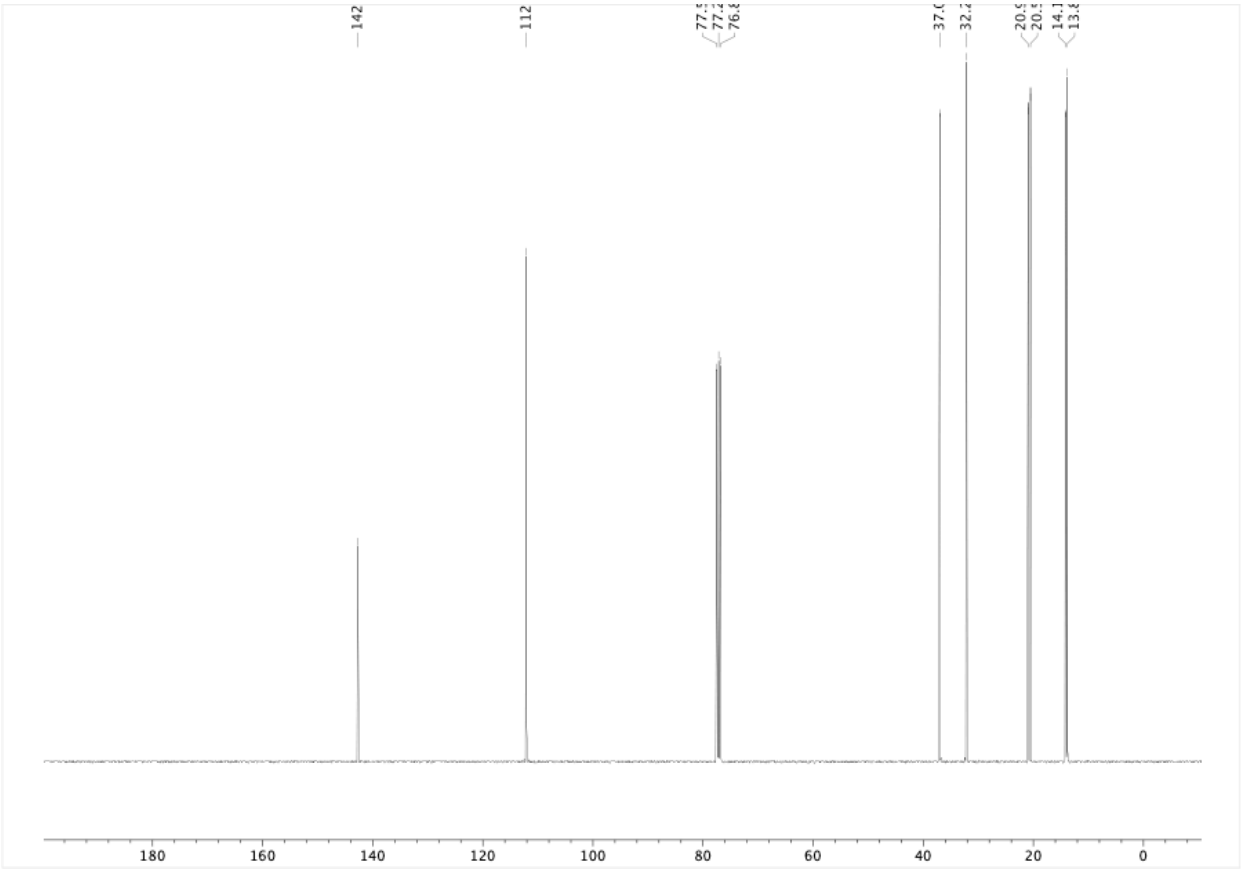

Figure A3.19. *^{13}C NMR (100 MHz, $CDCl_3$) of compound* ***S6****.*

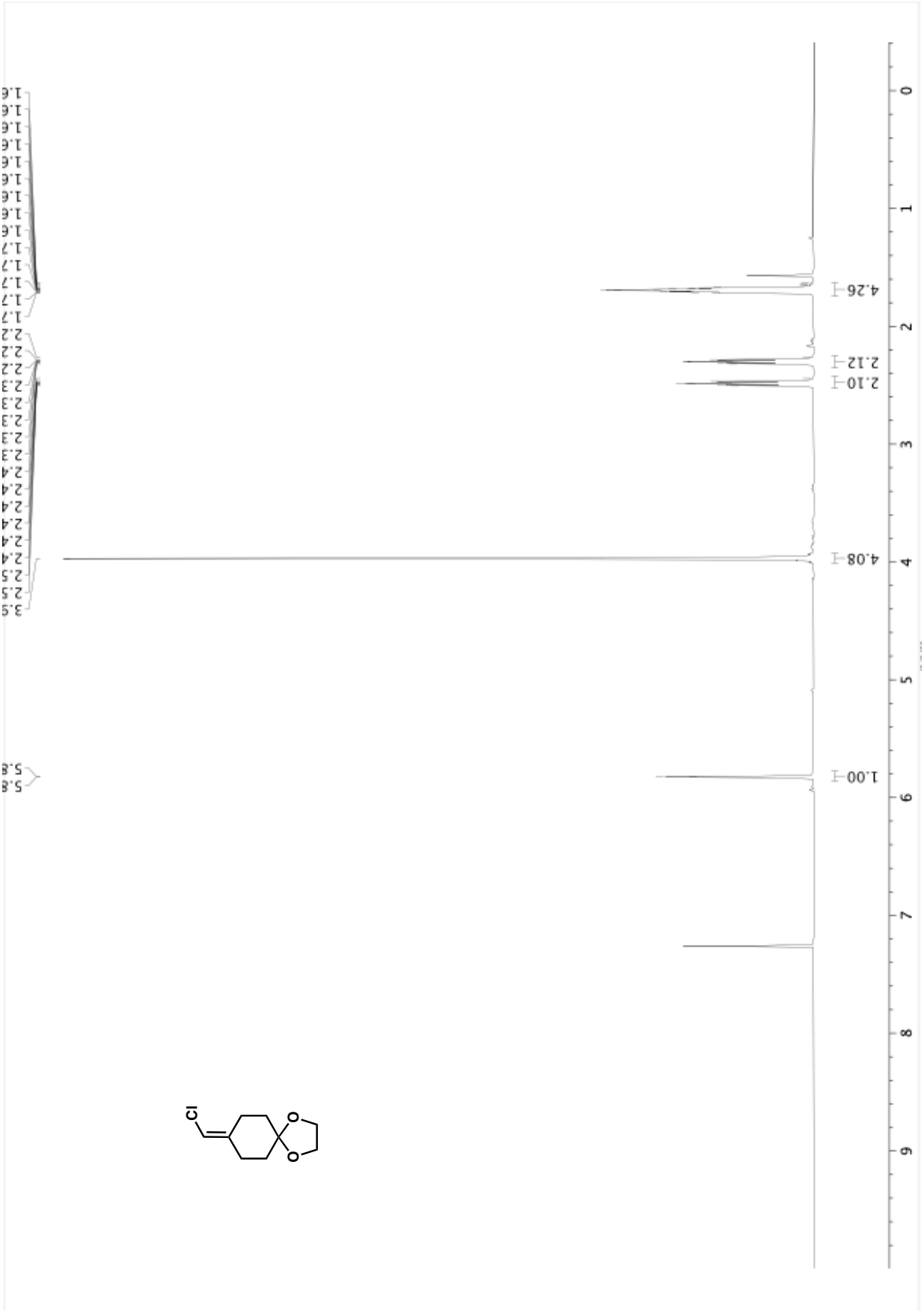

Figure A3.20. *^1H NMR (400 MHz, $CDCl_3$) of compound* ***S7****.*

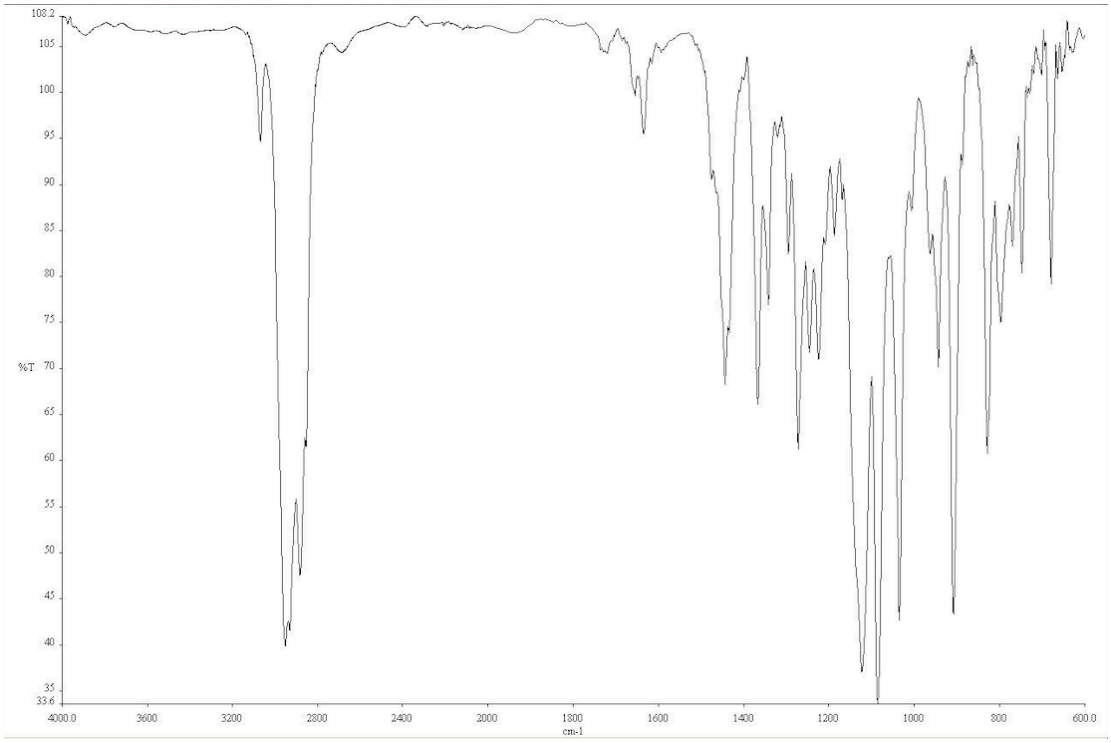

Figure A3.21. *Infrared spectrum (Thin Film, NaCl) of compound* ***S7****.*

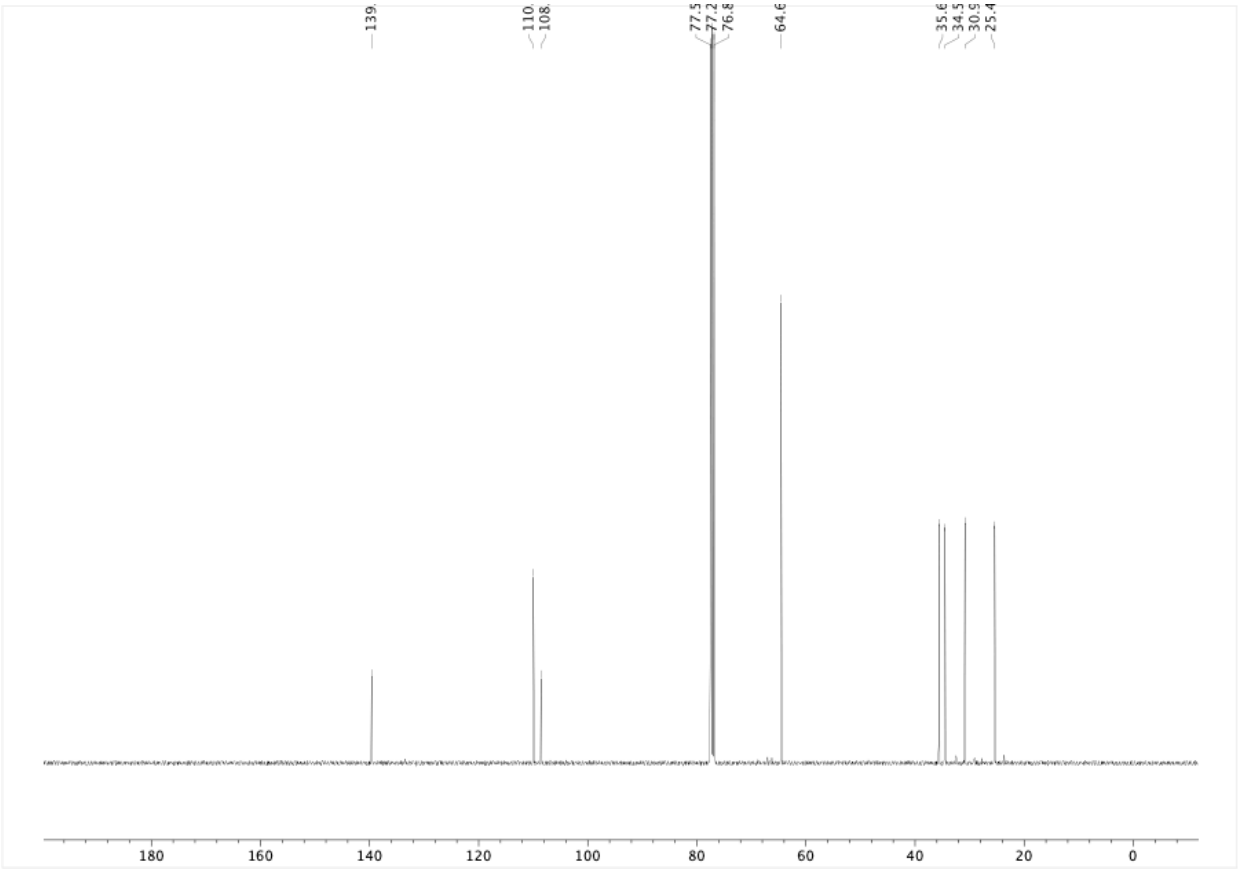

Figure A3.22. *^{13}C NMR (100 MHz, $CDCl_3$) of compound* ***S7****.*

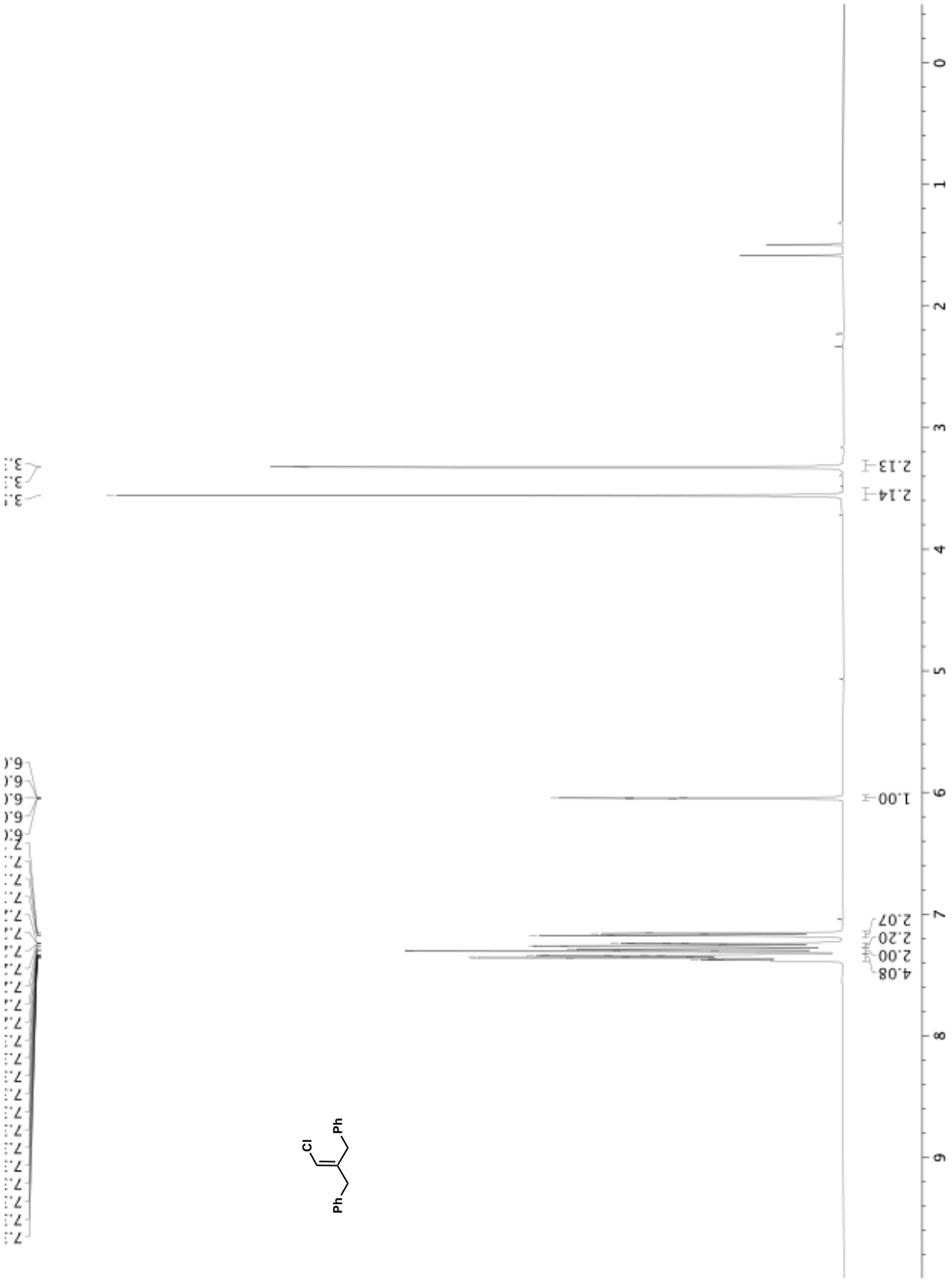

Figure A3.23. *^1H NMR (400 MHz, $CDCl_3$) of compound* ***S8****.*

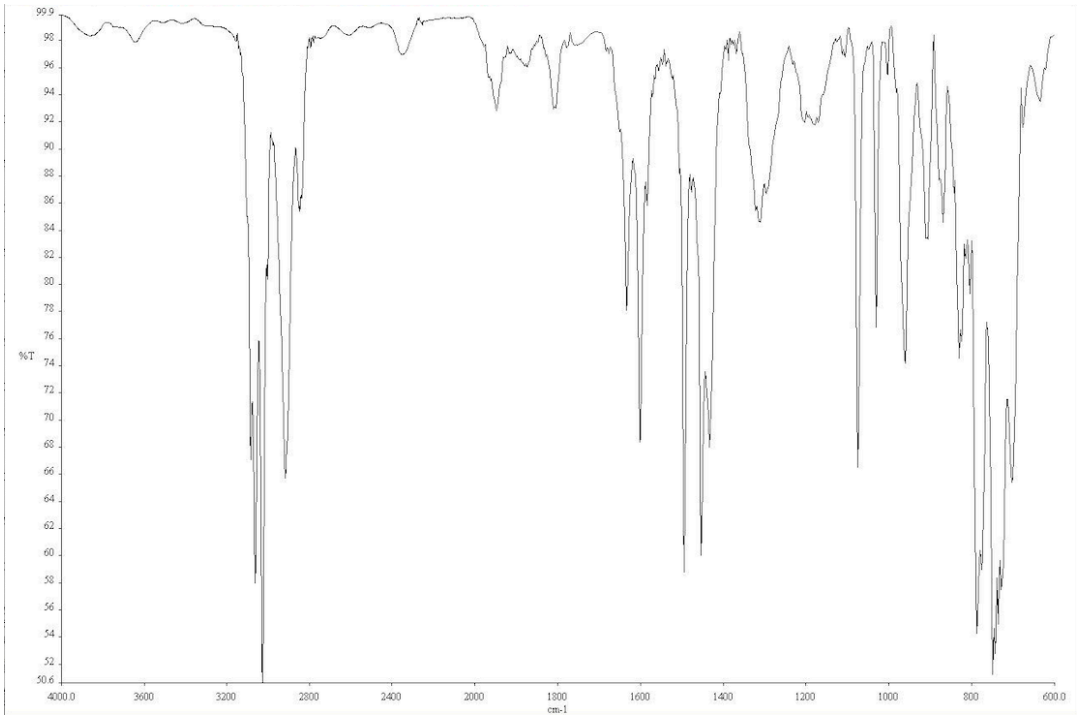

Figure A3.24. *Infrared spectrum (Thin Film, NaCl) of compound* ***S8****.*

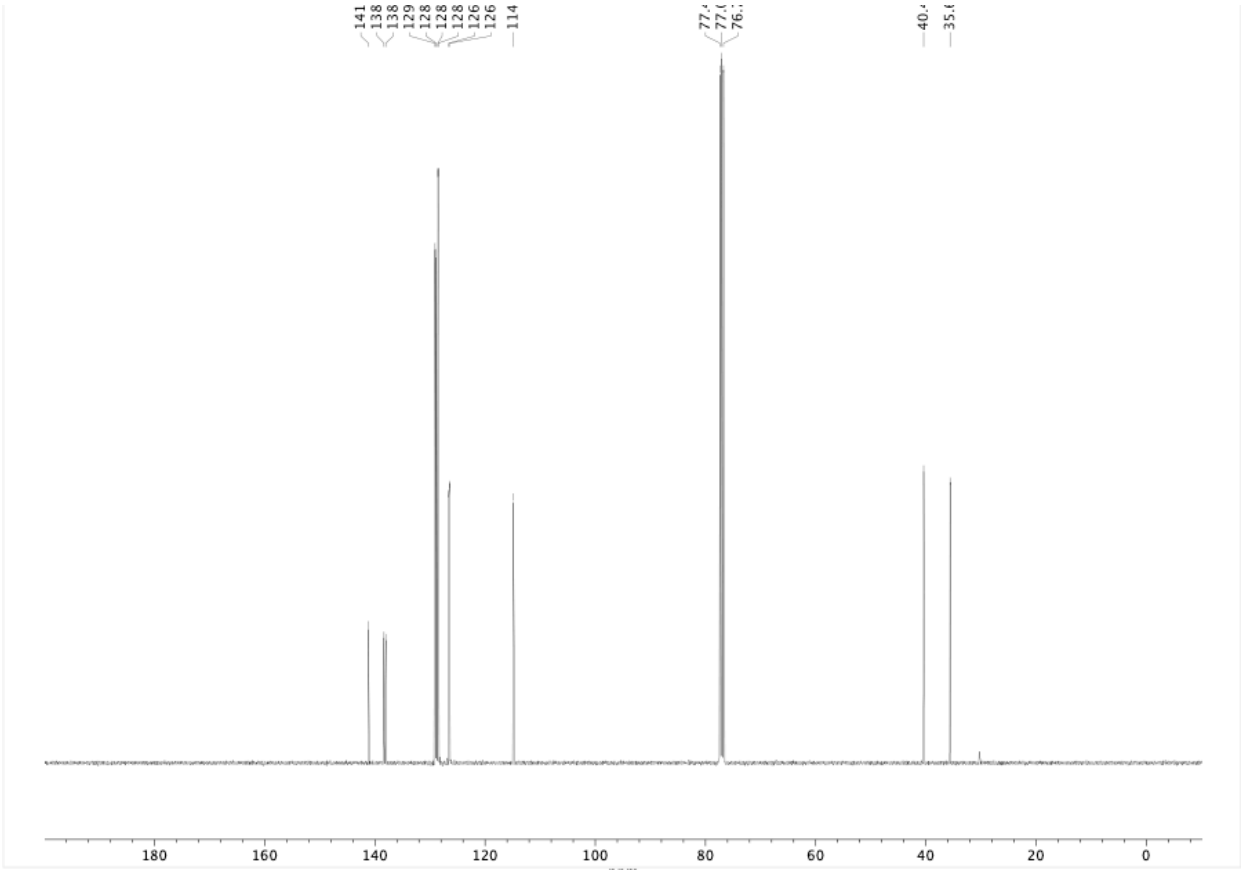

Figure A3.25. *^{13}C NMR (100 MHz, $CDCl_3$) of compound* ***S8****.*

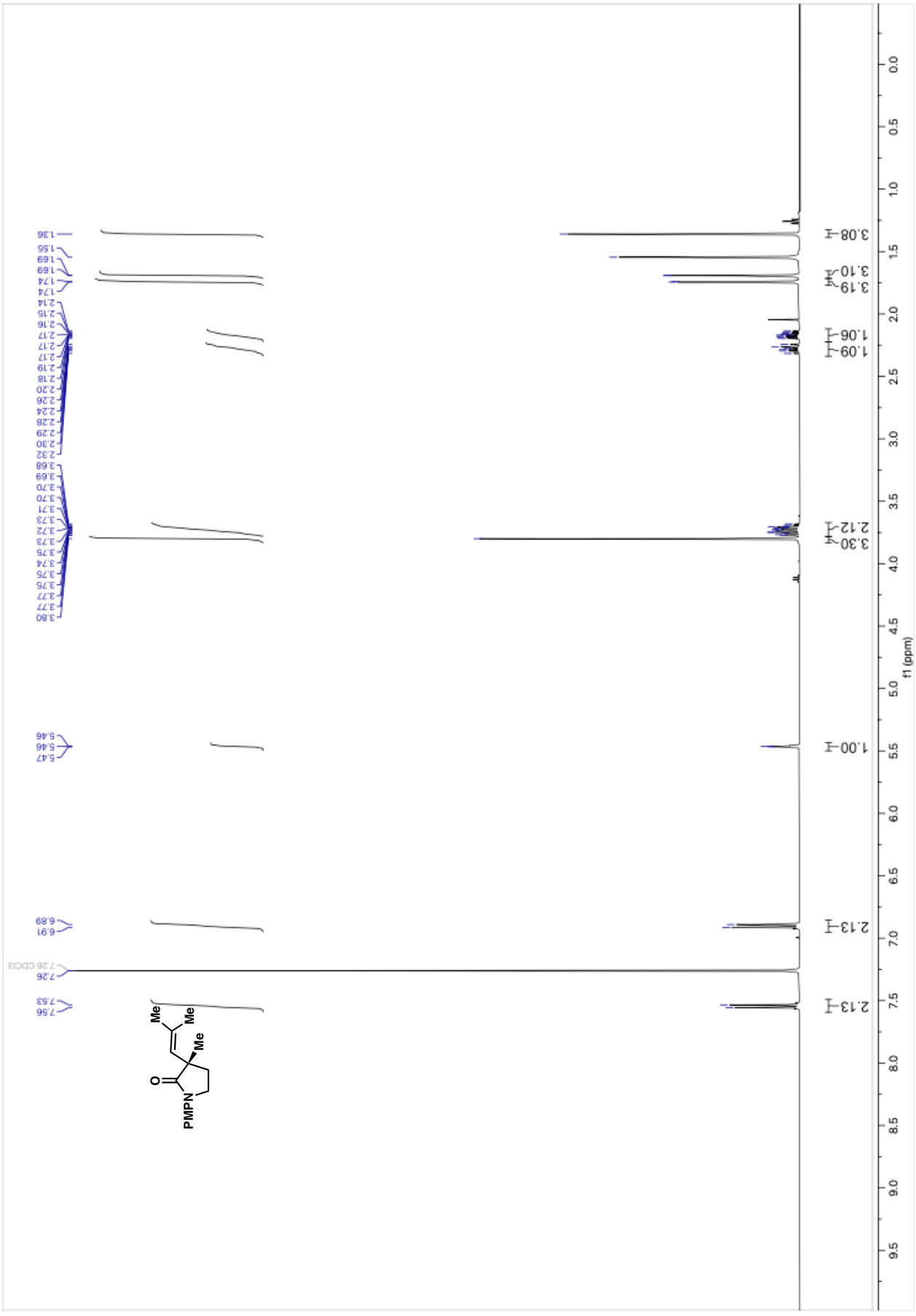

Figure A3.26. *^1H NMR (400 MHz, $CDCl_3$) of compound* ***53a****.*

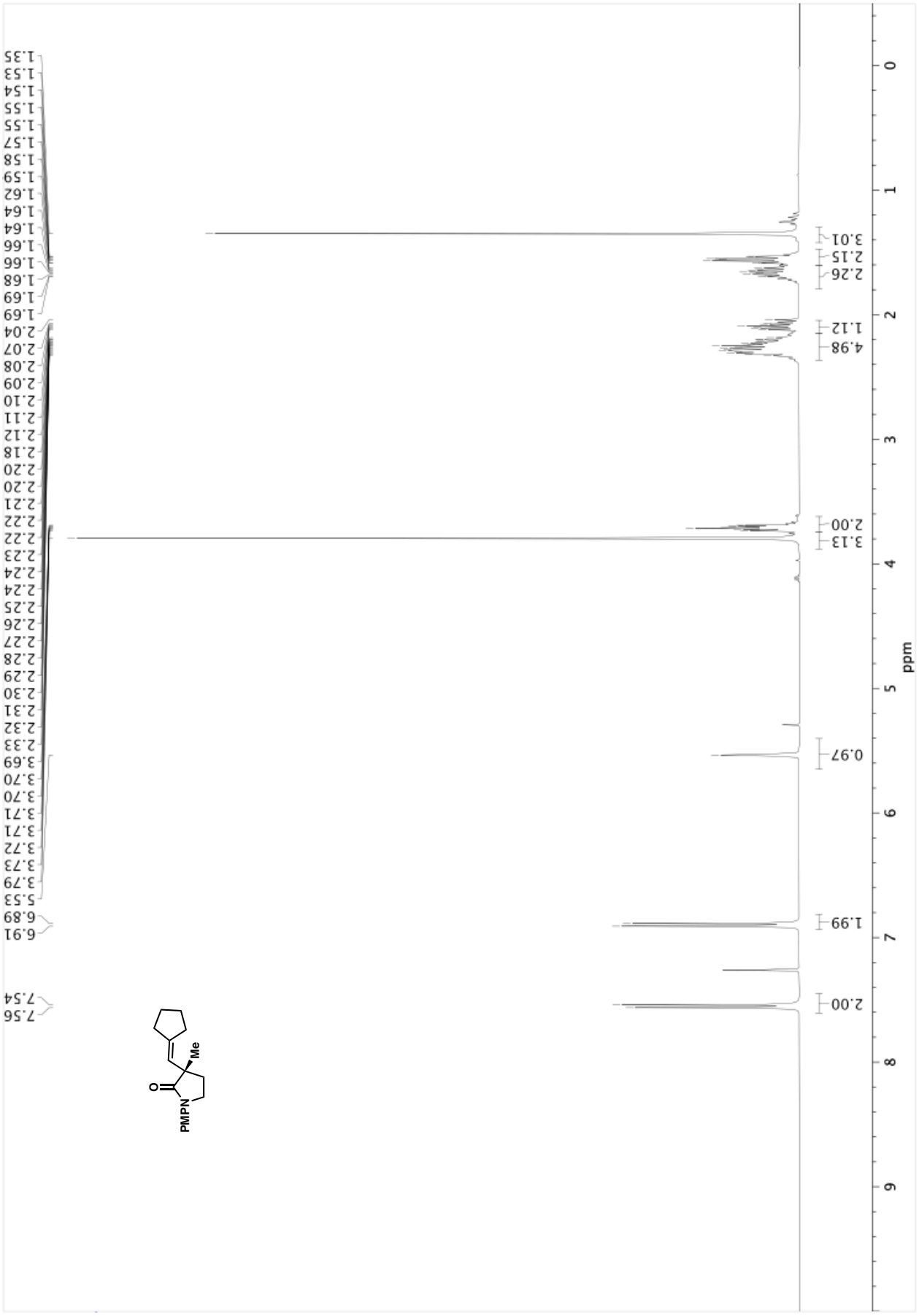

Figure A3.27. *^1H NMR (400 MHz, $CDCl_3$) of compound* ***54a****.*

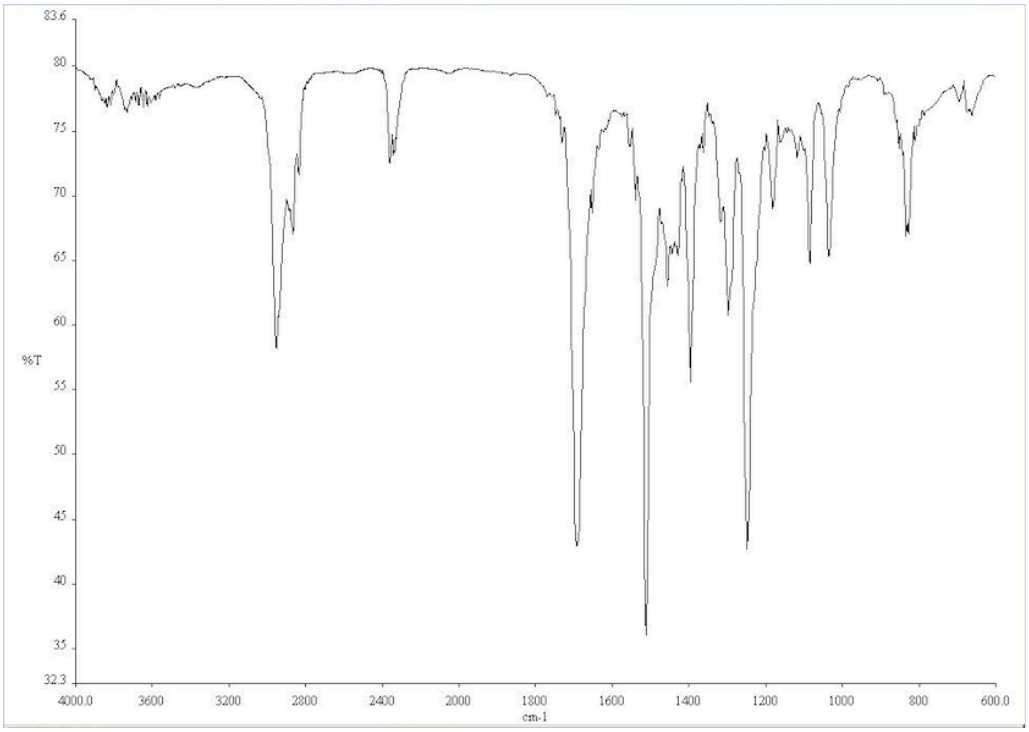

Figure A3.28. *Infrared spectrum (Thin Film, NaCl) of compound* ***54a****.*

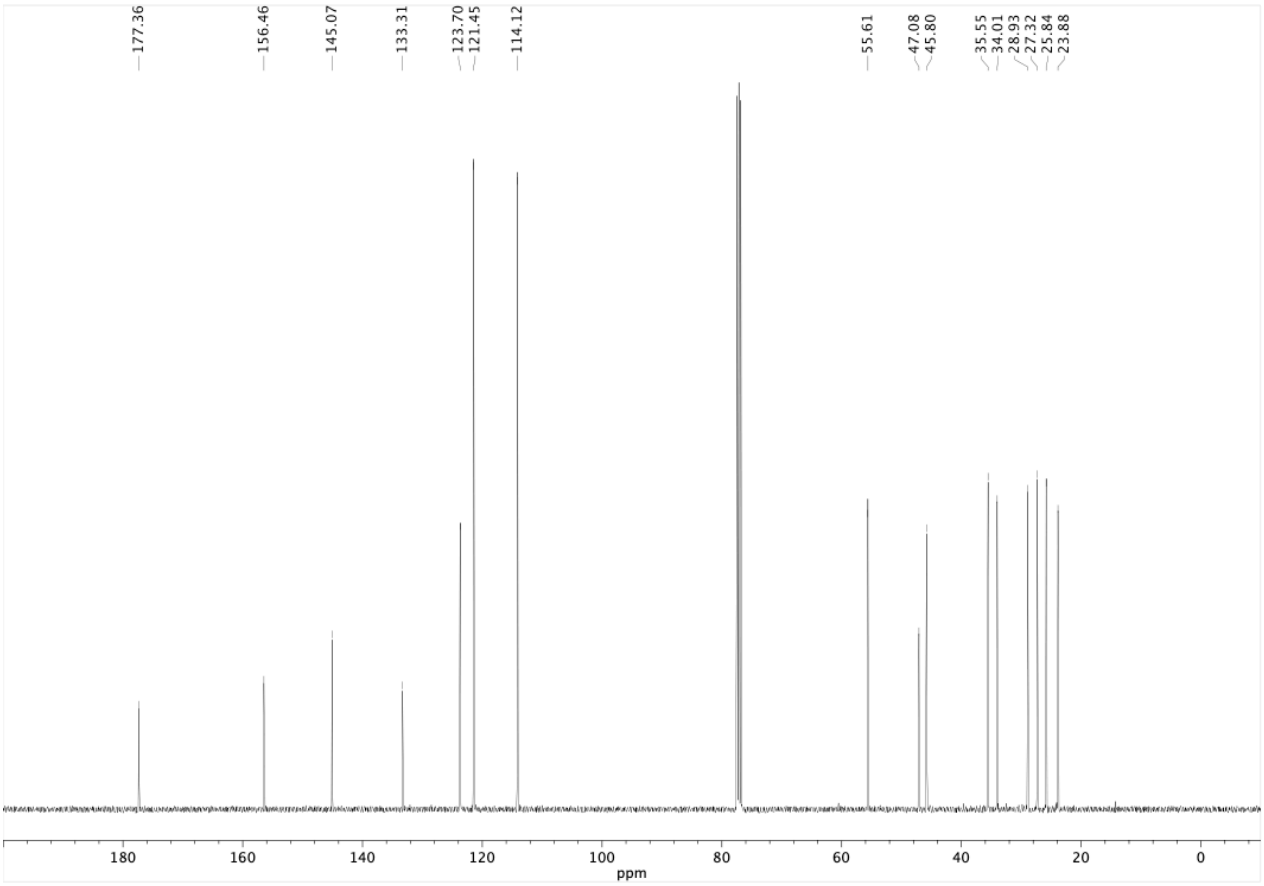

Figure A3.29. *^{13}C NMR (100 MHz, $CDCl_3$) of compound* ***54a****.*

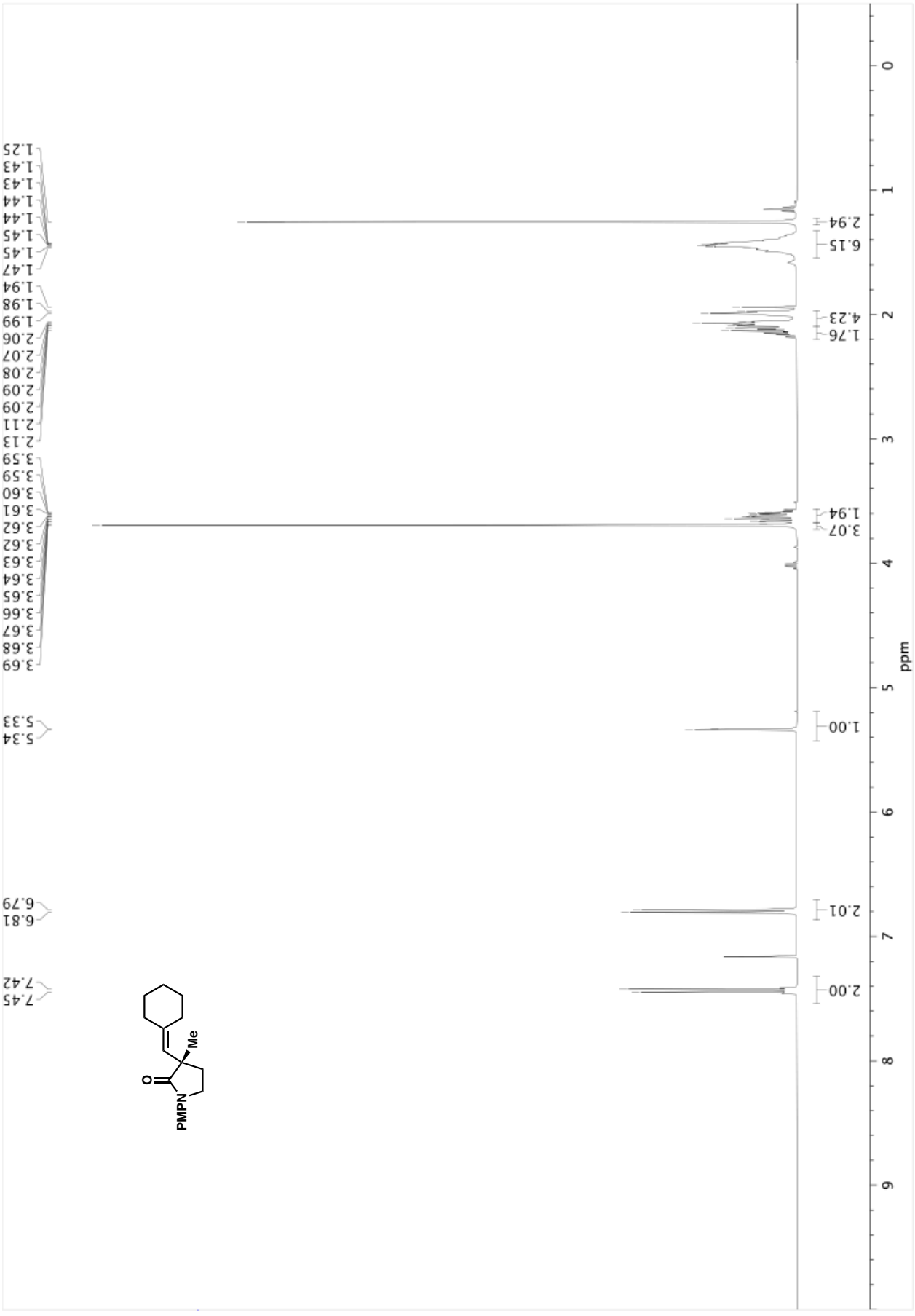

Figure A3.30. *^1H NMR (400 MHz, $CDCl_3$) of compound* ***55a****.*

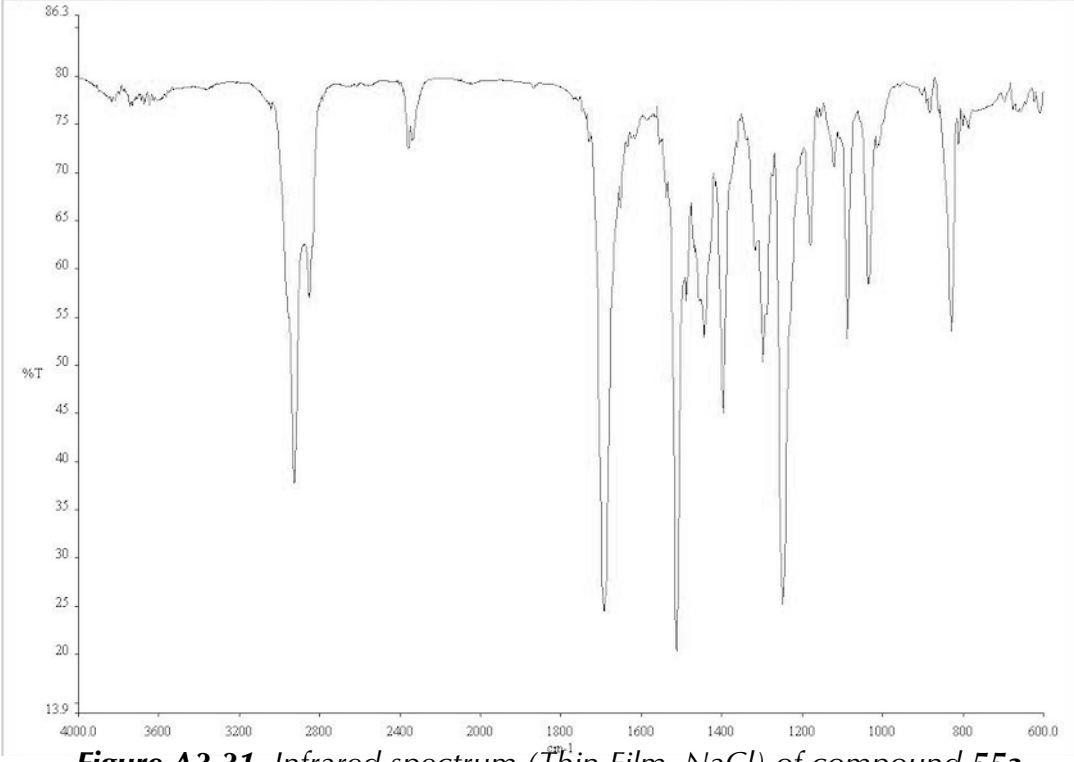

Figure A3.31. *Infrared spectrum (Thin Film, NaCl) of compound* ***55a****.*

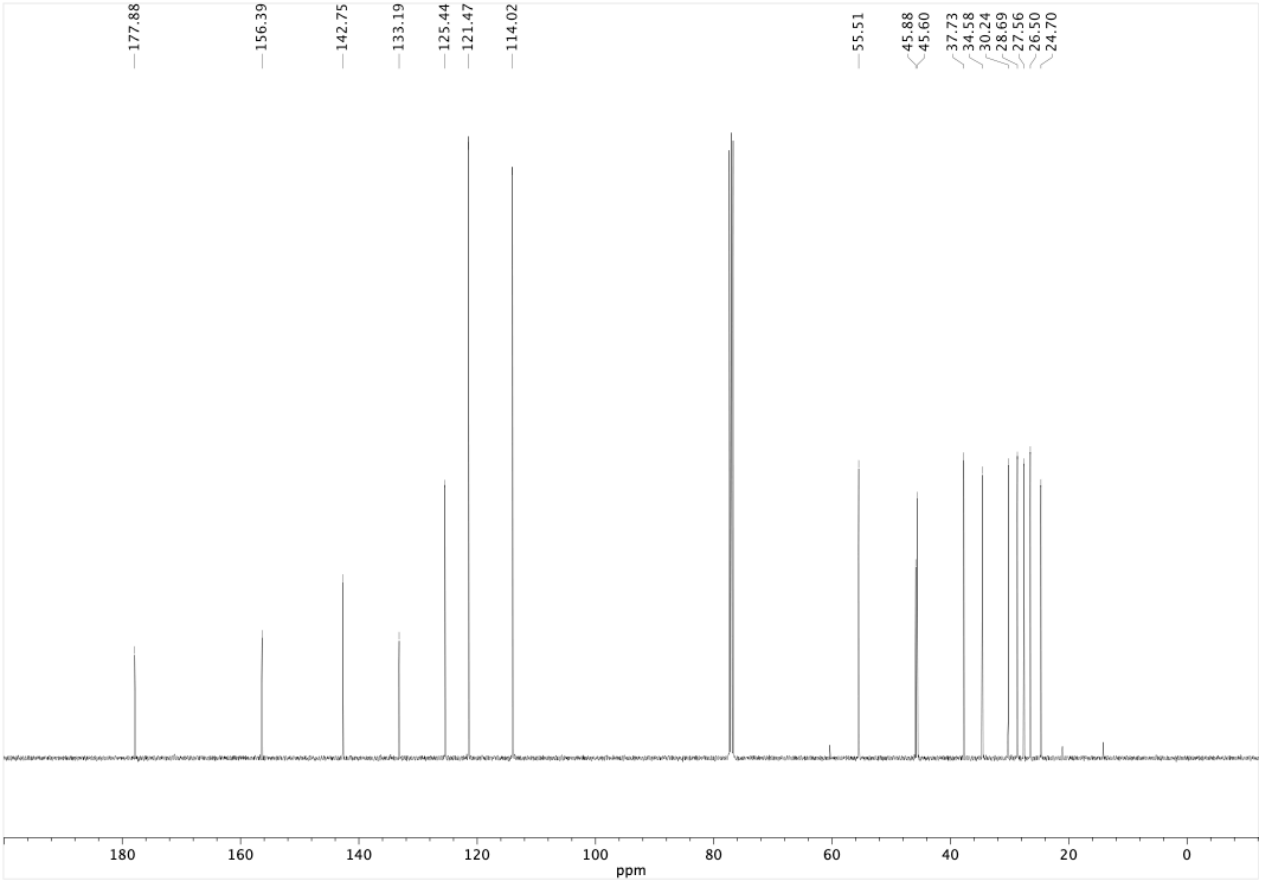

Figure A3.32. *^{13}C NMR (100 MHz, $CDCl_3$) of compound* ***55a****.*

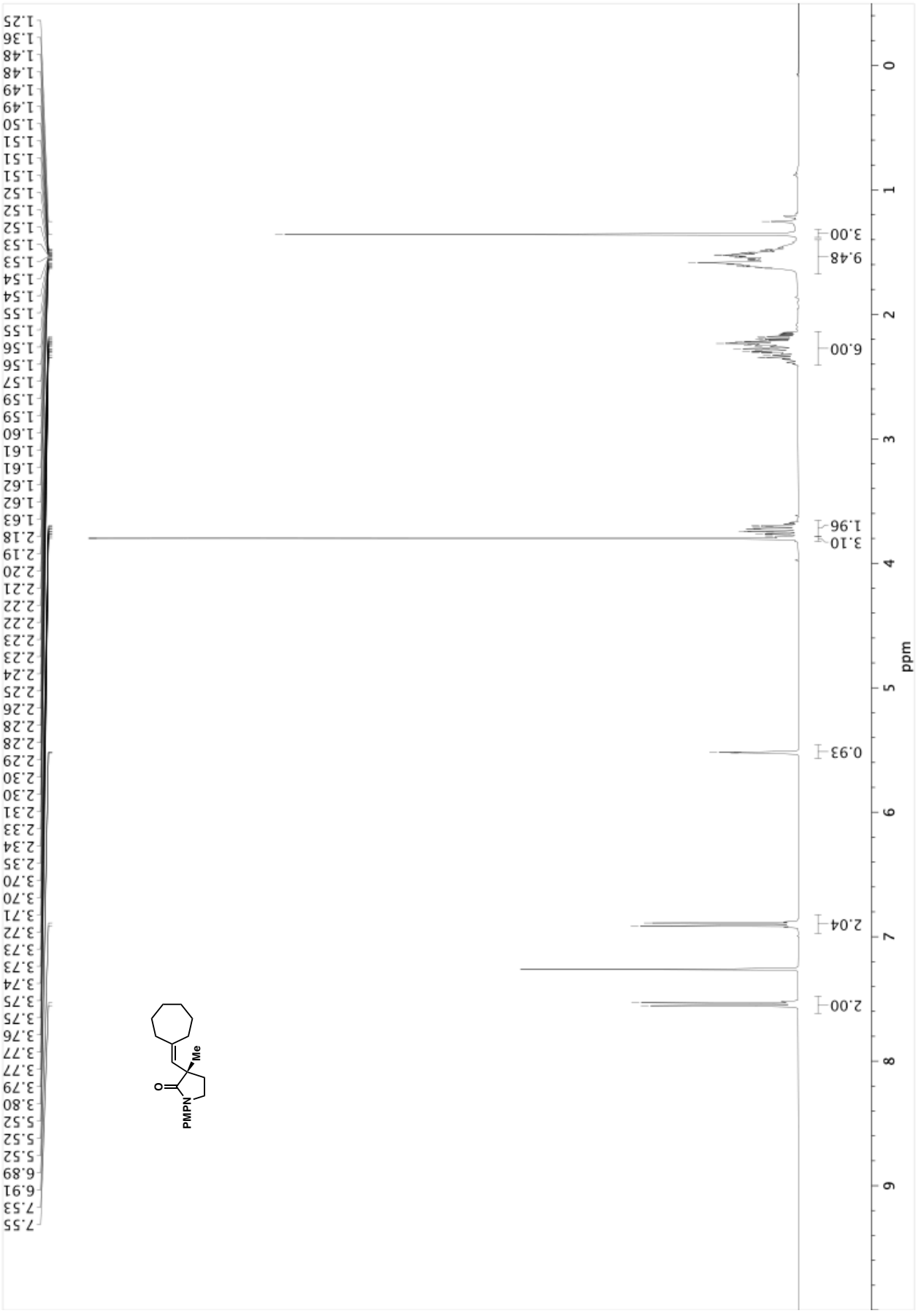

Figure A3.33. *^1H NMR (400 MHz, $CDCl_3$) of compound* ***56a****.*

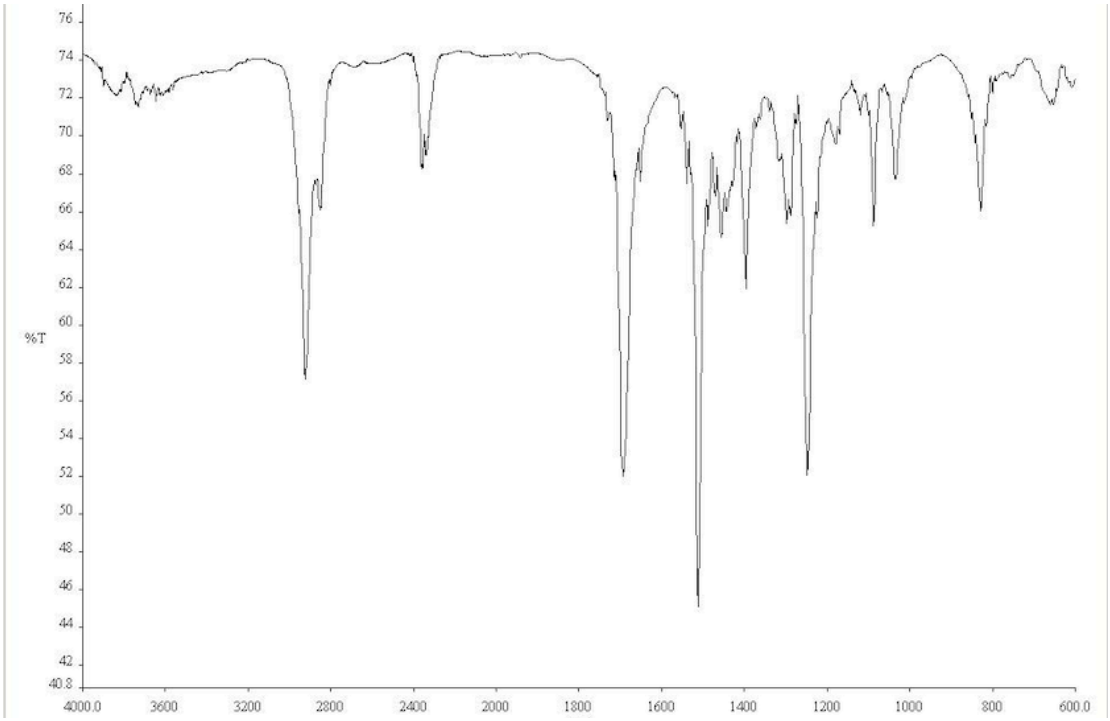

Figure A3.34. *Infrared spectrum (Thin Film, NaCl) of compound* ***56a****.*

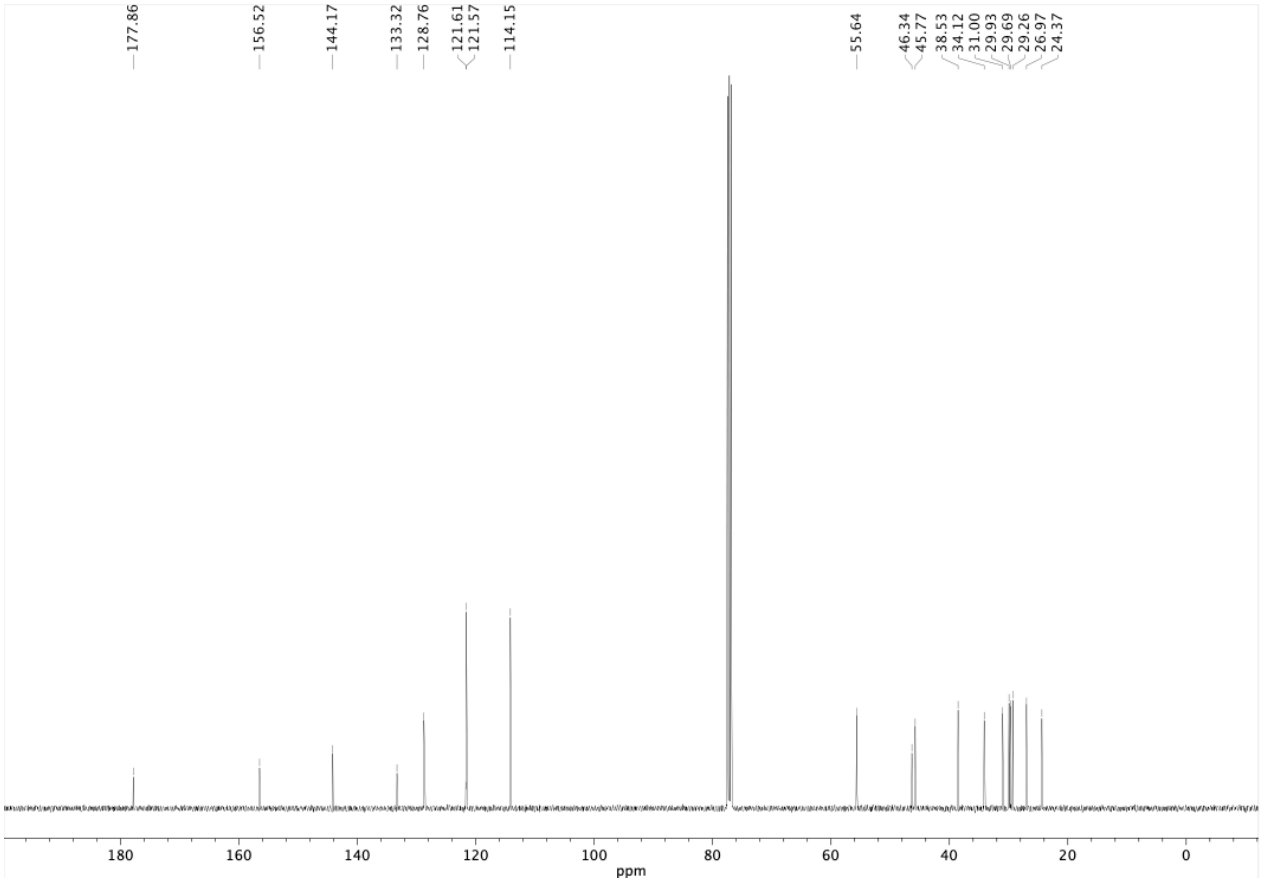

Figure A3.35. *^{13}C NMR (100 MHz, $CDCl_3$) of compound* ***56a****.*

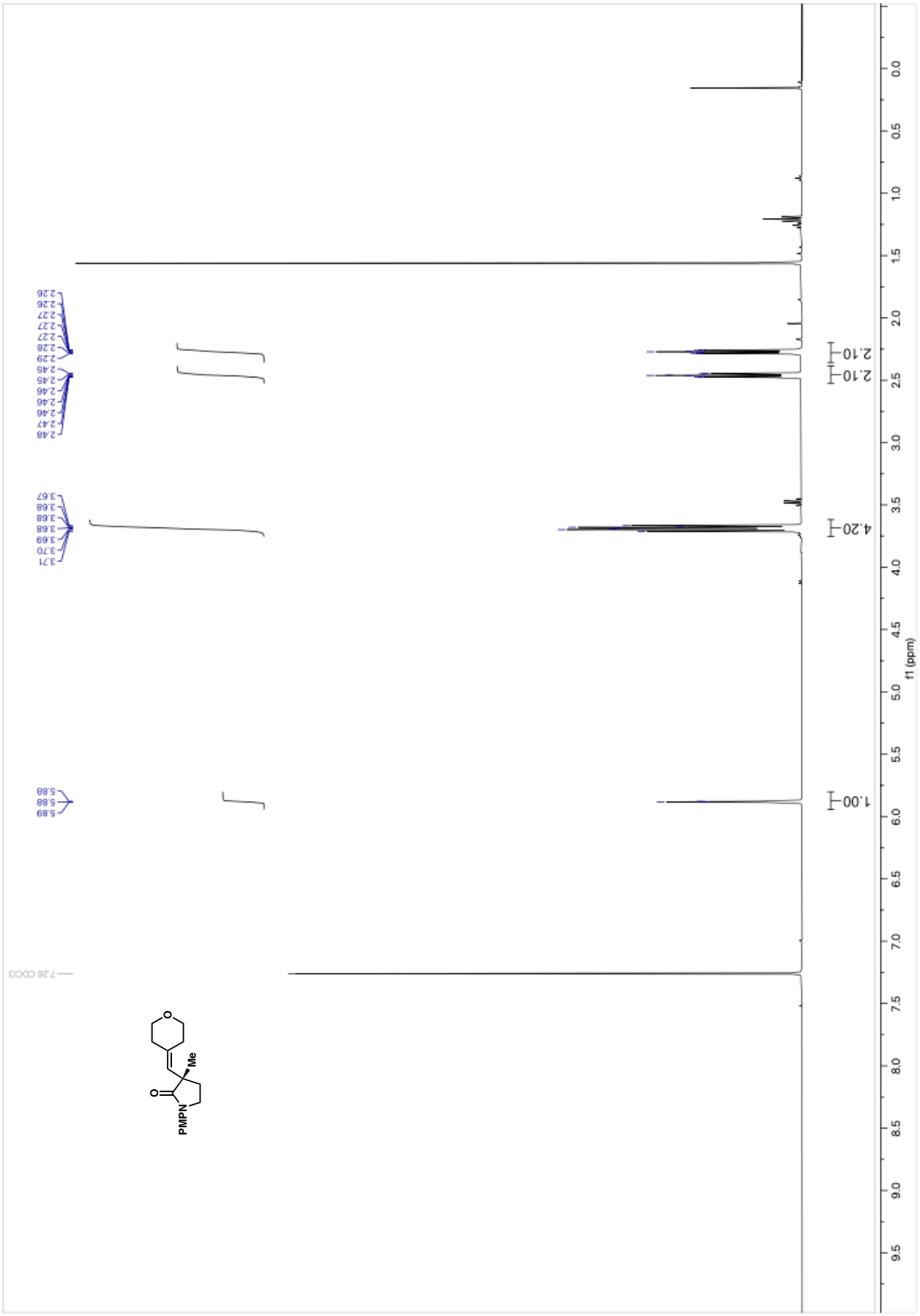

Figure A3.36. *^1H NMR (400 MHz, $CDCl_3$) of compound* ***57a****.*

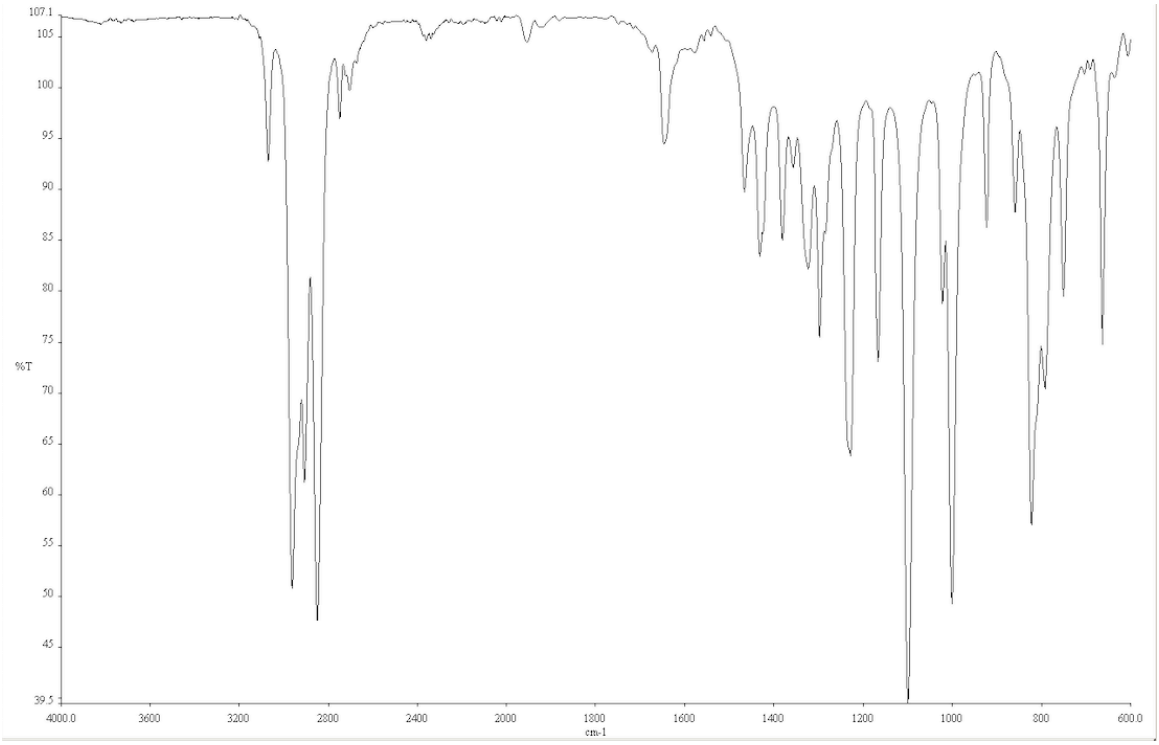

Figure A3.37. *Infrared spectrum (Thin Film, NaCl) of compound* ***57a****.*

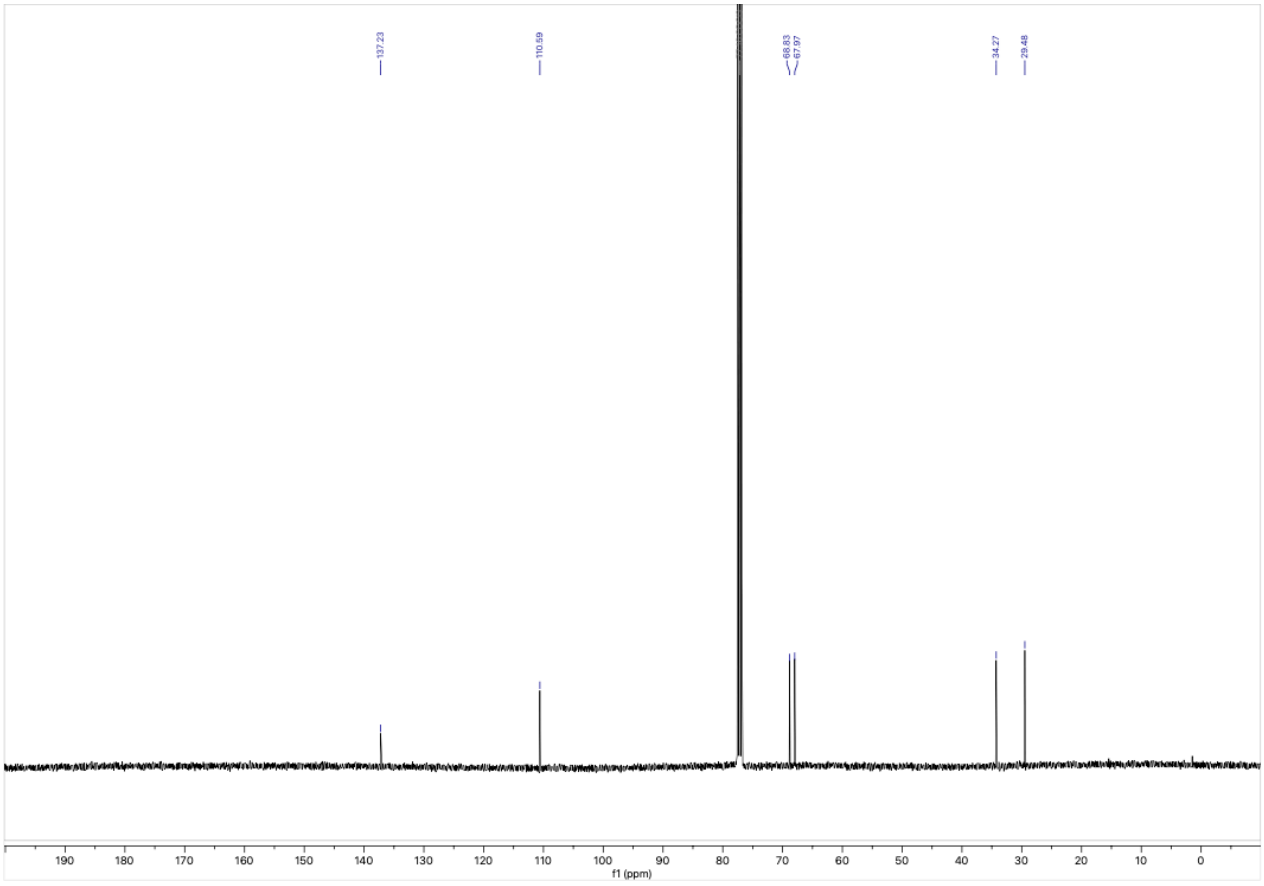

Figure A3.37. *^{13}C NMR (100 MHz, $CDCl_3$) of compound* ***57a****.*

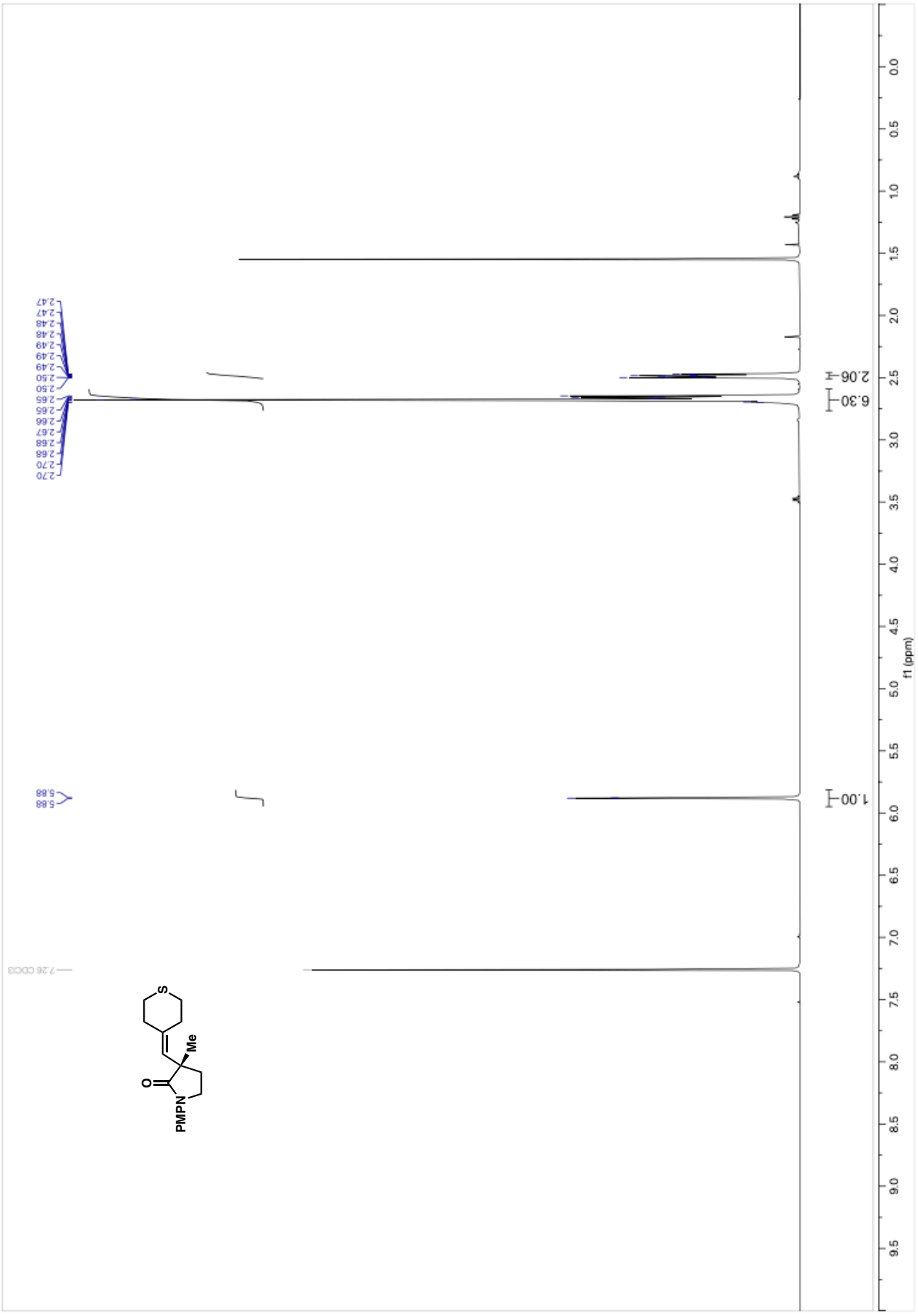

Figure A3.38. *^1H NMR (400 MHz, $CDCl_3$) of compound* ***58a****.*

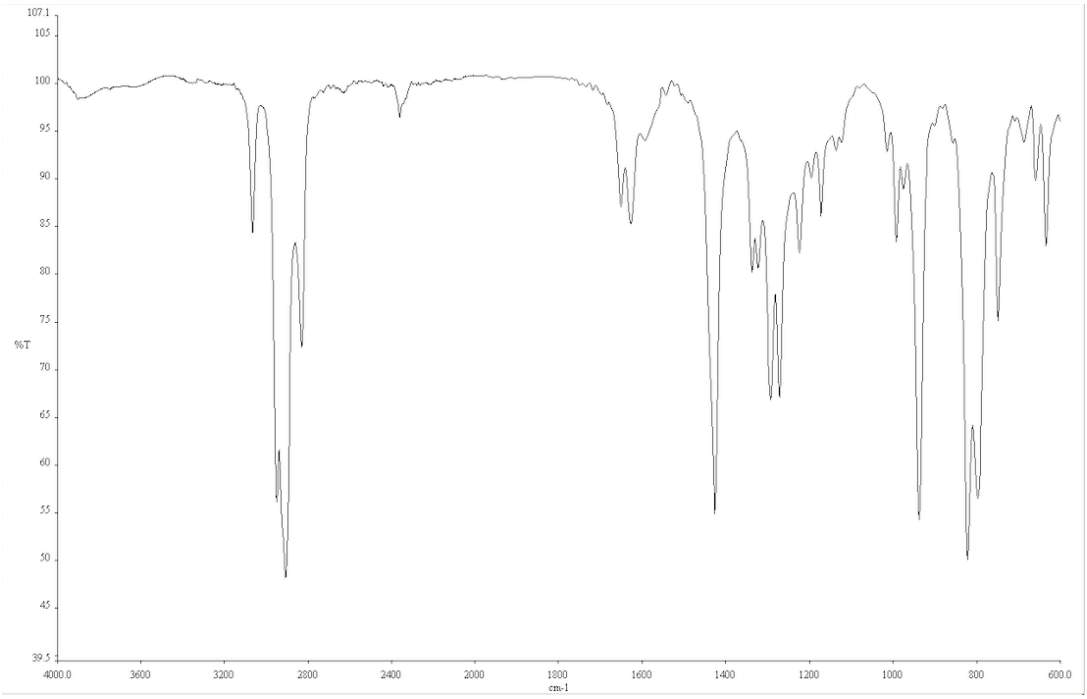

Figure A3.39. *Infrared spectrum (Thin Film, NaCl) of compound* ***58a****.*

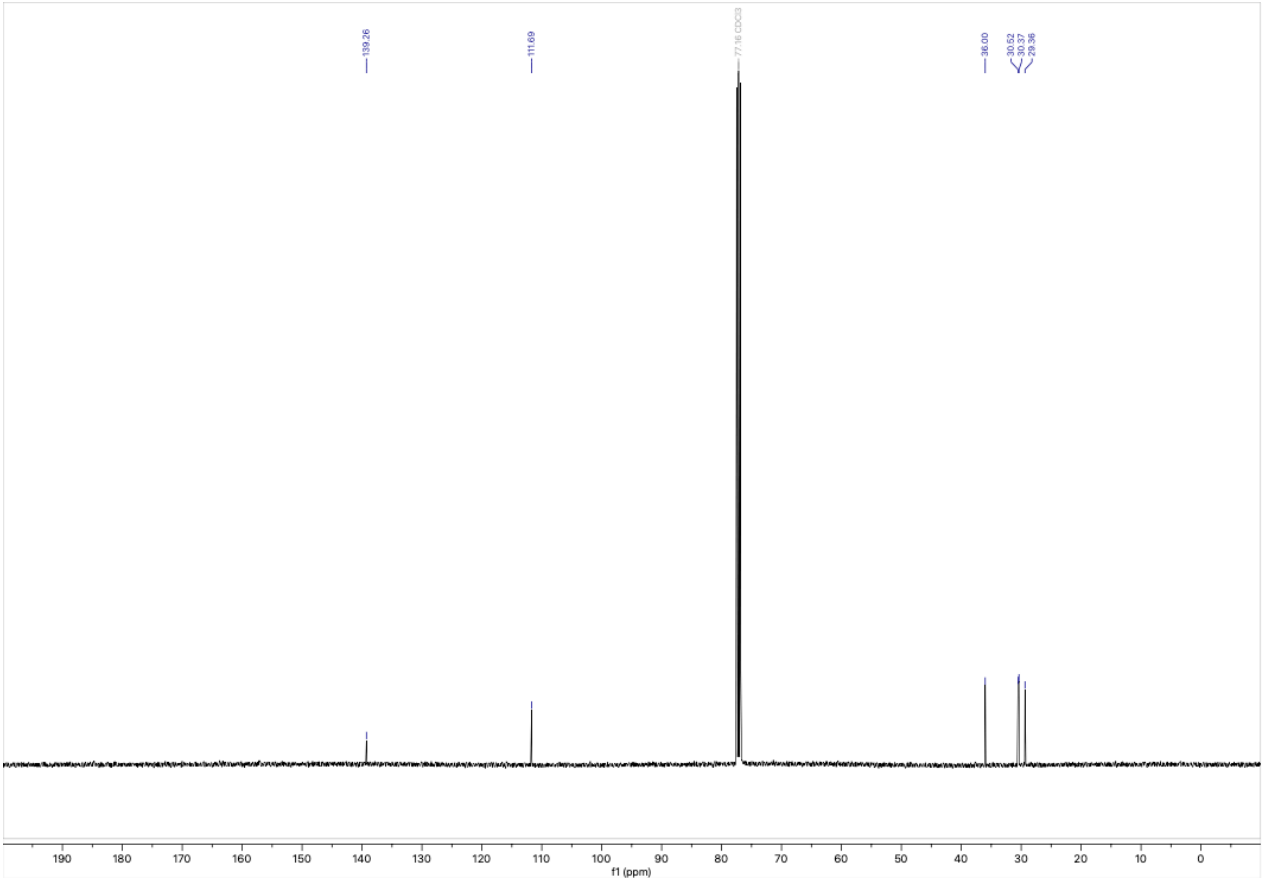

Figure A3.40. *^{13}C NMR (100 MHz, $CDCl_3$) of compound* ***58a****.*

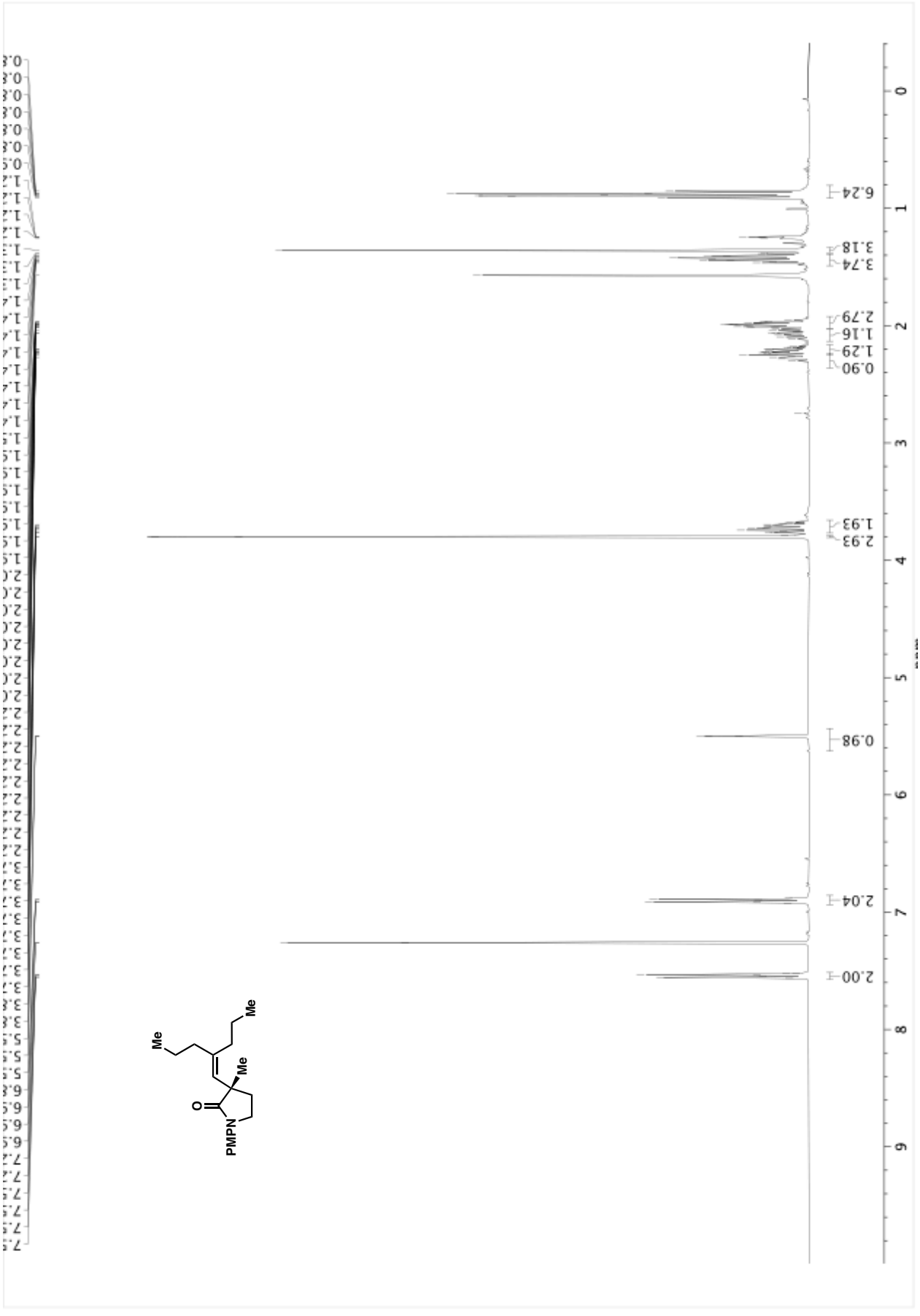

Figure A3.41. *^1H NMR (400 MHz, $CDCl_3$) of compound* ***59a****.*

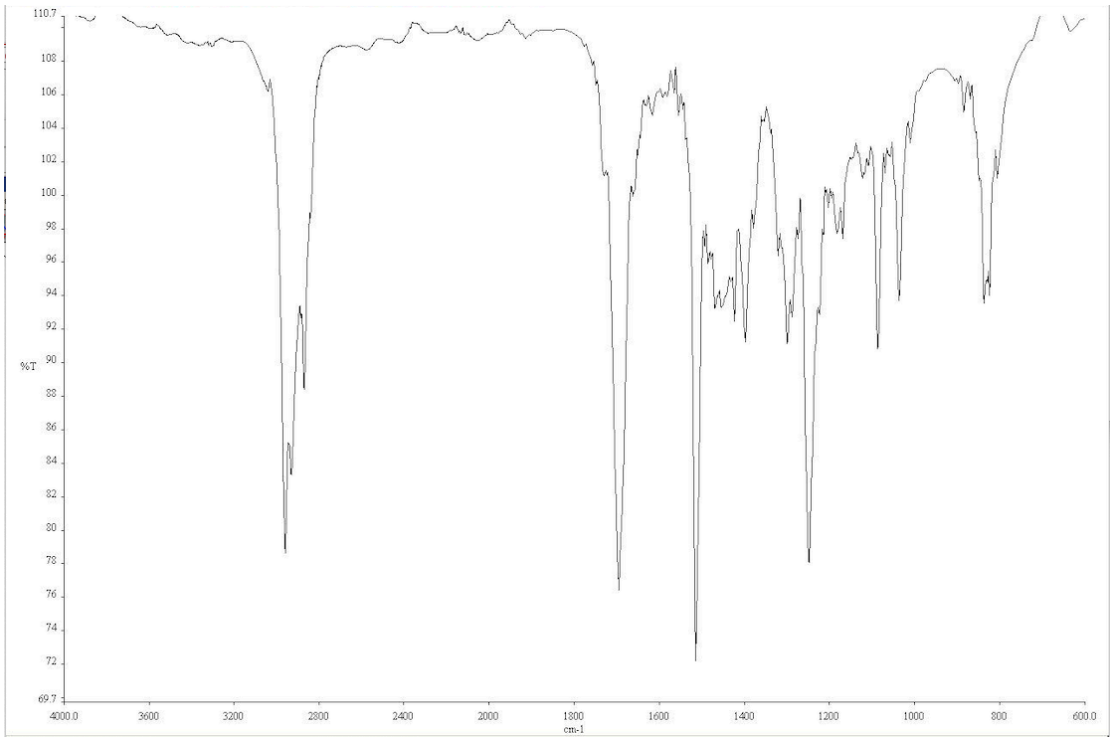

Figure A3.42. *Infrared spectrum (Thin Film, NaCl) of compound* ***59a****.*

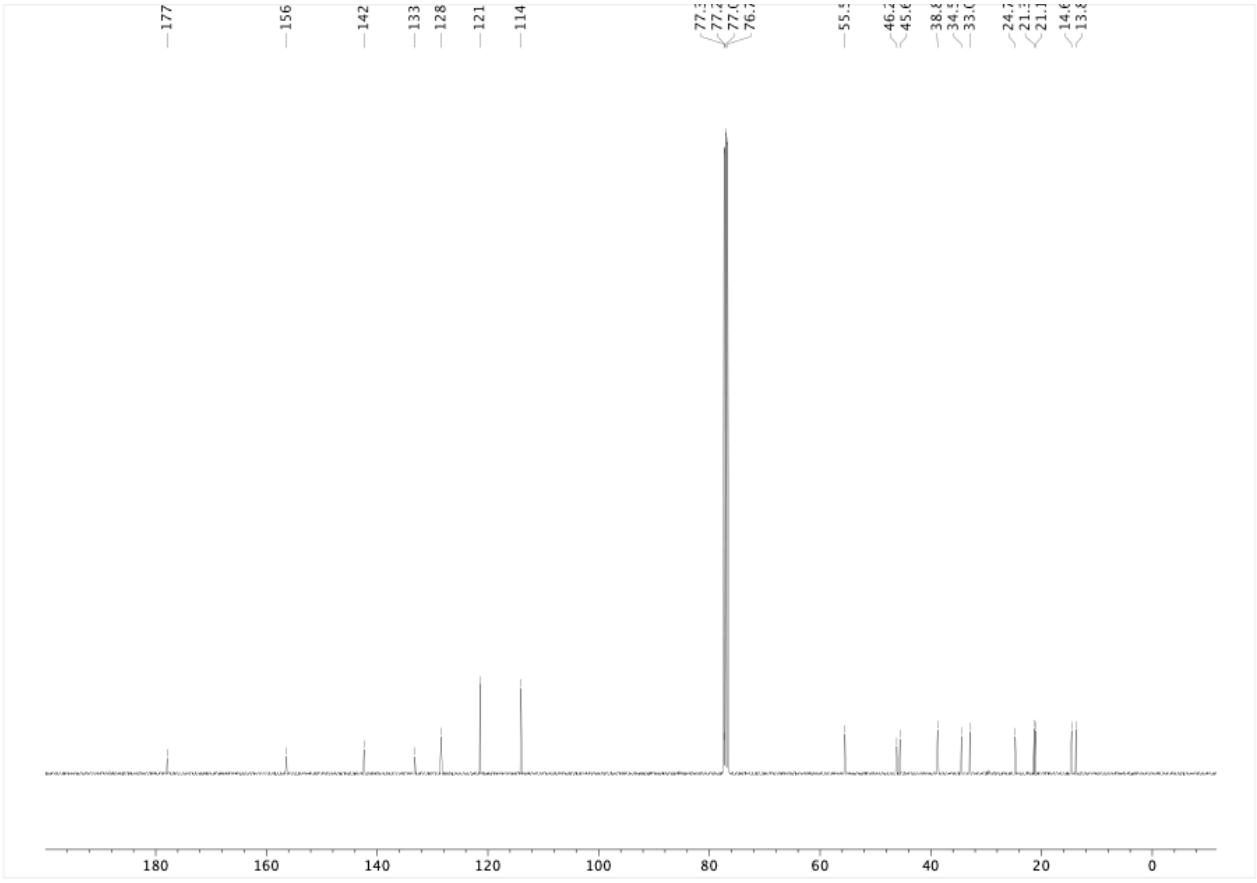

Figure A3.43. *^{13}C NMR (100 MHz, $CDCl_3$) of compound* ***59a****.*

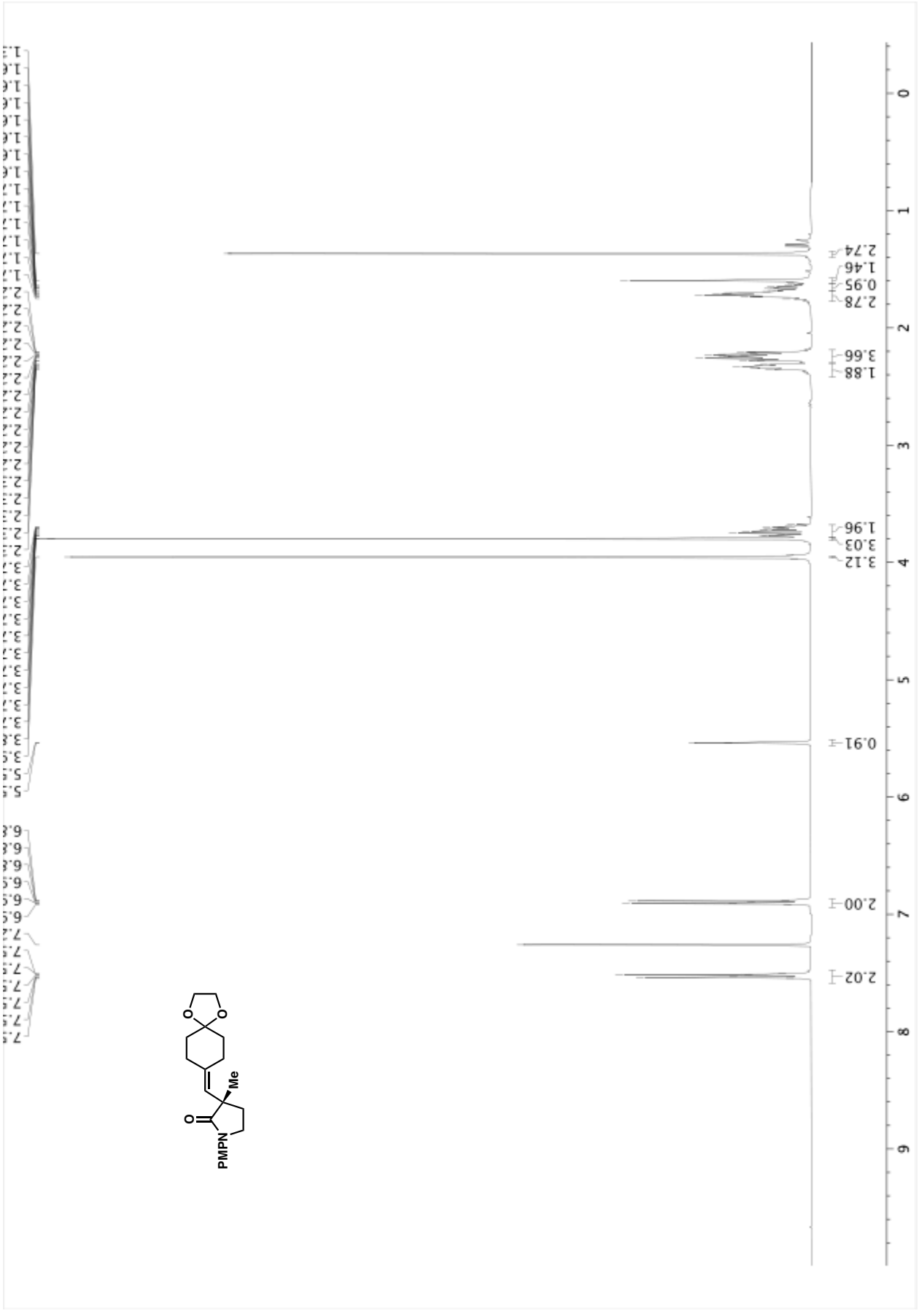

Figure A3.44. *^{1}H NMR (400 MHz, $CDCl_3$) of compound* ***60a***.

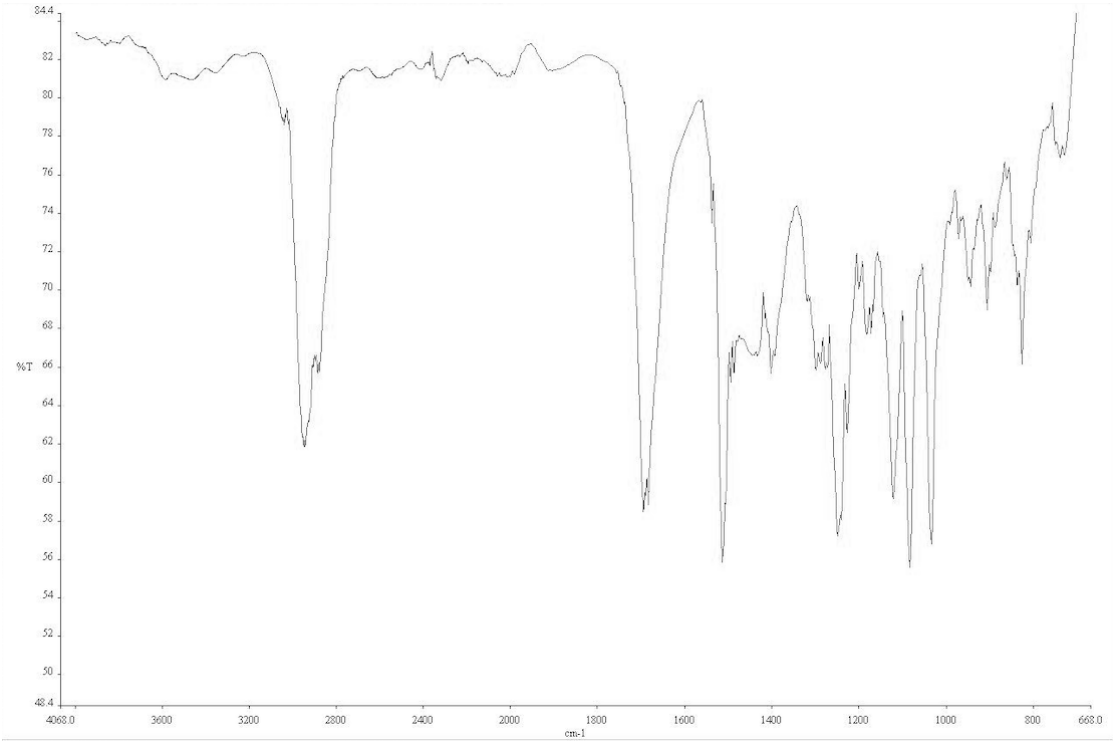

Figure A3.45. *Infrared spectrum (Thin Film, NaCl) of compound* ***60a****.*

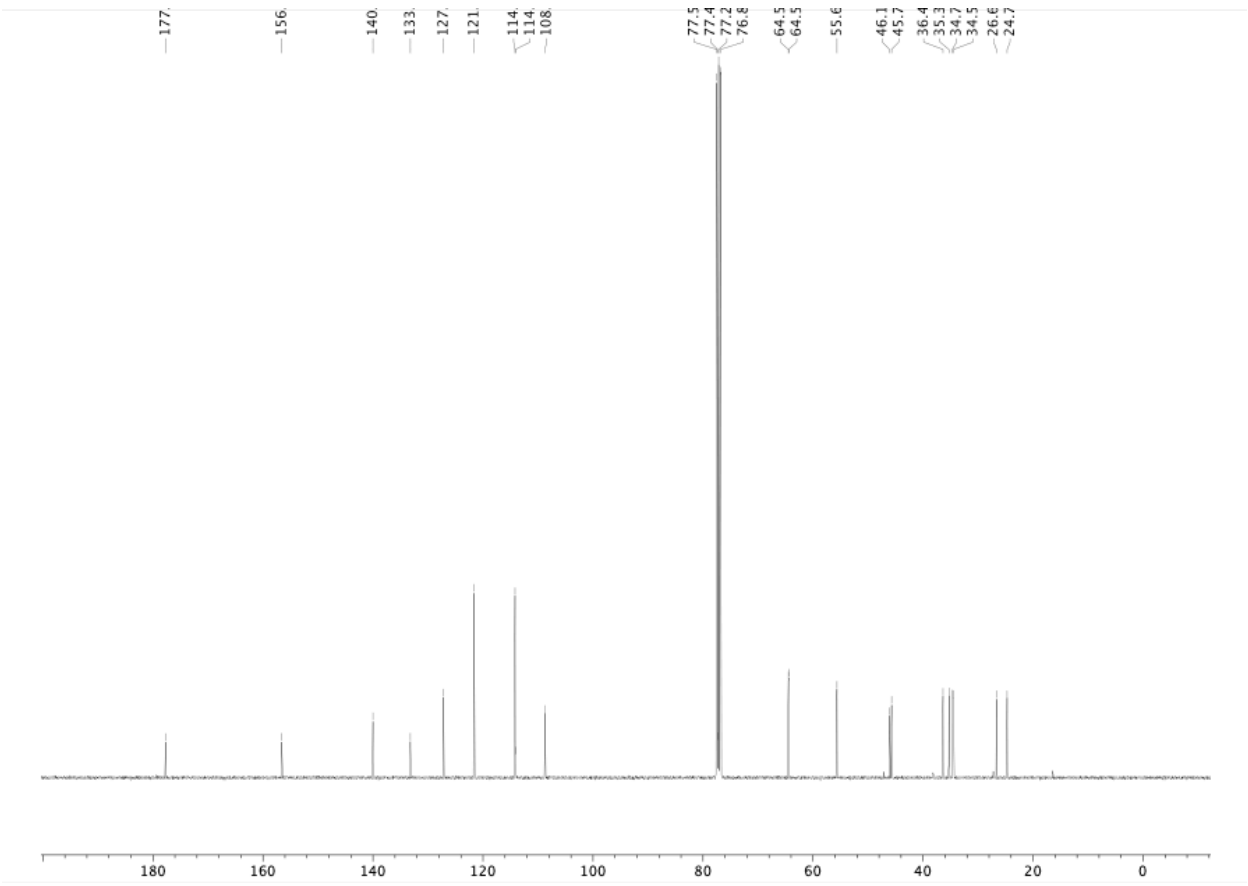

Figure A3.46. *^{13}C NMR (100 MHz, $CDCl_3$) of compound* ***60a****.*

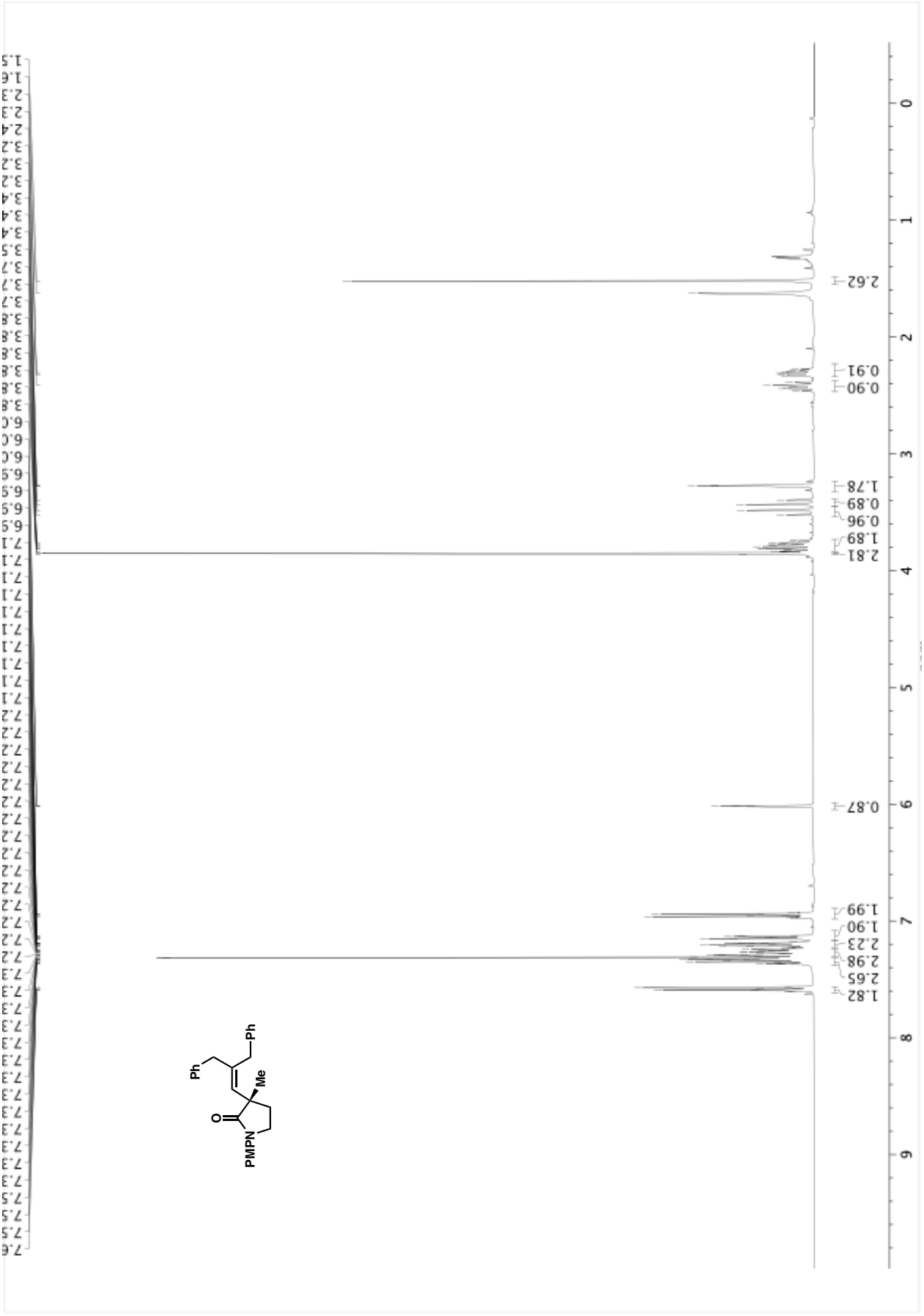

Figure A3.47. *^1H NMR (400 MHz, $CDCl_3$) of compound* ***61a***.

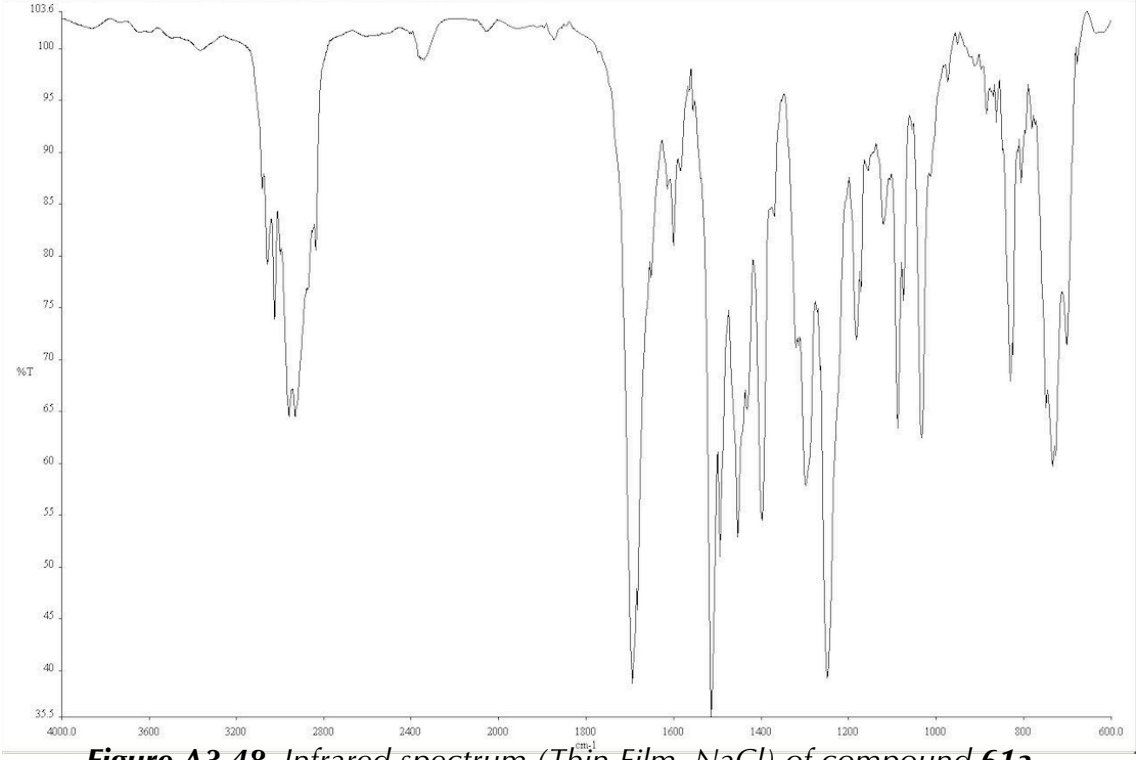

Figure A3.48. *Infrared spectrum (Thin Film, NaCl) of compound* ***61a****.*

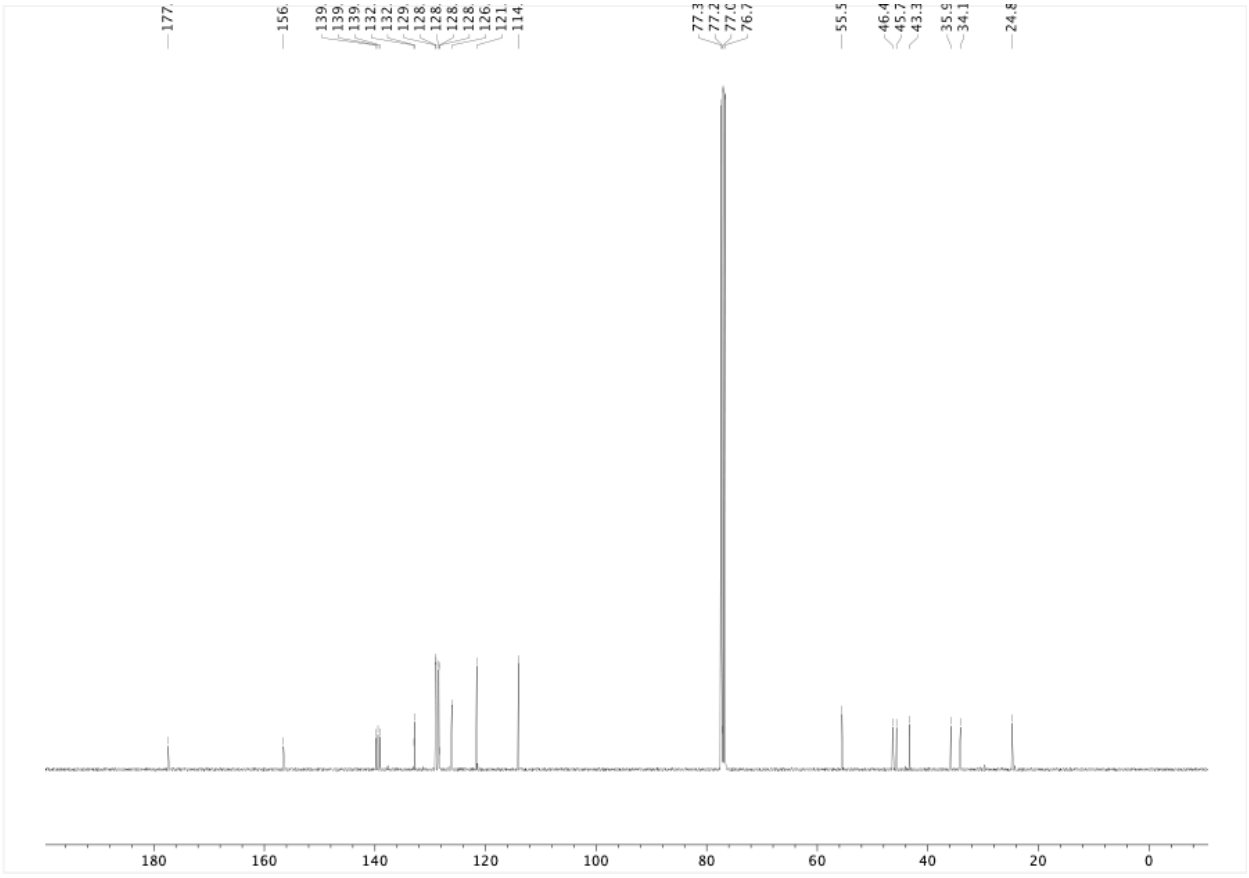

Figure A3.49. *^{13}C NMR (100 MHz, $CDCl_3$) of compound* ***61a****.*

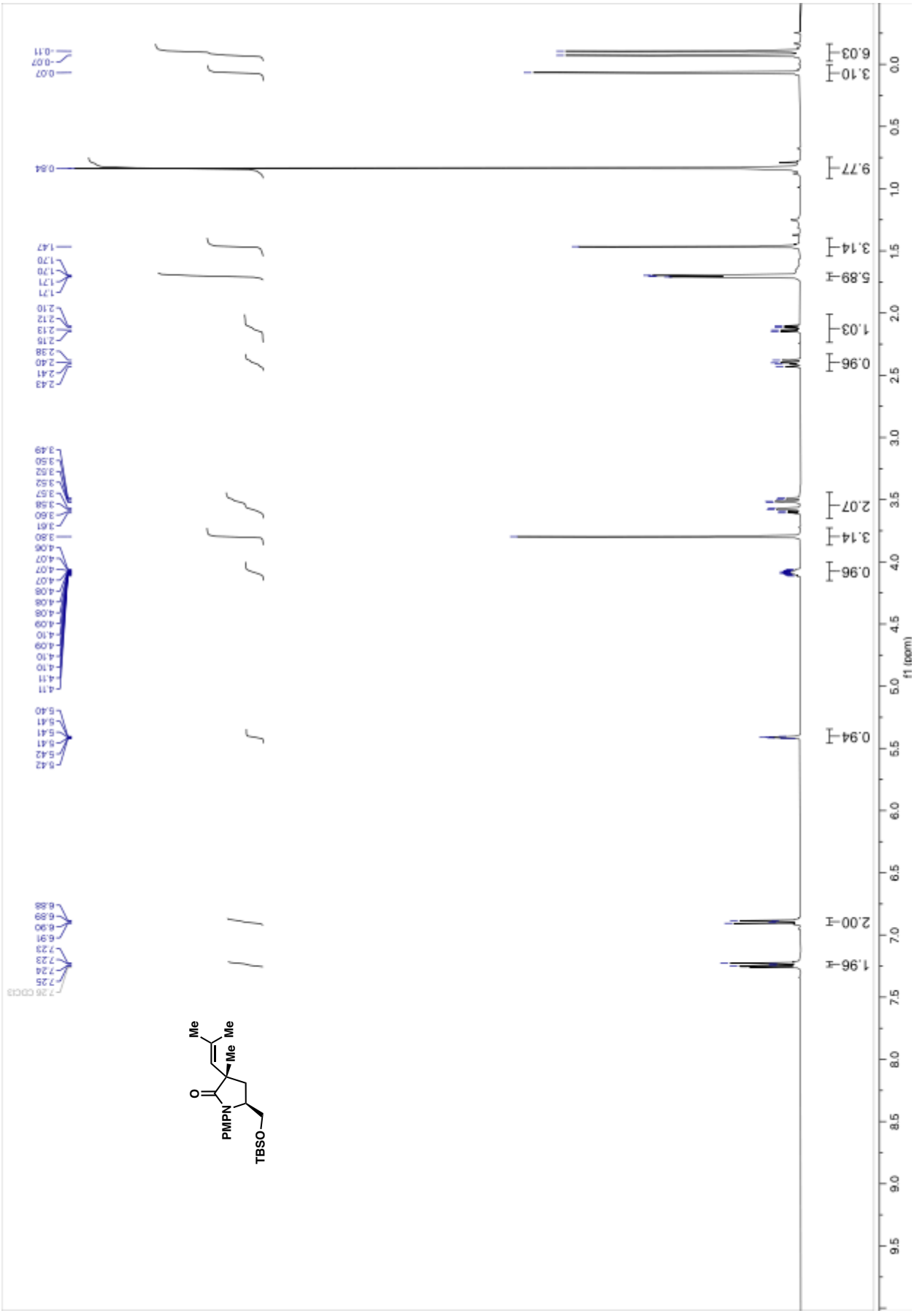

Figure A3.50. *^{1}H NMR (400 MHz, $CDCl_3$) of compound* ***62a****.*

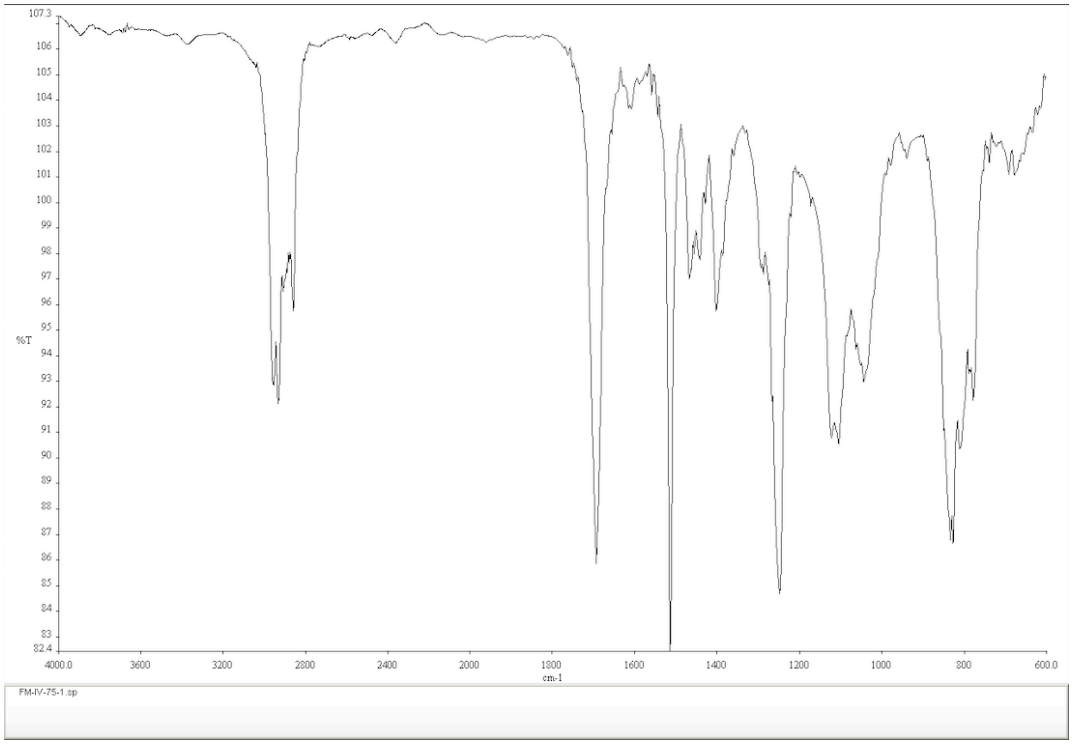

Figure A3.51. *Infrared spectrum (Thin Film, NaCl) of compound* ***62a****.*

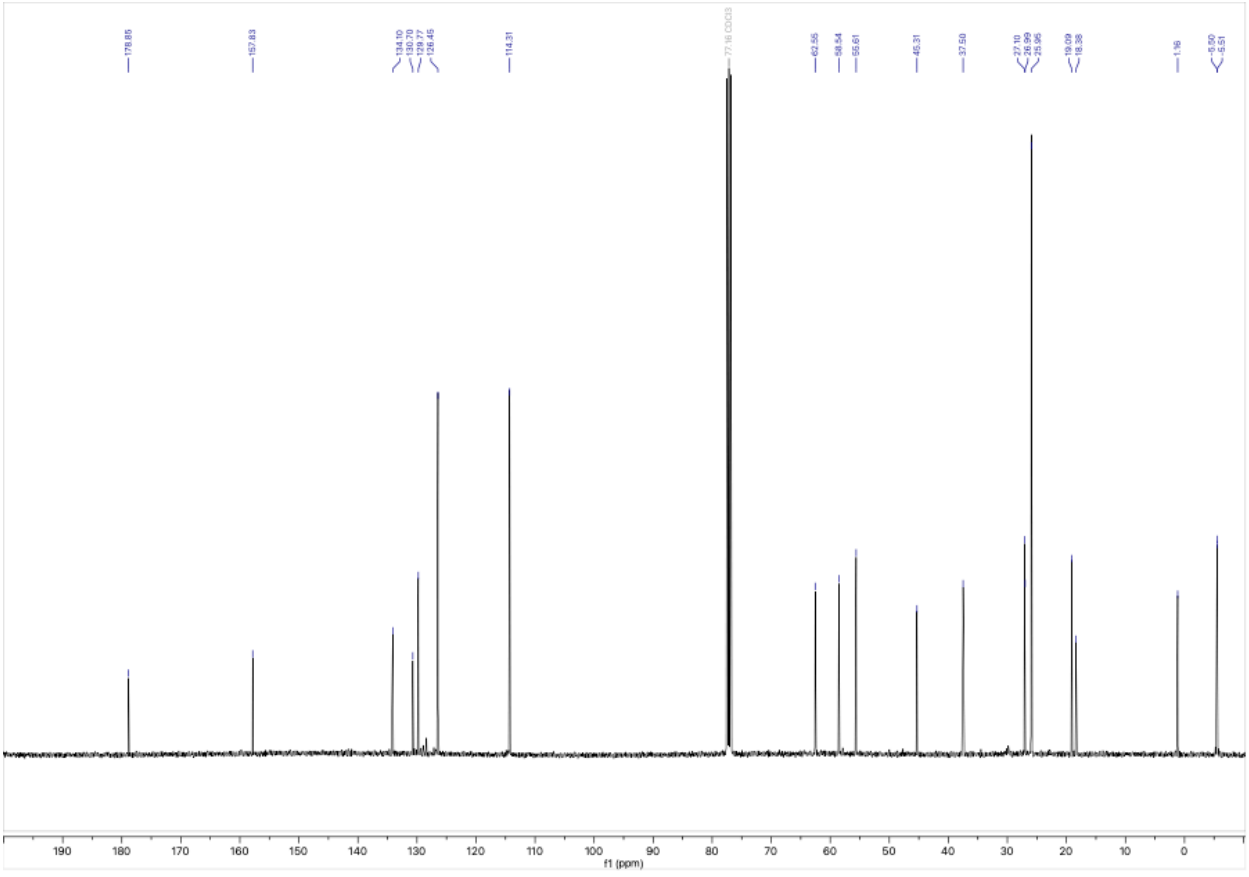

Figure A3.52. *^{13}C NMR (100 MHz, $CDCl_3$) of compound* ***62a****.*

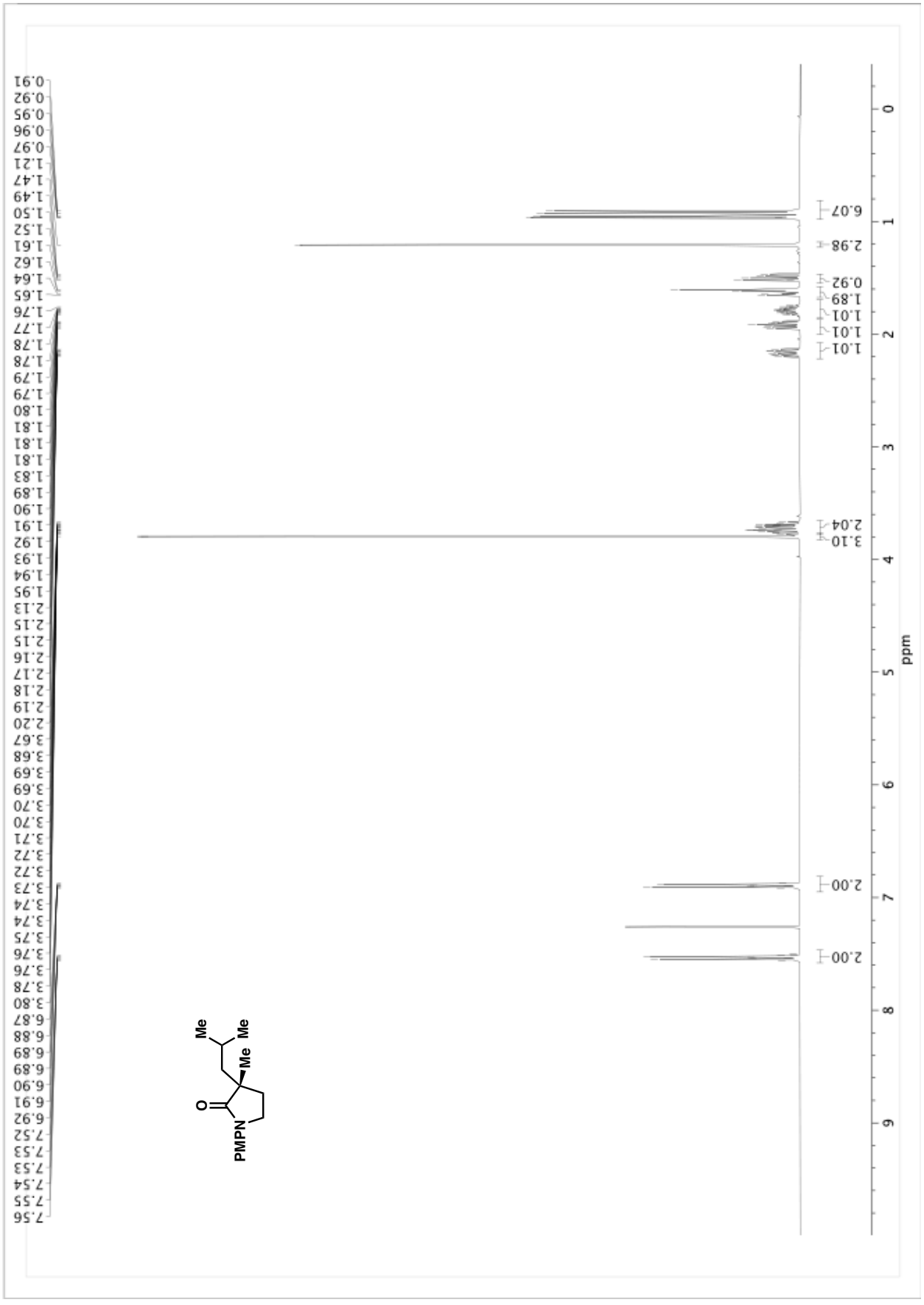

Figure A3.53. *^1H NMR (400 MHz, $CDCl_3$) of compound* ***64****.*

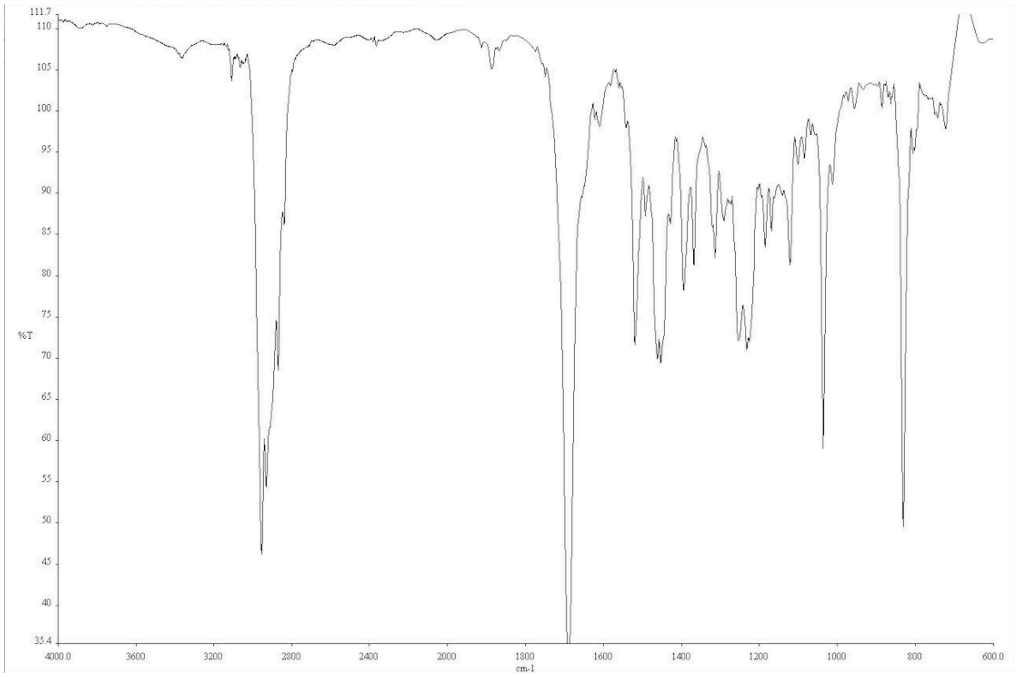

Figure A3.54. *Infrared spectrum (Thin Film, NaCl) of compound* ***64****.*

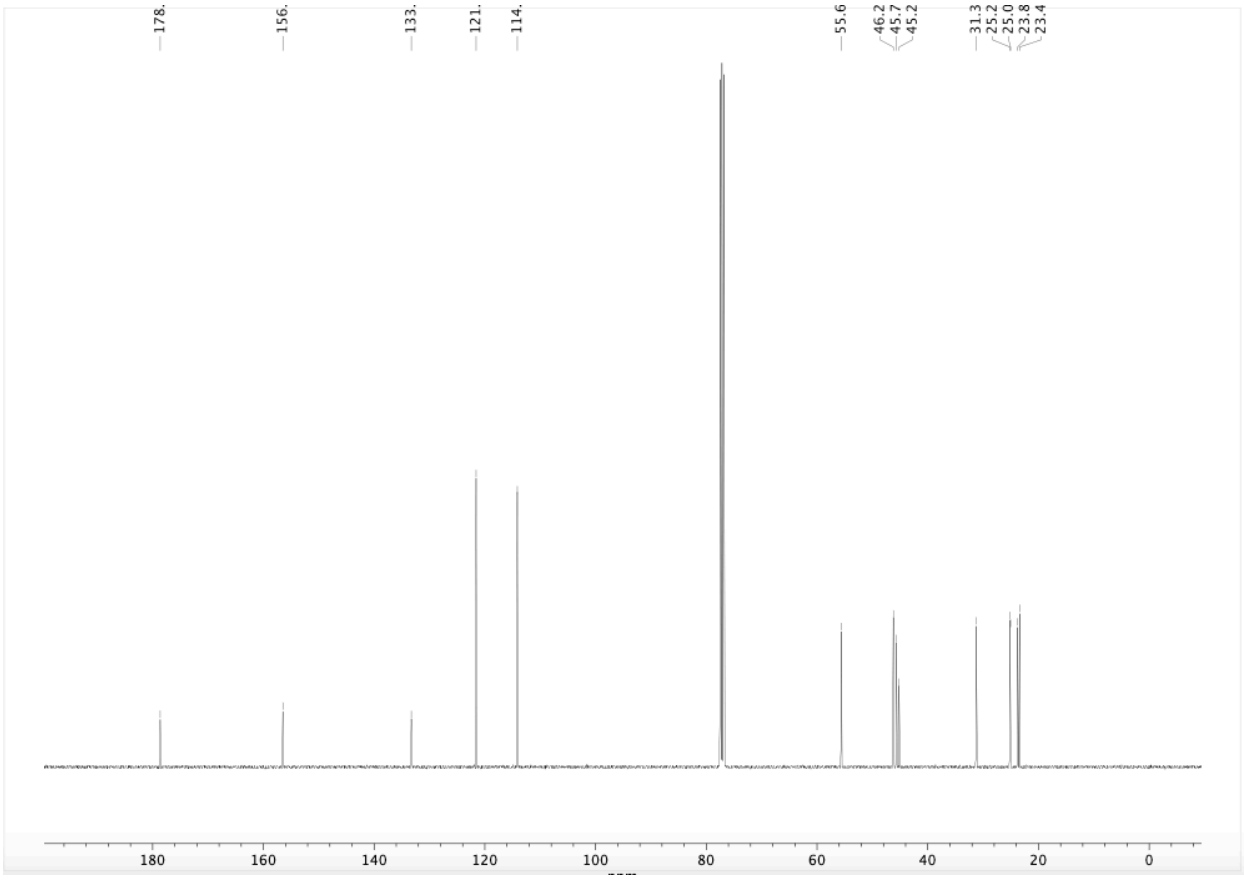

Figure A3.55. *^{13}C NMR (100 MHz, $CDCl_3$) of compound* ***64****.*

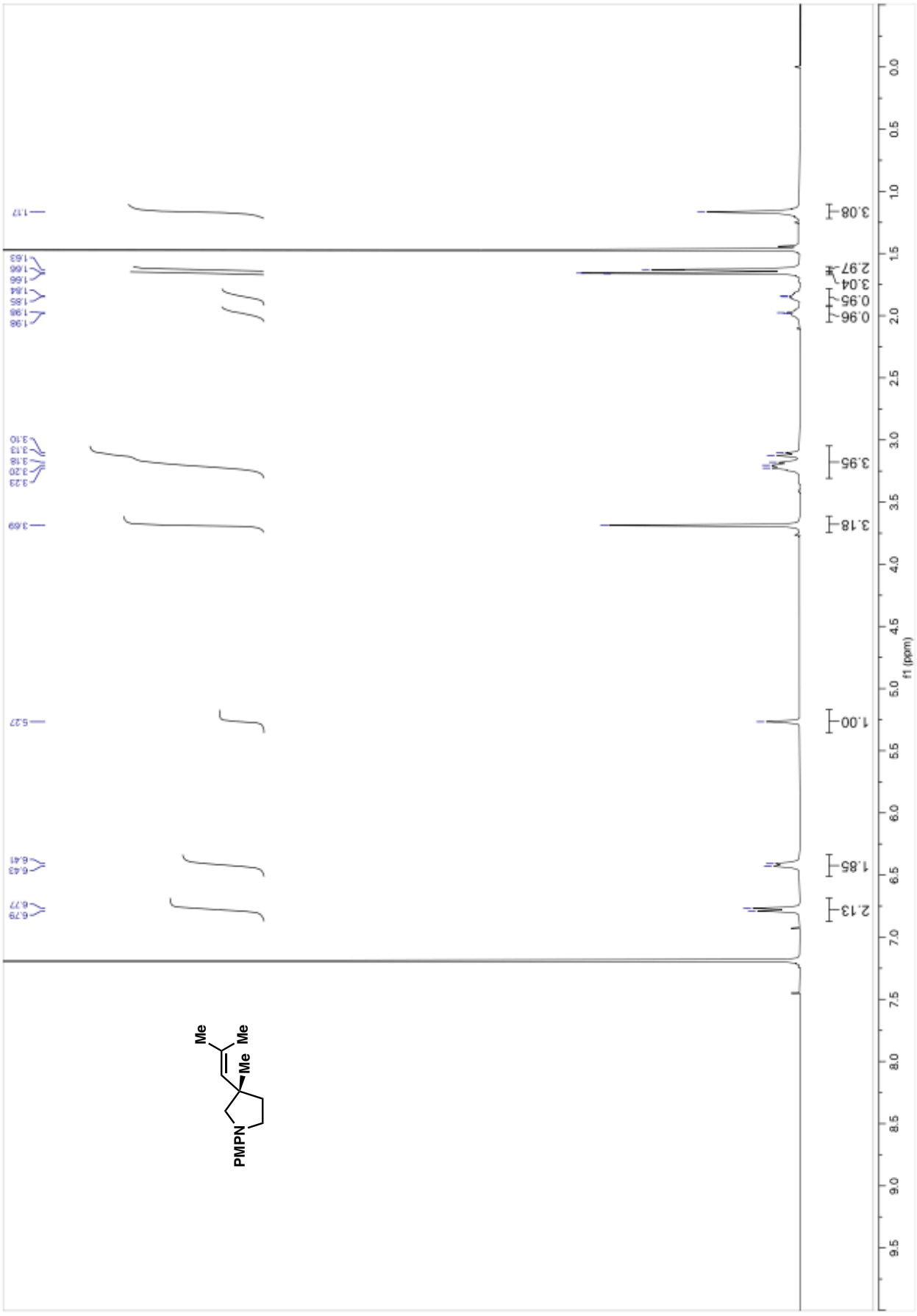

Figure A3.56. *^1H NMR (400 MHz, $CDCl_3$) of compound* ***65****.*

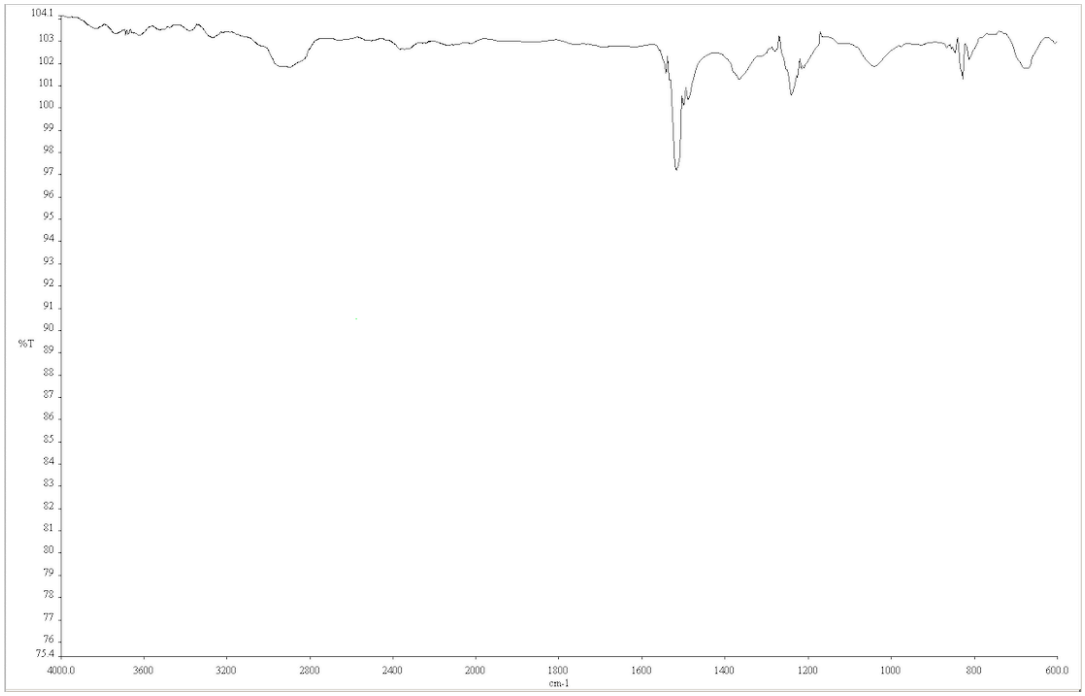

Figure A3.57. *Infrared spectrum (Thin Film, NaCl) of compound* ***65****.*

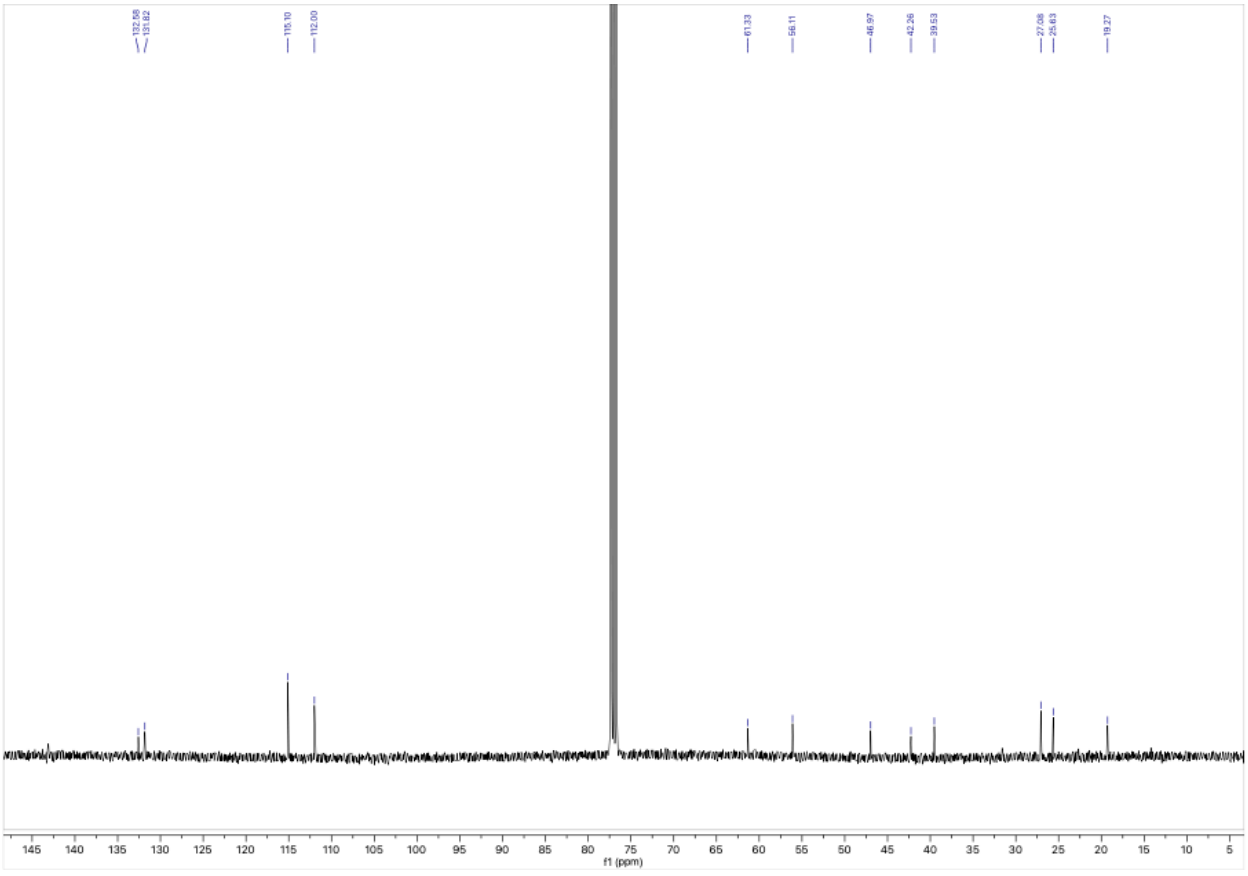

Figure A3.58. *^{13}C NMR (100 MHz, $CDCl_3$) of compound* ***65****.*

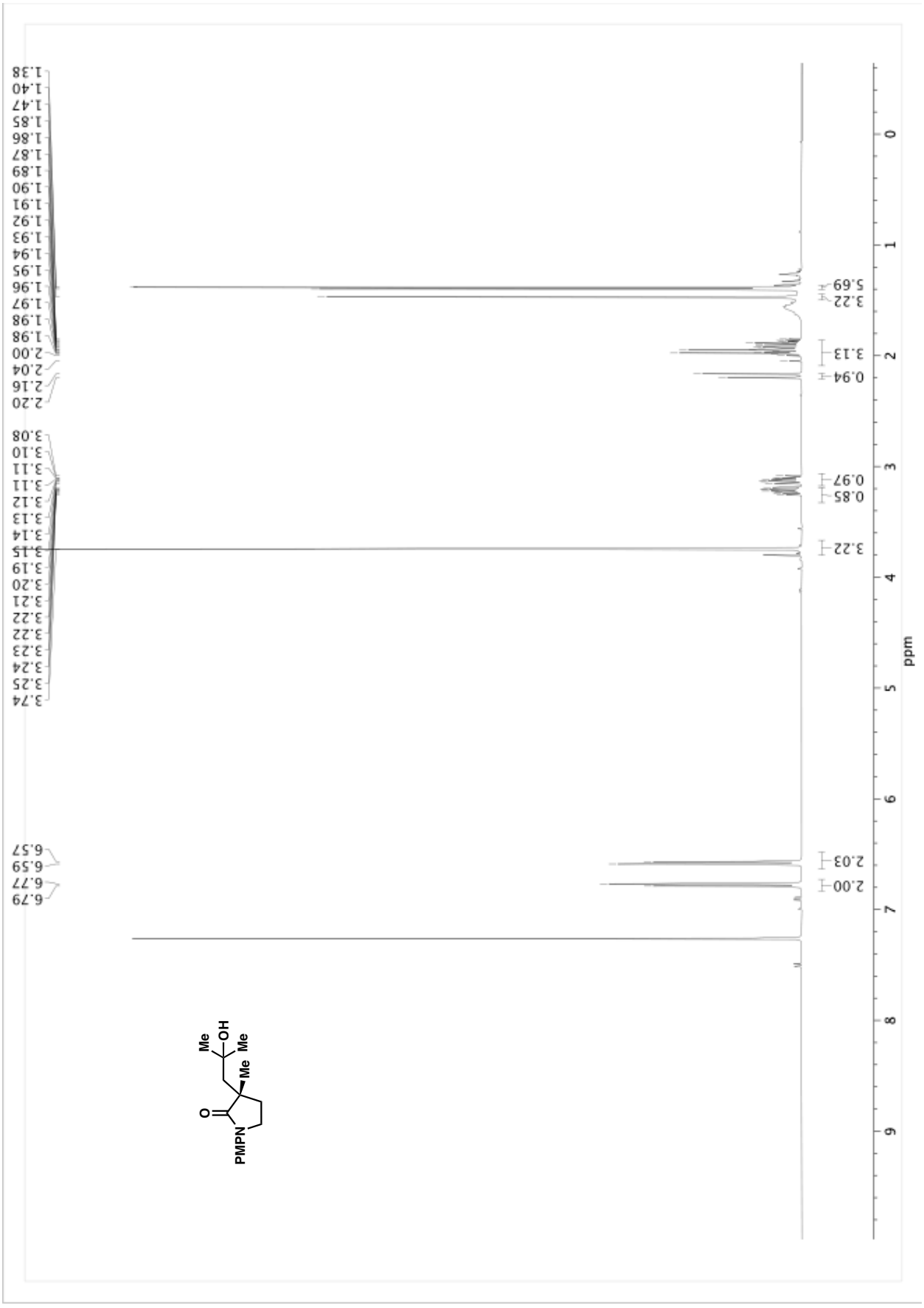

Figure A3.59. *^1H NMR (400 MHz, $CDCl_3$) of compound* ***66****.*

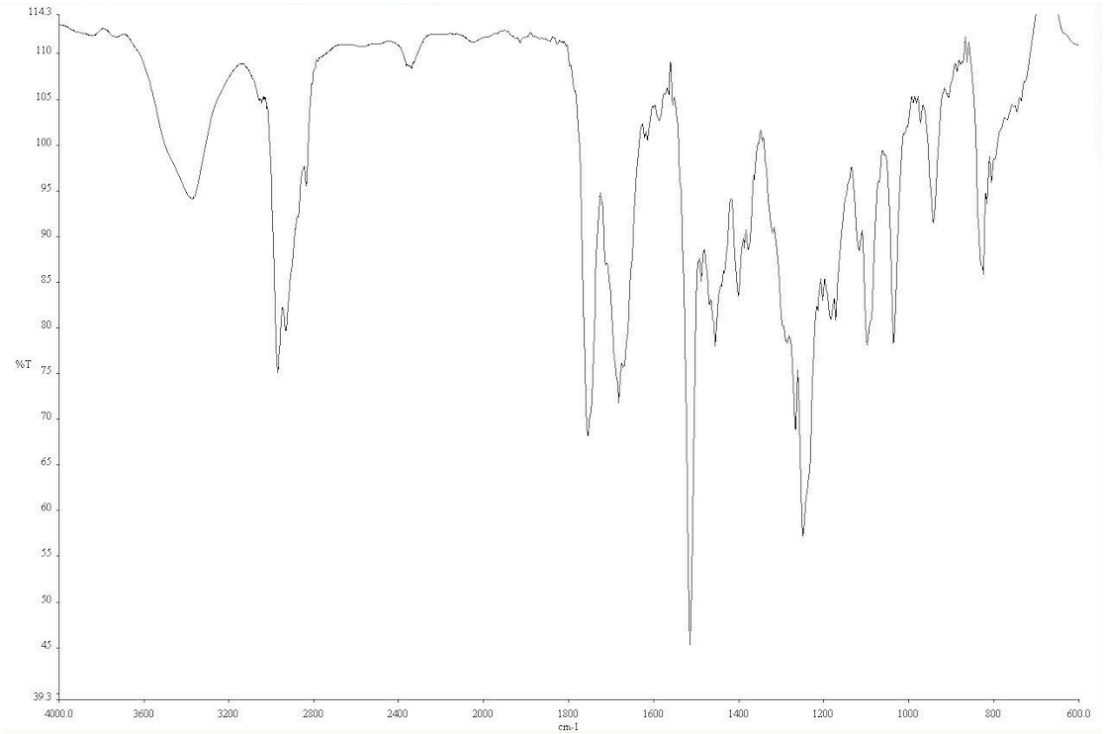

Figure A3.60. *Infrared spectrum (Thin Film, NaCl) of compound* ***66****.*

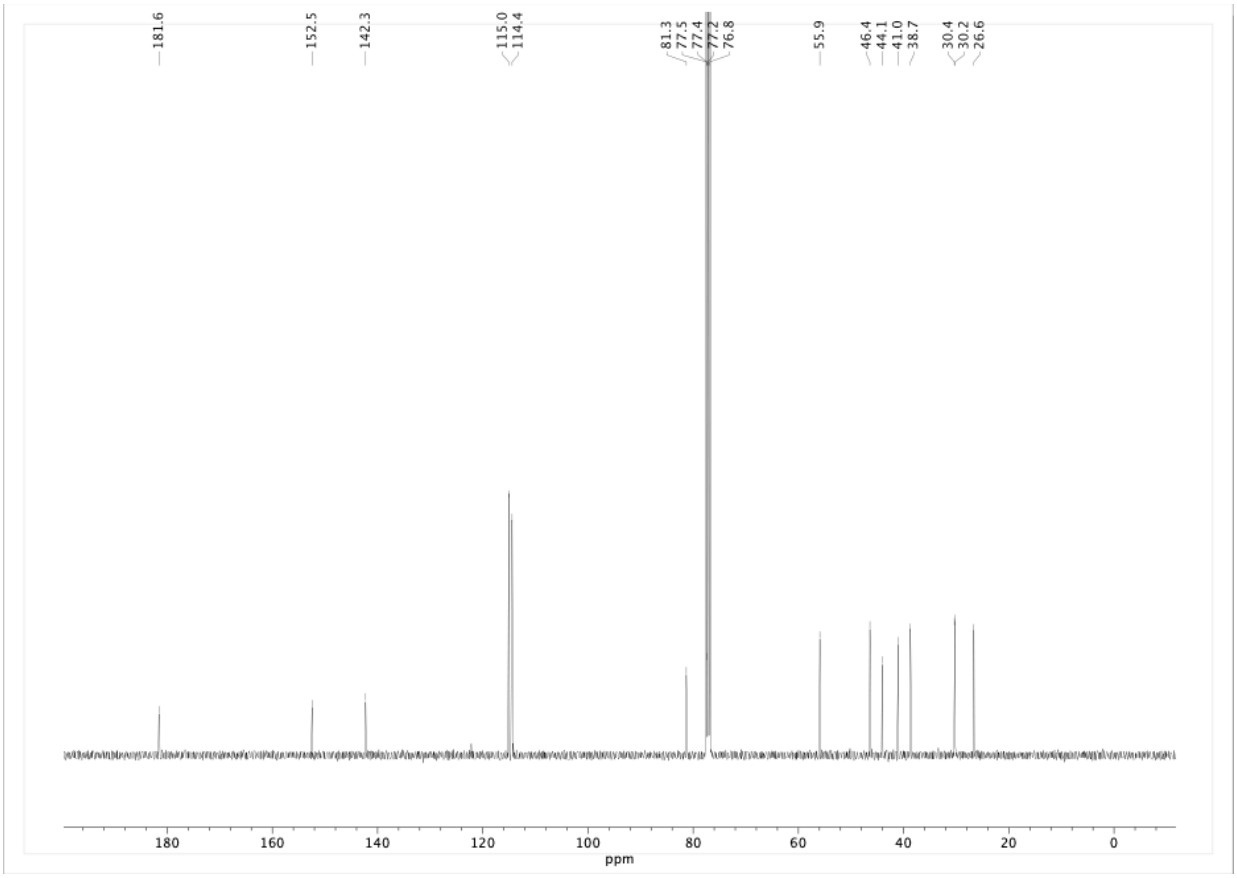

Figure A3.61. *^{13}C NMR (100 MHz, $CDCl_3$) of compound* ***66****.*

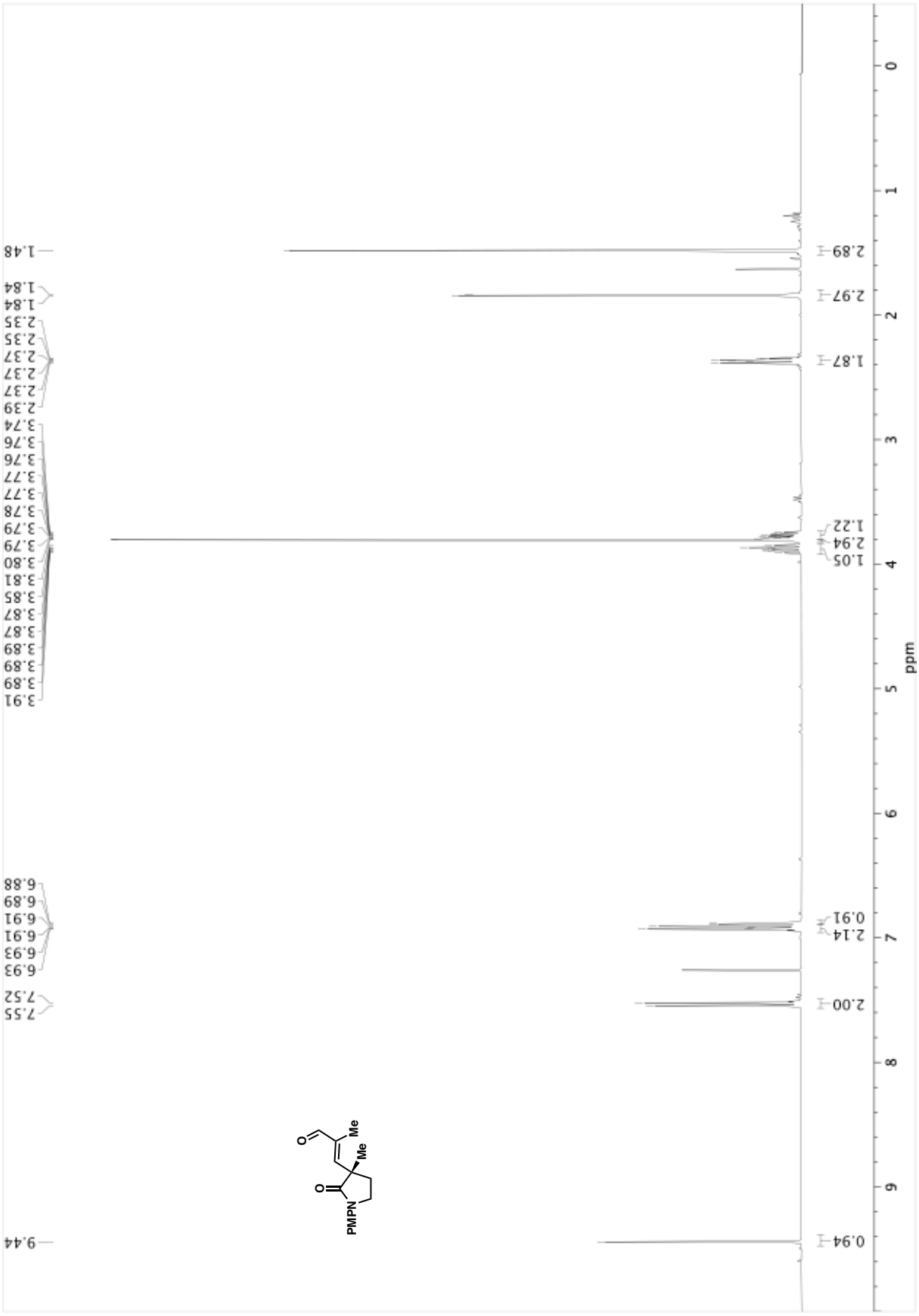

Figure A3.62. *^1H NMR (400 MHz, $CDCl_3$) of compound* ***69***.

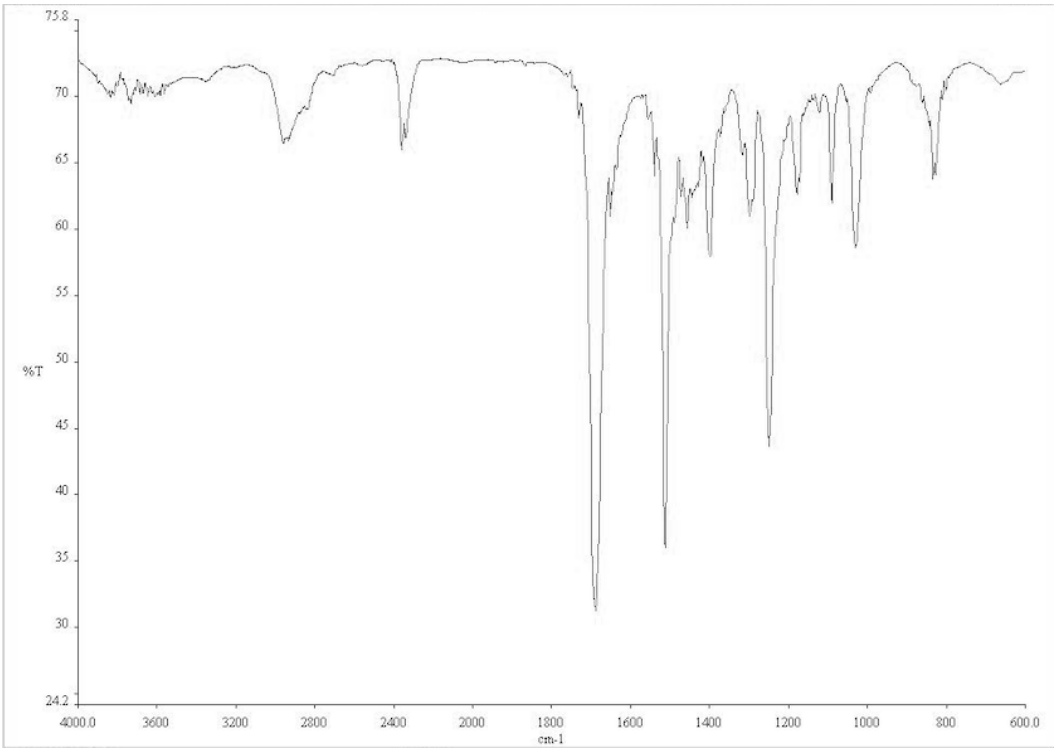

Figure A3.63. *Infrared spectrum (Thin Film, NaCl) of compound* ***69****.*

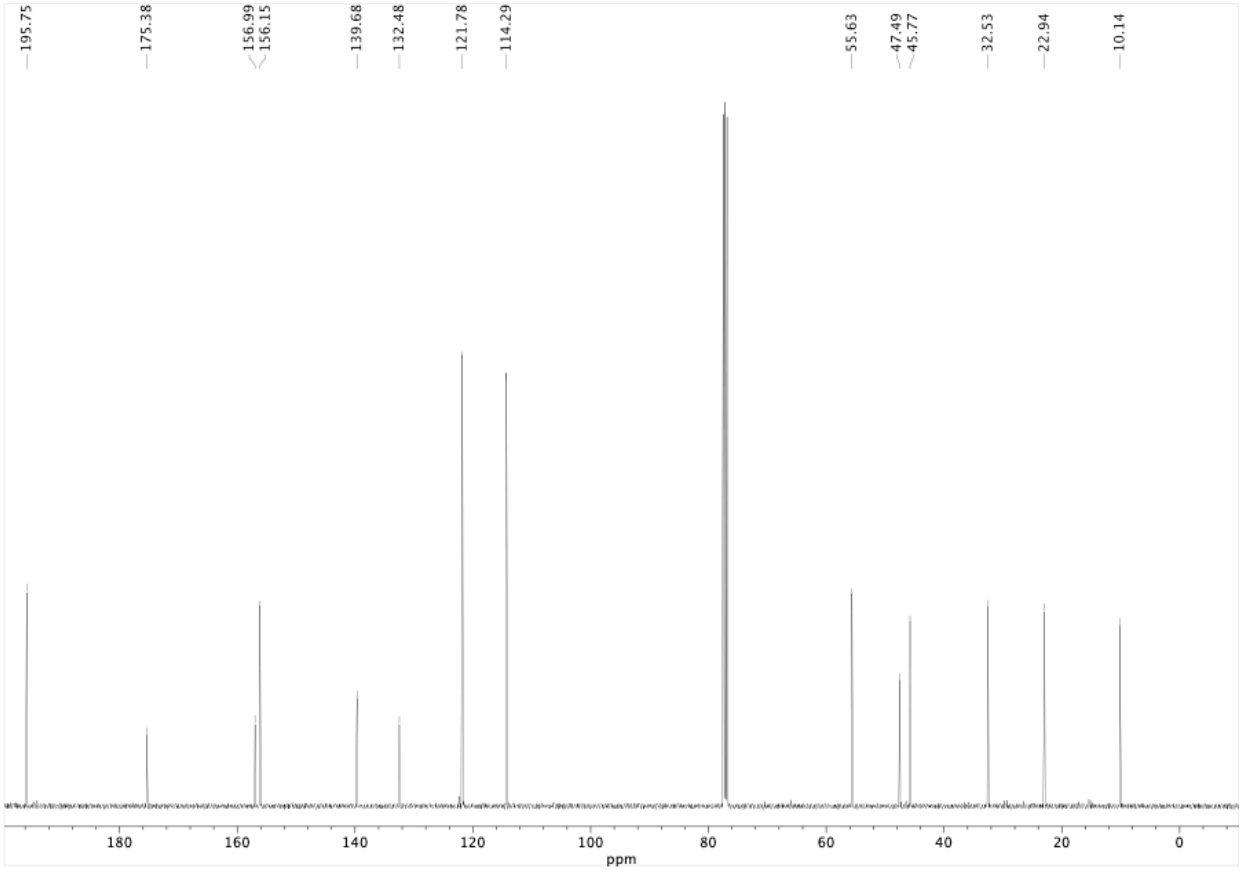

Figure A3.64. *^{13}C NMR (100 MHz, $CDCl_3$) of compound* ***69****.*

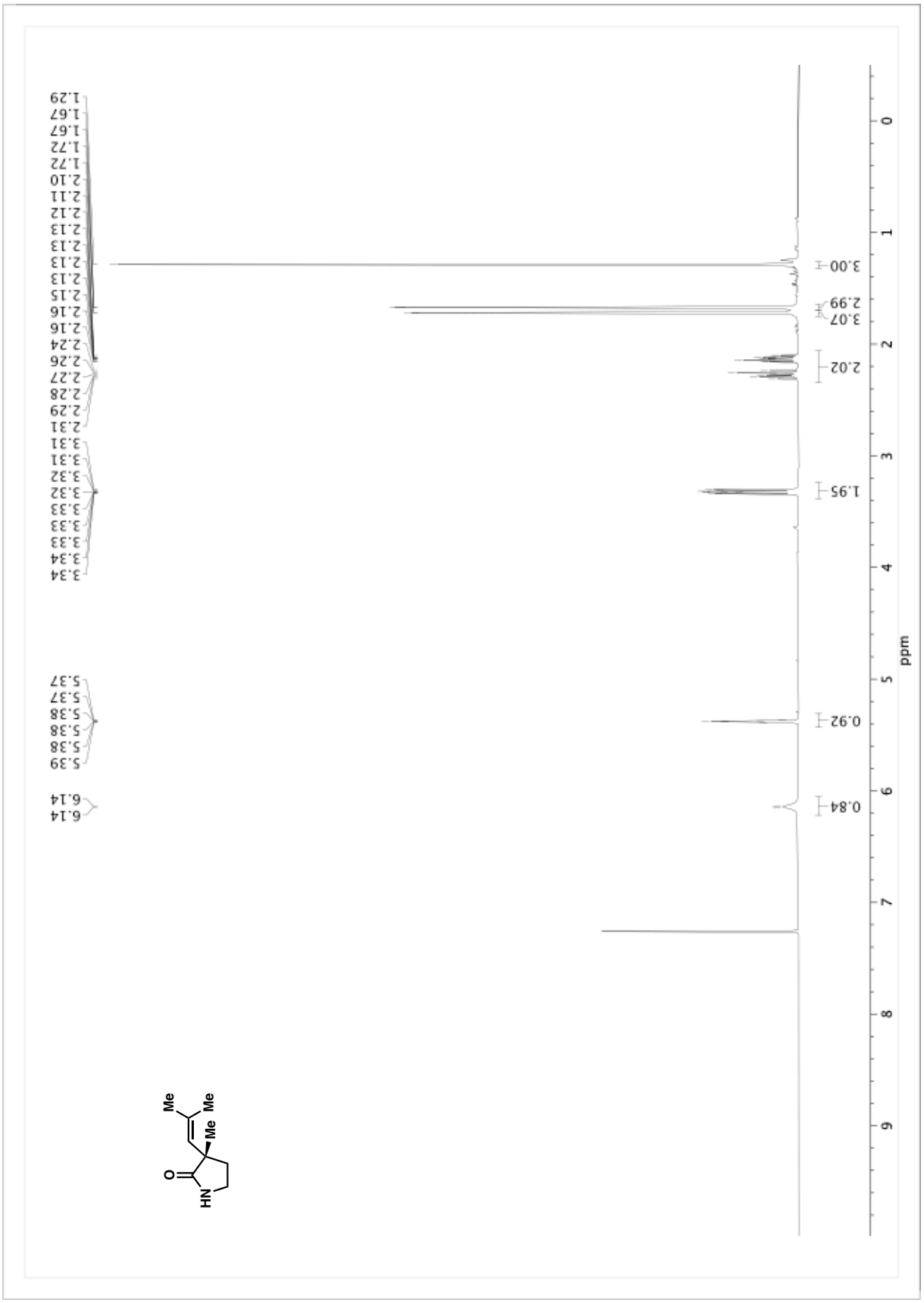

Figure A3.65. *^1H NMR (400 MHz, $CDCl_3$) of compound* ***70****.*

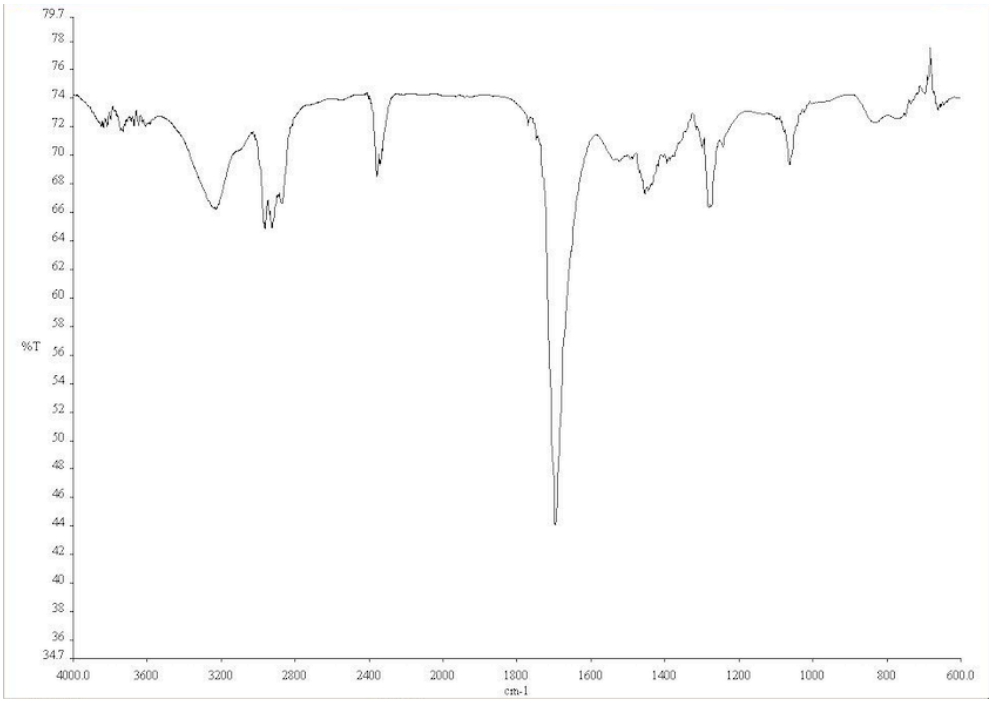

Figure A3.66. *Infrared spectrum (Thin Film, NaCl) of compound* ***70****.*

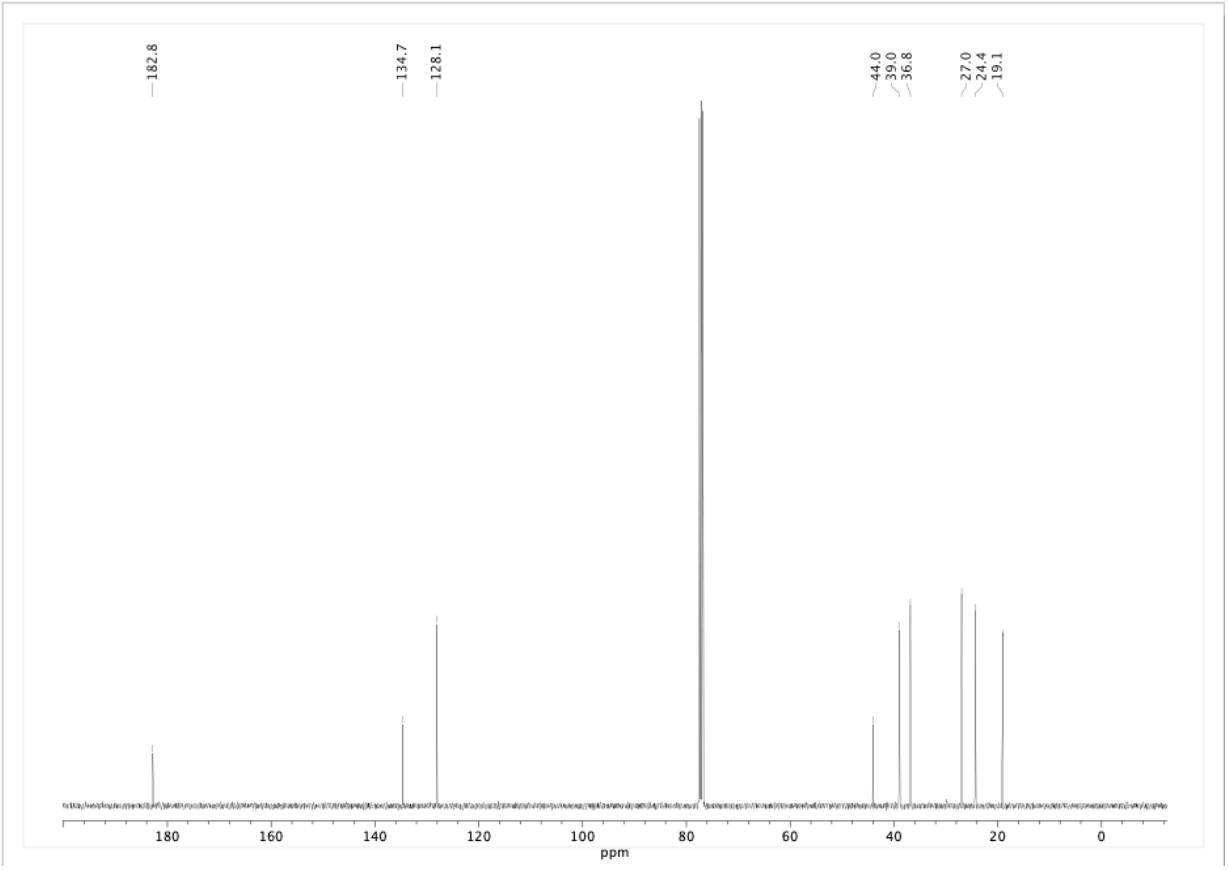

Figure A3.67. *^{13}C NMR (100 MHz, $CDCl_3$) of compound* ***70****.*

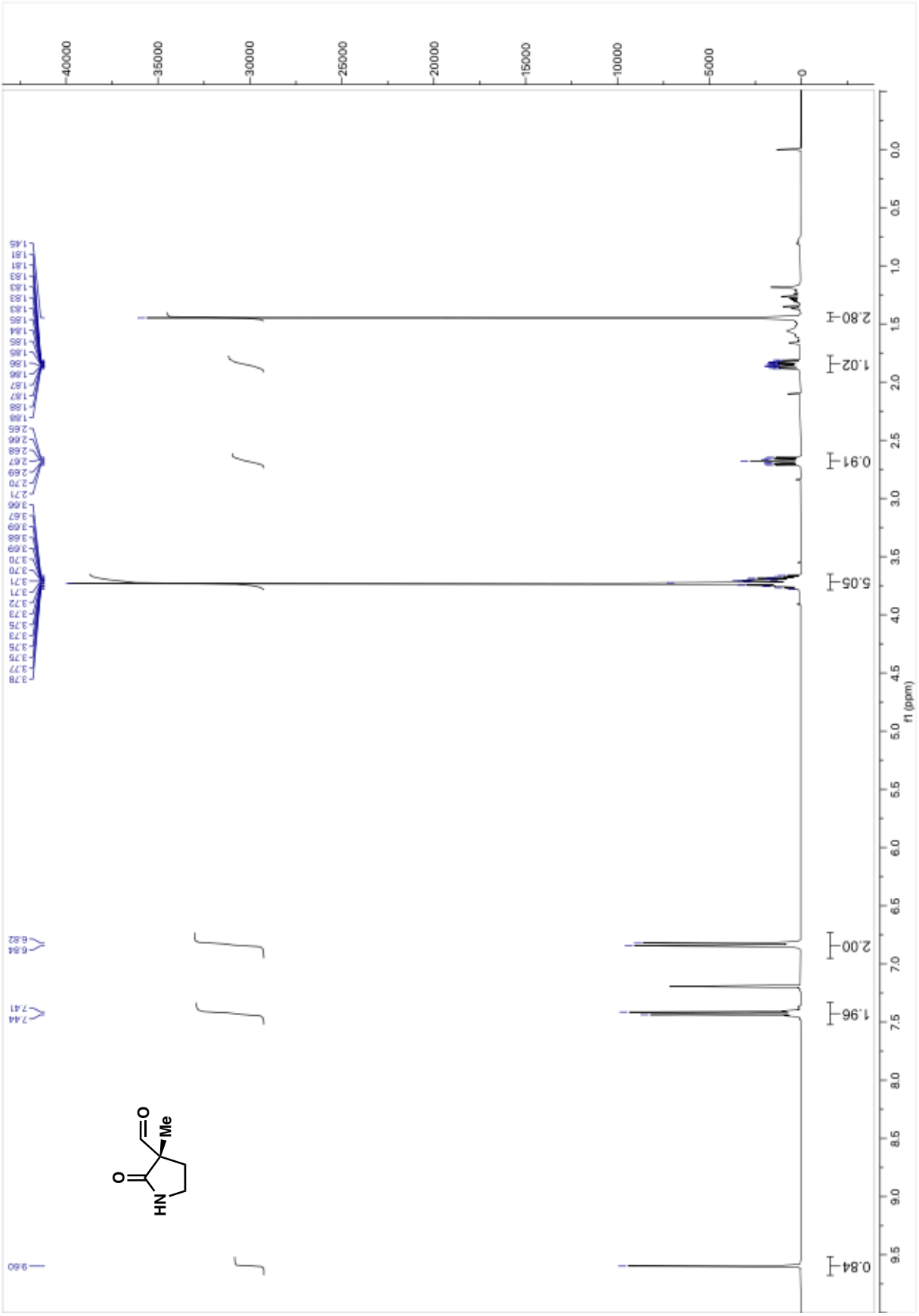

Figure A3.68. *^1H NMR (400 MHz, $CDCl_3$) of compound* ***67****.*

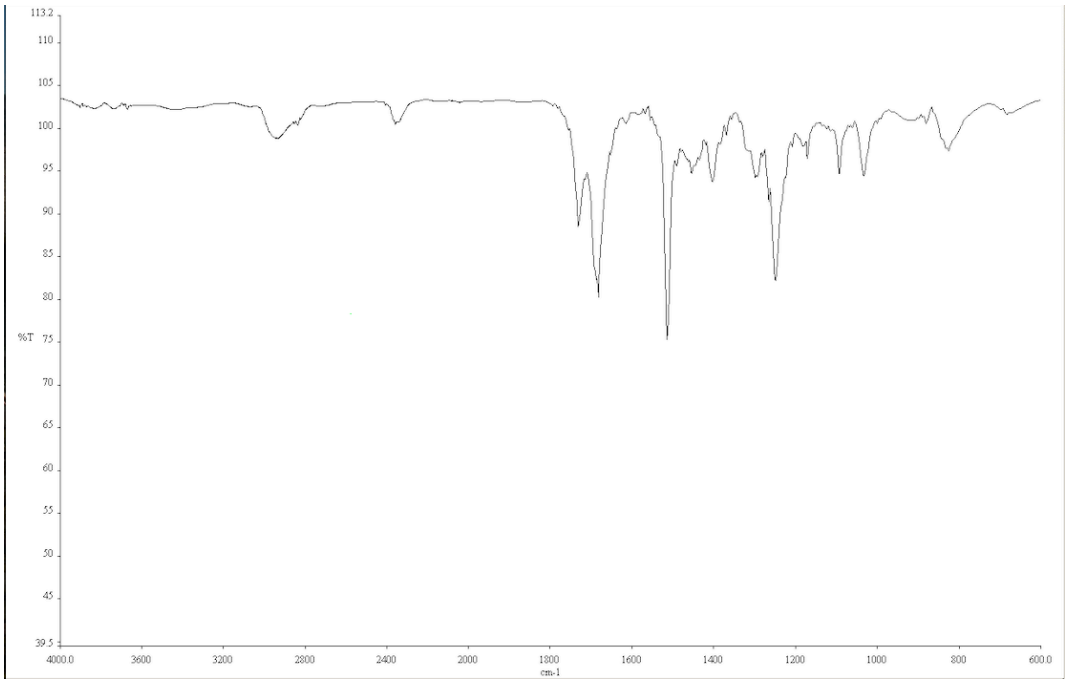

Figure A3.69. *Infrared spectrum (Thin Film, NaCl) of compound* ***67****.*

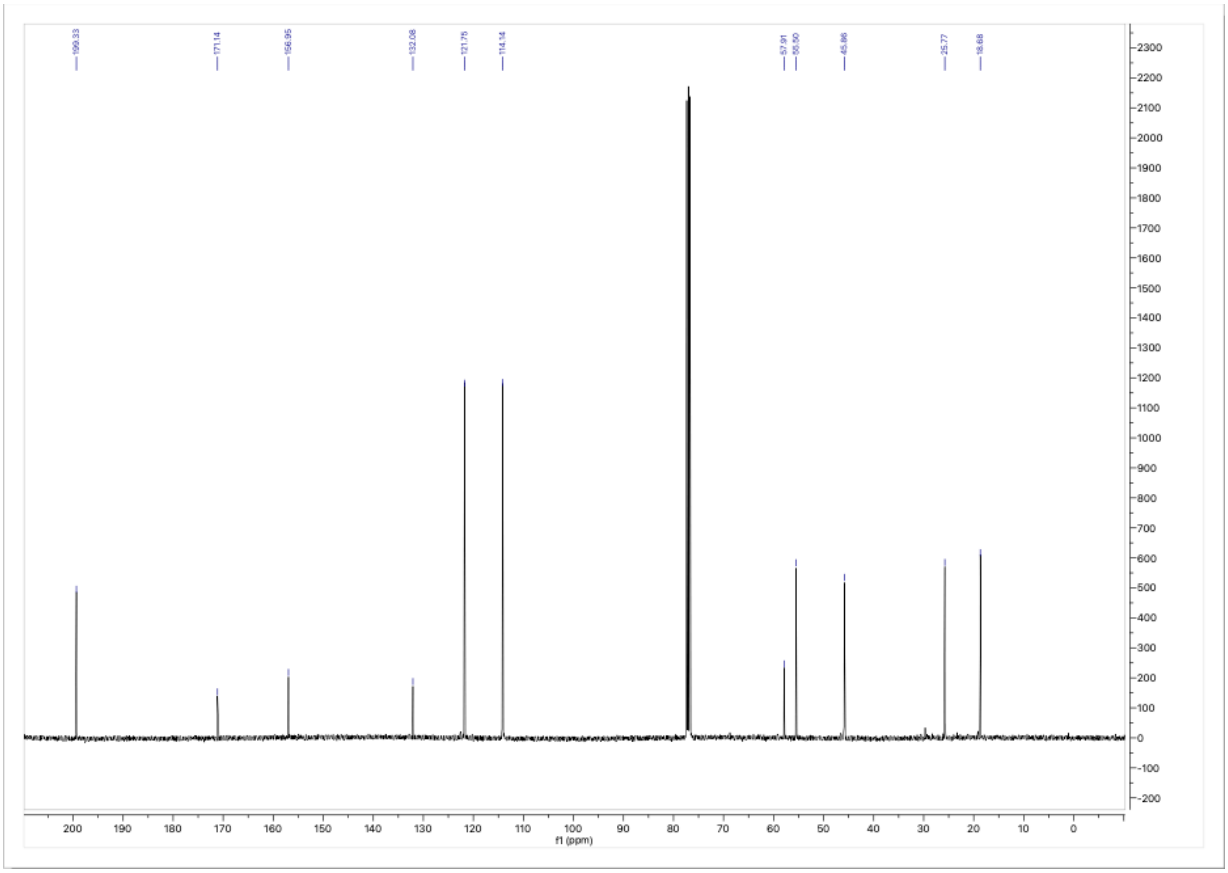

Figure A3.70. *^{13}C NMR (100 MHz, $CDCl_3$) of compound* ***67****.*

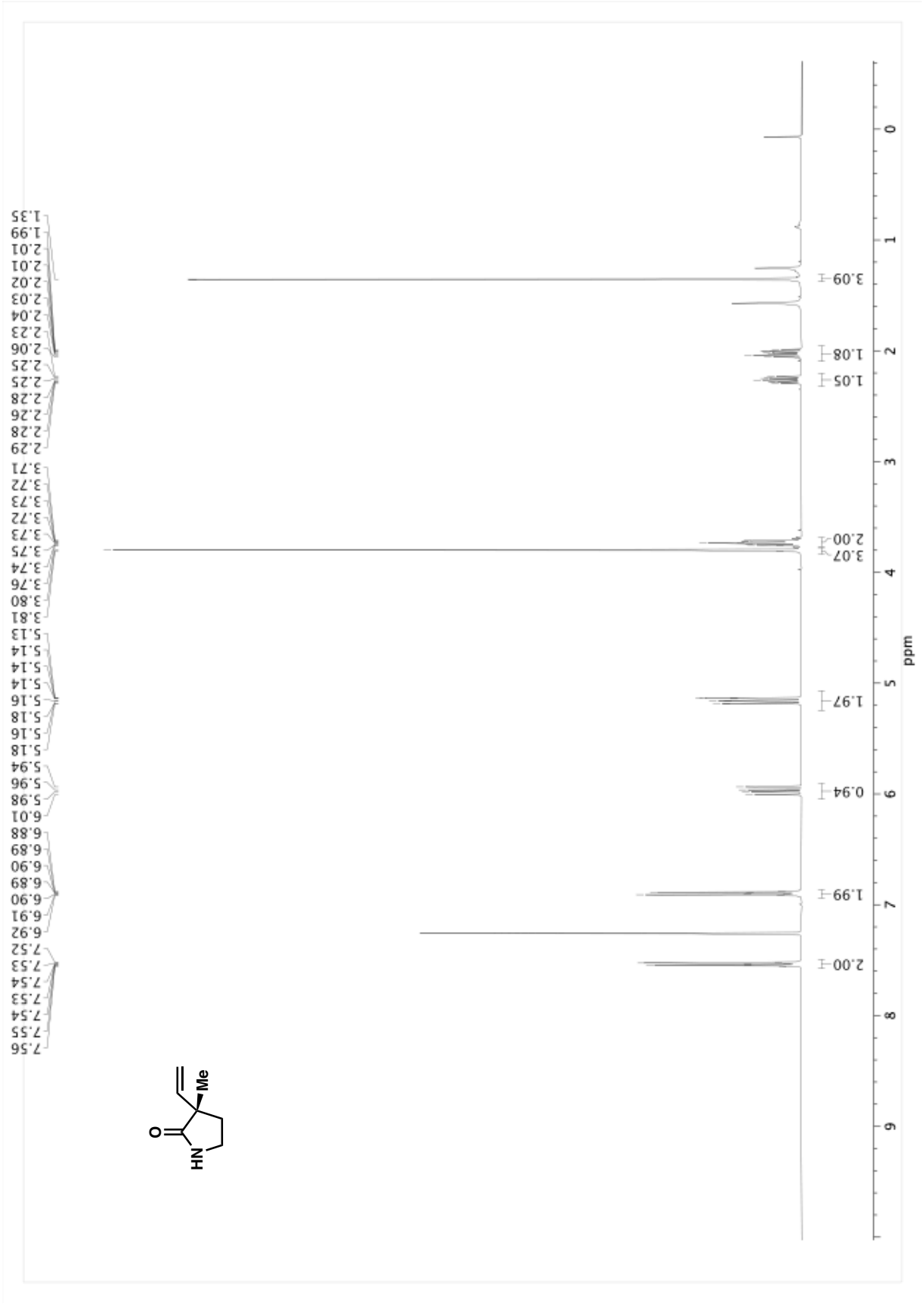

Figure A3.71. *^1H NMR (400 MHz, $CDCl_3$) of compound **68**.*

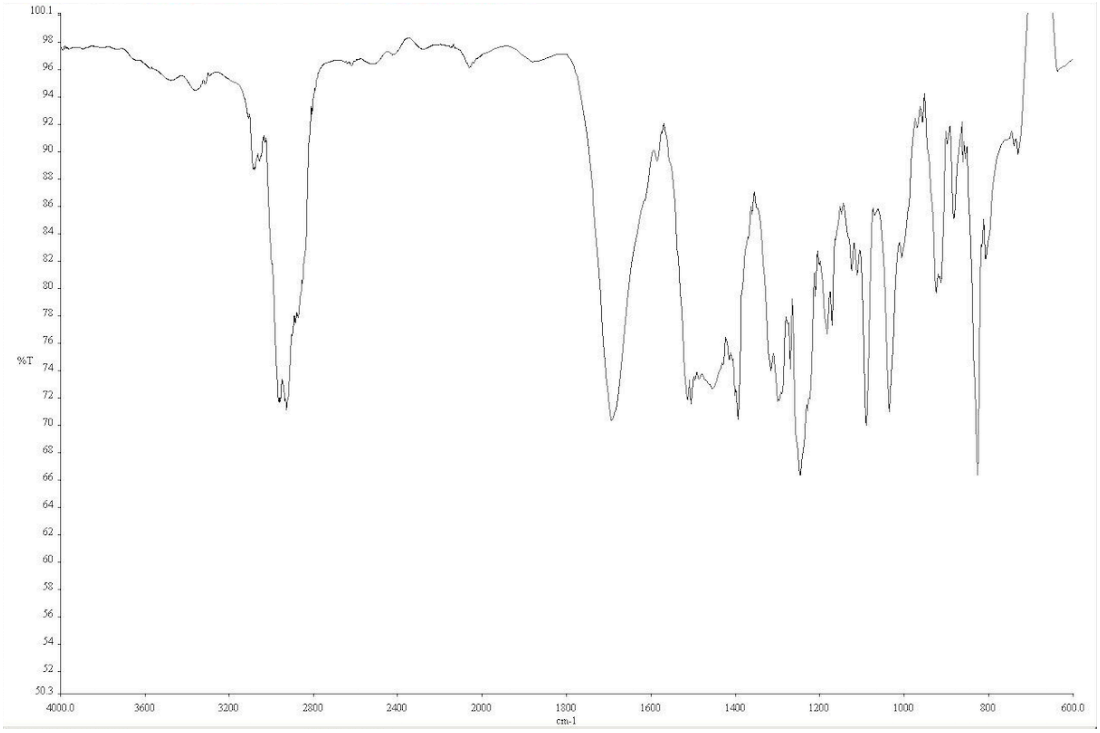

Figure A3.72. *Infrared spectrum (Thin Film, NaCl) of compound* ***68****.*

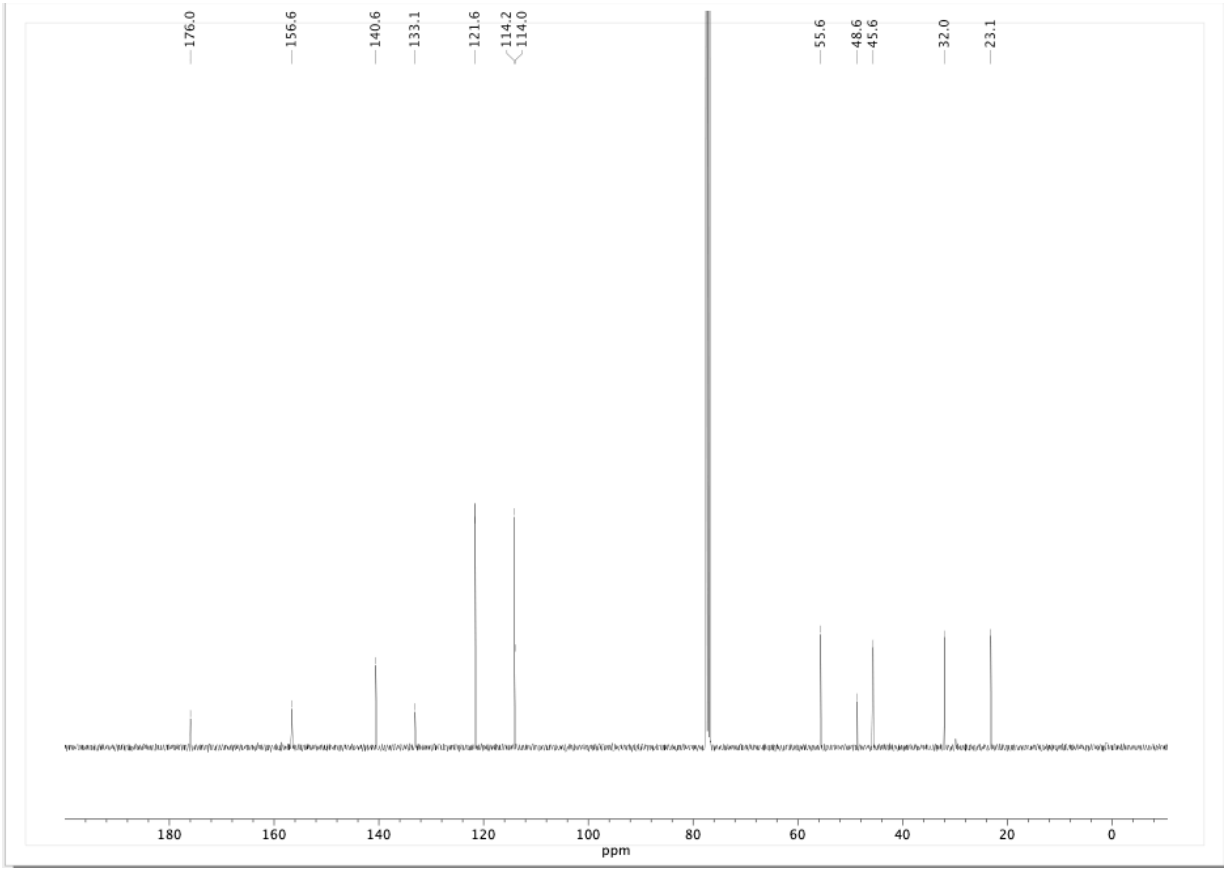

Figure A3.73. *^{13}C NMR (100 MHz, $CDCl_3$) of compound* ***68****.*

CHAPTER 4

Synthesis and X-ray Structural Characterization of C-Bound Palladium Enolate with Chiral PHOX Ligand

4.1 INTRODUCTION

Organometallic compounds have had a great impact in modern synthetic methodology and are commonly used as catalysts for the generation of small molecules, pharmaceuticals, and materials.[1] These organometallic processes also offer the opportunity to construct complex molecules efficiently and with high selectivity, which might be challenging to achieve otherwise. Thus, advancements in catalysis can improve the sustainability of reaction transformations. In fact, the application of catalysis is so ubiquitous that it is rare to find a natural product synthesis that do not incorporate organometallics in their synthetic routes.[1]

In the realm of catalytic reactions leading to new C–C bond formation, palladium-catalyzed allylic substitutions, also known as the Tsuji–Trost reaction, have been highly efficient and widely explored.[2] Many asymmetric variants of the Tsuji–Trost reaction have been developed. For example, our lab reported the Pd-catalyzed enantioconvergent decarboxylative allylic alkylation of racemic β-ketoesters in 2005 using

†This research was performed in collaboration with Alexander Q. Cusumano and Stephen R. Sardini.

phosphinooxazolines (PHOX) ligands and Tris(dibenzylideneacetone)dipalladium(0) [$Pd_2(dba)_3$] as Pd source (Scheme 4.1.1).[3]

Scheme 4.1.1 *Catalytic enantioconvergent decarboxylative allylic alkylation of α-substituted 2-carboxyallylcyclohexanones.*

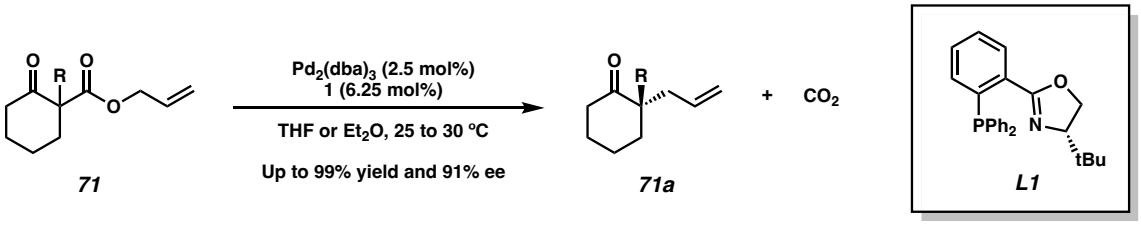

Bond formation proceeds through an inner sphere mechanism via the formation of a chiral O-bound palladium enolate derived from β-keto ester **71**.[4] However, despite our best efforts, the isolation and characterization of this fleeting intermediate remains elusive.

Previous accounts of isolated transition metal enolates are very limited. Some recent examples include a cationic Cp*Rh(III) enolate reported by Ellman and coworkers[5], and a series of palladium fluroenolate complexes were isolated and studied by Hartwig and coworkers[6]. To our best knowledge, C-bound Pd-enolate with PHOX ligands have yet been isolated or reported in literature. Herein, we report the synthesis, isolation, and single-crystal x-ray structure determination of a C-bound Pd-enolate with the *(S)-t*-BuPHOX (**L1**) ligand.

4.2 Synthesis and Characterization

The (PHOX)Pd(enolate) complex (**73**) was prepared from an in situ-generated (PHOX)Pd^0(dba) precursor ($Pd_2(dba)_3$ and *(S)-t*-BuPHOX in benzene at 25 ºC). Subjecting 2-bromoacetophenone **72** to this mixture generates the C-bound Pd- enolate complex via oxidative addition (Scheme 4.2.1). The resulting Pd-enolate solution was filtered through a plug of Celite and solvent was then removed in vacuo. The crude mixture was purified by trituration (hexanes, then 1:1 hexanes:diethyl ether) to remove remaining dba. This yields **73** as a yellow solid. Single crystals suitable for X-ray diffraction were grown via vapor diffusion using THF as the non-volatile solvent.

Scheme 4.2.1 *Synthesis of chiral ((S)-t-BuPHOX)Pd(enolate) complex 73.*

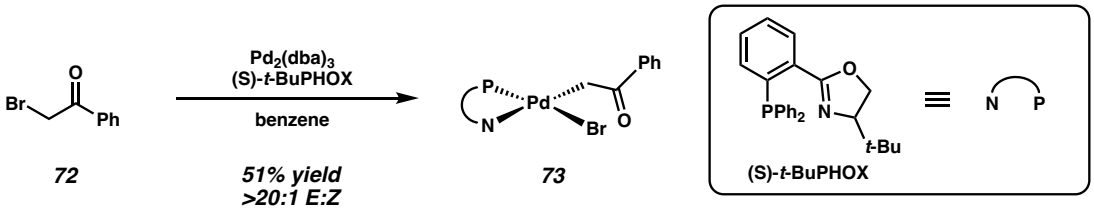

Complex **73** was characterized by NMR spectroscopy, and the connectivity was confirmed by single-crystal X-ray diffraction (Figure 4.2.2). In accord with the *trans* effect, **73** is formed as a single isomer with the strong σ-donating enolate *trans* to nitrogen rather than the better σ-donating phosphorus. The steric environment of the ligand sphere may also contribute to this selectivity.[7]

Figure 4.2.2 *ORTEP diagram of ((S)-t-BuPHOX)Pd(enolate) complex 73. Selected bond lengths: a) Pd1–P1, 2.211 Å; b) Pd1–N1, 2.120 Å; c) Pd1–C41, 2.096 Å; d)*

Pd1–Br1, 2.495 Å. Solvents of crystallization and hydrogen atoms are omitted for clarity.

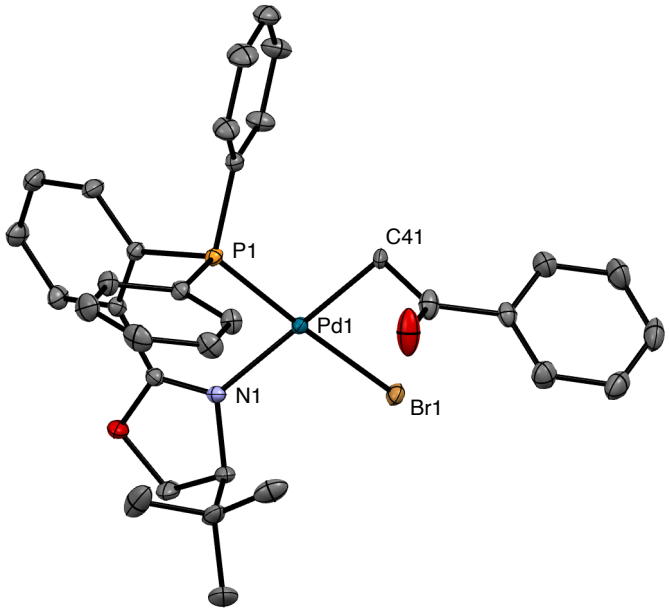

In conclusion, we report the first synthesis and characterization of an isolated (PHOX)Pd enolate complex (**73**). Due to the important role of Pd enolates in asymmetric catalysis, the isolation of this novel complex offers valuable insights into its structural intricacies and inherent properties. Such insights are crucial for unraveling its reactivity and potential applications, paving the way for the exploration of new asymmetric catalytic reactions involving this class of complexes in future research endeavors.

4.3 SUPPORTING INFORMATION

4.3.1 MATERIALS AND METHODS

Unless otherwise stated, reactions were performed in flame-dried glassware under a nitrogen atmosphere using dry, deoxygenated solvents. Solvents were dried by passage through an activated alumina column under argon. Reaction progress was monitored by thin-layer chromatography (TLC). TLC was performed using E. Merck silica gel 60 F254 precoated glass plates (0.25 mm) and visualized by UV fluorescence quenching, p-anisaldehyde, or $KMnO_4$ staining. Silicycle SiliaFlash® P60 Academic Silica gel (particle size 40–63 μm) was used for flash chromatography. 1H NMR spectra were recorded on Varian Inova 500 MHz and 600 MHz and Bruker 400 MHz spectrometers and are reported relative to residual CHCl3 (δ 7.26 ppm), C6D6 (δ 7.16 ppm) or CD3OD (δ 3.31 ppm). 13C NMR spectra were recorded on a Varian Inova 500 MHz spectrometer (125 MHz) and Bruker 400 MHz spectrometers (100 MHz) and are reported relative to CHCl3 (δ 77.16 ppm), C6D6 (δ 128.06 ppm) or CD3OD (δ 49.01 ppm). Data for 1H NMR are reported as follows: chemical shift (δ ppm) (multiplicity, coupling constant (Hz), integration). Multiplicities are reported as follows: s = singlet, d = doublet, t = triplet, q = quartet, p = pentet, sept = septuplet, m = multiplet, br s = broad singlet, br d = broad doublet. Data for 13C NMR are reported in terms of chemical shifts (δ ppm). IR spectra were obtained by use of a Perkin Elmer Spectrum BXII spectrometer or Nicolet 6700 FTIR spectrometer using thin films deposited on NaCl plates and reported in frequency of absorption (cm^{-1}). Optical rotations were measured with a Jasco P-2000 polarimeter operating on the sodium

D-line (589 nm), using a 100 mm path-length cell. High resolution mass spectra (HRMS) were obtained from the Caltech Mass Spectral Facility using a JEOL JMS-600H High Resolution Mass Spectrometer in fast atom bombardment (FAB+) or electron ionization (EI+) mode, or using an Agilent 6200 Series TOF with an Agilent G1978A Multimode source in electrospray ionization (ESI+), atmospheric pressure chemical ionization (APCI+), or mixed ionization mode (MM: ESI-APCI+).

List of Abbreviations:

TLC – thin-layer chromatography, Dr – dram**,** LCMS – liquid chromatography/mass spectrometry, NMR – nuclear magnetic resonance, THF – tetrahydrofuran.

4.3.2 EXPEPRIMENTAL PROCEDURES AND SPECTROSCOPIC DATA

Experimental Procedures

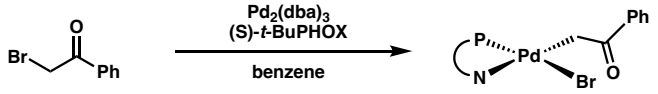

72 *73*

Enolate 9: To a one-dram vial with stir bar, $Pd_2(dba)_3$ (150 mg, 0.16 mmol, 0.5 equiv) and (*S*)-*t*-BuPHOX (140 mg, 0.36 mmol, 1.05 equiv) was charged in benzene (3.24 mL, 0.1M) in the glovebox. The mixture was stirred at rt for 20 minutes and added bromo-acetophenone **72** (64.5 mg, 0.32 mmol, 1.0 equiv) and stirred for another 10 minutes. The resulting Pd-enolate was purified by celite filtration to remove any excess Pd black. The filtrate was concentrated under vacuum in the glovebox, and the resulting solid is triturated with hexane x 3 and hexanes:diethyl ether (1:1) mixture x 3 to remove excess dba to afford enolate **73** (110 mg, 51% yield) as a powdery yellow solid; ^{1}H NMR (400 MHz, C6D6) δ 9.17 – 8.62 (m, 1H), 7.74 (ddd, J = 7.9, 3.8, 1.4 Hz, 1H), 7.55 (dtd, J = 11.7, 4.9, 2.4 Hz, 1H), 7.36 – 7.24 (m, 1H), 7.07 – 7.00 (m, 2H), 7.00 – 6.95 (m, 2H), 6.85 (tt, J = 7.6, 1.4 Hz, 1H), 6.80 (ddd, J = 9.6, 7.8, 1.3 Hz, 1H), 6.64 (tt, J = 7.6, 1.3 Hz, 1H), 5.64 (dd, J = 10.1, 4.4 Hz, 1H), 5.20 (dd, J = 6.0, 1.2 Hz, 1H), 3.72 (dd, J = 9.1, 4.4 Hz, 1H), 3.60 (dd, J = 10.1, 9.1 Hz, 1H), 2.55 (dd, J = 7.8, 5.9 Hz, 1H), 0.50 (s, 5H); ^{13}C NMR (101 MHz, C6D6) δ 204.09, 142.72, 140.39, 135.31 (d, J = 31.9 Hz), 134.72 (d, J = 11.0 Hz), 134.31

(d, J = 12.0 Hz), 132.37 (d, J = 7.7 Hz), 132.22, 131.42, 130.98 (d, J = 7.8 Hz), 130.25, 129.11 – 128.95 (m), 128.61, 126.21, 75.50, 69.82, 34.48, 25.96, 23.12. IR (thin film, NaCl) 3424, 3447, 2098, 1636, 683 cm^{-1}; HRMS (ESI) m/z calc'd (Note: HRMS indicated a strong signal for –Br ion) $C_{33}H_{33}NO_2PPd$ $[M–Br]^-$: 612.13, found: XX; $[\alpha]_D^{25}$ – 332.0880 ° (*c* 0.20, $CHCl_3$).

4.4 REFERENCES AND NOTES

[1] Cadierno, V. Recent Advances in Organometallic Chemistry and Catalysis. *Catalysts* **2021**, *11*, 646.

[2] Pàmies, O.; Margalef, J.; Cañellas, S.; James, J.; Judge, E.; Guiry, P. J.; Moberg, C.; Bäckvall, J.-E.; Pfaltz, A.; Pericàs, M. A.; Diéguez, M. Recent Advances in Enantioselective Pd-Catalyzed Allylic Substitution: From Design to Applications. *Chem. Rev.* **2021**, *121*, 4373–4505.

[3] Mohr, J. T.; Behenna, D. C.; Harned, A. M.; Stoltz, B. M. Deracemization of Quaternary Stereocenters by Pd-Catalyzed Enantioconvergent Decarboxylative Allylation of Racemic β-Ketoesters. *Angewandte Chemie International Edition* **2005**, *44*, 6924–6927.

[4] Cusumano, A. Q.; Stoltz, B. M.; Goddard, W. A. I. Reaction Mechanism, Origins of Enantioselectivity, and Reactivity Trends in Asymmetric Allylic Alkylation: A Comprehensive Quantum Mechanics Investigation of a C(Sp3)–C(Sp3) Cross-Coupling. *J. Am. Chem. Soc.* **2020**, *142*, 13917–13933.

[5] Boerth, J. A.; Ellman, J. A. Rh(III)-Catalyzed Diastereoselective C–H Bond Addition/Cyclization Cascade of Enone Tethered Aldehydes. *Chem. Sci.* **2016**, *7*, 1474–1479.

[6] Arlow, S. I.; Hartwig, J. F. Synthesis, Characterization, and Reactivity of Palladium Fluoroenolate Complexes. *J. Am. Chem. Soc.* **2017**, *139*, 16088–16091.

[7] Armstrong, P. B.; Dembicer, E. A.; DesBois, A. J.; Fitzgerald, J. T.; Gehrmann, J. K.; Nelson, N. C.; Noble, A. L.; Bunt, R. C. Investigation of the Electronic Origin of Asymmetric Induction in Palladium-Catalyzed Allylic Substitutions with Phosphinooxazoline (PHOX) Ligands by Hammett and Swain–Lupton Analysis of the 13C NMR Chemical Shifts of the (π-Allyl) Palladium Intermediates. *Organometallics* **2012**, *31*, 6933–6946.

APPENDIX 4

Spectra Relevant to Chapter 4:

Synthesis and X-ray Structural Characterization of C-Bound Palladium Enolate with Chiral PHOX Ligand

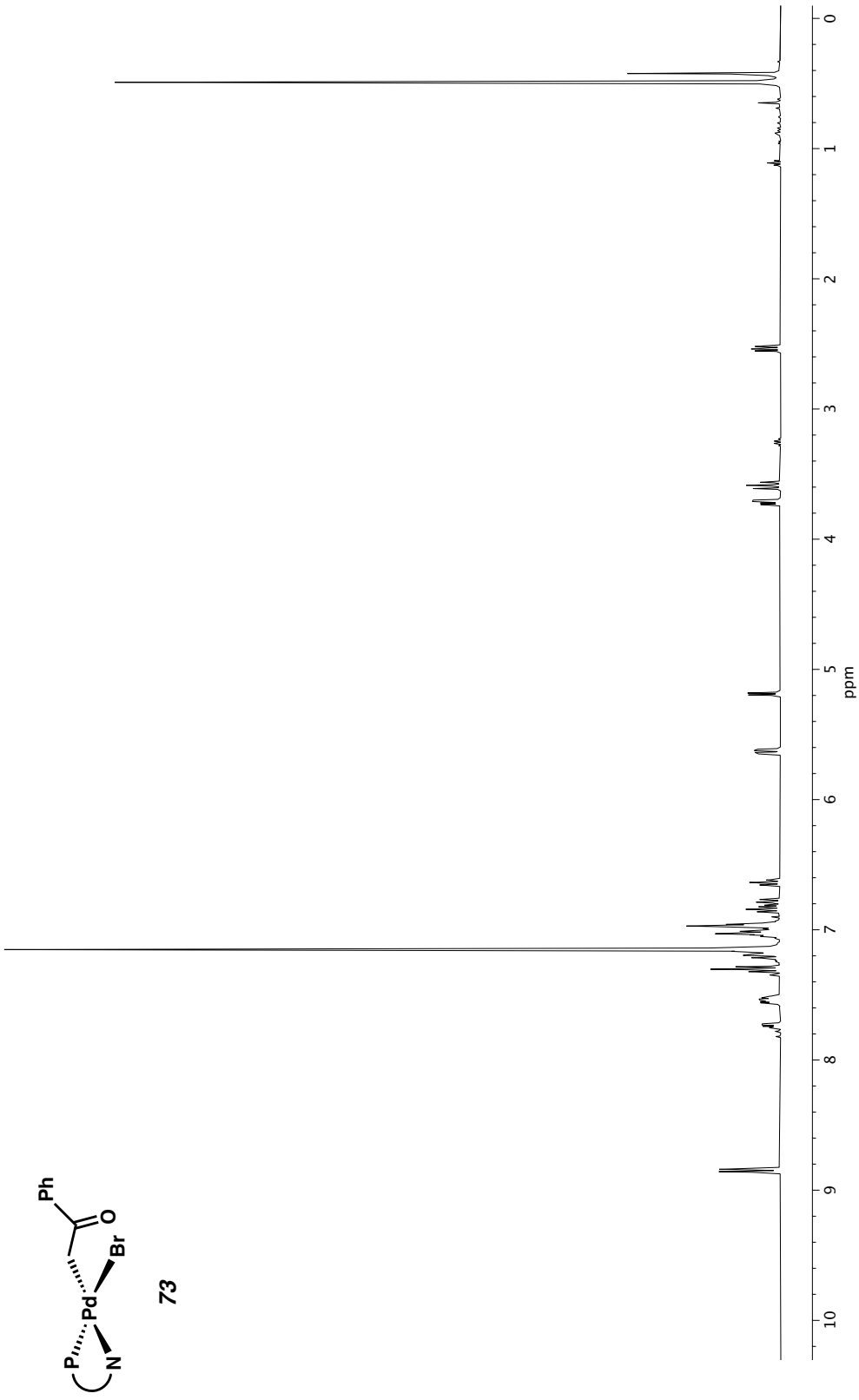

73

Figure A4.1. *^1H NMR (400 MHz, $CDCl_3$) of compound **73**.*

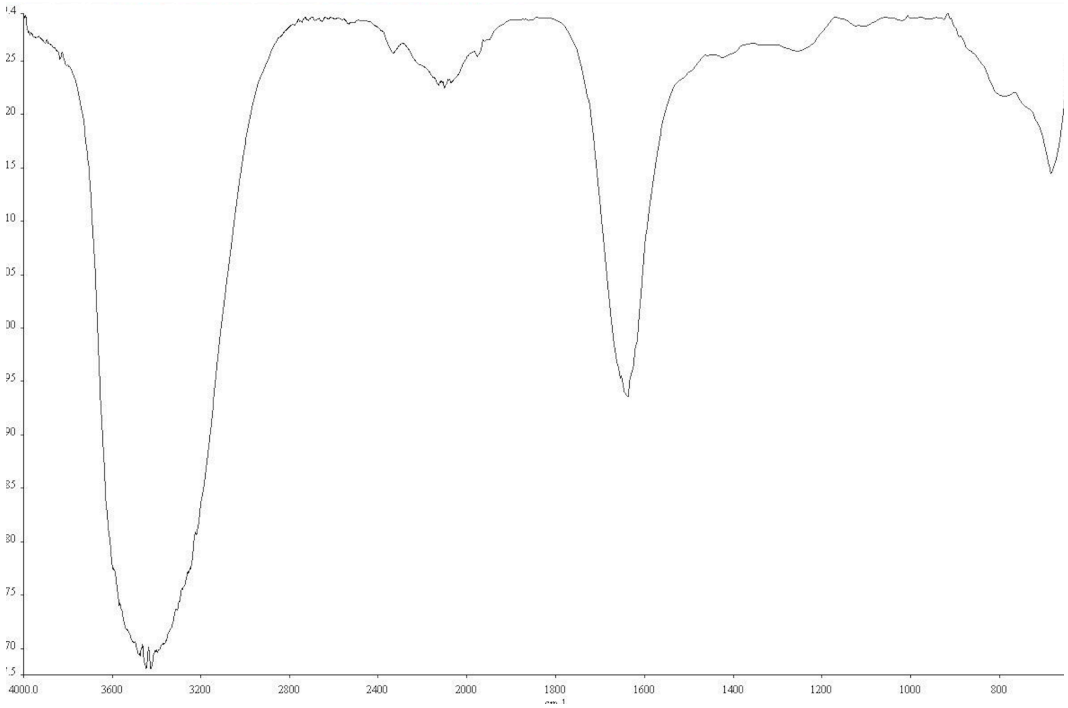

Figure A4.2. *Infrared spectrum (Thin Film, NaCl) of compound* ***32***.

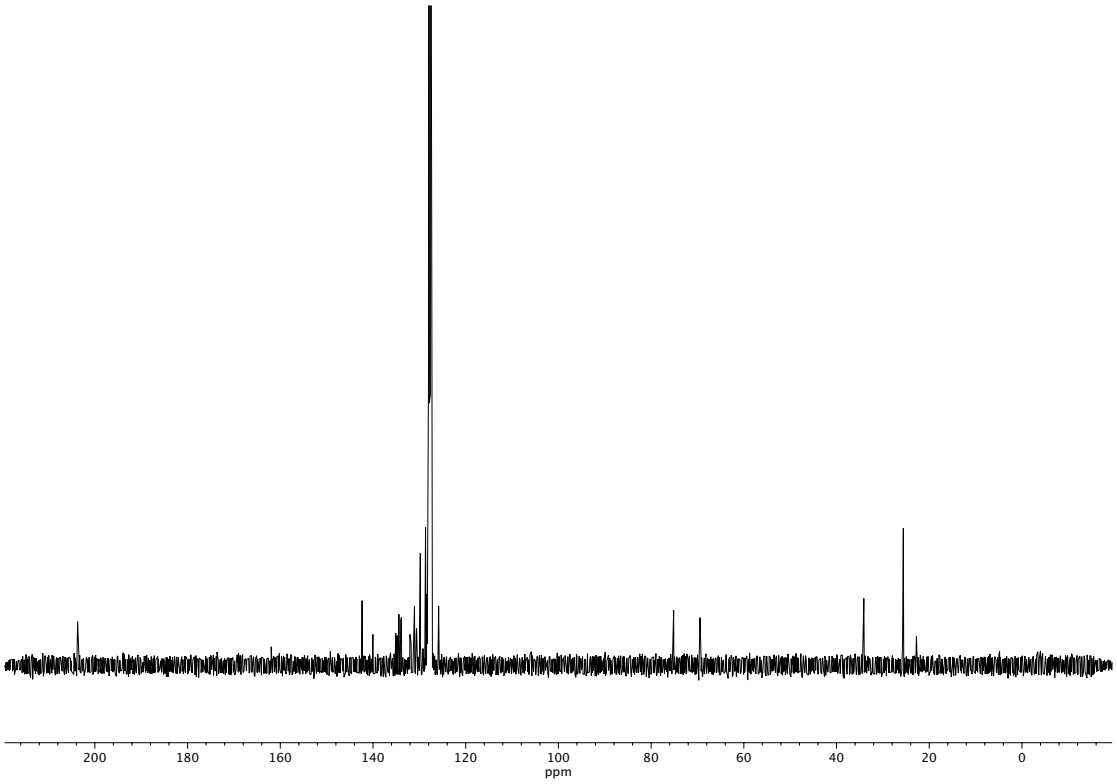

Figure A4.3. *^{13}C NMR (100 MHz, $CDCl_3$) of compound* ***32***.

CHAPTER 5

Unity in Diversity: Day of Inclusion[†]

5.1 INTRODUCTION

The landscape of academia has undergone significant transformation in recent years, largely propelled by the concerted efforts toward Diversity, Equity, and Inclusion (DEI). Across various disciplines, including chemistry, the demand for fostering diversity has become increasingly evident, with numerous cases illustrating its profound impact on academic advancement. Within this evolving framework, publications within the chemistry community have emerged as powerful advocates for diversity, articulating the need for proactive initiatives to drive meaningful change. For instance, in 2020, Professors Reisman, Sarpong, Sigman, and Yoon collaborated on an editorial piece advocating for transformative shifts within the chemical sciences field. Their publication called for the cultivation of a more diverse, equitable, and inclusive culture, while condemning longstanding exclusionary practices that have pervaded the discipline.1

Within the CCE division at Caltech, we place particular emphasis on the critical role of DEI within laboratory settings. Recognizing DEI as fundamental components, we aim to cultivate an environment that fosters inclusivity and collaboration among all individuals. By prioritizing DEI, our division aims to establish a culture where every

†This research was performed in collaboration with Jacob Parres-Gold,† Camila A. Suarez,† Marva Tariq,† Kevin J. Gonzalez,† Juliet A. Lee,† Noor Naji,† Omar S. Reyes,† Douglas C. Rees, Lindsey Malcom-Piqueux, Meagan Heirwegh, Brian M. Stoltz.

student, irrespective of background, feels valued, respected, and supported. This commitment is especially crucial for underrepresented minorities (URMs), who often encounter unique challenges stemming from systemic inequities.

The Diversity in Chemistry Initiative (DICI) within the CCE division is dedicated to supporting students who identify as URMs by providing a community support network. Additionally, DICI serves as an advocate for diversity in STEM fields and the URM experience, organizes outreach programs to enhance diversity in science both at Caltech and beyond, and highlights the achievements of URMs through seminars featuring exceptional speakers from across the country. Through years of involvement in DEI-related efforts, the DICI executive board has recognized the scattered nature of DEI participation within the CCE division. This realization underscores the need for division-wide unity regarding the significance of DEI and the specific initiatives to pursue. In response, DICI has taken the initiative to host the inaugural Day of Inclusion event for CCE, aiming to foster cohesion and collective action toward advancing DEI goals.

Organizing such a large-scale event with numerous new and unfamiliar components presented its challenges, yet our team was driven by passion and supported by a strong network. We were fortunate to secure funding from the CCE DEI committee and the Caltech Center for Inclusion and Diversity (CCID), along with additional contributions from the CCE Division's Office and Women in Chemistry (WiC), another DEI-focused student organization within CCE.

In selecting keynote speakers, our aim was to feature URM professors of chemistry who could share their unique experiences within academia, including the challenges they've faced and the solutions they've implemented. We sought to facilitate an open

dialogue where they could candidly discuss their personal struggles and their efforts to promote diversity, offering valuable insights that have shaped their careers. With this criterion in mind, we extended invitations to faculty members who not only excelled in their fields but also represented diverse backgrounds. We were privileged to have Professor Sarpong from UC Berkeley and Professor Isaacs from the College of the Holy Cross graciously accept our invitation to join us as keynote speakers.

Professor Sarpong, born in Ghana in 1974, was deeply influenced by his father's work with the World Health Organization in distributing the drug ivermectin to combat river blindness, which he described in his TEDxBerkeley talk in 2015.2 This early exposure sparked his interest in chemistry. Sarpong's research focuses on synthesizing bioactive organic molecules, particularly natural products with therapeutic potential.3 He is committed to improving diversity in the chemistry community and has received numerous awards for his research and teaching, including a Guggenheim Fellowship in 2017. Sarpong considers the achievements of his students as his greatest professional accomplishment.

Professor Isaacs, born in Kingston, Jamaica in 1981, utilizes the social media platform, TikTok, with a significant following, for educational and advocacy purposes, shedding light on organic chemistry and discussing the chemistry behind pharmaceuticals affecting marginalized communities.4 As a Black, queer chemist, Isaacs advocates for diversity in STEM and academia, actively supporting minority students in his lab group. He emphasizes the importance of embracing mistakes and finding a supportive community to thrive in STEM.

An additional vital aspect of the event is our collaboration with various partners for the workshops, including the CCID, the Center for Teaching, Learning, and Outreach (CTLO), Student-Faculty Programs (SFP), the Equity and Title IX (Title IX) Office, Caltech Accessibility Services for Students (CASS), and a fellow graduate student in CCE, Kim Pham, who led an inclusive teaching workshop.

5.2 IMPLEMENTATION

After we confirmed the participation of our keynote speakers, we proceeded to finalize the event schedule, crucial for securing space reservations. The schedule was structured to commence at 1 PM with a general seminar featuring opening remarks, followed by presentations from our esteemed speakers (Figure 1). This was succeeded by a panel discussion moderated by Lindsey Malcom–Piqueux, the assistant vice president for Diversity, Equity, Inclusion, and Assessment at Caltech. The panel, predominantly comprised of pre-prepared questions by Lindsey, allowed for audience interaction toward the end of the allotted time. Following the general session, the day transitioned into nine workshop sessions, including an exclusive session tailored for faculty and staff members. Each workshop was offered twice (session A and session B) to enable attendees to freely select two workshops of interest without scheduling conflicts.

Figure 5.2.1. *Finalized schedule of the Day of Inclusion event hosted on January 19, 2024.*

Day of Inclusion 2023-24	
Date 1/19/24	
Time	Event
1:00 PM	Opening Announcements
1:20 PM	Keynote Presentation
1:50 PM	Keynote Presentation 2
2:20 PM	Guided Panel with Keynote Speakers
3:00 PM	Workshop Session A
4:00 PM	Workshop Session B
5:00 PM	Closing Remarks: Dinner Social & Raffle Prizes

The workshops offered include Actionable Allyship and Unconscious Bias, hosted by the CCID office; Decoding Title IX: How Title IX Can Help You Thrive and Promoting Lab Cohesion, hosted by the Title IX office; Inclusive Teaching (for graduate students), hosted by Kim Pham; Inclusive Teaching (exclusive to faculty and staff members) hosted by the CTLO office; Balance Activism with Research and Imposter Syndrome, hosted by the SFP office; and Introduction to Neurodiversity and Universal Design, hosted by the CASS office. Furthermore, the workshops were categorized by size. The larger workshops, such as Actionable Allyship and Decoding Title IX, focus on providing educational and informational content. They are designed to accommodate a larger number of participants to ensure that everyone can attend a workshop during each session. In contrast, the small workshops are geared toward fostering interactive, hands-on participation, encouraging active engagement from attendees.

In the initial stages of planning this event, our foremost task was to secure sources of funding. Unlike other DEI-focused student organizations, DICI lacked an endowment or consistent funding stream. However, we had previously received support from the DEI

committee in CCE for smaller, routine events. For an event of this magnitude, we estimated our total expenses to be between 10 to 12k, including significant costs such as travel and accommodation for keynote speakers, room reservation at the Beckman Auditorium at Caltech, and catering for various activities throughout the week. With these considerations in mind, we reached out to several offices and organizations to request additional funding support. Fortunately, the CCID office generously covered the cost of the Beckman Auditorium, while WiC graciously agreed to cover the expense of raffle prizes.

Once our funding sources were secured, our next step was to arrange travel logistics for our keynote speakers. Recognizing the opportunity to showcase their expertise beyond the Day of Inclusion event, we decided to integrate their participation into the DICI's regular programming. We organized for both speakers to serve as special Organic Chemistry Seminar presenters, allowing them to share their research alongside their contributions and advice on DEI for the Day of Inclusion. Consequently, Professor Sarpong's session took place on Wednesday, January 17, featuring a series of one-on-one faculty meetings, student group coffee hours, and a scientific seminar. Similarly, Professor Isaacs' session occurred on Thursday, January 18, following the same format.

The subsequent phase of planning involved close collaboration with all participating offices to organize workshops. This entailed scheduling regular meetings to brainstorm topics, develop outlines, and conduct practice runs with DICI board members to gather feedback. Securing room reservations well in advance for the afternoon of January 19 was crucial, given the potential competition for space from other seminars and classes. In terms of event promotion, we opted for diverse advertising strategies, considering it was our inaugural event and unsure which would yield the best results.

Initially, we focused on garnering support from graduate students and postdocs by ensuring endorsement from their Principal Investigators (PIs). This involved working closely with the Division Chair's office, led by Professor Dennis A. Dougherty and Grace Liang-Franco, to advertise the event during faculty meetings, coordinate with faculty assistants to block off schedules for the Day of Inclusion, and encourage faculty members to endorse student attendance. Additionally, we employed traditional advertising methods such as creating flyers and a webpage (https://cce.caltech.edu/dei-in-cce/dei/day-of-inclusion), drafting emails, and leveraging word of mouth from DICI board members to reach the wider community. To further incentivize participation, we offered a complimentary dinner and entry ticket for raffle to win exciting raffle prizes ranging from iPads and Beats headphones to benzene ring coasters and beaker wine glasses.

The DICI board collaborated closely with Paolina Martinez, the communications specialist at CCE, to develop the event's website, registration link, and check-in platform, as well as to procure swag and goodies for attendees, all provided free of charge. As the event date approached, the DICI board has enlisted the help of 16 volunteers, including DICI general members, graduate students, and staff, to assist with various tasks throughout the day, such as facilitating registrations, distributing maps, and assisting with food setup and cleanup after the dinner social. On the day of the event, we were delighted to welcome approximately 200 attendees, a remarkable turnout considering the total number of graduate students in CCE is 356.

The registration process for the general seminar proceeded smoothly, and we were honored to have Division Chair Professor Dougherty deliver a warm welcome address, followed by insightful remarks from Professor Sarah Reisman, Theo Agapie, and Scott

Cushing, who introduced some of the DEI initiatives they oversee or have initiated in CCE. The general seminar concluded with two exceptional keynote presentations. During the guided panel session, we received an overwhelming number of live questions, unfortunately, time constraints allowed only few to be featured. The workshops were also well-attended, and the day concluded with a delightful Mediterranean feast provided by Caltech Dining Services, accompanied by generous swag and raffle prizes. It was truly a celebration for all organizers and participants, marking the success of our inaugural event.

5.3 DATA ANALYSIS AND FEEDBACK

As previously mentioned, our event exceeded our expectations with over 200 attendees participating in all planned activities from start to finish. To provide context, CCE typically hosts Safety Day every other year with mandatory attendance, drawing an average of about 300 students. Our attendance figures are particularly encouraging given that our event was not mandatory and marked our inaugural hosting. To gather feedback on both logistics and content, we distributed a post-event survey to all attendees. While the response rate was approximately 30%, we aim to improve this in future years by offering incentives for survey completion. Despite the modest response rate, we received valuable feedback from a diverse range of participants, including graduate students, postdocs, staff, and faculty members.

Figure 5.3.1 *Day of Inclusion Feedback Survey Results: Survey respondents' affiliation at Caltech.*

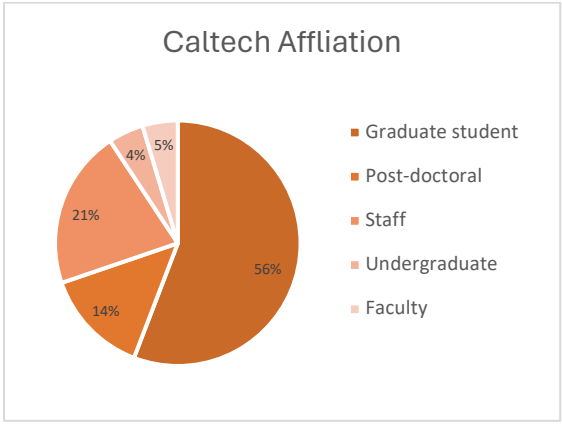

In order to enhance our future event advertising strategies, we included a question in our survey asking participants how they learned about the Day of Inclusion. Interestingly, responses revealed six distinct channels through which individuals became aware of the event. Notably, word of mouth and emails sent from the Division Office emerged as the most effective methods, each garnering 28% of responses. This was followed by emails from DICI, DICI flyers, emails from the DEI lab coordinator, and emails from PIs. Additionally, DICI spearheaded the DEI coordinator program, which designates a point person in each lab to serve as a liaison for DEI-related matters. These coordinators facilitate discussions on DEI initiatives and events within their respective labs, ensuring a supportive and inclusive environment for all members.

Scheme 5.3.2 *Day of Inclusion Feedback Survey Results: Effectiveness of event advertisement.*

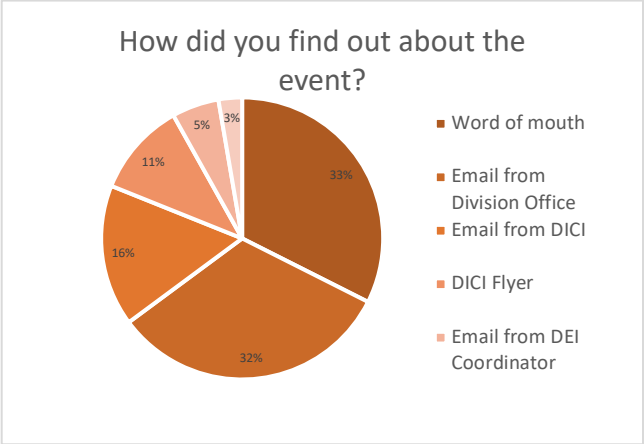

In the subsequent section of the survey, we inquired about various aspects of the event, including the ease of online registration, the efficiency of the check-in process, and the structure and pacing of the event schedule, including appropriate breaks. Overall, most respondents reported that online registration and check-in were straightforward, although some expressed feeling rushed during the transition from the general seminar to the workshops. Notably, the survey revealed that 100% of respondents found the volunteers to be exceptionally helpful, indicating the event's smooth execution and supportive atmosphere. Additionally, 83% of respondents expressed feeling supported by their labs to attend the event, often reflecting positively on the supportiveness of their PIs. Most significantly, 93% of survey participants expressed a desire for the Day of Inclusion to become a recurring event in CCE, underscoring the profound impact of the event on students and its effectiveness in fostering inclusivity and community engagement. The survey also encompassed feedback specific to each of the keynote presentations, the panel discussion with the speakers, and the individual workshops. These comments were

meticulously analyzed and subsequently conveyed to the respective speakers and workshop hosts by DICI board members for internal review and improvement purposes.

5.4 CONCLUSION

In conclusion, the inaugural Day of Inclusion event, organized by DICI with support from the DEI committee at CCE, aimed to foster division-wide unity in advancing diversity, equity, and inclusivity initiatives. Recognizing the importance of such an event, akin to the biennial Safety Day hosted by the division, we sought to send a powerful message of support for DEI efforts, demonstrating CCE's commitment to embracing and welcoming individuals from diverse backgrounds. The event's resounding success, with over half of the entire CCE division—comprising students, staff, and faculty—participating, underscores the significant strides made in promoting inclusivity. Encouragingly, the DEI committee has already committed to funding future iterations of the event, slated for 2025-26. While there is room for improvement, as highlighted by survey feedback, it is heartening to note that 93% of respondents expressed a strong desire for the event to continue in CCE, signaling its enduring impact and importance within the community.

By sharing our experience with the wider community, we extend an invitation for all to embark on their own "Day of Inclusion" event at their respective institutions, while also encouraging feedback on such initiatives. Given the unprecedented nature of these events, it is imperative that our community openly shares both failures and successes, fostering a collective pursuit of a more inclusive system in the chemical sciences and

beyond. We emphasize the critical role of consistent funding sources for student organizations like DICI and established committees such as the DEI committee at CCE. Such support ensures the longevity of existing events and facilitates the launch of new initiatives, thereby contributing to a more diverse, equitable, and inclusive environment for all members within institutions.

5.6 ACKNOWLEDGMENTS

This chapter stands as a testament to the collective commitment to fostering diversity and inclusivity within the STEM community and is dedicated to all URMs currently pursuing or aspiring to careers in STEM.

The authors thank Professor André K. Isaacs and Professor Richmond Sarpong for graciously serving as keynote speakers at this inaugural event. Their contributions were invaluable, and we are deeply appreciative of the inspiring and educational keynote presentations they delivered. Additionally, we thank them for their willingness to share insights from their remarkable journeys in STEM as underrepresented minorities (URMs) during the speaker panel discussions and coffee chats held throughout the week of their visit to Caltech.

The authors express their deepest gratitude to the CCID, CCE DEI committee, and WiC for their invaluable financial support and guidance. The authors thank David A. Cagan, the former president of DICI, who brought the idea of a "Diversity Day" to light during his administration.

Special recognition is extended to Elyse Garlock, Grace Liang-Franco, and Anya Janowski for their significant contributions and administrative assistance. Additionally, the authors acknowledge Paolina Martinez for her expertise in website design and event coordination. Furthermore, the authors wish to convey their appreciation to the various offices and workshop leaders who participated in this endeavor, including Hiliary Tribbs, Sarah Figorski, Jasmine Bryant, Tashiana Bryant, Devon Dobbs, Maria Manzanares, Kim Pham, Sean Cutting, Jocelyn Vargas, Candace Rypisi, and Hima Vatti.

The authors also extend their heartfelt thanks to the dedicated volunteers who generously contributed their time and efforts to support this initiative, including Audrey J. Washington, Rahuljeet S. (RJ) Chadha, Stanna K. Dorn, Kaylin N Flesch, Clara C. Seo, Sarah L. Weisflog, Jay P. Barbor, Maia R. Helterbrand, Kimberly Sharp, Maria S. Blankemeyer, Kerry A. Gomez, and Annette Luymes.

5.7 REFERENCES

1) Reisman, S. E.; Sarpong, R.; Sigman, M. S.; Yoon, T. P. Organic Chemistry: A Call to Action for Diversity and Inclusion. *J. Org. Chem*. **2020**, *85*, 10287–10292.

2) Sarpong, R. A Face of Disease in Sub-Saharan Africa. TED Conferences. **2015.**

3) The Sarpong Group | Synthetic organic chemistry lab at UC Berkeley. https://sarponggroup.com/ (accessed 2024-05-01).

4) Issacs Lab. https://www.isaacslab.com/ (accessed 2024-05-01).

APPENDIX 5

Pd-Catalyzed Asymmetric Protonation of δ-Lactams†

A5.1 INTRODUCTION

In recent decades, palladium-catalyzed reactions have emerged as a promising field for new organometallic transformations. Over the years, our group has devoted significant effort to the development of decarboxylative asymmetric allylic alkylation[1], which has shown high utility in the preparation of chiral building blocks for the synthesis of complex molecules.[2] This transformation undergoes an inner-sphere mechanism that involves a reductive elimination from a chiral O-bound Pd enolate to generate enantioenriched ketones (Figure A5.1.1).[3,4]

There are several advantages to forming this Pd enolate compared to traditional enolate formation methods. First, this Pd enolate is generated catalytically from achiral precursors, such as allyl enol carbonates and β-ketoesters[5] (**71**). Secondly, the Pd enolate is accessed under neutral conditions instead of basic conditions, expanding the functional group tolerance of this reaction. Lastly, the enolate is formed in a regiospecific fashion. In contrast, canonical enolate formations often face challenges with regioselectivity and typically require the use of a strong base or Lewis acid. Given the intrinsic benefits of this Pd enolate generation, we decided to exploit its reactivity beyond allylic alkylations into more asymmetric transformations.

†This research was carried out with Dr. Stephen R. Sardini and Dr. Alexander Q. Cusumano.

For instance, our lab has developed the enantioselective conjugate additions using this Pd enolate to build quaternary centers (**71a**)[6] and the intramolecular aldol reactions to construct chiral spirocycles (**76**). [7] Recently, we have reported the asymmetric intramolecular [4+2] reaction using divergent catalysis further underscores the application of utilizing Pd enolates as stereogenic nucleophiles.[8]

Figure A5.1.1 *Examples of divergent reactivity from Pd enolate XX.*

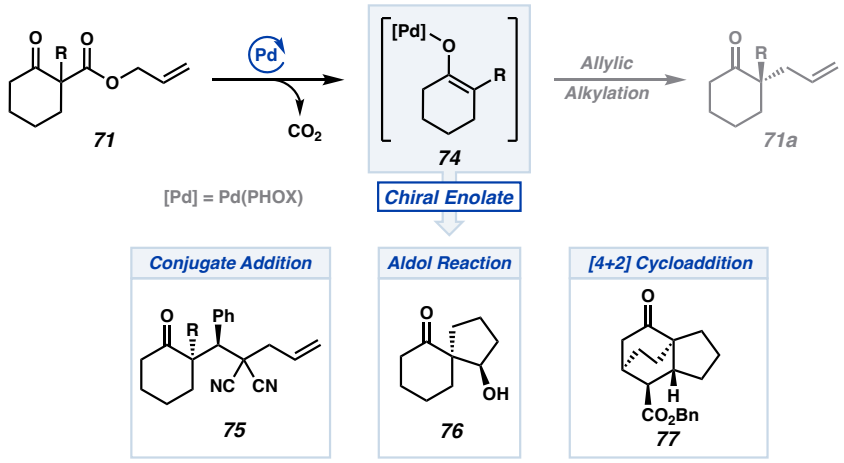

During the development of the [4+2] cycloaddition, we investigated the use of stoichiometric acidic additives to facilitate catalyst turnover, aiming to capture the cinnamyl fragment of ester **78**. Specifically, the addition of 4-methylaniline[7] led to the desired endo cycloadduct as a single diastereomer with high yield and ee (see Figure A5.1.2). Surprisingly, subjecting prenyl β-ketoester to the same reaction conditions resulted in the desired cycloadduct formation without generating alkylated 4-methylaniline (**80**) as a byproduct. Intrigued by this outcome, we conducted a control reaction excluding additive, yielding the desired product with similar yield and ee. This suggests an alternative turnover mechanism of the catalyst in the reaction.

Figure A5.1.2 *A) Reaction conditions of cinnamyl β-ketoesters with additives; B) Unexpected additive-free catalyst turnover with prenyl β-ketoesters.*

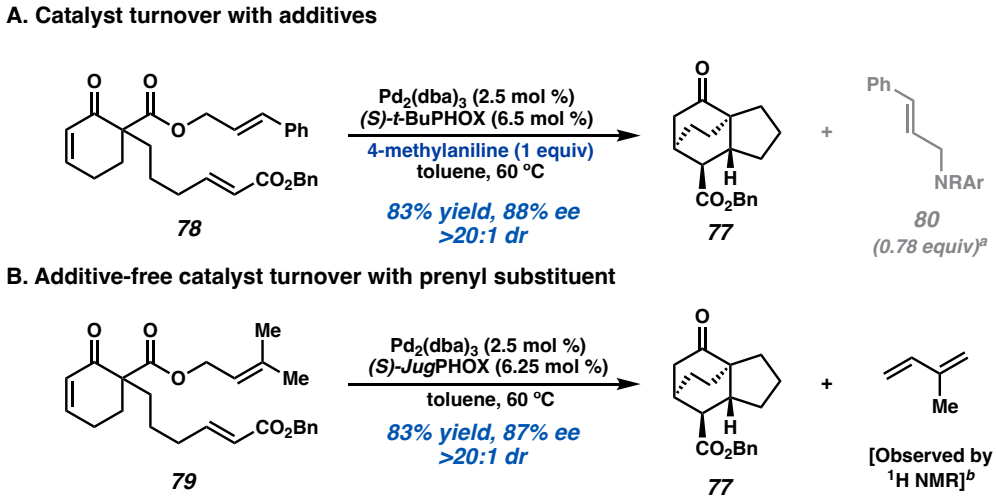

Upon conducting further NMR experiments, gradual generation of isoprene was accompanied by product formation, suggesting that a proton transfer from the prenyl group was the key to catalyst turnover. We then explored this reaction condition on other systems such as β-ketoester **93**, and to our delight, the formation of ketone **94** was observed in excellent yield of 95% and modest ee of 60% (Figure A5.1.3). Similarly, δ-lactams also give a promising hit of 60 yield and 80% ee.

Figure A5.1.3 *Initial hit with prenyl β-ketoester and benzoyl δ-lactams for the asymmetric protonation reaction.*

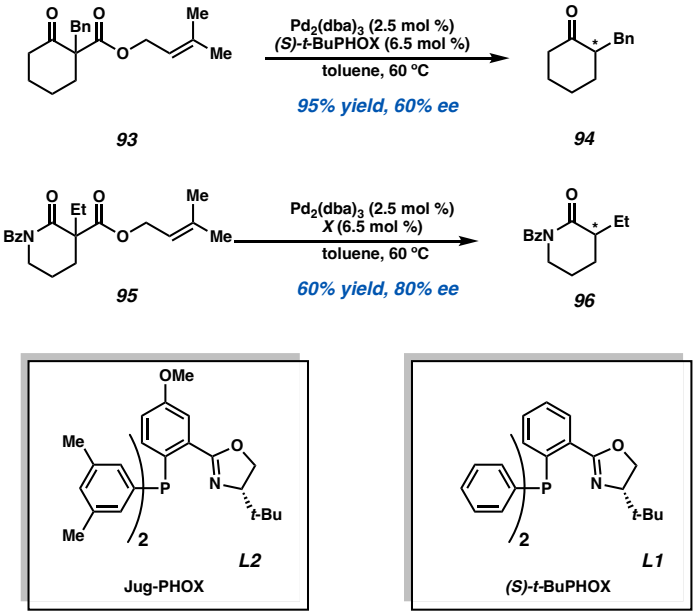

These findings are exciting for us because although the enantioselective protonation of β-ketoester has been achieved by our lab (Figure A5.1.4), the reaction required the additive of Meldrum's acid as a proton donor, and the developed conditions was unfruitful for lactam substrates.[9]

Figure A5.1.5 *Examples of natural products containing a-tertiary stereocenter motifs.*

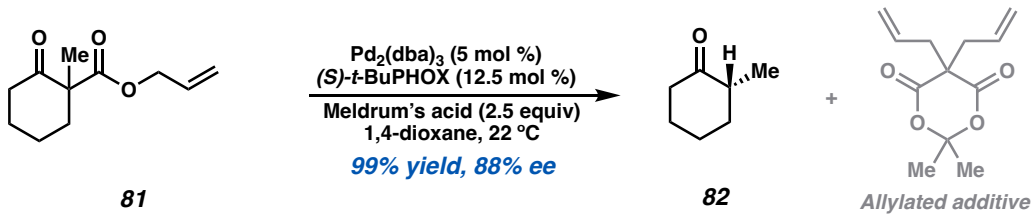

Because of the lack of need of additives, the reaction can be greatly generalized with high tolerance of substrates substitution and functionality. The α-tertiary stereocenter

motif in the product is also a common feature in many natural products and drug molecules such as the ones demonstrated in Figure A5.1.5 highlighted in red.[10]

Figure A5.1.5 *Examples of natural products containing α-tertiary stereocenter motifs.*[10]

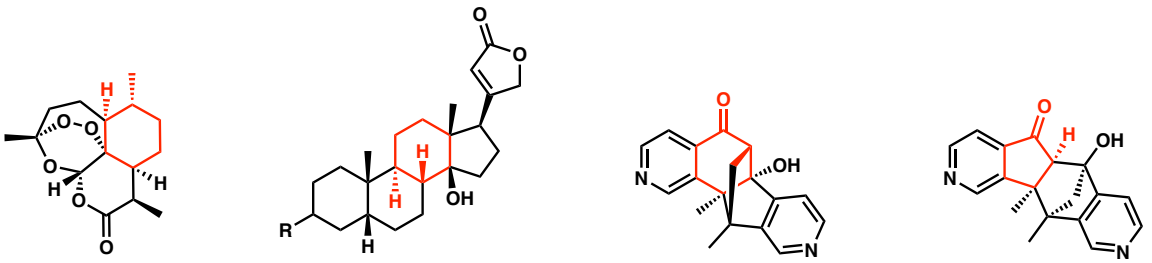

Therefore, our goal for this study is to develop a Pd-catalyzed enantioselective protonation reaction for both β-ketoesters and lactam substrates which would have great potential in its utility in natural product and pharmaceutical compound syntheses.

A5.2 RESULTS AND DISCUSSION

A5.2.2 SUBSTRATE DESIGN AND SYNTHESIS

Due to the lack of prior art, we opted to initiate with benzoylated δ-lactams due to our prior success in utilizing these lactams to achieve enantioselective Pd-catalyzed decarboxylative allylic alkylation of lactams (as illustrated in Figure A5.2.2.1).[11]

Figure A5.2.2.1 *Substrate synthesis of δ-lactams with prenyl substituents*

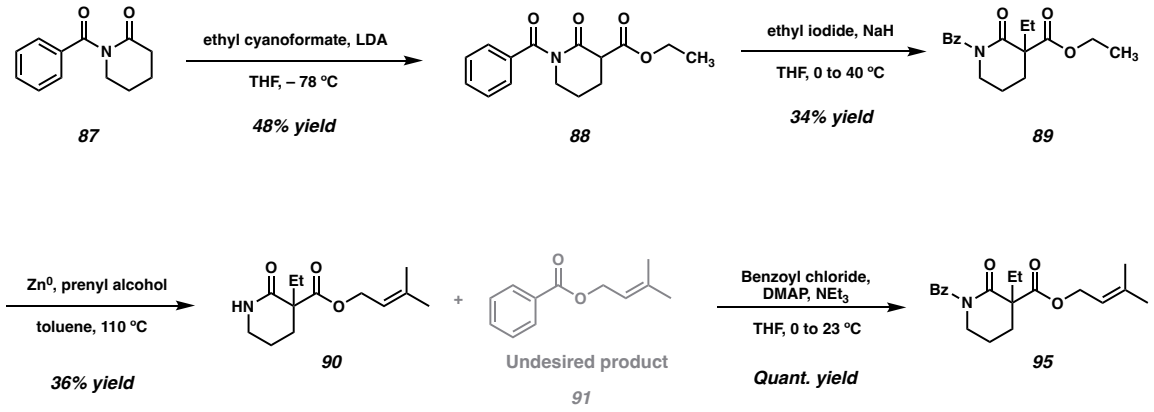

By subjecting the commercially available benzoyl-protected lactam **87** to basic acylation conditions with ethyl cyanoformate, we were able to obtain acylated lactam **88** in a modest yield of 48%. Alkylation of lactam **88** with ethyl iodide resulted in the formation of tetrasubstituted lactam **89**.[9] A transesterification reaction with zinc metal successfully synthesized prenyl ester **90**, albeit with an unexpected deprotection of the benzoyl group and the formation of the undesired side product **91**. Re-protecting amine **90** with benzoyl chloride led us to obtain product **95** in quantitative yield.

A5.2.3 REACTION DESIGN AND OPTIMIZATION

Initial hit of the β-keto ester and lactam were a great starting point for optimization (Figure A5.1.4). Modifying the electronics and the steric effect of the ligand was one of the first focuses of our optimization efforts (Figure A5.2.3.1). We found that although electronically rich ligands such as Jug-PHOX (L2) and trimethoxy-PHOX (L4) provides promising ee, the electronically withdrawing ligands such as CF_3-PHOX (L3) gives high conversion of the starting material and higher yields of the desired product. Similar pattern

is also observed with tBu-PHOX (L1), but for both CF_3- and tBu- PHOX ligands, a unsaturated side product **92** is observed, which could further complicates the analysis of the transformation.

Figure A5.2.3.1 *Ligand screen testing ligands with different electronics.*

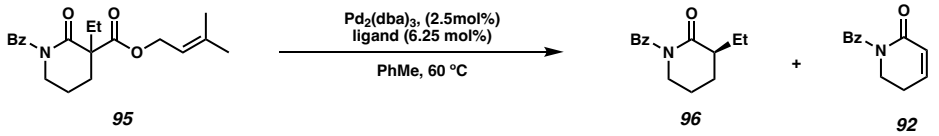

Entry	Ligand	NMR yield	ee	notes
1	CF_3-PHOX	82	63	formed the side product XX
2	tBu-PHOX	81	61	formed the side product XX
3	Jug-PHOX	60	80	not going to full conversion
4	trimethoxy-PHOX	46	71	not going to full conversion

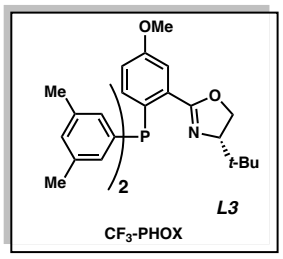

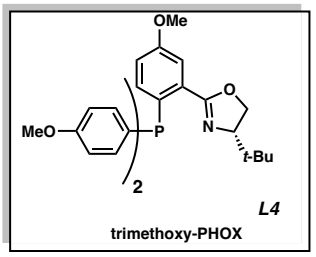

We have also explored different solvent mixtures and temperatures. Unpleasantly, the reaction yield decreases with temperature (Figure A5.2.3.2).

Figure A5.2.3.2 *Solvent and temperature screen.*

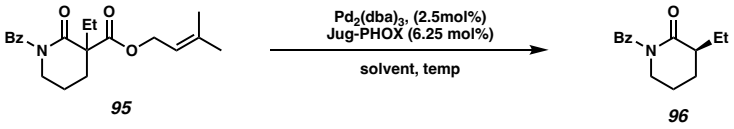

Entry	solvent	temperature	NMR yield	ee
1	PhMe	60	60	80
2	PhMe:Hex	50	52	63
3	PhMe:Hex	45	36	71

Unfortunately, it was also around this time that we were running the reactions side by side with the control reaction which is the conditions described in the initial hit in Figure A5.1.3, and we observed inconsistency regarding the ee of the control reaction. Specifically, we cannot reproduce the original finding of 80% ee. Many things have been tried to reproduce the data such as remaking substrate and changing the heating method to ensure consistent heating throughout reaction. Interestingly, by trying different sources of Pd was explored, different gloveboxes (both the Reisman Lab glovebox and the 3CS glovebox), and different batches of ligand, we started seeing full conversion of starting material and quantitative yield of desired product, but bigger fluctuations in ee.

We hypothesized that the inconsistency could be due to several reasons. Firstly, we have previously found that different bottles of Pd_2dba_3 could exhibit significant differences in the actual catalyst-to-dba ratio. This disparity could result in inconsistencies in reactions where dba plays an important role in the mechanistic cycle. Secondly, based on very preliminary computational calculations, we have learned that this proposed protonation reaction follows a new mechanistic pathway wherein the N atom of the PHOX ligand

detaches from Pd. This mechanism is fundamentally different from the canonical Pd-catalyzed decarboxylative allylic alkylation mechanisms.[4] This observation could indicate the potential involvement of a facile, low enantiomeric excess, or outer-sphere mechanism that contributes to the inconsistent enantiomeric excess observed under the presented reaction conditions.

Figure A5.2.3.3 *Failed attempts to resolve irreproducibility in ee.*

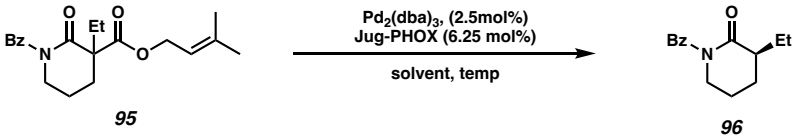

Entry	NMR yield	ee	notes
1	60	80	original pass
2	52	63	new batch of substrate
3	36	71	changing from heating block to oil bath
4	quant	53	new bottle of Pd_2dba_3
5	quant	50	tried different glovebox
5	quant	53	different batch of Jug-PHOX

Without any luck with the parent substrate, we decided to investigate different protecting groups on the lactam. Using the route developed in Figure A5.2.2.1, we have synthesized the corresponding benzylated lactam XX (Figure A5.2.3.4A). Not only that the transesterification step decreased in yield significantly, we were also surprised to see no desired product formation under the asymmetric protonation conditions (Figure A5.2.3.4B).

Figure A5.2.3.4 *A) Synthesis of benzylated lactam XX. B) Failed protonation reaction with lactam 101.*

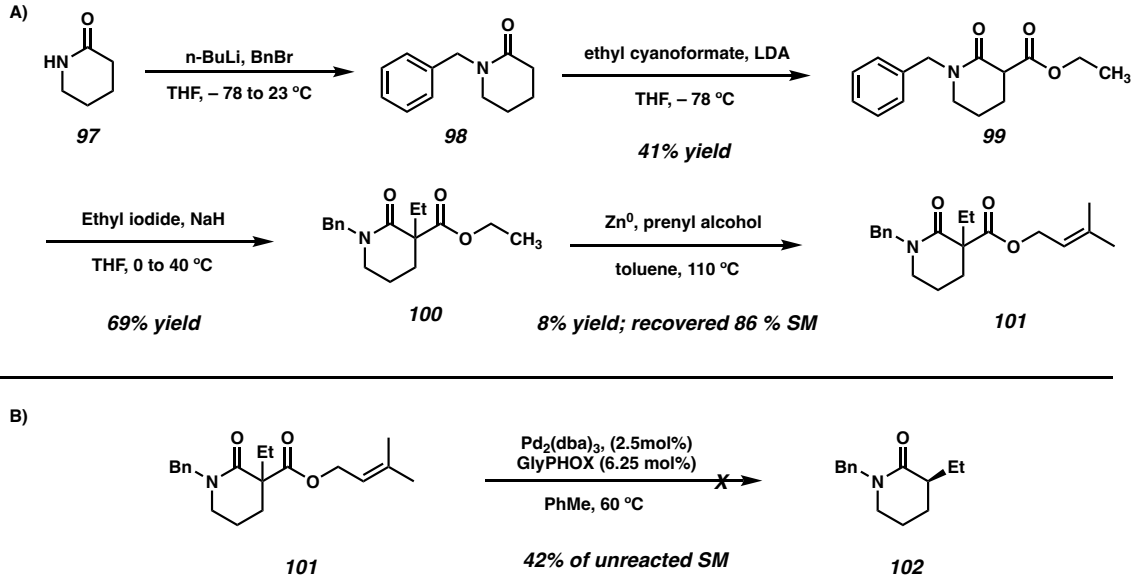

Similarly, we have made lactams with tosyl and p-Methoxyphenyl (PMP) protecting groups, and the reaction resulted in poor yield/ee (Figure A5.2.3.5).

Figure A5.2.3.5 *Attempted asymmetric protonation reaction with lactams of PMP and tosyl protecting groups.*

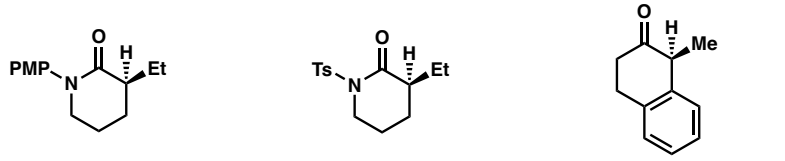

103 ***104*** ***105***

quant. yield, 51% ee ***35% NMR yield, 14% ee*** ***N/A product unstable***

A5.3 CONCLUSION

In conclusion, we have demonstrated the efforts of the development of the asymmetric Pd-catalyzed protonation of benzoylated δ-lactams. Though the reaction had

an intial hit of 60% yield and 80% ee, research efforts have shown that ee is extremely irreproducible. We hypothesized that perhaps the inconsistency could be due to a facile, low ee mechanistic pathway under the current reaction conditions. Further investigation on the reaction mechanism would be required to gain insights into how to fix the irreproducible issue of the reaction.

A5.4 REFERENCES AND NOTES

[1] Behenna, D. C.; Stoltz, B. M. The Enantioselective Tsuji Allylation. *J. Am. Chem. Soc.* **2004**, *126*, 15044–15045.

[2] Liu, Y.; Han, S.-J.; Liu, W.-B.; Stoltz, B. M. Catalytic Enantioselective Construction of Quaternary Stereocenters: Assembly of Key Building Blocks for the Synthesis of Biologically Active Molecules. *Acc. Chem. Res.* **2015**, *48*, 740–751.

[3] Cusumano, A. Q.; Stoltz, B. M.; Goddard, W. A. Reaction Mechanism, Origins of Enantioselectivity, and Reactivity Trends in Asymmetric Allylic Alkylation: A Comprehensive Quantum Mechanics Investigation of a $C(sp^3)$–$C(sp^3)$ Cross-Coupling. *J. Am. Chem. Soc.* **2020**, *142*, 13917–13933.

[4] (a) Keith, J. A.; Behenna, D. C.; Mohr, J. T.; Ma, S.; Marinescu, S. C.; Oxgaard, J.; Stoltz, B. M.; Goddard, W. A. The Inner-Sphere Process in the Enantioselective Tsuji Allylation Reaction with *(S)-t*-Bu-Phosphinooxazoline Ligands. *J. Am. Chem. Soc.* **2007**, *129*, 11876 11877. (b) Keith, J. A.; Behenna, D. C.; Sherden, N.; Mohr, J. T.; Ma, S.; Marinescu, S. C.; Nielsen, R. J.; Oxgaard, J.; Stoltz, B. M.; Goddard, W. A. The Reaction Mechanism of the Enantioselective Tsuji Allylation: Inner-Sphere and Outer-Sphere Pathways, Internal Rearrangements, and Asymmetric C–C Bond Formation. *J. Am. Chem. Soc.* **2012**, *134*, 19050–19060. (c) McPherson, K. E.; Croatt, M. P.; Morehead, A. T.; Sargent, A. L. DFT Mechanistic Investigation of an Enantioselective Tsuji–Trost Allylation Reaction. *Organometallics* **2018**, *37*, 3791–3802.

[5] Mohr, J. T.; Behenna, D. C.; Harned, A. M.; Stoltz, B. M. Deracemization of Quaternary Stereocenters by Pd-Catalyzed Enantioconvergent Decarboxylative Allylation of Racemic

β-Ketoesters. *Angew. Chem. Int. Ed.* **2005**, *44*, 6924–6927.

[6] Streuff, J.; White, D. E.; Virgil, S. C.; Stoltz, B. M. A Palladium-Catalysed Enolate Alkylation Cascade for the Formation of Adjacent Quaternary and Tertiary Stereocentres. *Nature Chem.* **2010**, *2*, 192–196.

[7] Inanaga, K.; Wollenburg, M.; Bachman, S.; Hafeman, N. J.; Stoltz, B. M. Catalytic Enantioselective Synthesis of Carbocyclic and Heterocyclic Spiranes via a Decarboxylative Aldol Cyclization. *Chem. Sci.* **2020**, *11*, 7390–7395.

[8] Flesch, K. N.; Cusumano, A. Q.; Chen, P.-J.; Strong, C. S.; Sardini, S. R.; Du, Y. E.; Bartberger, M. D.; Goddard, W. A. I.; Stoltz, B. M. Divergent Catalysis: Catalytic Asymmetric [4+2] Cycloaddition of Palladium Enolates. *J. Am. Chem. Soc.* **2023**, *145*, 11301–11310.

[9] Marinescu, S. C.; Nishimata, T.; Mohr, J. T.; Stoltz, B. M. Homogeneous Pd-Catalyzed Enantioselective Decarboxylative Protonation. *Org. Lett.* **2008**, *10*, 1039–1042.

[10] A) Cao, S.; Kingston, D. Biodiversity Conservation and Drug Discovery: Can They Be Combined? The Suriname and Madagascar Experiences. *Pharmaceutical. Biology.* **2009**, *47*, 809–823. B) Mishig, D.; Gruner, M.; Lübken, T.; Ganbaatar, C.; Regdel, D.; Knölker, H.-J. Isolation and Structure Elucidation of Pyridine Alkaloids from the Aerial Parts of the Mongolian Medicinal Plant Caryopteris Mongolica Bunge. *Sci. Rep.* **2021**, *11*, 13740.

[11] Behenna, D. C.; Liu, Y.; Yurino, T.; Kim, J.; White, D. E.; Virgil, S. C.; Stoltz, B. M. Enantioselective Construction of Quaternary N-Heterocycles by Palladium-Catalysed Decarboxylative Allylic Alkylation of Lactams. *Nature Chem.* **2012**, *4*, 130–133.

PROTON NMR FOR NEW COMPOUNDS RELEVANT TO APPENDIX 5

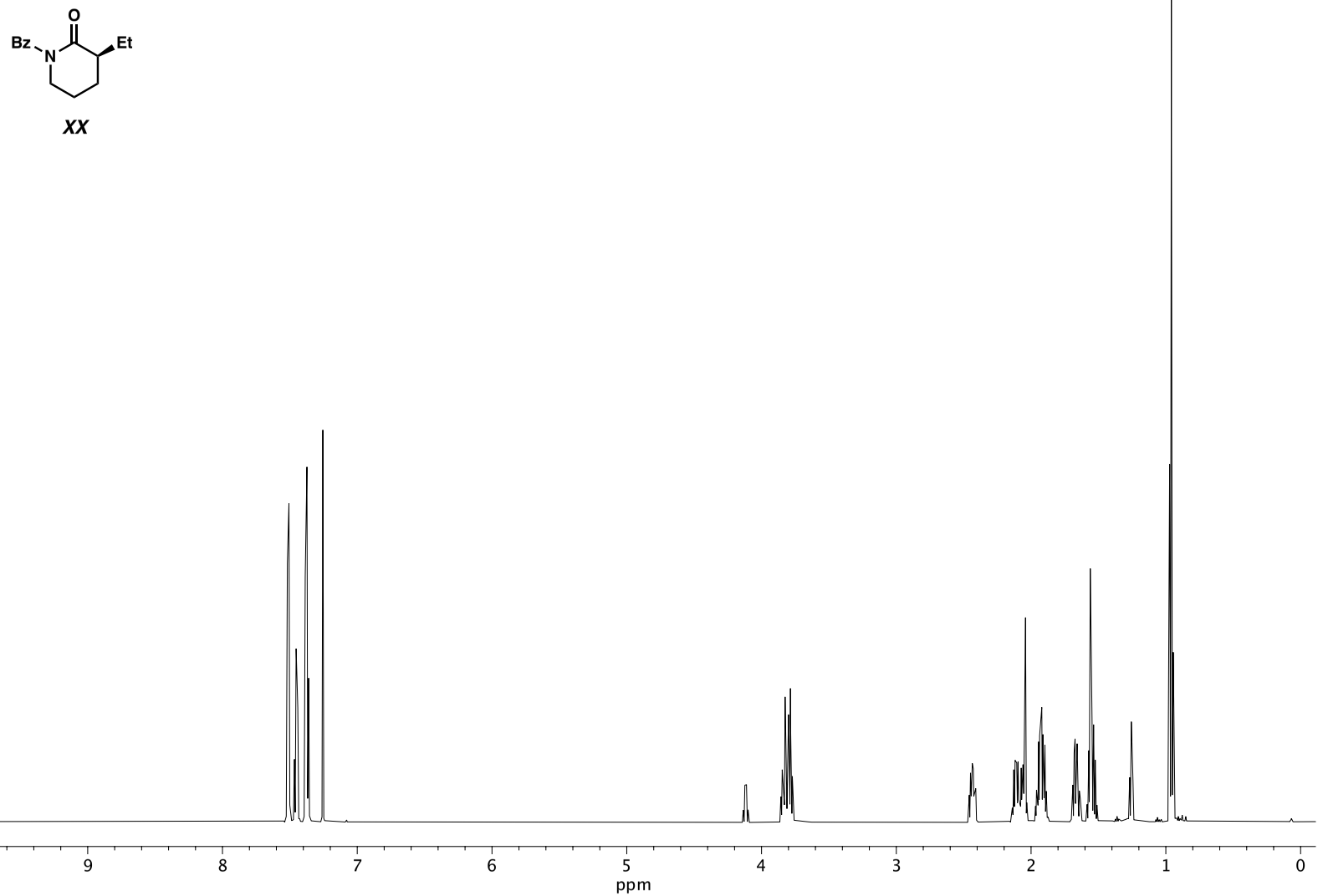

Figure A3.1. *^{1}H NMR (400 MHz, $CDCl_3$) of compound* ***160a***.

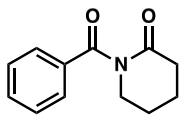

XX

Figure A3.1. *^{1}H NMR (400 MHz, $CDCl_3$) of compound* ***160a****.*

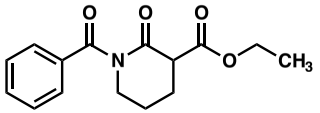

XX

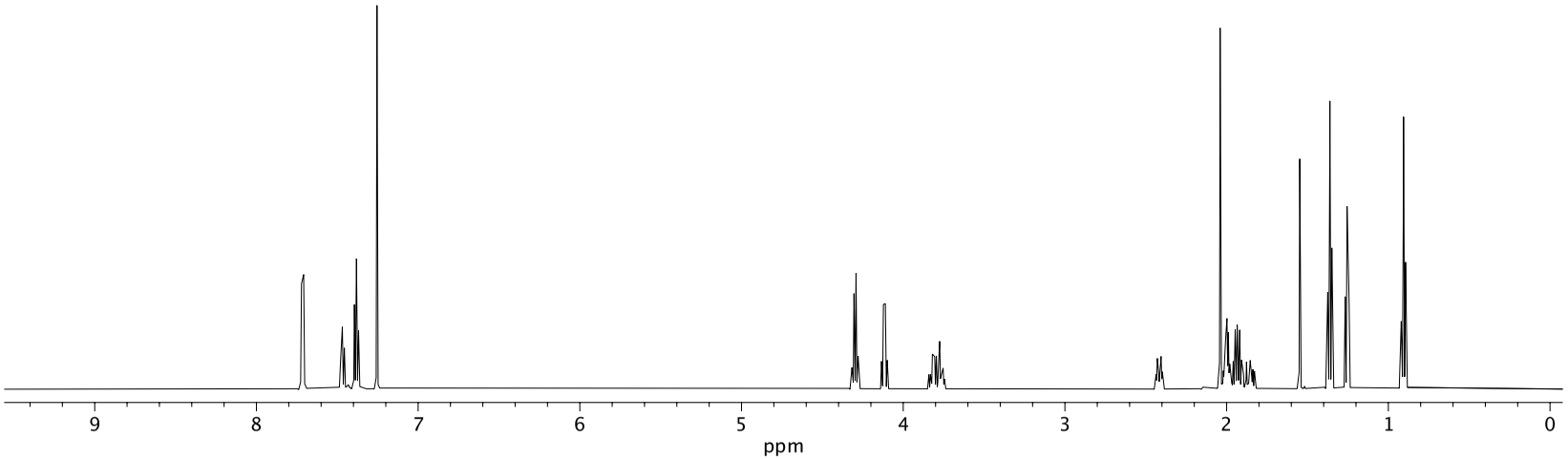

Figure A3.1. *^{1}H NMR (400 MHz, $CDCl_3$) of compound* ***160a***.

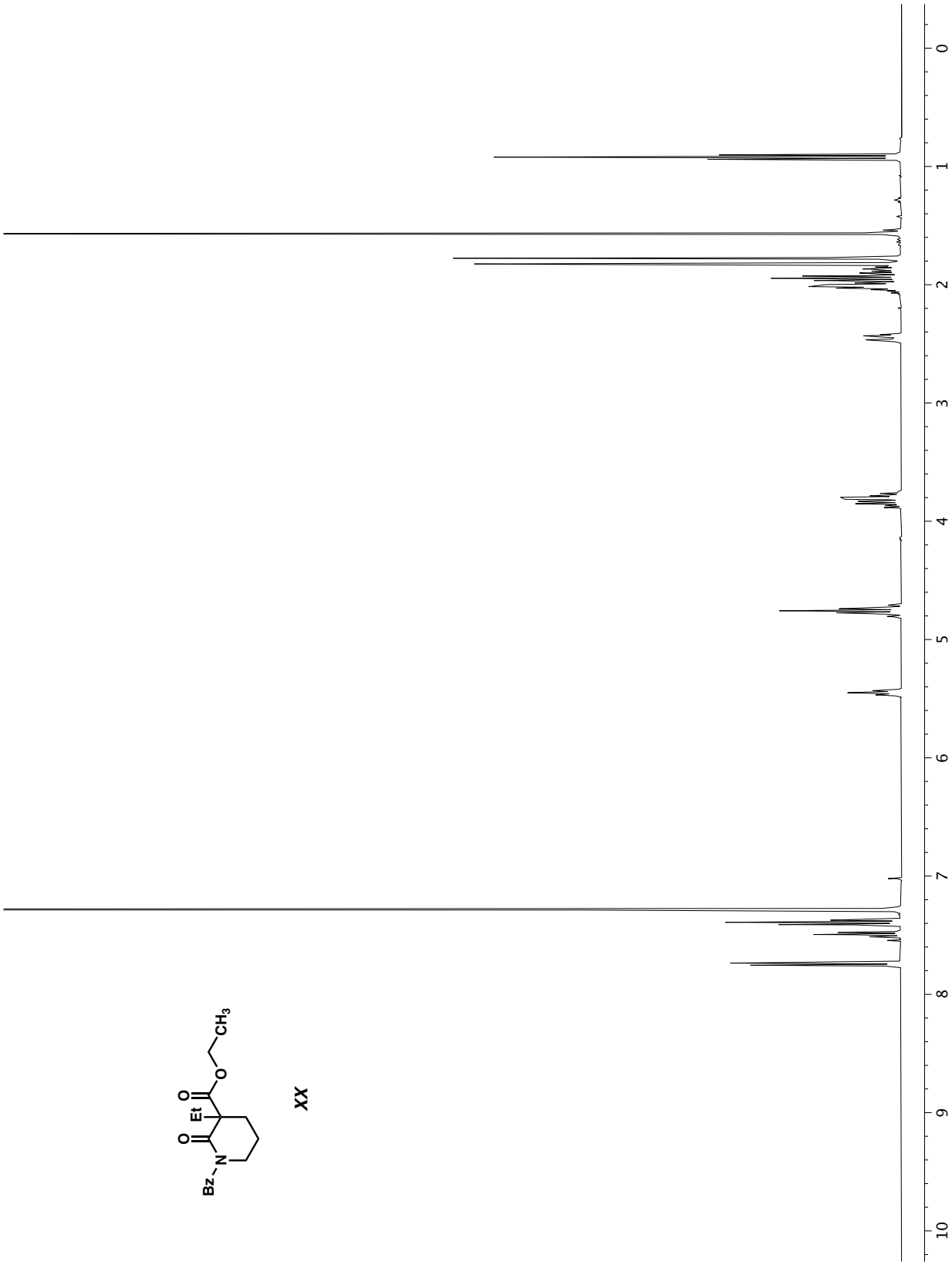

XX

Figure A3.1. *^{1}H NMR (400 MHz, $CDCl_3$) of compound* ***160a***.

Figure A3.3. *^{13}C NMR (100 MHz, $CDCl_3$) of compound* ***160a***.

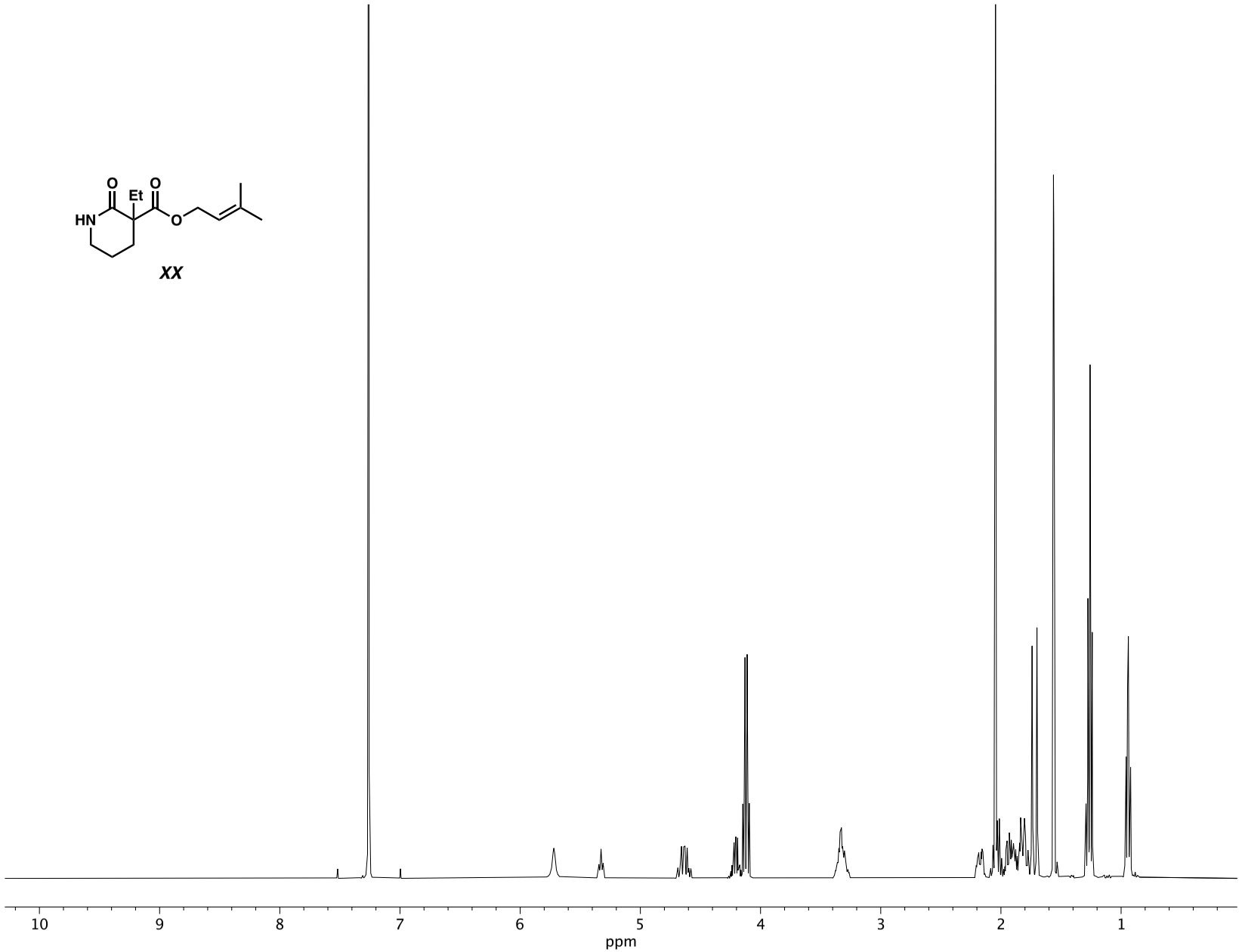

XX

Figure A3.1. *^{1}H NMR (400 MHz, $CDCl_3$) of compound* ***160a***.

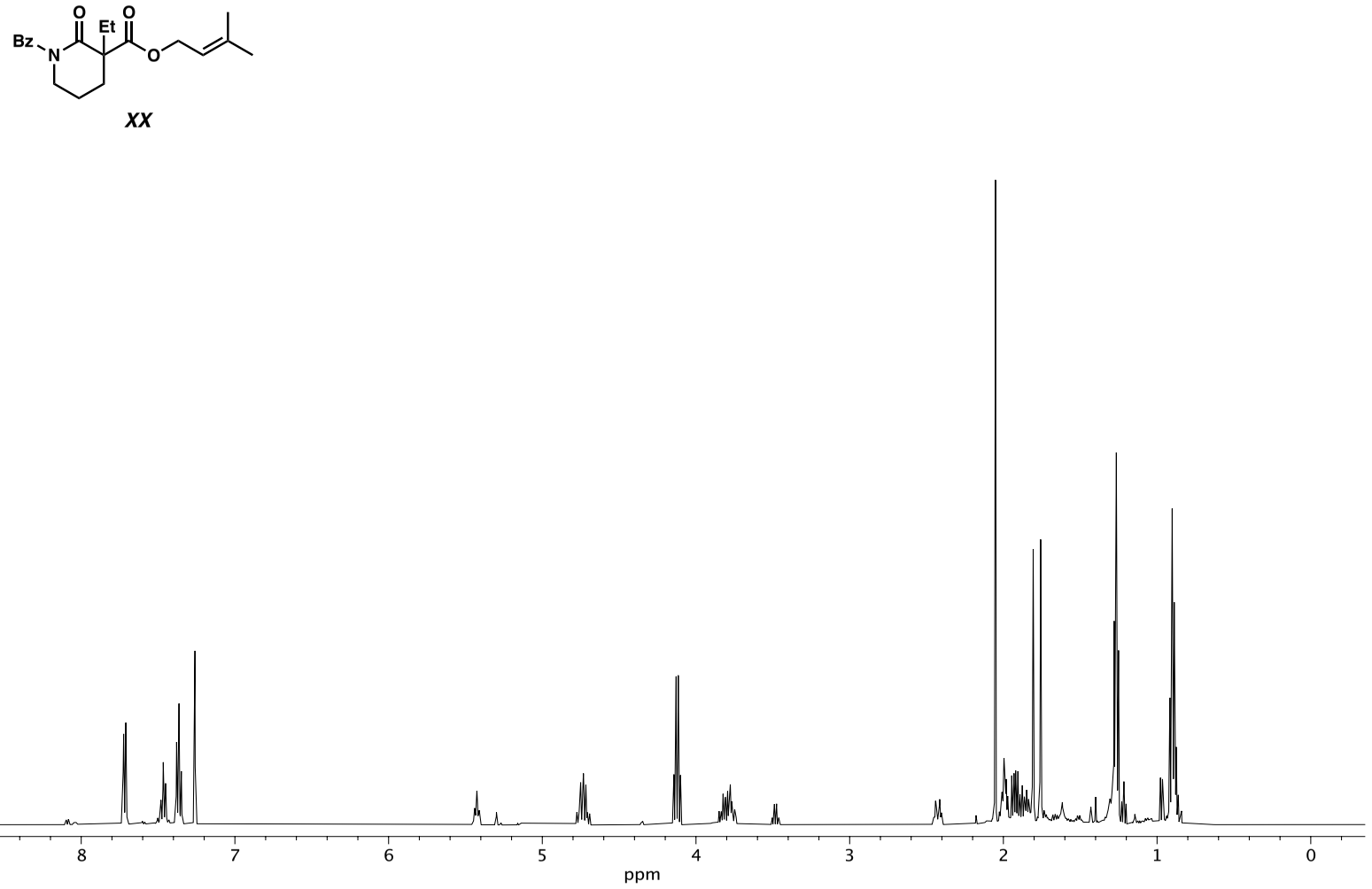

Figure A3.1. *^{1}H NMR (400 MHz, $CDCl_3$) of compound* ***160a***.

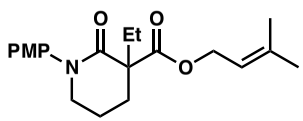

XX

Figure A3.1. *^{1}H NMR (400 MHz, $CDCl_3$) of compound* ***160a****.*

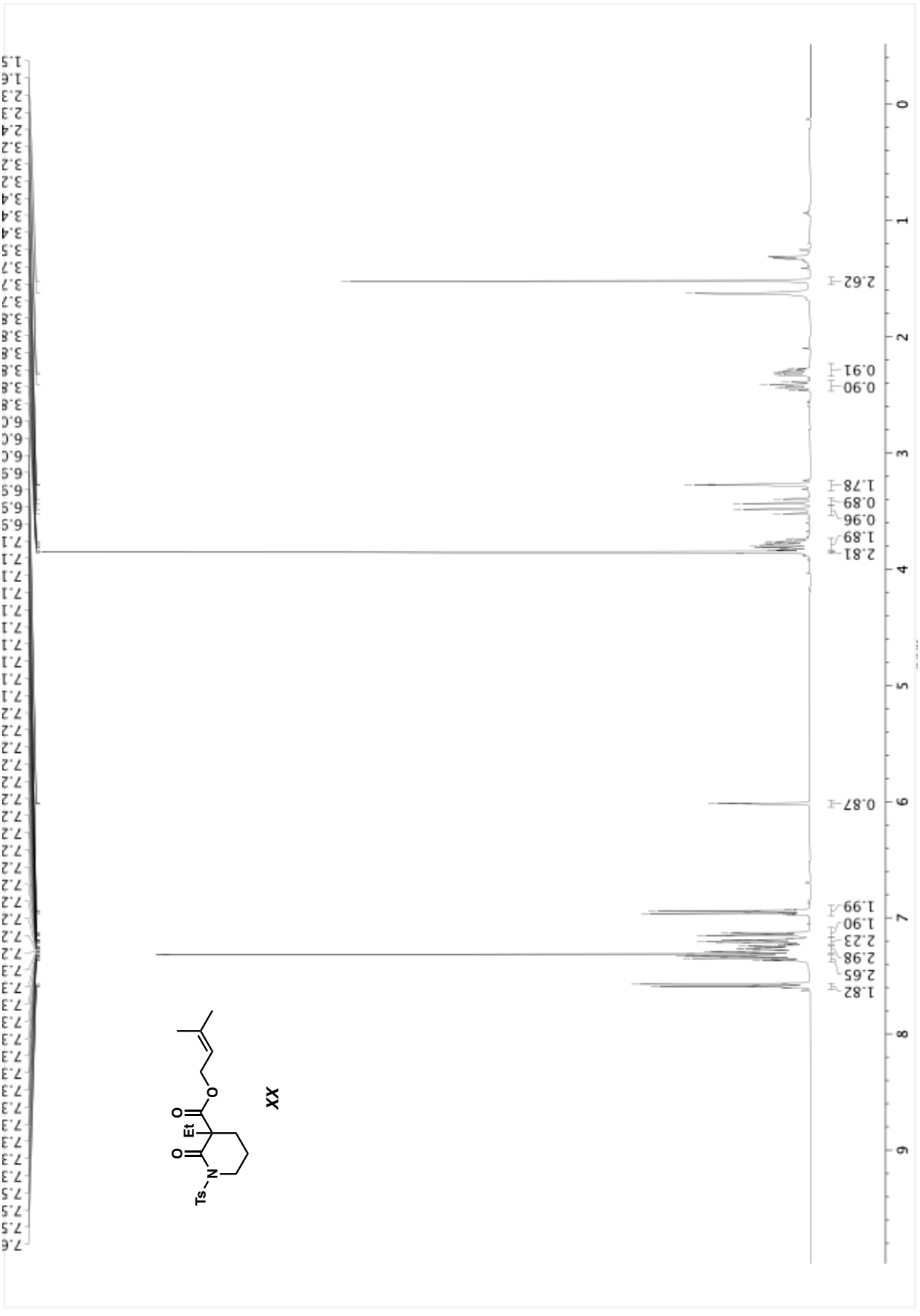

Figure A3.1. *^1H NMR (400 MHz, $CDCl_3$) of compound* ***160a***.

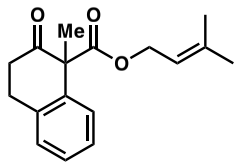

XX

Figure A3.1. *^{1}H NMR (400 MHz, $CDCl_3$) of compound* ***160a****.*

APPENDIX 6

Progress Toward an Asymmetric Double Michael Addition of Palladium Enolates†

A6.1 INTRODUCTION

All-carbon quaternary stereocenters are abundantly present in complex molecules, yet their asymmetric construction remains a persistent challenge in the synthetic chemistry community. Notable examples of natural products and drug molecules featuring this motif include Naloxone, (+)-Limaspermidine, (+)-Hamigeran B, and (–)-Cyanthiwigin F, as illustrated in Figure Z.1.1.[1] Consequently, our group has dedicated significant interest to the development of methodologies that enable the synthesis of these intricately substituted substrates with high efficiency and enantioselectivity from prochiral starting materials.

Figure A6.1.1 *Examples pharmaceuticals and natural products that bears all-carbon quaternary stereocenters.*

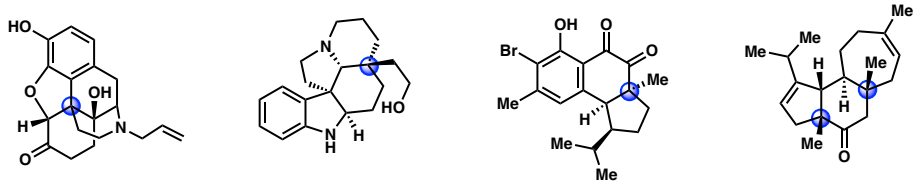

Naloxone (+)-Limaspermidine (+)-Hamigeran B (–)-Cyanthiwigin F

We have conducted thorough investigations into Pd-catalyzed allylic alkylation methods, which showcase a distinctive inner-sphere reductive elimination from the chiral Pd-enolate (refer to Figure A6.1.2). These methodologies commence from racemic starting materials such as β-keto ester **81**, enol carbonate **109**, or silyl enol ether **110**. The resultant

†This research was carried out with Kaylin N. Flesch and Jay Barbor.

products can subsequently serve as enantioenriched synthetic building blocks for the construction of more intricate molecules.[2]

Figure A6.1.2 *Pd-catalyzed decarboxylative asymmetric allylic alkylation.*

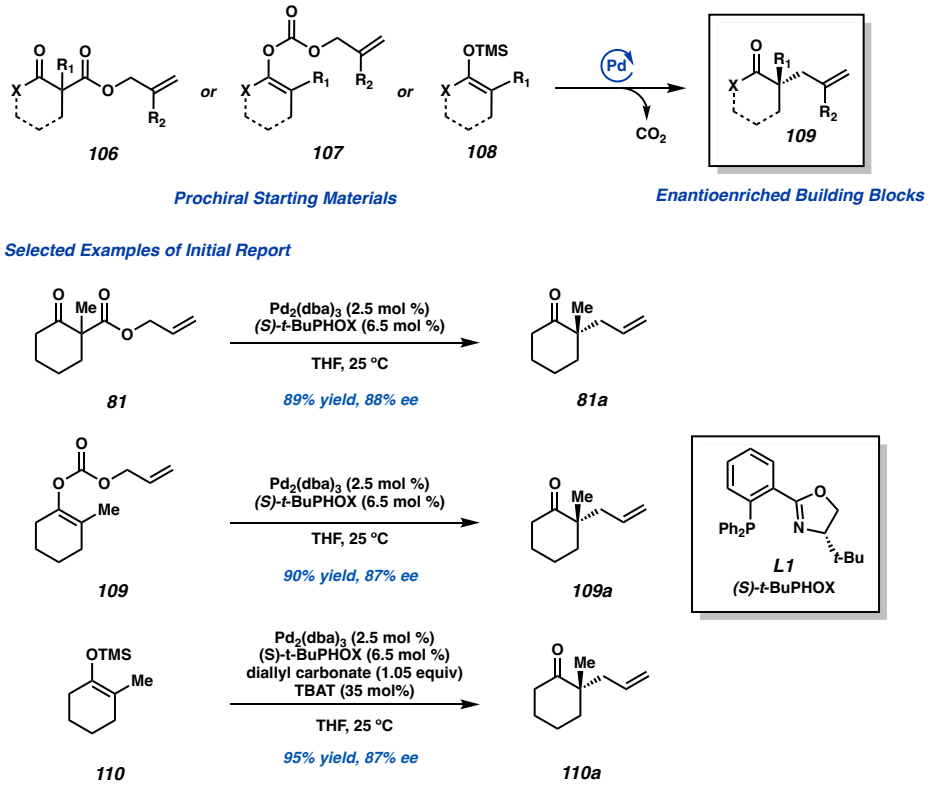

The proposed mechanism of this transformation initiates with oxidative addition to generate the Pd π-allyl species (Figure A6.1.3, X). Subsequent decarboxylation leads to the formation of the chiral Pd enolate (**C**). The enantio-determining step occurs during C–C bond formation, resulting in the formation of the all-carbon quaternary center. Lastly, ligand exchange with another β-keto ester starting material facilitates the construction of product **71a**, achieved in good yield and enantiomeric excess.[3]

Figure A6.1.3 *Proposed catalytic cycle of the Pd-catalyzed asymmetric decarboxylative allylic alkylation.*[3]

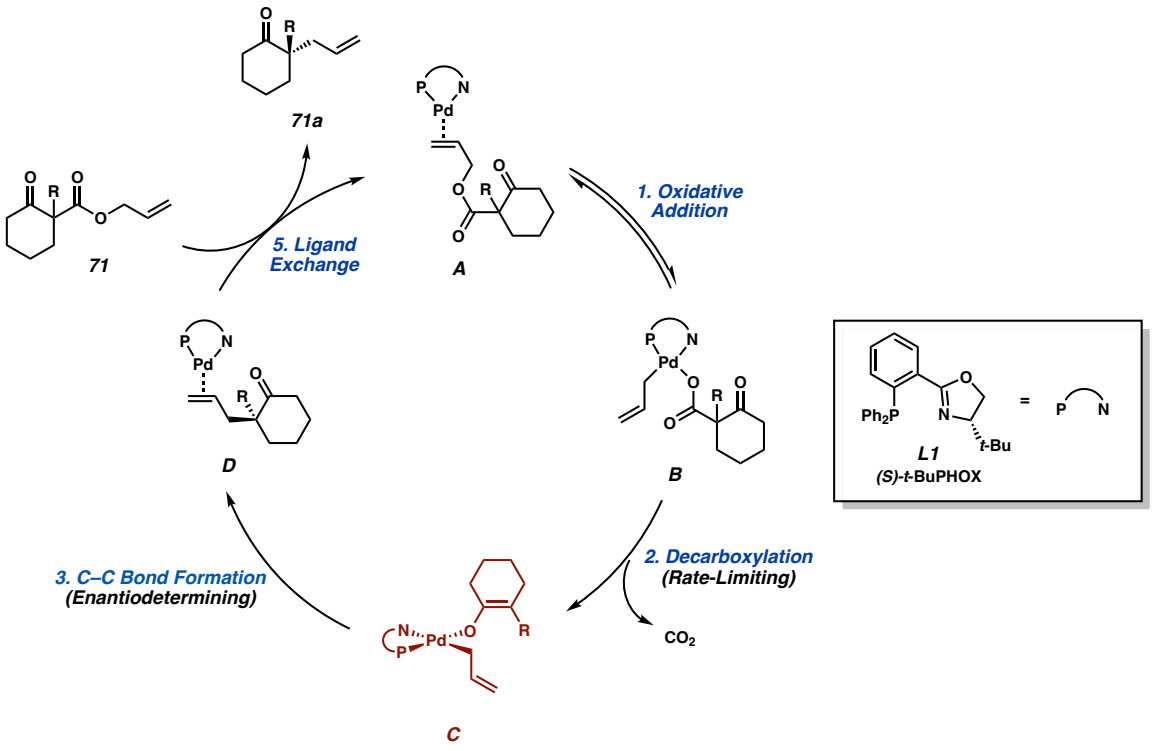

In recent years, our group has directed its attention toward divergent catalysis, with the main focus on harnessing the chiral O-bound Pd enolate intermediate (**C**, highlighted in red in Figure A6.1.3) and extending its application to reactions beyond allylic alkylation. Notably, this Pd enolate holds unique significance as it is formed without the need for exogenous base and originates from racemic enolate precursors. This characteristic endows it with immense potential for synthetic utility. With the concept of divergent catalysis by intercepting the original catalytic cycle, we have reported several asymmetric transformations that utilize Pd enolate X such as conjugate addition[4], intramolecular aldol reaction[5], intramolecular Diels–Alder reaction,[6] and protonation[7].

Figure A6.1.4 *Examples of divergent catalysis from Pd enolate* ***74****.*

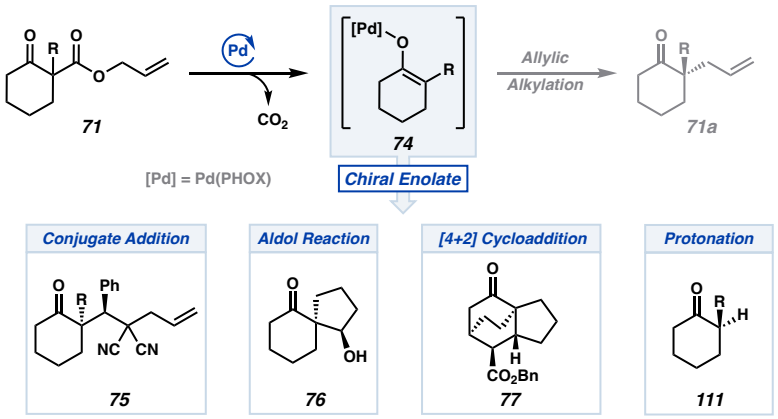

In this research, we present the efforts conducted to further utilize Pd enolate **74** for an asymmetric double Michael addition. In one single step, we are able to form two stereocenters with high ee and a bridged molecule that has great synthetic potential in the field of natural product and drug synthesis.

Figure A6.1.5 *This research.*

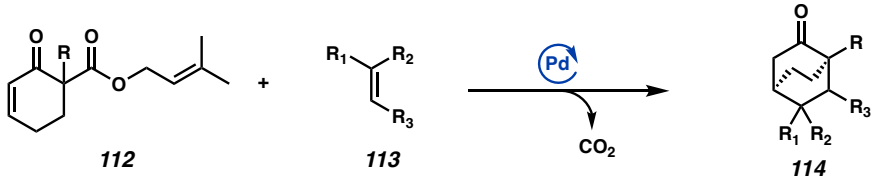

The initial hit of the reaction commences an allylated β-ketoester (**115**) and malononitrile **116**. Upon subjecting to Pd_2dba_3, (S)-tBu-CF3-PHOX ligand, and 3,5-dimethylephenol as an additive, the desired bridged product (**117**) is formed in 55% yield and 60% ee.

Figure A6.1.6. *Initial hit.*

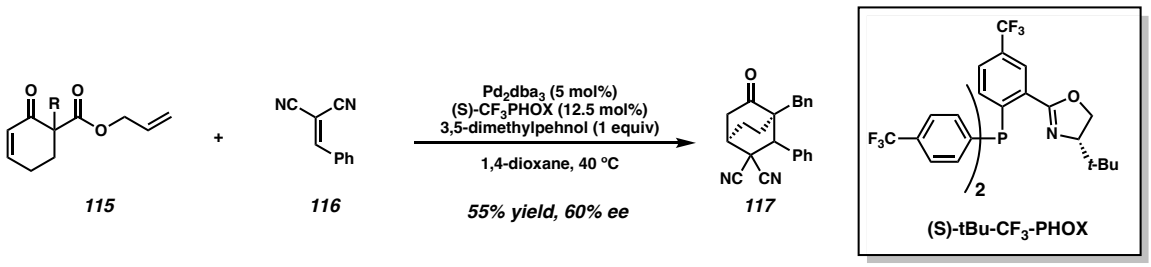

A6.2 RESULTS AND DISCUSSION

A6.2.1 REACTION DEVELOPMENT

Based on earlier findings from our group, stoichiometric Bronsted acid type additives are good agents to turn over the Pd catalyst by trapping the pendant allyl group on Pd and to protonate the final negatively charged species and allow for ligand change.[8] However, in the study of the catalytic asymmetric [4+2] cycloaddition of Palladium enolates published by our group[4], we learned that prenylated β-ketoesters such as **71** has an alternative catalyst turnover mechanism, as the same result was achieved without the addition of exogenous additive. Upon NMR experiment investigations, stoichiometric generation of isoprene was observed, rendering the protonation of the final enolate and turn over the catalytic cycle.

Table A6.2.1.1 *Optimization table regarding different ligands and temperatures with prenylated β-keto ester.*

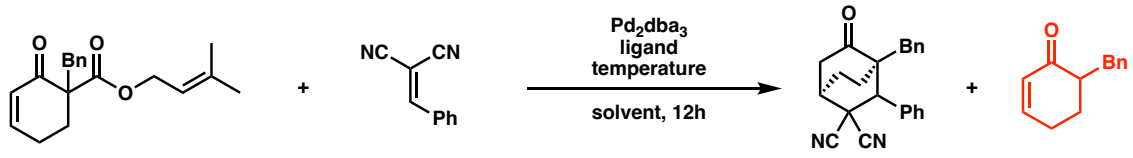

118 ***116*** ***2.3:1 dr*** ***117*** ***119***

Ligand	temp	solvent	NMR yield*	ee	notes
tBu-PHOX	100 °C	toluene	50	80	not full conversion from SM
tBu-PHOX	reflux	toluene	55	84	no SM, 21% protonation product
CF_3-PHOX	100 °C	toluene	52	91	no SM, 48% protonation
OMeJug-PHOX	100 °C	toluene	10	67	90% SM

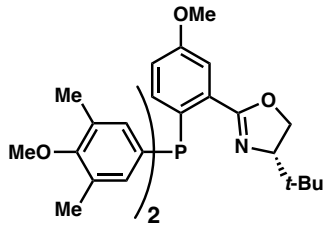

OMeJug-PHOX

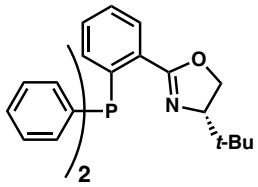

***t*-Bu-PHOX**

Commencing from the prenylated β-beto ester **118**, we were delighted to see that our desired product was formed in modest yield and high ee, which was greatly improved from its allylated β-ketoester counterpart. However, the major area of improvement for this condition is two-fold: 1) the product are a 2.3:1 mixture of diastereomers at the arylated beta position; 2) most of the mass balance goes to the protonation product, which is the undesired reactivity that was also observed with prenylated β-ketoesters in the asymmetric intramolecular Diels–Alder reaction mentioned previously.[4]

We have also explored the effect of varying temperature for the reaction, hoping to find an optimal temperature where the desired product is formed without the formation of the protonation product (**119**) in high ee. Unfortunately, lowering the temperature resulted in very little to no formation of the desired product (Table A6.2.1.2)

Table A6.2.1.2 *Varying temperature with CF3PHOX.*

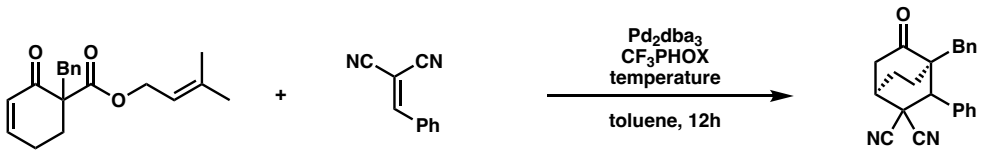

118 *116* *117*

temp	NMR yield* (dr)	Protonation	ee	notes
40	N/A	4	N/A	no conversion
60	N/A	6	N/A	pretty much no conversion
80	21 (15:6)	8	92	not full conversion
100	47 (33:14)	32	94 (75 for minor)	

Since CF3PHOX provided the best results thus far in terms of ee, we explored other electron-withdrawing PHOX ligands (Table A6.2.1.3). However, most of the other ligands gave no product and a lot of Pd black formation was observed quickly after addition, indicating a pretermination of the reaction. We hypothesized that this was potentially due to the steric effect of the highly substituted aryl rings on the ligand.

Table A6.2.1.2 *Screen of different electron deficient PHOX ligands.*

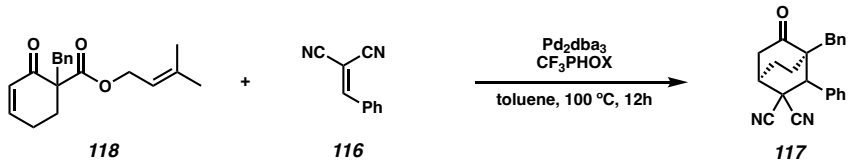

118 + *116* → *117*

Ligand	NMR yield* (dr)	ee	notes
L_5	N/A	N/A	
L_6	N/A	N/A	most reactions turned into Pd black very quickly
L_7	15	TBD	no product observed besides L_3
L_8	N/A	N/A	

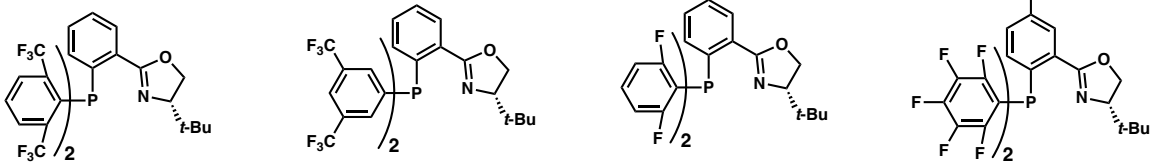

L5: VH-II-211 L6: VH-II-207 L7 L8

Though the prenylated β-keto ester can turn over the catalyst, we have found in our previous studies of the asymmetric aldol reaction that the additives might play additional roles in the catalytic cycle rather than just turning over the catalyst and offer as a proton source.[5] We then investigated several additives used in the aldol reaction.

Table A6.2.1.3 *Additives screen.*

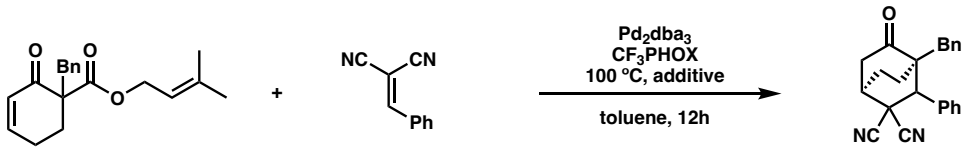

118 ***116*** ***117***

additive	NMR yield* (dr)	Protonation
none	56	40
1	20	80
2	60	38
3	32	90

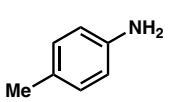

additive 1

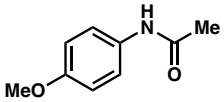

additive 2

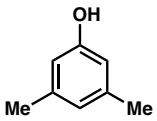

additive 2

We then hypothesized that different substitution pattern of the "prenyl-type" β-keto ester could affect the outcome of the transformation. To test our hypothesis, we have synthesized the cyclohexyl derivative of the "prenyl"-type β-keto ester via the developed route for substrate synthesis (Scheme A6.2.1.4A). First, the CDI reagent (**124**) was synthesized via the presented route of wittig reaction to give α,β-unsaturated ester **122**, which is reduced subsequently to the alcohol with DIBAL, and finally the alcohol is subjected to CDI and generate the corresponding CDI reagent **124**. Acylation with the newly synthesized CDI reagent with cyclohexenone **125** affords β-keto ester **127**. Finally, alkylation with BnBr forms the resubstituted substrate **128**. To our dismay, when subjecting the newly synthesized substrate, we were unable to observe desired product

formation but saw only formation of the undesired protonation product X with 60% NMR yield (Scheme A6.2.1.4).

Scheme A6.2.1.4 *Synthesis of other "prenyl"-type β-keto esters.*

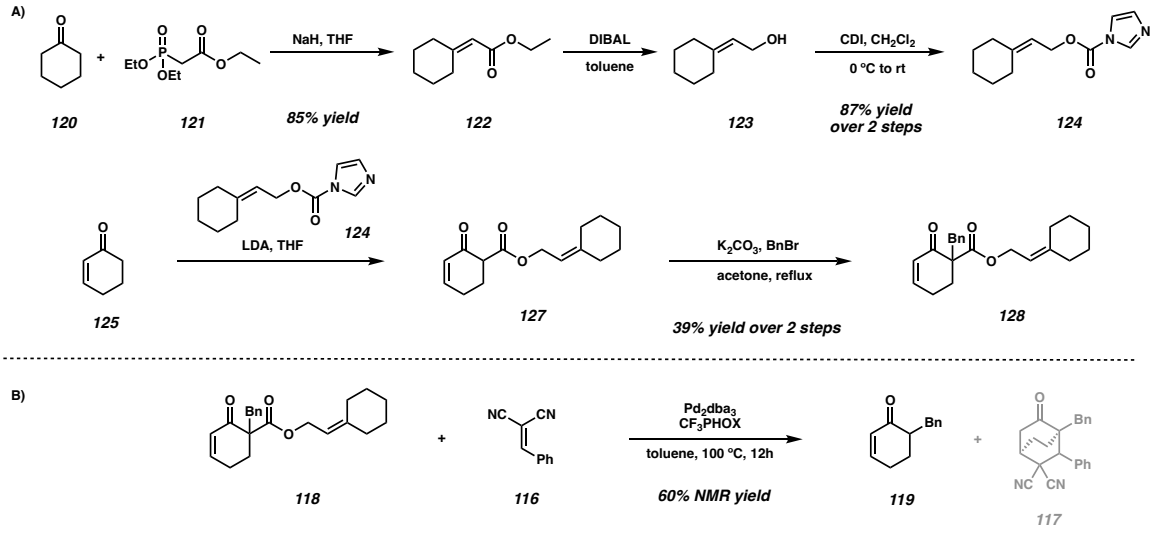

Lastly, we have also tested different electronics on the Michael acceptor to see if it causes any effect on the reaction. However, we have observed that most of the changes made resulted in an increase yield of the undesired protonation product and decrease of the desired Michael addition product (Scheme A6.2.1.5).

Scheme A6.2.1.5 *Changing the electronics on the electrophile.*

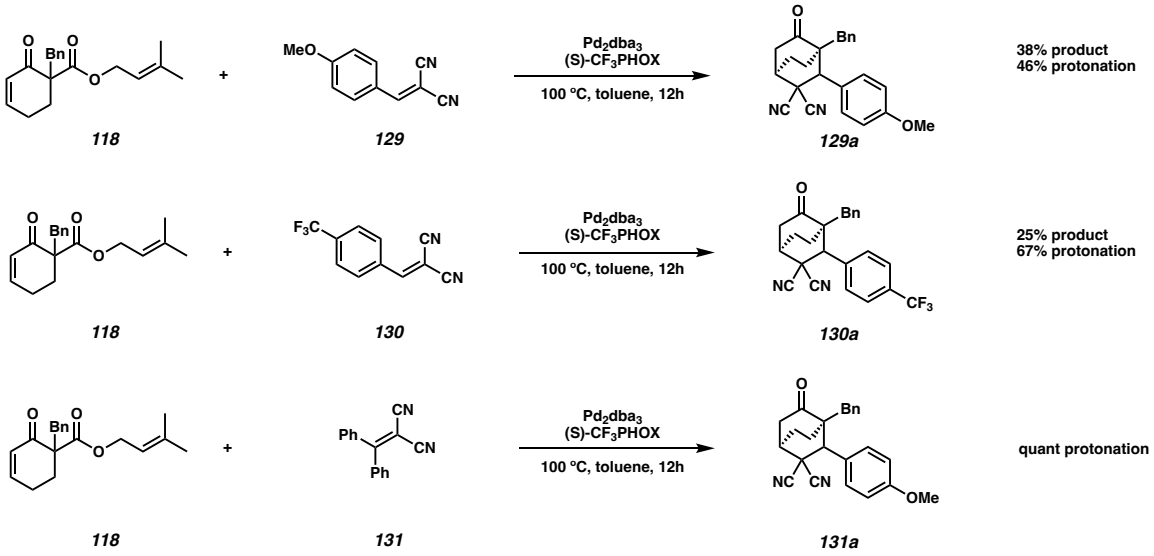

A6.2.2 FUTURE DIRECTION

Despite our best efforts, we were unable to improve the initial findings the double Michael addition from enone **118**, and one of the problems being the inseparable mixture of diastereomers. To address this issue, we have also turned our interest into the using alkyne as a Michael acceptor since that eliminates the generation of the new stereocenter and thus could potentially yield in a single diastereomer.

We have explored a few alkynes, and we have found that the diethyl propiolate **133** gives no product potentially due to its strong pi-acidic nature that has high coordination with the Pd complex, rendering the reaction difficult to proceed at lower temperatures. However, at higher temperature, **133** is susceptible to polymerization, making it unreactive. Other alkynes such as aldehyde **134** might not be stable toward the high temperature

conditions of the reaction. Therefore, further investigation is suggested to further explore this area.

Scheme A6.2.2.1 *Future direction of project – exploring alkyne Michael Acceptors.*

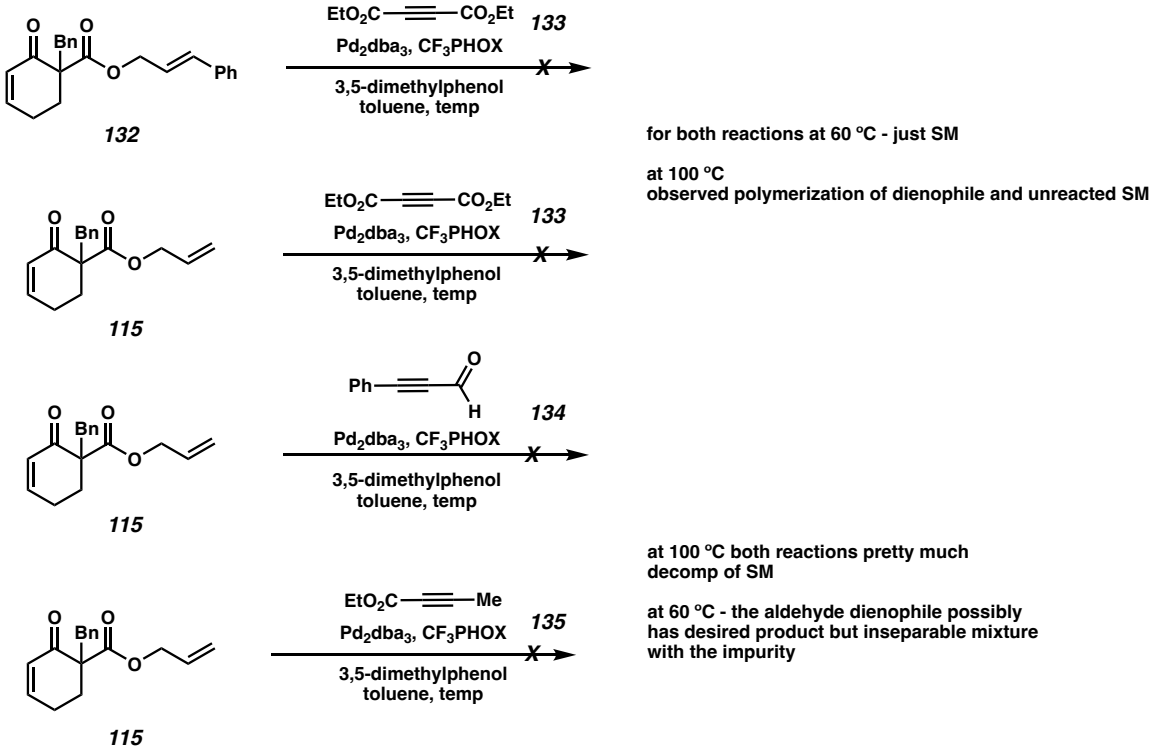

A6.3 CONCLUSION

In conclusion, we have demonstrated the efforts of the development of the asymmetric Pd-catalyzed double Michael addition into α,β-unsaturated β-keto esters. Though the reaction had an initial hit of 52% yield and 92% ee, we were unable to improve the reaction outcome further with this substrate, and the products are 2.3:1 mixture of inseparable diastereomers which complicates data analysis. A future direction of the product has been identified to use alkynes as electrophile to eliminate the issue with

forming diastereomers and the product formed from such transformation could offer more synthetic value as the canonical methods of asymmetric double Michael addition into alkynes are limited in the literature due to the poor facial selectivity of alkynes as a Michael acceptor.

\

A6. 4 REFERENCES AND NOTES

[1] Liu, Y.; Han, S.-J.; Liu, W.-B.; Stoltz, B. M. Catalytic Enantioselective Construction of Quaternary Stereocenters: Assembly of Key Building Blocks for the Synthesis of Biologically Active Molecules. *Acc. Chem. Res.* **2015**, *48*, 740–751.

[2] A) Behenna, D. C.; Stoltz, B. M. The Enantioselective Tsuji Allylation. *J. Am. Chem. Soc.* **2004**, *126*, 15044–15045. B) Behenna, D. C.; Mohr, J. T.; Sherden, N. H.; Marinescu, S. C.; Harned, A. M.; Tani, K.; Seto, M.; Ma, S.; Novák, Z.; Krout, M. R.; McFadden, R. M.; Roizen, J. L.; Enquist Jr., J. A.; White, D. E.; Levine, S. R.; Petrova, K. V.; Iwashita, A.; Virgil, S. C.; Stoltz, B. M. Enantioselective Decarboxylative Alkylation Reactions: Catalyst Development, Substrate Scope, and Mechanistic Studies. *Chemistry – A European Journal 2011*, 17, 14199–14223.

[3] Sherden, N. H.; Behenna, D. C.; Virgil, S. C.; Stoltz, B. M. Unusual Allylpalladium Carboxylate Complexes: Identification of the Resting State of Catalytic Enantioselective Decarboxylative Allylic Alkylation Reactions of Ketones. *Angewandte Chemie International Edition* **2009**, *48*, 6840–6843.

[4] Zhang, T.; Nishiura, Y.; Cusumano, A. Q.; Stoltz, B. M. Palladium-Catalyzed Asymmetric Conjugate Addition of Arylboronic Acids to α,β-Unsaturated Lactams: Enantioselective Construction of All-Carbon Quaternary Stereocenters in Saturated Nitrogen-Containing Heterocycles. *Org. Lett.* **2023**, *25*, 6479–6484.

[5] Inanaga, K.; Wollenburg, M.; Bachman, S.; Hafeman, N. J.; Stoltz, B. M. Catalytic Enantioselective Synthesis of Carbocyclic and Heterocyclic Spiranes via a Decarboxylative Aldol Cyclization. *Chem. Sci.* **2020**, *11*, 7390–7395.

[6] Flesch, K. N.; Cusumano, A. Q.; Chen, P.-J.; Strong, C. S.; Sardini, S. R.; Du, Y. E.; Bartberger, M. D.; Goddard, W. A. I.; Stoltz, B. M. Divergent Catalysis: Catalytic Asymmetric [4+2] Cycloaddition of Palladium Enolates. *J. Am. Chem. Soc.* **2023**, *145*, 11301–11310.

[7] Mohr, J. T.; Hong, A. Y.; Stoltz, B. M. Enantioselective Protonation. *Nat Chem* **2009**, *1*, 359–369.

8 Inanaga, K.; Wollenburg, M.; Bachman, S.; Hafeman, N. J.; Stoltz, B. M. Catalytic Enantioselective Synthesis of Carbocyclic and Heterocyclic Spiranes via a Decarboxylative Aldol Cyclization. *Chem. Sci***. 2020***, 11*, 7390–7395.

PROTON NMR FOR NEW COMPOUNDS RELEVANT TO APPENDIX 6

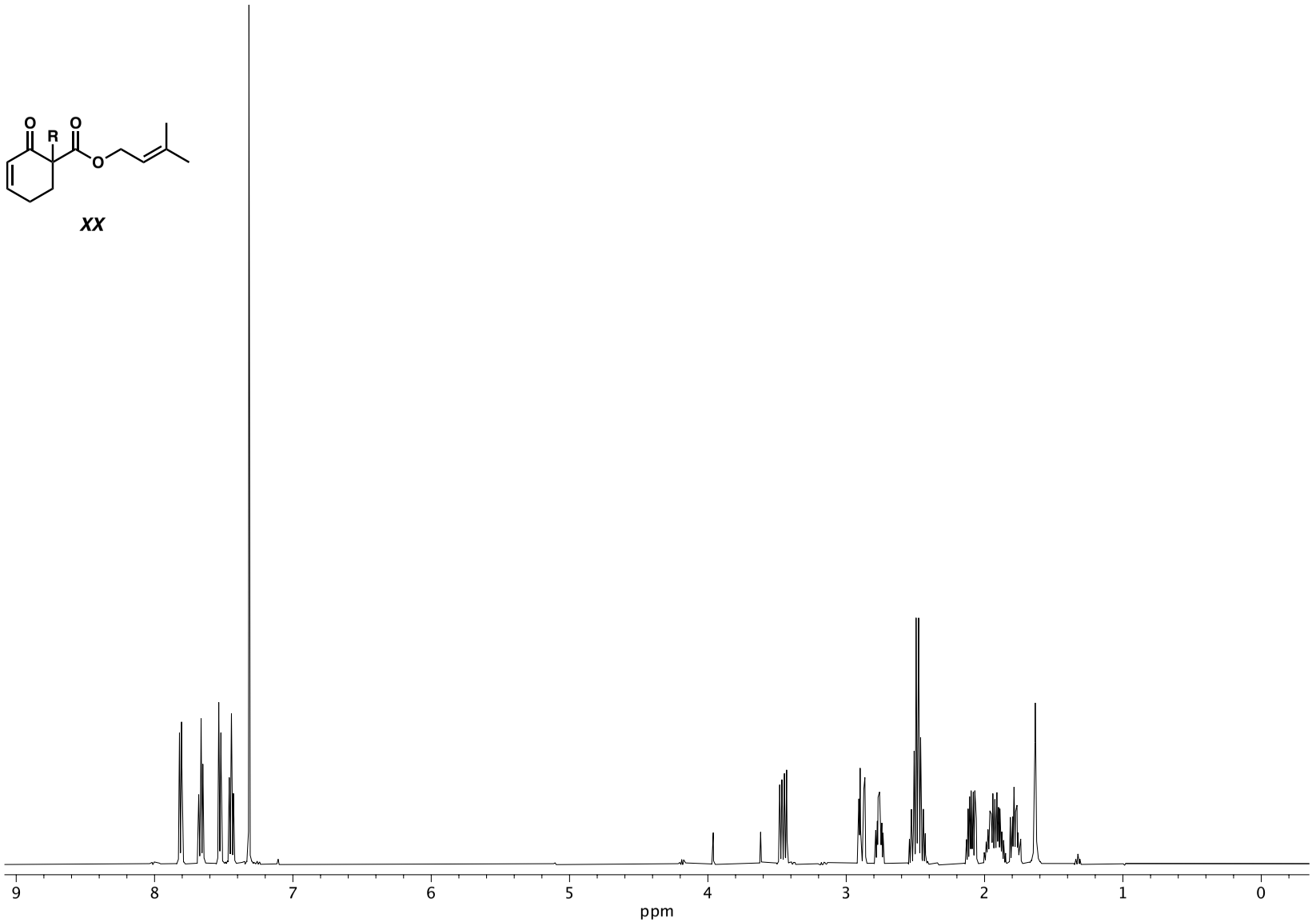

Figure A3.1. *^{1}H NMR (400 MHz, $CDCl_3$) of compound* ***160a***.

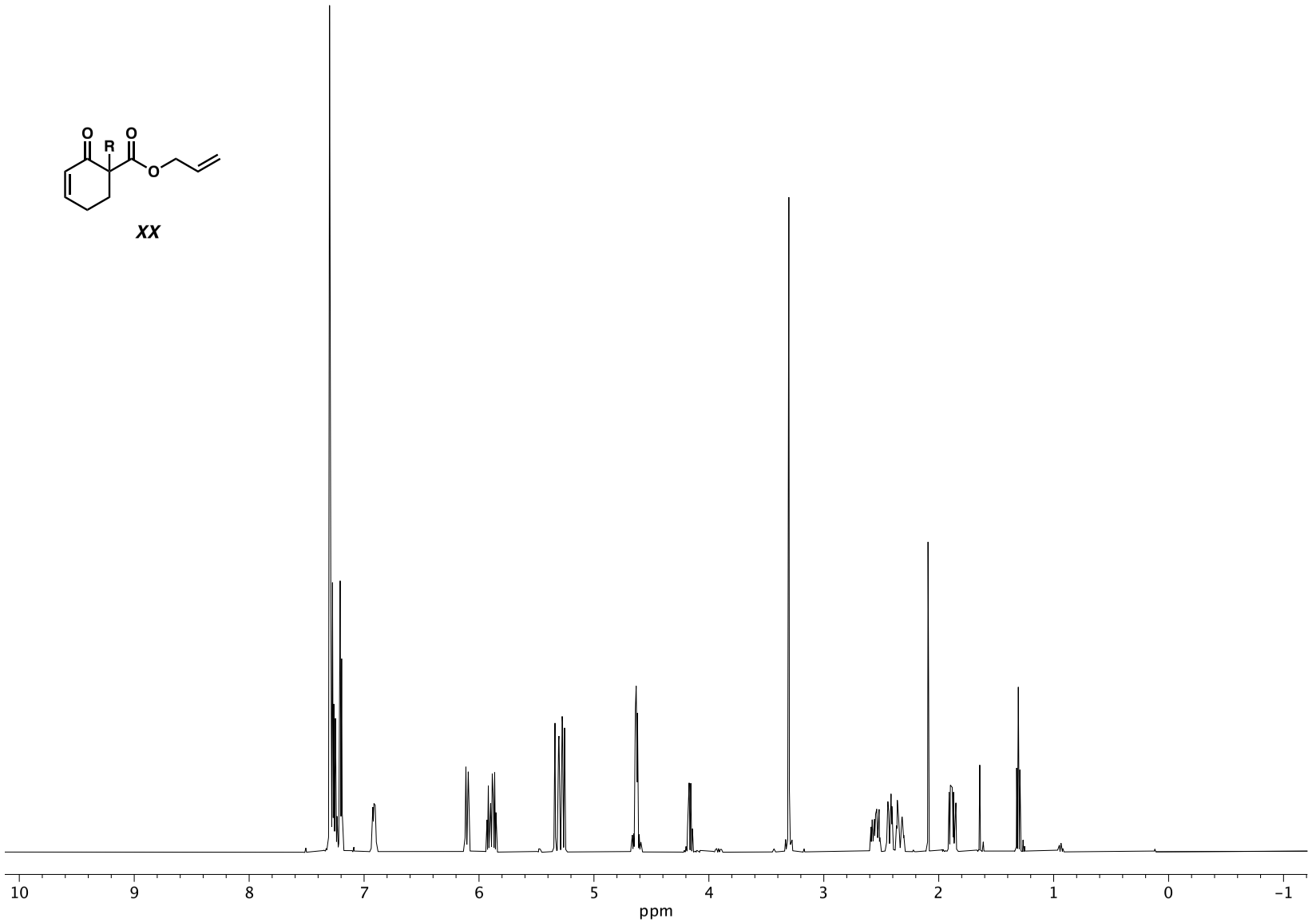

XX

Figure A3.1. *^{1}H NMR (400 MHz, $CDCl_3$) of compound* ***160a****.*

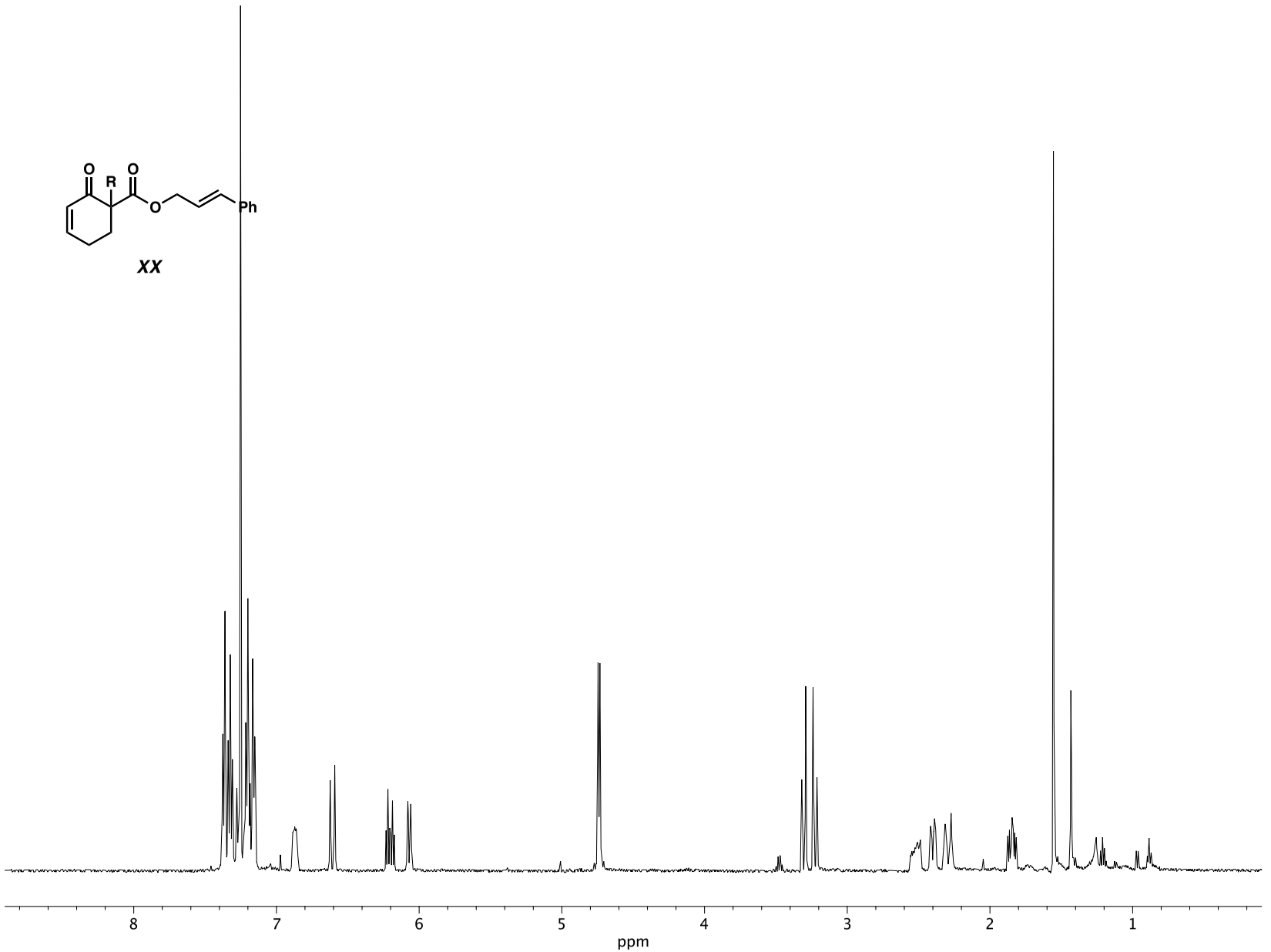

Figure A3.1. *^{1}H NMR (400 MHz, $CDCl_3$) of compound* ***160a***.

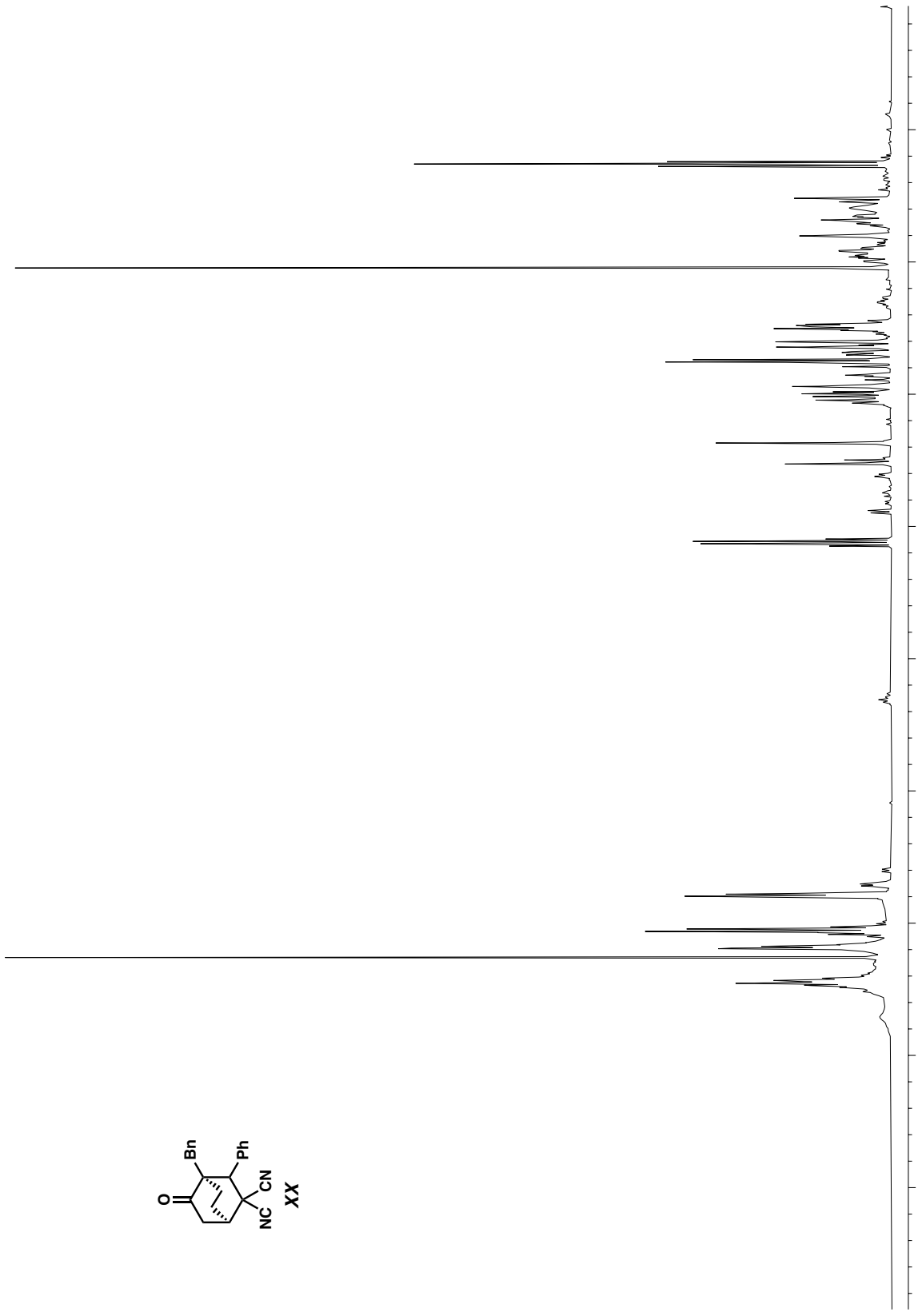

Figure A3.1. *^{1}H NMR (400 MHz, $CDCl_3$) of compound* ***160a***.

Figure A3.3. *^{13}C NMR (100 MHz, $CDCl_3$) of compound* ***160a***.

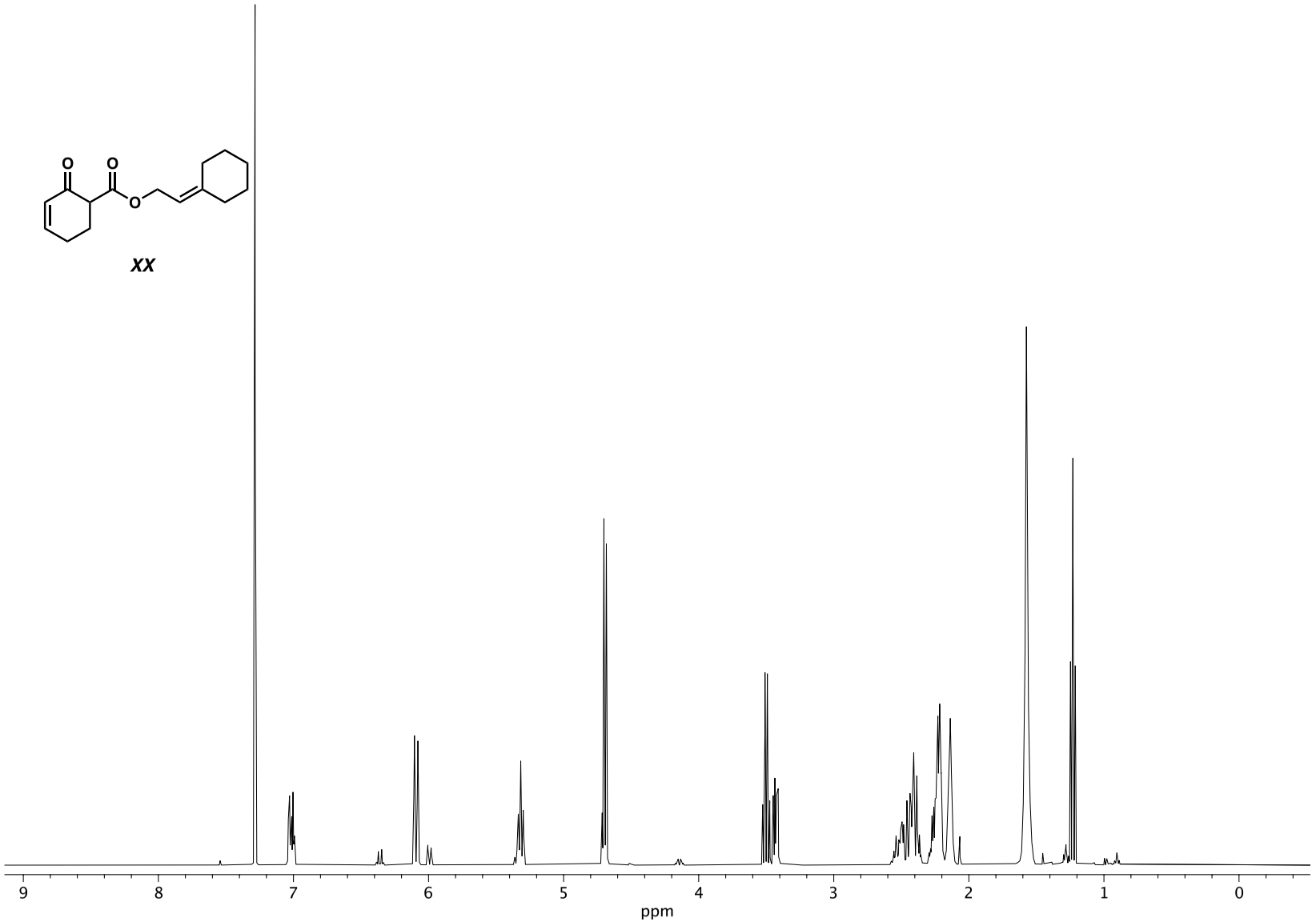

Figure A3.1. *^{1}H NMR (400 MHz, $CDCl_3$) of compound* ***160a***.

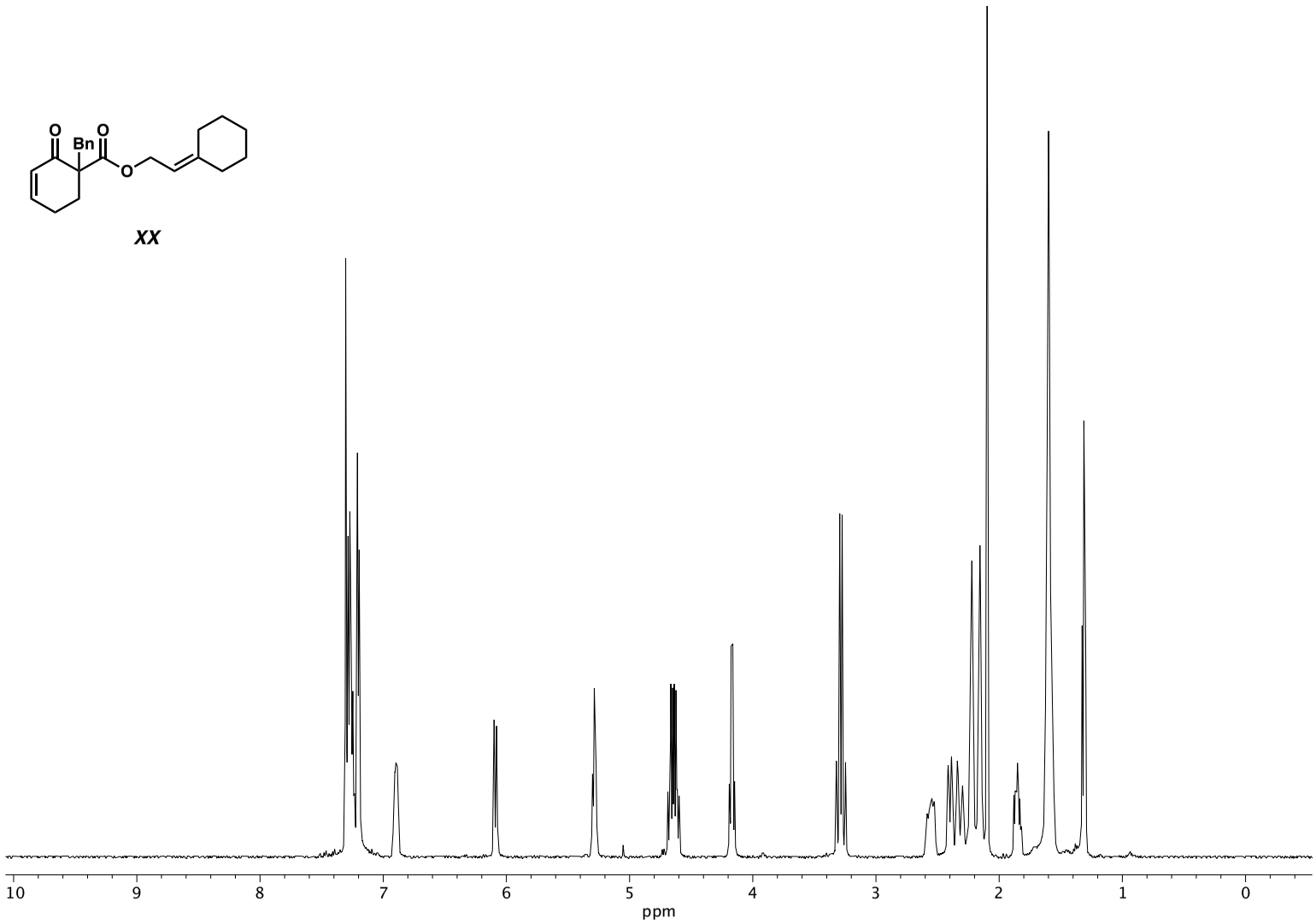

Figure A3.1. *^{1}H NMR (400 MHz, $CDCl_3$) of compound* ***160a***.

APPENDIX 7

Progress Toward an Asymmetric Spirocyclization of Pd Enolates†

A7.1 INTRODUCTION

All-carbon quaternary stereocenters are abundantly present in complex molecules, yet their asymmetric construction remains a persistent challenge in the synthetic chemistry community. Notable examples of natural products and drug molecules featuring this motif include Naloxone, (+)-Limaspermidine, (+)-Hamigeran B, and (–)-Cyanthiwigin F, as illustrated in Figure A7.1.1.[1] Consequently, our group has dedicated significant interest to the development of methodologies that enable the synthesis of these intricately substituted substrates with high efficiency and enantioselectivity from prochiral starting materials.

Figure A7.1.1 *Examples pharmaceuticals and natural products that bears all-carbon quaternary stereocenters.*

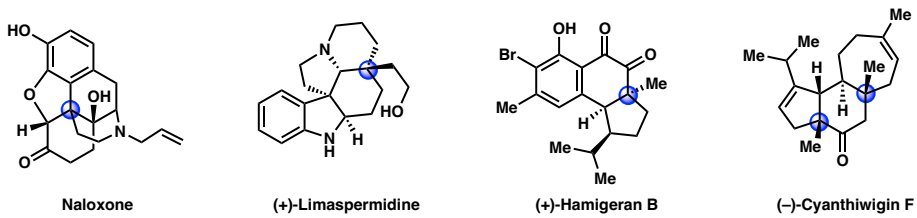

We have conducted thorough investigations into Pd-catalyzed allylic alkylation methods, which showcase a distinctive inner-sphere reductive elimination from the chiral Pd-enolate (refer to Figure A7.1.2). These methodologies commence from racemic starting materials such as β-keto ester **81**, enol carbonate **109**, or silyl enol ether **110**. The resultant

†This research was carried out with Jay Barbor and Kaylin N. Flesch.

products can subsequently serve as enantioenriched synthetic building blocks for the construction of more intricate molecules.[2]

Figure A7.1.2 *Pd-catalyzed decarboxylative asymmetric allylic alkylation.*

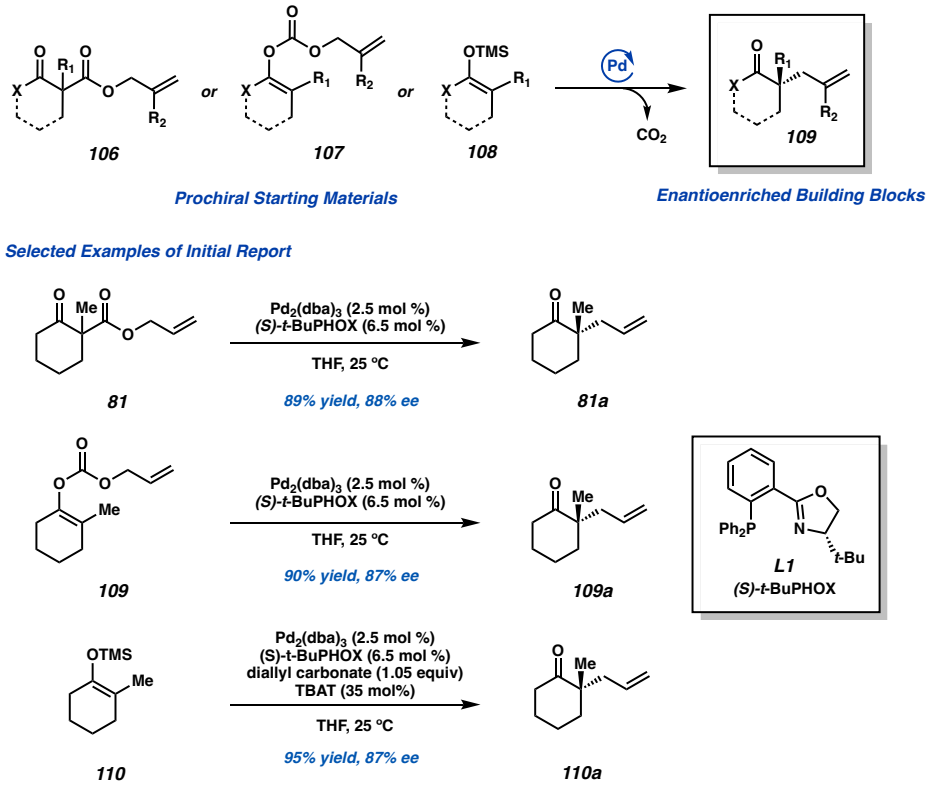

The proposed mechanism of this transformation initiates with oxidative addition to generate the Pd π-allyl species (Figure A7.1.3, X). Subsequent decarboxylation leads to the formation of the chiral Pd enolate (**C**). The enantio-determining step occurs during C–C bond formation, resulting in the formation of the all-carbon quaternary center. Lastly, ligand exchange with another β-keto ester starting material facilitates the construction of product **71a**, achieved in good yield and enantiomeric excess.[3]

Figure A7.1.3 *Proposed catalytic cycle of the Pd-catalyzed asymmetric decarboxylative allylic alkylation.*[3]

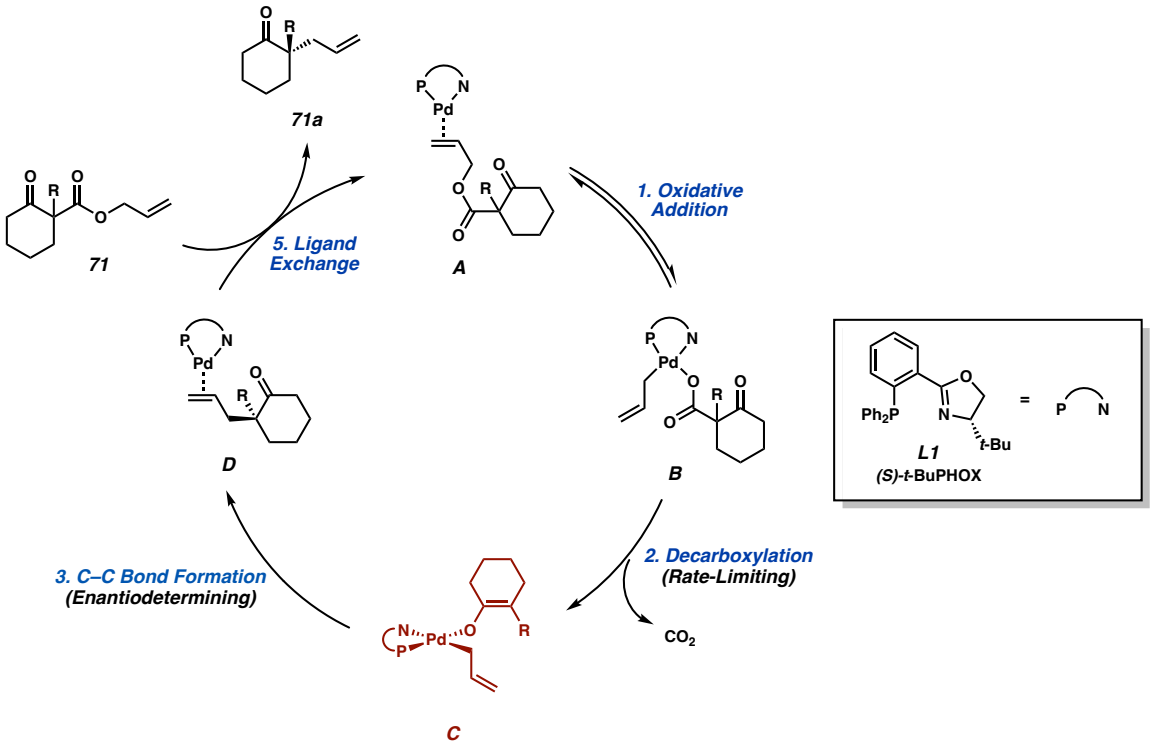

In recent years, our group has directed its attention toward divergent catalysis, with the main focus on harnessing the chiral O-bound Pd enolate intermediate (**C**, highlighted in red in Figure A7.1.3) and extending its application to reactions beyond allylic alkylation. Notably, this Pd enolate holds unique significance as it is formed without the need for exogenous base and originates from racemic enolate precursors. This characteristic endows it with immense potential for synthetic utility. With the concept of divergent catalysis by intercepting the original catalytic cycle (Figure A7.1.4), we have reported several asymmetric transformations that utilize Pd enolate 74 such as conjugate addition[4], intramolecular aldol reaction[5], intramolecular Diels–Alder reaction,[6] and protonation[7].

Figure A7.1.4 *Examples of divergent catalysis from Pd enolate 74.*

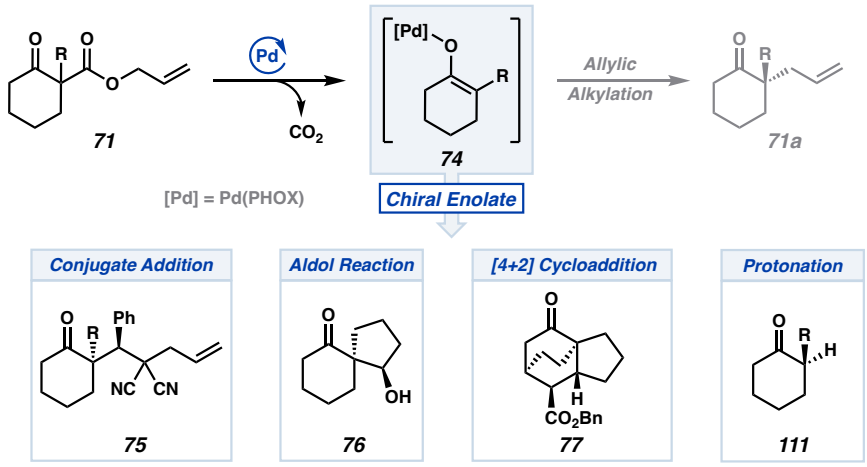

In this research, we present the development of an asymmetric spirocyclization of Pd enolate **74** using β-keto ester (**136**) with a tethered azide as starting material to generate spirocyclic lactams (**136a**) (Figure A7.1.5)

Figure A7.1.5 *This research.*

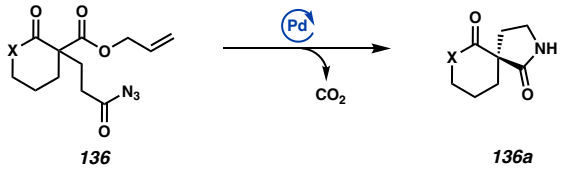

In addition to generating an all-carbon quaternary stereocenter, spirocyclic lactam is also a synthetic motif that is very prevalent in natural products and drug molecules. Many FDA-approved drugs such as Minalrestat[8] and complex molecules such as Horsfiline[9] and (+)-Aspergillin PZ[10] possesses this feature as shown in Figure A7.1.6.

Figure A7.1.6 *Selected examples of drug molecules and natural products that contain spirocyclic lactam motifs.*

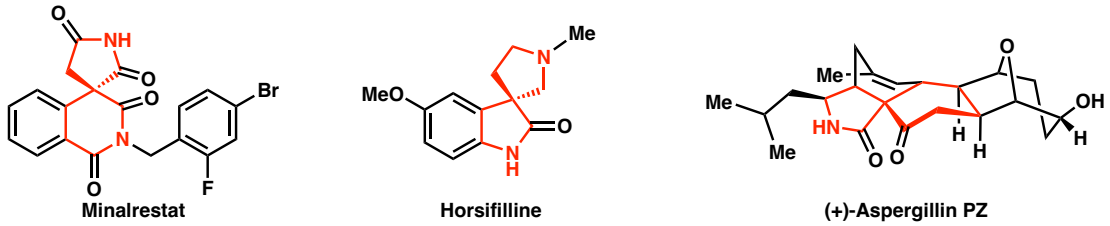

Despite of spirocyclic lactams being a common feature of complex targets, most of the literature precedents do not offer asymmetric synthesis of the spirocycle, and even for racemic cases, existing approaches are hindered by substantial substrate scope limitations. Notably, Rihs and colleagues demonstrated a Schmidt rearrangement employing sodium azide to convert carboxylic acid **137** into 2,4-diazocine **138** (Figure A7.1.7A), which eventually leads to the synthesis of the drug CGP 48508 (**139**) with negative chronotropic effect.[11] In a separate study in 2015, Xue and coauthors showcased the synthesis of spirocyclic lactams from β-keto carboxylic acid X on a racemic basis; however, product formation was confined to γ-pyrrolidines and with only moderate yields (Figure A7.1.7B).[12]

Figure A7.1.7 *Literature precedents of forming spirocyclic lactams. A) Rihs and coworkes synthesis of CGP 48508 which utilizes spiry cycle formation as a key step. B) the development of spirocyclization of β-keto carboxylic acids to form spirolactams.*

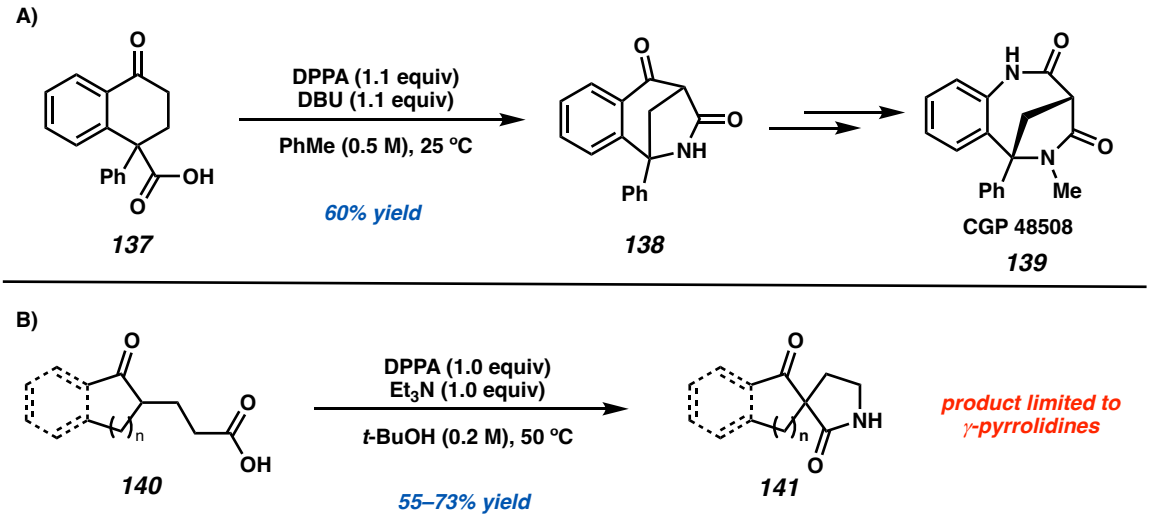

The initial hit of the transformation described started from acyl azide **142** and the Curtius rearrangement was triggered upon heating in 1,4-dioxane for 5 hours, then the corresponding isocyanate is formed in situ and subjected to $Pd(OAc)_2$ and (S)-tBuPHOX ligand (L1) to obtain spirocyclic product **143** in 10% yield and excellent 89% ee (Figure A7.1.8). Most of the mass balance of this transformation was attributed to the formation of biproducts **144** and **145** which is a hydrolysis dimer and a product/isocyanate dimer, respectively.

Figure A7.1.8 *Initial Spirocyclization results.*

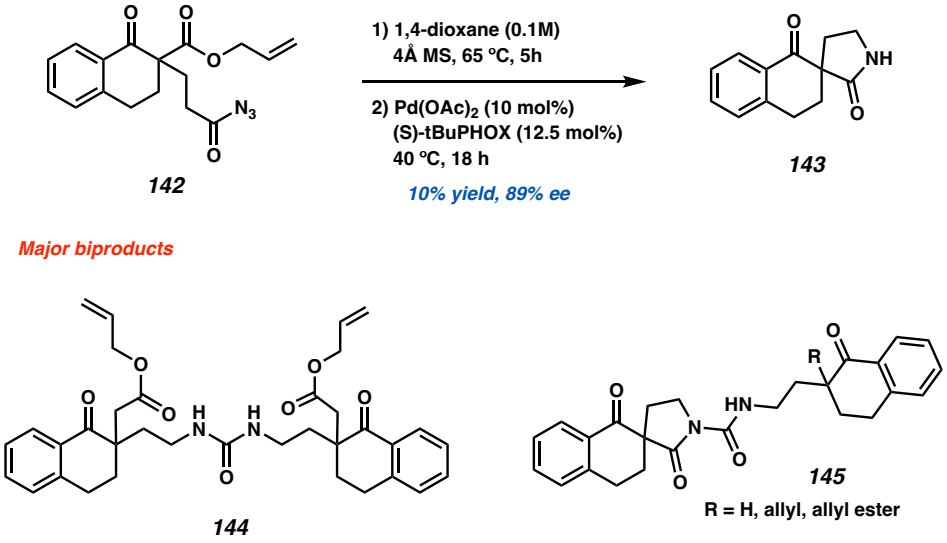

Another major focus was to induce reductive deallylation via adding an allyl trapping additive (Figure A7.1.9A). In the asymmetric aldol reaction reported by our group, 3,5-dimethylphenol was utilized to turn over the catalytic cycle by deallylating and protonating the resulting alkoxide. Similarly, in the asymmetric protonation report, Meldrum's acid was identified as a competent additive for the reaction. Upon trying several similar Bronsted acid additives, we have identified Meldrum's acid being one of the superior choices of a good starting point for optimization with the initial result of 31% yield and 89% ee (Figure A7.1.9B).

Figure A7.1.9 *Examples of allyl-trapping additives reported previously.*

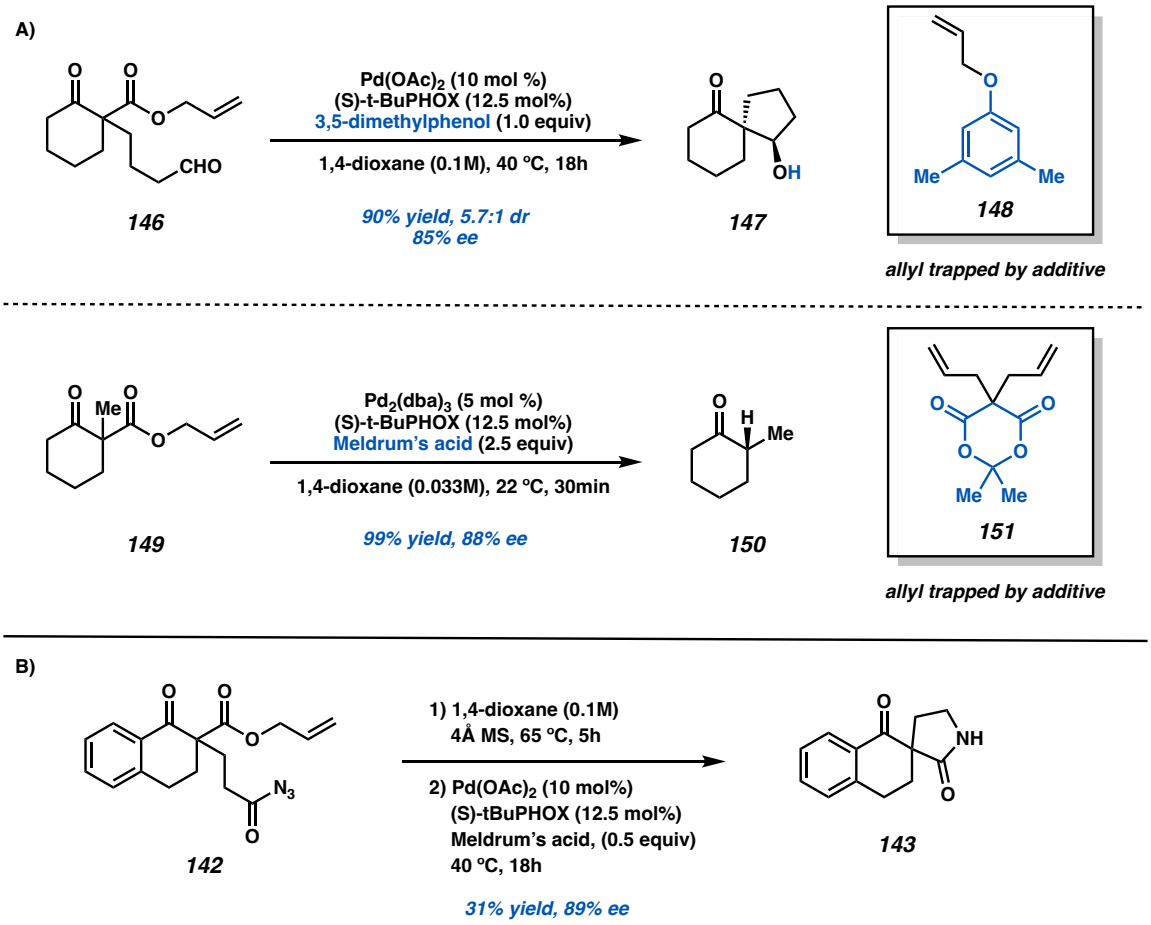

A7.2 RESULTS AND DISCUSSION

A7.2.1 OPTIMIZATION

After recognizing the potential advantages of employing Bronsted acid-type additives such as Meldrum's acid, our focus shifted toward optimizing the reaction utilizing these conditions as a starting point. Initially, we encountered variability in reaction yield, as depicted in Table A7.2.1.1. Subsequent investigation revealed the critical importance of precise Meldrum's acid quantities for the reaction's success.

Consequently, we adopted a strategy of preparing a freshly made stock solution rather than relying on weighed-out reagents. This adjustment proved instrumental in enhancing the accuracy and consistency of our results.

Table A7.2.1.1 *Examples of allyl-trapping additives reported previously.*

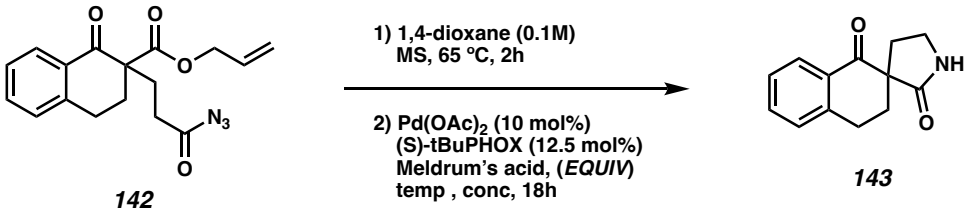

142 ***143***

Entry	Meldrum's Acid Equiv	Yield	ee%
1	0.5 equiv	59	93
2	0.6 equiv	59	92
3	0.7 equiv	48	91
4	1.0 equiv	19	90
5	2.0 equiv	trace	N/A

Knowing the criticalness of Meldrum's acid concentration, we decided to perform an assay with very carefully weighted Meldrum's acid stock solutions to see if a slightly higher concentration would be preferred. However, we have found that 0.5 equiv to be optimal, as the higher concentrations diminish the reaction yield tremendously (Table A7.2.1.2).

Table* A7.*2.1.2 *Different concentrations of Meldrum's acid.*

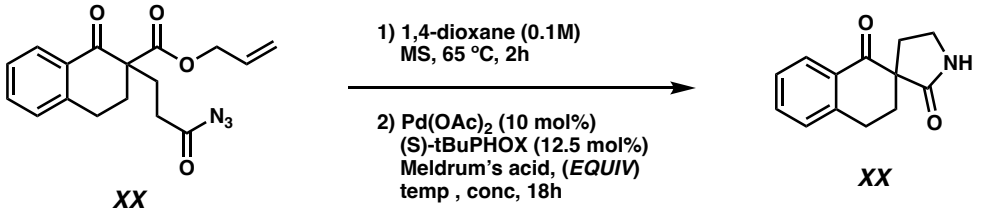

XX ***XX***

Entry	Meldrum's Acid Equiv	Yield	ee%
1	0.5 equiv	59	93
2	0.6 equiv	59	92
3	0.7 equiv	48	91
4	1.0 equiv	19	90
5	2.0 equiv	trace	N/A

Having success with Meldrum's acid, we have also explored other Bronsted acid additives such as dimedone, acac, methane sulfonylacetone, and we have found that Meldrum's acid is still the superior choice of additive for this transformation (Table A7.2.1.3).

Table* A7.*2.1.3 *Different concentrations of Meldrum's acid.*

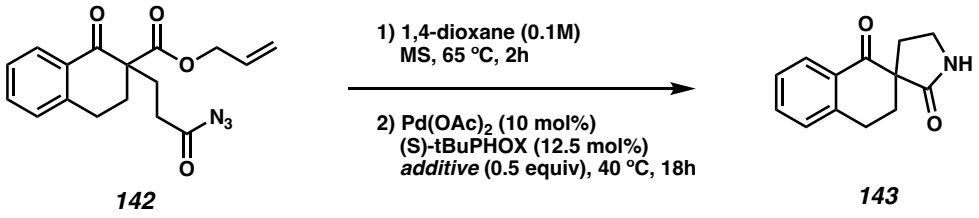

142 ***143***

Entry	Additive	Yield	ee%
1	dimedone	43	31
2	acac	32	58
3	methane sulfonylacetone	N/A	N/A
4	Meldrum's acid	44	93

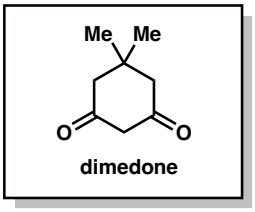

dimedone

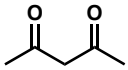

acac

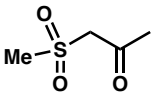

methane sulfonylacetone

During our search for the optimized conditions for the proposed reaction, we have also turned our interest in benzoylated δ-lactams for a potential area of exploration. However, we found that using the conditions developed with tetralone **142**, the ee is significantly lower with the lactam substrate (entry 1, table A7.2.1.4) with only 40% ee. We then synthesized many derivatives of Meldrum's acid and have tested them against the lactam substrate (**144**) with both (S)-tBuPHOX and (S)-tBu-CF3PHOX. To our delight, additive D significantly showed improvement toward the yield and the ee of the reaction for both tBuPHOX (entry 5) and CF3PHOX (entry 11).

Table* A7.*2.1.4 *Synthesized derivatives of Meldrum's acid and their reactivity.*

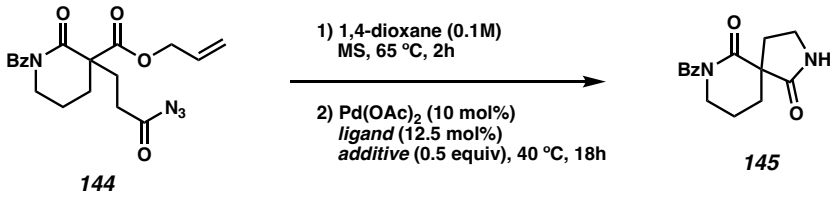

144 ***145***

Entry	Ligand	Additive	Yield	ee%
1	(S)-CF3-tBuPHOX	Meldrums acid	79	40
2	(S)-tBuPHOX	A	69	62
3	(S)-tBuPHOX	B	20	52
4	(S)-tBuPHOX	C	quant	7
5	(S)-tBuPHOX	D	98	63
6	(S)-tBuPHOX	E	77	61
7	(S)-tBuPHOX	F	84	62
8	(S)-tBuPHOX	G	82	21
9	(S)-CF3-tBuPHOX	A	73	60
10	(S)-CF3-tBuPHOX	B	4	N/A
11	(S)-CF3-tBuPHOX	C	83	10
12	(S)-CF3-tBuPHOX	D	71	66
13	(S)-CF3-tBuPHOX	E	57	58
14	(S)-CF3-tBuPHOX	F	74	58
15	(S)-CF3-tBuPHOX	G	13	-3

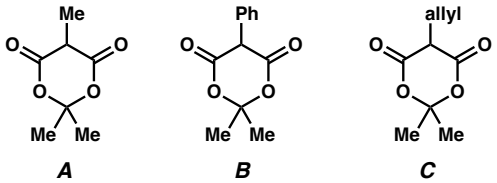

A ***B*** ***C***

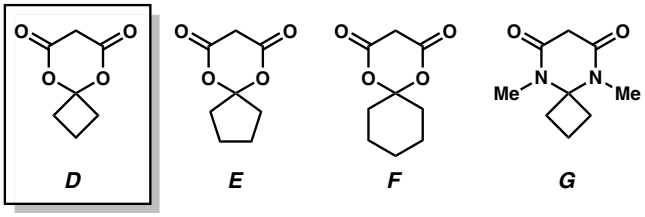

D ***E*** ***F*** ***G***

However, despite our extensive efforts, we were unable to advance the lactam substrate further to improve the ee including changing ligands, protecting groups, etc. We were delighted to see that when subjecting the newly discovered additive D to the parent tetralone substrate (**142**), we saw a significant improvement in yield to about quantitative yield without sacrificing ee (Table A7.2.1.5).

Table* A7.*2.1.5 *Additive D with tetralone substrate (142).*

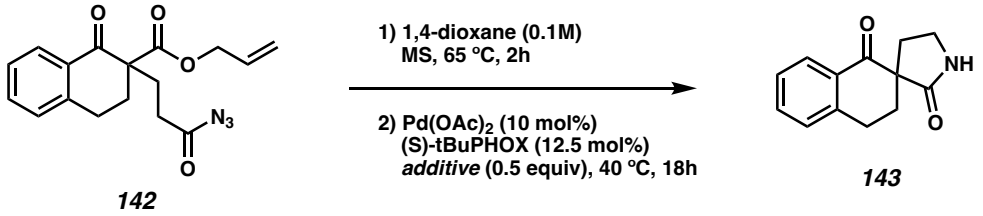

142 ***143***

Entry	Additive	Yield	ee%
1	Meldrum's acid	59	93
2	additive D	99	95

A7.2.2 SUBSTRATE SCOPE & MECHANISTIC INVESTIGATION

The current stage of the reaction development focuses on synthesizing substrate scope and conducting experiments to gain insights on mechanistic pathway of the proposed transformation. The established route of synthesizing the acyl azide starting material starts with β-keto ester **142** that is either achieved via acylation or cyclization. Alkylation with tBu acrylate **148** to afford tetrasubstituted β-ketoester **149**. Upon acid hydrolysis, carboxylic acid **150** is obtained in quantitative yield. Lastly, treatment with sodium azide, triphenylphosphine, and trichloroacetonitrile, azide **151** is formed in modest yield.

Scheme* A7.*2.2.1 *Developed route for substrate synthesis using cyclohexanone 151 as an example.*

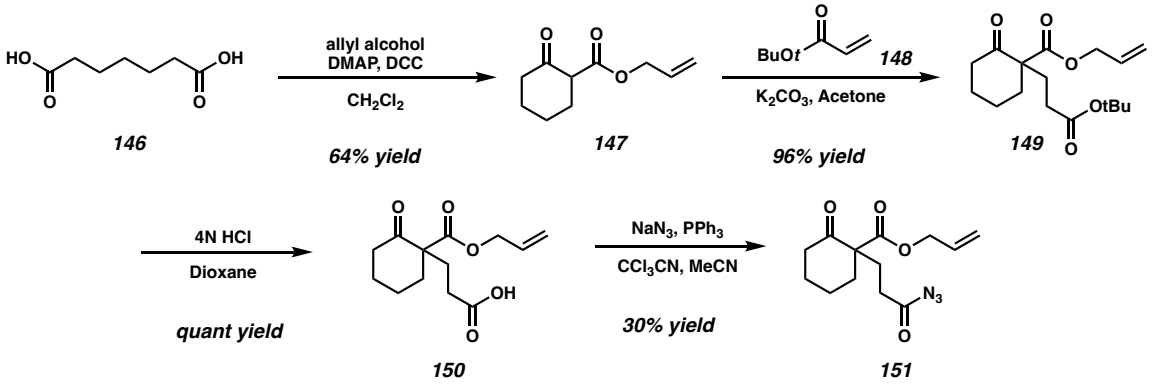

Efforts are ongoing to expand the substrate scope of the reaction. As we are trying the developed reaction conditions, we have learned several limitations of the reaction and mechanistic insights of the reaction.

A7.3 CONCLUSION

In conclusion, this is ongoing research in the development of the Pd-catalyzed asymmetric spirocyclization. Under the optimized reaction conditions, the parent tetralone substrate exhibits 99% yield and 95% ee. Currently, we are conducting mechanistic studies along with developing substrate scope.

A7.4 REFERENCES AND NOTES

[1] Liu, Y.; Han, S.-J.; Liu, W.-B.; Stoltz, B. M. Catalytic Enantioselective Construction of Quaternary Stereocenters: Assembly of Key Building Blocks for the Synthesis of Biologically Active Molecules. *Acc. Chem. Res.* **2015**, *48*, 740–751.

[2] A) Behenna, D. C.; Stoltz, B. M. The Enantioselective Tsuji Allylation. *J. Am. Chem. Soc.* **2004**, *126*, 15044–15045. B) Behenna, D. C.; Mohr, J. T.; Sherden, N. H.; Marinescu, S. C.; Harned, A. M.; Tani, K.; Seto, M.; Ma, S.; Novák, Z.; Krout, M. R.; McFadden, R. M.; Roizen, J. L.; Enquist Jr., J. A.; White, D. E.; Levine, S. R.; Petrova, K. V.; Iwashita, A.; Virgil, S. C.; Stoltz, B. M. Enantioselective Decarboxylative Alkylation Reactions: Catalyst Development, Substrate Scope, and Mechanistic Studies. *Chemistry – A European Journal 2011*, 17, 14199–14223.

[3] Sherden, N. H.; Behenna, D. C.; Virgil, S. C.; Stoltz, B. M. Unusual Allylpalladium Carboxylate Complexes: Identification of the Resting State of Catalytic Enantioselective Decarboxylative Allylic Alkylation Reactions of Ketones. *Angewandte Chemie International Edition* **2009**, *48*, 6840–6843.

[4] Zhang, T.; Nishiura, Y.; Cusumano, A. Q.; Stoltz, B. M. Palladium-Catalyzed Asymmetric Conjugate Addition of Arylboronic Acids to α,β-Unsaturated Lactams: Enantioselective Construction of All-Carbon Quaternary Stereocenters in Saturated Nitrogen-Containing Heterocycles. *Org. Lett.* **2023**, *25*, 6479–6484.

[5] Inanaga, K.; Wollenburg, M.; Bachman, S.; Hafeman, N. J.; Stoltz, B. M. Catalytic Enantioselective Synthesis of Carbocyclic and Heterocyclic Spiranes via a Decarboxylative Aldol Cyclization. *Chem. Sci.* **2020**, *11*, 7390–7395.

[6] Flesch, K. N.; Cusumano, A. Q.; Chen, P.-J.; Strong, C. S.; Sardini, S. R.; Du, Y. E.; Bartberger, M. D.; Goddard, W. A. I.; Stoltz, B. M. Divergent Catalysis: Catalytic Asymmetric [4+2] Cycloaddition of Palladium Enolates. *J. Am. Chem. Soc.* **2023**, *145*, 11301–11310.

[7] Mohr, J. T.; Hong, A. Y.; Stoltz, B. M. Enantioselective Protonation. *Nat Chem* **2009**, *1*, 359–369.

[8] Akamine, E. H.; Hohman, T. C.; Nigro, D.; Carvalho, M. H. C.; Tostes, R. de C.; Fortes, Z. B. Minalrestat, an Aldose Reductase Inhibitor, Corrects the Impaired Microvascular Reactivity in Diabetes. *J. Pharmacol. Exp. Ther* **2003**, *304*, 1236–1242.

[9] Jossang, A.; Jossang, P.; Hadi, H. A.; Sevenet, T.; Bodo, B. Horsfiline, an Oxindole Alkaloid from Horsfieldia Superba. *J. Org. Chem.* **1991**, *56*, 6527–6530.

[10] Reyes, J. R.; Winter, N.; Spessert, L.; Trauner, D. Biomimetic Synthesis of (+)-Aspergillin PZ. *Angewandte Chemie International Edition* **2018**, *57*, 15587–15591.

[11] Herold, P.; Herzig, J. W.; Wenk, P.; Leutert, T.; Zbinden, P.; Fuhrer, W.; Stutz, S.; Schenker, K.; Meier, M.; Rihs, G. 5-Methyl-6-Phenyl-1,3,5,6-Tetrahydro-3,6-Methano-1,5-Benzodiazocine-2,4- Dione (BA 41899): Representative of a Novel Class of Purely Calcium-Sensitizing Agents. *J. Med. Chem.* **1995**, *38*, 2946–2954.

[12] Yang, W.; Sun, X.; Yu, W.; Rai, R.; Deschamps, J. R.; Mitchell, L. A.; Jiang, C.; MacKerell, A. D. Jr.; Xue, F. Facile Synthesis of Spirocyclic Lactams from β-Keto Carboxylic Acids. *Org. Lett.* **2015**, *17*, 3070–3073.

ABOUT THE AUTHOR

Tsam Mang Melinda Chan was born in Hong Kong on December 17th, 1996, to Ngai Lam Cheung and Chuen Chan. Shortly after birth, she moved to Beijing, China, with her parents, where she attended elementary school through high school. During her high school years, she developed a strong interest in chemistry and economics but eventually decided to pursue a career in chemistry because of her high school chemistry teacher, Mr. Cav. She was also a competitive softball player, fielding the position of Left Center on the varsity team in high school.

In the fall of 2015, Melinda moved to San Diego, California by herself to pursue her undergraduate degree, initially as a general chemistry major. In her freshman year, she joined the lab of Elizabeth Komives, studying the structure, synthesis, and dynamics of Ubiquitin E3 Ligase. During her second year, she developed a keen interest in organic chemistry after taking the class series and changed her major to pharmacological chemistry. She then joined the lab of Dionicio Siegel at the Skaggs School of Pharmacy and worked on the synthesis of Fatty Acid Esters of Hydroxy Fatty Acid (FAHFA) derivatives. Her mentor, Andrew Nelson, in the Siegel lab, along with her passion for organic synthesis, inspired her to pursue a PhD in Chemistry.

In the summer of 2018, Melinda interned at Takeda Pharmaceuticals in the Medicinal Chemistry department, where she learned many industry-level organic synthesis techniques. In 2019, Melinda moved to Pasadena to pursue her PhD at the California Institute of Technology. She joined the lab of Professor Brian Stoltz, where she first worked on a total synthesis project, followed by Pd enolate synthesis and applications. She was on the summer softball team for two years, and she developed a passion for fostering diversity and inclusion in STEM. In the spring of 2022, she joined the DICI executive board, and during her two and a half years in DICI, she had

the pleasure of working with many amazing, passionate, and talented individuals ranging from students, postdocs, staff, and faculties.

Following graduation, Melinda will begin her career as an Associate at McKinsey & Company in the Southern California office. She has always had an interest in economics/finance, which propelled her to obtain a business minor in undergraduate studies. She found that consulting is a great field to combine her passion for STEM, business building, and problem-solving altogether. Melinda currently lives in Downtown Los Angeles with her boyfriend, Derek Ruan, and their cat, Pusheen, and dog, Mochi. Her hobbies include hiking, skiing, building Legos and jigsaw puzzles, and going to escape rooms.